CONF-971014 -- Vol.1

Proceedings of the 6th International Conference on Stability and Handling of Liquid Fuels

Vancouver, B. C., Canada
October 13-17, 1997

Volume 1

Edited by Harry N. Giles
Operations and Readiness Office
Deputy Assistant Secretary for Strategic Petroleum Reserve
Assistant Secretary for Fossil Energy

MASTER

DISTRIBUTION OF THIS DOCUMENT IS UNLIMITED

U.S. Department of Energy
Washington, DC

1998

Printed with soy ink on recycled paper

Previous Conferences

Conference on Long Term Storage Stabilities of Liquid Fuels, Tel Aviv, Israel, July 11-14, 1983. Proceedings published by the Israel Institute of Petroleum and Energy, Nahum Por, editor; Tel Aviv, Israel, December 1983.

2nd International Conference on Long-Term Storage Stabilities of Liquid Fuels, San Antonio, Texas, USA, July 29-August 1, 1986. Proceedings published by the Southwest Research Institute, Leo L. Stavinoha, editor; San Antonio, Texas, USA, October 1986.

3rd International Conference on Stability and Handling of Liquid Fuels, London, England, September 13-16, 1988. Proceedings published by the Institute of Petroleum (London), R. W. Hiley, R. E. Penfold, and J. F. Pedley, editors; London, England, November 1988.

4th International Conference on Stability and Handling of Liquid Fuels, Orlando, Florida, USA, November 19-22, 1991. Proceedings published by the U. S. Department of Energy, Harry N. Giles, editor; Washington, DC, USA, 1992.

5th International Conference on Stability and Handling of Liquid Fuels, Rotterdam, the Netherlands, October 3-7, 1994. Proceedings published by the U. S. Department of Energy, Harry N. Giles, editor; Washington, DC, USA, 1995.

DISCLAIMER

This report was prepared as an account of work sponsored by an agency of the United States Government. Neither the United States Government nor any agency thereof, nor any of their employees, makes any warranty, express or implied, or assumes any legal liability or responsibility for the accuracy, completeness, or usefulness of any information, apparatus, product, or process disclosed, or represents that its use would not infringe privately owned rights. Reference herein to any specific commercial product, process, or service by trade name, trademark, manufacturer, or otherwise does not necessarily constitute or imply its endorsement, recommendation, or favoring by the United States Government or any agency thereof. The views and opinions of authors expressed herein do not necessarily state or reflect those of the United States Government or any agency thereof.

DISCLAIMER

Portions of this document may be illegible in electronic image products. Images are produced from the best available original document.

Contents

Corresponding Authors' Addresses xi
Author Index .....
Preface .....

Volume I

Opening Address - I. A. King 1

Opening Address - II. H. U. Schellhase 5

Aviation Fuels - I. Dr. Cyrus P. Henry, Jr., Chair

Removal of Copper from Fuel by Immobilized Heterogeneous Chelating Agents.
D. B. Puranik, Y. Guo, A. Singh, R. E. Morris, A. Huang, L. Salvucci, R. Kamin, J. Hughes, V. David, and E L. Chang* 13

Effectiveness of MDA on Jet Fuel Thermal Stability as Determined Using the Gravimetric JFTOT: Effects of Extended Duration Testing and Time of Addition of MDA.
S.G. Pande & D.R. Hardy* 31

Retention of Metal Deactivator Additive Performance During Storage of Aviation Turbine Fuels.
C. P. Henry, Jr 51

The "Black Avtur" Incident in Northern Australia (1994/95); Report on the AMRL Investigation (1995/97).
A. J. Power*, P. M. Rawson, M. G. O'Connell, L. W. Hillen, and G. G. McVea 61

Jet Fuel Contamination by Diesel Fuel Dye.
K. H. Strauss 73

Impact of Caustic Treating on the Filterability of Jet Fuel.
L. D. Palmer*, K. M. O'Callaghan, and B. C. Springthorpe 87

*Author to whom correspondence should be addressed.

Aviation Fuels - II. Dr. J. M. Bauldreay, Chair

Measurement of Dissolved and Total Water Content in Advanced Turbine Engine Fuels With a Gas-Liquid Chromatographic OTC Technique.
S. D. Anderson, W. A. Rubey*, and R. C. Striebich 103

Aviation Fuel Handling: New Mechanistic Insight to the Effect of Surfactants on Water Coalescer Performance.
V. B. Hughes 113

An Analytical Approach to Water Separation from Jet Fuels and Coalescer Disarming.
P. David, S. E. Taylor*, and A. J. Woodward 129

Stadis 450® in Aviation Fuel Applications - Updated.
C. P. Henry, Jr 141

The Effect of Phenolic Impurities in Jet Fuel on the Behaviour of Conductivity Improvers.
B. Dacre and J. I. Hetherington* 151

Copper Contamination of Jet Fuel From Ships' Heating Coils.
P. David*, A. Goddard, S. E. Taylor, and A. J. Woodward 171

Aviation Fuels - III. Dr. J. I. Hetherington, Chair

Characterisation and Quantification of Deposits from Thermally Stressed Aviation Fuels.
C. Baker, P. David, I. Love, R. Mogford, S. E. Taylor*, and A. J. Woodward 185

Impact of Fuel Recirculation on Thermal Stability.
E. G. Jones*, W. J. Balster, and L. M. Balster 201

Comparison of the Effects of Storage Conditions, Type of Soluble Copper, and MDA on JP-5 Fuel Thermal Stability.
S.G. Pande* and D. R. Hardy 211

Investigation of the Effects of Time on the Physical Collection of Aviation Fuel Deposits in a Scaled Turbulent Flow System.
J. E. Colbert* and C.J. Nowack 231

Evaulation of JP-8+100 Fuel Compatibility with Aircraft Fuel System Materials: The Effect of Detergent/Dispersant on Aircraft Materials.
D. H. Kalt 251

JP-8+100: The Development of High Thermal Stability Jet Fuel.
S. P. Heneghan* and W. E. Harrison, III 271

Additive Stability in JP8 Metal Alloy Systems at Elevated Temperatures.
M. D. Vangsness* and S.P. Heneghan 285

Aviation Fuels - IV. Dr. P. David, Chair

High Reynolds Number Thermal Stability (HiReTS) Rig for Realistic, Rapid Evaluation of Distillate Fuel Thermal Oxidative Stability.
J. M. Bauldreay*, R. J. Heins, G. Houlbrook, and J. Smith 295

Electrical Conductivity of HITTS Additive Packages for the JP8+100 Programme.
B. Dacre* and J. I. Hetherington 315

Testing JP-8+100 Packages in European Jet Fuels - Evaluating and Understanding Benefits and Drawbacks.
J. M. Bauldreay*, W. G. Blundell, R. J. Heins, G. Houlbrook, and J. Smith 333

Experimental Evaluation of the Two-Tiered JFTOT Temperature Provision for Jet A Fuel.
C. Moses*, S. Seto, and S. Anderson 353

Studies of Jet Fuel Oxidation Using Oxidation Monitoring and Chemical Kinetic Modeling.
S. Zabarnick*, S. D. Whitacre, M. S. Mick, and J. S. Ervin 363

Numerical Simulations of Jet Fuel Oxidation and Fluid Dynamics.
J. S. Ervin* and S. Zabarnick 385

Long-Term and Strategic Storage. Dr. E. David, Chair

Eighteen Years of EBV's Handling and Quality Experience.
J. W. J. Koenig 403

Long-Term Storage Stabilities of Crude Oil Reserved by Japan National Oil Corporation.
T. Hara*, N. Hinata, Y. Imagawa, M. Kawai, Y. Imai, Y. Kon, and T. Seiki 419

Long-Term Gasoline Storage at Geosel Manosque Salt Cavern Field
E. David* & G. Le Ricousse 439

Assessing the Potential for Oxidative Crude Oil Degradation During Long-Term Storage.
J.B. Green*, J. Y. Shay, K. Q. Stirling, and H. N. Giles 459

Volume II

Fuel Blending and Compatibility. Dr. J. Ben-Asher, Chair

Controlling Residual Marine Fuel Composition by TGA
J.D. Bacha 479

Fuel Blending - How to Minimize Risk of Incompatibility
R. Kassinger 489

A Computerized System for Prediction of Compatibility of Fuel Oils.
J. Ben-Asher*, D. Luria, G. Krenis, and G. Kirpichnikov 503

General - I. Dr. J. D. Bacha, Chair

An Improved Fuel Filterability Test.
E.J. Beal*, J. M. Hughes, and D.R. Hardy 513

Rapid Detailed Chemical Analysis of Transportation Fuels by GC-FIMS.
R. Malhotra*, M. J. Coggiola, S. E. Young, and C. A. Spindt 527

Studies on the Nature of Gum Formed in Cracked Naphthas.
J. M. Nagpal*, G. C. Joshi, I. D. Singh, and K. Kumar 543

An Expert System to Predict Fall-Outs From Crude Oil in Storage.
J. Hartman* and J.W.J. Koenig 561

United States Tank/EPA Regulations, Tank Inspection Methods, Tank Remediation Techniques and Strategies (Abstract).
E.J. Guthrie 575

Tank Cleaning Strategies and Techniques
H.L. Chesneau 577

Middle Distillates. Dr. A. L. Pickard, Chair

The Acid Catalysed Formation of Existent Soluble Gums and Particulate Matter in Diesel Fuels.
R. Pardede and B. D. Batts* 591

The Relationshop Between Conductivity and Lubricity in "New" European On Road Diesel Fuels.
S.C.P. Ashton*, W. M. Thomson, and S. Dixon 611

The Effects of Moderate to Severe Hydrotreating on Diesel Fuel Properties and Performance.
J. B. Green, K. Q. Stirling*, D. L. Ripley, and J. Vanderveen 629

Effect of Increasingly Severe Hydrotreating on Stability-Related Properties of No. 2 Diesel Fuel.
J. A. Waynick 649

Diesel Fuel Thermal Stability at 300°F.
J.D. Bacha* and D.G. Lesnini 671

Thermo-Chemical and Thermo-Oxidative Stability of Diesel Fuels Containing Components of Light Catalytic Gas Oil.
Zh.D. Kalitchin*, Sl. K. Ivanov, M. I. Boneva, A. Ivanov, K. Kanariev, P. T. Georgiev, and S. K. Tanielyan 685

Studies on Gum Formation Tendencies of Middle Distillate Diesel Fuels.
Y.K. Sharma*, I. D. Singh, K. P. Bhatt, and K. M. Agrawal 699

A Bit of History - The Development of Storage Stability Tests for Middle Distillate Fuels Since World War II.
E.W. White 717

Stability of Diesel Fuels With Improved Low Temperature Characteristics.
Sl.K. Ivanov*, Zh. D. Kalitchin, A. Ivanov, K. Kanariev, M. I. Boneva, P. T. Georgiev, and S. K. Tanielyan 731

Improvement in Diesel Fuel Quality Through Additives.
S. Nandi*, V. K. Sharma, R. Manoharan, P. Bhatnagar, B. R. Tyagi, S. P. Srivastava, and A. K. Bhatnagar 745

Microbiology. Dr. K. Bosecker, Chair

Microbial Deterioration of Hydrocarbons.
K. Bosecker 763

Ability of Fuel and Water Soluble Biocides to Prevent Microbial Succession Changes to Oxygenated Gasoline and Synthetic Tank Water Bottom Chemistry in Laboratory Microcosms (Abstract).
F.J. Passman*, B.L. McFarland, and M. J. Hillyer 775

A New On-Site Quantitative Test for Microorganisms in Fuel
E.C. Hill*, G. C. Hill, and D. Collins 777

Alternative Fuels. Dr. P. Hödl, Chair

Stability and Handling of Sasol Semi-Synthetic Jet Fuel.
P. Roets*, J. J. Botha, C. A. Moses, and L. L. Stavinoha 789

Evaluation of the Stability, Lubricity, and Cold Flow Properties of Biodiesel Fuel.
J.A. Waynick 805

Oxidation Stability of Fatty Acid Methyl Esters Used as Diesel Fuel Substitute (Abstract).
P. Hödl*, M. T. Rodo-Cima, H. Schindlbauer, N. Simkovsky, and W. Tuechler 831

Biodiesel, An Environmental Blessing or a Biodegradation Headache for Long-Term Storage.
J.W.J. Koenig 833

General - II. Mr. C. J. Martin, Chair

Storage Stability of Reformulated Gasolines (RFG).
L.L. Stavinoha*, M. E. LePera, R. L. Gray, L. H. Hicks, and L. Turner 851

Summary Findings of the Property/Compositional Results of a Worldwide Commercial Marine Distillate Fuel Survey.
R.M. Giannini, R. Gray, L. Hicks, N. Lynn*, and R. Strucko 869

Survey of Diesel Fuels and Aviation Kerosenes from U. S. Military Installations.
S.R. Westbrook* and M.E. LePera 887

Recent Developments in the Production of Stable Fuel From H-Oil Process Bottoms (Abstract).
J.J. Colyar, R. O. Koseoglu*, and A. Quignard 909

The Elimination of Color in Kerosene Fraction Derived from Duri and Minas Crude Oil Mixture by Exposure to Light.
Adiwar*, M. Rahman, and H. P. Sihombing 911

Development of Field Analytical Procedures for BetzDearborn Spec•Aid 8Q462, a Jet Fuel Thermal Stability Additive.
W. L. Parker* and N. R. Calvert 923

Poster Presentations. Dr. D. R. Hardy, Chair

A Comparison of Jet Fuel Thermal Oxidation Test Visual Tube Ratings with Deposit Measurements by Ellipsometry.
K. A. Bower, P. S. Brook*, and J. O. Whitby 939

Development of an Ellipsometric JFTOT Tube Analyser (ETA).
P. David, R. Mogford, P. Paduschek, S. E. Taylor*, and A. J. Woodward 947

The Autoxidation of Phenalene (Abstract).
J. P. Guo and B. Beaver* 957

Follow-up Study of an Occupational Health Problem When Handling Jet Fuel After Initiate Actions.
H. Kling* and P.-Å. Skoog 959

Microbial Succession and its Impact on Oxygenated Gasoline in Laboratory Microcosms (Abstract).
B.L. McFarland, F. J. Passman*, and M. Hillyer 967

A Novel Test Kit for Determination of Hydrogen Sulfide in Liquids.
R. A. Neihof* and H. N. Giles 969

Liquid-Phase Oxidation Kinetics for a Paraffin Blend.
J. M. Pickard* and E. G. Jones 975

Experiences in Use of Automatic Heavy Fuel Oil Stability Analyzer.
O. Pilviö*, L.-Å. Larsson, and J. Vilhunen 985

Tests to Evaluate and Test Diesel and Gasoline Engine Fuel System Deposits.
L. L. Stavinoha* and P. I. Lacey 987

The Measurement of Antioxidant Performance in Aviation Turbine Fuel Using the Quartz Crystal Microbalance and Near Isothermal Flowing Test Rig (Abstract).
S. Zabarnick*, E. G. Jones, and S. Anderson 989

•••

Corresponding Authors' Addresses

Adiwar Research and Development Center for Oil and Gas Technology (Lemigas), P.O. Box 1089/JKT, Jakarta 10010, INDONESIA

Ashton, S. C. P. The Associated Octel Co. Ltd., Fuel Technology Centre, Watling Street, Bletchley, Milton Keynes MK1 1EZ, UK

Bacha, J.D. Chevron Products Co., 100 Chevron Way, Richmond, CA 94802-0627, USA

Batts, B.D. School of Chemistry, Macquarie University, Sydney, NSW 2109, AUSTRALIA

Bauldreay, J.M. Shell Research Ltd., Shell Research & Technology Centre, Thornton, P.O. Box 1, Chester CH1 3SH, UK

Beal, E.J. Naval Research Laboratory, Code 6181, Washington, DC 20375-5342, USA

Beaver, B.D. Department of Chemistry and Biochemistry, Duquesne University, Pittsburgh, PA 15282, USA

Ben-Asher, J. The Israel Institute of Petroleum and Energy, P.O. Box 17081, Ramat Aviv 61170, ISRAEL

Bosecker, K. Federal Institute for Geosciences and Natural Resources (BGR), Stilleweg 2, D-30655 Hannover, GERMANY

Brook, P. S. UK Ministry of Defence, Fuels and Lubricants Centre, Building 442, DERA Pyestock, Farnborough, Hants GU14 0LS, UK

Chang, E. L. Center for Bio/Molecular Science and Engineering, Naval Research Laboratory, Code 6930, Washington, DC 20375-5348, USA

Chesneau, H.L. Fuel Quality Services, Inc., P.O. Box 1380, Flowery Branch, GA 30542, USA

Colbert, J. E. Naval Air Warfare Center, 1440 Parkway Avenue, Trenton, NJ 08628, USA

Dacre, B. Rutherford Laboratory, Royal Military College of Science, Cranfield University, Shrivenham, Swindon, Wilts. SN6 8LA, UK

David, E. SAGESS, B.P. 282, 3 rue E. et A. Peugeot, 92505 Rueil Malmaison Cedex, FRANCE

David, P. BP Oil, Chertsey Road, Sunbury-on-Thames, Middx. TW16 7LN, UK

Ervin, J. S. University of Dayton Research Institute, Aerospace Mechanics Division, 300 College Park, Dayton, OH 45469-0210, USA

Giles, H. N. U. S. Department of Energy (FE-43), 1000 Independence Avenue, SW, Washington, DC 20585-034,0 USA

Green, J. B. BDM Petroleum Technologies, P. O. Box 2543, Bartlesville, OK 74005, USA

Guthrie, E. J. FQS Environmental Services, Inc., 3063 Hartley Road, Suite 2, Jacksonville, Fl 32257, USA

Hara, T. Department of Chemical Engineering, Yokohama National University, 79-5 Tokiwadai, Hodogaya-ku, Yokohama 240, JAPAN

Hardy, D.R. Naval Research Laboratory, Code 6181, Washington, DC 20375-5342, USA

Hartman, J. 18 Hazanhanim St., Rehovot 76212, ISRAEL

Heneghan, S.P. University of Dayton Research Institute, Aerospace Mechanics Division, 300 College Park Avenue, Dayton, OH 45469-0151, USA

Henry, C.P. Octel America, Inc., 200 Executive Drive, Newark, DE 19702, USA

Hetherington, J.I. Rutherford Laboratory, Royal Military College of Science, Cranfield University, Shrivenham, Swindon, Wilts. SN6 8LA, UK

Hill, E.C. ECHA Microbiology Ltd., Unit M210 Cardiff Workshops, Titan Road, Cardiff, CF1 5EJ, UK

Hödl, P. Research Institute for Chemistry and Technology of Petroleum Products, Arsenal Objekt 214, P. O. Box 8, A-1031 Vienna, AUSTRIA

Hughes, V. B. Shell Research Ltd., Shell Research & Technology Centre, Thornton, P.O. Box 1; Chester CH1 3SH, UK

Ivanov, Sl. K. SciBulCom, Ltd., P.O. Box 249, 1113 Sofia, BULGARIA

Jones, E.G. Innovative Scientific Solutions Inc., 2786 Indian Ripple Road, Dayton, OH 45440-3638, USA

Kalitchin, Zh. D. SciBulCom, Ltd., P.O. Box 249, 1113 Sofia, BULGARIA

Kalt, D. H. University of Dayton Research Institute, 300 College Park, Dayton, OH 45469-0148, USA

Kassinger, R. DNV Petroleum Services, 111 Galway Place, Teaneck, NJ 07666, USA

King, A. BC Hydro, P. O. Box 8910, Vancouver, B. C. V6B 4X3, CANADA

Kling, H. CSM Materialteknik AB, Box 13 200, S-580 13 Linköping, SWEDEN

Koenig, J.W.J. Erdölbevorratungsverband, Postfach 30 15 90, 20305 Hamburg, GERMANY

Koseoglu, R. O. HRI, Inc., 100 Overlook Center, Suite 400, Princeton, NJ 08540, USA

Lynn, N. Naval Surface Warfare Center, Carderock Division, Code 859, 3A Leggett Circle, Annapolis, MD 21402-5067, USA

Malhotra, R. SRI International, 333 Ravenswood Avenue, Menlo Park, CA 94025, USA

Moses, C. A. Southwest Research Institute, P. O. Drawer 28510, San Antonio, TX 78228-0510, USA

Nagpal, J. M. Indian Institute of Petroleum, P. O. Box IIP, Mohkampur, Dehradun 248005, INDIA

Nandi, S. Indian Oil Corporation Ltd., R & D Centre, Sector-13, Faridabad-121 007, INDIA

Neihof, R.A. Geo-Centers, Inc., Washington Operations, P. O. Box 441340, Ft. Washington, MD 20706, USA

Palmer, L. D. Ampol Refineries (Q'land) Ltd., P. O. Box 40, Wynnum Central, Qld 4178, AUSTRALIA

Pande, S.G., Geo-Centers, Inc., Washington Operations, P. O. Box 441340, Ft. Washington, MD 20706, USA

Parker, W. L. BetzDearborn Hydrocarbon Process Group, 9669 Grogans Mill Road, The Woodlands, TX 77380, USA

Passman, F.J. FQS Limited, Inc., 228 Alexander Street, Princeton, NJ 08540-7121, USA

Pickard, J. M. Kinetica, Inc., Mound Advanced Technology Center, 720 Mound Avenue, Miamisburg, OH 45343, USA

Pilviö, O. Neste Oy, Corporate Technology, P.O. Box 310, FIN-06101 Porvoo, FINLAND

Power, A.J. Airframes and Engines Division, Aeronautical and Maritime Research Laboratory (AMRL), P. O. Box 4331, GPO Melbourne, Victoria 3207, AUSTRALIA

Roets, P. Sasol Oil Research & Development, P. O. Box 1, Sasolburg 9570, SOUTH AFRICA

Rubey, W. A. Environmental Sciences and Engineering Laboratory, University of Dayton Research Institute, 300 College Park, Dayton, OH 45469-0132, USA

Schellhase, H. U. Powertech Labs., Inc., 12388-88th Avenue, Surrey, BC V3W 7R7, CANADA

Sharma, Y.K. Indian Institute of Petroleum, P. O. Box IIP, Mohkampur, Dehradun 248005, INDIA

Stavinoha, L.L. TARCOM Fuels & Lubricants Research Facility, Southwest Research Institute, P.O. Drawer 28510, San Antonio, TX 78228-0510, USA

Stirling, K. Q. BDM Petroleum Technologies, P. O. Box 2543, Bartlesville, OK 74005, USA

Strauss, K. H., 69 Brookside Road, Portland, ME 04103-4609, USA.

Taylor, S.E. BP Oil, Chertsey Road, Sunbury-on-Thames, Middx. TW16 7LN, UK

Vangsness, M. D. University of Dayton Research Institute, 300 College Park, Dayton, OH 45469-0148, USA

Waynick, J.A. Amoco Petroleum Products, 150 West Warrenville Road, Naperville, IL 60563-1460, USA

Westbrook, S.R. U. S. Army TARDEC Fuels & Lubricants Research Facility, Southwest Research Institute, P.O. Drawer 28510, San Antonio, TX 78228-0510, USA

White, E.W. 908 Crest Park Drive, Silver Spring, MD 20903-1307, USA

Zabarnick, S. University of Dayton Research Institute, Aerospace Mechanics Division, 300 College Park, Dayton, OH 45469-0140, USA

• • •

Author Index

Adiwar 911
Agrawal, K. M. 699
Anderson, S. D. 103, 353, 989
Ashton, S. C. P. 611
Bacha, J. D. 479, 671
Baker, C. 185
Balster, L. M. 201
Balster, W. J. 201
Batts, B. D. 591
Bauldreay, J. M. 295, 333
Beal, E. J. 513
Beaver, B. 957
Ben-Asher, J. 503
Bhatnagar, A. K. 745
Bhatnagar, P. 745
Bhatt, K. P. 699
Blundell, W. G. 333
Boneva, M. I. 685, 731
Bosecker, K. 763
Botha, J. J. 789
Bower, K. A. 939
Brook, P. S. 939
Calvert, N. R. 923
Chang, E. L. 13
Chesneau, H. L. 577
Coggiola, M. J. 527
Colbert, J. E. 231
Collins, D. 777
Colyar, J. J. 909
Dacre, B. 151, 315
David, E. 439
David, P. 129, 171, 185, 947
David, V. 13
Dixon, S. 611
Ervin, J. S. 363, 385
Georgiev, P. T. 685, 731
Giannini, R. M. 869
Giles, H. N. 459, 969
Goddard, A. 171
Gray, R. L. 851, 869
Green, J. B. 459, 629
Guo, J. P. 957
Guo, Y. 13
Guthrie, E. J. 575
Hara, T. 419
Hardy, D. R. 31, 211, 513
Harrison, W. E., III 271
Hartman, J. 561
Heins, R. J. 295, 333
Heneghan, S. P. 271, 285
Henry, C. P. 51, 141
Hetherington, J. I. 151, 315
Hicks, L. H. 851, 869
Hill, E. C. 777
Hill, G. C. 777
Hillen, L. W. 61
Hillyer, M. J. 775, 967
Hinata, N. 419
Hödl, P. 831
Houlbrook, G. 295, 333
Huang, A. 13
Hughes, J. M. 13, 513
Hughes, V. B. 113
Imagawa, Y. 419
Imai, Y. 419
Ivanov, A. 685, 731
Ivanov, Sl. K. 685, 731
Jones, E. G. 201, 975, 989
Joshi, G. C. 543
Kalitchin, Zh. D. 685, 731
Kalt, D. H. 251
Kamin, R. A. 13
Kanariev, K. 685, 731
Kassinger, R. 489
Kawai, M. 419
King, A. 1
Kirpichnikov, G. 503
Kling, H. 959
Koenig, J. W. J. 403, 561, 833
Kon, Y. 419
Koseoglu, R. O. 909
Krenis, G. 503
Kumar, K. 543
Lacey, P. I. 987
Larsson, L. -Å. 985
Le Ricousse, G. 439
LePera, M. E. 851, 887
Lesnini, D. G. 671
Love, I. 185
Luria, D. 503
Lynn, N. 869
Malhotra, R. 527
Manoharan, R. 745
McFarland, B. L. 775, 967
McVea, G. G. 61
Mick, M. S. 363
Mogford, R. 185, 947
Morris, R. E. 13
Moses, C. A. 353, 789
Nagpal, J. M. 543
Nandi, S. 745
Neihof, R. A. 969
Nowack, C. J. 231
O'Callaghan, K. M. 87
O'Connell, M. G. 61
Paduschek, P. 947
Palmer, L. D. 87
Pande, S. G. 31, 211
Pardede, R. 591
Parker, W. L. 923
Passman, F. J. 775, 967
Pickard, J. M. 975
Pilviö, O. 985
Power, A. J. 61
Puranik, D. B. 13
Quignard, A. 909
Rahman, M. 911
Rawson, P. M. 61
Ripley, D. L. 629
Rodo-Cima, M. T. 831
Roets, P. 789
Rubey, W. A. 103
Salvucci, L. 13
Schellhase, H. U. 5
Schindlbauer, H. 831
Seiki, T. 419
Seto, S. 353
Sharma, V. K. 745
Sharma, Y. K. 699
Shay, J. Y. 459
Sihombing, H. P. 911
Simkovsky, N. 831
Singh, A. 13
Singh, I. D. 543, 699
Skoog, P. -Å. 959
Smith, J. 295, 333
Spindt, C. A. 527
Springthorpe, B. C. 87
Srivastava, S. P. 745
Stavinoha, L. L. 789, 851, 987
Stirling, K. Q. 459, 629
Strauss, K. H. 73
Striebich, R. C. 103
Strucko, R. 869
Tanielyan, S. K. 685, 731
Taylor, S. E. . 129, 171, 185, 947
Thomson, W. M. 611
Tuechler, W. 831
Turner, L. 851
Tyagi, B. R. 745
Vanderveen, J. 629
Vangsness, M. D. 285
Vilhunen, J. 985
Waynick, J. A. 649, 805
Westbrook, S. R. 887
Whitacre, S. D. 363
Whitby, J. O. 939
White, E. W. 717
Woodward, A. J. 129, 171, 185, 947
Young, S. E. 527
Zabarnick, S. 363, 385, 989

...

Preface

The association's international conferences continue to be the premier forum for papers on stability and handling of liquid fuels, and attract the world's leading authorities on these topics. The 170 delegates from 24 countries on all five continents who attended IASH '97, the 6th of these conferences, attest to their importance.

Within the North America and much of Europe, legislative initiatives and an enlightened environmental awareness have resulted in stringent product specifications and stricter practices at fuel handling and storage facilities. In the U. S., for example, gasoline marketed in certain ozone nonattainment areas is required to contain at least 2 percent oxygen, and less benzene and other aromatics than previously allowed. By the year 2000, the entire U.S. gasoline pool may be reformulated. In many countries, diesel fuel must have an ultra-low sulfur content, and it is possible that even home heating oil may eventually have to conform to this new standard. Stringent product specifications and environmental and statutory requirements are compelling refineries to upgrade their processes to produce cleaner burner fuels.

In the U.S., some refineries have been shutdown rather than investment made in their upgrading. Although reformulated fuels have been in the marketplace for several years now, we still do not fully know how some of them will withstand the rigors of handling and storage, or stand up to microbial attack. Complicating the need to produce cleaner fuels, the world crude oil stream is getting heavier and higher in sulfur. More severe processing is necessary, therefore, to obtain specification products. Moreover, there is a greater tendency to upgrade the bottom of the barrel to provide more transportation fuels in response to rapid growth in demand. These trends are exacerbating problems with product quality and stability.

Despite the dramatic changes in the composition of the gasoline and diesel fuel pools and the relative sparsity of data on their stability, papers on aviation fuels dominated this conference as they did at the 5th conference in Rotterdam. Hopefully, the 7th conference in the year 2000 will have more papers on handling and environmentally-friendly fuels.

I thank the following companies and organizations that provided generous financial support for this conference: Angus Chemical Co.; the Arabian Fuels Center; BDM Oklahoma; BetzDearborn Hydrocarbon Process Group; BP/Plasmos; Chevron Products Co.; Emcee Electronics, Inc.; Ethyl Petroleum Additives; the FQS Group, Inc.; ITS-Caleb Brett; Nalco/Exxon Energy Chemicals, L.P.; Octel America; Oiltanking Houston, Inc.; Saybolt Nederland BV; SGS Canada; Varlen Instruments, Inc.; and the U. S. Air Force Wright Laboratory.

I am also grateful to the many people and organizations that assisted me in organizing this conference. Among them are Ms. Tamika Green of the U. S. Department of Energy, Mrs. Shirley Bradicich and Mrs. Jan Tucker of the Coordinating Research Council, Dr. Edmund W. White, consultant, and Ms. Erna J. Beal of the Naval Research Laboratory. The Canadian Embassy in Washington, DC and Tourism *Vancouver* provided support and assistance in bringing this conference to Vancouver. Finally, I thank everyone that attended the conference. Their interest and support ultimately make these conferences successful.

In opening the 4th conference in Orlando, FL, I reminded the delegates of the words of Francis Bacon, founder of the scientific method, that "science makes books, not books science." I have noted that Powertech Labs. Inc., employer of one of the opening keynote speakers, includes another quote from Bacon in its literature, namely "knowledge is power." I am confident the knowledge gained at the 6th conference will help power our quest for a better understanding of fuel instability and improved handling practices.

Harry N. Giles
Conference Chairman

IASH '97, the 6th International Conference
on Stability and Handling of Liquid Fuels
Vancouver, B. C., Canada
October 13-17, 1997

OPENING ADDRESS - I

Dr. Alan King

B. C. Hydro, P. O. Box 8910, Vancouver, B.C. V6B 4X3, CANADA

Good morning ladies and gentlemen. It is my pleasure and honour to welcome you to Canada, to British Columbia and particularly to Vancouver. I am delighted that your committee has chosen Vancouver as the host city for your conference. I hope that you will be able to take the opportunity to explore and enjoy a little of British Columbia and Vancouver during your stay.

You are in good company, in recent years the City has hosted the leaders of the G7 nations, a Clinton - Yeltsin summit, and next month will be hosting the leaders of the eighteen countries that constitute the Asia Pacific Economic Cooperation Trade Group. This latter is an organization that includes the majority of the Pacific Rim Countries including Canada, the U.S. and Japan.

For those of you who are unfamiliar with this part of the world, I would like to give a brief introduction. Forgive me if I brag a little. Canada, as you no doubt know is physically the second largest country in the world, second only to Russia. It spans six time zones and stretches north to the high arctic, and south, surprisingly, to the latitude of northern California. Canada is blessed with abundant natural resources and is a major producer of natural gas and oil, with the tar sands of Alberta holding potential petroleum reserves that rival the Middle East.

British Columbia has the greatest geographical diversity of any part of the country, ranging from a deeply indented and island studded mainland coast line, to the heights of the Rocky Mountains. With coastal rain forests contrasting with inland deserts and mountain ice fields. The Province is home to three and a half million people, a population growing with a steady influx of newcomers from other parts of Canada and around the world, attracted by the Province's prosperous economy and respect for it's cultural diversity.

Vancouver is, certainly by world standard, a new city. It was incorporated on April 6th 1886 and was burned to the ground on June 13th 1886; a process that took all of twenty minutes, which says something of the size of the place at that time. Not a very auspicious start. However, we have grown a little since then and are proud to have been recently ranked by the Corporate Resources Group of Geneva as the second most livable city in the world and the top ranked city in North America for public service, efficiency and infrastructure.

Vancouver's strategic location has helped it to take a leading position in trade. It is near the midpoint on the west coast of North America and equidistant by air between London and Tokyo. Vancouver boasts a major port and is the top exporting port to foreign countries in North America. Seventy-two million metric tonnes of cargo are handled annually and seven hundred thousand cruise ship passengers pass through the city each year. It is not, howeve,r a major handler of petroleum products, two million metric tonnes compared with twenty three million metric tonnes of coal and twelve million metric tonnes of grain.

Our focus is primarily on the Pacific Rim with nearly a third of the city's residents able to trace their origins to other Pacific Rim countries. Moreover, Vancouver is a city of immigrants with a population in which over thirty distinct ethnic origins are represented by a significant number of people and incidentally, each of these groups is served by at least half a dozen restaurants. No matter where you come from in the world it is probable that you will be able to find some home cooking somewhere in the city.

My work at B.C. Hydro, the electrical utility that supplies power to most of British Columbia, involves me in the generation of power in the more remote parts of the Province. Power to communities that are not integrated with the power grid. These communities are typically served by diesel engine powered generating stations.

Similarly, seven Provincial and Territorial utilities serve approximately one hundred and fifty communities across northern Canada and face formidable logistical problems, particularly in the handling and stability of fuel. Probably the best example is that of the Northwest Territories Power Corporation. The NWTPC operates forty-nine diesel stations , many of which are in the High Arctic. None of the stations are interconnected and all operate on a continuous basis throughout the year in

temperatures that range from plus thirty to minus fifty Celsius. The stations burn eighty-five million litres of fuel annually. Fuel costs anywhere from twenty-three cents to seventy-three cents a litre depending on the location of the respective power stations. Ensuring a reliable supply of appropriate fuel is the main concern. Delivery is either by truck over winter roads (ice roads) during the coldest months of the year, or by barge and ship during the short summer period when the rivers and sea are relatively ice free. Given the extremes of weather, the emphasis on environmental protection of very sensitive ecosystems, and the absolute criticality of electrical supply to the communities involved, it can be seen that the logistics of fuel supply to the arctic can be quite a challenge.

While B.C. Hydro does not face such severe fuel supply logistical problems as some of the other utilities across the country we do have our own set of concerns, particularly those of fuel stability. We operate a network of micro wave repeater stations. Information carried on the microwave system is vital to the protection and control of the electrical transmission system and associated generating stations located throughout the province. Most of the microwave stations are located on mountain tops and are not easily accessible. Each has an associated small diesel generation station, a few for prime power but most on standby to back up supply by cable up the mountain. The fuel can be in storage for many years and presents potential stability concerns.

B.C. Hydro is encouraging the use of independent power producers in some of our remote areas that historically have been supplied with diesel generation. Typically these are small hydro electric operators. Because of the lack of water storage in these small plants we have to maintain a back up diesel station to ensure continuity of supply to our customers. Again the need to keep fuel on hand for several years presents stability concerns. We operate two relatively large gas turbine powered generating stations, each of which is on standby duty to protect communities fed by a single radial transmission line. The stations maintain approximately two million and four million litres of middle distillate fuel respectively in single tanks. The fuel had been in storage at both sites for over twenty years and during this time it began to give indications of loss of stability and we become concerned that we would run into filter plugging and nozzle varnishing problems, which of course would show up just when we needed power. We have since replaced the fuel at both stations to facilitate tank inspection.

Our operating requirements and the use of middle distillate fuels have presented us with two basic concerns.

I. How to maintain and ensure the continuing stability of fuel in long term storage and, in particular, what commercially available fuel stabilizing product was most effective for the particular fuel in question; and

II. How to determine what fuel would be most stable over long storage periods before the fuel was purchased.

For answers to these problems I turned to the research arm of B.C. Hydro, Powertech and, in particular, to my colleague here this morning Hans Schellhase. We have taken the liberty of sharing this welcoming address between us. The user with his problems and the research chemist, the supplier of solutions. An illustration of both sides of the fuel stability coin.

IASH '97, the 6th International Conference on
Stability and Handling of Liquid Fuels
Vancouver, B.C., Canada
October 12–17, 1997

OPENING ADDRESS - II

Hans U. Schellhase

Powertech Labs Inc., 12388 - 88th Avenue, Surrey, B. C. V3W 7R7, CANADA

Ladies and Gentlemen, Mesdames et Messieurs. It gives me great pleasure and honor to follow my partner, Dr. Alan King, in welcoming all of you to the Pacific Rim City, Vancouver, and to British Columbia and Canada.

By Way of Introduction:

A highly interesting week is ahead of us, and I consider it fair game to muse in my welcoming address about the topic or, at least, some aspects of the topic that this conference, which was founded by Nahum Por in Tel Aviv, Israel in 1983, will address.

I had the pleasure of attending the 2nd International Conference on Long-Term Storage Stabilities of Liquid Fuels in San Antonio, Texas in July/August of 1986, and I remember with fondness both the excellent presentations and the hospitality of the chairman at that time, Leo L. Stavinoha, of Southwest Research Institute.

But, I am getting ahead of myself and had better start at the beginning.

Using a historical example, let me demonstrate to you how we dealt here in British Columbia with a severe problem of storage stability in the eighties.

Dr. Alan King initiated a project on fuel stability in 1982 which he alluded to a few minutes ago. Not long after the project had been undertaken, a middle distillate fuel (diesel) in one of the storage tanks at B.C. Hydro's Keogh Station started to foul in a bad way. A large amount of fuel (about 1 million imperial gallons, six years in storage) was rapidly turning sludgy and endangering emergency power generation at the associated power plant. Alan called upon us, at what came to be called Powertech Labs Inc., to participate in the clean-up and stabilization of the fuel. Our first line of defense was filtration; our final goal was stabilization of the stored fossil fuel.

We reinvented the wheel and duplicated work that had been done by D. Milson, A.R. Rescorla et al. from "Cities Service Research and Development Company", New York, N.Y. in 1952 to 1956 (1).

At that time, an ASTM method to measure the storage stability of middle distillates did not exist, and whatever one intended to do had to be validated. This study equipped us with the tools to evaluate

systematically storage stability of fuels before and after stabilization, and it resulted, for the fuel in question, in a recommendation to Dr. King to use a commercial multifunctional additive package at a concentration of about 100ppm.

During our work it became clear that not all commercial additives were equally successful in stabilizing a given fuel. The additive package that we recommended was composed of an antioxidant, a color stabilizer, a detergent and a metal deactivator. Sediments that formed initially at a rate of 45mg/L (43.3°C, 12 weeks) were reduced to less than 0.5mg/L annually and maintained at that level without further re-inhibition for at least three years.

Personal computers and Internet were still a few years off, and what had to be done in our research was done on the main frame. The outcome of our work was presented at a meeting of the Society of Automotive Engineers (S.A.E.) as a technical paper in 1983 (2), a fitting year in retrospect. It was the founding year of this association.

At about this time of our investigation, Leo L. Stavinoha, Steven R. Westbrook et al. were in the midst of comprehensive reviews and studies of middle distillate fuels. For example, they published jointly with D.W. Brinkman: "Accelerated Stability Test Techniques for Diesel Fuels" (3). This was and, perhaps, still is the most comprehensive work of this nature to date and had been commissioned by the U.S. Department of Energy (DOE).

Sludge deposition (generalist's view)

Why are straight-run fuels generally of greater stability than those of synthetic, cracked and blended nature? This question plagued some of us, especially petroleum processing engineers. I think, and believe, what I have to say is true for most conventional crude oils. During the geological creation of these fossil fuels the most stable organic compounds survived the numerous reactions under the changing chemical and physical environment of the petroleum reservoir. It is estimated that this lasted millions of years, and resulted in an increase of the carbon/hydrogen ratio, especially in the case of the sludge (asphaltenes). The sludge became more graphite-like, while the crude as a whole assumed the state of a stable, partially colloidal solution. From this point of view, the conventional crude oil is in a stable equilibrium, chemically as well as physically; one might call it cured and well-aged. In addition, it frequently contains compounds that act as natural inhibitors to fuel degradation.

Atmospheric distillation of these conventional crude oils followed by traditional refining techniques results in so-called straight-runs, which frequently show better storage stability than the equivalent cracked or synthetic fractions. In my view, the fast processes of the modern and sophisticated refining techniques that are applied to non-conventional crude oils and heavy feed stocks freeze multicomponent systems in equilibria that have not maximized the entropy of the reaction mixture. They are, as the American physicist Gibbs might have said more than a hundred years ago, in a state of labile thermodynamic equilibrium. Not only that, catalytic cracking, hydrotreating and all the other applied process chemistries reduce the chances of natural inhibitors surviving the chemical onslaught.

I would apply similar reasoning to the blending of fuels of different origins; the resulting blend is not necessarily in thermodynamic equilibrium and may result in storage and thermal instability.

Peroxides and free radicals are formed in petroleum products, once the same are exposed to air, water, catalytic metals and light. They complicate the chemistry of petroleum-based fuels. I am not addressing the issue of which come first, the peroxides or the free radicals? Nor am I exploring whether both are independently active.

What do Middle Distillate Fuels have in Common?

Strictly speaking, the name! The performance characteristics such as cetane number, density, flash point, distillation performance etc.. define the product.

What I said is especially interesting in view of the fact that the United States Department of Energy (DOE), Office of Heavy Vehicle Technologies is developing a vision for the heavy vehicle industry of the future (4). This future is to be based on "diesel fuels":

Diversity of Feedstocks	→	**A Common Diesel Fuel Specification**	→	**One Energy Conversion System**
• Petroleum		Cetane Number		Diesel Cycle Engine
• Natural Gas		Energy Density		
• Coal		Emissions Characteristics		
• Biomass		Cost Competitive etc.		

Here, one of the driving forces is the fact that the diesel engine is the highest efficiency engine today (44% versus 24 % for the gasoline engine). The hopes are to raise this efficiency to 55% or, perhaps, to 63%!

As we can all see, there is going to be lots of work for the respective industries and R&D centers.

An Unorthodox Approach to Correlate Middle Distillate Fuel Properties, Statistics of Populations.

Having introduced middle distillate fuels thus, I would like to share with you a brief reflection. Let me explain.

I used the approach of a generalist in an older study, which came about due to an unsolicited proposal to the Canadian Electrical Association (CEA) in 1984. It resulted in a two-year study into the fuel stability and storage life of middle distillate fuels. Based on the work that had been done for B.C. Hydro, specifically Dr. Alan King, we investigated middle distillates, "Canadian Middle Distillate Fuels" (5), if there is such a thing.

As you can see from Figures 1 and 2, we collected from coast to Canadian coast (about six to seven thousand km apart) 64 middle distillate fuels (14 from the Atlantic Region, 19 from Central Canada, 16 from the Prairie Regions, 14 from the Pacific Region and eight from the Northwest Territories). Oil companies as well as utilities cooperated generously and delivered gallon amounts of fuels that went into cold storage at our place. Yes, in those years common sense prevailed; only one company

inquired if, aside from providing the sample containers, we would also reimburse handling and freight charges.

We assessed their qualities, including long-term storage stability. I failed, like many other investigators before me, in correlating single parameters and stability. The best correlation R^2 I was able to come up with equaled 0.25, but in attempting to do the impossible, we learned a lot. If one sorted the database according to increasing total insolubles (43.3°C, 12 weeks), and divided these into six sub-ranges of about ten fuels each, the correlations for the six mean values improved. Case in point: the R^2 equaled 0.94 for the relationship of sulfur to total insolubles. I hear the argument (from my alter ego), that this is bad science! If I plot the non-manipulated data, I will get the true answer, there is no correlation ($R^2 = 0.25$). I refute this argument by stating that my alter ego is neglecting the fact that I sorted the data first! We are dealing with a population. If I were to investigate the distribution of false teeth in the Canadian Society, I would set up age groups first and then develop correlations between false teeth and these age groups. (Of course I could widen the scope and investigate false teeth, eating habits and ethnic groups!).

It became evident that these 64 fuels formed, just like our Canadian Society, a rather heterogeneous population. The Canadian cross section of middle distillate fuels that we had assembled had not much in common except certain performance characteristics. As a generalist I sorted my database (Lotus 1-2-3) for hours looking for common factors to appear encouraged by the success of this view.

Let me explain to you what I found in this matrix of data which was about 64 lines by 32 columns. Classifying the 64 investigated fuels, 15 fuels (24%) had both a sulfur content greater than 0.15% and a final boiling point greater than 340°C. Eleven of these fifteen fuels were classified as of low stability. The total insolubles were greater than 9mg/L by the accepted storage test of 12 weeks and 43.3°C (110°F). Only one fuel did not fit these criteria and was unstable. We had by our definition a total of 12 severely unstable fuels.

Thus, 92% of the unstable fuels (11 fuels) belonged to the sub-set just described, while 8% (one fuel) of the unstable fuels did not belong. The latter had a significant copper content (catalyst) of 1.5ppm instead. (Also nine of the unstable fuels belonged to a sub-set of 14 fuels of high aromaticity). Seven of the 11 unstable fuels contained synthetic or cracked components, while the other four were of unknown Eastern Canadian feedstock and treatment.

Encouraged by these findings, the data were statistically evaluated by a professional statistician (K. Wensauer, now of B.C. Hydro) using the SAS (Statistical Analysis Software) standard regression package. We reached the conclusion that this is a viable method of combining laboratory tests of some variables with statistical regression theory to arrive at a practical tool that estimates insolubles within a certain acceptance/rejection region.

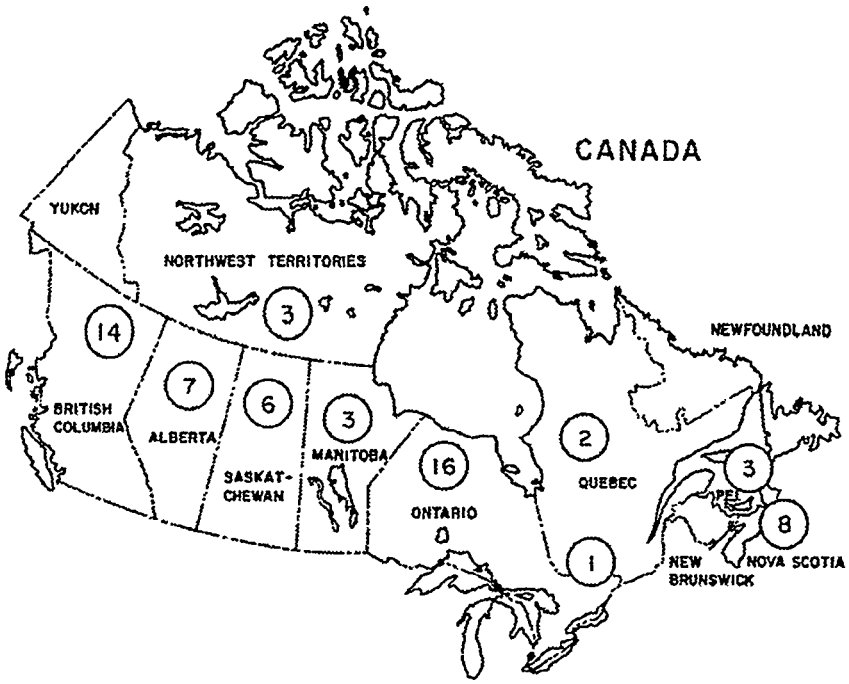


FIGURE 1
NUMBER OF FUELS ACCORDING TO PROVINCE OR TERRITORY

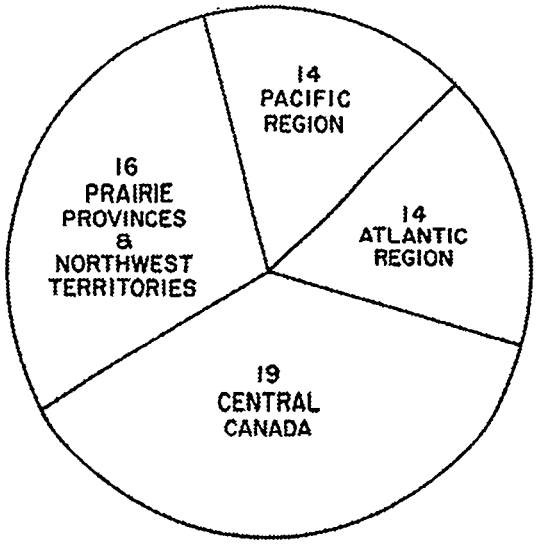


FIGURE 2
NUMBER OF FUELS ACCORDING TO REGIONS

Detailed characterization of 14 test fuels resulted in 63 variables (including NMR - data). We attempted to improve upon the prediction of the storage stability of a fuel beyond the prediction by a single test using regression models with up to three variables. We proved it is possible to assemble:

- improved statistical models from two or three variables (which included a newly developed, accelerated stability test)
- a less satisfactory but still reasonable model from ASTM D2274 and one of the other commonly used, accelerated stability tests (example: 16 hrs/100°C)

Points of Interest

I mentioned the previous findings for high sulfur and total insoluble to staff of the Lawrence-Livermore Laboratories at SAE's International Fuel and Lubricants Meeting and Exposition in Toronto, 1987. I was told that a similar correlation exists between particulate emission and kinetic combustion parameters. From this eagle's view, the restrictions in sulfur content and high boilers for middle distillates became even more meaningful. Our R&D findings were implemented early on in the purchase specifications of middle distillates at B.C. Hydro. These specified a low sulfur content.

It is hoped that the new initiative by the DOE's 'Dieselization' strategy will lead to programs that are similar to the Auto/Oil Air Quality Improvement Research Program (AQUIRP) in the United States (6) which investigated gasolines in great detail. We hope that diesel engine manufacturers, oil companies and government agencies will cooperate in increasing and deepening the knowledge about diesel fuels, diesel composition, engine performance and engine emissions as it has been done by IASH in the areas of stability and the handling of liquid fuels during these past sixteen years.

Where do we go from here?

I hope that it will be possible to establish an international database on distillate fuels into which all recognized laboratories can compile middle distillate fuel data. These databases, if accessible to appropriate research teams, would permit the development of algorithms and expert systems by industrial R&D and academia. The rational upgrading of liquid fuels, equipment and the development of predictive software is in the interest of the public and all parties concerned.

Conclusion and Welcome

If we had the genius of Josiah Willard Gibbs and could apply all thermodynamic principles to chemical equilibria and solutions par excellence; and if we had the gift of an idiot savant, we could evaluate hundreds of thermodynamic data, equilibria and phase relationships in our heads. Indeed, we would not only be able to predict storage stability, thermal stability, and combustion processes but could select the correct additive package as well as many other neat things. Nicole Tesla, a Serbian-American genius and inventor was, reputedly, the only person who was capable of doing things of that nature!

Following far-out thoughts of this kind, we should be able to look at the most up-to-date GC/MS chromatograms as well as the identification and quantitative evaluation of the respective compounds for fuel-x, and voila, we know!

What I try to allude to is this: in my opinion, the time has come to establish national and/or international databases for different liquid fuels. In the case of middle distillate fuels, these databases will combine detailed fuel description and data from gas chromatography, mass spectrometry, ASTM tests etc. and will be available to qualified software teams to develop effective algorithms and expert systems.

This is the reason why I chanced to bore you, the experts, with work that was completed ten years ago. I was not trying to sneak an old paper into this conference and to misuse this platform as invited speaker. I believe the time has come to design expert systems in these fields of study.

The know-how is there or under development and so is the idiot savant (the computer)!

As a postscript (P.S.): You should accept into your association researchers in the field of insulating oils. These oils are chemically similar to middle distillate fuels and many areas of study are useful to both investigating groups.
Thank you for your attention!

Ladies and Gentlemen. Welcome to Vancouver, to British Columbia and the 6th conference -IASH '97' - which is about to begin!

References:

(1) *Daniel Milsom and A.R. Rescorla "Determination of Fuel Oil Stability", Cities Service Research and Development Co., New York, N.Y.; presented before the Division of Petroleum Chemistry, American Chemical Society, Atlantic City Meeting, 17-21 September 1956.*

(2) *J.R. Bentley and H.-U. Schellhase "Fuel Stability and Storage Life of Middle Distillate Fuels", B.C. Hydro R&D Centre, Surrey, B.C.; SAE Technical Paper Series No. 831205; Reprinted from SP-548-Fuel Alternatives for Spark Ignition and Diesel Engines, Vancouver, August 1983.*

(3) *Stavinoha, L.L., Westbrook, S.R. , Southwest Research Institute, San Antonio, Texas. Brinkmann, D.W., Bartlesville Energy Technology Center, Bartlesville, OK. "Accelerated Stability Test Techniques for Diesel Fuels", DOE/BC/10043-12. Prepared for the Department of Energy, under Contract No. DE-AC19-79BC10043, October 1980.*

(4) *The CLEAN FUELS and Electric Vehicles REPORT, Comprehensive Coverage of Business, Government and Technology Issues for Transportation Fuels and Electric Vehicles; J.E. Sinor Consultants Inc.; Volume 9, No. 3, June 1997*

(5) *H.U. Schellhase "Storage Stability of Middle Distillate Fuels", B.C. Hydro and Power Authority, Surrey, B.C.; Report for the Canadian Electrical Association, Montreal, Quebec; CEA No. 341 G 469, Volume I & II; August 1988.*

(6) *Auto/Oil Air Quality Improvement Research Program; Published by: Society of Automotive Engineers, Inc.; SAE SP-920; February 1992.*

6TH International Conference
on Stability and Handling of Liquid Fuels
Vancouver, B.C., Canada
October 13-17, 1997

REMOVAL OF COPPER FROM FUEL BY IMMOBILIZED HETEROGENOUS CHELATING AGENTS

Dhanajay B. Puranik[1,2], Yan Guo[1,3], Alok Singh[1], Robert E. Morris[4], A. Huang[5], L. Salvucci[5], R. Kamin[5], Janet Hughes[2], V. David[2], and E. L. Chang[1]*

[1]Center for Bio/Molecular Science and Engineering, Naval Research Laboratory, Code 6930, Washington, D.C. 20375-5348; [2]Geo-Centers Inc., 10903 Indian Head Hwy., Ft. Washington, MD 20744; [3]Department of Biochemistry and Molecular Biology, University of Georgetown, 3900 Reservoir Road NW, Washington, D.C. 2007-2197; [4]Navy Technology Center for Safety and Survivability, Naval Research Laboratory, Code 6181, Washington, D.C. 20375-5348; [5]Naval Air Warfare Center, Code PE33, 1440 Parkway Ave., Trenton, NJ, 08628

ABSTRACT

As a potential alternative to the addition of metal deactivating additives to jet fuels, the removal of dissolved copper by passing fuel over a solid surface functionalized with an optimized chelant structure has been investigated. This approach allows for the use of optimized insoluble chelants with very high binding constants. Since nothing is added to the fuel, the impact of the resulting complex on fuel thermal stability is not a concern. A direct benefit of solid-supported heterogeneous chelant technology is that copper removal is achieved without introducing surface-modifying soluble chelants which can affect the outcome of thermal stability qualification tests that employ heated metal surfaces. Several different substrates have been functionalized with polyamine ligands. Copper extraction from JP-5 and dodecane with surfaces functionalized with a macrocyclic ligand, 1,4,7,11-tetraazacyclotetradecane, and an acyclic ligand, N-3-trimethoxysilylpropyl diethylenetriamine, are reported in this paper. Initial uses are targeted towards cleanup of contaminated fuel stores, with the ultimate goal of applying this technology to perform in-line copper removal at aircraft fueling points. The performance of these chelant systems in both static and flow tests demonstrates the potential of immobilized chelants to accomplish these goals.

INTRODUCTION

Jet fuel undergoes autoxidative degradation at elevated temperatures in the presence of oxygen. Sub-part per million levels of dissolved copper can promote this process, resulting in the formation of insoluble gums and/or sediments. Since copper bearing alloys are used in

components of fuel handling systems, there are ample opportunities for the introduction of copper into aircraft fuel. There is also evidence that dissolved copper can promote certain prerequisite chemical reactions in jet fuel during storage which enhance the autoxidation process and result in thermal degradation[1]. The addition of soluble metal chelants has been the basis for present measures in counteracting the catalytic effects of dissolved copper in fuels. This approach is based upon the assumption that the copper is effectively tied up in a soluble catalytically-inactive complex. Copper catalyzes autoxidation through an electron transfer mechanism[2], although the influence of coordination on the redox potential of the copper atom is not explicitly known in organic media. It is been proposed[3] that catalytic deactivation of the copper may be a consequence of the increased energy of activation for the change in valency. Therefore, the conversion of copper(II) disalicylidene to copper(I) disalicylidene would be unfavored, due to the difficulty of undergoing the change in geometry within the complex, thus rendering the copper catalytically inactive.

Findings from long-term high temperature turbulent rig studies[4,5] have indicated that these metal deactivating additives are not effective under flow and temperature conditions that exist in certain regions of a typical military aircraft fuel system. Other reports have indicated that the effectiveness of a soluble copper chelant at the elevated temperatures reached in jet engines is limited by the thermal stability of the complex[6,7]. Thus, there are many advantages to eliminating the reliance on soluble copper chelators to provide acceptable levels of thermal stability of jet fuels in the presence of copper.

The approach investigated in this study involves the removal of copper from jet fuel without otherwise changing the fuel constituency. We have examined the feasibility of immobilizing metal chelators on a solid substrate and passing fuel over the surface-modified solids to remove complexed copper from hydrocarbon liquids and jet fuel. The chelators are actually composed of three sections, the chelating group itself, a linker arm, and an attachment site for binding to a solid support. Each of these aspects can be optimized for a particular application or environment. The chelating groups we report here are polyamines, both acyclic and macrocyclic with a linker chain that varies from three to sixteen carbons long, with a variety of substrate linkages.

Polyamine chelators, particularly the macrocyclic forms, are among the strongest metal chelators known[8]. While the acyclic polyamines have an enhanced stability for complexing metal ions through the "chelator effect", azamacrocyclic molecules have additional thermodynamic stabilization attributable to the "macrocyclic effect", as first described by Cabbiness and Margerum[9]. The high metal affinity and selectivity of the polyamines make them attractive as systems for metal sensors[9], redox systems[11], or for water remediation as in ionflotation collectors[12]. Adsorption or chemical attachment of chelators to solid supports have been reported previously for chromatography[13-15] and for removal of metal ions from aqueous waste streams[16-20].

The advantages of this approach are that the chelators are highly specific for only transition metal ions, that the copper ions are directly removed from the fuel, that no metal ions need to be exchanged for binding copper, that no chemicals need to be added to fuel, and that the copper may be recovered after treatment of the fuel. In designing this alternative cleanup method, we have tried to consider carefully both the chemistry of the process and the economics of implementing such a technology. The positive results obtained from these studies are encouraging and demonstrate the potential of this approach as a plausible alternative to present methods.

EXPERIMENTAL

Materials

Technical grade DETA -silane, N-3-trimethoxysilylpropyl diethylenetriamine was purchased from Aldrich (Milwaukee, WI). All other standard chemicals and materials were purchased from commercial chemical providers including Aldrich, Fluka, Pierce, Sigma, Polychem and Kodak and were used as obtained without further purification, unless otherwise stated.

A copper-bearing JP-5 fuel used in flow testing was prepared by introducing copper by long-term immersion with copper plates until a copper concentration of 368 ppb was reached. Static tests were conducted with n-dodecane and a copper-free JP-5 doped with 20 ppm copper from copper(II) ethylacetoacetate (Eastman).

Procedures

Static exposure tests. In a typical procedure, a sample of the functionalized polymer was combined with the test solution, either dodecane or JP-5 that was doped with up to 20 ppm copper from the addition of copper acetoacetate. After stirring for a predetermined time, the liquid was recovered by filtration through glass wool and a 0.45 micron microporous nylon filter. The resulting filtrate was analyzed for copper content by graphite furnace atomic absorption.

Dynamic flow tests:

Aqueous tests: Initial flow tests were conducted in the laboratory using 250mm x 10mm tempered borosilicate Omnifit glass LC columns (Supelco, Bellefont, PA) packed 8.5g of the modified or unmodified silica. A variable peristaltic pump was calibrated for each mesh silica and used to pass known copper solutions through packed modified-silica gel. Eluates were taken periodically and copper concentrations measured using the above described method.

JP-5 tests: An Isco model 2350 HPLC pump was used to pass the copper-bearing JP-5 fuel through polyethylene drying tubes packed with approximately 30g of silica or modified silica at a flow rate of 20 ml/min at typically 20 - 30 psi. Samples were taken periodically and analyzed for copper content by graphite furnace atomic absorption.

Large scale JP-5 flow tests: Approximately 30 g of modified silica was packed into drying tubes closed off at each end by glass wool. JP-5 was pumped at the rate of 10 mL/min for 8 hours. Mixtures of modified silica used were: 70-230 mesh DETA-silica, 70-230 mesh DETA-silica/30-60 mesh DETA-silica (1:1), 70-230 mesh DETA-silica/30-60 mesh DETA-silica (1:1), aminopropylsilica, aminopropylsilica/70-230 mesh DETA-silica (1:1), aminopropylsilica/30-60 mesh DETA-silica (1:1) and 70-230 mesh unmodified silica.

Determination of binding capacities for DETA-modified silica in aqueous media. The general procedure was to mix a sample of DETA-modified silica, typically 0.5 g, with 15 mL of 3000 ppm Cu(II) and let stand overnight. The supernatent was then assayed for copper content spectrophotometrically as described below.

Spectrophotometric copper assay method

Aqueous media. The bathocuporine disulfonic acid (disodium salt) complex with Cu(I) is a yellow colored, water-soluble complex used for one-phase aqueous assays of copper. This method gives very sensitive and reliable results. Standard curves had least-squares regression factors of up to 0.999+ for the range of 40 ppb to 5 ppm Cu(I). The assays were verified by comparison with ICP-furnace.

Hydroxylamine hydrochloride was used as a reductant for Cu(II). Since the pH affects the stability of Cu(I)-bathocuproine complex, ammonium acetate was used as a buffer. Absorption measurements were obtained at 480nm. A typical procedure for 10 mL samples was as follows: a 1 ml sample was transferred into a test tube and the following aliquots added sequentially to the tube, mixing well after each addition: 1 ml 10% hydroxylamine hydrochloride solution, 1 ml 0.1 % bathocuproine solution, 1 ml 10 % ammonium acetate solution, and 6 ml of water for a 1:10 dilution. The solution was mixed and the absorption measured at 480-483 nm. Reagent blanks were prepared by substituting 1 ml water for the sample.

The sample results were compared to a linear standard curve. From the difference between the initial and measured Cu(II) concentrations, the total amount of copper absorbed and the mass of copper absorbed per gram of modified silica were obtained.

Organic media. A bathocuproine solution consisting of 225 ppm bathocuproine in ethanol and a 10% hydroxylamine solution were mixed in a 7:3 ratio, respectively. To a 16 ml portion of the copper-bearing hydrocarbon sample, 1 ml of the bathocuproine solution was added and mixed vigorously for 5-10 min. After standing for 24 h at room temperature, absorbance was measured at 475 nm. Copper content was calculated by comparison with a standard curve.

Aqueous formation constants. Formation constants in aqueous media were obtained[21] by titration and analysis of the titration data with HYPERQUAD[22], a suite of programs designed for analyzing chemical equilibria. Briefly, 1.0 mM of the fully protonated chelator was titrated with sodium hydroxide to obtain metal-free titration curves. These curves were analyzed by HYPERQUAD to obtain the protonation constants for the polyamines. Subsequent titration of

the chelator-metal complex with sodium hydroxide and application of HYPERQUAD yielded the formation constants.

RESULTS AND DISCUSSION

Copper extraction from JP-5 and a model fuel with surfaces functionalized with a macrocyclic ligand, 1,4,7,11-tetraazacyclotetradecane (cyclam) and an acyclic ligand, N-3-trimethoxysilylpropyl diethylenetriamine (DETA-silica) were examined. The structures of these compounds are shown in Figure 1. They were attached to a silica via a hydrocarbon bridging group, as shown schematically in Figure 2 for the acyclic ligand, DETA. The bonding model shown is one of several possible mechanisms where the vacant coordination site could be filled with an ion or an organic fuel constituent. If the DETA density were sufficient, participation by adjacent DETA molecules is also feasable.

Cyclic Polyamines (cyclam)

The results of the slurry (static) tests with different cyclam-attached materials are shown in Table 1. Tests were carried out with n-dodecane and JP-5 doped with copper from copper ethylacetoacetate. In tests with soluble cyclam which was not immobilized to a solid substrate, significant amounts of copper remained after filtering, particularly in the JP-5. This is probably due to the inability of filtration to remove all the unimobilized chelator-metal complex from the liquid

All the materials modified with cyclam performed well. The agarose control appeared to be efficient in adsorbing copper from dodecane, but was not as effective in JP-5, where the copper was more tightly bound. One of the variables examined was the length of the hydrocarbon linker arm that connects the ligand molecule to the surface. This was examined by correlating the copper removal efficiency with the length of the linker arm. The link has to be sufficiently long to provide adequate exposure of the chelant to the soluble copper in the fuel, but not so long as to impair the mechanical stability of the linkage. The length of the linker arm, as varied in the acrylate polymer series, did not appear to make a great deal of difference within the n = 2 to 8 range. However, the presence of a long linker versus the absence of any linker arm may account for much of the differences observed in the results between cyclam and cyclam-C_{16}.

Generally, the silanized silica showed the lowest levels of copper, although the agarose-coupled material was comparable, especially when one takes into consideration that there was a higher ratio of doped copper to agarose for the 0.1 g samples of agarose.

The survey results from the slurry tests demonstrated the feasibility of this approach for removal of copper from non-aqueous liquids. It is interesting to note that significant amounts of copper were still left in JP-5 fuel after treatment with free hexadecylcyclam, where less copper was left in solution when treated with free underivitized cyclam. This can be attributed to the higher affinity of cyclam, than its modified analogs, for copper[21]. However, given that several of the immobilzed cyclam results are even lower, another likely factor may be the greater degree of solubilization of the free alkylated cyclam, with its long hydrophobic chain, and the consequent difficulty of removing the soluble complex by filtration.

Acyclic Polyamines

Subsequent studies have been focused on the acyclic ligands, triethylenetetramine (TETA), diethylenetriamine (DETA), and silica modified with DETA. The structures of the acyclic ligands are shown in Figure 1. There are several advantages to the use of these acyclic polyamines: TETA and DETA have very high formation constants for Cu(II), both chemicals were available commercially in large quantities, and, in particular, trimethoxysilylpropyl-DETA, which is the chelator with a trimethoxypropyl linker arm, is also available commercially. The last point is important from a cost-effectiveness point of view because it decreases the number of steps in the immobilization chemistry.

We first sought to ascertain whether derivatization at the amine nitrogen atoms of the DETA and TETA with an alkyl group would significantly reduce the required high stability of their respective copper complexes. The tests were conducted in aqueous solutions by titration as described above. The results from Table 2 show that while both DETA and TETA have significantly lower copper formation constants than cyclam, although the mono-alkylated forms of cyclam (HDC), DETA (HDDETA), and TETA (HDTETA) were much closer together in their binding constants. Since it is the alkylated analogs of the chelators that are relevant, we felt that the DETA and TETA would make good alternates to cyclam. The selectivity of HDDETA for copper versus that of Mg(II) or Ca(II) is also included in Table 2 . While the Ca(II) value is

surprisingly high, it is still four orders of magnitude lower than that for Cu(II). The affinity of HDDETA for Mg(II) is negligible. As far as we are aware, these are the first measurements for the formation constants of Mg(II) and Ca(II) with a polyamine.

Static Tests

Trimethoxysilylpropyl-DETA was chemically immobilized to silica as described above. A slurry test in tetradecane, similar to the cyclam tests, was performed for the modified DETA-silica, varying the amount of time for mixing the slurry and standing time (Table 3). As was observed with the cyclam, decolorization of the copper ethylacetoacetate in the tetradecane occurred almost immediately. This was confirmed by undetectable amounts of copper even after only 150 seconds of exposure. These results indicated that DETA-modified silica was a suitable candidate for further flow studies.

Aqueous Flow Tests

Initially, 30-60 mesh silica was used to maximize the flow rate and keep the backpressure as low as possible, but we found that modified 70-230 mesh silica performed much more effectively in removing copper. Therefore, most of the subsequent flow tests were done using the finer mesh silica. We have also examined other parameters, such as choice of solvent, silane to silica ratio, baking time, temperature, and other factors to optimize for the capacity of the modified materials. For the flow tests reported here, we used DETA-silica with a capacity of 50 mg Cu/g modified silica.

Flow tests were done with aqueous copper solutions and with copper-bearing JP-5. The aqueous flow rates were kept between 4-5 ml/min through tempered borosilicate Omnifit glass LC columns packed with approximately 8.5 g modified DETA-silica. Figure 3a shows the breakthrough point at 590 ml for a 527 ppm Cu solution corresponding to a capacity under flow of 36 mg Cu/g of modified silica. A test performed with a 1:1 mixture of DETA-silica and aminopropyl-silica (Figure 3b) showed similar results: 580 mL breakthrough with a 520 ppm Cu solution, indicating a flow capacity of 36 mg Cu/g of modified silica.

The column flow tests were performed using aqueous 500 ppm $CuSO_4$ solutions. The high copper concentration was chosen to keep the volume of solution down to a reasonable

amount. At this concentration, one could see a. deep blue band move down the column as the DETA-silica became saturated with copper ions. The column capacity for the 70-230 mesh modified silica was lower than the slurry capacity due to the more limited contact time of the solution with the silica.

JP-5 Flow Tests

Flow tests were conducted with the JP-5, containing initially 368 ppb copper, over DETA and aminopropyl chelants on 30-60, 70-230 mesh silica at 10 ml/min for 8 hours. The copper contents of the effluents, shown in Table 4, illustrate the loss in column efficiency when the larger 30-60 mesh silica was used. By mixing equal parts of the two mesh sizes, the copper content went from 0.1 to 1.3 ppb with DETA. The results also show that the aminopropyl silica was generally not as effective as DETA and this difference was also larger when the 30-60 mesh silica substrate was used. Moreover, most of the column efficiency of the aminopropyl silica columns was lost after allowing to sit in contact with the fuel for two days; whereas the DETA surfaces retained their copper specificity.

Thermal Stability Testing

The benefits of copper removal on the quality of the JP-5 test fuel were demonstrated by evaluating the thermal stability of the effluent after passing through the modified silica columns. This fuel had contained soluble copper for approximately nine months and at the time of the test contained 317 ppb copper. The fuel was passed through column containing the 70-230 mesh DETA-silica and unmodified silica gel. A total of four liters of fuel was passed through each column and each liter of sample was collected and tested for thermal stability by the Gravimetric JFTOT apparatus, described elsewhere[23], at a flow rate of 3 ml/min at 260°C (500°F) for 2.5 hours. The fuel was passed through at a rate of 20 ml/min, with each column containing approximately 30 grams of the silica or DETA-silica. The results are shown in Table 5, for the filterable, adherant and total insoluble products for each fraction of fuel that passed thorough the column. From Table 5 the benefit of DETA-silica treatment of this fuel is clearly shown, with a decrease from an initial total insoluble content of 3.4 mg/L in the untreated copper-doped fuel to less than 1 mg/L. While initial reductions in thermal oxidation products were obtained with the

unmodified silica, stability began to increase as the copper passed through the column when the capacity was exceeded. It is interesting that, although there were undetectable levels of copper in all fuel samples after passing through the DETA-SiO_2 column, higher amounts of insolubles were formed from the first 2 liters of fuel. Comparison with the thermal products formed in the effluent from the unmodified silica column suggests that this is not a consequence of interactions with underivitized silica surface sites. This will be further investigated as we continue to characterize the relationship of ligand surface density and column efficiency.

CONCLUSIONS

We have studied the potential of polyamines chemically immobilized on solid supports to remove copper from both aqueous and non-aqueous solutions, particularly from jet fuel. In the process, we have examined a number of chelator-modified materials for their ability to bind copper in solution and found that they were all effective, to varying degrees, in extracting the soluble copper. While cyclam showed great promise, the high cost of the starting materials required that we focus on DETA, a more cost-effective acyclic polyamine. We found the DETA-silica system to be suitable for adsorbing copper from jet fuel, potentially at just pennies per gallon. It is envisioned that these types of functionalized surfaces will be employed as column packings.

There are still a number of remaining issues to be addressed. Underivatized silica will remove polar constituents, including stabilizing additives, along with natural and added lubricity enhancers from jet fuel. To minimize the contact of fuel with silica sites, synthetic procedures will be investigated to maximize the density of chelator linkages on the surface. It may also be possible to chemically block, or end-cap remaining free silica surface sites. A possible added advantage to end-capping would the freeing up of some amines that could form hydrogen bonds to silanol functionalities on the surface[24]. While silica has some obvious advantages as a solid support, a polymerized chelator may have an edge in other areas. In order to be practical for field use, flow rates on the order of tens of gallons per minute must be achieved. Efforts are currently underway to determine how to increase the flowrate through the relatively small-sized 70-230 mesh silica. In order to reach the flow rates required to utilize such a column packing for field

use, a balance must be reached between column efficiency and throughput. However, these are considered engineering issues and beyond the scope of this preliminary study.

In terms of cost-effectiveness of this approach, the material cost of the modified silica is approximately $0.09 per gram of modified silica, with the most expensive material being the silane. If one were to use the breakthrough data at 500 ppm Cu(II) to extrapolate the cost for removing 1000 ppb of copper from jet fuel, it is estimated that the cost would be about $0.01 per gallon, depending on the exact flowrate.

ACKNOWLEDGEMENTS

The authors would like to acknowledge support of this project from the Office of Naval Research and the Naval Air Propulsion Center, Trenton.

REFERENCES

(1) Pande, S. G. and Hardy, D. R. *Energy & Fuels*, **1997**, 11, 1019.
(2) Scott, G. "Atomspheric Oxidation and Antioxidants"; Elsevier Publishing Company, Amsterdam, 1965; p.179-80.
(3) Chalk, A. J. and Smith, J. F. *Nature*, 174, **1954**, 802.
(4) Kendall, D. R.; Houlbrook, et al., Presented at the 1987 Tokyo International Gas Turbine Congress, October 26-31, Tokyo, Japan, 1987.
(5) Moses, C. A. Southwest Research Institute report No. 281, contract DAAK70-92-C-0059, August 1992.
(6) Morris, R. E. and N. H. Turner. *Fuel and Science Technology Int.* **1990** 8(4), 327-350.
(7) Morris, R. E.; Hasan, M. T.; et al., submitted for publication in *Energy & Fuels*.
(8) Kodama, M. and E. Kimura. *J. Chem Soc. Dalton* **1978,** 1081-85.
(9) Cabbiness, D. K. and D. W. Margerum . *J. Am. Chem. Soc.* **1969,** 91, 6540-1.
(10) Singh, A., L.-I. Tsao, et al. *Langmuir* **1992,** 8, 1570-7.
(11) De Santis, G., M. Di Casa, et al. *J. Am. Chem. Soc.* **1989**, 111, 2422-7.
(12) Yamada, K., Y. Koide, et al.. *Bull. Chem Soc. Jpn.* **1989**, 62, 2867-74.
(13) Zhou, X. C., C. Y. Wu, et al. *J. Chromatography* **1994** ,662, 203-18.
(14) Lamb, J. D. and R. G. Smith *J. Chromatography* **1991**, 546, 73-88.
(15) Blain, S., P. Appriou, et al. *Analytica Chim. Acta* **1990**, 232, 331-6.
(16) Izatt, R. M., J. S. Bradshaw, et al. *Pure & Appl. Chem.* **1995**, 67(7), 1069-74.
(17) Tuncay, M., S. D. Christian, et al.. *Langmuir* **1994**, 10, 4688-92.
(18) Izatt, R. M., R. L. Bruening, et al.. *Pure & Appl. Chem.* **1990**, 62(6), 1115-18.
(19) Schlapfer, C. W. U.S Patent 5 102 640, 1992.
(20) Macedo, P. B. and A. Barkatt U.S. Patent 4 659 512, 1987.

(21) Puranik, D. B., A. N. Singh, et al. *J. Coord. Chemistry*, in press.
(22) P.Gans; A.Vacca and A.Sabatini, *J.Chem.Soc., Dalton Trans.*, 1196, **1985**.
(23) Beal, E. J.; Hardy, D. R.; Burnett, J. C. *Proceedings of the 4th International Conference on Stability and Handling of Liquid Fuels*, Orlando, FL, Nov 1991, pp 245-59. *Aviation Fuel: Thermal Stability Requirements*, ASTM STP 1138; Kirklin, P. W. and David, P., Eds.; American Society for Testing and Materials, Philidelphia, PA, 1992, pp. 138 - 50.
(24) Kahn, F. J. *Appl. Phys. Lett.* **1973**, 22, 386-8.

Table 1. Summary of Slurry Tests with Cyclam-Modified Substrates

Chelant	Substrate[1]	Chain Length[2]	Chelant derivitive, grams[3]	Dodecane Cu, ppb[4]	JP-5 Cu, ppb[4]
CYCLAM	polystyrene	16	--	8	--
CYCLAM	[none]	[none]	--	1	52
CYCLAM	[none]	16	--	16	319
[none]	Epoxy-activated aragose	[none]	0.2	1	45
CYCLAM	Epoxy-activated aragose	16	0.1	0	6
CYCLAM	Epoxy-activated aragose	16	0.1	0	17
CYCLAM	Epoxy-activated aragose	16	0.2	0	5
CYCLAM	Silica	8	0.4	0	1
CYCLAM	Silica	8	0.4	0	0
CYCLAM	Silica	8	0.4	0	1
CYCLAM	methacyrlate polymer	2	0.8	2	--
CYCLAM	methacyrlate polymer	8	0.8	2	9
CYCLAM	methacyrlate polymer	6	1.1	3	6

[1]All initial copper concentrations were 20 ppm and volumes of dodecane and JP-5 were 5.0g, except for aragose samples which used 3.5g. [2] Length of hydrocarbon chelant-substrate bridging group in number of methylene groups. [3] Grams of immobilized chelant treated with 20 ppm copper solutions. [4] Typical errors are ± 5 ppb.

Table 2. Comparison of Formation Constants for Cyclic and Acyclic Chelators in Aqueous Media

Chleator	Log $K_{cu(II)}$	Log $K_{Mg(II)}$	Log $K_{Ca(II)}$
Cyclam*	27.0		
TETA	20.0		
DETA	16.0		
HDC**	20.0		
HDTETA	16.0		
HDDETA	14.0	3.0	10.0

TETA=triethylenetetramine, DETA=diethylenetriamine, HDC=hexadecylcyclam HDTETA=hexadecyl triethylenetetramine, HDDETA=hexadecyldiethylenetriamine *Cyclam value from Bianchi[x], *et al. (1991).* **HDC value from Puranik, et al.[21]

Table 3. Copper Content of 10 ml Solutions of Copper in Tetradacane after Static Exposure to 2 g DETA-Silica

Mixing time	Standing time	Initial [Cu] = 5 ppm	Initial [Cu] = 20 ppm
30 s	2 min	0 ± 2 ppb	0 ± 2ppb
5 min	10 min	0 ± 2ppb	0 ± 2ppb
5 h	overnight	0 ± 2ppb	0 ± 2ppb

Control (neat tetradecane)= 1 ± 2 ppb. Samples filtered through Magna nylon filter.

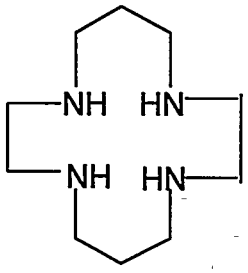
Table 4. Copper Remaining in JP-5 after Passing Through Columns Packed with Various Modified Silica Surfaces*.

Liters	F1	F2	F3	F4	F5	F6
0.0	1	1	2	2	6	3
0.6	1	1	2	3	8	41
1.2	1	1	2	3	9	183
1.8	1	1	1	3	11	229
2.4	1	1	2	3	11	325
3.0	0	2	1	3	12	283
3.6	0	2	1	3	12	256
4.2	0	2	1	3	16	238
4.8	0	2	1	3	18	234
After 48 hour soak						
10.8	0	0	60	129	--	--
20.4	0	2	233	137	--	--
30.0	0	17	258	140	--	--
36.0	0	15	271	129	--	--

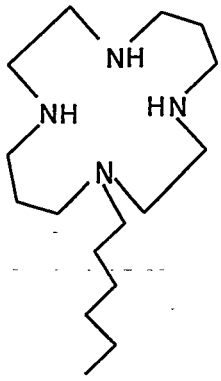
*Flow rate was 10 ml/min for 8 hours, total volume = 4.8 L. Initial [Cu] = 368 ppb.
F1 = 70-230 mesh DETA-silica; F2 = (1:1) 70-230 + 30-60 mesh DETA-silica;
F3 = aminopropyl silane; F4 = (1:1) 70-230 mesh DETA-silica + aminopropyl silane;
F5 = (1:1) 30-60 mesh DETA-silica + aminopropyl silane; F7 = unmodified silica.

Table 5. Insoluble Products Formed in GravJFTOT Testing of JP-5 after Passing Through Columns Packed with DETA-Modified and Unmodified Silica

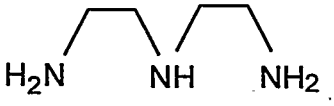
Treatment	Volume		Insoluble Products, mg/L		
		Cu, ppb	Filterable	Gum	Total
before copper exposure	--	<2	0.26	0.01	0.27
after copper exposure	--	177	3.39		3.41
SiO_2	0 -1 liters	2	0.15	0.55	0.70
SiO_2	1 - 2 liters	57	0.97	<0.01	0.97
SiO_2	2 - 3 liters	26	2.62	0.02	2.64
SiO_2	3 - 4 liters	20	2.51	<0.01	2.51
DETA-SiO_2	0 -1 liters	<2	1.94	0.19	2.13
DETA-SiO_2	1 - 2 liters	<2	1.16	0.21	1.37
DETA-SiO_2	2 - 3 liters	<2	0.64	0.23	0.87
DETA-SiO_2	3 - 4 liters	<2	0.87	0.12	0.99



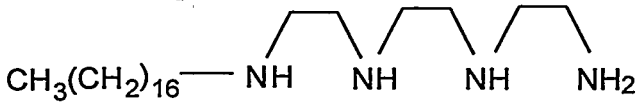
1,4,7,11-tetraazacyclotetradecane
(CYCLAM)



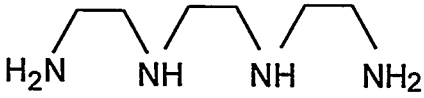
N-1-hexyl-1,4,7,11-tetraazacyclotetradecane



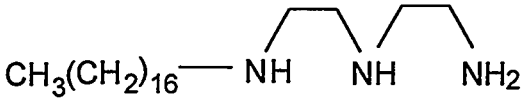
diethylenetriamine
(DETA)



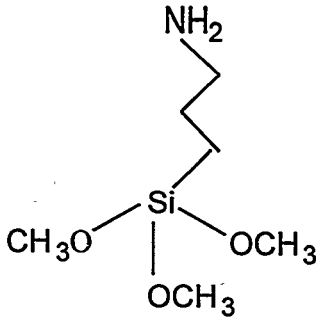
N-3-hexadecyltriethylenetetramine
(HDTETA)



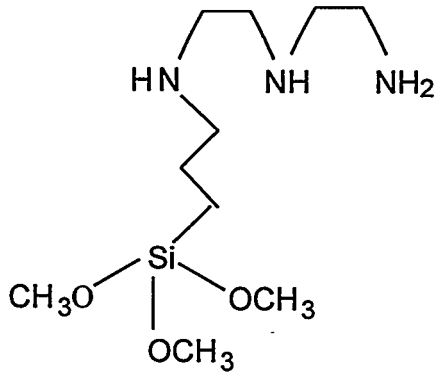
triethylenetetramine
(TETA)



N-3-hexadecyldiethylenetriamine
(HDDETA)



N-trimethoxysilylpropylamine
(aminopropyl silica)



N-3-trimethoxysilylpropyl diethylenetriamine
(DETA-silane)

Figure 1. Cyclic and acyclic chelants used in this study.

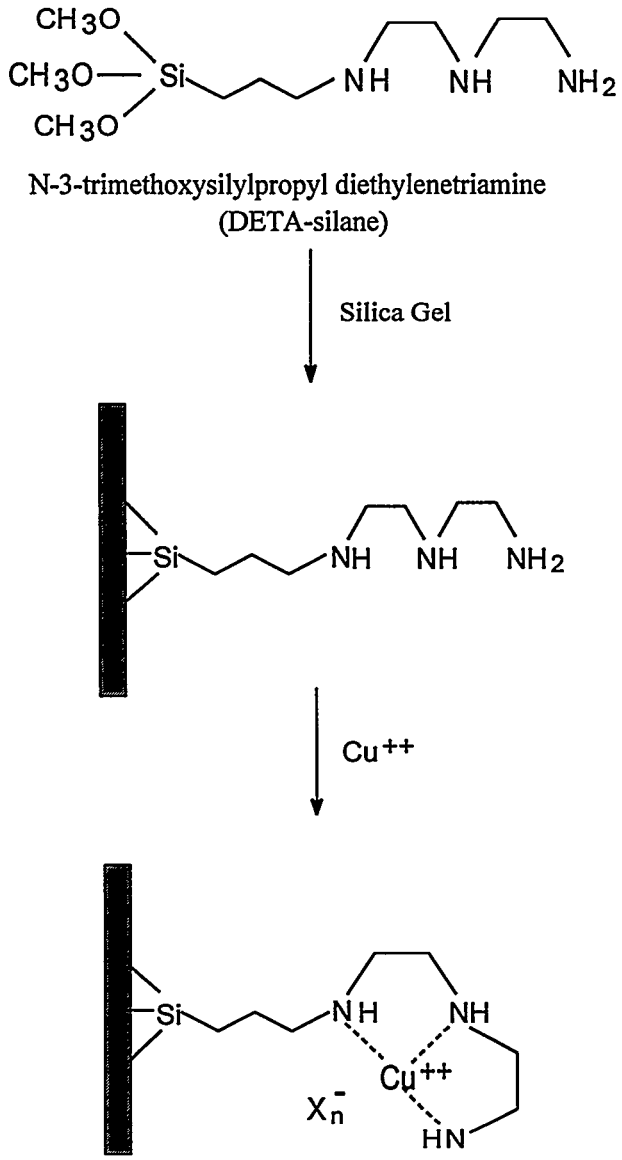


Figure 2. Schematic representation of the DETA-silica surface. X = a charged species, which forms an ion-pair or an organic species which can coordinate with the copper.

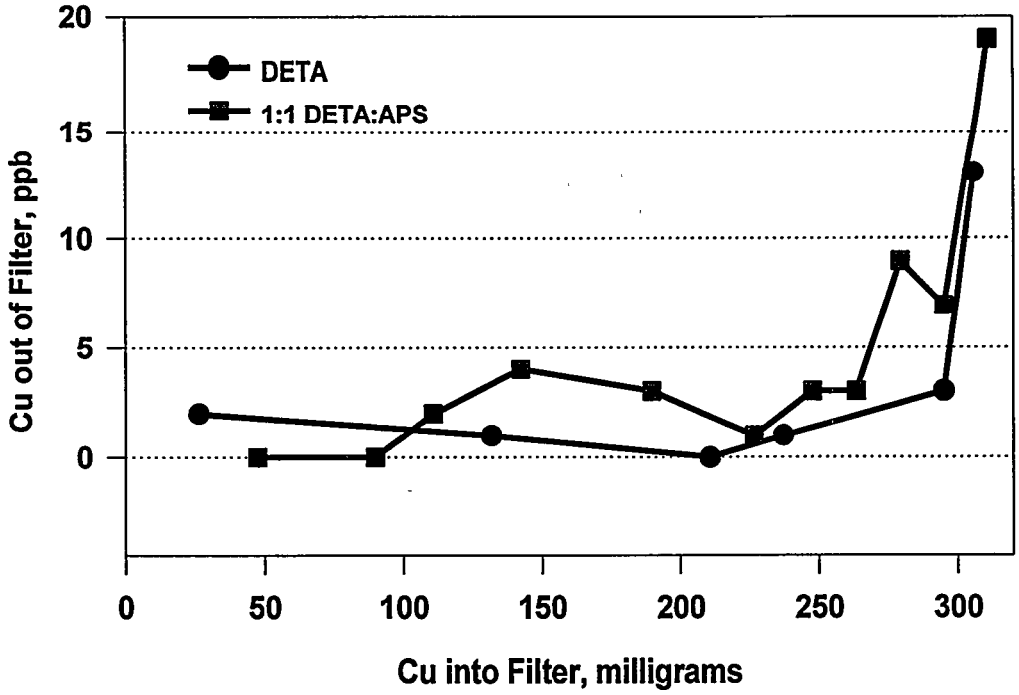


Figure 3. Copper breakthrough in effluent from 4 - 5 ml/min flow of aqueous 500 ppm $CuSO_4$ through 250 mm x 10 mm columns packed with modified silica. Breakthrough patterns shown for 70-230 mesh DETA-silica and a 1:1 mixture of 70-230 mesh DETA-silica and aminopropyl-silica.

6th International Conference
on Stability and Handling of Liquid Fuels
Vancouver, B. C., Canada
October 13-17, 1997

EFFECTIVENESS OF MDA ON JET FUEL THERMAL STABILITY AS DETERMINED USING THE GRAVIMETRIC JFTOT: *EFFECTS OF EXTENDED DURATION TESTING AND TIME OF ADDITION OF MDA*

Seetar G. Pande[1] and Dennis R. Hardy*[2]

[1]Geo-Centers, Inc., 4601 Presidents Drive, Lanham, MD 20706. [2]Code 6181, Naval Research Laboratory, Washington, D.C. 20375.

Abstract

Two studies were conducted on the effects of the metal deactivator, N,N'-disalicylidene-1,2-propane diamine (MDA) on jet fuel thermal stability. Study 1 focused on the effects of MDA on extended duration thermal stability testings ranging from 120 to 152 hours. The test fuel was a Jet A, and the effects of MDA were examined with and without the addition of the antioxidant, BHT (2,6-di-*tert* -butyl-4-methyl-phenol) as well as with and without added copper. For study 2, the thermal stability test duration was 2.5 hours, and the effect of time of addition of MDA, which was also investigated in study 1, was further examined in a test matrix that comprised two JP-5 fuels, two sources of copper and three concentrations of MDA. Thermal stability was determined using the gravimetric JFTOT. The results of the extended duration testings indicate that even at the relatively high MDA concentrations examined (15 and 35 ppm), MDA exhibited a beneficial effect in the non copper doped commercial (Jet A) and Navy type fuel (Jet A +BHT). The results of the time of MDA addition studies indicate that early addition of MDA is more effective than late addition for copper-contaminated stored jet fuels.

Introduction

The beneficial effects of the metal deactivator additive, N,N'-disalicylidene-1,2-propane diamine, commonly known as MDA, in counteracting the detrimental effects of copper on fuel thermal stability are well recognized.[1] However, on extended duration thermal stability tests of a non copper doped jet A-1 fuel, MDA was interpreted as having no effect after 30 hrs,[2] and, for a non copper doped JP-5 fuel, as having a potentially detrimental effect after 120 hrs.[3] These findings are based on injector feed-arm rig (IFAR) studies,[2] and on flow reduction studies of two atomizers,[3] respectively.

Because of the possible impact of these results on the use of MDA - which is both an optional military specification (MIL-T-5624) thermal stability additive, and an optional commercial fuel additive (ASTM D1655) - the effect of MDA on extended duration testing was reinvestigated (study 1). In the re-investigative study, we revised the protocol used in the initial extended duration

testings.[2,3] These revisions, which include storage of the test fuels prior to determining their thermal stabilities, the time of addition of MDA, and its concentration are subsequently described.

Revision 1 involved storing the test fuels in the presence of the test additive(s) prior to determining their thermal stabilities. The objective of this revision was to decrease the neat fuels' inherent thermal stabilities, such that the effects of the test additives could be better differentiated. This approach is based on the results of an earlier study,[4] which indicated that precursors that lead to thermal instability are predominantly formed during long term storage of the fuel in the presence of copper, and not during the thermal stability test itself.

Revision 2 involved the early addition of MDA and hence the use of a freshly refined jet fuel. This adoption is also based on the results obtained from the earlier study[4] wherein we found that the early addition of MDA to be especially important for fuels that are stored in the presence of copper. The early addition of MDA is consistent with Pedersen's recommendation[5] for gasolines, viz., MDA should be added at the earliest possible moment. The late addition of MDA, i.e., after storage, was examined to determine the effect of time of addition of MDA to non copper doped fuels.

Revision 3 was the addition of MDA at higher concentrations (~35 ppm) compared to the military specification[6] level of 5.8 mg /L. High concentrations of MDA were used for the following reasons: (a) To compensate for possible depletion on the long term storage conducted, e.g., losses of MDA may occur due to adherence on the walls of the samples' containers. And (b), to ensure that the amounts of MDA added, will be in excess of the concentration of solubilized copper in the copper dissolution studies.

Experimental Section

Test Matrices for studies 1 and 2. Common to the test matrices for studies 1 and 2, are the following: (a) the use of jet fuels that were freshly refined, where the term freshly refined refers to an interim period of 0-4 weeks after refining; (b) the early addition of the test additives, i.e., prior to storage unless otherwise stated; (c) the addition of MDA at relatively high concentrations ranging from 15-40 ppm: 15 ppm were used only for those studies involving the late addition of MDA, i.e., after storage, since compensation for possible losses due to depletion on storage was not relevant; and (d) storage of the test fuels at room temperature conditions for a period of approximately 13-16 months prior to determining their thermal stabilities. In study 1, storage of the additized test fuels extended over an interim period of a few months due to the length of time taken to complete the extended testings of the neat and doped fuels in the test matrix. The overall test matrices for both studies, 1 and 2 are summarized in Table 1.

Gravimetric JFTOT. Fuel thermal stability was determined using the gravimetric JFTOT. The method is based on the weight of the total thermal deposits (mg/L) formed when the filtered fuel flowing at 3 mL/min, under a back pressure of 500 psi, is heated at 260°C for 2.5 hours. This was the test duration used in study 2 (see below for the extended duration testing). Further details of the method are described elsewhere.[4,7]

Extended duration testing using the gravimetric JFTOT (study 1). For the extended duration testings, at the start of each gravimetric JFTOT test, and after each subsequent start-up, we employed a warm-up period of approximately 15 minutes during which the effluent was not collected. Extended gravimetric JFTOT testing was conducted for a duration period of 120 hours for the neat fuel, which was the first fuel examined. Subsequent testings were extended to a maximum of 152 hours, in the effort to monitor MDA's performance on further increasing the test duration (see Figures 2-5). To monitor the trend in deposit formation, with time, for each test fuel after known time intervals, the thermal deposits formed on the strip, and the filterables collected in the effluent were determined. To simulate continuity of the test, the same strip was reused until the test duration was completed. A new/clean strip was used per test fuel.

Copper analyses (studies 1 and 2). The concentrations of fuel solubilized copper from the copper doped/storage studies, with and without MDA present, were determined at periodic intervals (see Figure 1). Copper analyses were performed using graphite furnace atomic absorption spectroscopy at the Naval Air Warfare Center, Aircraft Division, in Trenton, NJ.

Results and Discussion

Study 1. Extended Duration Thermal Stability of a Stored Jet A Fuel: With and without the Presence of the Test Additives

Data presentation. To better understand the effects of the additives on increasing test duration, the cumulated strip and filterable deposits formed, in mg/L (i.e., total weight of deposits ÷ total volume of fuel used), were plotted versus the test duration (see Figures 2 and 3, respectively). As shown in these plots, after approximately 96 hours test duration, the rate of thermal deposition appears to level off for all the tests conducted, indicating a constant rate of deposit formation. Consequently, the test durations, including the 120 hours minimum, were more than adequate to study the effects of the additives on extended testings. From a maintenance perspective, the weights in milligrams of the cumulated strip and filterable deposits were also plotted versus the test duration (Figures 4 and 5, respectively).

General evaluation. As illustrated in the thermal deposit profiles versus time, for plots based either on mg/L (Figures 2 and 3), or from a maintenance standpoint, on milligrams (Figures 4 and 5), except for "BHT alone", most of the remaining test additives/additive combinations decreased both the strip and filterable thermal deposits of the reference fuel (see below). The extent of the decrease varied with the test additive/additive combination. Furthermore, the consistency in the trend of the extended duration test profiles, i.e., an apparent lack of scatter in the data (Figures 2-5), suggests that the apparent decreases are likely real. Moreover, what is significant is that MDA was neither detrimental nor innocuous in any of the cases examined. Instead, MDA was found to be beneficial.

Evaluation of the test additives by *ranking.* The relative effectiveness of the various test additives, individual and combined - on extended duration thermal stability testings - were evaluated by ranking their cumulated total thermal deposits formed for similar test durations (Table 3). Listed in order of decreasing fuel thermal stability, from best to worst, the test additives are ranked as follows:

1. Early addition of MDA alone≈ BHT/late addition of MDA
2. BHT/early addition of MDA
3. BHT/MDA/~2500ppb Cu ≈ BHT alone ≈ None: neat fuel

Note: Based on the repeatability of the gravimetric JFTOT (± 15%), we have ranked the neat fuel similar to that of BHT/MDA/Cu and BHT alone.

Based on the extended gravimetric JFTOT tests conducted on the stored doped test fuels examined, the above rankings indicate the following: For the *non copper doped* Jet A fuel, the two most effective additive/additive combination were: (1) the early addition of MDA alone, and (2) the combination of BHT/late addition of MDA. Both these additive/additive combination further decreased the thermal deposits of an inherently stable non copper doped Jet A fuel by approximately 60-70% (Table 3). Furthermore, the similarity in their effectiveness indicates that the observed efficacy is attributable to MDA. This premise is supported by the lesser performance of BHT alone (see Figures 2-5).

Pertinent to the above discussion are the results of a preliminary investigation (Table 4) that was also conducted on the thermal stabilities of the same Jet A fuel, but which was copper doped and stored using accelerated conditions that simulate ambient storage for approximately one year (viz., 90°C/50 psig air for 48 hrs). Accelerated storage was conducted in the presence of 400 ppb copper from CuEA in conjunction with each of the following additive/additive combination, viz., BHT, MDA, and BHT/MDA. The thermal stability test duration was 2.5 hours. As shown in Table 4, MDA appears to be the operative additive in significantly decreasing the thermal deposits of the copper/BHT doped stored fuel. However, these findings need to be confirmed in future studies using an ambient mode of storage.

The effects of the remaining additives are subsequently addressed with respect to the roles of MDA and the effects of BHT. However, the effect of early versus late addition of MDA is discussed later in conjunction with the results from study 2, because of the common link between the two studies.

Roles of MDA.

Copper doped fuel/chelation mechanism. On extended duration thermal stability testings, similar thermal stabilities were observed between the Jet A fuel that was stored in the joint presence of BHT, MDA, and copper (approximately 4000 ppb measured after 13 months storage), and that stored in the presence of BHT alone. Since MDA was present in an excess molar ratio relative to copper (based on a copper concentration of 4000 ppb and 35 ppm added MDA, the mole ratio of MDA:Cu is 1.96:1), these results suggest that MDA was effective in chelating the copper such that the net result was similar to that of BHT alone. Such an explanation is consistent with MDA's well known copper chelation mechanism,[1,4,5,8] in the autoxidation of fuels. Note, extended duration testing of the copper-doped stored fuel, with no MDA present, would have been useful for reference purposes. This test was not done, along with other pertinent studies, because of the time constraints in conducting the extended duration tests of an already large matrix, and because the primary objective was to investigate whether MDA would be detrimental on long term testing as was reported.[3]

Non copper doped test fuels/alternative mechanisms of MDA. The role of MDA in increasing thermal stability is not limited to a metal chelation mechanism. Supporting this position are the results from independent studies which demonstrate the effectiveness of MDA in fuels that contain negligibly low levels of copper. Examples include the following: (a) our current findings, wherein MDA improved the thermal stability of a Jet A, and JP-5 type fuel (Jet A+BHT) by as much as 60-70% (Table 3); the copper content of the Jet A fuel was 3 ppb; (b) the substantial decrease in thermal deposits due to the addition of MDA at 5.8 ppm, in a JP-5 fuel with a copper content of <1ppb, as reported by Morris *et al.*;[9] and (c), MDA's concentration effect identified by Clark.[8] In the latter case, when MDA was added at 0.3 and 5.7 ppm to a Jet A-1 fuel that contained no added catalytic metals (inherent copper content was <2 ppb), relative to the neat fuel, the 5.7 ppm-MDA doped fuel was found to exhibit a fivefold benefit in the Single Tube Heat Transfer Rig across all temperatures. No improvement was observed when the MDA concentration level was 0.3 ppm.

The mechanism whereby MDA is effective in fuels that contain negligibly low levels of copper, has not been elucidated, to date. Possible suggestions include interactions in the liquid phase,[10] e.g., that of an antioxidant,[9] though this effect appears to be fuel dependent;[11] and surface effects,[12] such as passivation.[8,13,14]

Effects of BHT. Of the test additives examined, BHT was the least effective and its decreased performance is particularly apparent from the extended duration test profiles of the strip deposit (see Figures 2 and 4). These results suggest that BHT is not an effective antioxidant at the 260°C test temperature. Thus, whereas BHT's hindered phenol structure serves well as an antioxidant for fuel storage stability, it may not be effective for thermal stability. In fact, Heneghan and Zabarnick's[15] proposed mechanistic pathways indicate that BHT may contribute to thermal deposits. Nevertheless, it is difficult to explain why the combination of BHT/addition of MDA after storage, is more beneficial than the combination of BHT/early addition of MDA, since BHT was present in both cases. Further discussion on the effects of BHT is beyond the scope of this study.

Significance of the results of MDA addition to non copper doped fuels on extended duration testing in the gravimetric JFTOT. As discussed earlier, consistent with other findings, MDA significantly decreased the thermal deposits of a typical thermally stable non copper doped Jet A fuel, by as much as 64% (Table 3), in the extended duration tests conducted. These results are significant from the following two aspects:

(a) The beneficial effects of MDA that were obtained, even on extended duration testings, the maximum being 152 hr. Since the operating conditions in the gravimetric JFTOT are similar to the JFTOT's (ASTM D3241), our results do not support the previously held interpretation[8] that the beneficial effects of MDA, observed in the JFTOT, is due to the JFTOT's short test duration of 2.5 hr. Specifically, the JFTOT (D3241) has been characterized as being over responsive to MDA (i.e., it supposedly gives false passes for MDA additized fuels) due to its short test duration. Furthermore, as indicated in the profiles of the test plots of the filterable deposits, which comprise the bulk of the

total deposits, based on mg/L (Figure 3), the MDA additized fuels depict either a decrease or nochange in the filterables with increasing test duration. These results are significant for they substantiate the beneficial effects of MDA observed in the JFTOT at the test temperatures employed.

(b) The applicability of MDA. This includes its future use in commercial jet fuels, where neither copper nor storage is of concern, and its ongoing use in Navy fuels at higher concentrations, where copper and storage are. The potential economic advantage in the use of MDA is well illustrated in the plots, based on milligrams, of the cumulated strip and filterable deposits, which represent the surface and bulk fuel deposits, respectively (Figures 4 and 5). The impact of such decreases in the thermal deposits of an inherently stable fuel includes decreased maintenance requirements, hence decreased downtime and, decreased maintenance costs for both commercial and Navy fuels.

Study 2. Effect of Early versus Late Addition of MDA on Jet Fuel Thermal Stability with and without the Presence of the Test Additives

Fuel solubilization of copper from 90:10 Cu-Ni alloy for two JP-5 test fuels. The solubilized copper concentrations of the Cu-Ni doped JP-5 test fuels, with and without MDA present, on long term storage are shown in Table 5. The results indicate that, in general, during the first six months of storage in the presence of six and eighteen Cu-Ni rods, the copper content of both test fuels did not increase significantly, with time. However, on extended storage (from approximately 6-12 months), the copper content did increase significantly for the TX test fuels that contained MDA, and for the LA test fuels that did *not* contain MDA. On further storage (13-16 months), the copper content of most of the test fuels exhibited some decrease. For fuels that *did not* contain MDA, copper absorption was greater in the LA fuel than in the TX fuel.

In general, copper solubilization appears to be dependent on the fuel (e.g., possibly, on the amount and type of organic acids present in the fuel), as well as on the amount of copper to which the fuel is exposed, the presence/absence of MDA, the MDA concentration when present, and the storage period. The difference in copper solubilization between the two fuels, when MDA was present focuses on possible fuel compositional differences. However, the similarity in total acid content of the two fuels (see Table 2) suggests that this parameter was not a contributing factor. Losses/decreases in the concentration of solubilized copper with time are likely due to adherence on the walls of the container as well as incorporation in the insolubles formed on storage.

Time of addition of MDA: studies 1 and 2. To facilitate the analysis of the overall results obtained from early versus late addition of MDA, the pertinent results from study 1 will be discussed jointly with those from study 2. Based on the collective results from studies 1 and 2, the time of MDA addition appears to be related to the presence/absence of copper. And, for the non copper doped fuels, which were thermally stable, on the presence/absence of an antioxidant and the test duration. The impacts of these factors on the time of addition of MDA for both non copper and copper doped fuels are discussed subsequently.

Non copper doped Jet A fuel/no antioxidant present (study 1). For fuels that do not contain an antioxidant (e.g., Jet A fuels), and provided they are storage stable, the overall extended duration test results suggest that the time of addition of MDA would not be critical. This interpretation is based on the following considerations: (a) high thermal stability effectiveness on the early addition of MDA alone; and (b) a similar effectiveness on the late addition of MDA (i.e., after storage). In the latter case, the Jet A fuel was stored in the presence of BHT, prior to the addition of MDA, but as discussed earlier, the observed beneficial effect is attributable to MDA. Also, the unchanged BHT concentration after long term ambient storage of the test fuel indicates that this fuel exhibited high storage stability. Consequently, BHT, which is used as an antioxidant for storage stability, is unnecessary for storage-stable fuels.

Non copper doped fuels/antioxidant present (studies 1 and 2). In the extended duration thermal stability study (study 1), late addition of MDA to the non copper doped Jet A fuel stored in the presence of BHT was more effective than early addition of MDA and BHT. But in study 2 (Table 6), the effect of the time of addition of MDA was not definitive for the non copper doped JP-5 fuels. This evaluation is based on the rationale that large percentage decreases/increases of small amount of deposits are not meaningful. Nonetheless, the disparity in the results between the two studies on the time of MDA addition may be related to the short test duration of study 2 *in conjunction with* the high thermal stabilities of the non copper doped JP-5 test fuels. Consequently, from a practical standpoint, based on the extended duration test results, for *non copper doped fuels that contain a hindered phenol antioxidant*, late addition of MDA appears more beneficial than early addition.

Copper doped fuels (study 2 only). For the TX and LA test fuels that were doped with copper either from CuEA or 90:10 Cu-Ni alloy, in general, the *early* addition of MDA was *consistently more* effective than the addition of MDA after storage in decreasing the total thermal deposits. Because of the inherent thermal stabilities of both the TX and LA fuels, the beneficial effect of early addition of MDA was generally not dramatic. A noted exception, however, was the 98% decrease in total thermal deposits (i.e., from 21.1 to 0.5 mg/L, see Table 6, cf., tests #14 *vs* #16) on *early* MDA addition to the TX fuel that was doped at an initial concentration of 2000 ppb copper from CuEA. In contrast, on MDA addition *after* storage, a small increase or, based on the ±15% repeatability of the gravimetric JFTOT, no change in the total thermal deposits was obtained relative to the reference copper doped fuel (Table 6, cf., tests #14 *vs* #15).

Comparison of the time of addition effect versus the MDA:Cu mole ratio effect. As discussed earlier, for copper doped fuels, the beneficial effect of MDA is attributable to its chelation of copper. Consequently, a minimum 1:1 mole ratio of MDA:Cu is required. As shown in Table 6, the molar ratios of MDA:Cu were in excess in all cases. However, although the extent of the excess varied, for both TX and LA copper doped fuels, the beneficial effect of MDA is consistently attributable to its early time of addition rather than to the extent of the mole ratio excess of MDA:Cu. Examples, include all the TX fuels' tests for which the MDA:Cu mole ratios were significantly higher for MDA addition after storage versus its addition before storage. For the LA fuel, in certain cases, although the MDA:Cu mole ratios were lower for MDA addition after storage versus its addition before storage (e.g., see Table 6: tests# 9 and 10, also #12 and 13), in other cases the corresponding mole ratios were fairly similar (Table 6: tests #6 and 7, also #15 and 16).

Significance of the results on the time of MDA addition to copper containing JP-5 fuels. The improved thermal stabilities on early versus late addition of MDA to copper doped JP-5 fuels further support our premise[4,16] that for copper containing fuels, the precursors that lead to thermal deposits are formed primarily during long term ambient storage; i.e., the copper promoted/catalyzed autoxidation reactions, whence the precursors are formed, occur primarily during storage. Thus, on *early* MDA addition such reactions are arrested due to copper chelation, thereby subsequently effecting improved thermal stabilities. These results are also particularly meaningful, since in the current investigations, storage was conducted using field conditions, viz., room temperature storage in the presence of 90:10 Cu-Ni alloy, whereas in our original study,[4] storage was conducted using laboratory test conditions, viz., accelerated storage in the presence of CuEA.

Impact of the Results Obtained onTraditionally Held Viewpoints

Areas of concerns that have in the past diminished/discounted the merits of MDA include: (a) increased copper solubilization in fuels due to MDA; and (b) the use of laminar flow test methods for determining thermal stability (e.g., the JFTOT: ASTM D3241, and the gravimetric JFTOT), whereas the fuel flow in jet engines is turbulent. Both these concerns are addressed below.

MDA/copper solubilization effect. The favorable results obtained at high MDA concentrations, even for non copper doped fuels, indicate that MDA is beneficial at concentrations well in excess of the current 5.8 ppm MDA military specification[6] level. Increasing the current military specification is particularly pertinent to US Navy fuels, for which, copper contamination is of concern. Nevertheless, anticipated opposition to such a revision may stem from the tendency of MDA to increase copper solubilization in fuels. However, the results in Table 5 indicate a fuel dependency. For example, whereas copper solubilization increased with time on storage in the presence of MDA for the TX fuel, a corresponding decrease was observed for the LA fuel. Nevertheless, as Pedersen has reported,[5] and our results attest to, despite the increased copper solubilization, MDA decreased the thermal deposits of the copper/MDA stored fuels.

Laminar versus Turbulent Flow Devices for Measuring Thermal Stabilities

The effects of flow velocity on heat transfer and deposition rates reviewed by Hazlett[17] indicate varying results. Nonetheless, it has been suggested[18] in the recent past that turbulent flow has some effect on the chemistry of fuel thermal instability deposition. This suggestion may be due to a temperature effect attributable to the mode of operation of the turbulent flow test devices, which tend to run at much hotter metal surface temperatures than laminar flow devices. For example, turbulent flow devices are designed to more closely simulate actual airframe and engine conditions from the standpoint of flow and the actual initial hot metal surface temperatures. However, as the test time progresses, these turbulent flow devices usually deviate to much higher than realistic metal surface temperatures. Consequently, the hidden variable between turbulent and laminar flow test devices is likely a temperature effect and it is this effect that may be the cause of the differences in thermal deposition between turbulent and laminar flow. In the gravimetric JFTOT, based on *the combination of*: 260°C wall temperature (the fuel temperature is approximately 250 °C for about 75% of the heated zone), six seconds residence time, 19 cm^{-1} surface/volume ratio, and the laminar flow, in general, the conditions employed are more severe than the initial conditions in the turbulent flow devices.

Conclusions

Based on the extended duration gravimetric JFTOT tests conducted, which ranged from a minimum of 120 hours for the stored neat Jet A fuel, and a maximum of 152 hours for most other tests, MDA, at the high concentration used (15-35 ppm), was not detrimental. Instead, MDA improved the thermal stability of a typical non copper doped commercial jet fuel by approximately 64%, based on the total deposits accumulated during a 125-hr test duration period. And, based on the individual and combined effects of MDA and BHT examined, the effectiveness observed appears to be attributable to MDA. Furthermore, based on the plots of mg/L versus time, after 96 hours, the rate of thermal deposition appears to level off. Consequently, the extended test durations employed, including the minimum of 120 hours, were more than adequate.

Since the operating conditions of the gravimetric JFTOT are similar to the JFTOT's (ASTM D3241), the beneficial effects of MDA observed in the extended duration gravimetric JFTOT tests do not support the interpretation that the JFTOT (D3241) is over responsive to MDA, due to its short duration test time of 2.5 hr. In addition, because the conditions employed in the gravimetric JFTOT are more severe than the initial conditions in the turbulent flow devices (viz., the combination of high fuel temperature, long residence time, surface/volume ratio, and laminar flow), the overall results obtained have even greater significance.

The apparent beneficial effect of MDA alone/early addition exhibited in the extended duration tests of a typical commercial jet fuel (Jet A: no antioxidant added) containing negligibly low copper content, appears promising with respect to decreasing maintenance costs and needs to be explored further. Although the effect of late addition of MDA (i.e., addition after storage) to the Jet A test fuel (no BHT present) was not examined, the overall data suggest that for storage stable Jet A fuels, the time of MDA addition would not be critical. For non-copper doped thermally stable JP-5 or JP-5 type fuels (BHT present), the effect of time of addition of MDA appears to be dependent on the test duration.

For *copper doped* JP-5 fuels, using copper derived from either copper II ethyl acetoacetate or 90:10 Cu-Ni alloy, the *early* addition of MDA appears to be more effective than late addition. These latter results are particularly significant because they further validate our premise that for copper contaminated fuels, the precursors that lead to thermal stability are formed primarily during storage. Finally, the overall thermal stability results obtained when BHT was present/absent focus on reassessing the use of BHT for storage stability. MDA may be a viable replacement in serving not only as a thermal stability enhancer, but as a storage stability additive. However, MDA's role in controlling peroxidation, on long term storage, needs to be established.

Acknowledgments

The authors thank the Office of Naval Research (Dr. M.Soto) for funding support, Dr. Alice Huang of the Naval Air Warfare Center, Trenton, NJ, for the great number of copper determinations, as well as for the BHT analyses, and Mr. Lindsay Hicks of the Defense Fuel Supply Center, in Alexandria, VA. for kindly providing the two freshly refined test fuels.

Literature Cited

1. Hazlett, R.N. *Thermal Oxidation Stability of Aviation Turbine Fuels*; ASTM Mongraph 1, American Society of Testing and Materials: Philadelphia, 1991, chapter 1X.

2. Kendall, D.R.; Houlbrook, G.; Clark, R.H.; Bullock, S.P.; Lewis, C. Thermal Degradation of Aviation Fuels in Jet Engine Injector Feed Arms. Part I - Results from a Full-Scale Rig. Paper 87-IGTC-49 presented at the *International Gas Turbine Congress*, Tokyo, October 1987.

3. Moses, C.A. Effect of a Metal Deactivator Fuel Additive on Fuel Deposition in Fuel Atomizers at High Temperature. Interim Report 281, Belvoir Fuels and Lubricants Research Facility (SwRI) Southwest Research Institute, San Antonio, TX, August 1992.

4. Pande, S.G.; Hardy, D.R. Effect of Copper, MDA, and Accelerated Aging on Jet Fuel Thermal Stability as Measured by the Gravimetric JFTOT. *Energy and Fuels* **1995**, *9*, 177-182.

5. Pedersen, C.J. Inhibition of Deterioration of Cracked Gasoline During Storage. *Ind. Eng. Chem.* **1949**, *41*, 924.

6. Military specification, MIL-T-5624.

7. Beal, E.J.; Hardy, D.R.; Burnett, J.C. In (a) *Proceedings of the 4th International Conference on Stability and Handling of Liquid Fuels:* Orlando, FL, Nov. 1991, pp245-259. (b) *Aviation Fuels Thermal Stability Requirements*, ASTM STP 1138; Kirklin, P.W.; David, P., Eds; American Society for Testing and Materials: Philadelphia, PA, 1992, pp. 138-150.

8. Clark, R.H. The Role of a Metal Deactivator in Improving the Thermal Stability of Aviation Kerosines. Presented at the *3rd International Conference on the Stability and Handling of Liquid Fuels*: London, September 1988, Paper No. 47, p.283, Institute of Petroleum, 1989.

9. Morris, R.E.; Hazlett, R.N.; McIlvaine, C.L. *Ind. Eng. Chem. Res.* **1988**, *27*, (8), 1524.

10. Schreifels, J.A.; Morris, R.E.; Turner, N.H.; Mowery, R.L. *Prepr.-Am.Chem. Soc., Div. Fuel Chem.* **1990**, *35*, (2), 555.

11. Morris, R.E.; Turner, N.H. *Fuel Science and Technology*, **1990**, *8*(4), 327.

12. Schreifels, J.A.; Gwynn, L.; Morris, R.E.; Interactions of a Metal Deactivator with Metal Surfaces at Elevated Temperatures. Presented at the *4th International Conference on the Stability and Handling of Liquid Fuels:* Orlando, FL., November 19-22, 1991.

13. Kendall, D.R.; Houlbrook, G.; Clark, R.H.; Bullock, S.P.; Lewis, C. Presented at the Tokyo International Gas Turbine Congress, October, 26-31, Tokyo, Japan, 1987, Paper 87-IGTC-49.

14. Clark, R.H.; Delargy, K.M.; Heins, R.J. *Prepr.-Am.Chem. Soc., Div. Fuel Chem.* **1990**, *35*, (4), 1223.

15. Heneghan, S.P.; Zabarnick, S. *Fuel* **1994**, 73, (1), 35.

16. Pande, S.G.; Hardy, D.R. Comparison of the Effects of Storage in the Presence of Copper Using Laboratory versus Field Conditions on Jet Fuel Thermal Stability As Measured by the Gravimetric JFTOT. *Energy and Fuels* **1997**, *11*, 1019.

17. Hazlett, R.N. *Thermal Oxidation Stability of Aviation Turbine Fuels, American Society of Testing and Materials*, ASTM Mongraph 1, American Society of Testing and Materials: Philadelphia, 1991, chapter V.

18. Clark, R.H.; Stevenson, P.A. *Prepr.-Am. Chem. Soc., Div. of Fuel Chem.* **1990**, *35*, 1302.

Table 1. Overall Test Matrix for the Two Studies Conducted

test matrix	extended duration testing (study 1)	early vs. late MDA addition follow-up study (study 2)
no. and type of fuel: id	1 freshly refined Jet A: Jet A	2 freshly refined JP-5s: TX, LA
room temp storage period:	13-16 months	14-15 months
non copper doped stored fuels:		
neat fuel	✓	✓
*test additives**	✓	✓
antioxidant (AO)	BHT added in lab at 24mg/L	AO added at refinery at 17mg/L
MDA: no AO	at 35 ppm	na**: JP-5s contain an AO
AO +: MDA before storage	MDA at 35 ppm	MDA at 20 ppm
AO +: MDA after storage	MDA at 15 ppm	MDA at 15 ppm
copper doped stored fuels:	Cu as copper wires	Cu as CuEA and Cu-Ni rods
Cu +AO +: MDA before storage	MDA at 35 ppm	MDA at 20 ppm +: (a) 400 ppb (CuEA) (b) 6 Cu-Ni rods MDA at 40 ppm+: (a)2000 ppb Cu (CuEA) (b) 18 Cu-Ni rods
Cu +AO: + MDA after storage	nd**	MDA at 15 ppm in all cases
grav. JFTOT test duration	min:120 hr max: 152 hr	2.5 hr

* Unless otherwise stated, all additives were added early, i.e., prior to storage. Antioxidants used at concentrations shown in all tests conducted. And, MDA concentrations are, as specified. ** na: not applicable; nd: not determined. ✓: tests conducted as identified.

Table 2. Available Properties and Compositional Data for the Two JP-5 Fuels Examined and Specification Limits for Jet A Fuels

properties/composition (ASTM method, MIL-T- 5624 specification limits for JP-5 fuels)	JetA* ASTM D1655	JP-5 fuels	
		TX	LA
aromatics, vol% (D1319, max: 25)	20 > 25	19	14.9
olefin, vol% (D1319, max: 5)	not reqd.	0.8	1.1
mercaptan sulfur, wt% (D3227, max: 0.0020)	0.003	0.0001	0.0012
total sulfur, wt% (D4294, max: 0.40)	0.3	0.0069	0.09
total acid, mg KOH/g (D3242, max:0.015)	0.1	0.003	0.002
density, g/mL (D4052, min-max: 0.788 - 0.845)	0.775-0.840	0.816	0.819
flash point, °C (D93, min: 60)	37.8	62.2	64
freeze point, °C (D2386, max: - 46)	-40	- 50.5	- 48.5
peroxide content, ppm (D3703, max: 8)	not reqd.	<0.001	<0.001
antioxidant	option	✓	✓
corrosion inhibitor	agreement	✓	✓
fuel system icing inhibitor, vol% (0.15-0.20)	agreement	0.13	not stated
copper content, ppb	3	4	2

* specification values only: actual values not available.

Table 3. Cumulated Deposits Formed after 120-128 Hours Extended Duration Thermal Stability Testings of the Specified Additives in the Jet A Test Fuel*

Thermal Stabilities Ranked from best to worst

additive/additive combination	cumulated deposits,** mg			%-decrease*** in total deposits
	strip	filterables	total	
BHT/MDA after storage	0.2	11.2	11.4	68
MDA	0.1	12.5	12.6	64
BHT/MDA before storage	0.1	23.3	23.4	34
BHT/MDA/~4000 ppb Cu	0.3	30.8	31.1	12
BHT	0.9	30.8	31.7	11
none (neat)	0.9	34.6	35.5	reference

* The test fuels were stored for approximately 13-16 months in the presence of the specified test additives prior to the extended duration thermal stability testings.

** For the neat fuel, the deposits shown are for a test duration of 120 hours. For the test additives/additive combinations, the deposits shown are for a test duration of 128 hours.

*** Relative to the reference neat fuel, i.e.,[(wt of total deposits of neat fuel) minus (wt of total deposits of additized fuel) x100]÷(wt of total deposits of neat fuel).

Table 4. Thermal Stability of the Jet A Test Fuel That Was Stored under Accelerated Conditions*in the Presence of the Specified Additives

test description**	grav. JFTOT deposits, mg/L		
	strip	filter	total
Cu/BHT	0.06	5.80	5.86
Cu/MDA	0.00	0.13	0.13
Cu/BHT/MDA	0.01	0.15	0.16

* The accelerated storage conditions are: 90°C/50 psig air/48 hrs.

** The respective concentrations of the additives are: Cu at 400 ppb derived from copper II ethyl acetoacetate; MDA at 5.8 mg/L; and BHT at 24 mg/L.

Table 5. Copper Levels on Storage at Room Temperature with and without MDA for Two Typical JP-5 Fuels

JP-5 fuel	description	copper concentration in ppb, at storage times shown:									
		1 mth	*2 mth*	*4 mth*	*5 mth*	*6.3 mth*	*8.4 mth*	*9.5 mth*	*11.5 mth*	*13 mth*	*16 mth*
TX	neat				4						3
	+ 6 Cu-Ni rods	37	45	54	75	70	97	96	99	75	38
	+ 6 Cu-Ni rods + 20 ppm MDA	55	56	74	86	98	200	340	631	477	401
	+ CuEA (400ppb Cu)	nd*	nd	nd	320	nd	nd	153	174	92	44
	+ CuEA (400ppb Cu) + 20 ppm MDA	nd	nd	nd	298	nd	nd	325	448	368	339
	+ 18 Cu-Ni rods	99	133	152	128	108	183	201	260	210	95
	+ 18 Cu-Ni rods + 40 ppm MDA	146	164	215	283	318	770	1382	2559	2093	2127
	+ CuEA (2000ppb Cu)	nd	nd	nd	1698	nd	nd	1462	665	226	9
	+ CuEA (2000ppb Cu) + 40 ppm MDA	nd	nd	nd	1464	nd	nd	1966	2290	1892	nd
LA	neat				2						3
	+ 6 Cu-Ni rods	92	111	117	155	169	562	831	1689	2172	1591
	+ 6 Cu-Ni rods + 20 ppm MDA	60	63	66	67	76	125	197	279	254	243
	+ CuEA (400ppb Cu)	nd	nd	nd	491	nd	nd	417	432	398	388
	+ CuEA (400ppb Cu) + 20 ppm MDA	nd	nd	nd	341	nd	nd	340	399	386	nd
	+ 18 Cu-Ni rods	256	305	342	425	455	1664	3058	3570	2731	2253
	+ 18 Cu-Ni rods + 40 ppm MDA	134	124	152	196	211	566	981	1467	1539	1390
	+ CuEA (2000ppb Cu)	nd	nd	nd	2173	nd	nd	1289	1411	763	763
	+ CuEA (2000ppb Cu) + 40 ppm MDA	nd	nd	nd	1871	nd	nd	2242	2257	2081	nd

* not determined

Table 6. Summary of the Total Thermal Deposits Formed for Two Stored JP-5 Fuels
Storage conducted for 14-15 months with and without the Test Additives as Stated
Effect of Early versus Late Addition of MDA*

test no.	test description ***	mole ratio** MDA:Cu TX	mole ratio** MDA:Cu LA	tot. deposit wt, mg/L TX	tot. deposit wt, mg/L LA
1	neat (reference): no additives/no storage	na ****	na	0.3	0.3
	Fuels stored in presence of test additives unless otherwise stated				
2	neat: storage without additives	na	na	0.2	0.4
3	15 ppm MDA added after storage	na	na	0.2	0.2
4	20 ppm MDA added before storage	na	na	0.3	0.1
	For fuels doped originally at 400 ppb Cu (CuEA)				
5	400 ppb Cu (CuEA): original Cu concentration added	na	na	0.6	2.3
6	92 and 398 ppb Cu (CuEA):+ 15.2 ppm MDA added after storage	37.2	8.8	0.4	1.2
7	400 ppb Cu (CuEA)+ 20 ppm MDA added before storage	11.2	11.3	0.1	0.5
	Cu concentration from Cu-Ni at the time of grav. JFTOT				
8	75 and 2170 ppb Cu (6 Cu-Ni rods)	na	na	0.7	2.8
9	75and 2170 ppb Cu (6 Cu-Ni rods): +15.5 ppm MDA added after storage	46.6	1.6	0.7	2.9
10	480 and 260 ppb Cu (6 Cu-Ni rods) + 20 ppm MDA added before storage	9.4	17.7	0.2	0.6
11	210 and 2730 ppb Cu (18 Cu-Ni rods)	na	na	0.5	5.3
12	210 and 2730 ppb Cu (18 Cu-Ni rods): +15.4 ppm MDA added after storage	16.5	1.7	0.5	3.1
13	2090 and 1540 ppb Cu (18 Cu-Ni rods) + 40 ppm MDA added before storage	4.3	5.8	0.3	1.1
	For fuels doped originally at 2000 ppb Cu (CuEA)				
14	2000 ppb Cu (CuEA): original Cu concentration added	na	na	21.1	3.5
15	230 and 760 ppb Cu (CuEA): + 15.1 ppm MDA added after storage	14.8	4.6	22.3	2.2
16	2000 ppb Cu (CuEA) +40 ppm MDA added before storage	4.5	4.5	0.5	0.9

* Early addition of MDA refers to its addition before storage; late addition, to its addition after storage.

**mole ratios are based on the MDA and Cu copper concentrations, at the time of addition of MDA.

*** For the sole purpose of calculating the mole ratios of MDA:Cu, for the CuEA doped fuels, the quoted copper levels are based on the time of addition of MDA. When MDA is added early, the quoted copper level is the original concentration added. When MDA is added late to the CuEA doped fuels, and for all cases of the Cu-Ni doped fuels, the quoted copper levels refer to the copper concentration at the time the grav. JFTOT tests were conducted. In cases where two copper concentrations are given, the first value pertains to the TX fuel, and the second, to the LA fuel.

**** na: not applicable

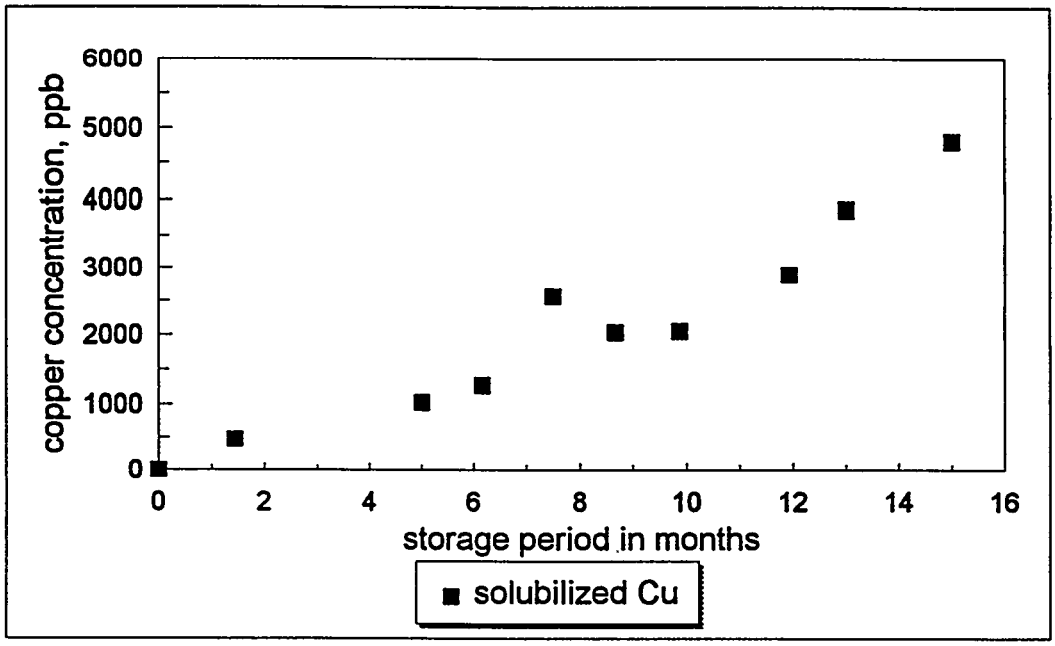


Figure 1. Fuel absorption of copper on storage. The Jet A test fuel was stored in the presence of copper as copper wires, BHT at 24 mg/L, and MDA at 30-35 ppm.

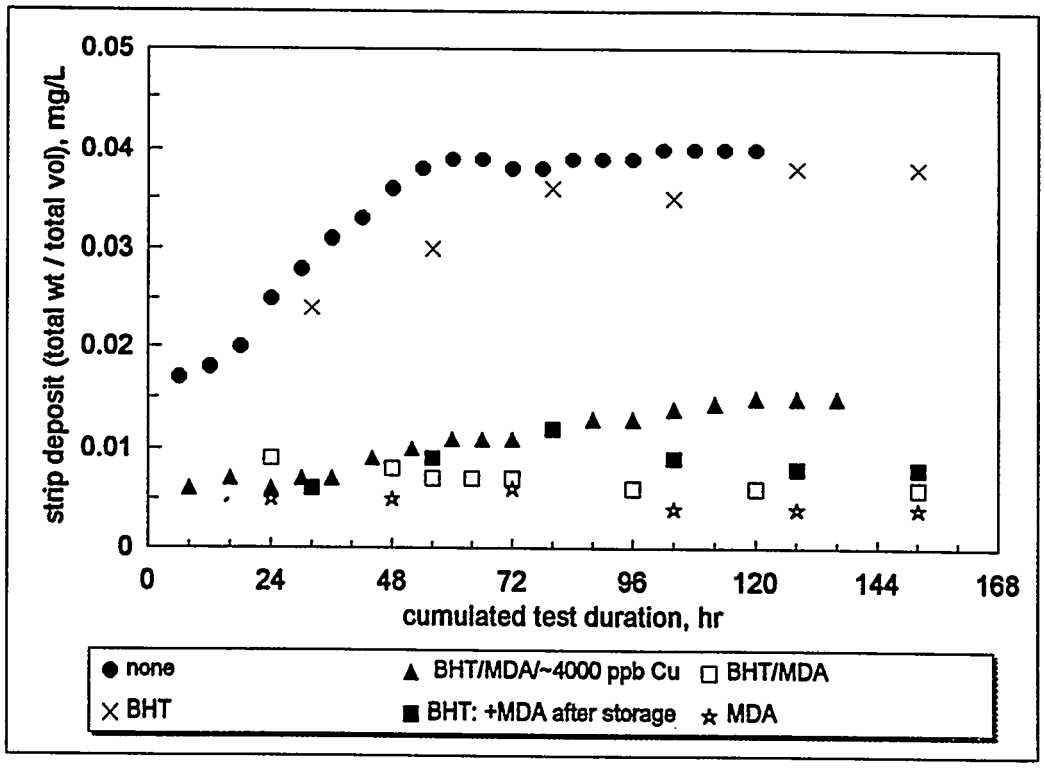


Figure 2. Cumulated strip deposits in mg/L. Effect of the test additives on the strip deposits formed on extended duration testings of the stored neat and doped Jet A test fuel.

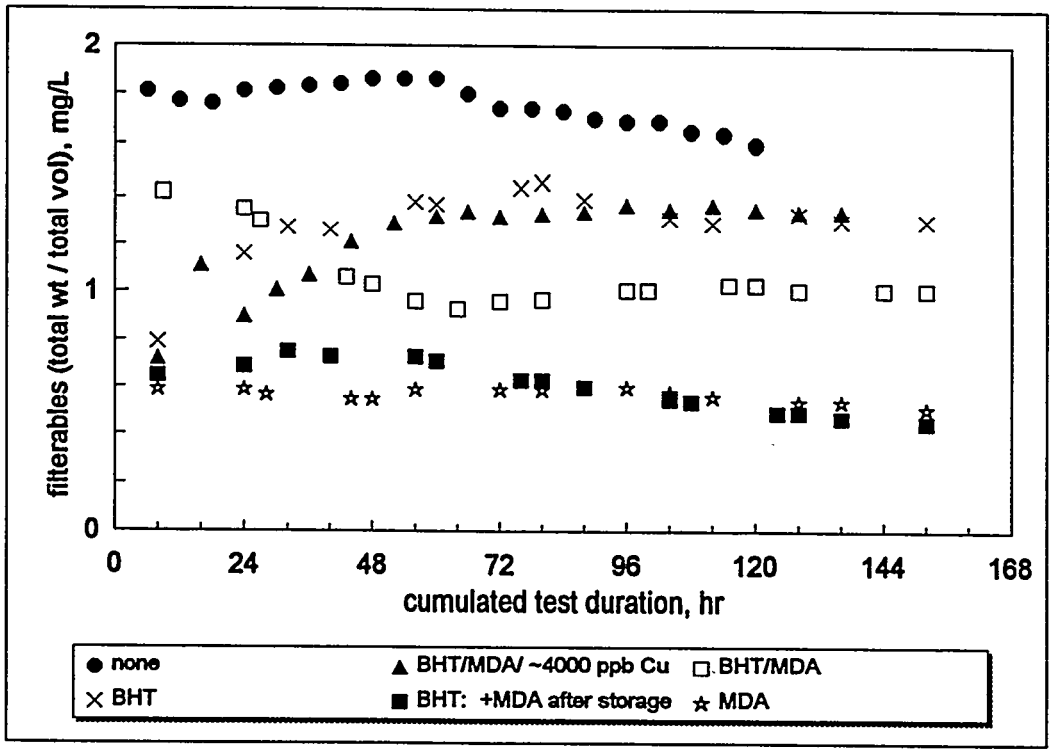


Figure 3. Cumulated filterable deposits in mg/L. Effect of the test additives on the filterable deposits formed on extended duration testings of the stored neat and doped Jet A test fuel.

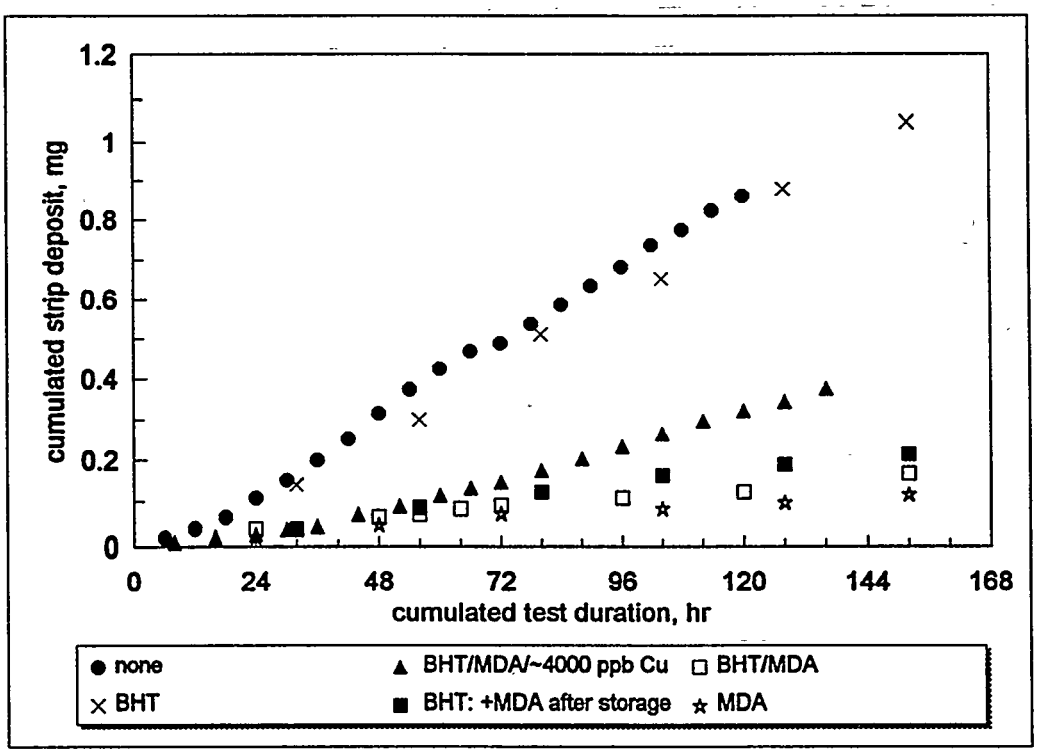


Figure 4. Cumulated strip deposits in mg: Effect of the test additives on the strip deposits formed on extended duration testings of the stored neat and dopedJet A test fuel.

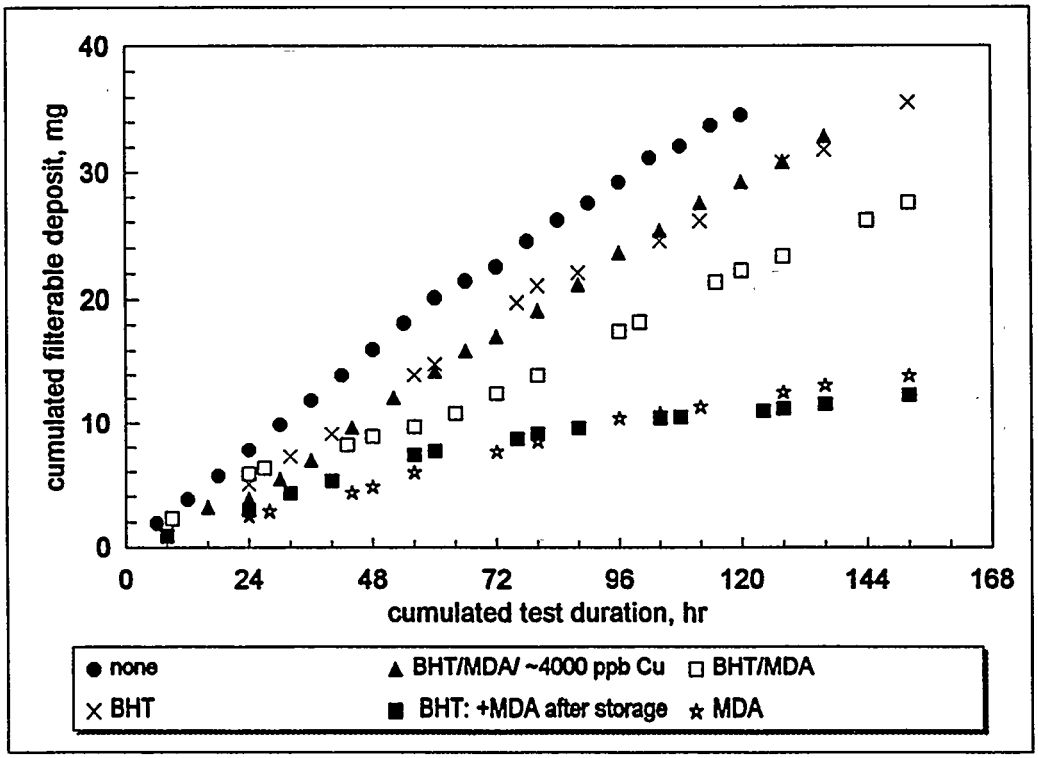


Figure 5. Cumulated filterable deposits in mg: Effect of the test additives on the filterable deposits formed on extended duration testings of the stored neat and doped Jet A test fuel.

6th International Conference
on Stability and Handling of Liquid Fuels
Vancouver, B.C., Canada
October 13-17, 1997

RETENTION OF METAL DEACTIVATOR ADDITIVE PERFORMANCE DURING STORAGE OF AVIATION TURBINE FUELS

Cyrus P. Henry Jr.

Octel America, Inc., 200 Executive Drive, Newark DE 19702 USA

The use of Metal Deactivator Additive (MDA) in aviation turbine fuels has continued to be controversial following the publication of Shell Thornton Research Centre data, which were presented in a paper at the 3rd International Congress. While benefits from MDA may be overstated in fuels with undetectable dissolved metal content in the ASTM D 3241 JFTOT test, there is also no question that use is fully merited when dissolved copper is present. Arguments have been presented that the allowed level in jet fuel should be significantly reduced, because the potential for copper contamination is lessened by the virtual disappearance of copper sweetening processes. There were concerns, however, about the possible loss of the additive during fuel storage, such that re-doping may be appropriate but not accommodated by reduced maximum use levels. To address that concern, samples of jet fuel containing MDA were stored and then challenged by the addition of soluble copper, followed by ASTM D 3241 JFTOT testing to determine whether the additive is still active.

INTRODUCTION

Use of up to 5.7 mg/L of Metal Deactivator Additive (MDA) has been permitted by most major civil aviation turbine fuel specifications for many years. Its primary purpose is to eliminate oxidation catalysis by dissolved metals, especially copper. Of the various metallic ions which might be dissolved in fuel, copper is generally regarded as the most potent oxidation catalyst. MDA is an extremely efficient chelating agent for copper, and for many years it has been used at low concentrations in aviation turbine fuel, motor gasolines, and other middle distillate fuels for that purpose. The MDA copper chelate is essentially inactive as an oxidation catalyst. In addition, copper sweetening processes were commonly used to reduce the odor of aviation kerosine; these fuels frequently contained traces of dissolved copper and effects were conveniently negated by addition of MDA. This practice was routinely followed for many years without controversy [1].

During the last twenty years, a chain of events has led to considerable debate about use of MDA in aviation fuels. In the mid 1970's, the D 3241 JFTOT thermal stability test method [2] was

accepted in aviation turbine fuel specifications as a suitable means to show that jet fuel has adequate thermal stability, and it is now the only method cited, except for Russian GOST specifications and those based on them. Copper sweetening processes have nearly disappeared and thus dissolved copper levels are lower; however, some fuels are still known to contain dissolved copper, primarily due to exposure to copper alloy heat exchangers or flow through copper alloy piping. Then during the 1980's, it became generally known that addition of MDA to aviation fuels could give a dramatic improvement in the thermal stability as determined by the D 3241 JFTOT test method, and its use as a "quick fix" became common when fuels failed to meet the specification requirements – even though dissolved copper content was frequently not determined by analysis. At that time, most specifications allowing MDA permitted its use at the discretion of the supplier, requiring only that its presence be declared on quality certificates. Growing use of MDA prompted the MOD (United Kingdom) to fund a project at Shells' Thornton Research Centre, to determine whether the apparent benefits of MDA as observed in the JFTOT test method were mirrored when fuel was then used in aviation turbines. A landmark presentation [3] of those results in 1988 suggested that benefits of MDA are overstated in the JFTOT test method.

As a consequence, a number of papers presented in this forum and elsewhere [4,5] have reported work on the use of MDA in aviation fuels, and some specifications have been altered to require permission for use [6] or reporting of test results before and after addition [7]. Studies previously reported by the author discussed results from eight jet fuels (three without measurable copper content) from field sources which all gave failing JFTOT test results at a test temperature of 260°C. All gave passing results when a small fraction of the allowed MDA concentration was added [8]. We also suggested that, while the apparatus no longer exists for direct comparison, old D 1660 [9] Coker thermal stability test data show much less effect from MDA.

While much has been learned, a fundamental conundrum remains: how should the use of MDA be limited to allow appropriate use when trace levels of dissolved copper are present, but avoiding indiscriminate use to satisfy a requirement for fuel quality – when it is known that the test method result might be unduly enhanced by the additive? Further complicating this question is the lack of adequate test methods (especially for field use) to determine parts-per-billion concentrations of copper or of MDA at use concentrations in fuel.

Finally, at the 1997 meeting of the MOD-UK Aviation Fuel Committee a proposal was advanced to limit the initial MDA concentration in aviation fuels to 2.0 mg/L, but allowing further re-doping up a cumulative maximum concentration of 5.7 mg/L. Since further addition of MDA is generally inconvenient, this action would generally result in a nearly 2/3 reduction in the typical concentration of MDA when used. We have recommended that a concentration of 2mg/L MDA is generally adequate in aviation turbine fuel for some time [10]. A question raised in response to this proposal was, however – will this concentration be maintained during storage of fuel or will loss of MDA due to degradation result in failing JFTOT test results after some period of time? We were aware that Hardy et al were also addressing this question and planned to discuss findings at this Symposium [11], but their work was not aimed at the suitability of this proposal.

EXPERIMENTAL

We were aware of early efforts by Hardy in which retention of metal deactivator was determined by an HPLC technique, and showed MDA disappeared over time [12]. However, there were concerns about the methodology. Instead, we focused on the performance of the additive over time. With rare exceptions, the concentration of copper in jet fuel samples from field sources is in the range < 5 – 100 parts per billion (higher levels are anticipated for JP-5 on board carriers, and might also be possible from extended exposure to copper alloy heat exchangers on board tankers). For many years, the concentration of copper in Jet A-1 fuels was limited to 150 parts per billion (ppb) in DERD 2494, United Kingdom Jet A-1 Specification which preceded the current Def Stan 91-91 Specification for Jet A-1 [1]. That requirement has been dropped from the current specification [7], because copper sweetening is very little practiced today, and to improve commonality between turbine fuel specifications. The amount of dissolved copper used to challenge MDA was therefore set at 80 and 160 ppb for this work on the basis that 80 ppb was in the upper range of typical copper contamination, and 160 ppb is the maximum concentration normally expected.

Fuels were aged under D 4625 [13] conditions in borosilicate glass containers, except one liter containers were used. Fuel samples were stored for 13 weeks at 43°C, conditions which are generally regarded equivalent to storage for one year at ambient temperature [13]. Since 2 mg MDA /L (active ingredient) is the proposed maximum concentration, all work was done using this amount. Tests were carried out where both MDA and 80 ppb dissolved copper (as copper

naphthenate) were added before storage, and in a second set of tests, an additional 80 ppb copper was also added so that a total of 160 mg/L soluble copper was used. These amounts were in addition to any adventitious copper already present in the base fuels.

D 3241 JFTOT tests were performed on un-aged fuels and on base fuels with added copper. In a second round of testing, samples with added copper and MDA were also tested prior to aging. For the second data set, the JFTOT apparatus being used malfunctioned, and the testing on aged samples was done at another site.

RESULTS AND DISCUSSION

A first set of preliminary data gave results shown in Table 1. The fuels used in these studies were three Jet A and Jet A-1 fuels available in our laboratory. These fuels had been in our hands for some time, and gave fair to poor results when tested without added copper or MDA. Addition of 80 ppb copper in the form of copper naphthenate to these fuels gave significantly poorer tube ratings, and in one case a failing ΔP result. When both copper and MDA were added to the fresh fuels, results were improved in terms of tube rating, but were still failing because of abnormally colored deposits. We have previously seen the high incidence of abnormally colored deposits from addition of copper naphthenate, and are puzzled these results which indicate inability of MDA to overcome the effects of dissolved copper.

Nonetheless, results showed that MDA was in fact retained after storage and in the case of Fuel B, the JFTOT rating was improved to a passing result (less than code 3 visual rating and not greater than 25 mm Hg pressure differential across the filter). In the case of Fuel B, abnormal tube deposits (and therefore a failing result) was obtained when fuel was aged with MDA and later copper addition, but passing results were obtained when the fuel was aged with both 80 ppb copper and MDA. Similarly, Fuel A gave better post-aging results when copper was added before aging, but Fuel C gave the reverse result.

We wanted to carry out additional tests in more fuels to supplement these data, and requested fuels from Steve Anderson, USAF for that purpose. He provided seven Jet A and Jet A-1 kerosines from a suite of fuels being used on the JP-8+100 program at Wright Patterson AFB which were then used for similar studies.

Table 1. Preliminary Data – Effect of Storing Fuel containing MDA and Dissolved Copper

Fuel Batch	Additive Treatment	Rating ASTM code	ΔP	
			Time	ΔP
A1	as is	< 2	150	2
A2	80 ppb Cu	< 4	125	123
A3 aged	80 ppb Cu + 2 ppm MDA	A, < 2	150	2
A4 aged	80 ppb Cu + 2 ppm MDA	<2	150	2
B1	as is	<4	150	2
B2	80 ppb Cu	A, heavy deposit	150	2
B3 aged	80 ppb Cu + 2 ppm MDA	A, < 3	150	3
B4 aged	80 ppb Cu + 2 ppm MDA	< 2	150	4
C1	as is	< 2	150	1
C2	80 ppb Cu	A, < 2	150	0
C3 aged	80 ppb Cu + 2 ppm MDA	< 1	150	2
C4 aged	80 ppb Cu + 2 ppm MDA	< 2	150	0

A3, B3, C3 – Aged with MDA, copper naphthenate addition after aging
A4, B4, C4 – Aged with MDA and copper naphthenate added before aging

These were tested as received, with 80 ppb copper as copper naphthenate, and with 80 ppb of copper and 2 mg/L of MDA before aging. Results from this testing is shown in Table 2, and also shows some unusual aspects – addition of excess MDA did not completely overcome the effect of added copper. As in the case of the first set of tests reported in Table 1, the fuels used for this study were not freshly produced, and had generally been stored under ambient conditions for some time. All seven fuels had satisfactory JFTOT results tested at 260°C before addition of copper or MDA; two failed on pressure drop after copper addition and six of the seven fuels failed due to pressure drop or abnormal deposits after copper addition.

Table 2. JFTOT Results on POSF As-received Base Fuels Before Aging of Samples

Fuel Batch (ppb Cu)	Additive Treatment	Rating ASTM code	ΔP	
			Time	ΔP
2827 (10)	as is	1	150	1
	80 ppb Cu	3 A	150	69
	80 ppb Cu + 2 ppm MDA	< 3 A	150	3
3219 (<5)	as is	1	150	3
	80 ppb Cu	1A	150	1
	80 ppb Cu + 2 ppm MDA	1	150	4
2926 (<5)	as is	1	150	1
	80 ppb Cu	1	61	125
	80 ppb Cu + 2 ppm MDA	< 2	150	2
3084 (6)	as is	< 2	150	0
	80 ppb Cu	3 A	150	4
	80 ppb Cu + 2 ppm MDA	< 2	150	0
3166 (5)	as is	< 2	150	0
	80 ppb Cu	3A	150	10
	80 ppb Cu + 2 ppm MDA	< 2	150	2
3305 (34)	as is	< 2	150	0
	80 ppb Cu	3 A	150	3
	80 ppb Cu + 2 ppm MDA	< 3	141	125
3119 (<5)	as is	2	150	1
	80 ppb Cu	< 3	150	1
	80 ppb Cu + 2 ppm MDA	---	---	---

Copper content of the as-received fuels was determined by ICP analysis and is shown with the fuel identification in Table 2.

Samples of these fuels, containing both 2 mg/L MDA (2 ppm) and 80 ppb dissolved copper, were aged as previously for 13 weeks at 43°C, and were again tested: however, the testing was done in another laboratory because our JFTOT apparatus had failed. The results of that testing are shown below in Table 3. Data are somewhat disconcerting, because the results

were generally better than that from un-aged fuels shown in Table 2. Although not shown, TDR data did not indicate that better results were due to differences between visual raters.

Table 3. JFTOT Results on POSF Aged Fuels

Fuel Batch	Additive Treatment	Rating ASTM code	ΔP	
			Time	ΔP
2827	Aged with 80 ppb Cu + 2 ppm MDA	< 2	150	0
	Aged with 80 ppb Cu + 2 ppm MDA; + additional 80 ppb copper	< 1	150	0
3219	Aged with 80 ppb Cu + 2 ppm MDA	< 1	150	0
	Aged with 80 ppb Cu + 2 ppm MDA; + additional 80 ppb copper	< 1	150	0
2926	Aged with 80 ppb Cu + 2 ppm MDA	< 1	150	0
	Aged with 80 ppb Cu + 2 ppm MDA; + additional 80 ppb copper	< 1	150	0
3084	Aged with 80 ppb Cu + 2 ppm MDA	< 1	150	0
	Aged with 80 ppb Cu + 2 ppm MDA; + additional 80 ppb copper	< 1	150	0
3166	Aged with 80 ppb Cu + 2 ppm MDA	< 1	150	0
	Aged with 80 ppb Cu + 2 ppm MDA; + additional 80 ppb copper	< 1	150	0
3305	Aged with 80 ppb Cu + 2 ppm MDA	1A	150	157
	Aged with 80 ppb Cu + 2 ppm MDA; + additional 80 ppb copper	< 2A	150	175
3119	Aged with 80 ppb Cu + 2 ppm MDA	< 1	150	1
	Aged with 80 ppb Cu + 2 ppm MDA; + additional 80 ppb copper	< 1	150	0

CONCLUSIONS

The data which were obtained with 10 jet fuels demonstrates that in general, fuels containing 2 mg/L of MDA can be stored for prolonged periods without loss in the ability of the MDA to chelate amounts of dissolved copper which can reasonably be expected in today's fuels. We therefore believe a limitation to allow 2 mg MDA/L for initial treatment of jet fuel is reasonable.

Several disturbing phenomena were encountered. We were mildly surprised that data obtained on a different instrument showed a systematic bias toward a milder result. The more disturbing JFTOT results were from treatment of fuel with a small amount of soluble copper and excess MDA – then finding that the resulting thermal stability was not as good as before either was added. This deserves further exploration; it may be due in part to use of older fuels for the study and formation of strongly acidic or other interfering species during aging.

ACKNOWLEDGEMENTS

Alan Garcia, Octel America, Inc. carried out all the experimental work on this project; his efforts are gratefully acknowledged.

REFERENCES

1. Smith, M., *Aviation Fuels,* G.T. Foulis & Co., Ltd., Cambridge UK **1970,** p. 284-287.
2. ASTM D 3241-96a "Standard Test Method for Thermal Oxidation Stability of Aviation Turbine Fuels (JFTOT Procedure), *1997 Annual Book of ASTM Standards, Vol. 5.02,* American Society for Testing and Materials, West Conshohocken PA, **1997.**
3. Clark, R.H., In *Proceedings of the 3rd International Conference on Stability and Handling of Liquid Fuels,* London, UK, 13-16 Sept. 1988, p. 283.
4. Baker, C., David, P., Hall, D., and Swatridge, R., In *Proceedings of the 4th International Conference on Stability and Handling of Liquid Fuels,* Orlando FL, Nov. 19-22, 1991, p. 316.
5. Schreifels, J.A., Gwynn, L., and Morris, R.E. In *Proceedings of the 4th International Conference on Stability and Handling of Liquid Fuels,* Orlando FL, Nov. 19-22, 1991, p. 661.

6. Performance Specification for Turbine Fuel, Aviation, Grades JP-4, JP-5, and JP-5/JP-8 ST, MIL-PRF-5624S, 22 November 1996.
7. Defence Standard 91-91/Issue 2, "Turbine Fuel, Aviation Kerosene Type, Jet A-1", Ministry of Defence Directorate of Standardization, Glasgow, UK, **1996**.
8. Henry, C.P., In Proceedings of the 4th International Conference on Stability and Handling of Liquid Fuels, Orlando FL, Nov. 19-22, 1991, p. 692.
9. ASTM D 1660, " Method of Test for Thermal Stability of Aviation Turbine Fuels", Discontinued, See *1993 Book of ASTM Standards,* Vol. 5.02, **1993**.
10. "Octel Additives for Use In Aviation Fuels", Octel America Tech Memo 10,001-96, Octel America, Inc., Newark DE, **1996**.
11. Pande, S.G., and Hardy, D.R., "Effectiveness of MDA on Jet Fuel Thermal Stability as Determined Using the Gravimetric JFTOT", Vancouver BC, Oct. 12-17, **1997**.
12. D.R. Hardy, private communication.
13. ASTM D 4625, "Test Method for Distillate Fuel Storage Stability at 43°C (110°F)", *1997 Annual Book of ASTM Standards, Vol. 5.02,* American Society for Testing and Materials, West Conshohocken PA, **1997**.

6th International Conference on
Stability and Handling of Liquid Fuels
Vancouver, BC, Canada
October 12-17, 1997

THE 'BLACK AVTUR' INCIDENT IN NORTHERN AUSTRALIA (1994/95); REPORT ON THE AMRL INVESTIGATION (1995/97)

Alan J Power*[1], Paul M Rawson, Michael G O'Connell, Lance W Hillen and Grier G McVea

Airframes and Engines Division, Aeronautical and Maritime Research Laboratory (AMRL), PO Box 4331, GPO Melbourne, Victoria, AUSTRALIA3207

ABSTRACT

The 'Black AVTUR' incident that occurred at a northern Australian Air Force base in late 1994 to early 1995, was the first known example in Australia of an aviation fuel throwing a sediment. The fuel was JET A-1 which had been additised to the military specifications of NATO Code F-34. The JET A1 fuel had been refined in Singapore from a Chinese crude oil. The black coloured fuel that formed at low point drains in ten 162,000 litre fuel tanks, after several months of storage, caused significant military logistic problems. From investigations by the above laboratory, it was established that the fuel was storage unstable, a characteristic that was responsible for the black colouration of the fuel. The bulk fuel temperature at the base was 32°C and at this temperature, the sediment particulate matter was apparently being held as a stable colloid that gave the fuel its black appearance. This report describes the investigation of this incident and provides details of work done in an attempt to identify the cause(s) of the 'Black AVTUR' incident. A major finding from this research was that an antioxidant present in the AVTUR fuel lubricity improver additive is strongly implicated as a component involved in the formation of the jet fuel sediment molecules that were responsible for the quarantining of the contaminated fuel for several months, at the military air base.

INTRODUCTION

The 'Black AVTUR' incident that occurred at RAAF Base Townsville in late 1994 to early 1995 was a unique event for the Air Force. The formation in AVTUR (F-34, JP-8) of a black coloured sediment was without precedent in jet fuel supplied to the RAAF. The consignment of fuel involved was an imported JET A-1, having been refined in Singapore from a Chinese crude oil. The fuel supplier additised the JET A1 fuel delivery to NATO F-34 specification requirements. The formation of black coloured fuel, after about five months storage, resulted in ten 162,000 L

[1] E-mail: alan.power@dsto.defence.gov.au

fuel tanks, up to 75% of the total fuel storage capacity at the base, being held in quarantine. This threatened supply of fuel for scheduled joint military exercises. RAAF personnel requested its Quality Assurance organisation and the fuel supply contractors for assistance with the black fuel problem. After no satisfactory resolution could be found from these agencies, the RAAF approached AMRL for assistance in solving and rectifying the black fuel problem.

TECHNICAL RESOLUTION OF THE 'BLACK AVTUR' INCIDENT

Samples of black AVTUR submitted to AMRL for investigation, on arrival, were observed not to be black, but were light straw in colour with a dark sediment at the bottom of the container. Clearly the fuel colour had changed in transit due to settling and/or temperature reductions. When the black fuel at Townsville was cooled in a refrigerator it was reported that the fuel changed from black to clear, indicating the contaminant was in a stable suspension at high ambient temperatures that settled out on cooling. A visit was made to the base to establish the history relating to details of the receipt and handling of the fuel, and to conduct contamination measurements in the field. AMRL was advised that black AVTUR (F-34, JP-8) had been first observed by RAAF personnel during the regular low point drain checks routinely carried out for removal of water from the tanks. This was reported about five months after fuel delivery. The colour intensity resembled an Indian ink black, as shown in the photograph displayed in **Figure 1**.

The extent of particulate matter contamination in the F-34 fuel storage tanks was measured and these ranged from low point drains (42 mgL^{-1}), middle level (1.9 mgL^{-1}) and upper level (1.5 mgL^{-1}). The fuel colour at middle and upper levels varied in colour from orange through to pale to straw-brown, whilst fuel at low point drains was Indian Ink black. It was evident from fuel storage tank inspections and laboratory measurements that a stable colloid of fine black particulate matter was forming in the fuel and settling to the bottom. This was occurring at the low point drains at intervals of 2-3 days, in volumes of about 20 litres.

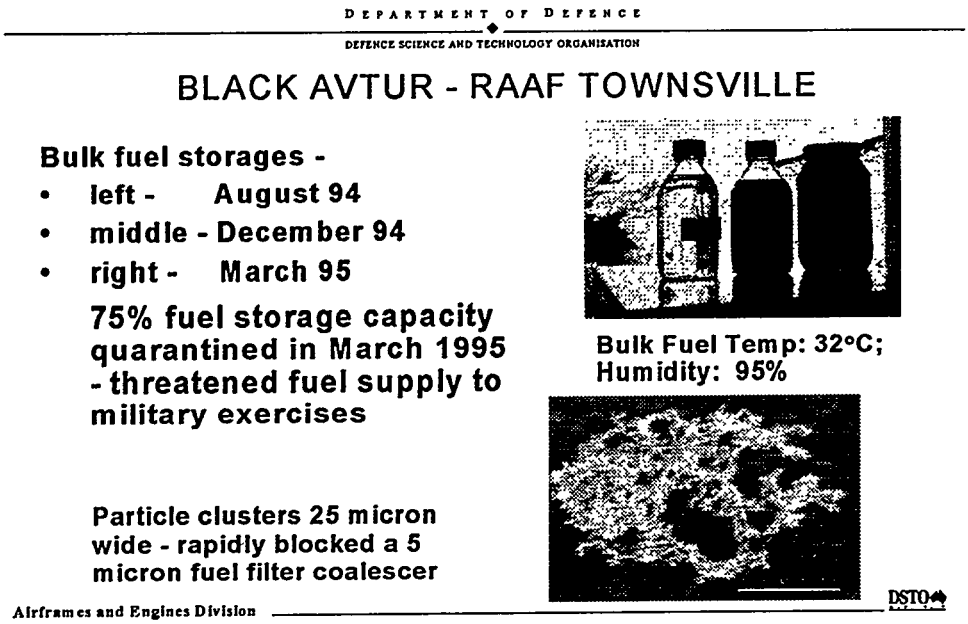


Figure 1: Visual examples of the 'Black AVTUR' fuel that was forming at the low point drains in the tanks, and a SEM microphotograph of typical clusters of sediment being thrown by the fuel

As the bulk of the fuel above the low point drains was not black, the RAAF was considering using this fuel in aircraft. To determine whether the fuel could be cleaned up by fine filtration and used before significant quantities of particulate matter re-formed, a coalescer filtration unit was used to transfer 30,000 L of the upper level fuel to a road tanker. The fuel particulate concentration in the bulk fuel was reduced to 0.03 mgL^{-1}. After three days storage, the particulate level in the tanker increased to more than 1 mgL^{-1}, about a thirty-fold increase, indicating that this batch of fuel was extremely unstable in storage.

Although AVTUR with this level of contamination could have been used immediately after filtration, it was concluded that if an aircraft was refuelled with this fuel, and then for some reason was not flown for an extended period, air safety may have been compromised when the aircraft re-entered service, due to accumulation of sediment over time in the aircraft's fuel systems. The particulate level found in the fuel farm tanks at low point drains was about 40 mgL^{-1}. When this is expressed as a total amount of solid in aircraft fuel tanks, of the order of 4,000L volume, accumulation of about 160g of sediment was possible. The possibility of a slug of this sediment entering an aircraft fuel system was of particular concern, because of the very small tolerances in fuel metering systems and nozzle orifices, such as in the F/A-18 F404 engine (diameter 38 μm).

Nozzles orifices of this dimension could have readily been blocked by a surge of fuel possessing such high particulate levels.

This risk was assessed as being potentially dangerous and as a result of the AMRL technical investigation, the RAAF decided that the suspect fuel above the black fuel forming at the low point drains was unusable. The fuel supplier then accepted the AMRL finding that there was a storage stability problem associated with this imported aviation fuel, and that there was a responsibility to take remedial action. The fuel (1.5 million L) was removed by the original fuel supplier.

AMRL Research into the Cause(s) of the 'Black AVTUR' Incident

The black AVTUR sediment was initially analysed by Fourier Transform infrared (FTIR) spectrometry to investigate its chemical composition. The FTIR spectrum (**Figure 2**) of the Black AVTUR sediment was consistent with sediment from secondary refined diesel fuels [1-3]. The large, broad absorbance centred at about 3400 cm^{-1} has been attributed previously either to stretching vibrations of hydrogen-bonded aromatic hydroxyl or amino groups.

Elemental analysis of the 'Black AVTUR' sediment was carried out for carbon (C), hydrogen (H), nitrogen (N), oxygen (O) and sulphur (S), with the following results:

C = 63.7%; H = 7.6%; N = 3.3%; O = 15.7%; S = 3.1%

These sediment elemental values are generally typical of those from storage unstable diesel fuels that result from unhydrogenated light cycle oil (LCO) blending stocks. In particular, the very high oxygen content of such LCO-derived fuel sediments has been discussed in a publication [1] that involved experimental derivatisation of LCO sediment using the reagents benzoyl chloride and acetic anhydride. The mass of the sediment increased significantly, and the IR spectra of the reaction products indicated conversion of the bulk of the sediment to benzoates and acetates.

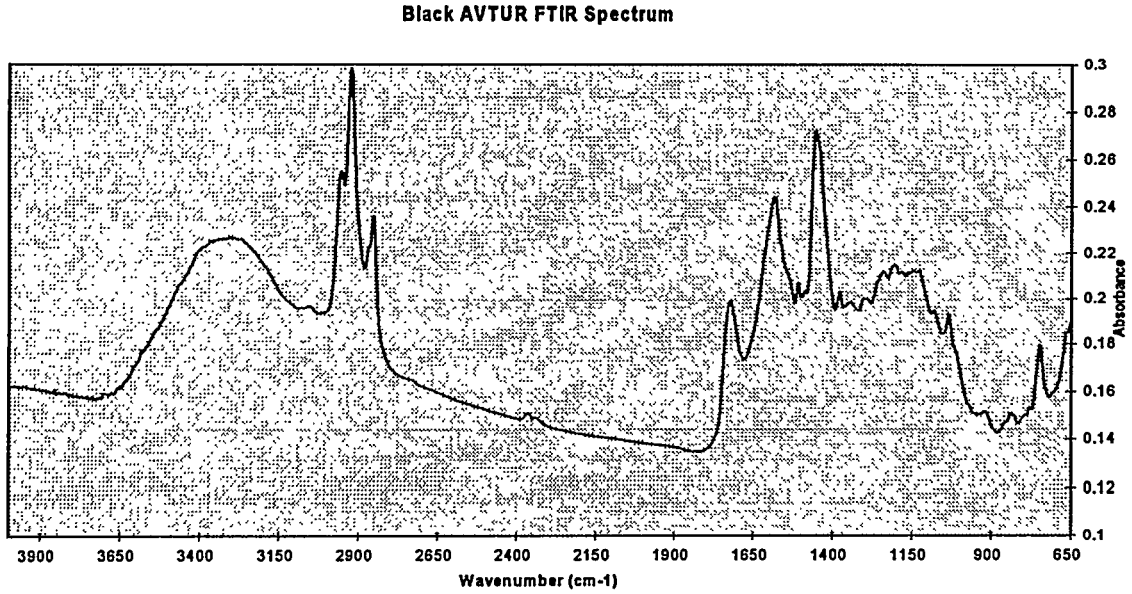


Figure 2. FTIR spectrum of the 'Black AVTUR' sediment exhibited IR absorbances that are characteristic of those published for diesel fuel sediments which form from unhydrogenated light cycle oil from the catalytic or thermal refinery cracker [1-3].

Conversion of indole species that may possibly exist in the sediment to amides was not indicated, while synthetic indolylphenalenone acid salt did convert to amide.

Blue-green coloured indolylphenalenone acid salts are very reliable indicators of insufficient hydrogenation of cracked stock in blends of LCO. However, it was concluded in that work that indolylphenalenone acid salts are not principal constituents of the total mass of fuel sediments. It was further concluded in that study that the broad FTIR peak at 3400cm^{-1} was attributable to aromatic hydroxyl groups from the fuel and not to amino species.

In the current study, it was therefore concluded that the chemical nature of the sediment from the black AVTUR was due, at least in part, to the presence in the fuel of unstable products of secondary refinery processing.

AMRL acquired a pyrolysis/gas chromatography/mass spectrometry (PyGCMS) facility to support investigation of the composition of the black fuel sediment. The intractable fuel sediment material that is shown in **Figure 1** is too involatile to be able to be examined by gas

chromatography (GC). To enable GC separation of sediment components, it was initially necessary to pyrolyse the sediment at high temperatures to volatilise the precursor molecules that had reacted in the fuel to form the solid deposit. This procedure could then lead to an attempt to elucidate potential precursor molecules in the fuel that may have been responsible for the 'Black AVTUR' incident.

Figure 3 demonstrates the capability of PyGCMS equipment to identify a candidate chemical participant in the formation of the black fuel sediment. The major component in the pyrogram was identified as an antioxidant from the fuel lubricity improver additive in the fuel. High precision in the spectral library match of the mass spectrum of the 4-amylphenol in the pyrogram was obtained. In **Figure 3**, the lower mass spectrum is from the electronic library. It was concluded that the presence of the 4-amylphenol, as a primary component of the sediment thrown by the 'Black AVTUR' sediment, was of synthetic origin. The smaller peak with an asterisk in **Figure 3** matched exactly with bis-2,4-amylphenol. A diagrammatic representation of chemical structures of the compounds identified is provided in **Figure 4**. It is rare in nature that a substituted alkylphenol derivative would be present, together with its related di-substituted derivative. Catalytic alkylation of phenols usually follows a chemical mechanism that leads to formation of a mono-substituted alkyl derivative, with minor amounts of the di-substituted derivatives being formed. It was on this basis that the 4-amylphenol was concluded to have been of synthetic origin. Several other alkylphenolic components were identified in the pyrogram, but none had related di-substituted homologues present.

In order to identify longer chain molecules in the Py/GC/MS pyrogram, which do not survive severe fragmentation caused by high voltage electron impact in the conventional electron impact (EI) mass spectrometric detector, AMRL has now acquired a soft ionisation source, namely a chemical ionisation (CI) source. This has now been trialed with standard organic chemicals, and has been found to work effectively. It can be seen from **Figure 5** that CI enhances the abundance of the molecular ion, at the expense of fragmentation seen in an EI mass spectrum. An example of the difference between EI and CI is shown in **Figure 5**, where the EI source (bottom picture) almost completely fragmented the decanoic acid methyl ester, giving only a very small molecular

ion at *m/z* 186, while the CI gave a large molecular ion (+ 1 for a hydrogen ion from the methane gas used in the CI source) at *m/z* 187.

Using a combination of electron impact and chemical ionisation detectors in the PyGCMS equipment, several longer chain alkylphenols were found in the pyrogram of the sediment. The presence of phthallic anhydride was also identified, indicating that cross-contamination of the fuel with phthallic acid esters, that are widely used as plasticisers of common plastics, may have occurred. At pyrolysis temperatures between 500-650°C, esters of phthallic acid would almost certainly be converted to phthallic anhydride. However, in recent investigations it has been found that phthallic anhydride, along with alkylanthracene and alkylphenanthrene, form the bulk of fuel thermal deposits from fuels that could not have been exposed to plasticisers [4]. The role of unreacted polycyclic fuel components in thermal deposits is being studied.

Treatment of 'Black AVTUR' with AMRL Fuel Stability Foam (FSF)

The 'Black AVTUR' was treated at 32°C (the bulk fuel temperature of the 'Black AVTUR - refer **Figure 1**) with AMRL Fuel Stability Foam (FSF), to investigate the absorptivity of the foam for the sediment and the possible removal of sediment from the black fuel. The FSF removed the sediment from the fuel sample, indicating that the known benefits of storing diesel fuel in contact with FSF may be applied to aviation fuels such as that involved in the 'Black AVTUR' incident. AMRL is currently studying absorptivity of FSF to F-34 fuel additives to ensure that, should FSF be used to protect AVTUR from build-up of sediment in future, the essential additives would still be present in the fuel. If FSF is found to be compatible with AVTUR, the RAAF will install this material in large fuel storages in northern Australia as additional protection against future potentially storage-unstable fuels.

SUMMARY OF CONCLUSIONS

1. The 'Black AVTUR' incident at RAAF Townsville occurred due to storage instability of the F-34 aviation fuel.

2. The chemical nature of the sediment is indicative that at least part of the fuel had been derived through secondary refinery processing, similar to the manufacture of diesel fuel.

3. The elemental analysis and the FTIR spectrum of the fuel sediment were very similar in nature to that which forms in diesel fuel that contains unhydrogenated light cycle oil.

4. The major fuel sediment precursor component in a pyrolysis/gas chromatography/ mass spectrometry pyrogram of the sediment was identified as a phenolic antioxidant from the fuel lubricity improver additive in the fuel.

5. The 'Black AVTUR' fuel that shed sediment can be rejuvenated by contact with FSF.

PRINCIPAL AUTHOR'S COMMENT

It has been suggested by a peer reviewer of this paper that conclusion 4, above, conflicts with conclusions 2-3. Consistent with our previous report [1] that phenolic species are involved in the formation of the bulk of fuel sediments derived from fuel blends that contain partially or fully unhydrogenated, unstable light cycle oil (LCO), it is relevant that the lubricity improver antioxidant identified in the PyGCMS work above is also phenolic. Competition between phenolic molecules derived from the LCO and that from the antioxidant, in the formation of the sediment, has now been found to have been approximately 3:1. This estimate was derived by summation of areas of the phenolic species found in the PyGCMS pyrogram (homologous series of C_1, C_2 and C_3 phenols from the LCO) and comparing the total area of those peaks with the area of the peak identified as 4-amylphenol, the lubricity improver antioxidant. Thus, conclusions 2-3 and 4 are considered to be both internally consistent and synergistic.

REFERENCES

1. Power, A J and Mathys, G I. **(1992)**. "Characterization of Distillate Fuel Sediment Molecules: Functional Group Derivatization", FUEL, **71**, 903-908.

2. Green, J B, Stirling, K Q and Ripley, D L, **(1991)**. "Storage Stability and Hydrotreating Chemistry of Phenolic Compounds Present in Mid-Distillate", 4th International Conference on Stability and Handling of Liquid Fuels, Orlando, Florida, USA, November 19-22, Ed H N Giles, Volume 2, 503-517.

3. Power, A J, **(1986)**. "Accelerated Oxidation of Diesel Distillate", FUEL, **65**, 133-137.

4. Power, A J, Rawson, P M and O'Connell, M G, unpublished results (draft in preparation).

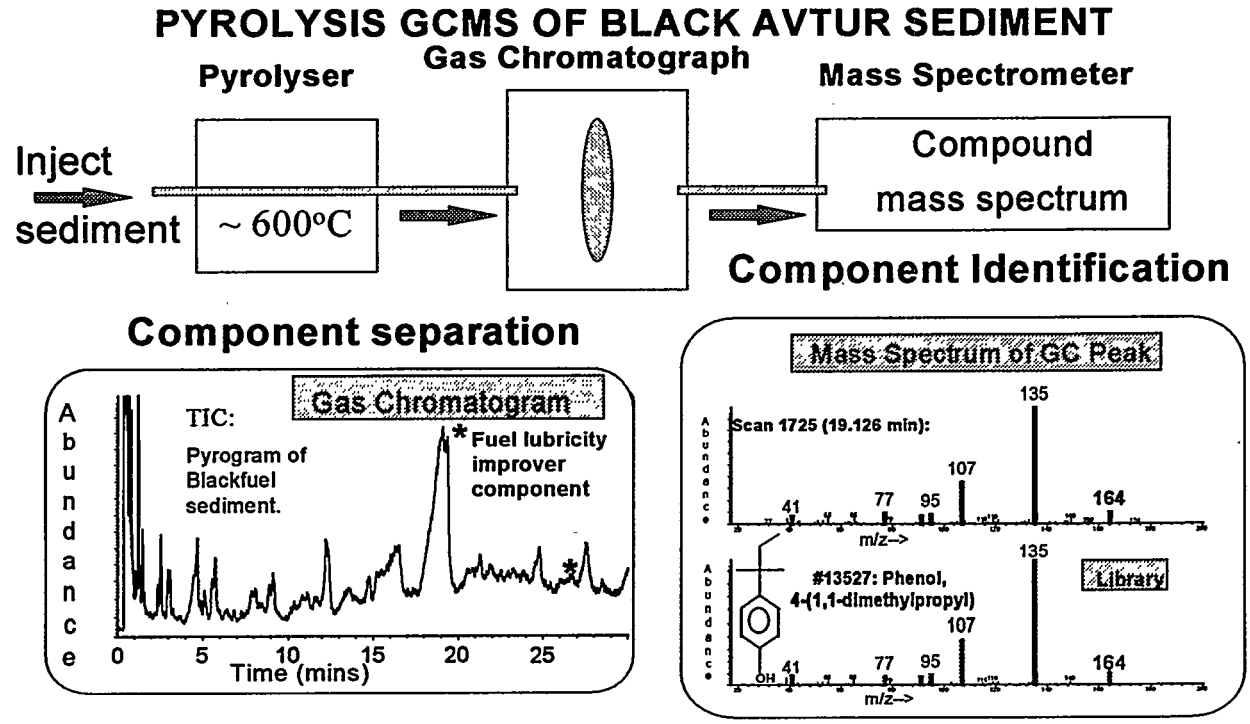


Figure 3. Pyrogram of the 'Black AVTUR' sediment, in conjunction with GC/MS separation / identification of the volatilised constituents from the sediment, implicate the presence of an antioxidant associated with the fuel lubricity improver.

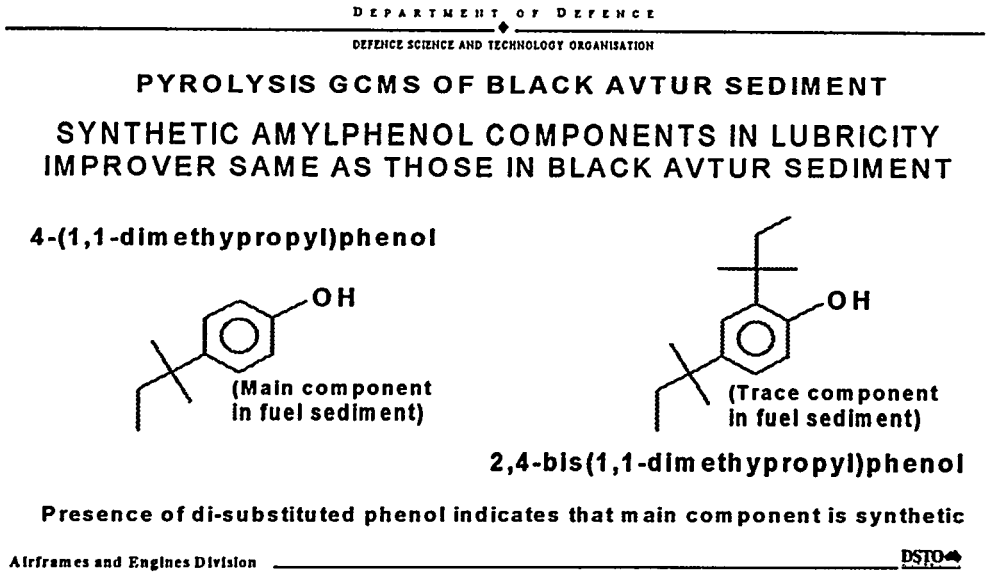


Figure 4. Identification of the di-substituted derivative of the 4-t-amylphenol shown in Figure 3 indicated that these sediment components were of synthetic origin.

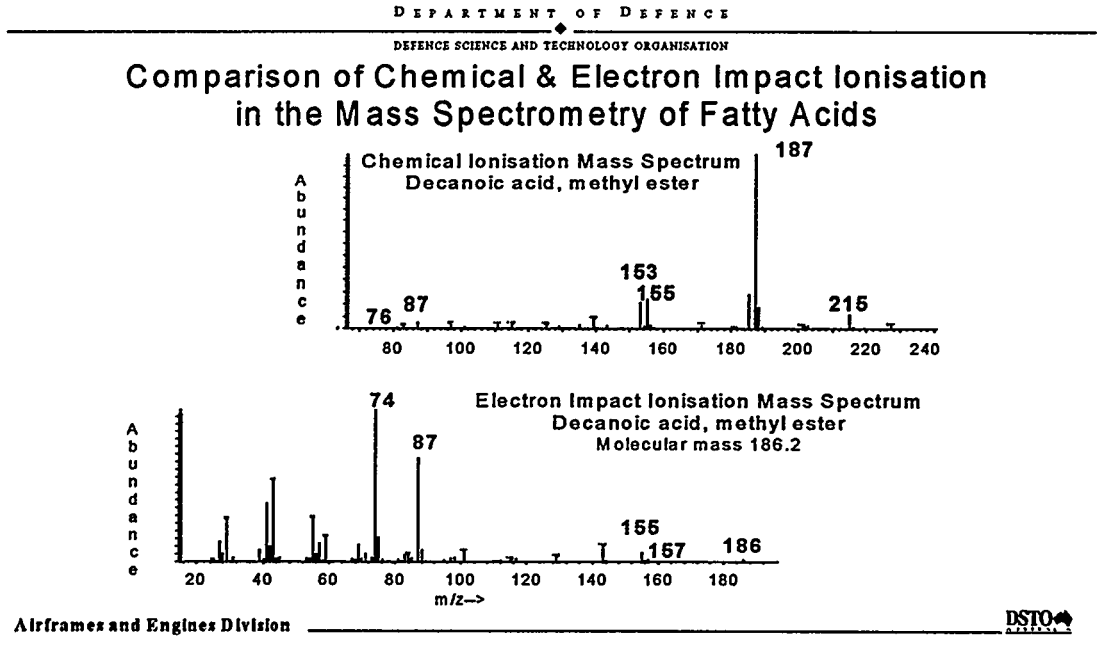


Figure 5. An example of the facility for correlating long chain chemical components in fuel, as seen by the Electron Impact (EI) detector, compared with the soft ionisation technique using Chemical Ionisation (CI).

6th International Conference
on Stability and Handling of Liquid Fuels
Vancouver, B. C., Canada
October 13-17, 1997

JET FUEL CONTAMINATION BY DIESEL FUEL DYE

Kurt H. Strauss
69 Brookside Road, Portland, ME 04103-4609

An investigation of jet fuel contamination by diesel fuel dye in the USA has been coordinated by the Coordinating Research Council since April 1994. During that time the CRC was instrumental in getting the dye color changed from blue to red to avoid confusion with aviation gasoline. Subsequent to that change laboratory tests were conducted to establish the effect of red dye on specification properties with high temperature stability being the only affected property. Based on these results aircraft operation with dye-containing fuel was severely restricted by airframe manufacturers. The paper reviews the test results and traces the chronology of industry actions to control the problem.

Background

Regulations published by the U. S. Environmental Protection Agency[1] (EPA) on August 21, 1990 required that, beginning on October 1, 1993, on-highway diesel fuel contain no more than 0.05 m% sulfur. Diesel fuel containing more than 0.05% sulfur was to be identified by the visible presence of a blue dye, 1,4-dialkylamino-anthraquinone. Simultaneously the Internal Revenue Service[2] (IRS) required the addition of the blue dye into diesel fuel or heating oil not subject to road tax. Following concerns by the aviation community about the possible misidentification of blue-dyed diesel fuel for 100 LL aviation gasoline, which is also dyed blue, both IRS[3] and EPA[4] changed the required dye to the solvent red 164 dye (alkyl derivatives of azobenzene-4-azo-2-naphthol), effective October 1, 1994. Currently EPA requires a "visible" dosage of red dye to be added to high sulfur diesel fuel (or high sulfur No. 2 heating oil), while the IRS minimum reference color strength dosage for color strength is 3.9 pounds per thousand barrels (PTB) of the solvent red 26 dye which is a better defined compound (methyl derivatives of azobenzene-4-azo-2-naphthol). The EPA dye level is to be added at the refinery, while the IRS dosage must be present when tax exempt fuel is delivered to the user at a refinery, at a terminal or at an import point. Although these requirements involve different fuel categories, sulfur levels vs. taxability, in practice

they tend to involve the same fuels in the U.S. Violation of either regulation involves heavy fines.

Neither regulation contains a dye requirement for aviation turbine fuel. Why then is there any concern in the aviation industry? The answer lies in the U. S. distribution system where differing fuels are not always physically separated from each other. Thus in large multi-product pipelines, different products follow each other with no separation. Cuts between products are usually made where there is a 50/50 mix of two products in the interface. The resultant interface is blended back into the product as long as the limited amount of mixed fuel does not drive either product off-specification. Mixing can also occur in manifolds, pumps and other shared components in pipelines as well as marine transports. Transport trucks which are not maintained in a single product can be another source of mixing. Because fuel appearance is a major component of aviation fuel quality control, particularly at airports, any discoloration due to diesel dye raises immediate questions regarding fuel acceptability by airframe manufacturers.

Industry Reactions

Subsequent to the issuance of the Federal regulations, the Boeing Company distributed an advisory letter[5] to its customers prohibiting the operation of Boeing aircraft on fuel containing the red dye because of the unknown effects of dye on aircraft operation. McDonnell-Douglas[6] issued similar prohibitions soon thereafter. These actions could result in shutting down an airport fuel system or running an airport out of fuel if any dye was found. For obvious reasons the actions caused major concerns among airlines and their fuel suppliers as no one had any way of forecasting the incidence of such contamination, but all agreed the results of airport shutdowns would be drastic.

Coordinating Research Council Activities

To answer a great variety of questions about dye effects on aviation turbine fuel performance, the Coordinating Research Council (CRC) organized a group to deal with the dye matter in June 1993. The Group membership is shown in Table 1. Among its first efforts[7] was an objection to the IRS and EPA to the use of blue dye because of possible confusion with 100LL Aviation Gasoline which is the major aviation gasoline in the North American market. Instead the letter suggested the use of red dye and requested a red dye dosage of less than 3 PTB. (Although the 80 grade aviation gasoline is dyed red, there is

little, if any, of this product available in the U. S.) While the two government agencies agreed to the dye color change, the IRS rejected a reduced dosage because of a desire to detect blending of taxable and nontaxable diesel fuels.

The second step was a cooperative program to ascertain the effect of red dye on specification properties. As a point of clarification it should be noted that the IRS dosage is expressed in terms of solid red dye (solvent red 26), a pure material. Commercially red dye is handled as a liquid in a carrier solvent. Both active ingredients and total liquid dye concentrations, therefore, differ from the solid dye concentrations. Equivalent dosages and various concentrations of both dye versions are shown in Table 2. In the program, 12 organizations ran a variety of specification tests, with most participants concentrating on thermal stability. Testing was done on Jet A fuels containing the dye but no diesel fuel. Fuel samples were selected at random but all dye samples came from the same supplier. The program established that the full IRS fuel dye dosage for tax-free diesel fuel affected no commercial specification properties except thermal stability. In addition to the specification requirements, Rolls Royce[8] and McDonnell-Douglas[9] tested the effect of dye on engine and airframe elastomers as summarized in Table 3. The Navy[10] found that the full dye dosage level gave higher readings in the Shipboard Contamination test than the neat fuel. (This test depends on light transmission through a wet membrane.) Tests by Boeing[11] showed the full IRS dosage to have no effect on freezing point or on turbidity at ambient temperatures.

Thermal stability was measured by conducting a series of Alcor JFTOT tests (ASTM D 3241) in which the control tube temperature was increased in 5°C steps until the test failed by exceeding the specification definition of either tube deposits or filter pressure drop. The minimum failure temperature was designated as the fuel break point. Dye effects were expressed as decreases in breakpoint temperature. Results are detailed in Table 4[10]. About 33% showed a breakpoint drop of 10°C or greater with the full dye dosage; a decrease of 5°C was considered within test repeatability. Four samples, which are shown in bold print, failed the specification minimum of 260°C tube temperature but passed the alternative ASTM D 1655 requirement of 245°C. However, two of these samples failed at 260°C without any dye.

The next step was to find the effect of reduced dye dosages. Those laboratories whose product in the first round had the 10°C or higher decrease repeated the testing with a 10% red

dye concentration. (Fuel samples J-7 and K-8 had been depleted in the earlier testing.) Those results are listed in the last column of Table 4. Although a number of fuels now showed no dye effects at the 10% dye level, 4 out of 10 samples still reflected a significant adverse effect of the red dye at this level. In addition, five laboratories ran additional fuels with wider concentrations of dye as shown in Table 5[12]. Here again, the higher dye dosages caused three of the fuels to have break points below 260°C.

At this point some comments on the program are in order. Fuel samples were selected at random. Although none of the fuels failed specification requirements even with the full IRS dosage, none of the fuels were a marginal pass in the absence of dye. Lastly, the testing did not include the effect of diesel fuel addition, although field contamination would normally take place through the inadvertent addition of dyed diesel fuel. The JFTOT results therefore raised a warning flag without answering the question of what was an acceptable industry maximum of dye contamination.

Field Problems

Over the history of red dye addition to specific grades of diesel fuel, quite a number of cases of dye-contaminated jet fuel occurred. Thus for the first half of 1996, one airline reported 22 cases of dye-contaminated product, including 4 cases where such product was received into airport storage. The remaining incidents were detected further upstream in the system. Most incidents involved tank truck deliveries, but several of the larger volumes were pipeline deliveries to an airport. In the last three years one airport in Alaska had to be shut down, but several other airports only avoided closure because not the entire receiving storage was contaminated. These cases included Dulles, LaGuardia and Miami Airports. At Boeing Field, Seattle, eight aircraft were fuelled with dye-contaminated fuel and had to be defuelled, but an alternate fuel system allowed other operations to continue.

Field Detection of Dye

The contamination incidents graphically illustrated differences in detection methods. At refineries and terminals product appearance is normally checked by the Clear and Bright or bottle test (ASTM D 4176), while airport personnel look at product appearance with the White Bucket test[13], using a white porcelain bucket. In the former color is determined by transmitted light through about 100 mm of product, while in the latter appearance is judged by transmitted and reflected light through about 150 mm of fuel. In addition the white bucket

rating includes a significant surface area integration factor. Comparisons have shown the white bucket to be more sensitive to red dye contamination than the Clear and Bright test, with a lower detectable level in the white bucket being about 1 volume of fuel dyed to the IRS minimum level in 3000 volumes of water-white jet fuel, although some have reported even lower detectable levels with this test[14].

However, both methods are subject to human judgment and an early CRC initiative was to encourage the development of a field meter capable of measuring these low dye levels. Such a meter is now available in the PetroSpec JT 100 and has been submitted to ASTM for standardization.

Industry Remedies

Pipelines and other fuel handling organizations have concentrated on eliminating contamination as much as possible. One major improvement has been a change in the injection points for the IRS dosage. Originally, the full IRS dye dosage was injected at the refinery to minimize the number of injection points. This practice created two problems. When dyed fuel preceded or followed jet fuel, normal cuts could not be made at the middle of the interface but had to be made where the interface mix was almost 100% jet fuel, resulting in a substantial loss of jet fuel. Refinery injection also meant handling a highly dyed fuel which could contaminate jet fuel in manifolds, pumps and other shared parts of the system. As of July 1996, the IRS dosage is now injected at the receiving terminals of two major pipelines. While this has reduced the problem, it does not eliminate it because the EPA dosage (roughly 25% of the IRS requirement) must still be injected at the refinery. Pipeline problems are compounded by the fact that the low sulfur, taxable diesel fuel cannot show any dye either, thereby limiting which products can follow or precede the dyed product.

Almost from the beginning, the airline industry has been searching for ways of avoiding airport shut downs. Early on it was proposed to the engine manufacturers that fuel containing a maximum of 2.5% dye or 0.40 mg liquid dye per liter be acceptable on an emergency basis and that a maximum of 0.5% (0.08 mg/L) be acceptable on a continuous basis. These proposals have not been agreed to at the date of this writing. A partial resolution has been made by a Boeing Service letter [15] which accepts fuel that does not show color in the White Bucket test. Such fuel is considered equivalent to satisfactory fuel made before the existence of the dye problem. However, the service letter does not answer the airline request

for an acceptable dye level which would avoid airport shutdowns. Being a high temperature problem, that answer has to come from the engine companies.

One engine company, General Electric, has conducted a 12 hour accelerated cycle test program with a CF6-80C2 engine and Jet A fuel containing 5% of the minimum IRS dosage of red dye or 0.80 mg of liquid dye per liter[16]. The thermal stability of this fuel by JFTOT exceeded the specification minimum by 30°C. The 12 hour program was followed by 44 hours of engine running on neat fuel to calibrate the test stands. Nozzle performance was checked at the beginning and the end of the dyed fuel testing for 15 of the 30 engine nozzles. Also at the end of the 44 hour test the same 15 nozzles were exercised on the flow stand and reevaluated. Out of the 15 fuel nozzles, 5 showed no degradation at the test's end, 6 were affected during the program but returned to normal performance after 44 hours on neat fuel, two were affected but showed only partial recovery and two nozzles did not recover original performance. In each case only the secondary flow schedule was affected and this at the point where the secondary nozzle flow started. It was, therefore, concluded that the dye was starting to cause deposits to form on the wall of the secondary orifice slot. These results are expected to play a major part in determining any decision regarding emergency operation.

Future Actions

Apart from eliminating the dyeing of certain diesel fuels, an extremely unlikely scenario, the development of an acceptable dye level for continuous engine use appears to be at least a partial solution. The Southwest Research Institute has proposed a program to develop such a dye limit. Each major engine manufacturer would select a critical fuel injector nozzle. As the hottest component in the engine fuel system, nozzles tend to be the most sensitive part of the fuel system. Four different nozzle feed arm and nozzle bodies would be subjected to heated air flow to duplicate severe engine conditions. These nozzles are identified in Table 5. Fuel would pass through the nozzles once and would not be burned. New nozzles would be used for each test run and every nozzle would be run in duplicate. Test variables would include air temperature, initial fuel temperature (fuel preheating), fuel quality and dye contamination levels in the presence and absence of diesel fuel. Nozzle condition would be checked by monitoring flow rate and pressure drop. Fouling life would be defined as the time required to obtain a 10% decrease in flow rate. Based on test results from each engine manufacturer's nozzles, a mutually acceptable maximum dye concentration would

be agreed upon. Consideration is also being given to the inclusion of servo valves from engine fuel controls as another sensitive engine component.

An important part of the program would be an extensive evaluation of a number of high temperature laboratory test procedures. The procedures are to include the JFTOT, the Shell HiRenTS test and the Southwest Institute Short-Tube, High-Heat-Flux Deposition Rig. In addition the JFTOT tube deposits will be rated by at least two different procedures. A comparison of these test results with the nozzle fouling results should lead to the validation of one or more of the tests which could then serve as a future high temperature screening test or possibly even a specification requirement.

Fuel handling organizations will have to continue to tighten their procedures to avoid any dye contamination of jet fuel. If contamination is found, a quantitative device should be used to accept or reject the fuel, a more acceptable approach than exists today.

Altogether the dye contamination problem has once again highlighted the need for constant attention to quality control in the handling of aviation turbine fuels.

Acknowledgements

The release of the CRC data cited above is greatly appreciated, but it should be emphasized that the comments, observations and conclusions in the paper represent only the author's own opinion and not those of any other organization or individual.

References

(1) Federal Register/ Vol. 54/ pp 35276 & following/ August 21, 1990,

(2) Federal Register/ Vol. 58, No. 228/ pp 63069 - 63080/ Nov. 30, 1993

(3) Dept. of the Treasury, IRS, 26 CFR Part 48, RIN 1545-AP48; 1545-AS32, Diesel Fuel Excise Tax; Dye Color and Concentration; Final Regulation

(4) Environmental Protection Agency, 40 CFR Part 80, Regulation of Fuels and Fuel Additives; Fuel Quality Regulations for Highway Diesel Fuel sold in 1993 and Later Calendar Years, Interim Final Rule, July 5, 1994

(5) Boeing Service Letter, dated 29 August 1994

(6) All Operator Letter by McDonnell Douglas, subject: Aircraft Use of Dyed Fuels, dated 23 August 1994

(7) Letter of W. F. Taylor to Margaret M. Richardson, IRS Commissioner, of June 23, 1993

(8) Unpublished CRC data of December 6, 1994

(9) Douglas Aircraft Company, Materials and Process Technology Laboratory Report No. 18112, dated 4/19/96

(10) Unpublished CRC data of 10/26/1994

(11) Unpublished CRC data of 10/11/95

(12) Unpublished CRC data of 4/26/95

(13) R. Waite, ed. *ASTM Manual MNL 5*, second edition, American Society of Testing and Materials, Philadelphia, PA, June 1995, pp. 1-2.

(14) Unpublished CRC data of 6/25/96

(15) Boeing Service Letter, dated 22 November 1996 (amending Service Letter of 29 August 1994)

(16) Unpublished CRC data of 6/25/96 and 12/10/96

Table 1

Membership of CRC Group on Dye in Aviation Turbine Fuel

K. H. Strauss, leader	Consultant
R. D. Anderson	Facet International
F. Barnes	Chevron Products
Y. Barshad	Applied Analytics
T. B. Biddle	Pratt & Whitney Aircraft
G. J. Bishop	Shell International Petroleum
K. Bower	Defence Research Agency (MOD)
J. E. Brown	Colonial Pipeline
S. Bullock	Rolls Royce
J. C. Callison	Amoco Oil
S. E. Casper	United Airlines
P. David	BP Oil International
W. G. Dukek	Consultant
W. L. Easton	Federal Aviation Administration
D. A. Fabry	Ashland Petroleum
H. Gammon	Gammon Technical Products
R. M. Garrett	Exxon Company USA
R. L. Gray	Defense Fuel Supply Center
O. J. Hadaller	Boeing Commercial Airplane Group
D. Hardy	Naval Research Laboratory
C. P. Henry	Octel America
A. Holden	British Airways
D. H. Hoskin	Mobil Technology
C. Tsao-Chin Huang	Pennzoil Products
R. Kamin	Naval Air Warfare Center
J. Kuebrich	Arco Products
R. Leisenring Jr.	Texaco
P. Liberio	U S Air Force
R. P. Lohmann	Pratt & Whitney Aircraft
J. E. McGettrick	Arco Products
S. McLemore	Delta Air Lines
J. W. Muzatko	Chevron Products
R. J. Organ	Caltex Petroleum
K. Polk	Hammonds
S. Seto	GE Aircraft Engines
W. Spitzley	Total Petroleum
C. Taucher	American Airlines
W. F. Taylor	Exxon Research & Engineering

Table 1 (continued)

Membership of CRC Group on Dye in Aviation Turbine Fuel

R. D. Tharby	Consultant
M. Thom	Allied Signal Aerospace
R. G. Thompson	Phillips 66
B. Visser	Shell Oil Products
R. Waite	Velcon Filters
G. Wendtland	Buckeye Pipeline
G. Wilson	Varlen instruments

Table 2

RED DYE CONCENTRATIONS IN DIESEL FUEL

Active Ingredient Basis

Percent of required red dye in non-taxed diesel fuel	Solid*	Liquid**	Solid*	Liquid**
	Lbs/1000 Bbls		mg/Liter	
100% (minimum IRS dosage)	3.9	5.6	**11.1**	16.0
50%	1.95	2.8	**5.55**	8.0
20%	0.78	1.12	**2.22**	3.2
10%	0.39	0.56	**1.11**	1.6
2.5%	***0.098***	***0.14***	***0.28***	***0.40***
2.0%	0.078	0.11	**0.22**	0.32
1.0%	0.039	0.056	**0.11**	0.16
0.5%	***0.019***	***0.028***	***0.055***	***0.08***

* Solid Red Dye SR 26 (active ingredient)

** Liquid Red Dye (estimated active ingredient)

Table 3

Elastomer Tests with Red Dye

	Dye Dosage	Effect
Airframe Materials[10]		
Sealant: DMS 2082, PR 1422 B-2	0, 0.08, 0.4, 0.8mg/L	none on adhesion to primer
Elastomers		
DPM 3710-70, MIL-R-6855, Class 1	same	none on hardness or volume change
DPM 3713-1, MIL-R-83248, Type 2, Class 1	same	none on hardness or volume change
DPM 3717, MIL-R-25988, Class 1, Grade 60	same	none on hardness or volume change
Fuel bladder: BTC 101	same	none on tensile strength or elongation
Tank coating: DMS 1580, composition A and C	same	none on adhesion or film hardness
Engine Materials[11]		
-113 O-rings	0, 16 ppm	
Nitrile		none on swell or embrittlement
Silicone		none on swell or embrittlement
Fluorocarbon		none on swell or embrittlement
Fluorosilicone		none on swell or embrittlement

Table 4
Thermal Stability Effects with Red Dye
Break Points by Alcor JFTOT, °C

Laboratory-Fuel No.	Liquid Dye Dosage 0mg/L	16.0 mg/L*	1.6 mg/L**
A-1	360	270 (-90)	285 (-75)
B-1	375	335 (-40)	375 (0)
C-1	350	350	-
D-1	295	300 (+5)	-
D-2	295	295	-
E-1	290	265 (-25)	280 (-10)
E-2	265	**245 (-20)**	**250 (-15)**
F-1	290	280 (-10)	285 (-5)
G-1#	282	280 (-2)	-
H-1	295	285 (-10)	285 (-10)
H-2	315	320 (+5)	-
I-1	300	285 (-15)	300 (0)
I-2	290	275 (-15)	280 (-10)
J-1#	293	293 (0)	-
J-2#	293	293 (0)	
J-3#	293	293 (0)	-
J-4#	274	274 (0)	-
J-5#	274	268 (-6)	-
J-6#	274	282 (+8)	-
J-7#	304	293 (-11)	-
J-8#	277	268 (-9)	-
J-9#	268	260 (-8)	-
K-1	285	280 (-5)	-
K-2	290	285 (-5)	-
K-3	295	290 (-5)	-
K-4	290	290 (0)	-
K-5	**250**	**250 (0)**	-
K-6	**255**	**255 (0)**	-
K-7	260	260 (0)	-
K-8	265	**255 (-10)**	-

* Minimum IRS dosage for tax-free diesel fuel
** 10% of minimum IRS dosage
Run at 5°F intervals

Notes: Numbers in parentheses indicate change in breakpoint after dye addition.
Bold numbers indicate breakpoints below 260°C.

Table 5

Thermal Stability Effects with Reduced Red Dye Levels

Break Points, °C

Laboratory-Fuel No.	Liquid Dye Concentration 0 mg/L	16.0 mg/L*	1.6 mg/L**	0.40 mg/l#	0.16 mg/L##
A-2	290	-	**250 (-40)**	**250 (-40)**	285 (-5)
C-1	350	-	-	350 (0)	350 (0)
C-2	270	-	-	260 (-10)	260 (-10)
E-3	275	**250 (-25)**	265 (-10)	270 (-5)	-
E-4	265	**245 (-20)**	**250 (-15)**	260 (-5)	-
F-2	295	-	-	290 (-5)	290 (-5)
H-3	285	-	-	280 (-5)	285 (0)
H-4	275[a]	-	-	290 (+15)	285 (+10)

* Minimum IRS dosage for tax-free diesel fuel

** 10% of minimum IRS dosage

2.5% of minimum IRS dosage

1% of minimum IRS dosage

[a] Possible reporting error

Notes: Numbers in parentheses indicate change in breakpoint after dye addition.

Bold numbers indicate breakpoints below 260°C.

6th International Conference
on Stability and Handling of Liquid Fuels
Vancouver, B.C., Canada
October 13-17, 1997

IMPACT OF CAUSTIC TREATING ON THE FILTERABILITY OF JET FUEL

Lawrence D. Palmer*[1], Kristina M. O'Callaghan[2], and Brian C. Springthorpe[1].

[1]Ampol Refineries (Q'land) Ltd, P.O. Box 40, Wynnum Central, Qld 4178, Australia;
[2]Chemistry Department, Queensland University of Technology, GPO Box 2434, Brisbane, Qld 4001, Australia.

ABSTRACT

Demand for jet fuel in Australia continues to increase, and refiners are seeking low-cost means of expanding their production capability. An existing caustic treater may be undersized and act as a production bottleneck. When the caustic treater is limited by flow rate and the jet fuel has minimal acidity, caustic treatment of only a part of the jet fuel is an attractive option. An Australian refinery performed refinery trials with the aim of proving that this approach could increase its jet fuel production. Filterability of jet fuel was severely affected, and electrical conductivity became more sensitive to light-induced decay. The filterability problems were caused by traces of sodium and calcium naphthenates in the fuel. A filter blocking tendency test was developed, and became an essential tool for developing a modified processing scheme which now produces 50% more jet fuel. During refinery trials, the filterability test minimised filtration problems at distribution terminals and airports, and it continues to serve a useful quality control role. Salt driers, located between the caustic treater and refinery storage tanks, acted as reservoirs for the filter blocking agent, which was released intermittently into jet fuel. Complete segregation of one of the salt driers from the caustic treater provided a simple means of eliminating the filterability problem.

INTRODUCTION

Demands for transport fuels in Australia continue to increase steadily, with jet fuel experiencing the highest percentage growth. Consequently, Ampol's Brisbane refinery has increased its crude oil distillation capacity by 40% during the past decade. By the mid-1990s, the flow rate of kerosine (unfinished Jet A-1) from the crude distillation units exceeded the capacity of the Jet A-1 caustic treating unit. The caustic treater, which removes traces of organic acids from kerosine to produce Jet A-1, therefore imposed a bottlenecking limit on jet fuel production. A new caustic treater would have required capital expenditure of several million dollars, so a team of engineers and chemists took up the challenge of finding a low-cost means of increasing the refinery's jet fuel production.

Although the prime function of the caustic treater is removal of traces of organic acids, the Jet A-1 acidity specification (< 0.015 mg KOH/g by ASTM D3242) was not limiting the maximum possible flow rate through the caustic treater. Instead, this limit was set by residence time considerations in the caustic settling vessel. Jet fuel flow rates exceeding the limit did not provide enough time for effective separation of the water and hydrocarbon liquid phases. At high jet fuel flow rates, traces of naphthenic acid salts from the caustic treating process could contaminate the treated jet fuel and downstream vessels and tanks, instead of remaining in the waste water phase.

Bypassing some of the kerosine stream around the caustic treater was suggested as a simple means of overcoming the bottleneck. Jet A-1 production would then be a mixture of say 70% caustic treated and 30% untreated jet, with the 30% bypass stream representing increased production. While appealingly simple in concept, implementation of this strategy was difficult, because of unforeseen effects on filterability and electrical conductivity.

JET FUEL PRODUCTION AND SPECIFICATIONS

Figure 1(a) shows the process scheme used for production of Jet A-1 at Ampol's Brisbane refinery prior to implementation of the process changes described in this paper. Figure 1(b) shows the current, improved process scheme. In the original scheme, kerosine rundown from two crude oil distillation units was combined and fed to a caustic treater/settler, followed by a water washing/settling vessel. Hazy (wet) jet fuel from the water wash was split into two streams and directed to two salt driers in parallel. Conductivity additive was injected after the salt driers, and finished jet fuel was directed to refinery tankage. Both the previous and the revised processing schemes are relatively simple, and do not include hydrodesulfurisation, Merox treatment for mercaptan removal, or clay filtration for removal of surfactants.

Ampol's Brisbane refinery is constrained to process only low sulfur crude oils. This has two consequences for jet fuel acidity. First, the average acidity of the kerosine fraction *prior to* caustic treating is 0.011 mg KOH/g, comfortably below the specification limit of 0.015 mg KOH/g. Second, none of the usual crude oils processed has acidity which greatly exceeds the

average. Hence, there appeared to be scope for bypassing a substantial proportion of kerosine around the caustic treater (as much as 100%) on a virtually permanent basis.

Prior to proceeding to refinery trials, laboratory blends of caustic treated and untreated (bypass) jet fuel were prepared from two refinery crude slates. The first of these crude slates contained 80% of Gippsland crude oil, which up to the mid-1990s, had been the refinery's principal feedstock. The second crude slate contained 77% Kutubu crude, which became the refinery's principal feedstock in the mid-1990s. In addition to acidity, properties which may depend on caustic treatment - via more subtle chemical effects - were also tested. These included copper and silver corrosion (ASTM D130 and IP 227), water reaction (ASTM D1094), mercaptan sulfur (ASTM D3227) and microseparometer rating (ASTM D3948). The results are shown in Table 1. It was concluded that for these two cases, Jet A-1 could have been produced with no caustic treating (100% bypass of the caustic treater). Table 1 provided the basis for proceeding to refinery production trials. The refinery trials confirmed the conclusions made from Table 1, but revealed two unforeseen quality problems:

- severe filter blocking problems occurred in terminal and airport filter/separators, and

- electrical conductivity was rendered more susceptible to light-induced decay.

FILTERABILTY

Jet fuel specifications do not contain explicit filterability requirements. Instead, high filterability quality is ensured by the presence of filter/separators in the distribution chain [1]. Filter/separators contain coalescer cartridges, which have the dual function of (i) removing dirt, and (ii) coalescing fine particles of water so that they settle or are separated from jet fuel by downstream separator cartridges. Jet A-1 produced by Ampol's Brisbane refinery during caustic wash bypassing trials passed all required specification tests, but caused severe reduction in the life of coalescer cartridges in filter/separators in the distribution system. In the worst instance, costly coalescer cartridges had to be replaced after a jet fuel throughput of only about 0.5 ML. This is only a few per cent of the normal total throughput (20 - 30 ML) before replacement is required because of pressure drop considerations.

Following the first notification of filterability problems, one of the blocked coalescer cartridges (Facet CA 43-3) from a distribution terminal was cut open for examination. Visual inspection indicated that it was free of gross contamination. In fact, the critical glass fibre element appeared to be remarkably clean. However, examination under a microscope (x40) revealed a layer of greasy material of thickness about 100 μm embedded in the upstream surface of the glass fibre element, which has thickness of about 700 μm. Fourier transform infrared (FTIR) analysis of the greasy material gave strong peaks at 1575, 1539, 1112 and 720 cm^{-1}, characteristic of salts of naphthenic acids. When dried to remove water and jet fuel, the contaminant hardened to a grey/brown solid. Semi-quantitative x-ray analysis in a scanning electron microscope (JOEL JXA 840A electron probe microanalyser) showed high concentrations of calcium, together with substantial peaks for chlorine, magnesium, sulfur, potassium and sodium.

Very similar FTIR and electron probe microanalysis results were obtained for:

- light brown solids filtered from jet fuel with high filter blocking tendency, produced during subsequent refinery trials,

- solids recovered from emulsion material present in the water phase of the refinery's water wash vessel, and

- solids recovered from emulsions on the surface of the rock salt and its gravel support bed in the salt driers.

A further identifying characteristic of this material is its distinctive odour, which is particularly persistent after it comes into contact with human skin.

It was concluded that the filter blocking material was a mixture of jet fuel, water and:

- sodium naphthenates and phenolates, formed when sodium hydroxide reacted with naphthenic acids and phenols (constituents of crude oil) in the caustic treater;

- calcium and possibly magnesium naphthenates, formed in the caustic treater. Brisbane's hard town water, used for diluting the commercial-grade caustic soda used in the refinery process, was the source of the calcium and magnesium; and

- lesser concentrations of inorganic salts such as sodium chloride.

These naphthenic acid salts are extremely strong agents for blocking glass fibre filters, including coalescer cartridges. They appear to have a strong affinity for glass fibres, and are trapped as a greasy layer embedded among the fibres, near the upstream surface. During bypassing trials, concentrations as high as 12 mg/L of naphthenic acid salts were intermittently entrained in jet fuel, necessitating special filtration of the fuel prior to its release from the refinery. So potent are these salts that we estimate that their concentration has to be kept below 0.2 mg/L to guarantee acceptable life for coalescer cartridges.

Refinery trials and mechanisms of fuel contamination

After investigating the first reports of filterability problems, there was ample evidence to indicate that the filterability problems experienced in the distribution system were a direct consequence of the first refinery caustic treater bypassing trial. However, the detailed mechanism by which the contamination occurred was far from clear. The central idea of the bypassing strategy was to *reduce* the carryover of emulsions containing salts of naphthenic acids and phenols, by allowing a longer residence time for phase separation in the caustic settling and water wash vessels. The intention of the refinery was to bypass about 30% of the total jet fuel production around the caustic treater, enough to have a strong beneficial effect on separation of the water and hydrocarbon phases in the caustic-wash and water-wash vessels.

Over a nineteen month period ending in mid-1996, eight refinery trials were conducted to develop an understanding of the mechanism by which the filterability of jet fuel had been so badly affected during the initial trial. The fact that it took a total of eight trials is a true reflection of the frustration involved in studying trace-component chemical reactions on a refinery scale. For example, in laboratory experiments, chemists ensure that reaction vessels are clean prior to experiments, but this is impractical for refinery production trials. Also, in laboratory-scale experiments, it is not too difficult to ensure homogeniety of products and

intermediates. The caustic bypassing trials involved flow rates of jet fuel of up to 1300 t/day, with the possibility that the contaminant was being introduced into the jet fuel intermittently. Hence, even with intensive and extensive sampling, there was always some doubt about the accuracy of surveys of contaminant concentrations.

After the initial refinery trial, several mechanisms were proposed to explain the disappointing outcome. These formed the basis for future trials, from which new or refined mechanisms arose. Among the possible mechanisms considered were:

- Existing sediments in the refinery's jet fuel storage tanks (or perhaps in downstream terminal tanks) were "solubilised" by the partly caustic-treated jet fuel produced during the trials. It was known that emulsions containing naphthenic acid salts accumulate on the floors of refinery jet fuel tanks even in the absence of refinery trials, necessitating tank cleaning every two years. When downstream filterability problems were experienced after the bypassing trial, there was speculation that the subtle change in jet fuel acidity could be responsible for entraining traces of these sediments in the jet fuel during the tank mixing process.[1]

- Naphthenic acids in the untreated jet fuel were reacting with sodium chloride in the salt driers. This potential mechanism arose from a 1977 Chicago conference paper on fuel treating processes. It states that some crudes, *eg.* Trinidad, contain troublesome naphthenic acids in their straight-run middle distillates, and that problems arise from the formation of sodium naphthenate when contacted with sodium hydroxide during refinery treating, or when contacted with salt water during shipment.

- Existing sediments in the salt driers were being released into jet fuel by the bypassed jet fuel, either because of subtle changes in the overall acidity and/or surfactant properties of the jet fuel, or by introduction of a higher concentration of water[2] in the jet fuel entering the drier.

[1] Tank mixing to ensure homogeniety for quality certification is accomplished by 600 mm propellers rotating at 420 rpm, mounted on the tank wall near the tank floor. A slow movement of the entire tank of jet fuel is induced, but in the vicinity of the mixer, the movement of jet fuel is fast enough to move floor sediments.

[2] Kerosine (untreated jet fuel) from the crude distillation units contains about 1600 mg/kg of water from steam stripping to control flash point. The water concentration is reduced to about 400 mg/kg by passage through the caustic and water wash vessels. Bypassing therefore raises the concentration of water in jet fuel entering the driers.

- The most potent filter blocking species were the calcium and magnesium salts of the naphthenic acids, with sodium naphthenate being less of a problem. This led to speculation that relief from the filtration problems could be available by switching from town water to demineralised water for dilution of caustic soda.

- Contamination of jet fuel was occurring intermittently, and particularly when the water in the water wash vessel was dumped and renewed[3].

Development of a filter blocking tendency test

Development of a jet fuel filter blocking tendency test was essential for determining which of the proposed mechanisms were in fact occurring, and to maintain customer satisfaction with the quality of the jet fuel. Standard test method ASTM D2068 *Filter Blocking Tendency of Distillate Fuel Oils* was adapted in the following manner:

- The filter element is cut from a commercial Facet CA 43–3 coalescer cartridge, using just the finest porosity glass fibre membrane, with nominal porosity of 0.5 μm. A single cartridge provides enough filters for thousands of tests, enough to last a laboratory for many years. Selection of this filter membrane was attractive because it provided a direct comparison with the field coalescer cartridges which had been so strongly affected by small concentrations of naphthenates in jet fuel.

- A jet fuel flow rate of 60 mL/min for 10 minutes is used, compared with 20 mL/min for 15 minutes for ASTM D2068. This provides greater sensitivity for detection of fuel contaminants.

A numerical value is obtained for the filter blocking tendency (FBT) of the jet fuel sample by using the appropriate equation:

$$FBT = [1 + (P/105)^2]^{1/2}$$

[3] Water was changed three times each day. When fresh water is admitted to the vessel, the flow rate of jet fuel entering the salt drier increases substantially.

where P (kPa) is the final pressure recorded after passage of 600 mL of jet fuel, or

$$FBT = [1 + (600 / V)^2]^{1/2}$$

where V is the volume recorded in cases when the pressure reaches 105 kPa prior to passage of 600 mL of fuel.

Table 2 shows the classifications for jet fuel filterability quality. This classification system was developed by direct correlation (Figure 2) of the total throughputs that were achieved through the field filter/separator between Ampol's Brisbane refinery and its products distribution terminal. It can be seen that jet fuel with an FBT rating of 1.002 - 1.003, which is the typical normal high quality, will allow the coalescer to pass more than 30 ML of jet fuel before replacement is required. On the other hand, if fuel of marginal quality (FBT = 1.005) passes through the coalescer, cartridges will have to be replaced after only about 10 ML of fuel has passed. Hence, this small increase from 1.002 to 1.005 in filter blocking tendency will increase the total cost of coalescer cartridges consumed by a factor of three.

Also shown in Figure 2 are the results of laboratory runs through the FBT test apparatus, in which we simulated a field filter/separator running until the differential pressure rose to 105 kPa, the pressure at which new cartridges must be introduced. These tests required the laboratory rig to be run for long times, especially for higher quality jet fuel. The simulated throughput for a commercial cartridge was calculated by scaling-up the laboratory throughput by a factor corresponding to the ratio of surface areas of the commercial coalescer cartridges and the laboratory filter. It can be seen that this predicts a shorter life (lower throughput) for coalescer cartridges than is actually obtained in field units. This serves to highlight the importance of directly correlating laboratory data against field experience when developing laboratory tests for fuel quality.

Benefits and conclusions derived from the filter blocking tendency test

The jet fuel filter blocking tendency test was progressively refined and used intensively during the eight refinery trials. This eventually led to a successful introduction of the caustic treating bypassing strategy and a 50 % increase in the refinery's jet fuel production capability. It

required only a very modest capital investment when compared with the cost of a new caustic treating plant.

The following conclusions were reached with respect to the proposed mechanisms discussed above:

- Filter blocking naphthenates residing in the salt driers were a particularly significant cause of the poor filterability of jet fuel produced during trials 2 through 7. In early trials, it was assumed that the poor jet filterability was caused by release of naphthenates distributed throughout the salt beds. When filterability problems persisted even after a trial with fresh salt and complete bypass of the caustic treater, it became apparent that there was a reservoir of naphthenates in the gravel distributing layer which supports the salt bed. During early trials, the gravel support layer had been assumed to be free of contaminants after being washed by an overhead fire hose for several hours. Inspections during preparations for a later trial revealed that this washing procedure was ineffective, apart from cleaning the surfaces directly exposed to the fire hose water.

- Contamination of jet fuel by release of naphthenates resident in the salt driers was induced mainly by the higher water content of the jet fuel entering the salt drier, rather than by subtle changes in the acidity of the jet fuel caused by partially bypassing the caustic treater.

- Sudden changes in the flow rate of jet fuel through the salt driers may release stationary deposits of naphthenates from the salt driers, resulting in short periods of grossly naphthenate-contaminated jet fuel being passed to refinery storage tanks. Fast changes of the water in the water wash vessel can cause such upsets. For water wash systems which do not have continuous withdrawal of dirty water and clean water makeup, it is preferable to decrease the water change-out frequency, and allow the wash water to become more contaminated with naphthenates.

- Naphthenic acids in jet fuel do not react with sodium chloride to yield filter blocking naphthenates.

- Sodium naphthenates are extremely potent filter blocking agents. While introduction of demineralised water for caustic dilution and water washing may have had some impact by eliminating calcium and magnesium naphthenates from jet fuel, jet fuel filterability was still severely degraded whenever it contained even trace concentrations of sodium naphthenates.

Complete segregation of one of the salt driers from the caustic-treated jet fuel stream [Figure 1(b)] provided a simple means of keeping it free of filter blocking naphthenates. At the same time, this segregation sends lower flow rates through the salt drier serving the caustic treated stream of jet fuel, thereby minimising contamination of this stream by naphthenates.

Current refinery procedure, implemented as a result of this study, is to measure the filter blocking tendency of all batches of jet fuel prior to release. Following testing, the appropriate response from Table 2 for non-bottom tank samples is enacted. There is also a classification system for dead-bottom tank samples, which is used for three-monthly surveys of jet tank cleanliness.

To be acceptable for release from the refinery, jet fuel should have a filter blocking tendency below 1.005. This corresponds to a very small but easily measured increase in the pressure differential across the test filter as a consequence of passing the 600 mL test sample through the filter. It is interesting to note that a common benchmark for acceptable filter blocking tendency of automotive diesel fuel is <1.4 by ASTM D2068. This highlights the extremely high filtration quality required of jet fuel.

ELECTRICAL CONDUCTIVITY

An operational quality control problem was observed during the first bypassing trial. With 30% of jet fuel bypassing the caustic treater, jet fuel electrical conductivity became much more sensitive to light-induced decay. To control conductivity within the specification range of 50 to 450 pS/m, the normal refinery practice was to take daily samples of the finished jet fuel stream going to refinery tankage, and also a tank average sample from the tank being filled. These samples were taken by refinery operators in clear glass bottles (poor practice), which typically stood in direct sunlight on a sample rack for an hour or so before collection by

laboratory analysts. Because of the sunlight-induced conductivity decay, the laboratory reported low conductivity results, and the refinery operators responded by increasing the concentration of Stadis 450 conductivity additive being injected into the jet fuel stream to tankage. Sampling for certification of the filled tank was done by the laboratory analysts, with the jet fuel receiving minimal exposure to sunlight. As a result of the extra additive dosing, conductivity of these samples exceeded the allowed upper limit of 450 pS/m.

Figure 3 shows the results of laboratory experiments in which jet fuel was dosed with conductivity additive in a 20 L steel drum, a 2.5 L brown glass bottle, and in normal one litre refinery sample bottles. For the normal bottles, experiments were conducted for the bottles (i) as received, (ii) as received but externally covered with aluminium foil, (iii) pre-rinsed with isopropyl alcohol according to ASTM D2624 to eliminate any water, and (iv) washed with methanol then dried at 160°C for an hour. All samples stood on a laboratory bench under typical fluorescent lighting for 20 h, after which the three unprotected clear bottles were exposed to 30 min of diffuse sunlight. After a further 30 minutes to allow the samples to re-equilibrate to laboratory temperature, conductivities were measured. At the 24 h point, the aluminium foil was removed from the two foil-covered bottles, and these samples (and some other samples) were exposed to diffuse sunlight for two periods of 15 minutes. The following conclusions are evident from Figure 3:

- Both fully caustic-washed jet fuel and jet fuel produced with 30% bypass of the caustic treater were prone to sunlight-induced conductivity decay.

- Jet fuel produced with 30% bypass of the caustic treater was particularly sensitive to sunlight-induced conductivity decay. More than half of the conductivity was destroyed by sunlight exposure for 30 minutes.

- Provided jet fuel is not exposed to light, jet fuel produced with 30% bypass of the caustic treater has stable electrical conductivity following dosing with conductivity additives.

Changing from glass to metal sample containers provided a simple solution, with only minor inconvenience.

CONCLUSION

By developing an understanding of the mechanisms involved in the formation of naphthenic acid salts, and their entrainment in jet fuel, a modified process scheme for jet fuel production was introduced at Ampol's Brisbane refinery in late 1996. The most important modification was the complete segregation of one of the two salt driers from the caustic treater. This ensures that the salt drier receiving untreated jet fuel remains completely free of naphthenic acid salts, and thereby eliminates the possibility that filter blocking contaminants can be released into jet fuel by causes such as high flow rates or high water content of jet fuel. Jet fuel production capacity was increased by 50% by introduction of the modified processing scheme, with a low capital investment.

This study has highlighted the extreme potency of naphthenic acid salts for causing blockage of coalescer cartridges in the jet fuel distribution system. It also shows that departures from recommended practices - in this case those listed in ASTM D2624 and ASM D4306 for conductivity sampling - are counterproductive.

While carryover of naphthenic acid salts with jet fuel as it moves from caustic treaters through process units such as salt driers can be minimised, it is probably inevitable that traces of filter blocking naphthenates will accumulate in jet fuel storage tanks. Even with the improvements made as a result of this study, it is likely that coalescer cartridge life in downstream filter/separators is still limited by extremely small concentrations of naphthenic acid salts. If so, the cost of manufacturing and distributing jet fuel could be decreased by eliminating the caustic treating process whenever permitted by jet fuel acidity requirements. Of course, other jet fuel properties, *eg.* thermal stability, would have to carefully assessed, but our experience suggests that it would be better to leave low concentrations of organic acids and phenols in jet fuel, rather than converting them to filter blocking salts, which are difficult to completely remove by water washing. In their unreacted acidic form, they present no filtration problems, and are simply burnt in jet engines along with bulk jet fuel.

REFERENCE

1. API Publication 1581 (1989). "Specifications and Qualification Procedures for Aviation Jet Fuel Filter/ Separators", third edition.

Table 1 Properties of laboratory blends of caustic treated and untreated (bypass) jet fuel

	Specification limit	Caustic treater bypass (Gippsland)			Treater bypass (Kutubu)
		0%	20%	100%	100%
Acidity, mg KOH/g	0.015 max	0.0010	0.0014	0.013	0.011
Copper corrosion, 2 h at 100°C	1 max	1a	1a	1a	1a
Silver corrosion, 4 h at 50°C	2 max	0	0	0	0
Separometer rating (MSEP-A)	70 min	84	99	99	94
Water reaction	1b(2)	-	1(1)	1(1)	1(1)
Mercaptans, mg/kg	30	9	9	9	3

Table 2 Classification of jet fuel by the Ampol jet fuel filter blocking tendency (FBT) test

Non-bottom tank samples

FBT	Rating	Response
1.002 - 1.003	Typical quality	Release to off-takers
<1.004	Acceptable quality	Release to off-takers
1.004 - 1.005	Marginal quality	Can be released, subject to off-taker sensitivity and recent history
1.005 - 1.01	Major filtration problem	Consider settling, filtration, segregation for Ampol Terminal

Dead-bottom tank samples

FBT	Rating	Response
<1.10	Acceptable	No action required
1.10 - 1.50	Major tank contamination	Monitor FBT of dead-bottom samples for each jet batch
>1.5	Extreme tank contamination	Consider tank cleaning

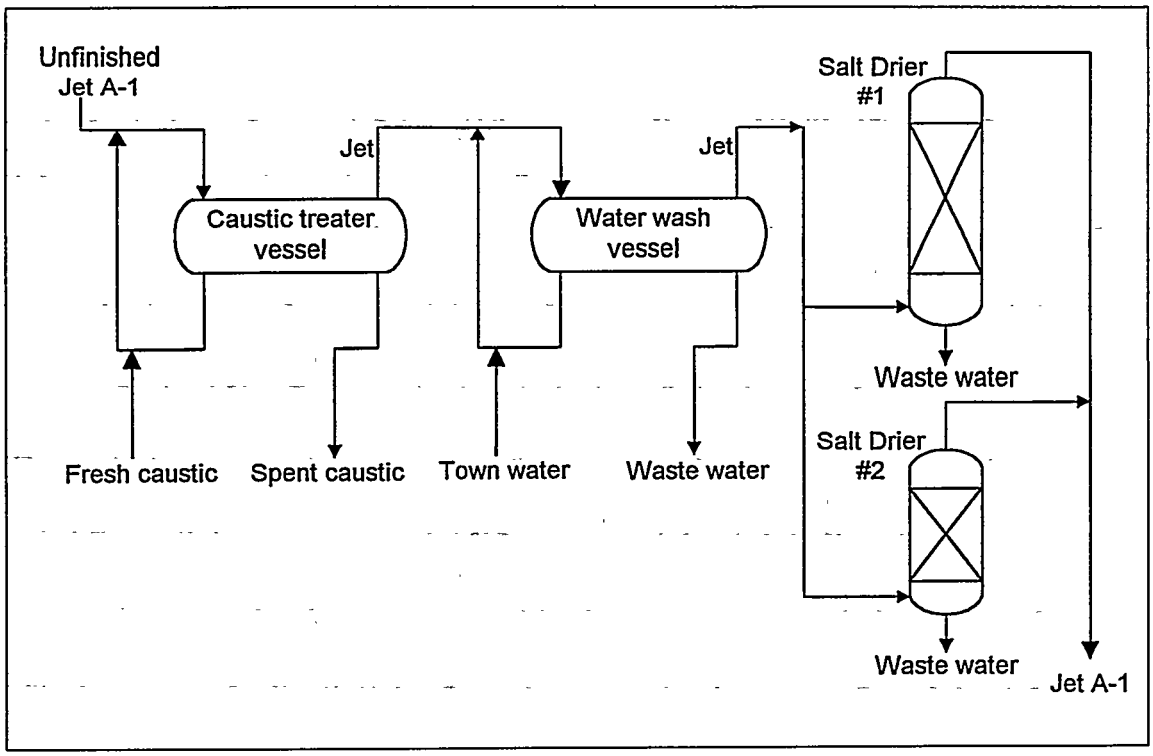


Figure 1 (a). Caustic treating and salt drying prior to introducing the bypass strategy.

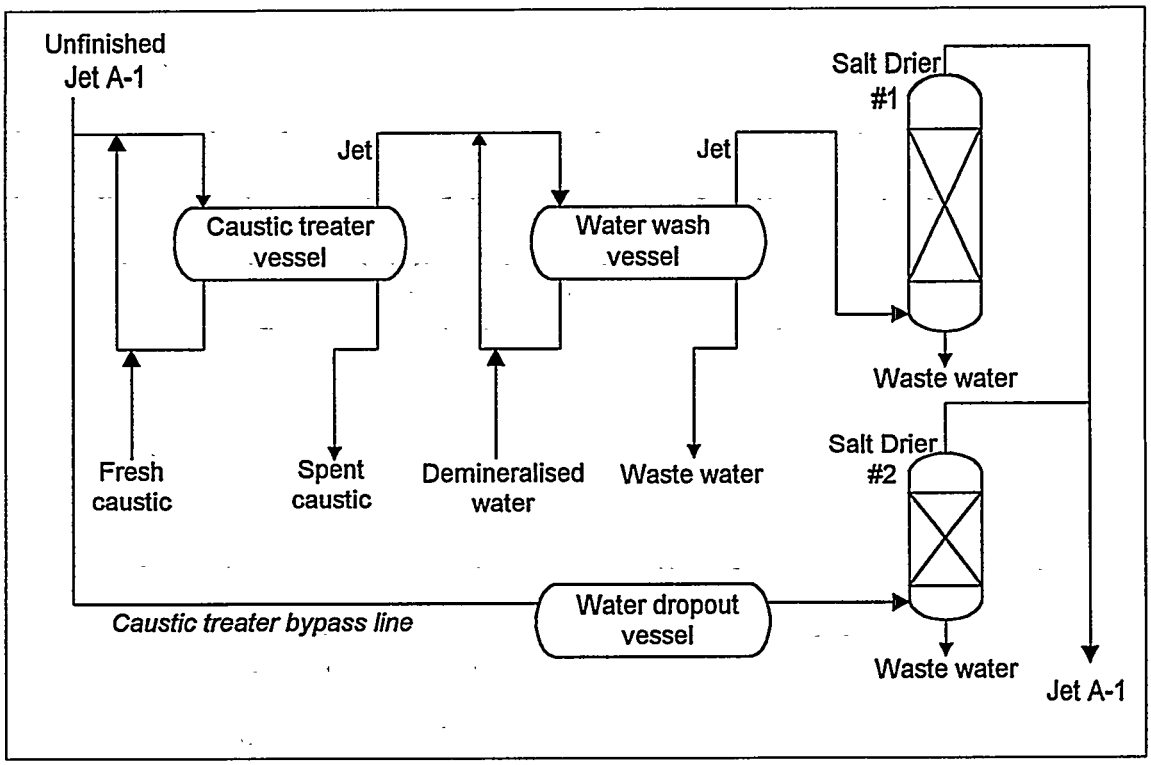


Figure 1 (b). The current caustic treating and salt drying process, with one drier completely segregated from the caustic system.

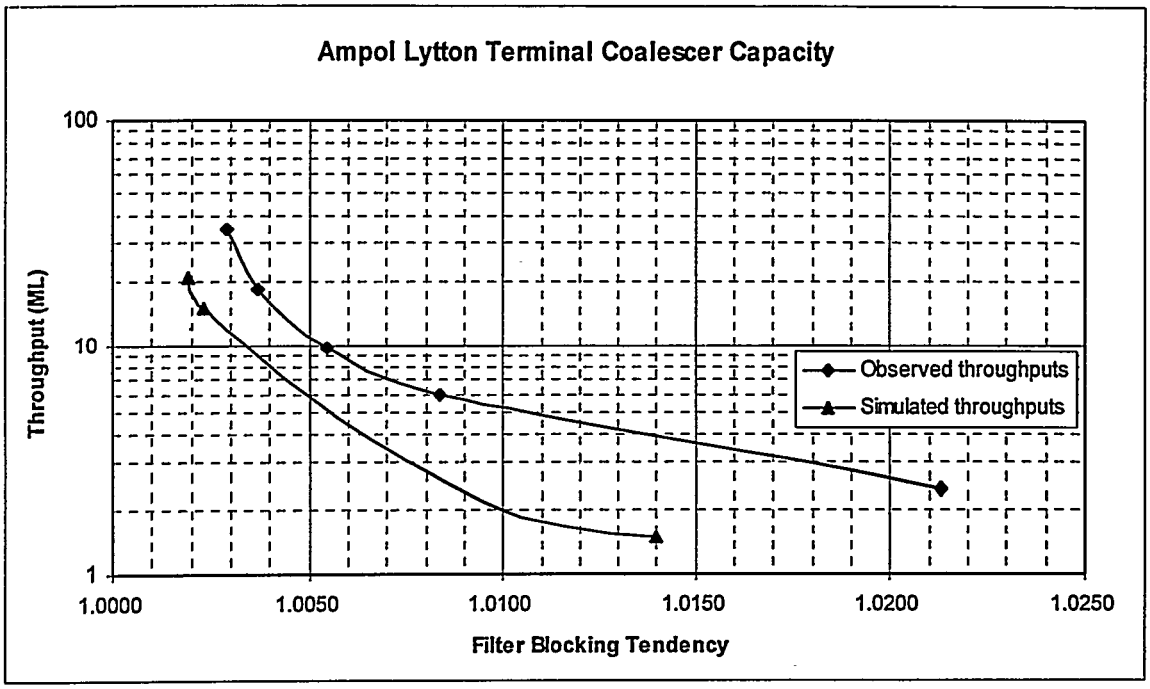


Figure 2 Limiting throughput of jet fuel through 0.5 micron coalescer cartridges as a function of jet fuel filter blocking tendency.

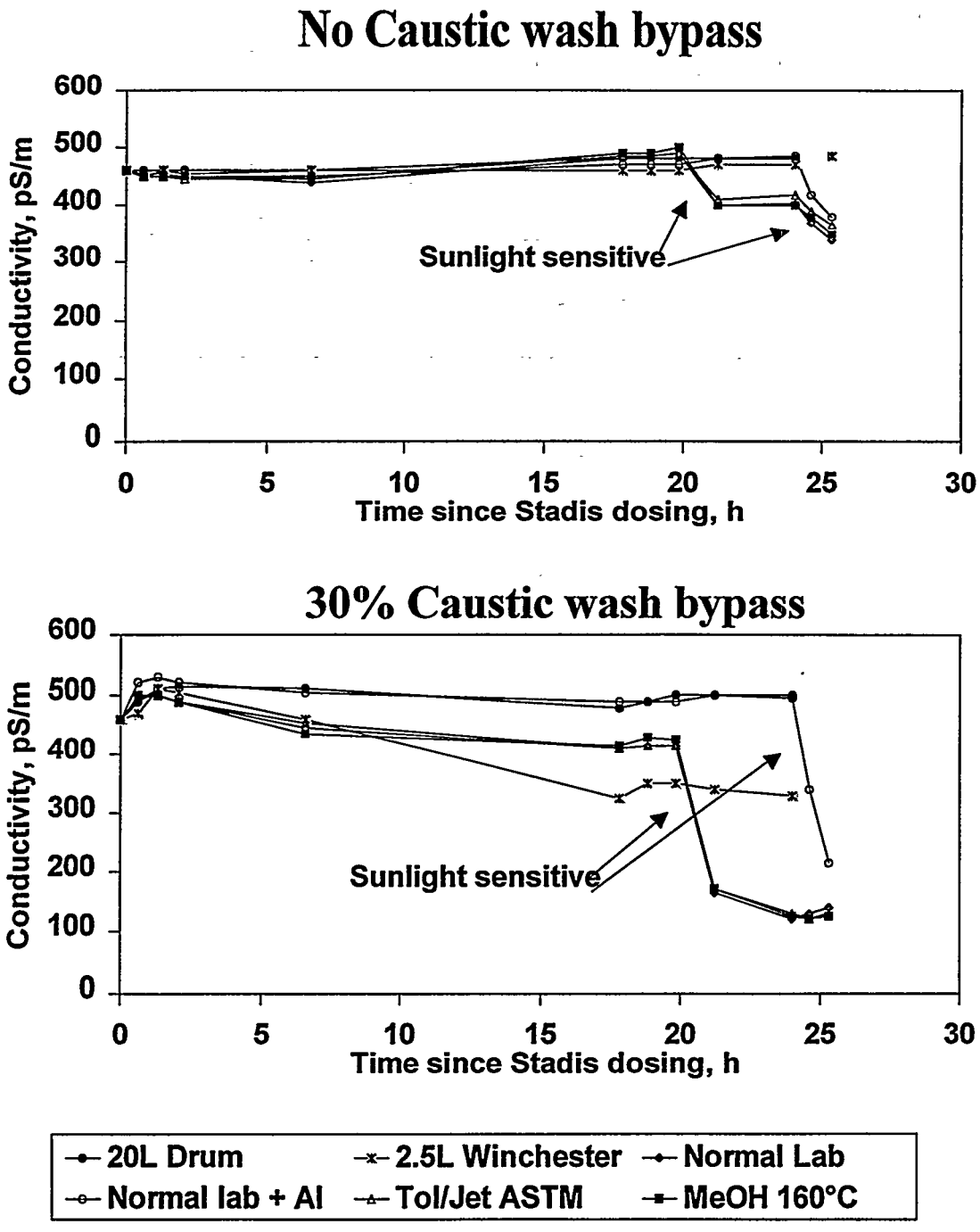


Figure 3. Conductivity changes for caustic treated jet fuel (top) and partially treated jet fuel (bottom).

6th International Conference
on Stability and Handling of Liquid Fuels
Vancouver, B. C., Canada
October 13-17, 1997

MEASUREMENT OF DISSOLVED AND TOTAL WATER CONTENT IN ADVANCED TURBINE ENGINE FUELS WITH A GAS-LIQUID CHROMATOGRAPHIC OTC TECHNIQUE

Steven D. Anderson[1], Wayne A. Rubey*[2], and Richard C. Striebich[2]

[1]Wright Laboratories, POSF, 1790 Loop Road North, Wright-Patterson AFB, OH 45433-7103.
[2]Environmental Sciences and Engineering Laboratory, Research Institute, University of Dayton, 300 College Park, Dayton, OH 45469-0132.

ABSTRACT

Significant capabilities have been developed over the past quarter century for detecting extremely trace quantities of organic compounds in water. However, accurate and precise analyses for water in complex organic mixtures continues to be an analytical challenge. Water is omnipresent and a thin film of adsorbed moisture usually coats every type particle and surface. The analysis for water content in a complex turbine engine fuel is complicated by water sorption onto fine particulate matter and also the presence of numerous fuel additives, e.g., corrosion inhibitors, fuel system icing inhibitors, static dissipators, metal deactivators, detergents, dispersants, etc. Many of these additives affect the interfacial surface tension and the water coalescing properties of the bulk fuel. Instrumental approaches for measuring water content in complex organic mixtures include titration techniques, optical spectroscopy, humidity sensing devices, diode lasers, light emitting diodes, liquid chromatography, and gas chromatography. There has been a real need for a laboratory technique that can provide appropriate water content measurements for turbine engine fuels which contain extensive additive packages. Accordingly, we pursued the gas chromatographic approach for measuring dissolved and free water. Initially, a reaction gas chromatography (RGC) technique was investigated in which water was converted to acetylene by way of a temperature controlled calcium carbide reactor. Although this RGC procedure exhibited considerable sensitivity via detecting water as acetylene using hydrogen flame ionization detection, significant irreproducibility was encountered. Accordingly, various gas-solid chromatographic (GSC) and gas-liquid chromatographic (GLC) scenarios were investigated. It was found that when a modified high-temperature splitter injector assembly is used in conjunction with a highly deactivated and low β value GLC open tubular column, that water can be well-behaved (symmetrical zone profile) and separated from other constituents. Measurement of water content in a variety of turbine engine fuels while using a modulating thermal conductivity detector was found to be both precise and sensitive, even into the sub-ppm region. Using standard addition procedures along with an internal standard, it is anticipated that this GLC analytical method can be simplified for eventual field-scale testing.

INTRODUCTION

Many analytical techniques have been developed for measuring trace levels of organic substances *in water*. Some of these instrumental procedures can measure certain organic constituents at the sub part-per-trillion level.[1,2] The situation is significantly different for measuring *water in* an organic mixture, as analytical techniques only have measurement capabilities down to the low ppm or high ppb measurement regions. Much of this difference in analytical capability is due to ease of contamination and the difficulty in quantitatively transporting trace quantities of water, particularly in various chromatographic scenarios.

With respect to advanced turbine engine fuels, dissolved and total water content represent important information with respect to transferring and refueling aircraft under a severe range of atmospheric conditions. There are many additives in advanced turbine engine fuels which can adversely affect the interfacial tension and the water coalescing properties of the bulk hydrocarbon fuel. They can also form emulsions or micelles as depicted in Figure 1. Example additives are fuel system icing inhibitors, static dissipators, metal deactivators, detergents, corrosion inhibitors/lubricant improvers, dispersants, etc. There has been a pressing need for a laboratory technique that can provide appropriate dissolved and total contained water measurements for turbine engine fuels, along with other complex organic mixtures which contain extensive additive packages.

Background. Under our earthly atmospheric conditions, water is omnipresent. Accordingly, precise measurement of water content is complicated by the physical and chemical nature of the various materials. A thin film of adsorbed moisture usually coats every type of particle and surface. In addition, water is present as a dissolved or dispersed contaminant in practically every organic mixture sample. Consequently, accurate measurement of low concentrations of water in an organic matrix needs to be accomplished with a minimum of atmospheric exposure, sample transfer, and further contamination.

There are a variety of instrumental techniques for measuring water in specific samples. However, an urgent need exists for a general technique which can address a wide range of organic matrices and particularly samples which contain fine particulate matter, assorted additives, and other interfering materials. The Karl Fischer titration procedure[3] has long been used for analyses where water can be liberated and reacted. Also, a variety of spectroscopy

procedures have found wide acceptance when water can be truly isolated from related materials, such as, alcohols, ketones, etc. A gas chromatographic technique was desired which could rapidly separate and detect low ppm concentrations of water in advanced turbine engine fuels. Initially, a precise laboratory procedure was desired in support of fuel research activities for high-performance aircraft. However, a field-portable unit would also be advantageous for monitoring fuel status at flight line facilities.

INSTRUMENTAL APPROACH

For several decades, ppm levels of water have been measured with a reaction gas chromatographic (RGC) procedure. Our laboratory and other research facilities have had considerable success measuring low levels of water using RGC techniques whereby water vapor is passed through a heated calcium carbide reactor.[4] This quantitatively converts the highly adsorbed water to acetylene which is thereafter readily transported and detected by a hydrogen flame ionization detector. High ppb levels of water in jet fuel can be measured using such a procedure. Even so, as the block diagram of the RGC system in Figure 2 shows, there are many stages involved in transporting water, acetylene, and the various associated inert and organic compounds through such an analytical system. It was found that significant and unpredictable error was associated with this particular multi-stage transport and RGC measurement procedure. Different forms of gas-solid chromatography (GSC) were also investigated and found to be unacceptable with respect to quantitatively transporting trace-levels of water. Consequently, a more straight forward gas-liquid chromatographic (GLC) analytical approach was pursued whereby inertness (relative to water) of the chromatographic flowpath was of primary concern.

Modified GLC-OTC Approach. Recent advances in column technology have permitted a different analytical approach for separating and measuring low levels of water. This instrumental approach utilized a modified GLC system which employed a highly deactivated and very thick film polydimethylsiloxane open tubular column (OTC). Detection was with the modulating thermal conductivity detector, although a variety of detection devices could be used, e.g., AED, PDID, etc. A special high-temperature splitter injector[5] was used for injecting approximately two microliters of fuel sample. This high- temperature split assembly used an inerted injector insert (with deactivated glass wool) which needed to be replenished after

approximately 50 injections. A high capacity, but coarse, in-line charcoal trap was used in the vent line of the injector.

The column specifics were the key to obtaining a separation of water from the other trace eluting constituents of the organic mixtures. Although the OTC was deactivated, the thick film of polydimethylsiloxane contributed significantly to the good symmetry of the emerging water zone. The importance of generating symmetrical solute zones is related to both the quantitative precision and accuracy. Specifically, Figure 3 presents a description of the various statistical moments that are associated with generating chromatographic zones. For this type of trace-water analysis, the third statistical moment describes the major criterion. The symmetry (or extent of asymmetry) that exists with an emerging zone is of extreme importance as the initiation and termination of the integration process is determined by the behavior of the extremities of the solute zone. Thus, symmetrical zone profiles always provide far better quantitative measurements in chromatography.

EXPERIMENTAL

We have a strong preference for the GLC separation mode. When chromatography is performed properly in the GLC mode, symmetrical elution profiles are generated.[6] Figure 4 shows a high resolution GC-MS tracing of a typical JP-8 fuel. Consequently, when water can be transported and eluted without skew (like these organic solutes) and analytically separated by GLC, then considerable instrumental simplifications can be obtained. Previously, most gas chromatographic procedures that involved a water separation (particularly the GSC methods) also included extensive solute zone "tailing", which would be extremely detrimental for precise quantitation of the trace amount of water.

The sample introduction mode is of major importance to a laboratory GLC analytical procedure. Two different procedures were investigated; an on-column injection technique, and a high-temperature split injection procedure. In both cases, an extremely thick film GLC-OTC was used as it has two distinct advantages for separating water from other constituents. By having a very thick film column, the water could be slightly retained relative to inert gases that would be dissolved in the jet fuel. Also, the thick film of stationary phase provides further deactivation of the fused silica OTC wall surface. Eventually, we decided upon the modified

high-temperature injector assembly shown in Figure 5. The instrumental arrangement for conducting water-in-fuel analyses consisted of a modified Hewlett Packard 5890 gas chromatograph with a reporting integrator (HP-3390A). This GC instrument had highly filtered helium as the carrier gas. With the splitter injector and a 15 meter megabore OTC having a polydimethylsiloxane substrate (of low phase ratio, or β value), water could be eluted with near-perfect symmetry (see Figure 6). Such an instrumental arrangement allowed water to be easily separated from the other constituents, and Figure 7 shows a typical chromatogram of a JP-8+100 fuel. Figure 8 also shows the early portion of chromatograms for other similar types of turbine engine fuels. These separations were performed with a GLC column temperature of 35°C. The only co-eluting species or interferent in this analysis scenario was propane. Consequently, a series of different jet fuels were analyzed for propane content using the highly sensitive hydrogen flame ionization detector, and here it was found that only extremely small quantities of propane (approximately 0.01 ppm) were encountered.

As water is an omnipresent contaminant, it was found that different syringe needles sorbed differing quantities of water. For example, while under laboratory conditions, a polyimide-clad fused silica needle could contain up to 100 nanograms of water, while a simple #26 stainless steel syringe needle sorbed approximately 10 nanograms of water. Recent information has shown that a special Silcosteel treated needle is especially inert with respect to water sorption, and only miniscule amounts of water have been detected using this syringe needle in conjunction with JP-8+100 fuels.

RESULTS

This particular gas-liquid chromatographic open tubular column method has been able to analyze a variety of turbine engine fuels. Thus far, measurements of water content have ranged from 33 to 144 ppm, by weight. The calibration procedure that is associated with this GLC method utilized a standard addition technique. The precision for the water measurement was found to be 2.48% RSD. It appeared that the largest source of error with the present method is associated with sample delivery. An automatic sampler or a digital syringe should reduce this error.

Water settling time has been observed to be a variable in high water-content analyses. The size of the formed water droplets appears to be especially important. Experiments are

planned for examining several aspects further. Investigations are underway to determine water settling time at different fuel temperatures and water/fuel equilibrium properties with various additive packages.

CONCLUSIONS

The measurement of water content in JP-8+100 fuel can be accomplished with precision using near-conventional GLC technology. Trace levels of water can behave well in an appropriate open tubular column and be measured to sub-ppm concentrations with the use of on-column injection. In this type of analytical work, precautions are needed for dealing with surface adsorbed water. Accurate calibrations for water are achievable using special standard addition procedures. With backflush capabilities, this measurement technique can be scaled down for field testing.

ACKNOWLEDGEMENTS

This work was supported by the Fuels Branch of the US Air Force Wright Laboratory. Part of this effort was performed under the Combustion and Heat Transfer Studies Program, F33615-87-C-2767.

REFERENCES

(1) Grob, K. *J. Chromatogr.* **1973**, *84*, 255-273.

(2) Tomkins, B. A. Griest, W. H., and Higgins, C. E. *Anal. Chem.* **1995**, *67*, 4387-4395.

(3) Fischer, K. *Angew. Chem.* **1935**, *48*, 394-399.

(4) Knight, H. S., and Weiss, F. T. *Anal. Chem.* **1962**, *34*, 749-751.

(5) Sandra, P. *Sample Introduction in Capillary Gas Chromatography: Volume 1*, Huthig: Heidelberg, 1985.

(6) Giddings, J. C. *Unified Separation Science*, Wiley: New York, 1991.

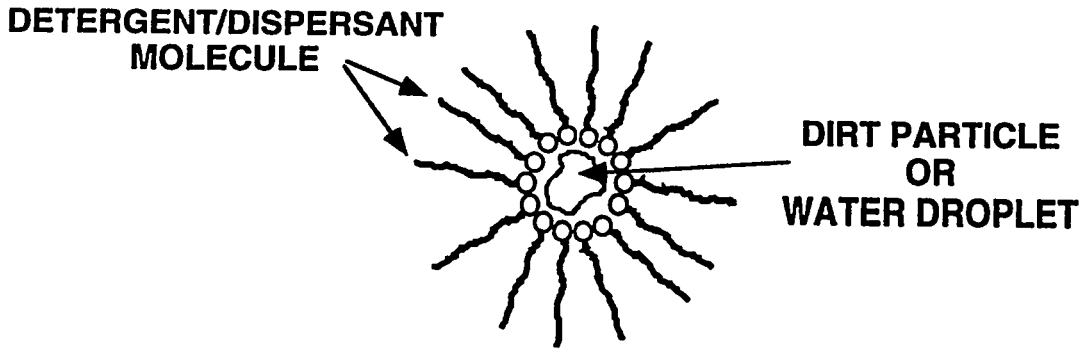


Figure 1. Detergent/dispersant additives can form micelles around dirt particles and water droplets. This prevents agglomeration of particles needed for removal in current filter/coalescer media.

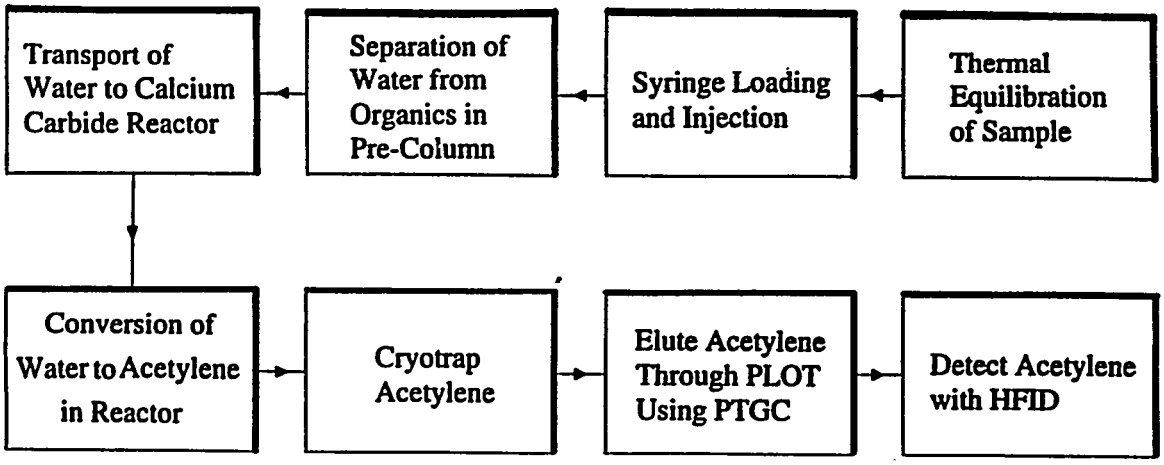


Figure 2. Block diagram of reaction gas chromatographic (RGC) procedure.

$$\bar{m}_k = \frac{\int_0^\infty c(\tau)(\tau - m_1)^k d\tau}{\int_0^\infty c(\tau) d\tau}$$

m_0 = zone area

m_1 = zone retention time

$\bar{m}_2$ = zone time variance

$\bar{m}_3$ = zone skew, or asymmetry

$\bar{m}_4$ = zone kurtosis, or flattening

Figure 3. Statistical moments of emerging GC solute zones.

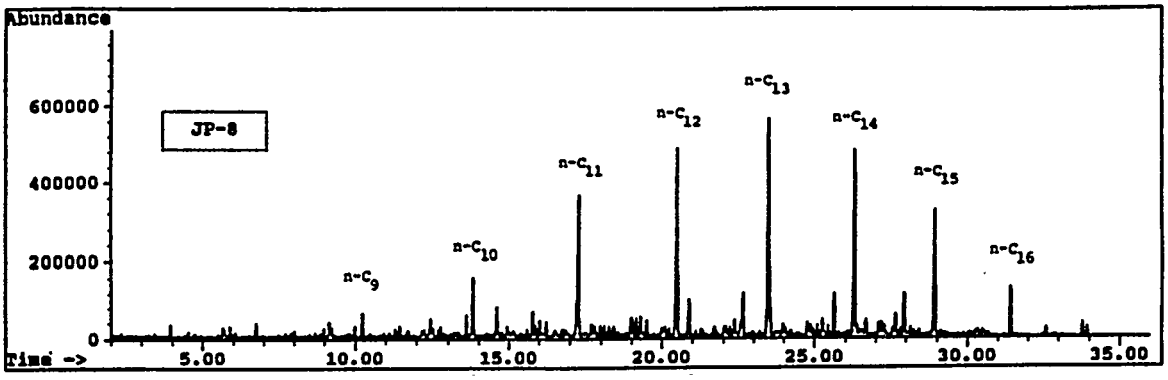


Figure 4. GC-MS output signal for a JP-8 fuel.

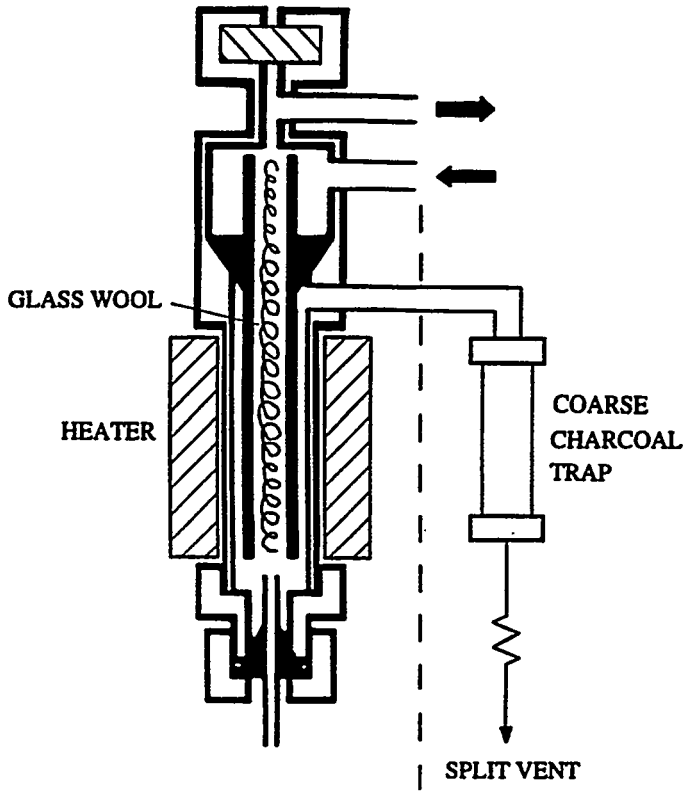


Figure 5. Modified high-temperature splitter injector assembly.

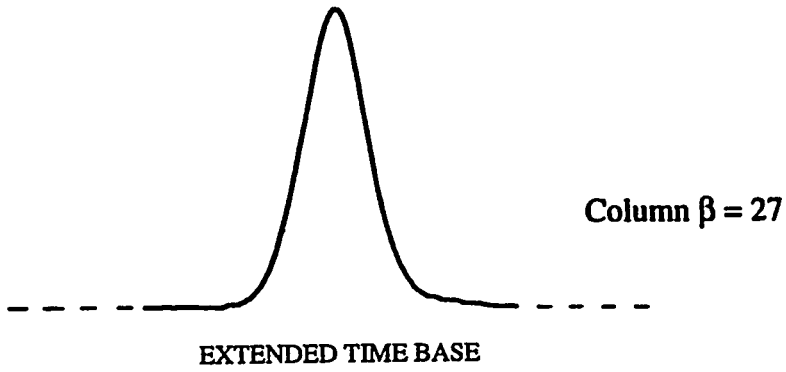


Figure 6. Near-perfect symmetry of water elution zone.

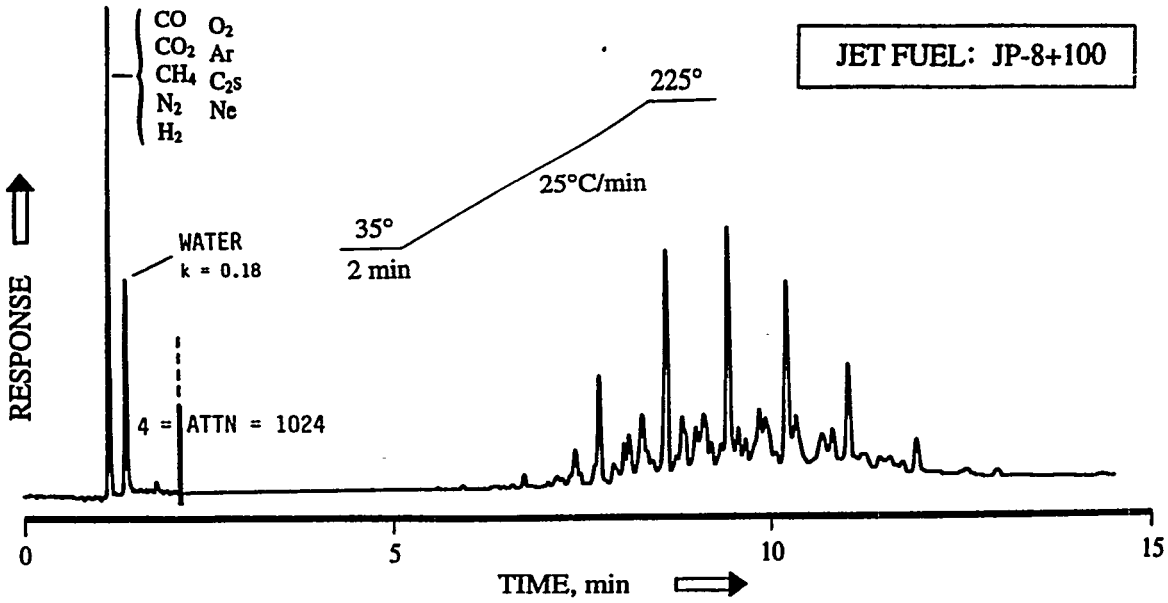


Figure 7. Typical GLC chromatogram of a JP-8+100 fuel.

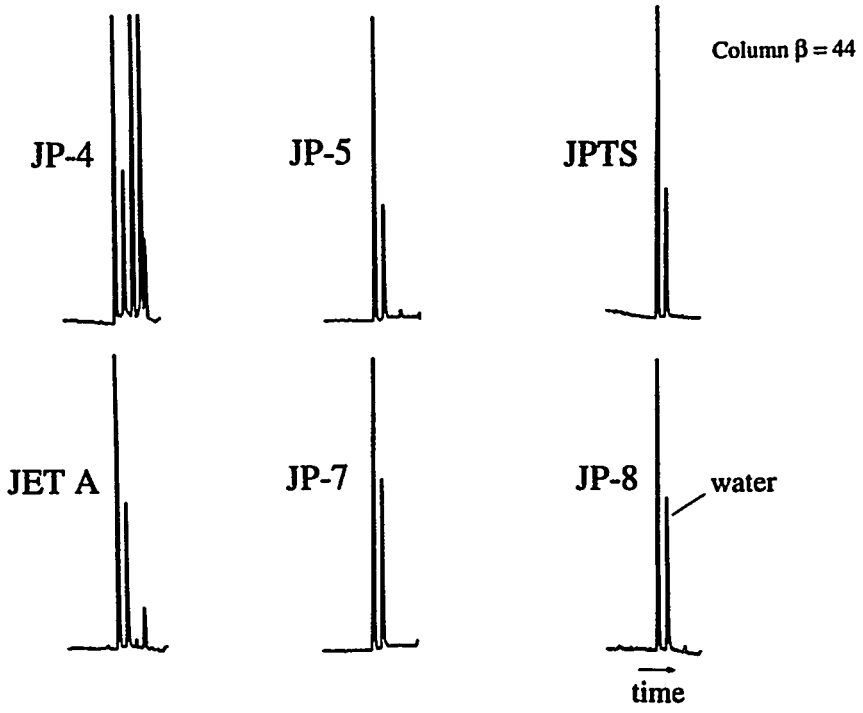


Figure 8. Early elution portion of GLC chromatograms of other types of jet fuels.

6th International Conference
on Stability and Handling of Liquid Fuels
Vancouver, B.C., Canada
October 13-17, 1997

AVIATION FUEL HANDLING: NEW MECHANISTIC INSIGHT INTO THE EFFECT OF SURFACTANTS ON WATER COALESCER PERFORMANCE

Victor B. Hughes

Shell Research & Technology Centre, Thornton, P.O. Box 1, Chester, CH1 3SH, U.K.

Aviation fuels may contain trace polar materials of a type and at a concentration sufficient to impair the performance of filter-water-coalescers in the removal of dispersed droplets of free water from the fuel. This process, commonly called "coalescer disarming" may cause the transmission of unacceptable levels of free water. There are a number of proposed mechanisms for this phenomenon, one of which invokes a change in "(water-)wettability" of the coalescer fibres as a result of surfactant adsorption. In this paper the results of fibre wettability changes observed using an Environmental Scanning Electron Microscope (ESEM) are presented. Bundles of fibres may be observed in the ESEM whilst the water vapour pressure is varied. Precipitation of water droplets onto the fibres may be induced by cooling the stage holding the fibres and increasing the water vapour pressure. Thence the contact angles made by water droplets may be assessed for fibres exposed to fuels with and without potent surfactants. Droplet growth may also be observed until coalescence occurs. Surprisingly the observations reveal that the trend in fibre wettability as a function of surfactant exposure does not go the way expected from considerations of currently proposed mechanisms. Fibres exposed to surfactants appear to be prone to water swamping rather than becoming hydrophobic. The implications of this observation will be discussed in terms of macroscopic coalescer performance observations.

1. Introduction

Water can become entrained in jet fuels as very finely divided droplets, often <40 μm in diameter. In this finely divided state, water will not readily settle out of the fuel under gravity alone. The Stokesian settling rate for 20 μm droplets in a typical jet fuel is approximately 15 mm/min. For even finer droplets gravity settling becomes totally ineffective as Brownian motion dominates.

The exclusion or removal of water from jet fuel is of major importance to the distribution and supply industry in order to guard against the delivery of contaminated fuel into-plane and the consequent potential catastrophic consequences of an in-flight failure. Increasing the droplet

size of fine water dispersions by fibre bed coalescence is one of the currently adopted solutions.

1.1. Filter/Water Separators

These devices (complying with an API 1581 specification) contain two types of element (Fig. 1). Firstly the fuel passes through a combined filtration and water coalescence element (in-to-out) where dirt particles >1μm in diameter are filtered out and finely dispersed water droplets are coalesced into larger droplets which easily settle out of the fuel under gravity. Secondly the fuel passes through a separator element (out-to-in) which is usually a simple hydrophobic (water-repelling) screen. Coalesced water drops settle out of the fuel rapidly and accumulate in the sump whence bulk water can be drained off. Vessels usually contain more than one of each element type. Each element has a maximum recommended flow rate and this value is used to calculate the numbers of elements needed for a particular flow rate.

2. Dispersed water coalescence:

Definition: "The process of joining together two or more bodies of the same fluid, separated by another immiscible fluid. One of the fluids must be a liquid, the other can be a liquid or a gas."

2.1. Coalescence Mechanisms.

Droplet-droplet coalescence (AUTOCOALESCENCE) may occur if the number population of water droplets is high enough and if there are no antagonistic components in the fuel.

The Hazlett model[1] for coalescence processes in a fibrous bed has remained unchallenged for many years. The model (Fig. 2) comprises four main steps:

- Approach of a droplet to a fibre,
- Attachment of the droplet to the fibre,
- Coalescence of droplets on the fibre and
- Release of enlarged droplets from the downstream side of the fibre bed.

In summary: PROXIMITY, INTERCEPTION, GROWTH, RELEASE.

Of the interception mechanisms, inertial, direct collision and diffusional, Hazlett considers that direct collision is the most likely and inertial impaction the least likely (on hydrodynamic

grounds). Diffusion is only likely to contribute with the smallest droplets and at low velocities. On this premise Hazlett developed a Langmuirian model for the interception of droplets at a single isolated fibre, derived from purely hydrodynamic considerations and for superficial velocities less than a critical value of about 1.5 cm/sec.:

$$E_S = \frac{1}{2(2-\ln N_R)}\left[2(1+r)\ln(1+r)-(1+r)+\frac{1}{(1+r)}\right] \qquad 1)$$

where: E_S = interception efficiency (%) i.e., the efficiency of collection by a single fibre from a fluid stream of a width equal to the diameter of the fibre,

N_R = Reynold's No. = $v\, d_f \rho / \mu$

v = superficial velocity,

d_f = fibre diameter,

d_p = droplet diameter,

$r = d_p / d_f$

However this model takes no account of any non-hydrodynamic effects which may reduce interception efficiency and assumes that every droplet/fibre interception is 100% successful. Hughes and Foulds[2] introduced an empirical correction factor, σ, to account for coalescence systems which failed to conform to the Hazlett model, when:

$$E'_S = \sigma E_S \qquad 2)$$

For aqueous emulsions σ was related to electrostatic effects only. In the jet fuel system, a similar factor could be related more comprehensively to both electrostatic and steric repulsion effects. More importantly Hughes and Foulds extended the Hazlett model to a number of non-interacting fibres in a fibre bed based on sequential probabilities of interception:

$$E_B = \left(1-E'_S\right)^n \qquad 3)$$

where: E_B = Coalescence Efficiency of the whole bed,

$$n = 2(1-\varepsilon)\left(\frac{d}{d_f}\right)$$

ε = porosity of the bed,

d = bed depth.

Not much is known about the subsequent stages of coalescence but in an effectively operating fibrous bed coalescer, water appears to be released from specific "active" sites on the downstream side. The coalesced dispersed phase has been observed to accumulate in the upstream part of the fibrous bed and to feed threads of liquid through the bed, bridging fibre-

to-fibre. Release of large coalesced drops of water remains "black-art" with most coalescer manufacturers providing a relatively coarse weave cotton "sock" as the final release medium.

2.2. Coalescer Disarming.

Experiments on a full-sized test rig have shown a dramatic reduction in coalescer efficiency in the presence of a model fuel surfactant (Aerosol OT, which is a sulphosuccinate). The results of these experiments are shown in Fig.3. The coalescer was subjected to a fuel in which 1% volume of water had been finely dispersed. The base fuel with no surfactants or additives transmitted only 5 ppmv water maximum during an extended test period. However, as can be seen in Fig.3, increasing the concentration of surfactant in the fuel caused increasing levels of water transmission.

Sodium naphthasulphonate (SNS) has long been known in the industry to produce the same effect at levels of only 0.4 ppm. Recent work commissioned by the Institute of Petroleum and carried out on the test facility at Thornton indicate the potency of this material in causing disarming (Table 1). Neither SNS nor AOT are likely components of jet fuel but are representative of those that are and as such can be used in laboratory and rig investigations of disarming.

Coalescer failures of this type are known as "coalescer disarming" and are thought to be the result of surfactant adsorption onto the glass fibre coalescer surfaces and also onto the hydrophobic water separator element altering the water-wetting properties of those surfaces in an adverse way. Jet Fuels may occasionally contain surfactants as a result of the type of crude oil used by a refinery or deficiencies in the processing steps. These can be quite potent in causing coalescer disarming and in the field many examples have been encountered. Additives which contain surfactant material such as Static Dissipators when used at their normal working dosage rates are not known to cause problems.

2.3. Proposed Mechanisms for "Disarming"

The two theories currently being advanced to explain coalescer disarming are based on droplet size and fibre wettability considerations respectively.

2.3.1. Droplet Size.

The Hazlett model clearly indicates that the smaller the droplet size for a given fibre diameter the less the probability for interception. Droplet size is related to mechanical shearing but also to the interfacial properties of the fuel/water interface. The lower the interfacial tension then the smaller the droplet size for a given shear regime. Interfacial tension (IFT) measurements for water and fuels containing either SNS or AOT indicate subtle differences in their behaviour (Fig.4). AOT is very effective in reducing IFT and has been extensively reported in literature to be a very powerful emulsifier. The IFT data for SNS indicates this material to be potentially much less effective as an emulsifier. This is very interesting in terms of coalescer disarming because it suggests that the disarming seen with AOT is much more likely to arise from a droplet size effect whilst for SNS, and materials of similar IFT response, another mechanism must be sought.

Conclusion: Surfactant materials active at the fuel/water interface are most likely to produce coalescer failure because of the smaller water droplet size produced by shear in such systems. This effect is purely hydrodynamic and is predicted by the Hazlett model. In the field, fuels behaving in this way could be identified by a simple water haze stability measurement.

2.3.2. Fibre "wettability".

The glass fibre medium used in conventional filter-coalescer elements presents a surface which has both hydrophilic (silicate) and hydrophobic (organic resin) regions. It is commonly thought that water interception and growth occurs at the hydrophilic sites. Surfactant adsorption can also occur at the hydrophilic sites because surfactants have polar groupings within the molecule. Such a process will alter the surface properties of the glass fibre. For many years it has been the view of many in the industry that the process produces a fibre surface with hydrophobic properties with the result that water droplets are not intercepted but migrate without coalescence through the media.

Conclusions: Surfactants especially active at the solid/fuel interface might be expected to dominate this disarming process. In the field, fuels behaving in this way would require a more

sophisticated and controlled method for identification, one in which the coalescer fibres have adequate exposure to the potent fuel components.

3. Characterisation of Fibre Surfaces by ESEM

To explore further the surface properties of glass-fibres used in water coalescence media a new approach was taken. The development of Environmental Scanning Electron Microscopy[3,4] in which a sample can be examined in a vapour space saturated with water (25 millibar at room temperature) permits the condensation of free water onto the specimen fixed to a cold mount. Further, the samples can be studied without the need for coating because the controlled environment ensures that surface charging is neutralised (Fig.5).

3.1. Experimental:

Dry coalescer fibres were taken from a Velcon Filters Inc. filter coalescer Model 85. Fibres were then immersed for 24 hours in either a clay-treated Jet A-1 fuel or the same fuel to which had been added 1%v/v Petronate L (Sodium Naphthasulphonate - supplied by Witco). The samples were allowed to dry and then glued to a conventional SEM stub.

The ESEM was operated with a water vapour pressure of 6-7 millibars and the sample was maintained at ambient temperatures during normal data aquisition. To initiate water droplet formation on the fibres the stage was cooled to 8°C and the water vapour pressure increased to saturation at 11 millibars.

Real time video imaging of the fibres was carried out during droplet formation and evaporation.

3.2. Results:

3.2.1. Fibres soaked in clay-treated Jet A-1

Condensing water formed discrete droplets on specific sites (Fig.6). Evaporation of the droplets followed by another condensation cycle resulted in the formation of water droplets on the same sites as previously observed. This indicated that the fibres possessed "islands" of hydrophilic surfaces within a hydrophobic "sea". Back-scattered X-rays (EDX) indicated the hydrophobic sites to be resinous and containing carbon and oxygen (CKa, OKa). To further verify that the droplets seen were water, an electron beam was focussed on individual droplets which then rapidly evaporated. Focussing the same beam on resinous structures had no effect

on the structure. As the condensed water increased, coalescence of adjacent droplets was observed and if the droplet size reached some critical size the drop fell off the fibre.

Conclusion: Water droplet interception and attachment occurs on specific sites in resin-coated fibre-glass media used in filter-coalescer elements.

3.2.2. Fibres soaked in Jet A-1 containing a sodium naphthasulphonate (SNS).

The dry fibres appeared structurally similar to those soaked in clay-treated Jet A-1.

In the first condensation cycle, no droplets formed on the fibre surfaces, instead thin films of water were observed to bridge across fibres (Fig.7). All fibre surfaces were wetted by the water, i.e. THE FIBRE SURFACES WERE COMPLETELY HYDROPHILIC. These water films ruptured on the evaporation cycle or when the film was subjected to a focussed beam of electrons. This observation was a complete surprise being in complete contradiction of commonly held theories of coalescer disarming. The observation does however explain one specific feature of coalescer disarming, viz. "Graping". Graping is the occurrence of released water structures comprising a fuel drop surrounded by a "skin" of water. Such structures have a near-neutral boyancy in a fuel continuous phase and are frequently observed in disarmed coalescers. Spontaneous rupture of the skin results in the formation of large numbers of extremely small (~1μm) droplets. Water films formed across a fibre framework could produce such structures when flowing fuel moves against the framework in an analogous manner to blowing soap-film bubbles (Fig.8).

Conclusion: Surfactant coated fibres prevent the normal interception and attachment of discrete water droplets. Instead, a continuous spontaneously spreading water film is produced suggesting that the fibres have become completely hydrophilic. This observation entirely contradicts currently held theories which suggest an increasing hydrophobicity on exposure to such surfactants but does explain the formation of some structures seen in cases of coalescer disarming which current theories do not. Further it suggests that the observed coalescer failures are in this case involves the droplet release stage rather than interception.

4. Conclusions

- Surfactants which are highly interfacially active at the water/fuel interface can cause filter-coalescer failure by producing fine water droplets. These remain on streamlines and cannot be intercepted by glass-fibres effectively.
- Some surfactants are not as highly interfacially active at the fuel/water interface but are active at the solid/fuel interface. Such surfactants also cause coalescer disarming, but by a mechanism which this work shows to be at variance with commonly held theories. Features of this mechanism are:

  (i) Rather than becoming hydrophic the fibres become completely hydrophilic.

  (ii) Water droplets intercepted by such fibres spontaneously spread to form water films.

  (iii) The water drop release stage is the more likely cause of the perceived coalescer performance failure.
- At least one disarming phenomenon, graping, can be explained by this new mechanism.

5. Acknowledgements

P.D.Rugen for the Interfacial Tension Measurements and the full scale rig coalescer performance data.

D. Park who for many years heralded the introduction of ESEM and who finally set up the contact with University of Manchester Institute of Science and Technology (UMIST) and who together with Mike Macknay and the technicians at UMIST conducted the ESEM study.

6. References

1. Hazlett, R.N., *Ind. Eng. Chem. Fundam.*, **1969,** *8*, 625, and **1970,** *9,* 520 and with Carhart, H.W., *Filt. Sep.*, **1972,** *9*, 456.
2. Hughes, V.B.; Foulds, A.W., *Proc. 4th World Filtration Congress*, **1986.**
3. Danilatos, G.D., *J.Microsc.*, **1991,** *162*, 391-402
4. Danilatos, G.D., *Microscopy Research & Technique,* **1993,** *25,* 529-534.

	FUEL TYPE	% Water (Inlet)	Facet CA 14-3SB	Velcon I614-85TB	Faudi F7-362
RUN 1	1.0 mg/l Stadis 450 + 2.9 mg/l Hitec 580 + 0.4 mg/l Petronate L	0.01	Fail	Fail	Not available
		3.0	Fail	Fail	for testing
RUN 2	1.0 mg/l Stadis 450 + 0.4 mg/l Petronate L	0.01	Fail	Fail	Pass
		3.0	Pass	Fail	Fail
RUN 3	4.5 mg/l Stadis 450	0.01	Pass	Pass	Not available
		3.0	Pass	Pass	for testing
RUN 4	2.9 mg/l Hitec 580	0.01	Pass	Pass	Not available
		3.0	Pass	Pass	for testing
RUN 5	1.0 mg/l Stadis 450 + 2.9 mg/l Hitec 580	0.01	Pass	Pass	Pass
		3.0	Pass	Pass	Pass
RUN 6	4.5 mg/l Stadis 450 + 2.9 mg/l Hitec 580	0.01	Pass	Not	Not
		3.0	Pass	Tested	Tested
RUN 7	0.4 mg/l Petronate L	0.01	Fail	Fail	Pass
		3.0	Fail	Fail	Fail

Table 1. Examples of commercial coalescer failures in fuels containing various additives including SNS (Petronate L). Failure is defined as the transmission of >15ppm free water downstream of the coalescer. Fuels containing approved additives such as Stadis 450 (a static dissipator additive) and/or Hitec 580 (a corrosion inhibitor) are not disarmed. The inclusion of only 0.4 mg/l SNS in the fuel causes failure at one or both of the inlet water addition rates.

Figure 1. Filter-Water Separator (schematic)

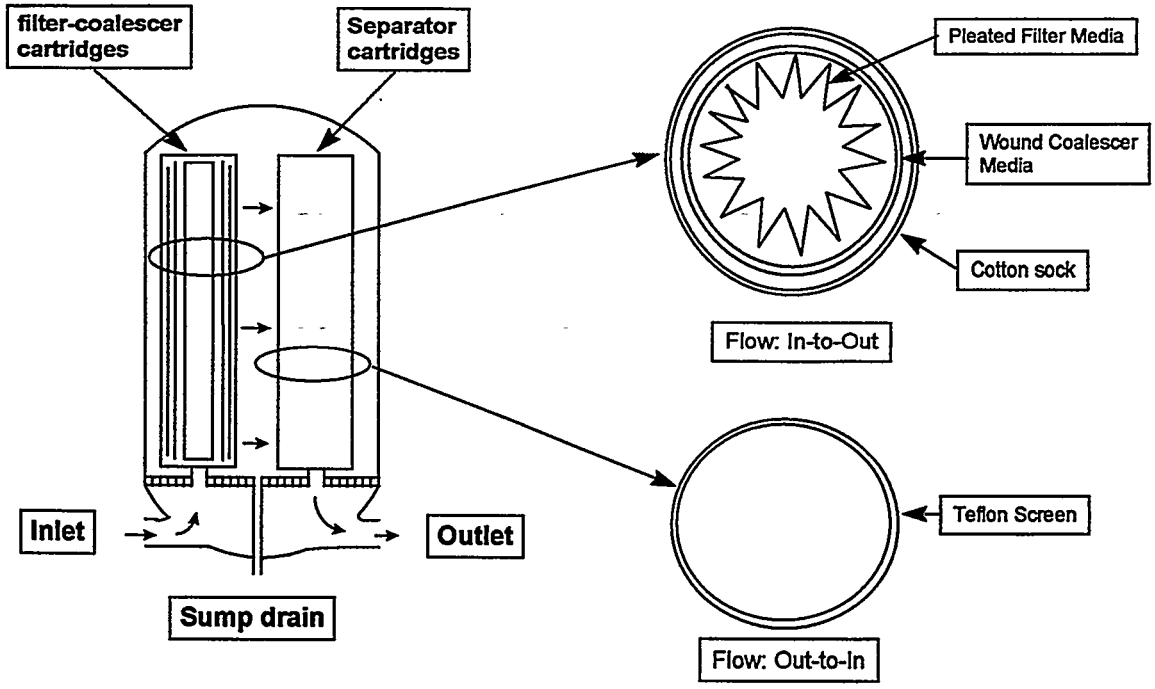
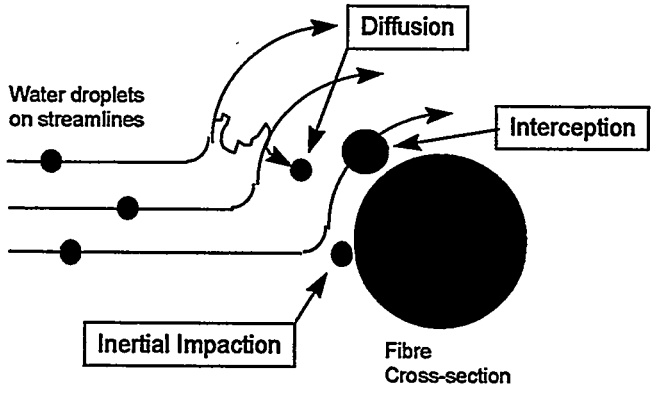


Figure 2. Dispersed Water Coalescence:



(Hazlett Theory)

PROXIMITY

INTERCEPTION

GROWTH

RELEASE

$$E_S = \frac{1}{2(2-\ln N_R)}\left[2(1+r)\ln(1+r) - (1+r) + \frac{1}{(1+r)}\right]$$

E_s = interception efficiency (%)

$r = d_p / d_f$

N_R= Reynold's No.

Figure 3. Effect of fuel surfactant level on the water coalescence performance of a commercial filter-coalescer, model Velcon 85.

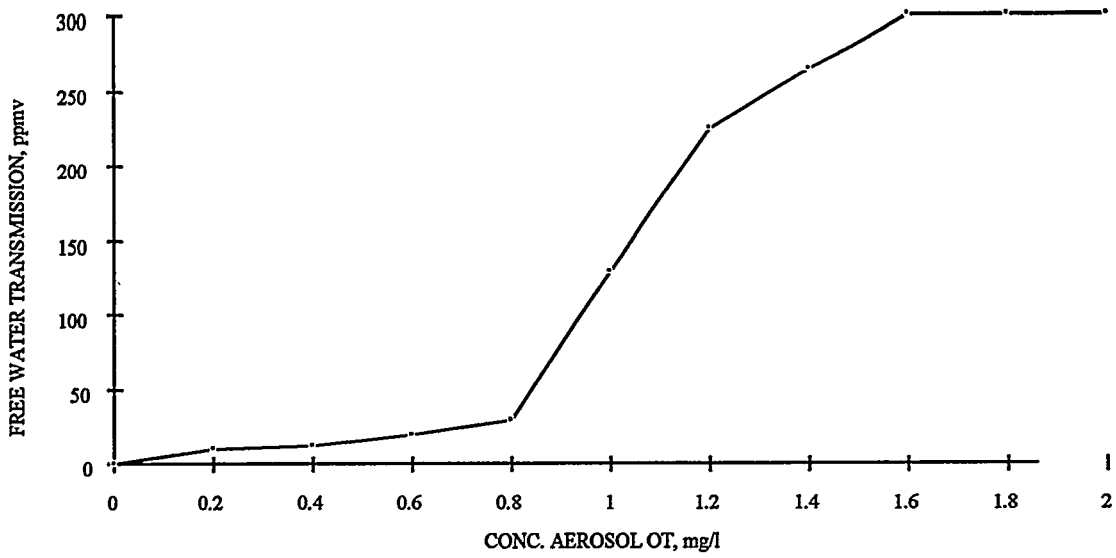


Figure 4. Water/Jet fuel Interfacial tension values for fuel containing AOT and SNS

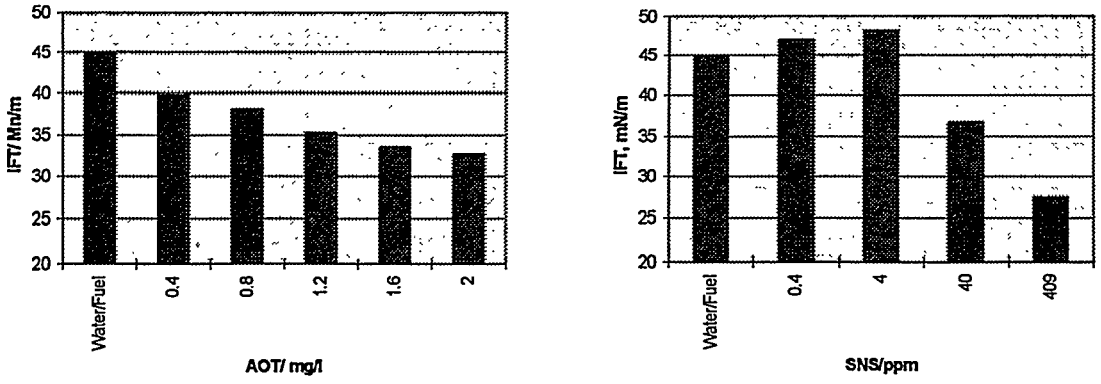


Figure 5. UMIST ElectroScan ESEM Model 20

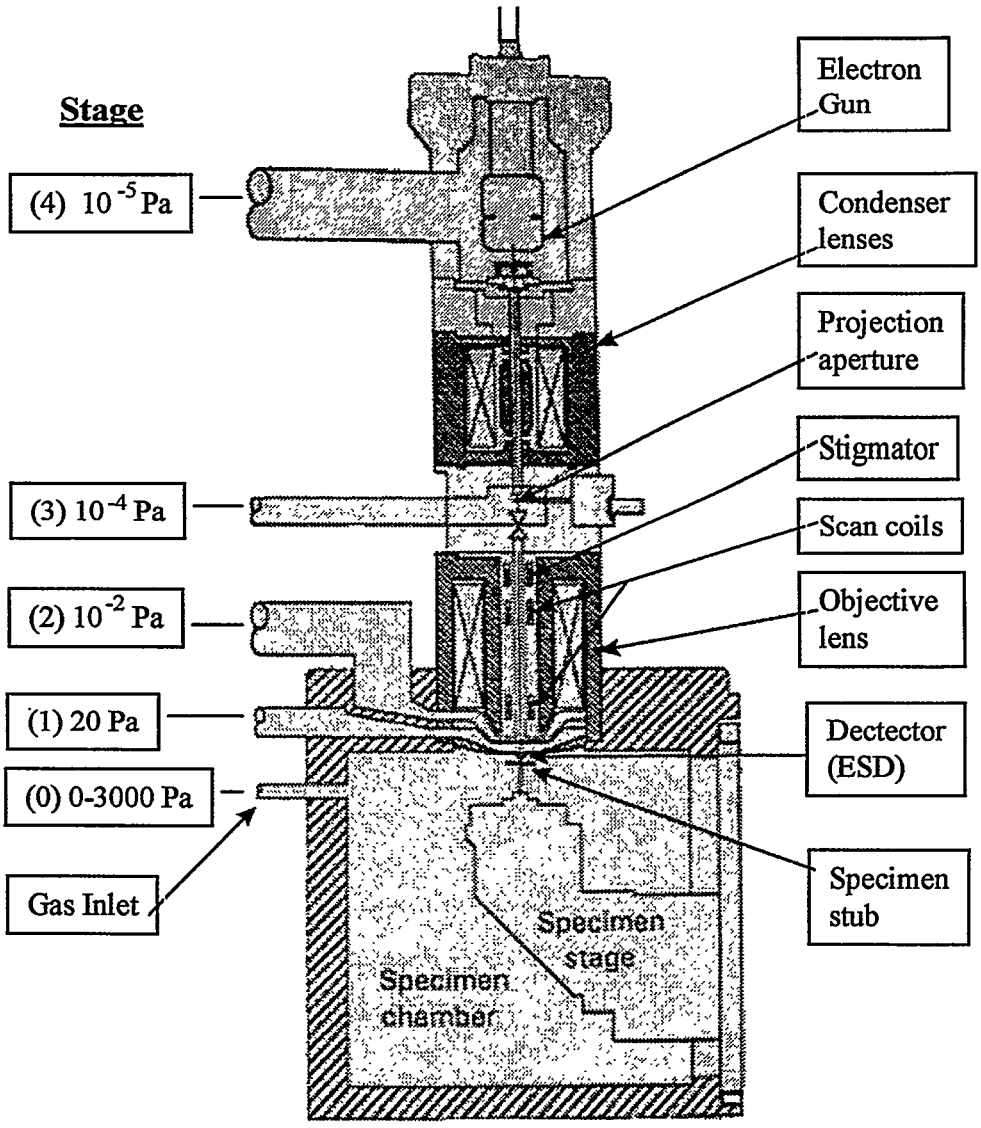


Figure 6. Water droplet formation on coalescer fibres after soaking in a clay-treated Jet A-1 fuel. Note the wide variation in droplet contact angle

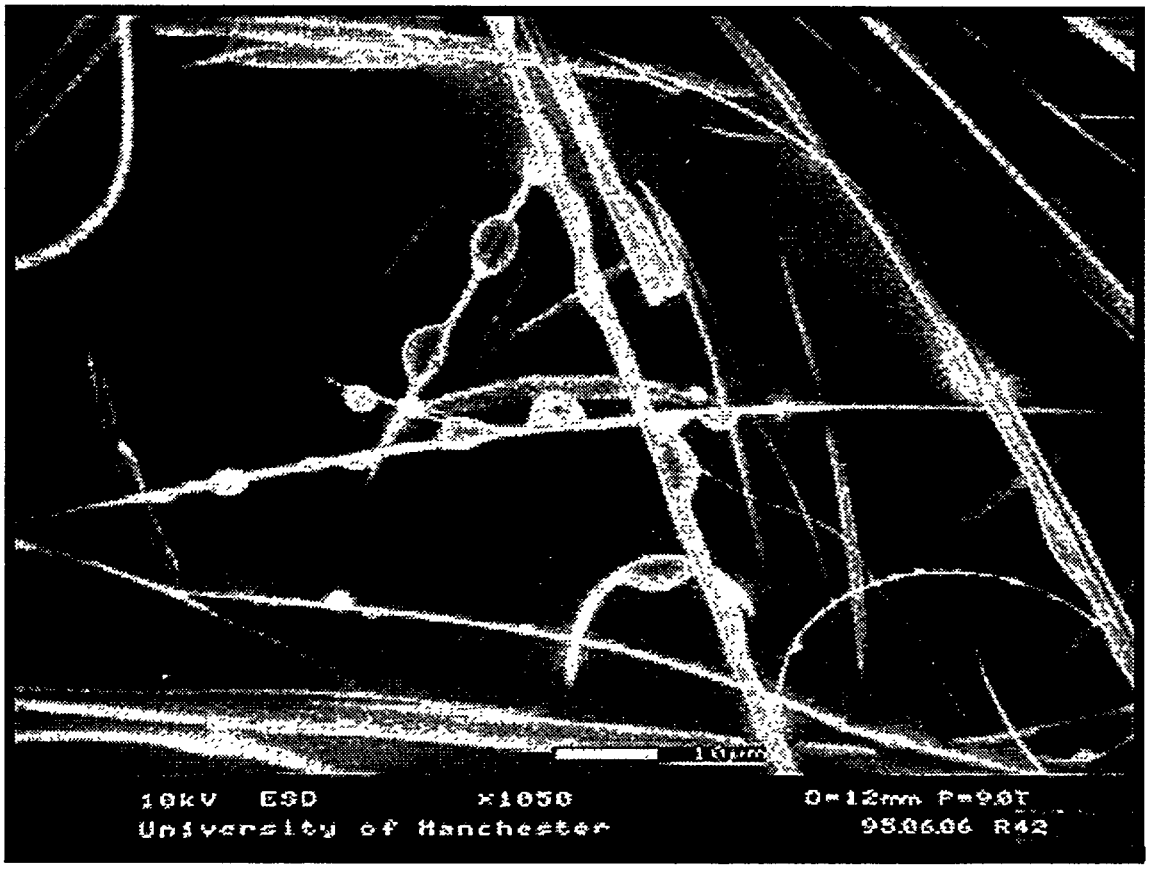
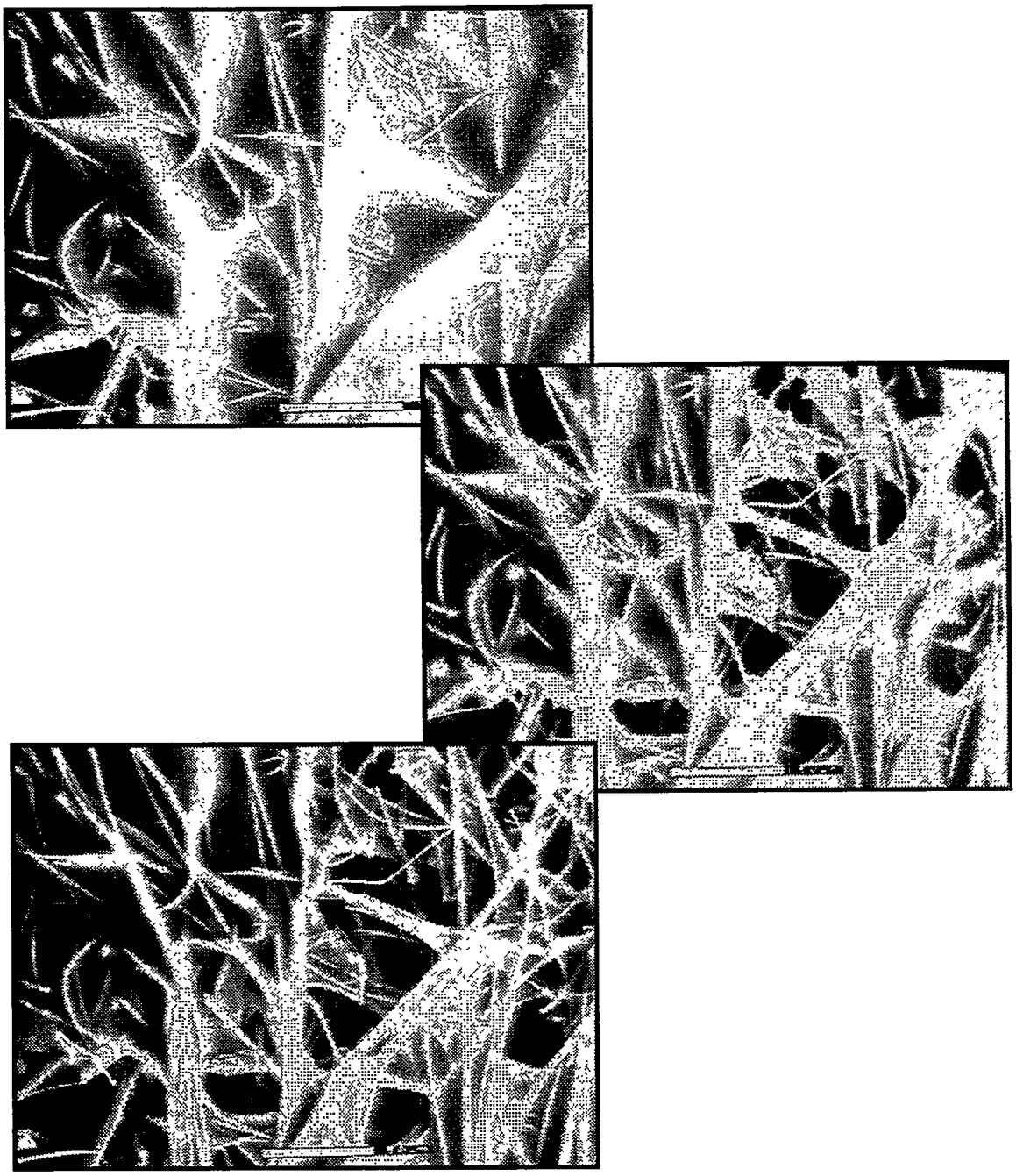


Figure 7. Water film formation on coalescer fibres after soaking in a Jet A-1 containing SNS. The sequence shows the progressive evaporation of water from the system.



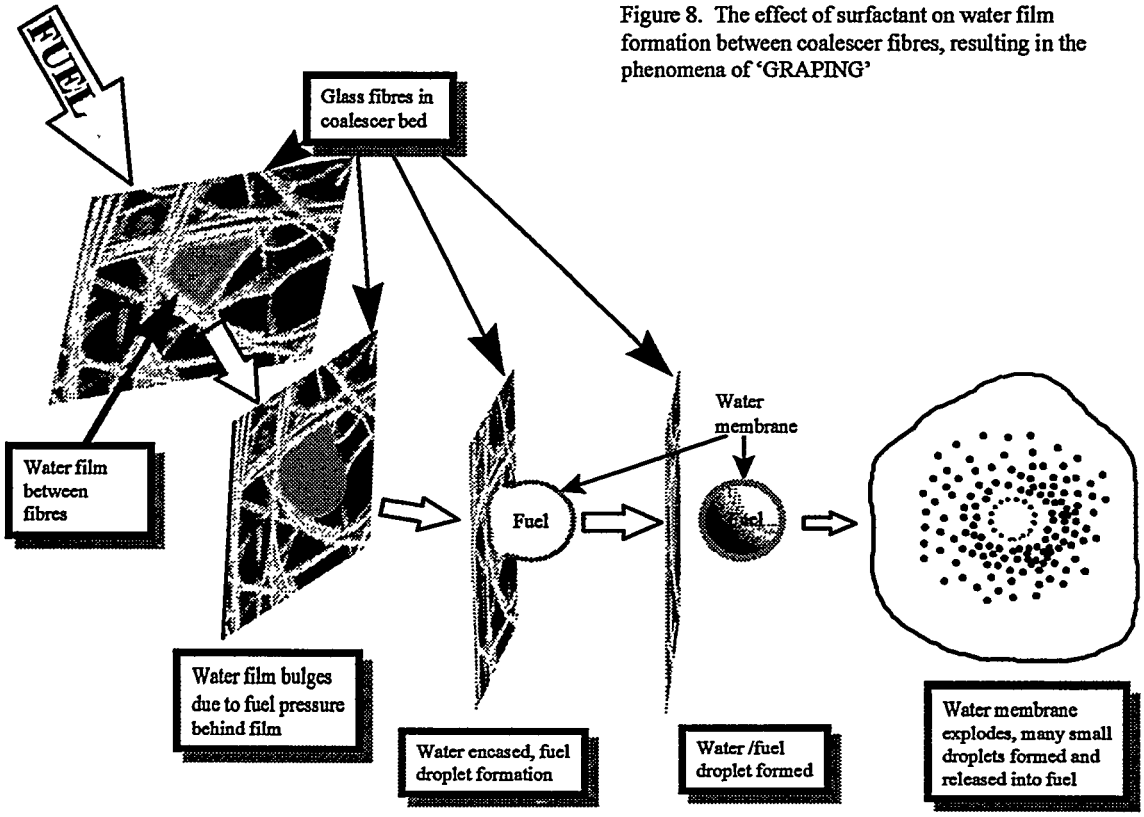


Figure 8. The effect of surfactant on water film formation between coalescer fibres, resulting in the phenomena of 'GRAPING'

6th International Conference
on Stability and Handling of Liquid Fuels
Vancouver, B.C., Canada
October 13-17, 1997

AN ANALYTICAL APPROACH TO WATER SEPARATION FROM JET FUELS AND COALESCER DISARMING

Peter David, Spencer E. Taylor* and Andy J. Woodward

BP Oil, Chertsey Road, Sunbury-on-Thames, Middlesex TW16 7LN, UK

Abstract

An analysis is presented of some aspects of fibre wetting and the possible implications for the operation of filter-coalescers. Two experimental approaches have been adopted in the present work. In the first, pre-treatment of single fibres by a Merox fuel and by a JP8+100 dispersant additive was followed by dynamic wetting measurements in water. The second approach, which is more representative of the practical situation, involves a "dual-liquid" system, in which the fibre first passes through an oil phase directly into water, *via* an oil/water interface. Specific wetting-related features arising from these single-fibre experiments have been identified.

Introduction

The operation of fibrous filters for removing dispersed water from jet fuels involves several distinct stages:[1]

1 Interception of the dispersed droplets by the fibrous media;
2 Droplet-fibre attachment as a result of wetting of the fibres following fuel displacement;
3 Coalescence between attached and incoming droplets;
4 Passage of coalesced drops through the bed; and
5 Release of coalesced droplets.

The interception process by which the droplets become physically attached to the fibrous media requires that *droplet-fibre contact* occurs, which will be dependent on physical factors such as the relative sizes of the droplets and fibres and the fibre

packing density, as well as the system hydrodynamics, controlled by fluid density and viscosity. Whether attachment of the droplet to the fibre occurs will necessarily be dependent on *wetting* of the solid fibre by the water (*ie* requiring that a *contact angle* of less than 90° is made with the fibre). The contact angle defines the wetting properties of a system, and relates to the *equilibrium* angle made by a liquid on a solid surface, as illustrated in Figure 1.

From a fundamental viewpoint, the wetting properties of individual fibres will govern the behaviour of a packed coalescer bed. However, the fibrous nature of coalescence media does not readily lend itself to an analysis of wettability in a bulk form. In the present study, therefore, a single-fibre approach has been taken to the analysis of the water wettability of glass fibres that have been exposed to a Merox-treated fuel and to a thermal stability dispersant additive. Whilst it is appreciated that coalescer action will be determined to some extent by the nature of packing of the fibre beds, the principal objective of this preliminary investigation was to identify general features of single-fibre wettability by fuel/water systems which could be important during the action of fibrous coalescers.

Experimental

Single-fibre wettability was determined using a Cahn Dynamic Contact Analyser (DCA) operating in the fibre balance mode. Two types of glass fibres have been used in the present work, one hydrophilic (denoted as type I) and one hydrophobic (denoted as type II). The type I fibres were from glass wool, obtained from BDH, Poole, whilst the type II fibres were extracted from heat-resistant insulation material and shown by scanning electron microscopy (SEM) and Electron Dispersive X-ray analysis (EDX) to be calcium-rich. Fibres suitable for examination were approximately 6 cm in length and had small wire loops secured to one end with epoxy resin for ease of attachment to the DCA. Optical microscopy was used to determine the fibre diameter. The DCA allows fibre immersion into the wetting liquid, whilst simultaneously monitoring the force exerted on the fibre and its immersion depth.

Two types of single-fibre wetting experiment were performed at ambient temperature (20 ± 2°C). The first, termed the *single-liquid* approach, involved pre-treating the fibre by immersion in appropriate liquids, either a Merox-treated jet fuel or (alumina-treated) *n*-heptane solutions of a JP8+100 dispersant additive. The force exerted on the fibre is given by

$$f = 2\pi r\gamma\cos\theta \qquad 1)$$

where γ is the surface tension of the test liquid and θ is the *dynamic* contact angle made by the liquid on the fibre, and a typical trace for *n*-heptane wetting is shown in Figure 2. Both *advancing* and *receding* dynamic contact angle behaviour can be studied in this way by immersing and withdrawing the fibre. During this process, adsorption of surface-active species can occur directly on to the fibre surface. This then allows the consequences of surface treatment on water wettability of the fibre to be determined.

The second approach, the *dual-liquid* method, which more accurately represents the practical situation, involves immersing the fibre attached to the DCA into an oil/water interfacial system. This is depicted in Figure 3. The attraction of this approach is that the fibre is pre-wetted by the oil phase before contacting the water, such that oil displacement is necessary before water wetting occurs, as in the "real" situation. As shown in Figure 4, a force is exerted on the fibre during immersion, first, from the effect of the oil (fuel) surface, which is then followed by the oil/water interface. Deconvolution of the effects of the surface and interfacial components is then possible with care. Analysis of the system is as follows.

The initial force exerted on the fibre is given by

$$f_{oil} = 2\pi r\gamma_{oil} \qquad 2)$$

where γ_{oil} is the surface tension of the oil phase and r is the fibre radius. The contact angle here is assumed to be zero, since hydrocarbons are regarded as completely

wetting liquids. Upon reaching the interface, the measured force is modified, such that the total force exerted on the fibre is given by

$$F_{total} = f_{oil} + f_{interface} = 2\pi r\gamma_{oil} + 2\pi r\gamma_{OW}\cos\theta \qquad 3)$$

where θ is now the contact angle for the oil/water/fibre system and $\gamma_{oil/water}$ is the interfacial tension. This latter situation exactly mimics the wetting interaction expected between a dispersed water droplet and a fuel-wetted fibre in the practical system. From equation 1, a knowledge of either r or γ_{oil} will enable the other parameter to be determined.

Results

Single-liquid systems

In Figure 2 are shown typical force-immersion depth traces for fibre wetting by hydrocarbon liquids. The traces can be seen to be relatively smooth in these cases, with the behaviour during immersion and withdrawal being almost identical, indicating that this type of liquid completely wets the fibres. Under these conditions, a knowledge of the surface tension of *n*-heptane (20.4 mN m^{-1}) allows the fibre radius to be calculated. For the fibres in the following example, the respective derived radii of 6.5 and 4.6 microns compare favourably with the microscopically-measured values (6.2 and 4.4 microns, respectively). The wetting behaviour found for hydrocarbons contrasts with the corresponding behaviour for water as the wetting liquid, shown for the same two fibres in Figure 5. Here, the wetting upon immersion (governed by the advancing contact angle) is seen to be erratic, which reflects the non-uniformity of the water contact angle along the length of each fibre. Figure 6 shows the corresponding advancing contact angle data for these two types of fibre which illustrates the essential difference between hydrophilic and hydrophobic fibres.

This is a typical finding for these types of fibre, and also suggests the difficulties which may arise when attempting to use other contact angle determination methods, *eg* direct observation of drops on fibres,[2] where, most likely, a range of values will be evident.

Upon retraction of the fibre, however, more uniform and larger forces are recorded, indicating that the receding contact angle is lower than the advancing angle, and in many cases, including the present examples, is almost zero. Also shown as dashed lines in Figure 5 are the expected retraction forces based on the zero contact angle hydrocarbon data and the ratio of the liquid surface tensions. Interestingly, it can be seen that the measured force is actually *higher* than the expected value, which has no physical significance in terms of the force due to surface tension. One explanation, however, is that a "wetting layer" is produced on the fibre, the weight of which contributes to the measured force. This is more evident in the case of the hydrophilic, type I fibre, as would be expected.

Figure 7 shows the average contact angle for the treated section of fibre as a function of the number of exposures to the Merox treated jet fuel. It can be seen that, although there is a relatively large increase in contact angle following the first treatment cycle, subsequent treatment cycles do not significantly affect the fibre wettability. From these data, this particular fibre radius is 6.1 microns (*cf* 6.5 microns by microscopy) and the Merox fuel surface tension is 25.5 mNm^{-1}.

However, pretreatment with different concentrations of the dispersant has a more dramatic effect on fibre water wettability. As shown in Figure 8, ppm levels of this surface-active additive cause a large effect on the advancing contact angle, which indicates that exposure of the fibre to approximately 10-20 ppm of the additive is sufficient to increase the contact angle to $\geq 90°$. Under these conditions, it would be expected that water droplets would not adhere to the fibres spontaneously upon contact. Correspondingly, the efficiency of coalescence by the fibrous media would be severely reduced.

Dual-liquid systems

In Figure 4, showing a typical force-immersion depth trace for type I fibres in the heptane/water system, the entry points into the oil phase and the oil/water interface can be clearly seen. From the oil surface data, the fibre radius in this case is determined as being 6.8 microns (*cf* 6.5 microns by microscopy). Upon retraction from the interface, and assuming a zero receding contact angle, the average heptane/water interfacial

tension is calculated to be 46.7 mN m^{-1} (*cf* 50.2 mN m^{-1}).[3] If the interfacial tension and fibre radius values are then used in analysing the immersion data, the contact angle profile for the interface shown in Figure 4 is produced, as shown in Figure 9, from which the heterogeneity of contact angle is evident, as also seen by the single-liquid approach. Surface-active materials can significantly affect the wettability in the dual-liquid systems also. In Figure 10 are shown advancing and receding contact angle data for successive immersion cycles in the Merox fuel, indicating the adverse effects of surface-active impurities in the fuel on wetting behaviour. More dramatic effects have been found in the *n*-heptane/water system in the presence of different concentrations of JP8+100 dispersant, again, leading to a decrease in fibre hydrophilicity.

Discussion

The two fibre wetting systems considered in the present work are contrasted by virtue of the predisposition of the surfactant with respect to interaction with the fibre. In the single-liquid situation, fibre surface modification by surfactant adsorption and subsequent water wetting are carried out in two separate stages. On the other hand, in the dual-liquid approach, oil wetting/surfactant adsorption and water wetting are consecutive processes occurring in the same system. The advantage of the latter approach, as far as understanding phenomena occurring during water coalescence is concerned, is that the fibre is pre-wetted by the oil (fuel) prior to contacting the water. Also, the measured contact angles reflect this situation, relating to the oil/water/fibre system, relevant to the practical application. From a surface chemical viewpoint the main difference between the two systems is the presence of the fuel/water interface in the dual-liquid situation. Such interfacial regions can often play important roles in surface chemical-dominated processes. Hitherto, little attention has been given to the fundamental aspects of the interfacial region during water coalescence processes. There are certain indications from the present work that the interfacial region is indeed playing an active role in influencing fibre wettability. For example, treatment with Merox fuel indicates that there is a greater effect on advancing contact angle data in the dual-liquid system compared with the single-liquid case, for which surfactant adsorption is the dominant mechanism. The presence of the interface is apparently

amplifying the influence of indigenous surfactants in the fuel. One mechanism for this is the more effective creation of a surface layer through surfactant *deposition* as opposed to adsorption. This is akin to the formation of Langmuir-Blodgett films on surfaces using well-defined surface-active molecules. As a consequence, it would be expected that fibre wettability would be adversely affected by such a deposition mechanism. The same general trends are true for the dispersant-treated fibres.

Conclusions

This work has identified some potentially important surface chemical features of the wetting of glass fibres by water. In addition, a new approach to water wetting in the presence of an oil phase in a dual-liquid situation is described for the first time. This has enabled the determination of a three-phase contact angle made with the fibre.

Acknowledgements

This project was funded by Air BP and the UK Ministry of Defence.

References

(1) Hazlett, R.N. *Ind. Eng. Chem. Fund.* **1969**, *8*, 625-632; *8*, 633-640

(2) (a) Taylor, S.E. unpublished observations; (b) Hughes, V. "Aviation Fuel Handling: New Mechanistic Insight to the Effects of Surfactants on Water Coalescer Performance", Presented at *6th International Conf. On Stability and Handling of Liquid Fuels*, Vancouver, 1997

(3) Ross, S.; Morrison, I.M. *Colloidal Systems and Interfaces*, Wiley-Interscience: New York, 1988; p 77

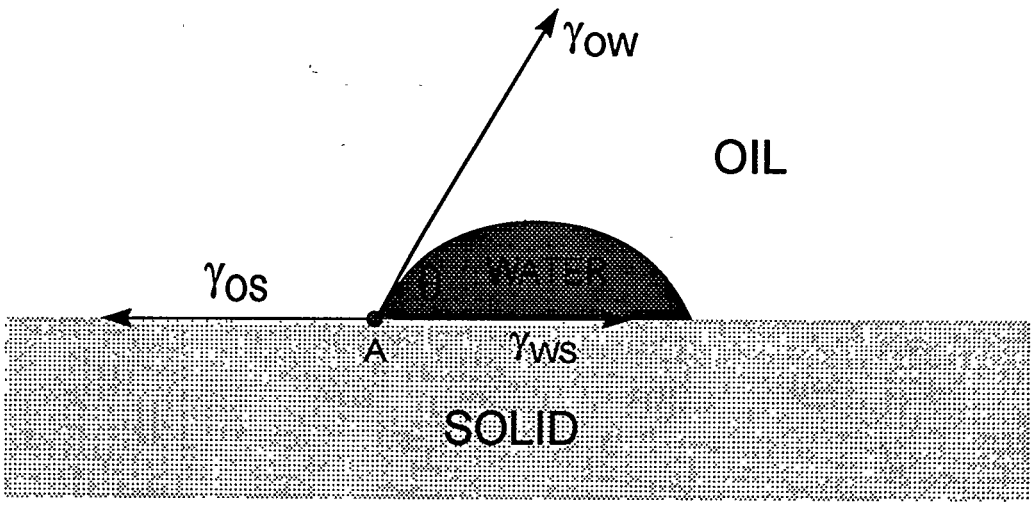


Figure 1. Schematic representation of a water drop at equilibrium on a solid surface, making a contact angle θ with the surface under the influence of the respective interfacial forces indicated.

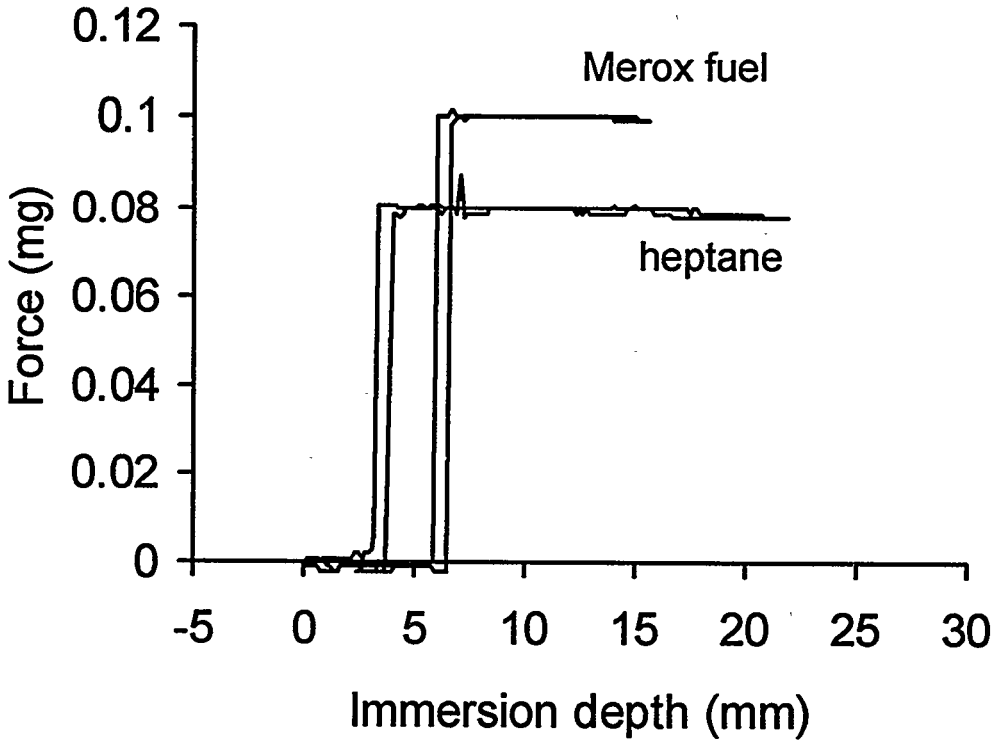


Figure 2. A typical force-immersion depth trace for fibre wetting by *n*-heptane and Merox fuel.

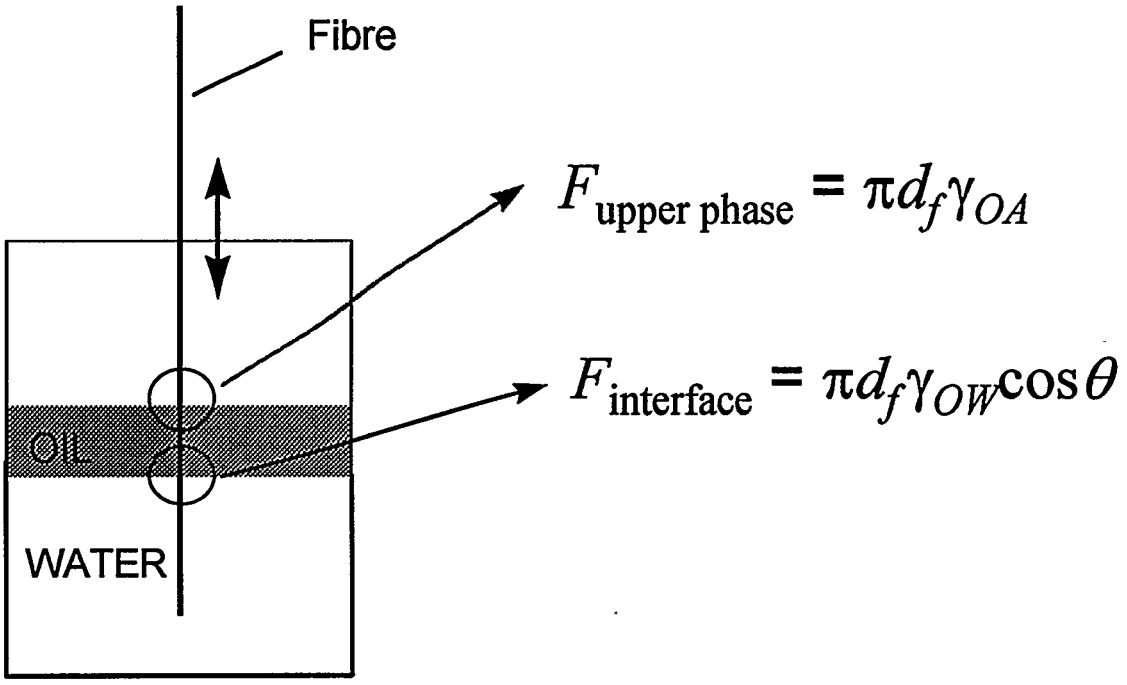


Figure 3. Schematic of the dual-liquid system.

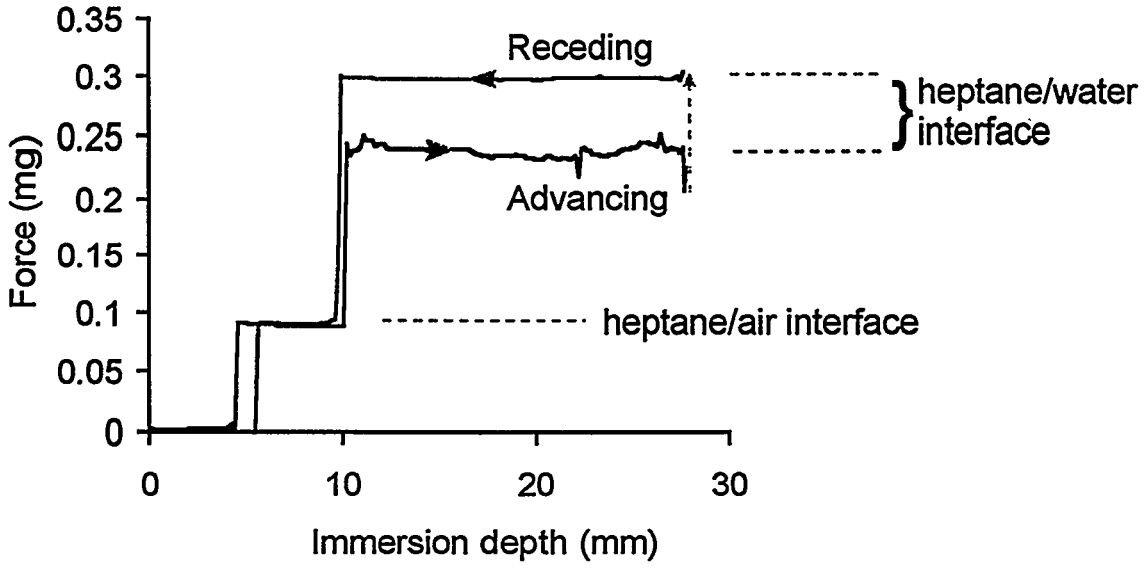


Figure 4. Typical form of fibre force-immersion depth profiles for an interfacial system in the dual-liquid approach.

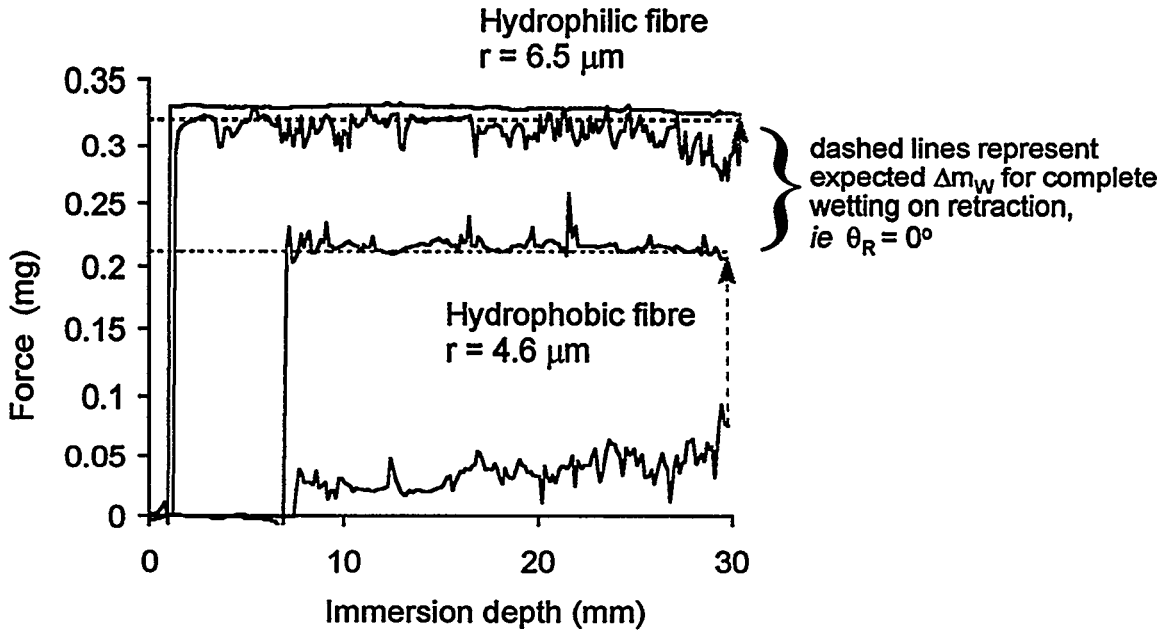


Figure 5. Force-immersion depth traces for types I and II fibres in water.

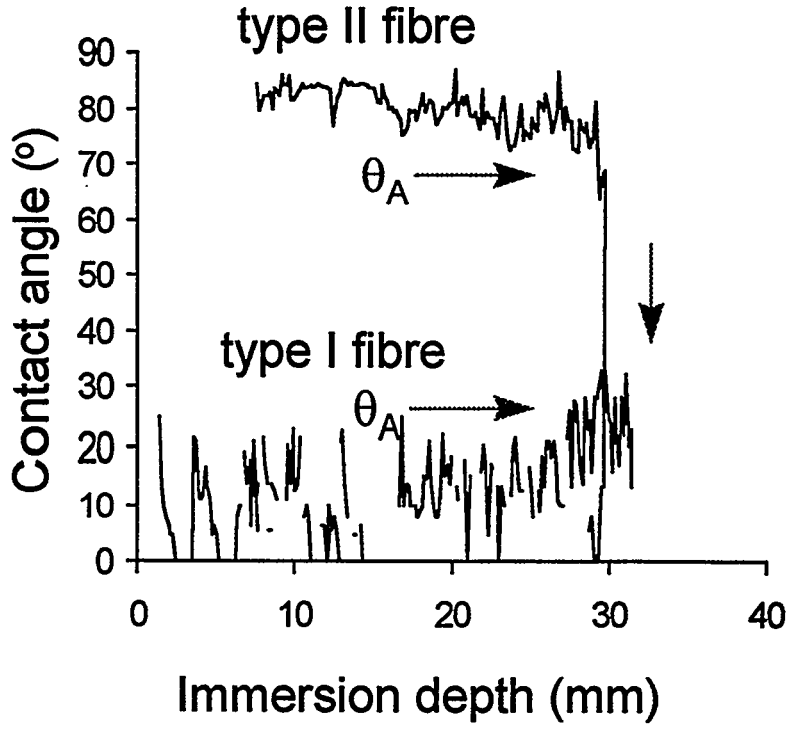


Figure 6. Advancing contact angle profile for types I and II fibres.

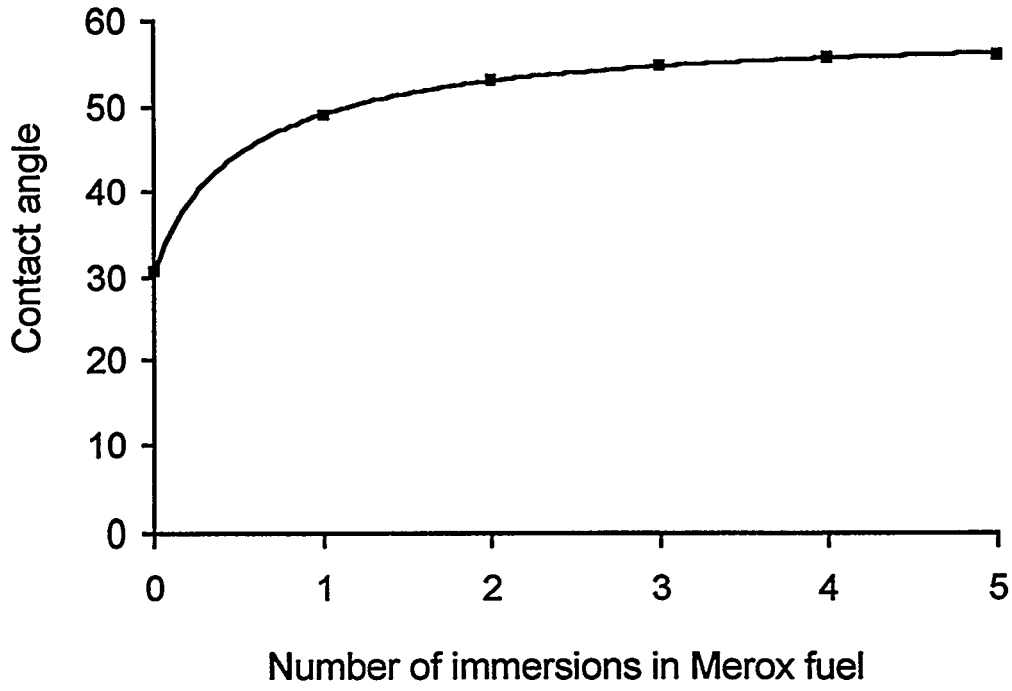


Figure 7. Effect of the number of immersion/drying exposures to Merox fuel on the resulting contact angle against water.

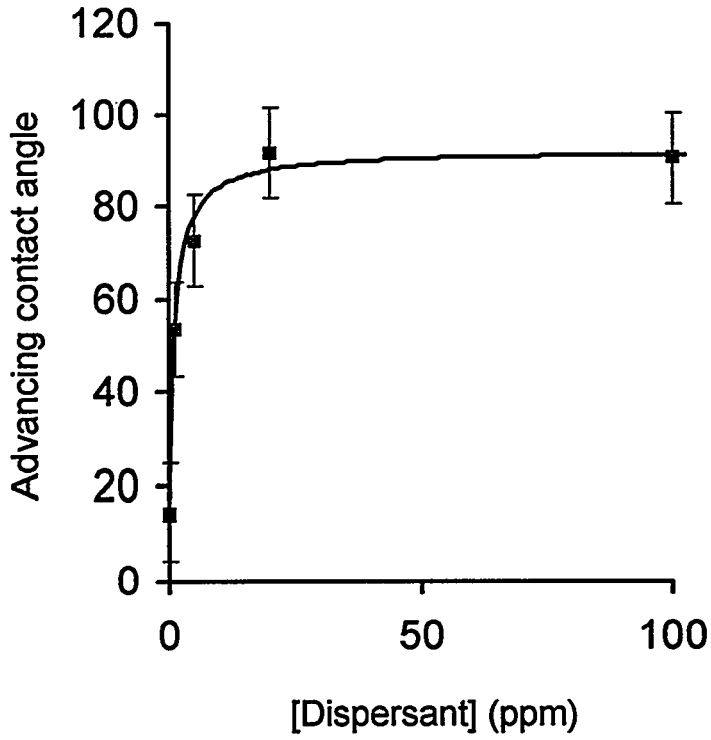


Figure 8. Effect of dispersant concentration on the mean advancing contact angle for a type I fibre.

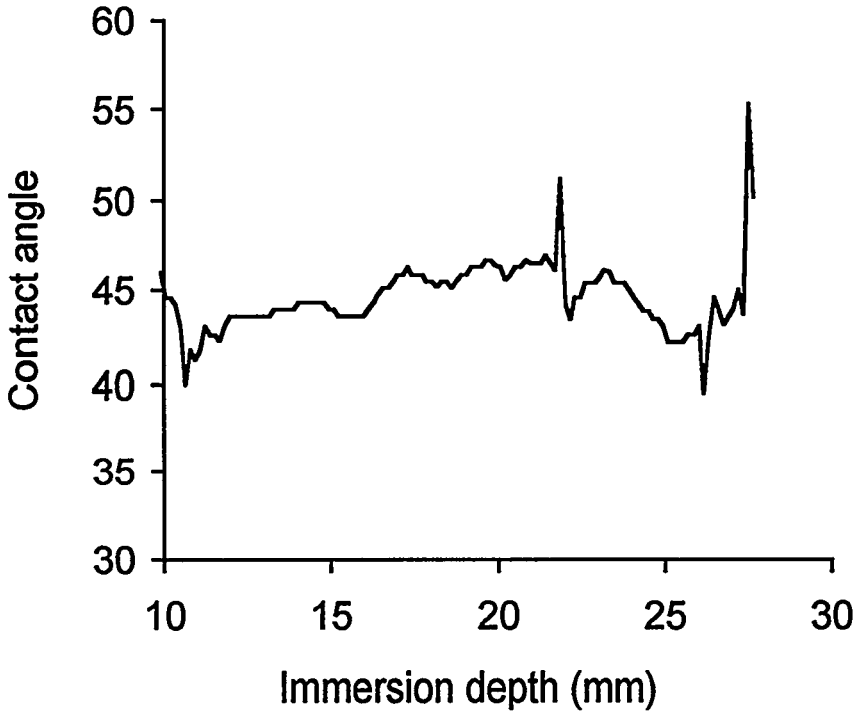


Figure 9. Example of an advancing contact angle profile along a type I fibre determined in the dual-liquid system.

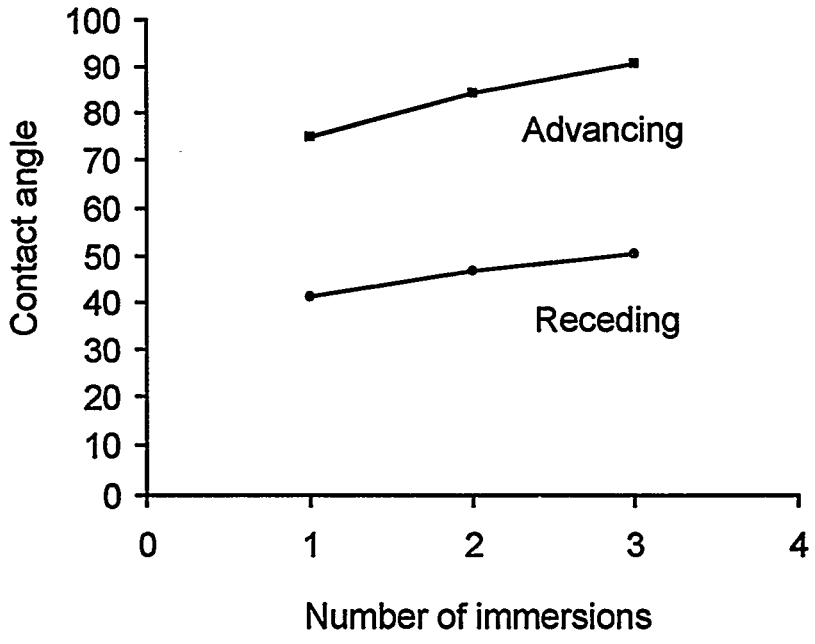


Figure 10. Effect of the number of immersion cycles in Merox fuel on the advancing and receding contact angles of a type I fibre.

6th International Conference
on Stability and Handling of Liquid Fuels
Vancouver, B.C., Canada
October 13-17, 1997

STADIS® 450 IN AVIATION FUEL APPLICATIONS - UPDATED

Cyrus P. Henry Jr.

Octel America, Inc., 200 Executive Drive, Newark DE 19702 USA

At the October, 1994 International Conference in Rotterdam, information was presented on the use of Stadis® 450 in certain fuels, mainly chemically sweetened, which contain interacting trace impurities resulting in several difficulties. A slightly modified product has now been introduced which overcomes a potential to form a precipitate containing a dodecylbenzene sulfonate. This modified additive has now been fully accepted by airframe and turbine manufacturers and is fully commercialized; production of the old formulation ceased in December 1996. The status of the transition to the modified product is reviewed. Additionally, progress has been made in understanding the relationship of the results from ASTM D 3948 water separation tests, and the actual performance of coalescers in the industry. This has lead to changes in aviation fuel specifications, and to a program in ASTM to better define an improved test method to predict coalescer performance. Overall, fewer difficulties are expected in the future.

INTRODUCTION

At the 5th International Conference on Stability and Handling of Liquid Fuels, a paper [1] was presented which detailed a number of concerns about Stadis® 450 in chemically sweetened aviation fuels, and efforts underway to understand and rectify them. Two fundamental problems and their various ramifications were discussed. The first dealt with disarmed coalescers found at the Munich airport, which was due to formation of an insoluble dodecylbenzene sulfonate in the fuel. This accumulated on coalescers while operating with dry fuel, but led to a failing result when a coalescer was removed from the fuel system and evaluated in the single element test. This was caused by the dodecylbenzenesulfonic acid component in Stadis® 450. A modification of Stadis® 450 was developed and discussed which overcame this problem, and consideration of changing over to its use was discussed. That has now been completed, and is reviewed.

The second problem was more general in nature; some Merox™-sweetened fuels containing Stadis® 450 show conductivity loss during storage. Stadis® 450 also tends to have a greater effect on the D 3948 [2] MSEP rating of these fuels. The combination of these effects

makes it difficult to assure supply of fuel to airports which meets both conductivity and water separation requirements. That work led to the conclusion that the fundamental aspects of testing to simulate coalescer performance needed to be addressed, and is also reviewed. This paper is a general review of the activities leading to resolution of these problems, and of other recent activities.

"DINNSA" STADIS® 450 INTRODUCED

The concept of replacing dodecylbenzenesulfonic acid (DDBSA) with dinonylnaphthylsulfonic acid (DINNSA) in the Stadis® 450 formulation was discussed at the last conference[1]. At that time the concept was shown viable in small scale testing, but a full-scale demonstration had not yet been carried out; a great deal of work was needed to fully verify suitability, and steps needed to implement a transition had not been defined. This has all been completed, as follows.

First, data were developed comparing performance of the two formulations. These results included properties of the modified additive, relative conductivity-improving performance, electrostatic charging properties, various aspects of water separation, effects on thermal stability, compatibility with other jet fuel additives in fuels and aircraft fuel system materials, and compatibility of the old and new additives. This was completed in July, 1995 and a report is available detailing the findings [3]. Lot 1 of modified Stadis® 450 was produced in September, 1995. Feasibility of manufacturing was demonstrated thereby, and an adequate store of material obtained for general testing and trial purposes, but not released for general use in aviation fuels.

Next, large-scale tests were carried out at the OMV refinery in Berghausen, Germany. These demonstrated that the modified product was indeed useful and solved the problem. On two occasions, 5,000 m^3 batches of Jet A-1 fuel containing the modified Stadis® 450 were circulated through a coalescer vessel then elements were removed and evaluated in the single element test. These were successful, and showed no signs of coalescer deactivation. These fuel batches were downgraded and not used as jet fuel, since the modified product was not fully accepted.

These results provided the necessary motivation for aircraft and turbine manufacturers to consider the acceptability of the modified product. Acceptance was requested from Boeing, Airbus Industries, Fokker, Lockheed, McDonnell Douglas, British Aerospace, General Electric,

Pratt & Whitney, Pratt & Whitney Canada, Rolls Royce, Garrett (Allied Signal), the United States Air Force, the British Ministry of Defence, CAA, and indirectly, FAA. All of these parties had accepted the use of DINNSA in place of DDBSA in the Stadis® 450 formulation by May, 1996. In the meantime, members of ASTM Subcommittee J on Aviation Fuels, the IATA Aviation Fuel Working Group, the Canadian General Standards Board Aviation Fuel and Related Products Committee, and the MOD Aviation Fuel Committee, and the CRC Coalescer Deactivation Panel were all fully apprised of the work in progress.

It was also agreed that the name of the additive would not be changed, and the modified product would still be identified as Stadis® 450; this resulted in no need to revise any specification or document which referred to "Stadis® 450". It was not possible to develop a satisfactory laboratory test to determine whether this form of coalescer deactivation might occur with DDBSA Stadis® 450. Because it was determined unsatisfactory to have two different forms of Stadis® 450 in use, Octel America agreed to a complete transition to DINNSA Stadis® 450 upon completion of trials.

During the period May to December 1996, these acceptances were the basis for limited use of the DINNSA Stadis® 450 in aviation turbine fuel at several sites where performance was carefully monitored. Commencing in October, 1996 modified Stadis® 450 was used in fuel produced at the OMV Burghausen refinery and sent to Munich airport. On two occasions during the period October – December 1996, coalescers were removed from the fuel distribution system and evaluated in the single element test; excellent results were obtained. The second testing was after 57,000 m^3 (approximately 360,000 barrels) of fuel had flowed through the coalescer vessels. The success of these trials fulfilled the final requirement to begin a complete transition to the modified product.

The last lot of DDBSA Stadis® 450 was manufactured in December 1996 and all customers were notified. Early in 1997 all supplies of DDBSA at Octel America, Inc. were exhausted, save a small reserve for non-aviation applications. We anticipate that it will take some time before all supplies of DDBSA Stadis® 450 are depleted in customers' hands. Further information is available on the transition [4]. No difficulties related to the modification have been reported as of this date.

IMPROVING THE CONDUCTIVITY/MSEP RATING TRADEOFF IN MEROX-SWEETENED FUELS

In the previous paper we noted that some, but not all, chemically-sweetened jet fuels exhibit loss of conductivity during storage following treatment with Stadis® 450. Results from several treatment options were discussed. These have been more extensively evaluated, and have not proven generally successful for refineries which have varied crude slates. These included filtration through alumina, acid washing, reduction of filming amine additive in the processing equipment, and improved water washing. At several refineries, conductivity retention and D 3948 MSEP test results were shown to vary substantially depending on the crude oil slate in use. This demonstrated that frequent changeout of the attapulgus clay tower is, in many cases, not a satisfactory solution. While absorbent clay removed interacting species, some are apparently not strongly absorbed and are quickly eluted. Strong surfactants, on the other hand, are very polar and absorbed permanently. Fuels were examined where each of these options gave acceptable improvement, but additional fuel samples from the same refinery often did not respond the same way. For a refinery producing 10,000 bbl/day of jet fuel, installing an additional absorbent tower for alumina, or an acid washing step, represents significant investment which might be acceptable if known to be a consistent solution – but not otherwise.

This led to a conclusion that a general solution to the conductivity/MSEP tradeoff difficulties could not be identified, mainly because the variable nature of the interacting trace materials in jet fuel. In the meantime, we were aware that API Publication 1581 "Specifications and Qualification Procedures for Aviation Jet Fuel Filter/Separators", 3rd Edition [5] had been amended to allow use of 3.5 mg/L of Stadis® 450 in place of 0.75 mg/L of ASA-3 during qualification testing. This level was set by determination of water coalescing performance in modern coalescers, and was intended to provide the same level of severity for coalescer vessel qualification purposes. Yet, we were well aware that most fuels containing these levels of conductivity additives would show vastly better D 3948 MSEP test results with ASA-3 than with Stadis® 450! Overall, this led to two conclusions which were discussed at the April 1997 meeting of the Coordinating Research Council (CRC) Aviation Fuel, Lubricant and Equipment Research Committee meeting [6].

- *The only universal remedy for the conductivity/MSEP problems encountered for Merox sweetened jet fuels produced at many refineries was to replace with hydrogen*

treating sweetening processes. Since there are about 150 jet fuel Merox units world-wide, the cost would be formidable.

- *The results of API / IP studies leading to the API 1581 amendment suggested that this was not necessary: a better remedy was to find a water separation test method which had a better correlation with field performance of coalescers.*

As a consequence of these discussions, several initiatives were quickly undertaken. At the June ASTM meeting, a Task Force on Water Separation Test Methods was established to determine if an improved D 3948 Test Method could be developed, or an alternative method could be defined which would better predict water separation properties of fuels in full scale coalescers. A CRC report was assembled which reviewed available literature and data and concluded that "the customary minimum MSEP of 70 can be relaxed when a drop in rating is ***specifically due to the addition of Stadis® 450"*** [7]. This led to a relaxation of MSEP requirements in Canadian and British aviation turbine fuel specifications [8,9]

The work of the Task Force on Water Separation Test Methods led to development of an improved version of the D 3948 Test Method, which is being evaluated. The modified method uses a mini-coalescer for the test which better mimics modern filter coalescer media, and is a promising lead toward providing a test method to assure jet fuel remains adequately free of coalescer-disarming surfactants during distribution. The modified test coalescer reflects current trends toward using a fiberglass-containing filter media, which initiates coalescence prior to flow through the outer fiberglass wraps. This material is much finer, and intercepts smaller water droplets. Other test work indicates that Stadis® 450 tends to cause smaller water droplets to form when water is emulsified with fuel. However, when the modified test coalescer is challenged with fuel containing Aerosol OT surfactant, it gives similar results to the current test coalescer. It is, however, necessary to re-evaluate the ratings obtained with the two versions of the method to establish correlation. This is especially important to assure that the aviation fuel industry knows what rating with the new method correlates with the 85 rating value traditionally thought to be the borderline for "surfactant-free" fuel.

OTHER RELATED ACTIVITIES

The changes which have been implemented in specifications which note MSEP requirements, and the ongoing D 3948 MSEP test method activities have reduced worries about

conductivity loss and MSEP effects for fuels containing Stadis® 450. We still view these problems as serious concerns which need further work to help refiners deal with any difficulties involving use of Stadis® 450, but the these are now reduced to the inconvenience of re-doping when necessary.

Conductivity and Light Exposure

Studies have shown that exposure to sunlight can cause dramatic, permanent loss in the conductivity of fuels containing conductivity improving additives. This has been demonstrated in borosilicate glass and in polytetrafluoroethylene bottles, and probably occurs in other transparent or UV transparent containers. Glass containers are frequently used on refineries to obtain quality control samples for laboratory measurement. The data in Table 1 were obtained for three kerosine jet fuel samples with conductivities of 385 - 550 pS/m obtained by treatment with Stadis® 450, in 500 mL borosilicate glass or in polytetrafluoroethylene (PTFE) containers after exposure to Mid-Atlantic Summer sunlight. Slower loss is expected from fluorescent lights or other uv sources. Similar effects were found with various other conductivity additives. An Octel Additive Brief has details of these findings [10].

Table 1. Conductivity Loss from Sunlight Exposure

Container	% Conductivity Loss at designated exposure interval		
	5 min	20 min	95 min
Amber Glass	0	0-16	1-47
Clear Glass	0-58	66-71	78-89
PTFE	22-70	76-80	81-90

These conductivity losses occur only with parts per million solutions of these additives in fuels. Thirty days daylight exposure of concentrated Stadis® 450 as supplied, or of a 5% solution in kerosine, did not result in a measurable conductivity loss when these were then used to treat fuels. Modification of D 2624 Conductivity Test Method and Practice D 4306 on containers for jet fuel has been recommended commensurate with these findings.

Fuel Temperature and Conductivity Loss

Some time ago we studied chemically sweetened jet fuel from a refinery in Canada which tended to exhibit rapid conductivity loss after treatment with Stadis® 450, but it was observed that such losses were especially troublesome during hot summer months. This led us to evaluate the rate of conductivity loss exhibited by jet fuels as a function of temperature. Five Jet A and Jet A-1 fuels were chosen, several of which were known to exhibit conductivity loss problems. These were treated to obtain a moderately high conductivity. Half-liter samples in Teflon™ bottles were then stored at 4.4°C, 21°C, and at 43°C, and conductivity measured at the stored temperature over time [11]. Rate of conductivity loss generally showed a temperature relationship which is typical for slow chemical reactions. The one exception was Fuel B when stored at 4.4°C. This was from a refinery which has typically low aromatics content (12-14%) jet fuel, and the results indicate that some degree of micell formation or other phenomena may play a role. Results are in Tables 2, 3, 4, 5, and 6. We then prepared fresh samples of four of these fuels at 21°, determined conductivity after Stadis® 450 doping, and stored them 16 hours at 79°C. The samples were cooled for 3 hours back t[illegible]C, and conductivity re-measured. Results were in good agreement with data obtained after 4 t[illegible] weeks at 43°C. This technique needs additional work, however, to assess the reliability of the correlation. Prior to this work, we believed that the trend of conductivity stability would be apparent after two weeks storage at ambient temperature. These results indicate longer storage is needed to fully assess the potential for conductivity loss. We plan further work to fully develop this methodology, which will help to determine an appropriate initial conductivity, and to assess the possible need for further re-doping to assure minimum conductivity requirements are met.

Table 2. Fuel A (Jet A, processing unknown; 1 mg/L Stadis® 450)

Storage Temp °C	Initial PS/m, 21C	3 Hr pS/m at Temp	% Conductivity Change During Storage (Compared to 3Hr Result)				
			1 wk	2 wk	3 wk	4 wk	5 wk
4.4	274	179	+2	-4	+18	0	+7
21	268	248	-5	-9	-14	-22	-30
43	269	434	-20	-30	-32	-24	-31

Table 3. Fuel B (Jet A-1, Merox sweetened, 2 mg/L Stadis® 450)

Storage Temp °C	Initial PS/m, 21C	3 Hr pS/m at Temp	% Conductivity Change During Storage (Compared to 3Hr Result)				
			1 wk	2 wk	3 wk	4 wk	5 wk
4.4	285	235	-43	-55	-48	-60	-66
21	282	253	+7	-9	-14	-22	-30
43	294	547	-3	-15	-36	-54	-69

Table 4. Fuel C (Jet A-1, Merox sweetened, 2.5 mg/L Stadis® 450)

Storage Temp °C	Initial PS/m, 21C	3 Hr pS/m at Temp	% Conductivity Change During Storage (Compared to 3Hr Result)				
			1 wk	2 wk	3 wk	4 wk	5 wk
4.4	297	188	-13	--	-3	-15	-11
21	322	272	0	-8	-14	-21	-29
43	305	618	-19	-68	-66	-64	-65

Table 5. Fuel D (Jet A-1, Merox sweetened, 2 mg/L Stadis® 450)

Storage Temp °C	Initial PS/m, 21C	3 Hr pS/m at Temp	% Conductivity Change During Storage (Compared to 3Hr Result)				
			1 wk	2 wk	3 wk	4 wk	5 wk
4.4	329	216	-4	-4	-2	-9	-8
21	340	321	-30	-11	-17	-27	-39
43	330	636	-16	-77	-75	-77	-76

Table 6. Fuel E (Jet A-1, Merox sweetened, 2 mg/L Stadis® 450)

Storage Temp °C	Initial PS/m, 21C	3 Hr pS/m at Temp	% Conductivity Change During Storage (Compared to 3Hr Result)				
			1 wk	2 wk	3 wk	4 wk	5 wk
4.4	438	260	-2	+23	+7	0	0
21	450	399	+5	-18	-22	-28	-45
43	430	816	-27	-84	-85	-87	-85

Table 7. Conductivity of Jet Fuels After Heating 16 Hours at 79°C, and Cooling

Fuel	S450 Conc., mg/L	Initial Cond., 21°C	Cond. After 16 Hr 70°C Aging, and cooling 3 Hr to 21°C
A - Jet A	1	262	172 (-34%)
B – Jet A-1	2	315	137 (-57%)
D – Jet A-1	1.5	328	80 (-76%)
E – Jet A-1	1.5	371	67 (-82%)

Based on these results, we suggest the following.

- *Conductivity loss in Merox-sweetened jet fuels will be minimal when fuel is stored at low temperature. Loss can be further minimized by delaying treatment with Stadis® 450 during cold weather until after the fuel has cooled.*
- *Under most conditions, the likely maximum loss in conductivity during extended storage of jet fuel can be estimated by storing samples at 80°C for 16 hours, cooling to room temperature, and re-measuring conductivity.*

CONCLUSIONS

The possibility that insoluble sulfonates will form in jet fuel resulting in disarming of coalescers has been successfully addressed by introduction of a slightly modified Stadis® 450 with a new sulfonic acid stabilizer. The transition to this modified product has proceeded smoothly with no known difficulties.

Difficulties with the conductivity – MSEP tradeoff have been successfully addressed. Work is progressing to improve or develop test methods to better predict coalescer performance. Data suggest that the rate of conductivity loss which occurs during storage of some fuels follows a temperature relationship. This relationship predicts fewer problems at low fuel temperatures, and suggests that conductivity loss can be predicted with an accelerated test method.

Octel America, Inc. maintains information on Stadis® 450 in aviation fuels on the world wide web; address is www.octel-petadd.com.

ACKNOWLEDGEMENTS

Many individuals contributed to the success of the work reported above. The author wants to especially acknowledge the efforts of Ed Matulevicius, Exxon R&E and Vic Hughes, Shell Research who co-chaired the CRC Panel on Coalescer Deactivation; Udo Lauks, OMV – Berghausen, whose full cooperation and expert handling was crucial to the refinery trials with modified Stadis® 450; and finally, Andy Holden of British Airways who was a great help in obtaining the necessary aviation equipment manufacturers' acceptance of modified Stadis® 450.

REFERENCES

1. Henry, C.P., *Proceedings of the 5th International Conference on Stability and Handling of Liquid Fuels,* Giles, H.N. (Ed); U.S. Department of Energy, Washington DC, **1995**, 59-73.

2. ASTM D 3948-93 "Standard Test Method for Determining Water Separation Characteristics of Aviation Turbine Fuels by Portable Separometer", *Annual Book of ASTM Standards Vol. 5.02,* American Society for Testing and Materials, West Conshohocken, PA.

3. Henry, C.P. "Modified Stadis® 450 – Supporting Information on Composition and Performance", PLMR-7-95, Octel America, Inc., Newark DE, **1995.**

4. Henry, C.P. "Transition Underway for Modified Stadis® 450 in Aviation Fuels", Octel America Additive Brief 97-01, Octel America, Inc., Newark DE, **1997.**

5. API *Specifications and Qualification Procedures for Aviation Jet Fuel Filter/Separators,* API Publication 1581, 3rd Edition, May 1989 and amendment, API, Washington DC.

6. Minutes of the Aviation Fuel, Lubricant and Equipment Research Committee of the Coordinating Research Council, April 27, **1995.**

7. "The Effect of Stadis® 450 on MSEP Rating and Coalescence – Technical Basis of Re-doping Turbine Fuels with Stadis® 450", CRC Report No. 601, CRC, Atlanta GA, **1996.**

8. Defence Standard 91-91/Issue 2, "Turbine Fuel, Aviation Kerosene Type, Jet A-1", Ministry of Defence Directorate of Standardization, Glasgow, UK, **1996**.

9. CAN/CGSB-3.23-93 "Aviation Turbine Fuel – Kerosine Type", Amendment No. 4, Canadian General Standards Board, Ottawa CANADA, **1997**.

10. Henry, C.P., "Conductivity of Fuels After Exposure to Sunlight", Octel America Additive Brief 97-07, Octel America, Inc., Newark DE, **1997**.

11. Henry, C.P., Garcia, A.W. , Montgomery, N.E., and Horack, J.J. "Guidelines for Laboratory Evaluations of Stadis® 425 and Stadis® 450 Conductivity Improver Additive", Octel America Additive Brief 96-09, **1996**.

6th International Conference
on Stability and Handling of Liquid Fuels
Vancouver, B.C., Canada
October 13-17, 1997

THE EFFECT OF PHENOLIC IMPURITIES IN JET FUEL ON THE BEHAVIOUR OF CONDUCTIVITY IMPROVERS

Brian Dacre and Janice I. Hetherington*.

Rutherford Laboratory, Royal Military College of Science, Cranfield University, Shrivenham, Swindon, Wiltshire,
SN6 8LA, United Kingdom.

ABSTRACT

The conductivity improver Stadis 450 is known to give a variable conductivity response in jet fuels which come from different crudes and refinery processes. The present work shows that certain phenolic impurities in the jet fuel may be responsible for these variations and that fuels with a high phenolic content could be particularly prone to poor conductivity response with Stadis. Conductivity measurements on Stadis in model systems have shown that certain phenols interact with Stadis to cause considerable reductions in the conductivity. The magnitude of the effect is highly dependent on the concentration and the structure of the phenol and especially on whether the phenol is hindered or unhindered. Unhindered simple phenols such as m-cresol, p-cresol and phenol, at concentrations above 50ppm, cause a large reduction in the conductivity response with Stadis. Highly hindered phenols, such as the types used as antioxidants (2,6-di-tert-butyl-4-methylphenol), cause almost no reduction in the conductivity. This confirms the findings of the antioxidant suppliers. Partially hindered phenols such as 2-tert-butyl-4-methylphenol are intermediate in their effect on the reduction of the conductivity. Jet fuels analysed by BP revealed total phenol concentrations as high as 700ppm, which is considerably higher than had previously been expected. Of these phenols, 80% were found to be of the simple, low molecular weight, unhindered type, such as m-cresol, which were found in the model systems work to have the most damaging effect on the conductivity of Stadis. The conductivity of Stadis was measured in fuels of known phenolic content. The response was found to be lower in fuels of high phenolic content, thus confirming the behaviour predicted from model phenol systems. The role of the phenols on the conducting mechanism of Stadis is discussed. It is proposed that the phenol is involved in a proton donor interaction with a component of the Stadis, possibly the sulphone and that this interferes with the normal ion producing mechanism which imparts conductivity to Stadis-doped fuels.

1 INTRODUCTION

Jet fuel has a very low natural electrical conductivity, normally less than $5pSm^{-1}$. It is well known that dangerous levels of electrostatic charge can accumulate during the high speed pumping and filtration of jet fuel[1,2]. This can be overcome by increasing the electrical conductivity of the fuel which is achieved by the use of a static dissipator additive. Only one static dissipator additive is approved for this purpose, namely Stadis, supplied by Octel America. However, considerable variation is observed in the conductivity response of fuels from different crude oils when doped with the same amount of Stadis.

In earlier papers[3,4,5] we have reported the influence of a wide range of possible fuel components on the performance of Stadis. Sodium salts of acid impurities in the fuel were found[4] to have a complex effect on the conductivity. The salts at low concentrations were found to reduce, by as much as 50%, the conductivity performance of Stadis, with a minimum value of the conductivity occurring when the ratio (in ppm) of sodium salt to Stadis was approximately unity. At higher concentrations of the salts the conductivity response was enhanced. The sodium salts have a significant, but complex, effect on the water separation characteristics of model systems.

Preliminary work on phenols[4] indicated that some phenolic impurities also caused considerable conductivity loss, as great as 70%, in Stadis. The conductivity decreased non-linearly with phenol concentration but did not exhibit the conductivity minimum found with the sodium salts. The magnitude of the effect was dependent on the type of phenol and appeared to contradict the well documented knowledge that commercial phenolic antioxidants such as BHT (2,6-di-tert-butyl-4-methyl phenol) had no effect on the conductivity response of Stadis.

2 AIMS OF THE WORK

This work continues the theme of our earlier published work[3,4,5] with the aims of:

- investigating the influence of fuel components on the performance of the static dissipator additive Stadis 450,

- attempting to understand the nature of the intermolecular interactions occurring in Stadis 450 which impart conductivity to a fuel,
- attempting to understand, in terms of the intermolecular interactions occurring, the role of fuel components and impurities in assisting and obstructing that mechanism.

Our earlier work on phenols suggested that Stadis was sensitive to some types of phenolic impurities. The effect was greater and showed a different concentration dependence to the sodium salt impurities which we have studied in detail[4]. These findings appeared to conflict with the knowledge that antioxidants of the hindered phenolic type had no effect on the conductivity response of Stadis.

It was to clarify these points that a comprehensive study has been made of the influence of a range of unhindered, partially hindered and highly-hindered phenols on the conductivity of Stadis in dodecane solutions. The parameters studied are: (a) phenol type, (b) phenol concentration, (c) time effects, (d) comparison of response of Original Stadis 450 and Reformulated Stadis 450, (e) pK_a of the phenol.

The study of phenols in model systems is compared with the role of phenols in jet fuels doped with Stadis. To support this work BP has supplied fuels, analysed for phenol concentrations, phenol type and sources of phenolic impurities. The conductivity behaviour of Stadis in these fuels is characterised for the effects of: (g) fuel phenol levels, (h) fuel viscosity, (g) methods of removal of phenolic impurities.

These results are used to support a theoretical treatment of the equilibria for the interactions of the phenols with the Stadis. By elucidating the nature of the reaction it is hoped to increase the understanding of the conducting mechanism of Stadis and the sensitivity to impurities which could destroy or enhance the conductivity.

3 EXPERIMENTAL

3.1 Materials

Original Stadis 450 was supplied by Octel. Reformulated Stadis 450 was supplied by DuPont. *m*-cresol (3-methylphenol) was purchased from BDH Chemicals. The following phenols were purchased from Aldrich Chemical Company: 2,6-dimethylphenol, 2,4,6-trimethylphenol, 2-*tert*-butyl-4-methylphenol, 2-*tert*-butyl-6-methylphenol, 2,6-di-*tert*-butyl-4-methylphenol, o-cresol (2-methylphenol), *p*-cresol (4-methylphenol), phenol, 2-nitrophenol, 3-nitrophenol, 4-nitrophenol.

Dodecane was supplied by BDH Chemicals / Merk and purified as described previously[3]. Toluene (Analar) and acetone (Analar) were supplied by BDH Chemicals / Merk.

Jet fuels were supplied by BP.

3.2 Conductivity Equipment and Conditions

Conductivity measurements were made at 25C using the apparatus and experimental procedures described in previous work[3,4]. The uncertainty in the conductivity measurements with the laboratory built apparatus is estimated to be ±4%.

Concentrated stock solutions (~2000ppm) of each of the phenols listed above but excluding the nitrophenols, were made up in toluene and these were added to the Stadis solutions in the conductivity cells at the concentrations indicated in Section 4. The effect of toluene on the conductivity of the Stadis solutions is negligible at the concentrations employed. In the case of the nitrophenols concentrated stock solutions were made in acetone due to their limited solubility in toluene. The contribution to the conductivity from the nitrophenol / acetone system alone was always below 15pSm^{-1}.

4 RESULTS AND DISCUSSION

4.1 Effect of Model Phenolic Impurities on the Conductivity of Stadis 450 in Dodecane

The effect of a range of phenols on the conductivity of a 3ppm solution of Stadis 450 in dodecane is given in Figure 1. The most significant feature is the difference in the effect of the hindered and unhindered phenols on the conductivity response of Original Stadis 450.

The highly hindered phenol 2,6-di-*tert*-butyl-4-methylphenol has no effect on the conductivity of the Stadis 450 solution. This supports the general view in the industry that the antioxidant 2,6-di-*tert*-butyl-4-methylphenol (BHT) does not affect the behaviour of Stadis 450. It suggests that any similarly hindered phenol with large groups on the 2-, 6- positions will have no effect on the performance of Stadis.

The unhindered, simple phenols, by contrast, greatly reduce the conductivity of the Stadis solution. Phenol and *m*-cresol show the most pronounced effects with concentrations of 100ppm causing reductions of 50% in the conductivity and higher concentrations of 750ppm causing reductions of 80% in the conductivity. The analysis of the BP fuels indicated that levels of 100ppm of simple phenols regularly occur in fuels and that levels as high as 750ppm have been found.

The partially hindered phenols reduce the performance of Stadis, with the magnitude of the effect being as expected from the steric restrictions imparted on the -OH group or the phenoxide ion by groups in the 2- and/or 6- position. For example, the effect of 2-*tert*-butyl-4-methylphenol on the conductivity is intermediate between that for phenol and 2,6-di-*tert*-butyl-4-methylphenol.

The same trends are apparent when equimolar concentrations of the phenols are considered.

It should be noted that where there is a decrease in the conductivity for a phenol, the effect is nonlinear with the concentration and that there is no minimum in the conductivity versus concentration plot as was reported for sodium salt impurities in the previous paper in this

series[4]

4.2 Time Effects on the Conductivity of Stadis Solutions Containing Phenols

The conductivity of Stadis solutions in dodecane containing 650ppm of *m*-cresol and 2,6-di-*tert*-butyl-4-methylphenol remained unchanged from the values in Figure 1 when measured over a period of seven days. This confirms the lack of response of the conductivity of the Stadis solutions to highly hindered phenols and rules out the possibility of mobility or diffusion effects accounting for the difference in behaviour compared with simple unhindered phenols such as *m*-cresol.

The phenol concentrations of 650 ppm in these model systems were chosen to be representative of the level of phenolics measured in a fuel identified as exhibiting a drop in conductivity over a period of several days. These data indicate that although a poor response of Stadis in some fuels may be attributed to high levels of simple phenols, the phenols are unlikely to be responsible for any long term drop in conductivity.

4.3 Comparison of the Effect of Model Phenolic Impurities on the Conductivity of Reformulated Stadis 450 and Original Stadis 450 in Dodecane

In the presence of phenolic impurities the Reformulated Stadis 450 shows the same conductivity behaviour as the Original Stadis 450. Figure 2 for the Reformulated Stadis and Figure 1 for the Original Stadis show that simple phenols such as *m*-cresol at concentrations of 100ppm and above, greatly reduce the performance of both types of Stadis. Hindered phenols, even at concentrations as high as 1000ppm, have very little effect or no effect on either type of Stadis.

4.4 Dependence of Conductivity on Stadis Concentration at Constant Phenol Concentration

The poor conductivity response of Stadis even at relatively high concentrations in the presence of unhindered or partially hindered phenols is illustrated in Figure 3. The phenol concentration of 550ppm is typical of that found in fuels with high levels of phenolic impurities.

The data for *m*-cresol are particularly significant by showing that increasing the concentration of Stadis from 1ppm to 5ppm, the maximum level used in the industry, produces very little increase in the conductivity. This mimics the poor conductivity response reported for some fuels on increasing the Stadis concentration. These results suggest that the fuels in question had a high level of phenolic impurities.

Partially hindered phenols also depress the response of Stadis, but the effect is intermediate between that for the unhindered phenols and that in the absence of any phenols, as illustrated by the data for dodecylphenol.

The previous paper in this series[4] discussed the effects of sodium salts on the conductivity of Stadis solutions. The depression of Stadis performance is considerably greater in the presence of unhindered phenols than sodium salts when each are considered at the concentrations likely to be encountered in fuels.

4.5 Effect of pKa of Phenolic Impurities on the Conductivity Perform ance of Stadis 450

The magnitude of the effect of a phenol in relation to its pK_a is unclear from the data presented in Figure 1. There the magnitude of the effect is in the order:

phenol > *m*-cresol > *o*-cresol > *p*-cresol

whereas the relative order expected from consideration of the pK_a values would be:

phenol (9.95) > *m*-cresol (10.08) > *p*-cresol (10.19) > *o*-cresol (10.28)

The previous paper[4] in this series,postulated a proton transfer process for the ion producing mechanism of Stadis. The interference with this mechanism by a phenol must involve the -OH group and consideration of the effect of pK_a is significant in this context since it provides a means of quantifying its proton donor ability albeit in aqueous media.

Nitrophenols were used to extend the range of pK_a and degree of hindering. Although they are not found in fuels, their effect on the behaviour of Stadis is nevertheless interesting and suggestive in elucidating the mechanism of the interaction of the phenols in general. Figure 4 shows the effect of some Nitrophenols on the conductivity of a solution of Stadis. By simply

considering the pK_a of the Nitrophenols, the magnitude of the suppressing effect on the Stadis conductivity is expected to be:

4-nitrophenol (pK_a 7.14) > 2-nitrophenol (pK_a 7.2) > 3-nitrophenol (pK_a 8.35) > *m*-cresol (pK_a 10.8)

The order found experimentally is:

4-nitrophenol ≥ 3-nitrophenol >> *m*-cresol >> 2-nitrophenol

This suggests that the pK_a does relate to the effect on Stadis performance, but where groups are introduced in the 2-, 6- positions on the benzene ring then steric and other effects predominate over the effects of pK_a. The phenolic compounds appear to be acting as proton donors in the absence of such neighbouring groups.

Relying on pK_a data to interpret the behaviour of phenolic compounds in a hydrocarbon solvent is open to question, although some data[6] show a parallel between acidity in aqueous and non-aqueous systems.

4.6 Effect of Fuel Phenol Levels on the Conductivity Response of Stadis 450

A useful way of comparing the work on model phenol systems with the effects of phenol levels in real fuels is required. Figure 5 presents the data in terms of a ratio R, where R is a measure of the performance degradation of the Stadis due to the presence of phenols. R is the ratio of the conductivity of the Stadis solution (in dodecane or fuel) *with phenol present* to the maximum possible conductivity for an ideal Stadis solution in dodecane *without phenols*. Incorporated into Figure 5 is the performance degradation of Stadis in a number of fuels analysed by BP for phenol content. In Figure 5 a correction has been made for the difference in viscosity of the fuels and the dodecane as outlined in Section 4.7.

The fuels show a significant degradation in Stadis performance as the levels of phenolic impurities become higher.

4.7 Significance of Fuel Viscosity when Comparing Conductivity Response to Stadis 450

A two or threefold variation in viscosity is not uncommon in fuels[7] and the subsequent effect

on the conductivity response to Stadis must be taken into account when comparing fuel properties or performing standard tests. Work by Henry[8] and subsequent analysis by Dacre[9] shows that the relationship between the conductivity κ and the viscosity ν can be approximated by:

$$\kappa \propto 1/\nu^{0.7}$$

This relationship is used as the viscosity correction in Figure 5.

4.8 Removal of Phenolic Impurities from Fuels

The change in response of Reformulated Stadis to fuels at different stages in the refining process is shown in Figure 6. The fuels were supplied by BP. The conductivity response of the Stadis increases with each stage in the refining process. The largest change occurs after the Merox unit, suggesting that the efficiency of this process is paramount in determining the performance of Stadis.

The phenolic impurities from the caustic wash were isolated by BP and redoped into BP fuels and dodecane. The response of Stadis to this phenolic extract at different concentrations is given in Figure 7. The similarity with the response to the model phenolic impurities is striking. The agreement is excellent, both in the magnitude of the effect and the concentration of the phenolic impurity required to produce a given fall in the conductivity. These results highlight the importance of changing the caustic wash frequently to prevent problems with Stadis.

Filtering through fresh clay is found to remove phenolic and polar impurities from the fuel and to improve the response to Stadis. However impurities extracted from a 'spent' refinery clay bed do not cause a reduction in the conductivity of fuel doped with Stadis (in fact a small increase in conductivity was found) but they do have a large effect on the water separation characteristics. This supports the idea that the caustic wash is the critical stage in the refining process for removing the phenolic impurities and preventing problems with the conductivity response of Stadis.

5 SPECULATION ON THE ROLE OF PHENOLS IN DESTROYING THE CONDUCTION MECHANISM OF STADIS

5.1 General Comments

In earlier papers[3,4] we have discussed a possible mechanism for ion production in Stadis 450 solutions. In this mechanism an activated sulphone group $-SO_2$ plays a central role as a proton acceptor for carbonyl hydrogen from another molecule. Any interaction which interferes with this process will change the ion concentration and hence the conductivity. We suggest that the antagonistic effect of phenolics is caused by their complexation with sulphone which is then not available for interaction with ion-producing carboxyl groups. We have considered several alternative mechanisms, but the one outlined below combines simplicity with ability to represent observed behaviour as described in the following paragraph.

5.2 Equilibrium Model

If P represents a phenol and S the sulphone group in Stadis, then the association interaction between them can be written :

$$\begin{array}{ccccc} P & + & S & \leftharpoondown & PS \\ (a-x) & & (b-x) & & x \end{array}$$

where PS is a phenol/sulphone complex and a and b are the weighed-in molar concentrations of P and S respectively. If the solutions are sufficiently dilute to be ideal then the equilibrium constant can be written :

$$K = \frac{[PS]}{[P][S]}$$

$$= \frac{x}{(a-x)(b-x)}$$

If we assume that the measured conductivity, κ, is proportional to the free sulphone concentration [S], then in the absence of phenol the conductivity, κ_0 is given by:

$$\kappa_0 = Ab \quad \textit{where } A \textit{ is a constant}$$

also

$$\kappa = A(b-x)$$

$$Let\ F = \frac{\kappa}{\kappa_0}$$

$$then \quad b-x = bF$$

$$so \quad x = (1-F)b$$

$$(a-x) = [a-(1-F)b]$$

$$Thus\ K = \frac{(1-F)}{[a-(1-F)b]\ F}$$

$$so \quad \frac{(1-F)}{F} = K\ [a-(1-F)b]$$

and so in principle from conductivity and concentration data it is possible to obtain the equilibrium constant K. Unfortunately b, the molar concentration of sulphone groups is not known with any certainty since the information required for its calculation is not available. However for a given fixed sulphone concentration and for low phenol concentrations such that (1-F) is less than ~0.15, then b(1-F) << a and (1-F)/F plotted against a should be linear and have a slope equal to K. Plots have been obtained in this way for all the phenols and values of K have been derived.

5.3 K Values and Their Dependence on Phenol Type

If this simple model has any validity then we expect the K values to depend on phenol structure and in particular to depend on the influence of ring substituents. To check this we have used

the Hammett equation[10] which quantifies the ability of ring substituents to influence a reaction centre, which in this case is phenolic -OH. One form of the Hammett equation can be written

$$\log K = \rho\sigma$$

in which K is an equilibrium constant, the substituent effect is expressed in terms of a σ-value and the reaction type is characterised by ρ. We have calculated total σ-values for the combinations of substituents present using published data[10] and these are shown in Table 1. Figure 8 is the Hammett plot of logK against Σσ. The plot, which spans a thousandfold range of K values is encouraging and is consistent with a complexation process involving the -OH group and which is assisted by electron-withdrawing substituents. One further point is that it is possible to assess the behaviour of molecules of the antioxidant type 2,6-di-tert-butyl-4-methylphenol by extrapolating the Hammett line to the appropriate value of Σσ, which is equal to -1.04. The predicted K value is ~3 and is clearly consistent with the absence of antagonistic effects observed with this compound.

The magnitude of antagonistic effects observed at higher phenol concentrations may require further elaboration of the simple equilibrium model to include association of a second phenol molecule at a sulphone site. This will be reported in full when more information is available.

6 SUMMARY AND CONCLUSIONS

6.1 Simple phenols such as *o*-cresol, *m*-cresol, *p*-cresol and phenol, at concentrations above 50ppm, greatly *reduce* the conductivity of Stadis 450 and Reformulated Stadis.

6.2 Highly hindered phenols have no effect on the conductivity of Stadis.

6.3 Both the *type of phenol* and the *concentration of the phenol* affect the performance of Stadis.

6.4 Analysis of fuels by BP has indicated phenolic levels as high as 750ppm, with 80% of the phenols being of a simple low molecular weight type such as cresols.

6.5 The response of Stadis was found to be poorer in fuels of high phenolic content.

6.6 The behaviour of Stadis in a limited number of fuels of known phenolic content fits with the behaviour of Stadis in model phenol systems. Further work on reliably characterised fuels is required to confirm the types and concentrations of phenols in the fuel which will give rise to problems with Stadis.

6.7 Phenolic extract from the caustic wash of the refinery behaved in a very similar manner to the model simple non-hindered phenol impurities.

6.8 To remove phenols from fuels effectively, the caustic wash should be replaced regularly to prevent high levels of phenols accumulating and being reincorporated into the fuel.

6.9 Where the conductivity response of fuels is being compared, the viscosity-corrected conductivity should be used.

6.10 It is speculated that phenols interact with sulphone groups present in Stadis 450 and that the resulting complexed sulphone has less ability to activate the ion production mechanism.

6.11 A model for complexation is suggested and is successfully treated by simple equilibrium theory. This permits the calculation of equilibrium constants.

6.12 The variation of the equilibrium constant with phenol structure, as represented by the Hammett σ-value, is consistent with a complexation model in which the phenol group is an interaction centre. As a consequence the equilibrium constants also correlate with the phenol pK_a values.

6.13 Some anomalous effects are observed for phenols with substituents adjacent to the phenolic group.

7 ACKNOWLEDGEMENTS

The authors wish to thank additive manufacturers and oil companies for there helpful cooperation and supply of additives and fuels. In particular they would like to thank BP for the analysis of the fuels and for many helpful and enjoyable discussions during the course of this work. They would also like to express their gratitude to the sponsors of this work, LSF4, DERA, Pyestock, Farnborough, UK, under contract LSF/E20093.

8 REFERENCES

(1) Klinkenberg,A; van der Minne,J.L. *Electrostatics in the Petroleum Industry*; Elsevier,1958.

(2) Bustin,W.M,:Dukek,W.G. *Electrostatic Hazards in the Petroleum Industry*; Research Studies Press, 1983.

(3) Dacre,B; Abi Aoun,W.G. The Effects of Fuel Components on the Behaviour of Conductivity Improvers in Jet Fuel, 4th International Conference on Stability and Handling of Liquid Fuels, Orlando, Florida, USA, November 1991.

(4) Dacre,B; Hetherington,J.I. Behaviour of Conductivity Improvers in Jet Fuel, 5th International Conference on Stability and Handling of Liquid Fuels, Rotterdam, The Netherlands, October 1994.

(5) Dacre,B; Abi Aoun,W.G. Effects of Fuel Components on the Performance of Conductivity Improvers in Hydrocarbons, *Journal of Electrostatics*, 1997, *39*, 89-110.

(6) US Department of Commerce NBS Monograph 105, *Acid-Base Behaviour in Aprotic Organic Solvents*, August 1968.

(7) Annual Reports by DQA/TS and DRA, *Quality of Aviation Turbine Fuels Available in the UK,* 1983 to 1992.

(8) Henry,C. CIT/MOD Seminar on Aviation Turbine Fuel Specification - History and Future Development, Bath, UK, September 1988

(9) Dacre,B, Unpublished Work

(10) Perrin,D.D.; Dempsey,B.; Serjeant E.P. *pK_a Predictions for Organic Acids and Bases*, Chapman and Hall, 1981.

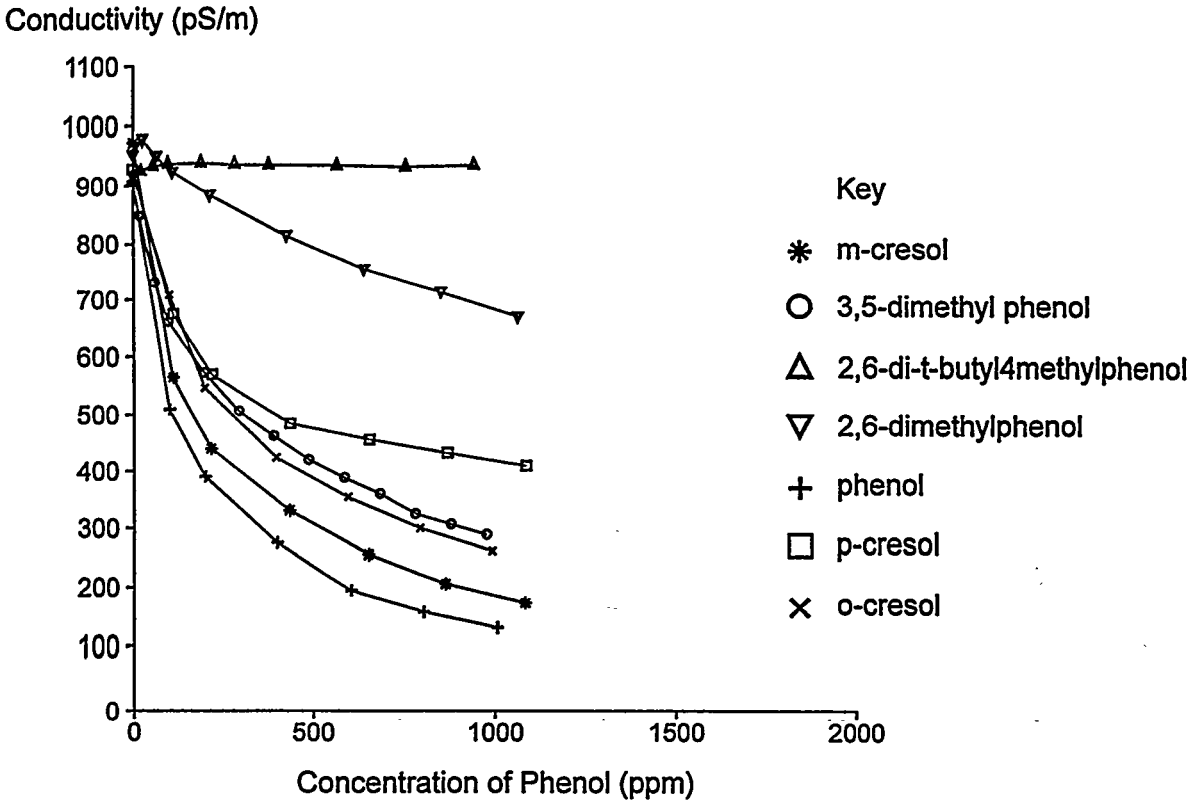


Fig. 1 Effect of Phenol Type on the Conductivity of 3ppm Original Stadis 450 in Dodecane

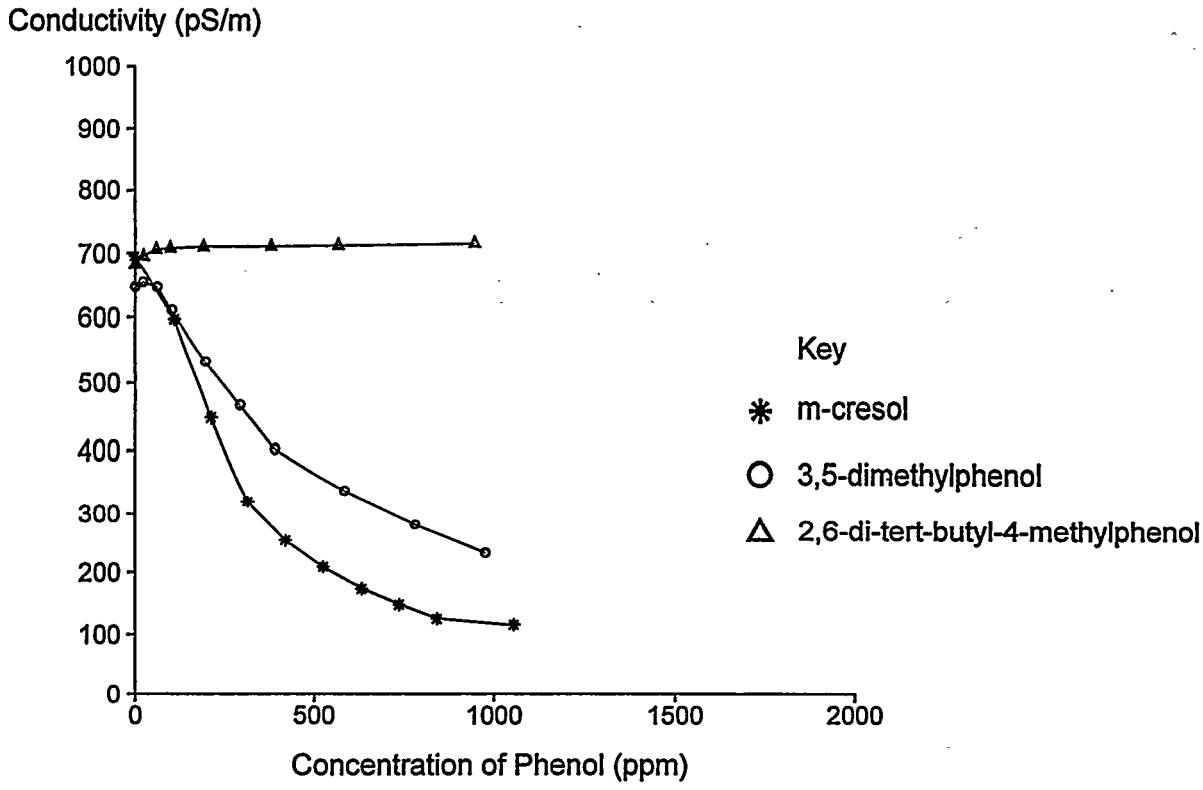


Fig. 2 Effect of Phenol Type on the Conductivity of 3ppm Reformulated Stadis 450 in Dodecane

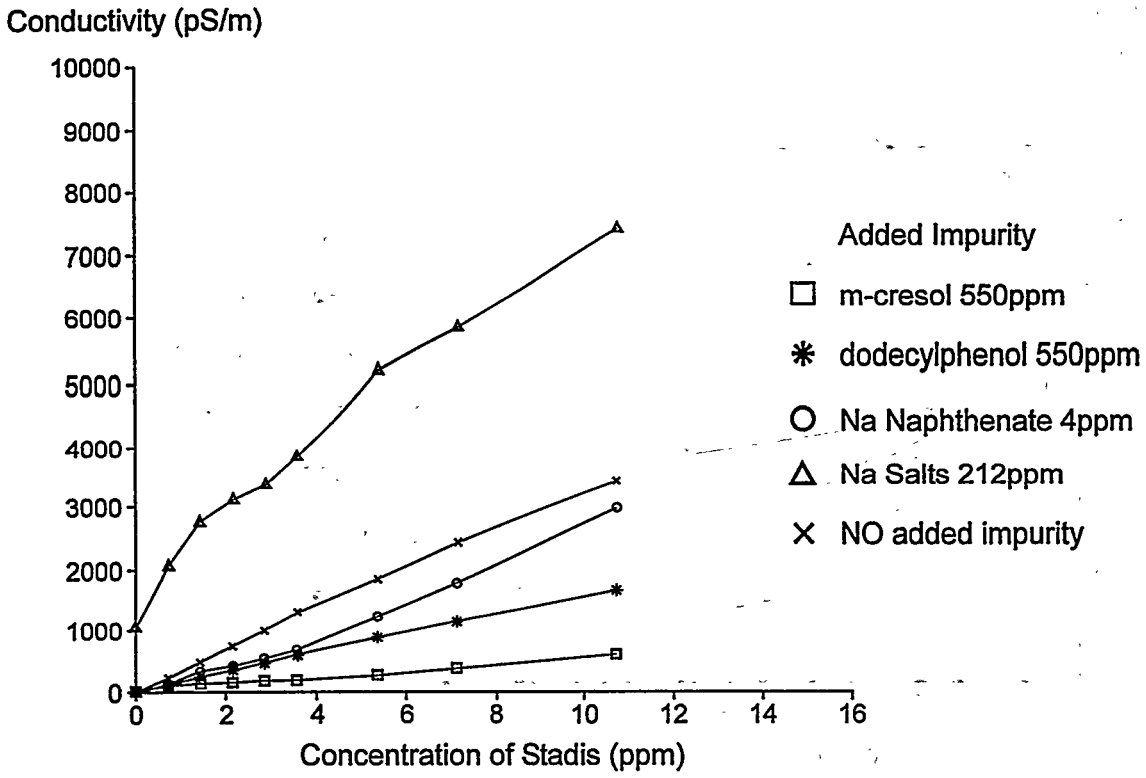


Fig. 3 Conductivity Response of Original Stadis 450 in Dodecane Containing Sodium Salt and Phenolic Impurities

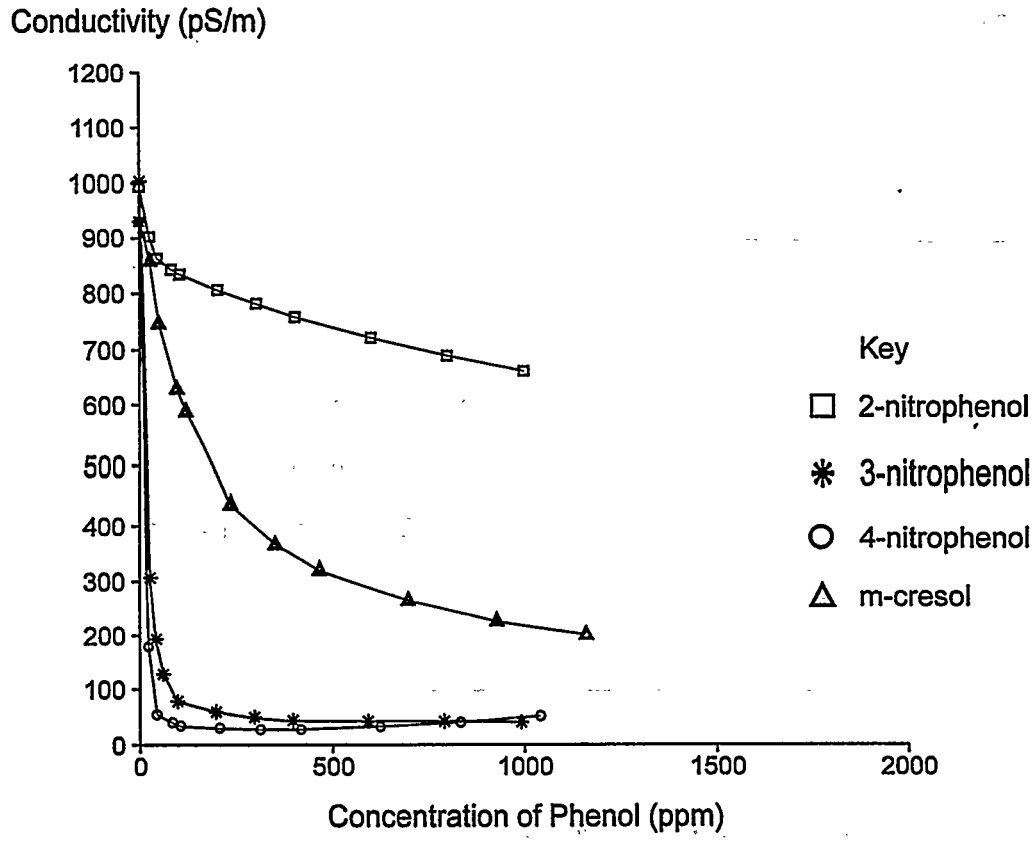


Fig. 4 Effect of Phenol Type on the Conductivity of 3ppm Original Stadis 450 in Dodecane

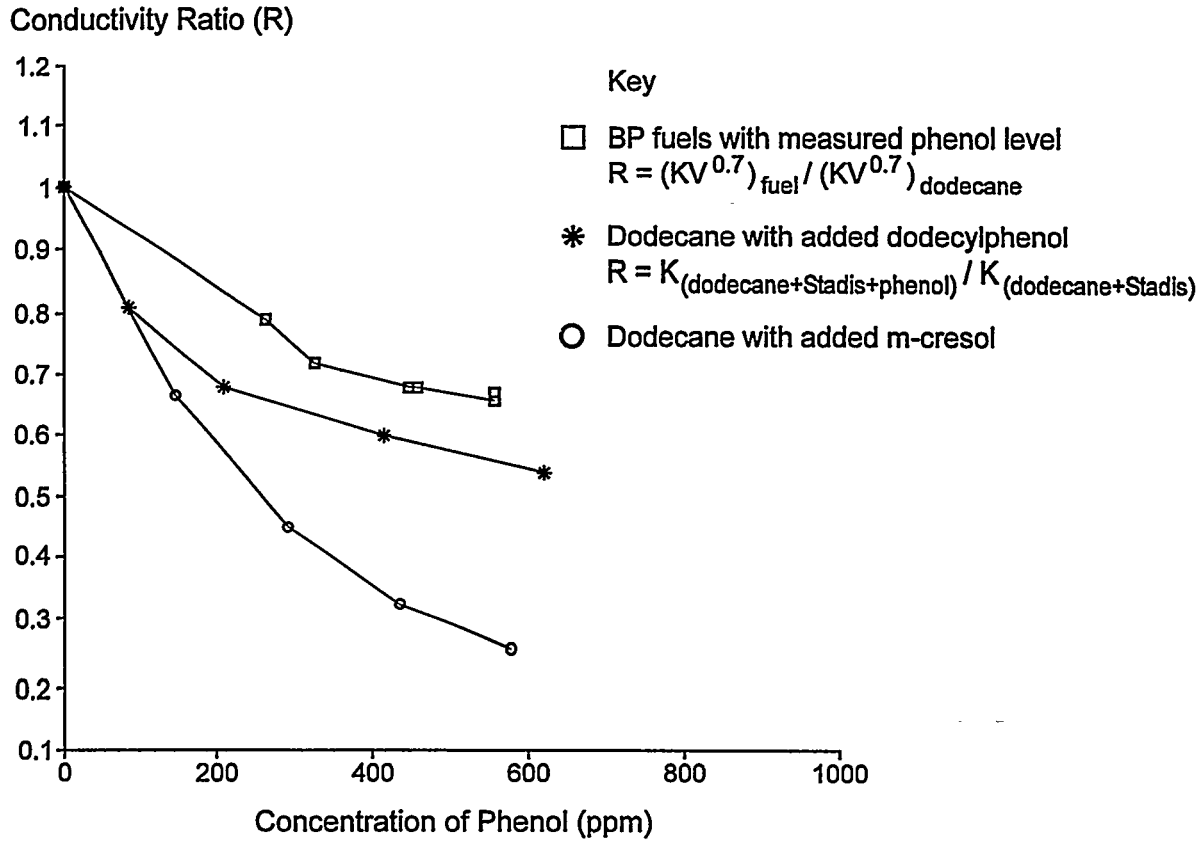


Fig. 5 Effect of Phenols on the Conductivity of 4.8ppm Original Stadis 450 in Fuels and Dodecane

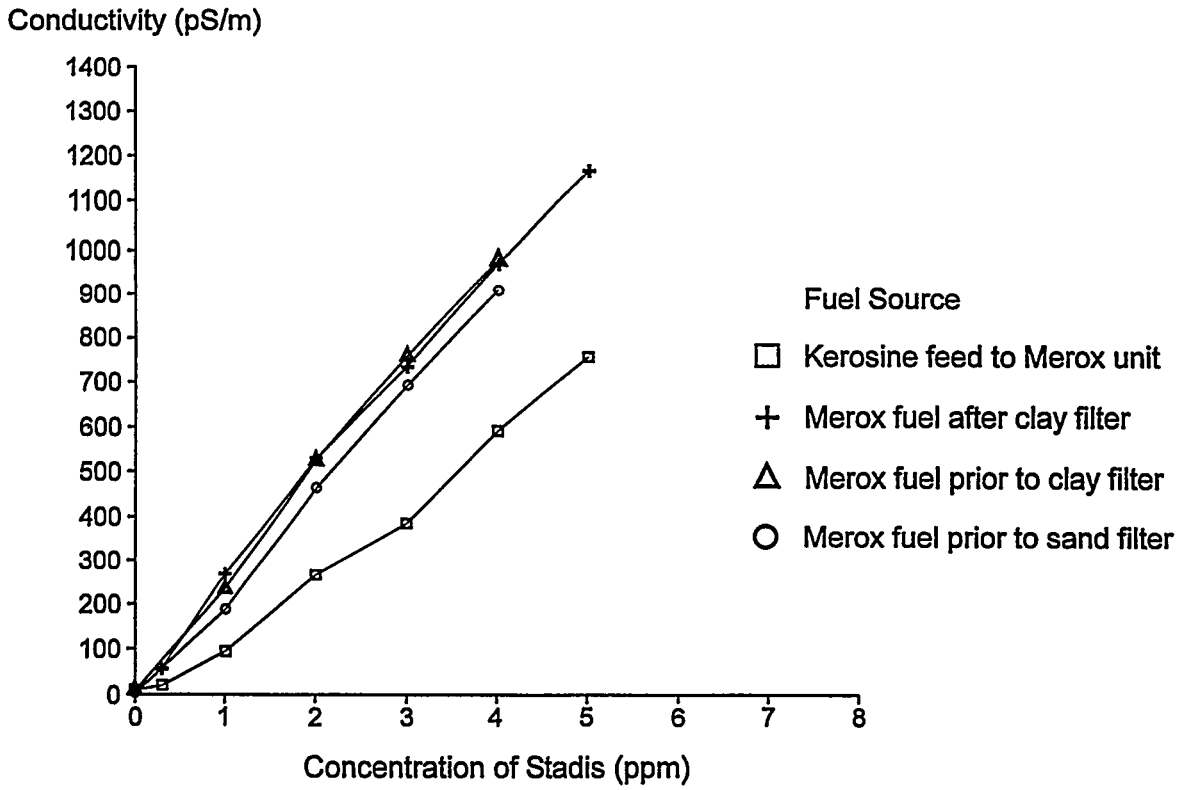


Fig. 6 Conductivity vs. Concentration for Reformulated Stadis 450 in Fuel from Different Stages in the Refining Process

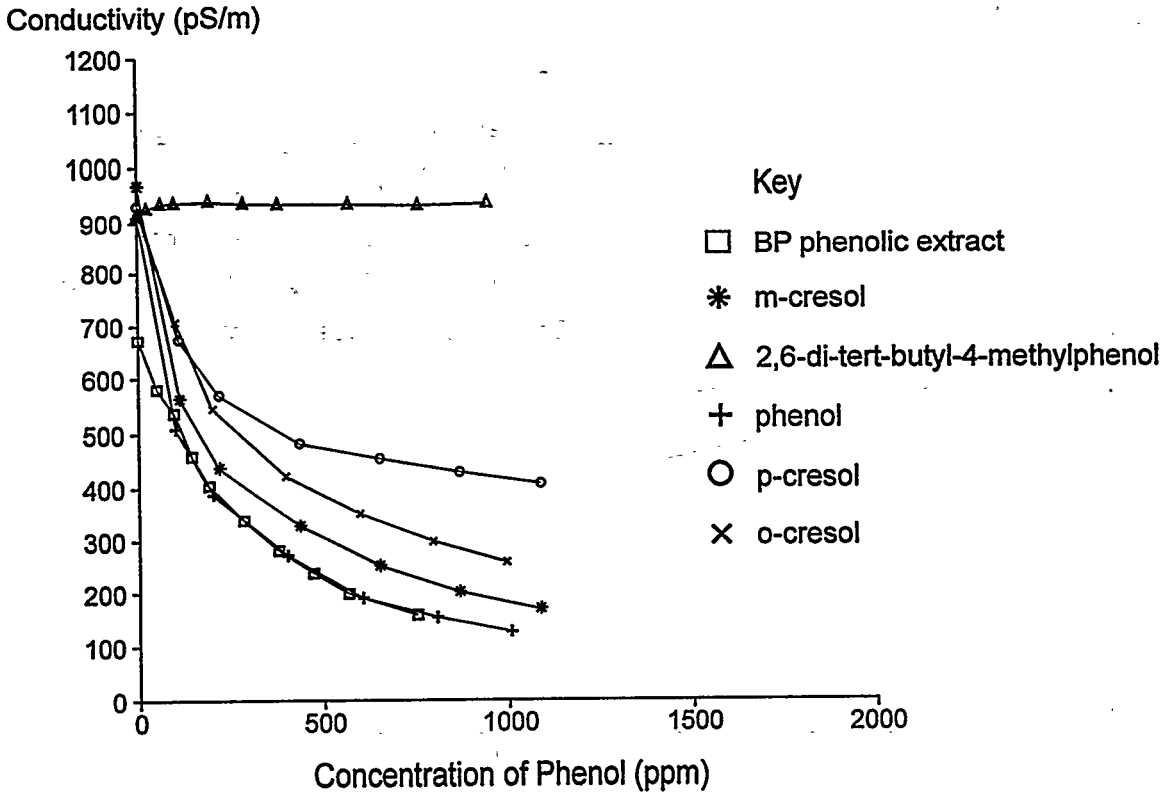


Fig. 7 Effect of Phenol Type on the Conductivity of 3ppm Original Stadis 450 in Dodecane

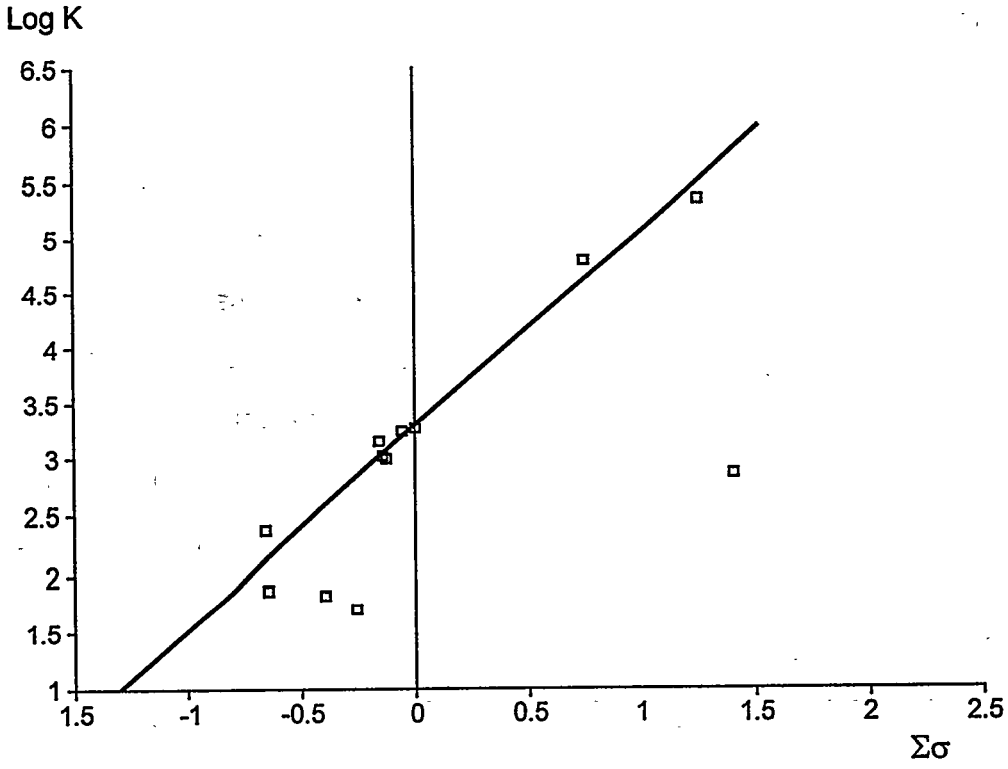


Fig.8 Variation of Equilibrium Constant (K) with Substituent Constant (σ)

Substituents	Σσ	Substituents	Σσ
4-methyl	-0.14	2,6-terbutyl	-1.04
3-methyl	-0.06	2-terbutyl,6-methyl	-0.65
2-methyl	-0.13	2,4,6-trimethyl	-0.4
4-dodecyl	-0.16	4-nitro	1.24
2,6- dimethyl	-0.26	3-nitro	0.74
2-terbutyl,4-methyl	-0.66	2-nitro	1.4

Values have been calculated from tables A1,A4 and A5 in reference 10. The value for 4-dodecyl has been assumed to be equal to that for butyl.

Table 1 Total Substituent Constants for Substituted Phenols

6th International Conference
on Stability and Handling of Liquid Fuels
Vancouver, B.C., Canada
October 13-17, 1997

COPPER CONTAMINATION OF JET FUEL FROM SHIPS' HEATING COILS

Peter David*, Alan Goddard, Spencer E. Taylor and Andy J. Woodward

BP Oil, Chertsey Road, Sunbury-on-Thames, Middlesex, UK, TW16 7LN

Abstract

Metal contamination of aviation fuels can sometimes occur during distribution to the extent that the fuel is rendered off-specification with respect to thermal stability. Such problems can occur during sea transportation and the effects can often be traced to on-board copper dissolution from ship's heating coils, employed for shipment of more viscous cargoes, such as residual fuel. Verification of the metal-leaching propensity of fuels has been based for the most part on the results from tests involving controlled storage of fuels over specimens of representative metallurgies, followed by metal analysis to determine the levels of contamination. Often these experiments are lengthy and by the time the results of the extended tests are known, failures in the JFTOT or other indicators of contamination are also known. There is therefore a requirement for a method which will rapidly determine a fuel's propensity for copper leaching, especially in cases where it is known that the likelihood is high of the fuel coming into contact with copper alloys. A simple laboratory test based on copper strip immersion with determination of fuel copper by a new in-house colorimetric method has been devised to predict the aggressive nature of fuels towards copper alloys. The relationship with fuel composition and processing route has been investigated. The quartz crystal microbalance (QCM) with copper crystals has also been used to study copper dissolution from fuel systems; results are generally in agreement with the immersion tests. Details of the studies are presented in the paper, together with recommendations on test implementation.

Introduction

Metals contamination of aviation fuels can sometimes occur during distribution to the extent that the fuel is rendered off-specification with respect to thermal stability. Such problems can occur during sea transportation and the effects can often be traced to on-board copper dissolution from ship's heating coils, employed for shipment of more viscous cargoes, such as residual fuel. The detrimental effects of copper on JFTOT breakpoint are well known[1].

In a recent example, a batch of Merox treated jet fuel was transported from Sardinia to the UK. The fuel satisfied specification requirements on loading, but after discharge, failed

JFTOT at 260°C. Upon investigation, the fuel had been carried on a ship with copper alloy heating coils in the product tanks and the copper content of the jet fuel had increased from 6ppb (μg/kg) to in excess of 60ppb. Not all the tanks contained heating coils, and the copper content of samples taken from these tanks indicated no uptake of copper. On this occasion, the fuel was treated with metal deactivator additive (MDA) in accordance with specification requirements, prior to release. The whole episode created considerable operational difficulties, which could have been minimised, or even avoided, if there had been some forewarning that copper contamination might have occurred. The incident prompted a study at the BP Oil research laboratories at Sunbury-on-Thames to investigate the propensity for fuels to leach metals from ships' heating coils and to develop a laboratory predictive test, details of which are given in this paper.

The study covered three areas of activity:

- Long term fuel storage over representative heating coil sections
- Laboratory short-term copper strip immersion tests
- Evaluation of quartz crystal microbalance (QCM) to study copper dissolution.

Long term fuel storage over heating coil sections

To simulate carriage of jet fuel in ships' tanks with heating coils, controlled laboratory immersion tests were performed. Test sections of typical heating coils were immersed in a range of Merox and hydrofined fuels contained in 1 litre glass bottles at 43°C for 12 weeks and the copper content monitored during the storage period. The composition of the heating coils is shown in Table 1. These analyses were obtained using X-Ray Fluorescence rubbing techniques and the data shown thus represent surface composition.

The heating coil sections were cut to size to give surface areas of *ca* 22cm^2, giving a surface area:fuel volume *ca* 100 times greater than in practice. This high ratio was chosen to allow ease of reproducing the same surface area sizes for the different heating coils and also to accelerate the metal leaching process to enable laboratory assessment. The test sections were lightly rubbed with emery paper to remove any surface oxides present, and thoroughly solvent washed beforehand.

Uptake of copper, zinc and iron was monitored using Inductively Coupled Plasma-Mass Spectrometry (ICP-MS). Only copper measurements are presented here; similar trends were observed for iron and zinc uptake.

Figure 1 shows that there was significant leaching of copper from the aluminium/brass and copper/nickel/iron heating coils by the Merox treated fuel which occurred within a matter of days and continued throughout the storage period. For the tests with the galvanised steel and stainless steel coils, there was no increase in copper content, as expected from the coil composition. The galvanised steel coil gave significant increases in iron and zinc contents; the stainless steel coil was the most inert of the coils examined, although even here there was a slight increase in iron content.

In contrast, Figure 2 shows that the hydrofined fuel was far less aggressive towards the coils, with no significant increase in copper uptake during storage. It is not precisely known how metal contamination of the fuels occurs, although it is suspected that polar species present in trace amounts may be aggressive to metals. Fuels are known to contain low residual levels of species which vary in acidity, such as phenates, naphthenates, sulphonates, and such species are likely to be present at higher levels in the Merox treated fuel than in the hydrofined fuel.

In Figure 3, the effect of MDA in the two fuels is shown; results are shown for the aluminium brass coil tests. The presence of the additive leads to a significant increase in uptake of copper compared with the base fuels. It is interesting to note that the copper level in the MDA treated Merox fuel after 12 weeks storage is at a higher level than might be anticipated on the basis of metal chelation alone. On a stoichiometric basis, 5.7 mg/l MDA will chelate with *ca* 1300 ppb copper, coincidentally the level in the MDA treated hydrofined fuel after 12 weeks. With hindsight, it would have been worthwhile continuing the storage period for this fuel beyond 12 weeks. These data indicate that under the conditions of the tests performed, there would have been high levels of unchelated copper present especially for the Merox treated fuel, suggestive of poor thermal stability. Unfortunately, JFTOT tests were not performed on the fuels during this study, the original purpose of which was to define the potential for copper uptake from heating coils.

It is recognised that differences in heating coil surface finish will strongly influence the metal leaching process. No attempt was made in the investigation to characterise the surface finish of the heating coil sections and thus comparisons of absolute metals content observed should be treated with caution. For the same reasons, no attempts are made to predict the extent of metal leaching which would occur in practice with full size heating coils. However, the trends observed between the various fuels and heating coils are likely to be valid and indicate that some fuels will be aggressive towards heating coils. On the evidence of field experience, such fuels may be rendered off-specification in terms of their thermal stability.

Laboratory short term screening tests

The metal leaching propensity of fuels can be established by controlled storage of fuels over specimens of representative metallurgies, followed by metal analysis to determine the levels of contamination. However, these experiments are lengthy, and by the time the results of the extended tests are known, failures in the JFTOT or other indicators of contamination are known. Such tests cannot therefore be used practically to predict the potential for copper contamination. On the basis of the results from the coil immersion tests, consideration was given to development of a laboratory test to predict the aggressive nature of fuels to heating coils. Such a test could find use to establish the acceptability of transporting fuels in product carriers with heating coils in situations where no other carrier is available.

A simple laboratory test based on the Copper Strip Corrosion test (IP 154/ASTM D130) was devised. The fuel is subjected to the standard test for jet fuels of 2 hours at 100°C with additional copper content measurement before and after strip immersion. The premise is that the extent of copper pick-up will be indicative of the propensity of the fuel to leach metals from heating coils.

Initially, copper contents were measured by atomic absorption spectroscopy, but it was recognised that such equipment might not be available in less well-equipped laboratories. Accordingly, a simple, laboratory test method for copper was developed. The method is based on:

- Ignition of the fuel remaining after the standard copper strip immersion test in the presence of sulphuric acid
- Ashing of the material remaining after ignition at 500°C
- Dissolution in sulphuric acid
- Complexation with 2,2-biquinoline
- Extraction into iso-amyl alcohol
- Measurement of absorption at 545 nm

Results for a hydrofined and Merox treated fuel are shown in Figure 4 and show that the Merox fuel was more aggressive in terms of copper pick-up than the hydrofined fuel. The trend is similar to that observed for the heating coil immersion tests, although comparison between absolute levels of copper pick-up cannot be made.

In blends containing both hydrofined and Merox components, the extent of metal leaching is dominated by the presence of the Merox component, and within the limits of experimental error, the relationship is linear (see Figure 5). The copper measurements are given in Table 2 where results by atomic absorption and the colorimetric method are compared. There is generally good agreement. The lower limit of detection of the colorimetric method is *ca* 25 ppb, restricted by the volume of fuel (30ml) arising from the standard copper strip corrosion test. By increasing the sample volume, the lower limit of detection may be reduced.

In order to compare the role of individual acidic species in determining the metal leaching propensity of fuels, copper strip immersion tests were performed on fuel containing various individual acidic reagents representative of those naturally occurring in fuels. These included:

- Phenols, as p-cresol, at levels up to 100 mg/l
- Naphthenic acids, molecular weight 190, at levels up to 100 mg/l
- Sulphonate as Aerosol OT (dioctyl ester of sodium sulphosuccinate) at levels up to 0.1 mg/l.

The effect of these reagents at the maximum addition rate given above on the copper strip immersion test is shown in Figure 6. The base fuel selected was a hydrofined jet fuel and the additional effect of MDA is also shown. In these tests, when added singly, the p-cresol and

AOT had little effect on copper pick-up, whereas the naphthenic acids were aggressive to some extent, resulting in levels of copper comparable with those observed for Merox fuels. MDA added singly had a similar effect. In contrast, very high levels of copper extraction occurred when the MDA was added in combination with the acidic reagents, with apparent synergism being observed. Definite conclusions cannot be drawn from the limited data available; a separate study at the BP Oil laboratories at Sunbury is currently underway to help clarify matters. The data do suggest that the presence of MDA can have a pronounced effect on the leaching of metals from heating coils. Unfortunately, as with the heating coil immersion tests described earlier, no assessment of the fuel thermal stability was made, and no conclusions regarding the state of the metal ions (whether chelated or not) can be drawn.

Finally, samples of Merox treated and hydrofined fuels were taken from the market and subjected to the copper strip immersion test. Whilst recognising that the quality of such fuels will be dependent on processing conditions and crude source, it is clear from Figure 7 that the three hydrofined fuels examined were not aggressive to copper, whereas the six Merox treated fuels showed varying degrees of propensity to leach out copper. The effect of approved jet fuel additives (added at the maximum permitted addition rate) is also shown in the Figure 7. As expected, the additives had little effect on copper corrosion, although it is possible that any effect might have been swamped by the corrosive properties of the base fuel.

Application of QCM to study copper dissolution

QCM offers the sensitivity to determine rapidly a fuel's propensity for copper leaching through ready detection of the dissolution of very small (ng) masses of copper. Previous experience with QCM has largely been directed at the use of "inert" metal electrodes (usually gold Au-QCM) for following deposition in jet fuel thermal degradation experiments. In the present study, copper dissolution was studied using copper electrodes (Cu-QCM).

QCM employs the piezoelectric resonant properties of a quartz crystal which change proportionately with small mass changes, either through deposition or dissolution on/from the active electrode surface. By measuring the change in frequency of the quartz crystal oscillator, a mass change can be quantitatively detected. The theory of QCM and practical details of QCM operation may be found elsewhere[2].

The fuels examined in this study comprised Merox treated and hydrofined basestocks and blends thereof. The QCM experiments were performed at 105+/-1°C. Whilst extremely small reductions in mass resulting from dissolution can be readily detected, any deposition from thermal degradation which may also be occurring may serve to complicate the observed behaviour. Thus both Cu-QCM and Au-QCM experiments were performed. It is assumed that results from the Cu-QCM will comprise contributions from both dissolution and deposition, whereas the Au-QCM results reflect deposition only.

For the Cu-QCM, there was a frequency change consistent with mass loss from the crystal. For the Au-QCM experiments performed under identical conditions, the frequency change was consistent with crystal mass increase, ie through deposition. Changes of frequency with time as a function of blend composition are shown in Figure 8. Positive values are indicative of mass loss; negative values indicate mass gain. The behaviour is interesting in that there is an apparent maximum rate of dissolution at approximately a 50:50 Merox:hydrofined blend. For the Au-QCM experiments, there is roughly a linear decrease in deposition rate with increase in hydrofined component, suggesting that the Merox component is the major contributor to the deposition behaviour. (This agrees with the results from the copper strip immersion tests described earlier.)

From the measured rates of frequency change given in Figure 8, an estimate of the dissolution rate in which deposition effects have been accounted for can be obtained. The resultant behaviour is shown in Figure 9 and is believed to be a more realistic measure of copper dissolution. Treated in this manner, the results suggest that as with deposition, the level of Merox component dictates the propensity for copper dissolution. Also shown in Figure 9 are results of copper strip immersion tests on the same samples as the Cu-QCM tests. The same general features are exhibited by both series of results providing strong support for the interpretations of the QCM approach.

Whilst recognising that a number of assumptions have been made in interpretation of the QCM data, these preliminary findings confirm the potential of QCM for the assessment of the copper dissolving propensity of aviation fuels towards heating coils. In particular, it has been

assumed that deposition rates will be identical on the gold and the copper crystals and no account has been made of the destabilising effect the dissolved copper will have on the fuel stability.

Conclusions

- Metal contamination from ships' heating coils can make fuels off specification in terms of their thermal stability. Heating coils comprising copper alloys are particularly hazardous; stainless steel coils are inert.
- In general, Merox fuels are more aggressive than hydrofined fuels in their propensity to leach metals from heating coils. Differences are related to the levels of trace acidic species present in the fuels.
- Laboratory strip immersion tests with copper determination can be used to identify potentially aggressive fuels.
- QCM is sufficiently sensitive to study copper dissolution.

Recommendations

- Whenever possible, ships with copper alloy heating coils should be avoided, especially for MDA treated fuels.
- If unavoidable, JFTOT tests should be performed before and after shipment.
- The fuel leaching potential of the fuel may be assessed by the copper strip immersion test.
- If deterioration in JFTOT performance has occurred through metal contamination, consideration may be given to the use of MDA after discharge to restore the fuel quality in accordance with specification requirements.

Acknowledgements

This project was funded by Air BP and UK Ministry of Defence.

References

(1) Hazlett, R.N.; Thermal Oxidation Stability of Aviation Turbine Fuels; ASTM, Ann Arbor, MI, 1991.

(2) Bruckenstein, S.; Shay, M.; Experimental Aspects of Use of the Quartz Crystal Microbalance in Solution, *Electrochim. Acta*, **1985**, 30, 1295-1300.

TABLE 1

HEATING COIL COMPOSITION

(%m, surface analysis)

	Al / Brass	Copper / Nickel / Iron	Galvanised Steel	Stainless Steel
Copper	75.4	86.1	-	0.7
Zinc	22.1	0.13	97.7	-
Iron	0.08	1.7	1.8	65.5
Aluminium	1.9	-	-	-
Nickel	-	10.7	-	11.6
Chromium	-	-	-	17.2
Others	0.5	1.37	0.5	5.0

Table 2

COPPER STRIP IMMERSION TEST RESULTS (µg/kg)

	AA COPPER	COLORIMETRIC COPPER
Merox treated Jet A-1	520	490
Hydrofined Jet A-1	40	40
80/20 v/v Merox/hydrofined	500	470
60/40 v/v Merox/hydrofined	360	340
50/50 v/v Merox/hydrofined	300	280
40/60 v/v Merox/hydrofined	280	250
20/80 v/v Merox/hydrofined	130	120

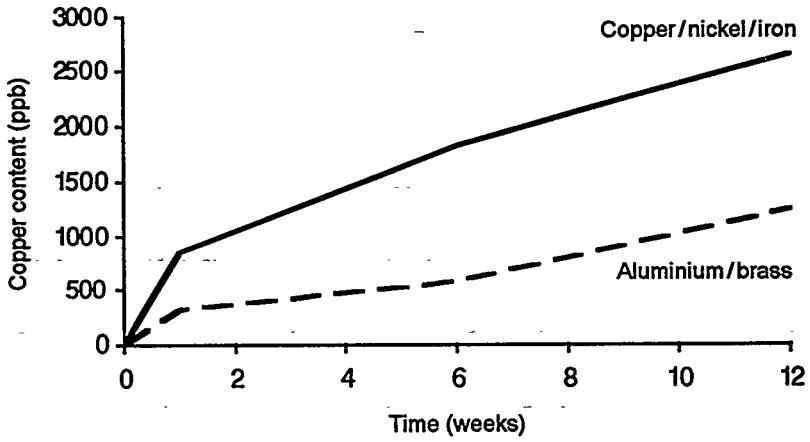


Figure 1. Heating coil immersion tests – Merox fuel

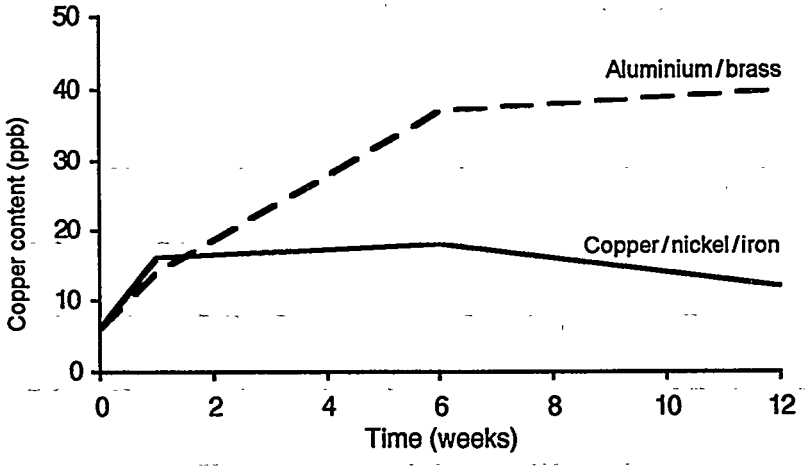


Figure 2. Heating coil immersion tests – Hydrofined fuel

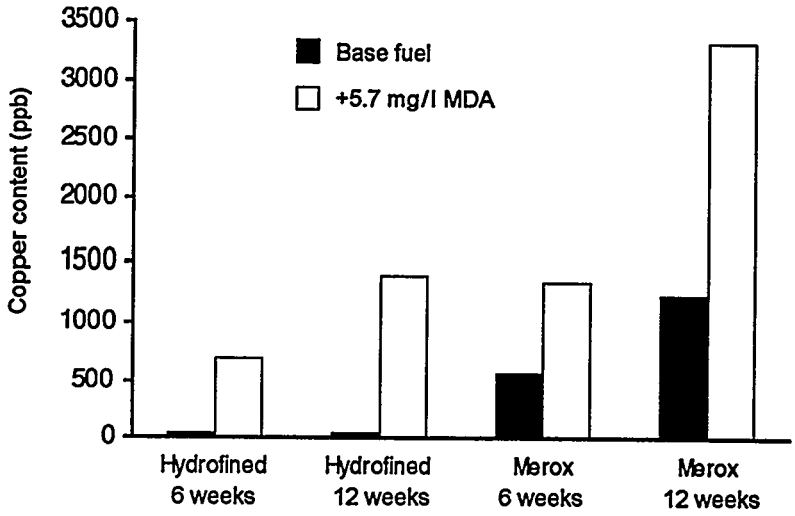


Figure 3. Heating coil immersion tests – Effect of MDA

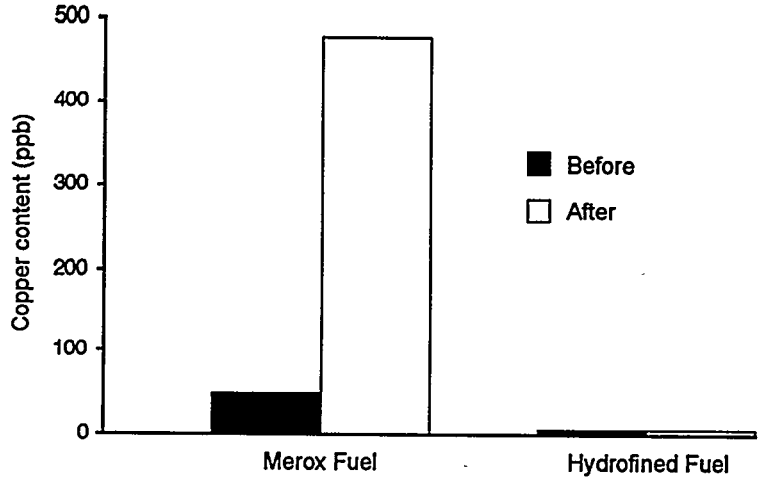


Figure 4. Laboratory copper strip immersion tests

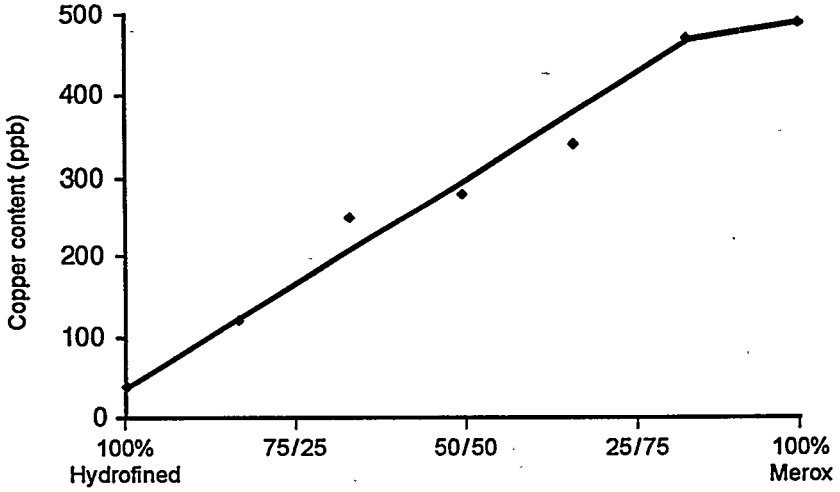


Figure 5. Copper strip immersion tests effect of blend composition

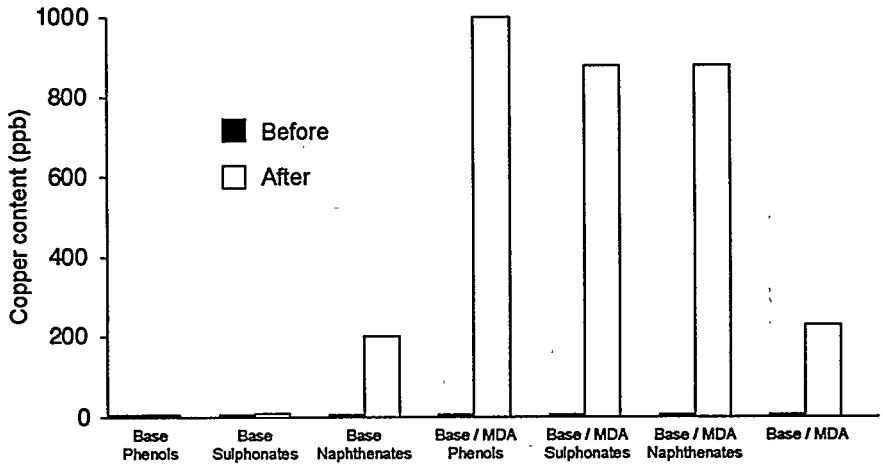


Figure 6. Copper strip immersion tests: Hydrofined fuel with acidic species / MDA

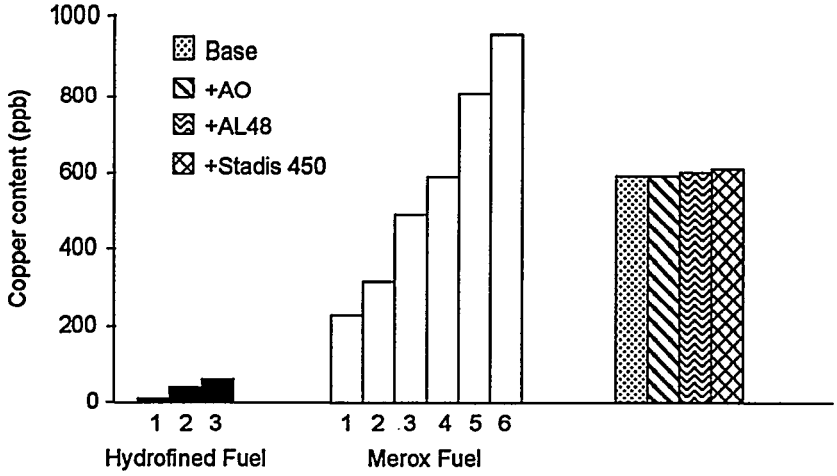


Figure 7. Copper strip immersion tests market samples / additive effects

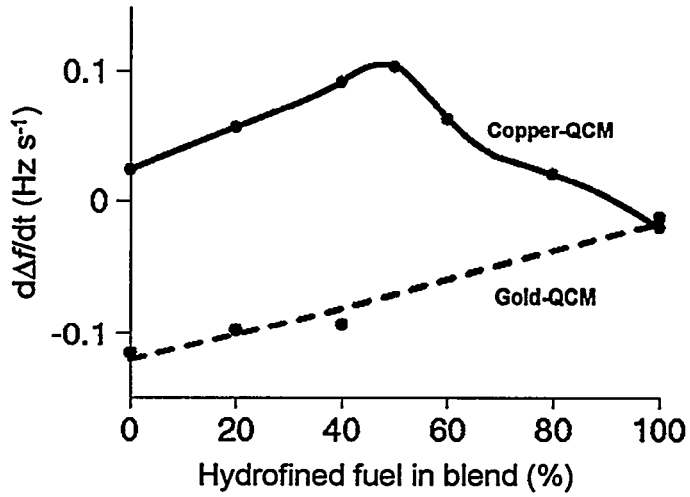


Figure 8. Frequency change rates – Copper and Gold QCM

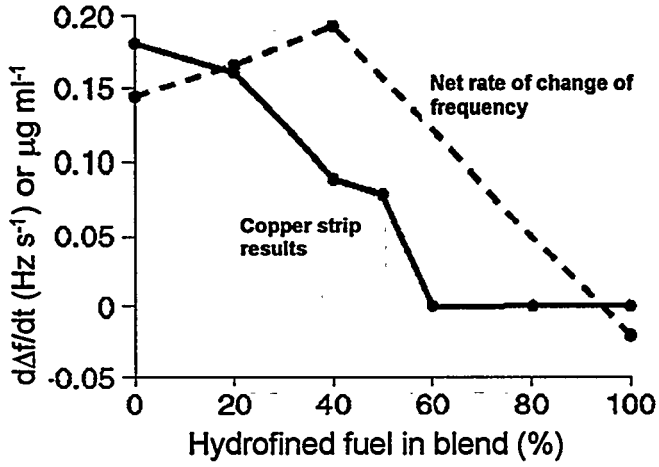


Figure 9. Copper dissolution results – QCM and strip immersion

6th International Conference
on Stability and Handling of Liquid Fuels
Vancouver, B.C., Canada
October 13-17, 1997

CHARACTERISATION AND QUANTIFICATION OF DEPOSITS FROM THERMALLY-STRESSED AVIATION FUELS

Clive Baker, Peter David, Ian Love, Robin Mogford, Spencer E. Taylor*
and Andy J. Woodward

BP Oil, Chertsey Road, Sunbury-on-Thames, Middlesex TW16 7LN, UK

Abstract

Using a combination of the Ellipsometric Tube Analyser (ETA), SEM/EDX analysis and the Jet Fuel Thermal Oxidation Tester (JFTOT), three aspects of thermally-induced deposit formation in jet fuels have been studied. These are (i) the quantification of surface deposits and bulk insolubles generated in the JFTOT test, and the extent to which metal deactivator additive affects deposition rates; (ii) the feasibility of characterising fuel thermal stability from single JFTOT runs; and (iii) a preliminary analysis of the composition and nature of *abnormal* deposits generated in JFTOT tests and the mechanism by which they are formed. The analyses have been based on results from a variety of fuel types.

Introduction

The action of thermally stressing jet fuels is well-known under operational conditions, and research to understand the phenomena involved is well-documented in the literature.[1] The laboratory study of these aspects of fuel thermal breakdown is restricted to a few specialised approaches. Traditionally, the Jet Fuel Thermal Oxidation Tester (JFTOT) is a laboratory device for evaluating the thermal oxidative stability of a jet fuel under a standard set of operating conditions. The device is used to identify the extent of fuel thermal breakdown through the formation of *surface deposits* on a heated metal tube, and also indicates the formation of particulates which cause an increase in pressure differential across a test filter. The ASTM D1655 specification for jet fuel takes into account both types of deposit formation through an assessment of the tube surface coloration and the differential pressure. In a previous

report,[2] the analysis of filterable deposits generated in the JFTOT was achieved by replacing the conventional *ca.*17 micron Dutch-weave filter with a 0.45 micron Millipore membrane and analysing the deposits gravimetrically. This approach usefully complements data provided by more labour-intensive rig testing, and thereby provides additional information on the mechanism and chemistry of fuel degradation under *quasi-dynamic* conditions of laminar flow. Results of previous work along these lines has shown that the rate of bulk particulate formation decreases with increasing JFTOT test time.[2]

Until very recently, routine quantification of JFTOT tube surface deposits was only possible under specific conditions, such as when sufficient deposit was present to allow its combustion and determination of the evolved CO_2, or through dielectric breakdown measurements. These approaches require that deposition occurs over relatively long periods in order to obtain measurable deposit levels, with the mean rates of deposition over the particular time period being quoted. Generally, it has been observed with the carbon burn-off technique that the quoted *deposition rates* initially increase with time, suggesting that different deposition processes are occurring during the experimental timescales. The disadvantage of this methodology, however, is its relative insensitivity to the *early stages of deposition*, which are likely to be formative for the overall course of deposition. One approach to overcome this problem has been through the use of ellipsometry for the analysis of the dimensions of surface films on JFTOT tubes. A description of the basic principles of the ellipsometric approach for characterising surface deposits was presented at the Rotterdam IASH meeting.[3] Since that time, an Ellipsometric Tube Analyser (ETA) dedicated to the handling and deposit quantification of JFTOT tubes has been developed in conjunction with Plasmos GmbH (Munich). This device is able to determine typical surface film thicknesses in the range 0 - 300nm, and is therefore able to characterise the early stages of deposition.[4]

The overall aim of the present study is therefore to quantify fuel breakdown and the formation of different types of deposits in the JFTOT. In particular, examples are described in which a combination of ellipsometric tube analysis, gravimetry and scanning electron microscopy (SEM) are used to investigate different aspects of fuel thermal oxidative stability. These include (i) the relationship between surface and bulk

deposits generated in the JFTOT test, and the extent to which these are affected by the presence of metal deactivator additive; (ii) characterisation of fuel breakdown in terms of the temperature-time course of deposition in the JFTOT; and (iii) a study of the chemical composition and physical nature of *abnormal* deposits produced in JFTOT tests, and the mechanism by which they are formed.

Experimental

Materials

The main fuels used in this study are listed in Table 1. The approved metal deactivator additive (MDA), *N,N'*-disalicylidene-1,2-propanediamine, was obtained from Octel. *n*-Dodecane was purified by passing it through an alumina column prior to use. *n*-Hexane thiol was obtained from Aldrich. The deposits formed on 6061 aluminium JFTOT tubes were largely freshly-generated, although in some cases older, retained tubes were used as illustrative examples.

Methods

A Hot Liquid Process Simulator (HLPS), modified to include a 0.45 micron filter downstream of the fuel outlet from the aluminium JFTOT tube, was used for the surface and bulk deposition studies. Temperature and time have been the two main variables used for any given fuel in the present work. Analysis of surface deposits was effected using the Ellipsometric Tube Analyser, ETA, described elsewhere.[4] Briefly, this method allows tube surface deposit thickness profiles to be measured, and integration under these profiles provides the total deposit volume. Typically *maximum* deposit thickness and deposit volume are the two parameters currently used to characterise the deposit.

JFTOT tube surface (compositional) analyses have been made using Scanning Electron Microscopy (SEM) in a grazing incidence mode at relatively low applied voltages of 3 kV and Electron Dispersive X-ray (EDX) analysis.

Results and Discussion

Comparative Production of Bulk Insolubles and Surface Deposits

A typical ellipsometric deposit thickness profile derived using ETA is shown in Figure 1 as a single slice for a typical fuel. Such profiles illustrate the increasing deposit thickness as the hottest position of the tube is reached (at a point 39.5mm from the inlet).[1] The deposit thickness then decreases beyond this point. ETA routinely measures 12 such longitudinal slices, enabling integration under the resultant surface profile to provide a measure of total deposit volume, V_{dep}. Deposit thickness, t_{dep}, and volume can therefore be used as quantification of the deposits. The time courses for deposit formation for fuel M1 are shown in Figure 2 and for fuel H at two temperatures in Figures 3 and 4; each figure includes data for particulates and surface deposits. Here, data are presented as deposition rates, either for the bulk insolubles (k_b) or surface deposits (k_s), and are based on the volume of fuel treated during a given test time and the residence time τ that the fuel is exposed to the heated tube region (*ie* 11.4s). The latter is calculated from the flow-rate f of 3 ml min^{-1} and the JFTOT test time t and the free volume between the tube and its holder calculated from the tube dimensions. Expressing the data in this way is consistent with other measures of deposit formation based on dynamic testing methods. This serves to normalise the data throughout a given JFTOT experiment, recognising that fresh fuel is being continuously passed over the heated tube, *ie*

$$k_s = \frac{V_{dep}}{ft\tau} \qquad 1)$$

and

$$k_b = \frac{w_{dep}}{ft\tau} \qquad 2)$$

for surface and bulk deposits, respectively, where V_{dep} and w_{dep} are the corresponding ETA deposit volume and weight of filtered bulk insolubles. In Figure 5 are results for M1 fuel containing (added) copper(II) naphthenate (CuM1) in the presence and absence of MDA to modify the thermal stability.

It is apparent from the deposition rate data shown in Figures 2 to 5 that complex behaviour occurs in both surface and bulk deposition regimes. For example, the bulk

insoluble deposit formation rate is seen to decrease during the early stages of the JFTOT experiments for all the fuels studied. For later JFTOT test times, the deposition rate for CuM1 shows signs of increasing. This appears to correspond reasonably well to an increase in surface deposits. These effects are illustrated for M1 and CuM1 fuels in Figure 6 in which the ratio of the rates of formation of surface deposits to bulk insolubles are presented.

It can be seen that, in the case of the highly-depositing CuM1 fuel (in the absence of MDA), the ellipsometric analyses show a steady rate of surface deposition, up to *ca.* 100 minutes into the test. Thereafter, an increase becomes apparent. Interestingly, this region coincides with the "secondary production" of bulk filterable deposits (Figure 5). Even allowing for the uncertainties associated with the quantification of the low levels of filterable deposits, the correspondence between these two sets of data is evident. It is tempting in this case to suggest that the increases in the two sets of deposits have a common origin. In the case of the corresponding MDA-treated fuel, there is little evidence for an increase in surface deposition rate over the time-scale of the experiments, with bulk particulate formation also being retarded. Deposit formation in all the fuels studied so far has been characterised by a high initial rate of bulk particulate formation, suggestive of an involvement of the clean tube surface. The reduction in the bulk deposition rate (Figure 6) appears to be accompanied by the slower rate of formation of surface deposits. The activity of the fresh tube surface may be influenced by surface metallurgical factors discussed later in this paper.

Single-run Thermal Stability Analysis

The JFTOT test is a non-isothermal method. Fuel flowing over the electrically-heated tube produces a temperature gradient as detailed in ASTM D3241. As a consequence, surface deposition generally approaches a maximum thickness at or around the "hot spot", some 40mm from the fuel inlet. Although attempts had been made with varying degrees of success in the past to quantify deposit thicknesses, only now does ETA analysis make this routine. In particular, it is now possible to determine deposit thicknesses at given positions along the tube surface which can be correlated with tube temperature profiles, thereby generating deposit thickness-tube temperature profiles from single JFTOT runs. An example of this transformation is given in Figure 7, from

which the asymmetry of the temperature profile is evident, with the upstream side of the deposit being thinner than the downstream side for the same temperature. This has been found for all of the tubes analysed in this way to date, and confirms previous SEM/EDX analyses,[2] and possibly arises from the finite kinetics of the surface deposition process. If this is indeed the case, it would seem appropriate that effects on the upstream side of the maximum deposit thickness will be indicative of the direct effects of temperature on the formation of depositing species and of deposition, and hence fuel thermal stability in general. The reproducibility of this portion of the deposition profile is illustrated in Figure 8 in which deposit thickness profiles for a single fuel at several different JFTOT operating temperatures are presented. It is evident that data on the fuel inlet side of the maximum tube temperature position are highly reproducible, whilst deviations are apparent on the outlet side. This type of analysis therefore creates the possibility of determining *from a single JFTOT run* a temperature which corresponds to a given deposit thickness *on the inlet side of the maximum deposit*. This has been done for a number of different fuels systems, and temperatures corresponding to a thickness of 120 nm (as an illustration of the approach only) are compared with the conventional visually-rated "breakpoint temperature", in Table 2. From these data, it can be seen that there is good directional agreement between results from "conventional" determinations and this new approach based on a single JFTOT run.

Analysis of "Abnormal" Deposits

The visual appearance of many abnormal deposits results from the scattering of light, suggesting the presence of some surface particulate material. Moreover, the consistent formation of abnormal deposits using fuel systems has been difficult to achieve in the laboratory. In view of the latter, in order to satisfy the requirement for reproducible abnormal deposits, a model system was developed. This comprised dodecane + 100ppm hexane thiol run at typically >300°C, for which the appearance of the deposits was similar to those observed for a sample of M1 fuel (at the lower temperature of 260°C). ETA and SEM/EDX analyses were carried out on each system. In each case, in the "abnormal" regions of the respective tubes, a high concentration of particulates in the size range 1-5 microns, comprising, predominantly magnesium and oxygen was

observed, as shown in Figure 9. Additionally, some carbon was often also found to be associated with these particles.

Figure 10 shows the "abnormal" ETA thickness profiles for a sample of fuel M1, in which the abnormal and normal regions are clearly distinguishable. Figure 11 shows comparative EDX spectra for a typical particle and the adjacent background for the M1 fuel. In this region, there is little carbon seen to be associated with the deposit, although in the background spectrum there is evidence for the presence of contaminant metals. (Cu or Zn in this instance). By way of contrast, Figure 12 shows a corresponding particle in the "normal" region at approximately 40mm from the fuel inlet, in which it can be seen that the level of carbon is substantially increased, in accord with the ellipsometric profile.

Figure 13 shows the deposit profile for the dodecane/*n*-hexane thiol system at three temperatures. The presence of magnesium-rich particles was confirmed by SEM/EDX, as above, and a representative EDX spectrum is shown for the 40mm position from the fuel inlet in Figure 14. On the basis of these observations, it is concluded that the presence of magnesium in particulate form on the tube surface must originate from the tube itself. The 6061 aluminium JFTOT tubes contain *ca.* 1% magnesium which is initially uniformly distributed throughout the aluminium matrix. Previous studies led to the conclusion that, under JFTOT conditions, magnesium "migration" to the surface occurred.[1] Although at a relatively early stage, results of recent SEM/EDX analyses, confirm changes to the surface metallurgy of aluminium tubes as a consequence of thermal/fuel treatment. A tentative explanation of the observed features of the process involves an initial redistribution, akin to a coalescence process, of the minor magnesium component of the 6061 alloy into Mg-rich surface domains, observable at the inlet end of the tube. Further along the tube, where the local surface temperatures are higher, these domains give way to pronounced Mg-rich particulates, as described above. Although initially located in the surface region, the particulates appear to be depleted further along the tube, only to be concentrated in specific regions, where their increased concentration results in an "abnormal" appearance. At the present time it is not clear whether the observations and interpretations of this part of the work is

related in any way to the increased rates of bulk particulate formation discussed earlier. These aspects are being addressed in continuing studies.

Conclusions

The present study has demonstrated the use of a combination of JFTOT/HLPS techniques and ellipsometric (ETA) analysis for characterising jet fuel thermal stability and breakdown mechanisms. The rate of formation of bulk insolubles is found to decrease as the volume of fuel treated is increased. Profiling JFTOT tube surfaces by ellipsometry has been shown to offer potential for determining fuel thermal stability from a single test. Abnormal deposits have been found to comprise mainly inorganic particulates, which have been found to be magnesium-rich in many instances. In the present work, the formation of magnesium-based abnormal deposits in a model fuel system which is devoid of magnesium, strongly implicates the JFTOT tube as the magnesium source. If this finding is confirmed during ongoing studies, this indicates that this thermal stability fail code may be an artefact of the test procedure using aluminium alloy tubes.

Acknowledgements

This project was funded by Air BP and the UK Ministry of Defence.

References

(1) Hazlett, R.N. *Thermal Oxidation Stability of Aviation Turbine Fuels*; ASTM, Ann Arbor, MI, 1991

(2) Baker, C.; David, P; Hall, D; Swatridge, R. *Proc. 4th International Conf. on the Stability and Handling of Liquid Fuels*, Orlando, FLA, 1991, 316-328

(3) Baker, C; David, P; Taylor, S.E.; Woodward, A.J. *Proc. 5th International Conf. on the Stability and Handling of Liquid Fuels*, Rotterdam, 1994, 433-447

(4) David, P.; Mogford, R.; Paduschek, P.; Taylor, S.E.; Woodward, A.J. "Development of an Ellipsometric JFTOT Tube Analyser (ETA)", Presented at *6th International Conf. On the Stability and Handling of Liquid Fuels*, Vancouver, 1997

Table 1. Fuels used in the present work.

Fuel (abbreviation)	Comments
Merox 1 (M1)	< 10ppb metals
Merox 2 (M2)	< 10ppb metals
Cu-doped Merox 1 (CuM1)	30ppb Cu added as copper naphthenate
Hydrofined (H)	< 10ppb metals

Table 2. Comparison between visually-rated breakpoints and single-run T_{120nm} values for several systems.

Fuel system	Tube number (JFTOT temperature /°C; VR)	T_{120nm} /°C	VR breakpoint /°C
M1 + 150ppb Fe naphthenate	1989 (255; <4)	238	-
Kerosene	2023 (250; <4)	250	245
CuM1	1988 (260; <4)	260	-
M1	96/113 (260; <4)	257	255
M2	2154 (290; <4P)	272	265
Jet A1/6% diesel	2016 (295; >4P)	293	285
JP8	3982 (296; <4)	296	291

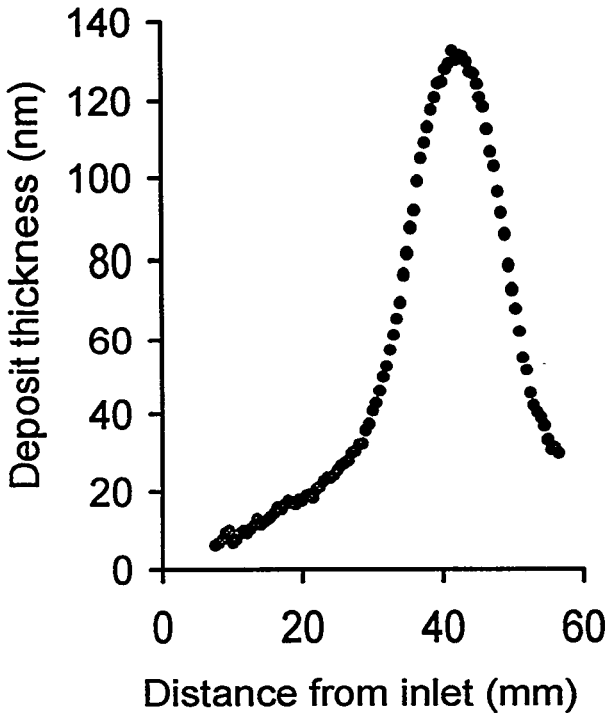


Figure 1. A typical single slice surface deposit profile for a coloured deposit.

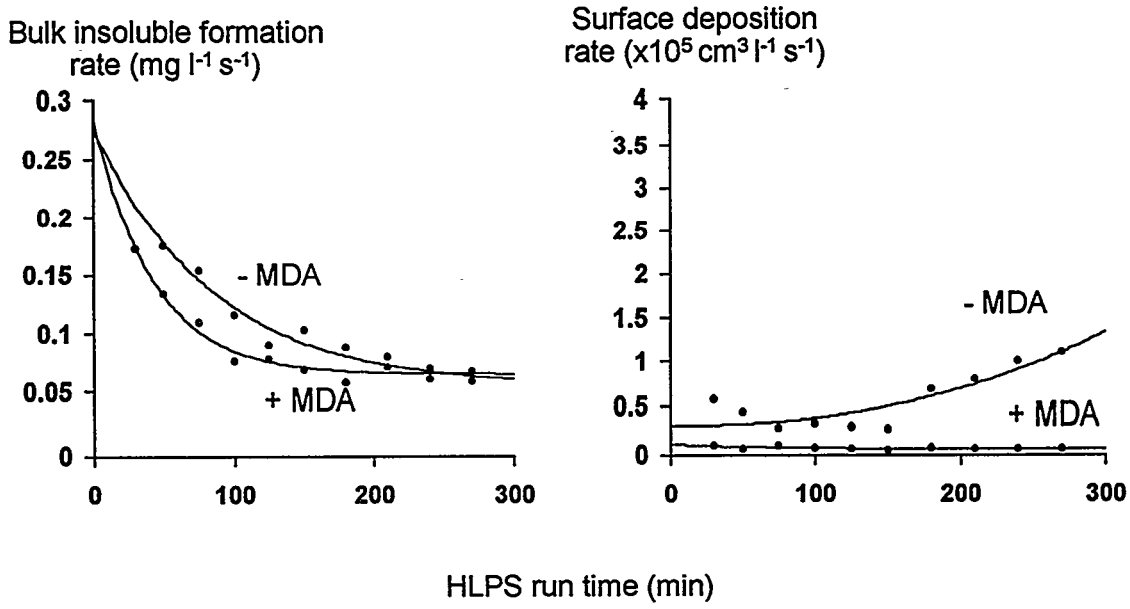


Figure 2. Surface and bulk deposition rates for Merox fuel M1 in the presence and absence of 5.7 mgl^{-1} MDA (255°C).

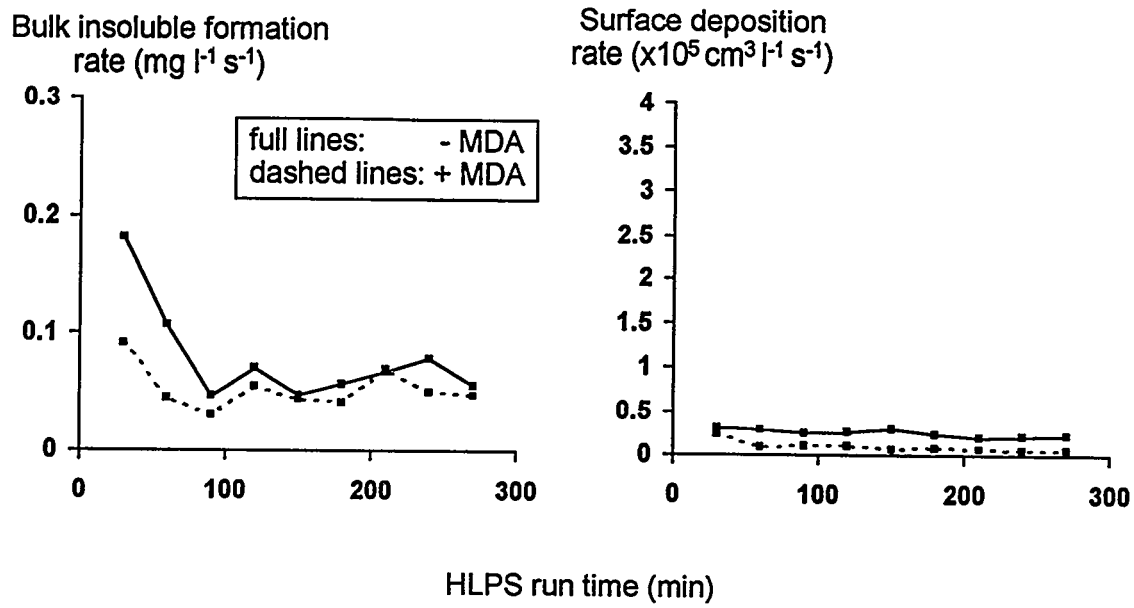


Figure 3. Surface and bulk deposition rates for hydrofined fuel H in the presence and absence of 5.7 mgl^{-1} MDA (280°C).

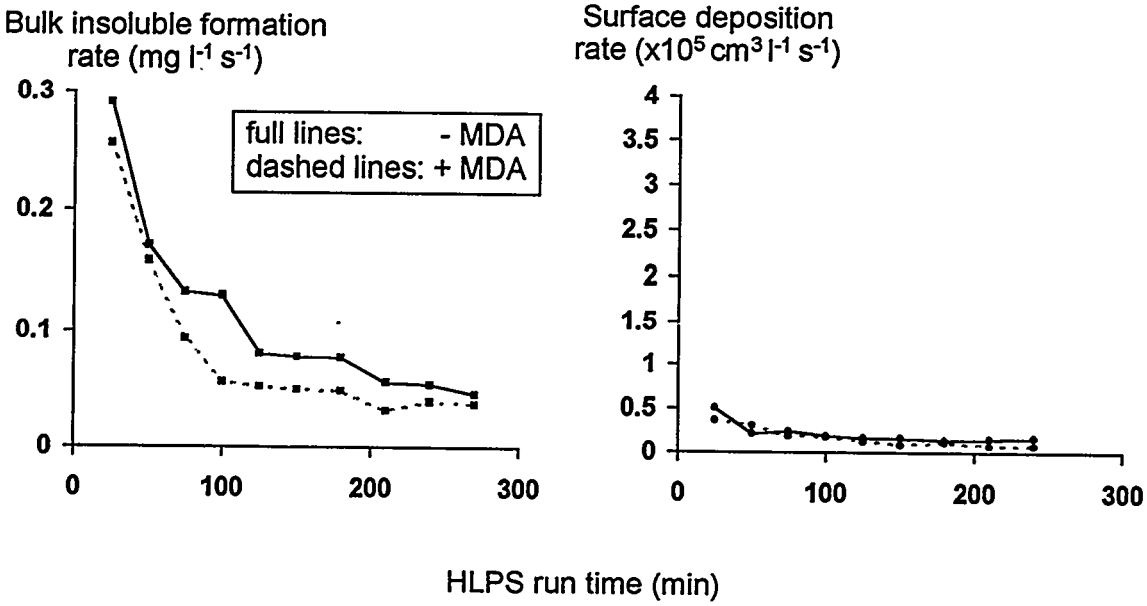


Figure 4. Surface and bulk deposition rates for hydrofined fuel H in the presence and absence of 5.7 mgl^{-1} MDA (340°C).

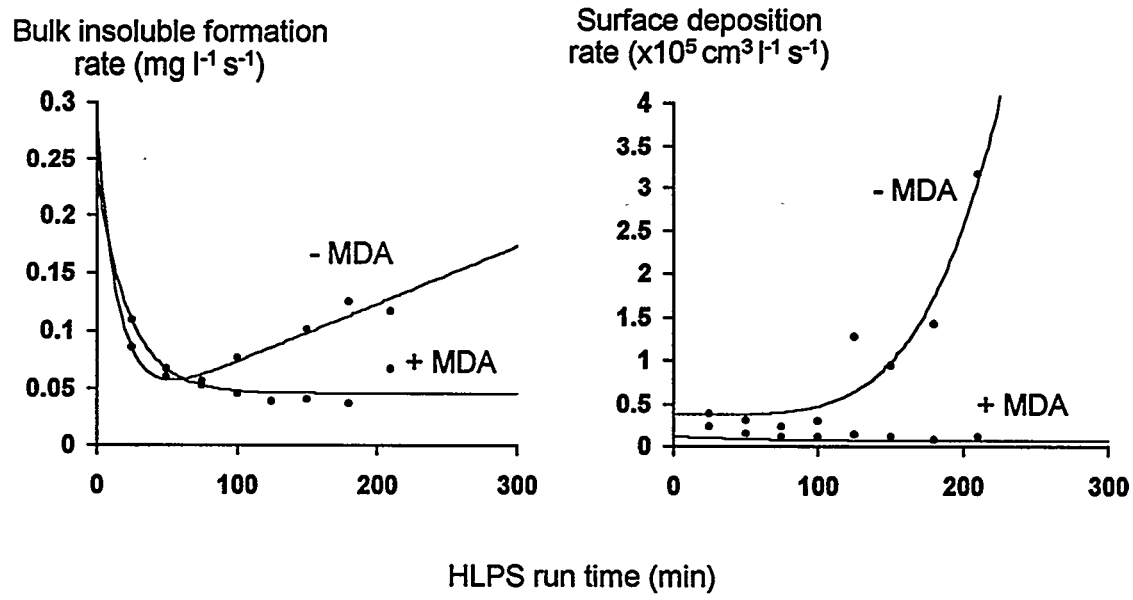


Figure 5. Surface and bulk deposition rates for CuM1 fuel in the presence and absence of 5.7 mgl^{-1} MDA (245°C).

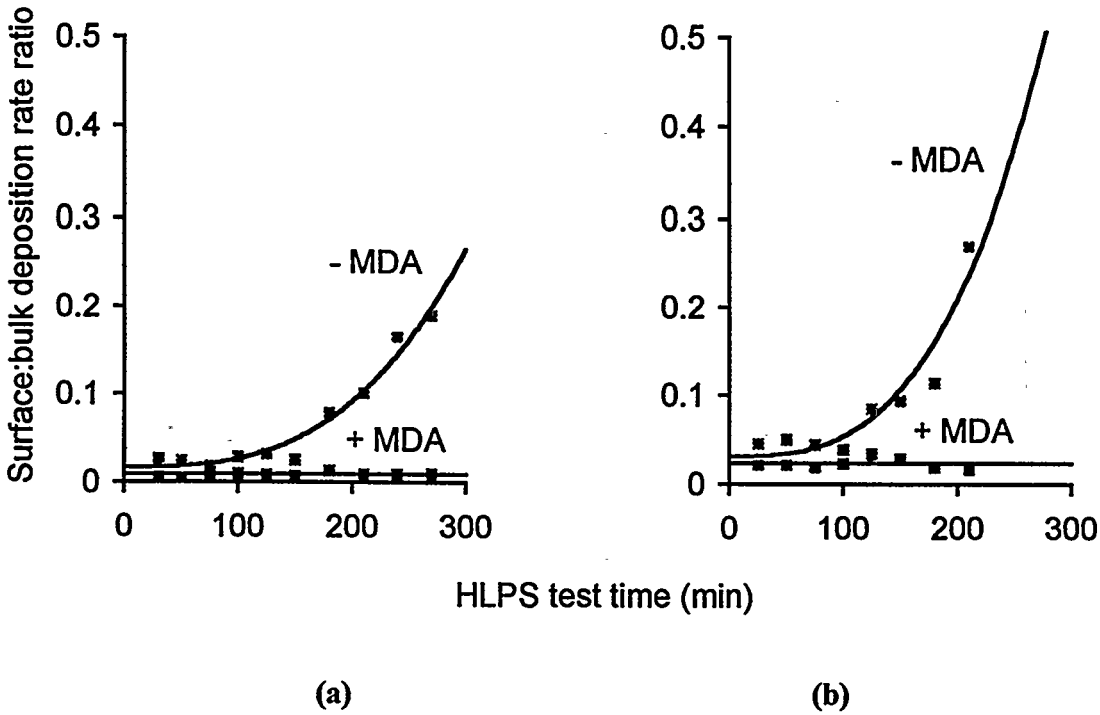


Figure 6. Ratio of surface to bulk deposition rates for (a) M1 at 255°C and (b) CuM1 at 245°C, in the presence and absence of 5.7 mgl^{-1} MDA

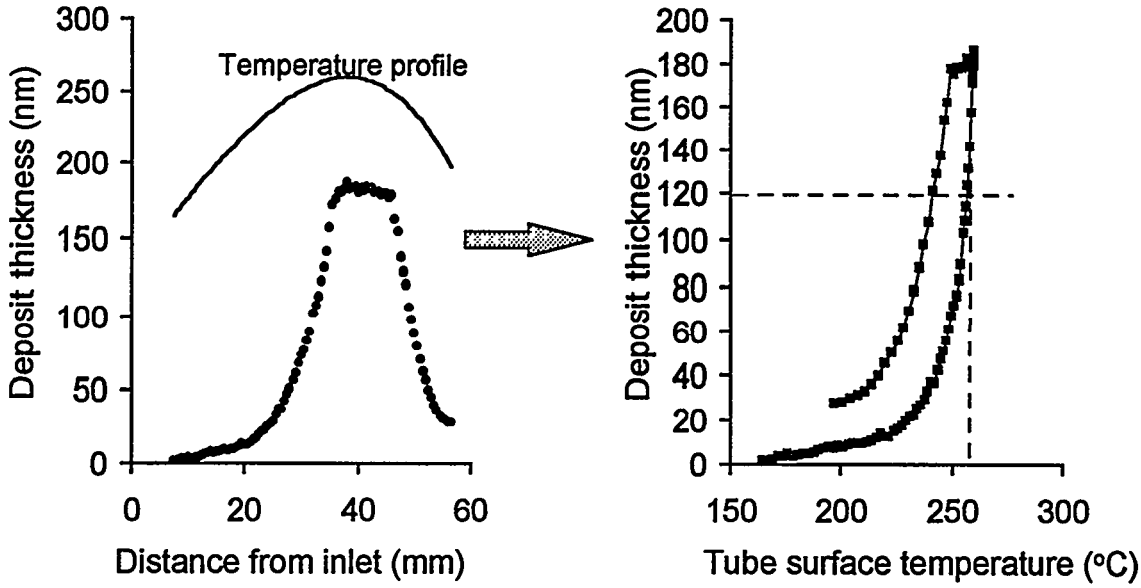


Figure 7. An illustration of the transformation between deposit thickness-distance data to thickness-temperature data for fuel M1 run at a JFTOT temperature of 260°C, indicating the "critical" temperature T_{120nm}.

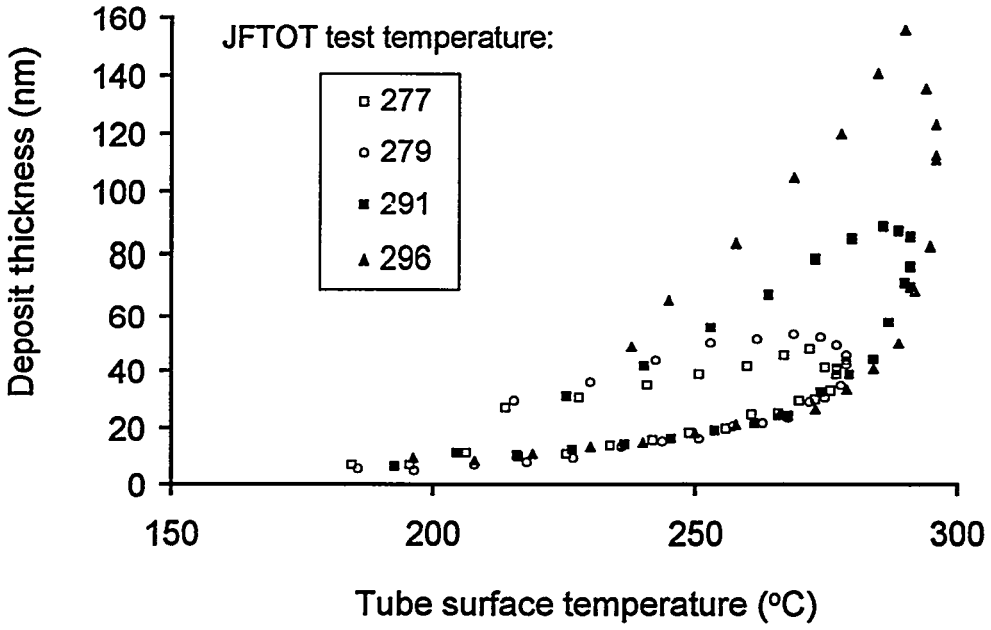


Figure 8. Deposition profiles for different JFTOT temperatures as a function of tube surface temperature.

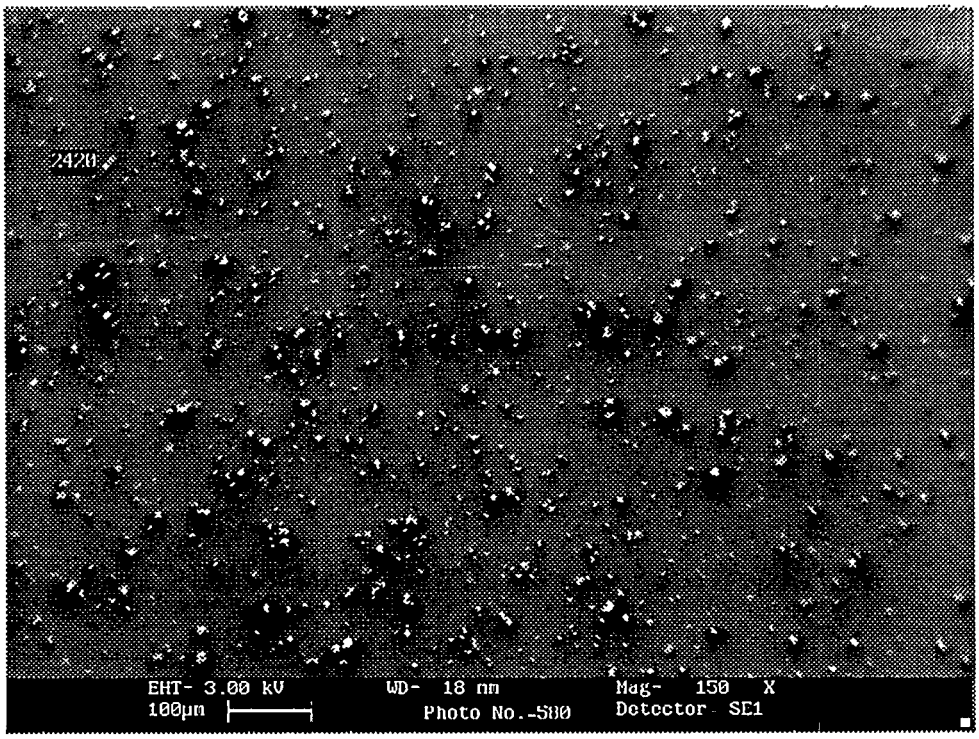


Figure 9. A scanning electron micrograph showing magnesium-rich particles in the "abnormal" region.

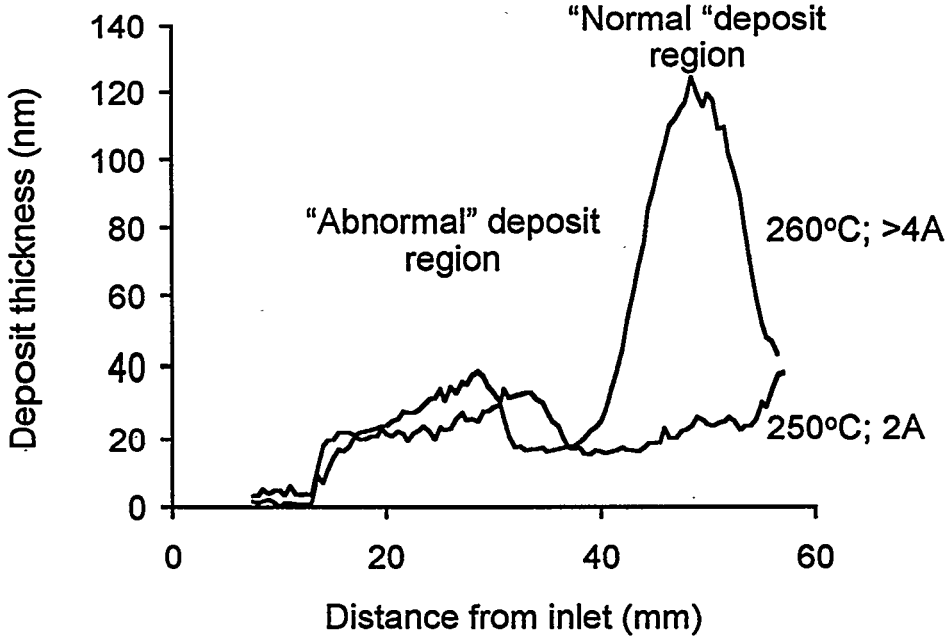
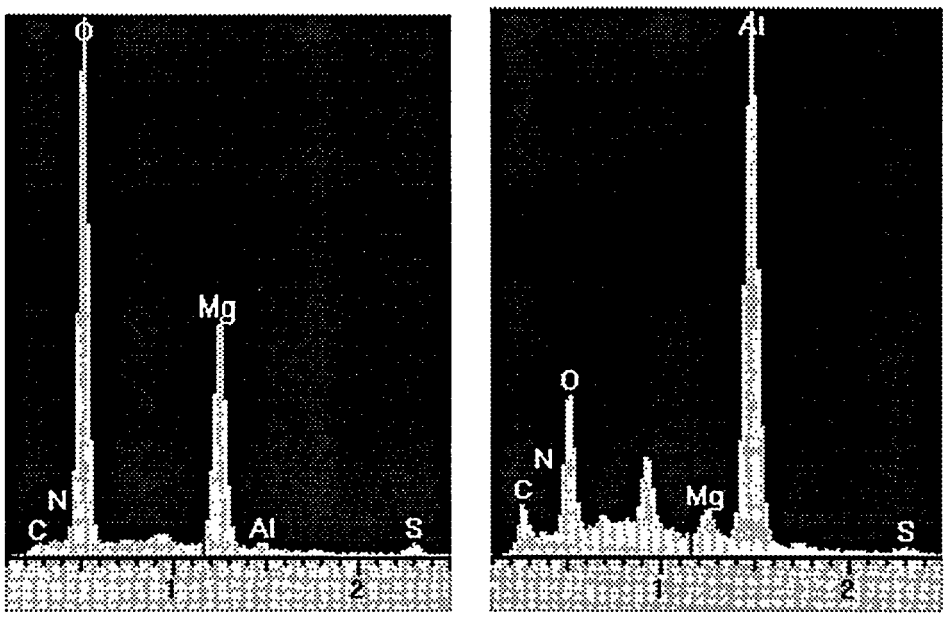
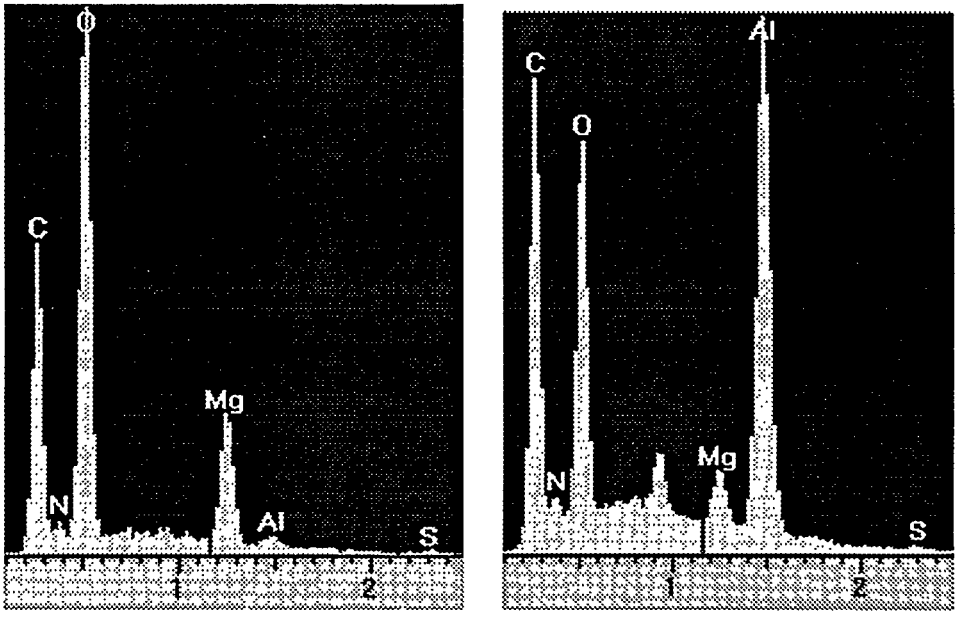


Figure 10. ETA thickness profile for a sample of fuel M1 at two different (indicated) temperatures.



(a) (b)

Figure 11. EDX compositional analysis of (a) a particle in the "abnormal" region at 30mm from the fuel inlet and (b) the adjacent background region for fuel M1 at 260°C.



(a) (b)

Figure 12. EDX compositional analysis of (a) a particle in the "normal" region at 40mm from the fuel inlet and (b) the adjacent background region for fuel M1 at 260°C.

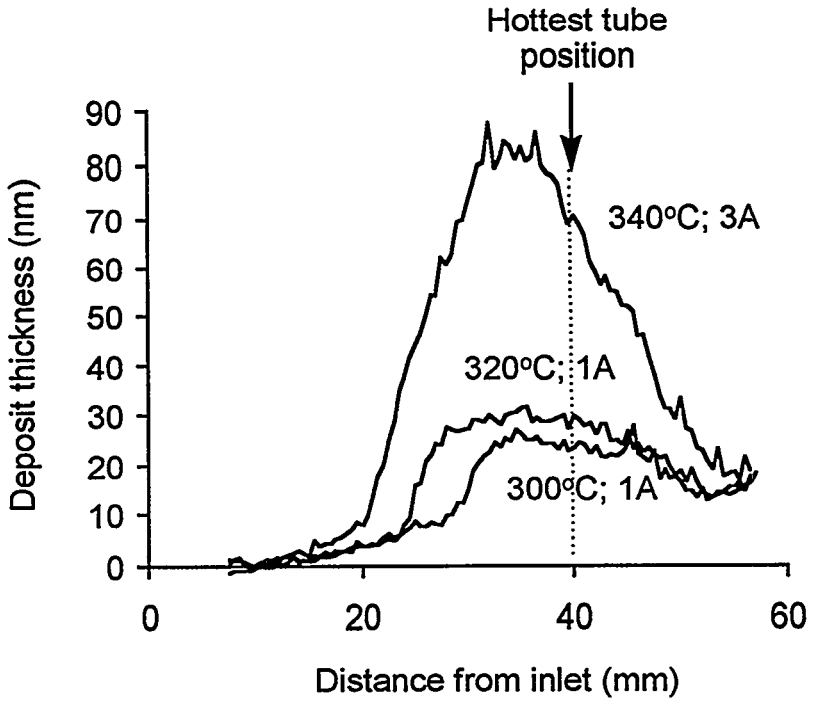
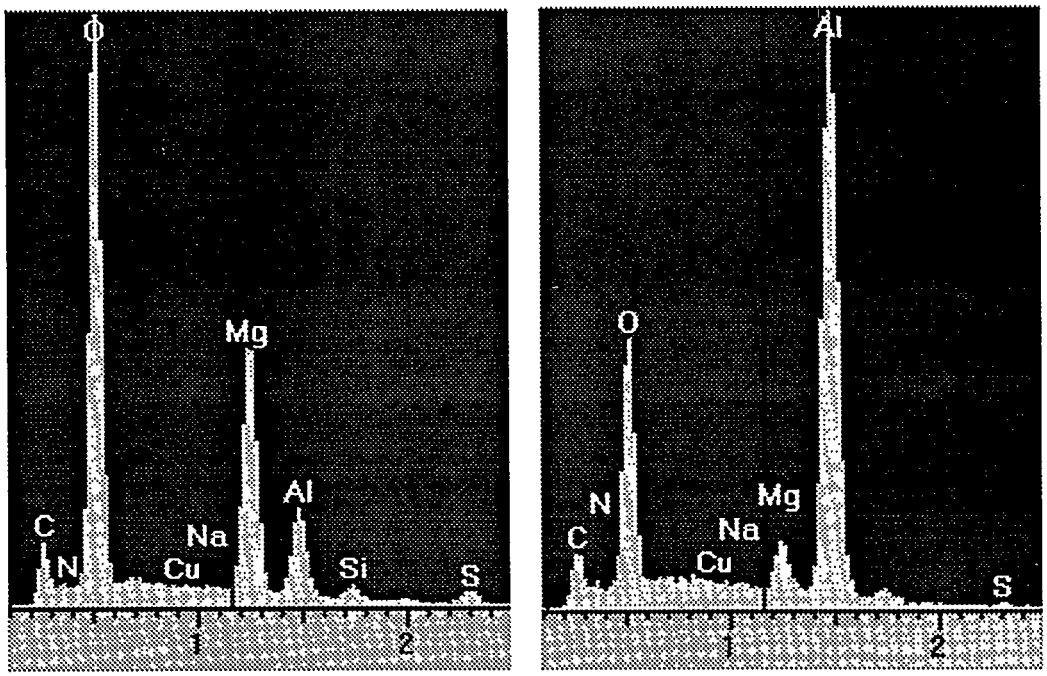


Figure 13. ETA thickness profile for dodecane + 100ppm *n*-hexane thiol at three different (indicated) temperatures. Visual ratings are also indicated.



(a) (b)

Figure 14. EDX compositional analysis of (a) a particle in the "abnormal" region at 40mm from the fuel inlet and (b) the adjacent background region for the dodecane/*n*-hexane thiol system at 320°C.

6th International Conference on
Stability and Handling of Liquid Fuels
Vancouver, B. C., Canada
October 12-17, 1997

IMPACT OF FUEL RECIRCULATION ON THERMAL STABILITY

E. Grant Jones*, Walter J. Balster, and Lori M. Balster

Innovative Scientific Solutions, Inc., 2786 Indian Ripple Road, Dayton, OH 45440-3638, USA.

ABSTRACT

Modern military aircraft utilize aviation fuel for combustion energy and also as a heat sink to cool component systems. On-board fuel management must satisfy both combustion and cooling requirements during all phases of a flight. Frequently, fuel that has been subjected to thermal oxidative stress must be diverted from combustion and recirculated back to the fuel tanks. The resultant pre-stressing can significantly reduce fuel thermal stability. Through an isothermal simulation under well-defined reaction conditions, the thermal stability of neat and pre-stressed or recirculated fuels has been measured. It was found that fuel recirculation seriously degrades thermal stability. The results of this study are reported, and possible corrective measures are discussed.

INTRODUCTION

In addition to providing combustion energy, fuel in modern aircraft is utilized as a heat sink to cool component systems.[1] Exposure to heated surfaces and the presence of dissolved oxygen can lead to the undesirable fouling of critical surfaces. As surfaces become fouled with carbonaceous deposits, the efficiency of heat transfer decreases, servo controls experience hysteresis, and nozzle performance is degraded. Methods of limiting fouling include improvements in fuel thermal stability through refining techniques such as hydrotreatment and through the use of fuel additives and additive packages. Efficient fuel management for limiting fuel exposure time at temperature and surface treatment to minimize catalytic effects have also been used in efforts to minimize this problem.

Additional complications arise because of fuel management, whereby a fraction of the fuel that has already been used for cooling is directed back to on-board fuel tanks for later use. In fact, certain flight conditions such as idle descent create high

heat dissipation needs at a time when combustion requirements are minimal. Under these latter conditions, most of the thermally stressed fuel is returned to the fuel tanks. As the flight progresses an increasingly larger fraction of pre-stressed fuel is utilized. Clearly, pre-stressed fuel will have reduced thermal stability. Binns and co-workers[2-5] have reported increased fouling related to recirculation of JP-8 fuels in a large-scale simulator. The present paper reports the results from a simple test simulation under well-defined isothermal test conditions at 185°C. The effects of fuel recirculation on thermal stability were determined by measurements of autoxidation behavior and surface and bulk insoluble formation for both neat fuels and recirculated blends. Potential sources of the problem are discussed, and results from the use of the JP-8+100 additive packages consisting of antioxidant, metal deactivator (MDA), and dispersant/detergent are presented.

EXPERIMENTAL

Two Jet-A fuels have been investigated; on the basis of the quantity of insolubles formed during stressing at 185°C (surface > 2.5 μg/mL; bulk > 1.8 μg/mL), these fuels have average to below-average thermal stability. Experiments were conducted at 185°C using NIFTR[6] single-pass heat exchangers. The basic experiments for deposition and oxidation measurements were described in detail previously.[7] A new recirculation configuration and related O_2 measurements will be described in more detail here. Four different types of experiments have been performed; the first two involve measurements of surface and bulk insolubles, and the last two relate to O_2 depletion. A total system pressure of 2.3 MPa was used in all experiments to ensure a single reaction phase.

Standard Single-Pass Test. Fuel, initially saturated with respect to air at room temperature, is pumped at 0.25 mL/min through stainless-steel (304) tubing (183-cm long, 0.216-cm i.d., 0.318-cm o.d.) maintained at constant wall temperature within a Cu-block heat exchanger. Because of the slow fuel flowrate, reaction occurs isothermally, and reaction time or stress duration can be calculated at each position along the tube, assuming plug flow. A complete pass through the block provides 22 min of stressing during which all of the dissolved O_2 is depleted. Fuel, after leaving the heated region, cools and passes through two in-line Ag-membrane filters (0.45 and 0.20 μm). After a 72-hr period and the passage of 1.08 L of fuel, the tube is removed, rinsed with heptane, and cut into 5.1-cm sections. Each tubing segment and filter is treated in a vacuum oven for 24 hr and then evaluated using surface-carbon

analysis. The quantity of carbon in the surface insolubles is summed along the tube, and the result is expressed as total surface carbon per unit volume of fuel as a function of residence time in minutes.

Recirculation Double-Pass Test. The new test configuration (Figure 1) is a variation on the single-pass test setup whereby Pump 1 passes fuel through the heat exchanger to provide the initial stressing. After exiting the heated block, fuel is cooled for 1 min, mixed with an equal flow of unstressed fuel from Pump 2, and directed back through a second channel in the heat exchanger. The second pass simulates the use of pre-stressed (and re-oxygenated) fuel as a heat sink. Since the initially stressed fuel contains no residual O_2, the resulting blend contains 50% stressed fuel and a dissolved O_2 concentration that is 50% of the air-saturated level. At the higher flowrate (0.5 mL/min), the recirculated fuel blend receives only 11 min of stressing. At the exit of the heated block, fuel cools and passes through in-line filters. After a 72-hr period during which 1.08 L of neat fuel have passed through the first tube and 2.16 L of the pre-stressed fuel blend through the second tube, tubes and filters are evaluated for surface carbon as described above.

Autoxidation of Neat Fuel. Autoxidation occurs as fuel passes through a fixed length (81.3 cm) of heated tubing within a Cu-block heat exchanger. Reaction time within the heated tube is varied by changing the flowrate. The initial dissolved O_2 concentration is equated to 100%, and the residual dissolved O_2 following reaction is measured at the end of the tube using GC detection. In one series of experiments using reduced (50%) initial O_2 concentration, fuel is sparged for 30 min with a 1/9 blend of O_2/N_2. For reducing surface catalysis in autoxidation experiments, tubing passivated by the Silcosteel[8] process is used.

Autoxidation of Pre-Stressed Fuel. Depletion of O_2 in the recirculated blend is tracked by diverting the blended fuel into a separate heater block (81.3 cm), as shown in Figure 1, and changing the residence time by adjusting the system flowrate. These measurements are much less accurate than those discussed above for neat fuels. Through the establishment of equal, progressively higher flowrates at Pumps 1 and 2, the initial dissolved O_2 entering the second block is maintained at 50%, and reaction time in the sampling block is correspondingly reduced. Data can be collected only at flowrates where the initial fuel from Pump 1 experiences 100% O_2 conversion before blending.

RESULTS AND DISCUSSION

Surface Fouling and Autoxidation of Neat Fuel. The total surface carbon measured for neat (air-saturated) fuels is represented by closed circles in Figure 2; the corresponding autoxidation data are given in Figure 3. Autoxidation is characterized by acceleration at higher conversion caused by self-initiation from thermal--and, in addition, possible metal-catalyzed--dissociation of hydroperoxides.

Surface Fouling of Recirculated Fuel. In the current test configuration, recirculated fuel is actually a 1/1 blend of neat fuel and fuel that has been stressed for 22 min at 185°C. Since all of the O_2 has been consumed in 22 min of stressing, the resultant blend contains only 50% of the O_2 present in air-saturated fuel. In isothermal experiments with complete O_2 conversion, the total quantity of insolubles is proportional to the amount of dissolved O_2. In the absence of other factors, total surface fouling from recirculated fuel will be only about one-half that from neat fuel.

Surface fouling for recirculated-fuel blends (see Figure 2) differs significantly from that for neat fuels, although the total quantities are in the expected range. Deposition from the pre-stressed fuel blend increases sharply from t = 0, whereas neat fuels exhibit some delay (induction time) before the highest rate of surface fouling is achieved. Because of this difference, total fouling in the recirculation pass exceeds that of the neat fuel over at least the first 5 min of reaction. In summary, despite a reduced O_2 concentration, surface fouling in the recirculation pass occurs at shorter reaction times with a rate similar to that eventually achieved with neat fuel.

Autoxidation of Neat and Recirculated Fuels at Reduced Initial O_2. Interpretation of the deposition data requires information on the autoxidation of both neat and pre-stressed fuels at reduced initial O_2. Results of O_2 measurements are given in Figure 3. The rate of autoxidation of neat, half-air-saturated fuel is never faster than that of neat, air-saturated fuel. However, because of reduced reactant concentration, the total time required for depletion of O_2 is always less. This finding indicates that the simple reduction of dissolved O_2 associated with this test configuration cannot account for the changes in deposition observed in Figure 2. These changes result from pre-stressing.

Autoxidation of recirculated fuels requires less time than that of neat fuels, although the maximum reaction rates achieved at high conversion are similar for both the neat and recirculated fuels, independent of O_2 content. Autoxidation times of pre-stressed fuels are expected to be shorter for two reasons. The first involves depletion of antioxidants. If antioxidants are totally consumed during pre-stressing, their overall

reduction in a 1/1 blend is 50%; this change alone may be sufficient to account for the observed differences. The second concerns the formation of catalytic products. It is doubtful that many hydroperoxides will survive 22 min of stressing at 185°C, but even small concentrations of dissolved metals will add to the free-radical pool.

Differences in fouling may be due only in part to oxidation. A potentially more important cause may be the presence of insolubles in the recirculated stream. Pre-stressing may effectively establish conditions for rapid deposition, thereby precluding the need for an induction time. This factor may account for the above observation that deposition from recirculated fuel displays little or no time delay.

Implications and Corrective Action. Two major factors are offered to account for differences in the thermal stability of neat and recirculated fuels. The first relates to increases in the rate of autoxidation caused by a combination of reduced antioxidant concentration and the formation of catalytic products. The second relates to reduction or elimination of the time delay in the formation of surface deposits. Surface fouling associated with fuel recirculation can be minimized by 1) slowing autoxidation through the use of effective primary and secondary antioxidants, 2) eliminating metal-catalyzed free-radical initiation through the introduction of a metal deactivator, and 3) reducing agglomeration of insolubles through the introduction of appropriate detergents/dispersants. The suggested methods to reduce fouling in recirculated fuel are virtually the same as those found to minimize fouling from neat fuels. Additive packages, developed as part of the USAF JP-8+100 program,[12] consisting of antioxidant, metal deactivator, and dispersant have been shown to reduce surface and bulk insolubles in both fuels studied.[9,10] Also, Binns and co-workers[2,4,5] have found reductions in surface fouling in a JP-8 fuel (POSF-2980) with the use of additive packages.

Changes in thermal stability for two candidate JP-8+100 additive packages is shown in Figure 4. In this comparison the relative change in surface fouling with the introduction of the additive package is plotted as a function of reaction time. The dashed line through the origin represents no change; positive and negative values indicate, respectively, increased and reduced fouling. Additive packages 1 and 2 differ only in the nature of the proprietary detergent/dispersant. The first is manufactured by Ethyl Corporation and the second by Betz Corporation. The two behave similarly and significantly reduce surface fouling and, by definition, improve thermal stability as measured at 185°C. Bulk insolubles are similarly reduced.

CONCLUSIONS

Small-scale isothermal rigs using only 2 L of fuel have been employed for comparing the behavior of two Jet-A fuels in a single-pass and in a recirculation test configuration to assess the effect of fuel recirculation upon thermal stability. Total insolubles collected for an extended reaction time and for complete O_2 consumption have been found to be independent of the test mode. However, recirculated fuel containing a pre-stressed fraction displays an increase in surface fouling, particularly over reduced stress times. We have identified three causes for this reduced thermal stability, all attributable to changes occurring during pre-stressing: 1) consumption of antioxidants, 2) formation of catalytic products, and 3) development of precursors to surface deposition. Changes 1) and 2) accelerate autoxidation, and change 3) reduces the delay time in surface fouling in isothermal tests. Two additive packages consisting of antioxidant, metal deactivator, and dispersant are shown to provide a simple means of reducing fouling in both single-pass and recirculation configurations. Conceivably, higher concentrations of synthetic antioxidant and dispersant may result in further reductions in fouling associated with fuel recirculation. A more detailed reporting of the effects of recirculation on these and other fuels is scheduled.[11]

ACKNOWLEDGEMENTS

This work was supported by Wright Laboratory, Aero Propulsion and Power Directorate, Wright-Patterson Air Force Base, Ohio, under USAF Contract No. F33615-95-C-2507. Valuable discussions with Mr. Steven D. Anderson (USAF) and Mr. K. Edward Binns (University of Dayton Research Institute) are gratefully acknowledged. The authors thank Mrs. Marian Whitaker (ISSI) for editorial assistance.

LITERATURE CITED

(1) Edwards, T.; Anderson, S. D.; Pearce, J. A.; Harrison, III, W. E. High-Temperature JP Fuels--An Overview, AIAA Paper No. 92-0683, Presented at the AIAA 30th Aerospace Sciences Meeting and Exhibit, Reno, NV, 6-9 January 1992.

(2) Dieterle, G. L.; Binns, K. E. Evaluation of High Thermal Stability Fuels for Future Aircraft, AIAA Paper No. 94-3171, Presented at the 30th AIAA/ASME/SAE/ASEE Joint Propulsion Conference, Indianapolis, IN, 27-29 June 1994.

(3) Binns, K. E.; Dieterle, G. L.; Williams, T. In *Proceedings of the 5th International Conference on Stability and Handling of Liquid Fuels*; Giles, H. N., Ed.; U.S. Department of Energy: Washington, D. C., 1995; Vol. 1, pp 407-422.

(4) Dieterle, G. L.; Binns, K. E. Extended Duration Thermal Stability Test of Improved Thermal Stability Jet Fuels, ASME Paper No. 95-GT-69, Presented at the International Gas Turbine and Aeroengine Congress and Exposition, Houston, Texas, 5-8 June 1995.

(5) Binns, K. E.; Dieterle, G. L. *Prepr.-Am. Chem. Soc., Div. Pet. Chem.*, **1996**, *41* (2), 457-460.

(6) NIFTR: Near-Isothermal Flowing Test Rig.

(7) Jones, E. G.; Balster, L. M.; Balster, W. J. *Energy Fuels* **1996**, *10*, 509-515.

(8) Silcosteel tubing, Restek Corp., Bellefonte, PA.

(9) Jones, E. G.; Balster, W. J.; Balster, L. M. Evaluation of the Effectiveness of a Metal Deactivator and Other Additives in Reducing Insolubles in Aviation Fuels, ASME Paper No. 96-GT-204, Presented at the International Gas Turbine and Aeroengine Congress and Exposition, Birmingham, U.K., 10-13 June 1996. ASME J. Eng. Gas Turb. Power, **1997**, *119*, 830-835.

(10) Balster, W. J.; Balster, L. M.; Jones, E. G. *Prepr.-Am. Chem. Soc., Div. Pet. Chem.* **1996**, *41* (2), 446-451.

(11) Jones, E. G.; Balster, W. J.; Balster, L. M. *Energy Fuels* **1997** (in press).

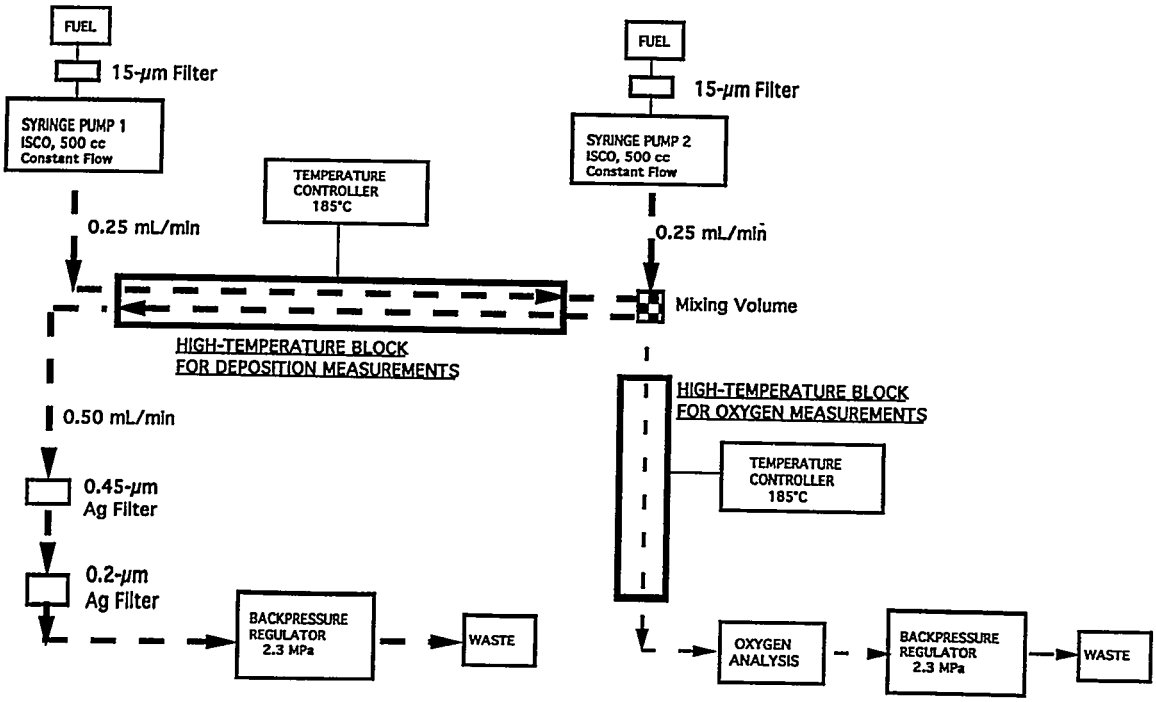


Figure 1. Schematic Diagram of Apparatus (NIFTR)

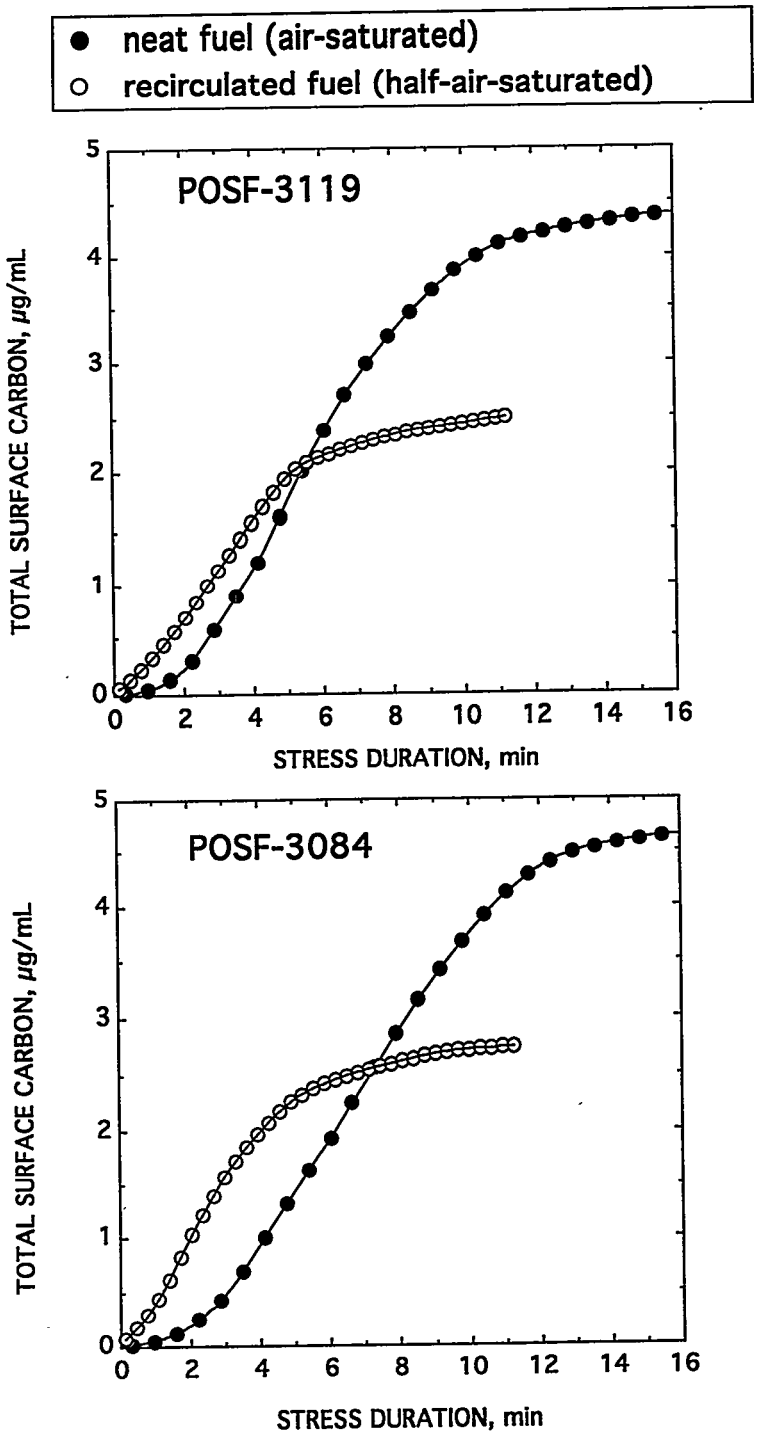


Figure 2. Surface Deposition Profiles at 185°C.

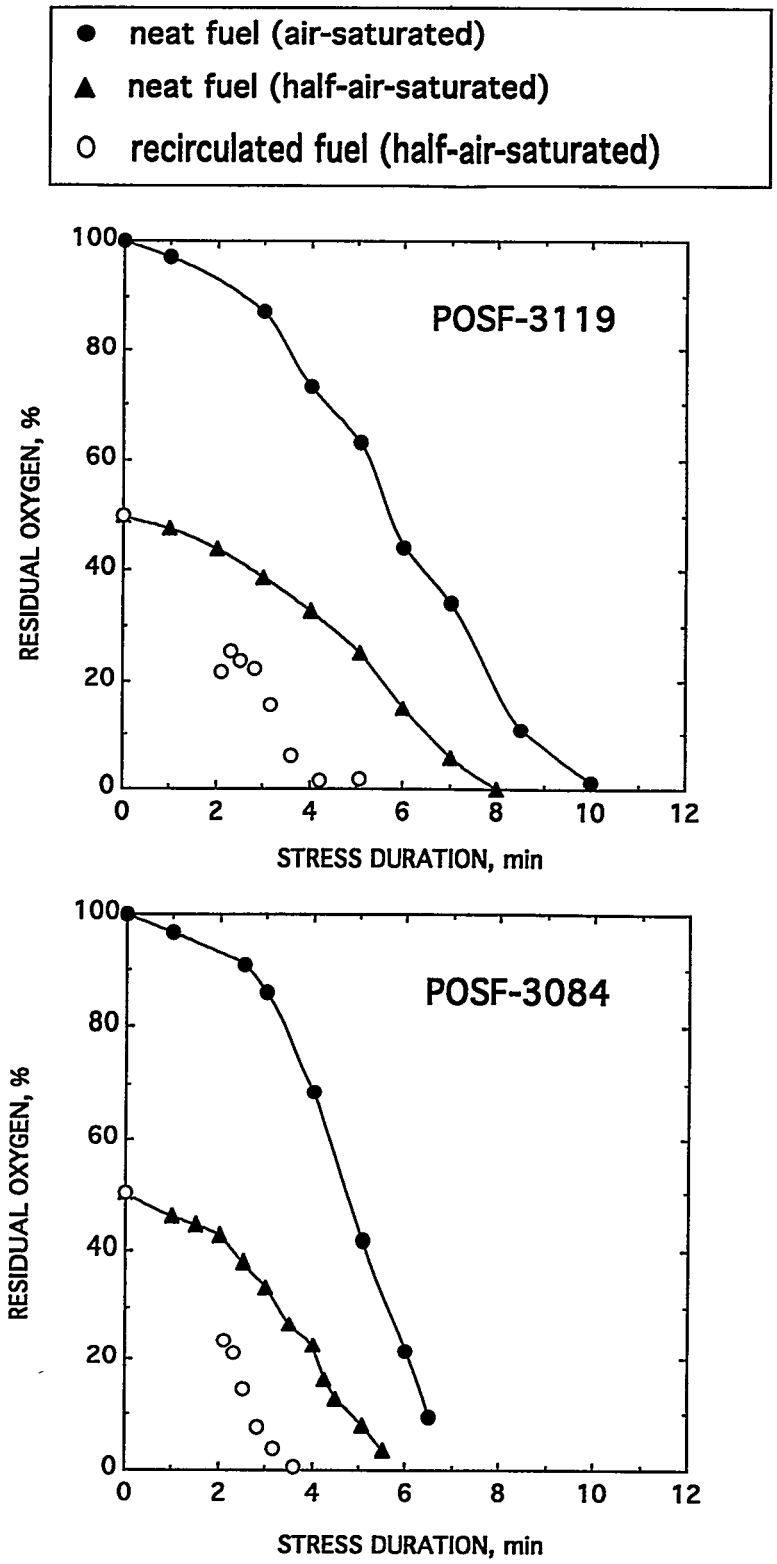


Figure 3. Autoxidation Profiles at 185°C

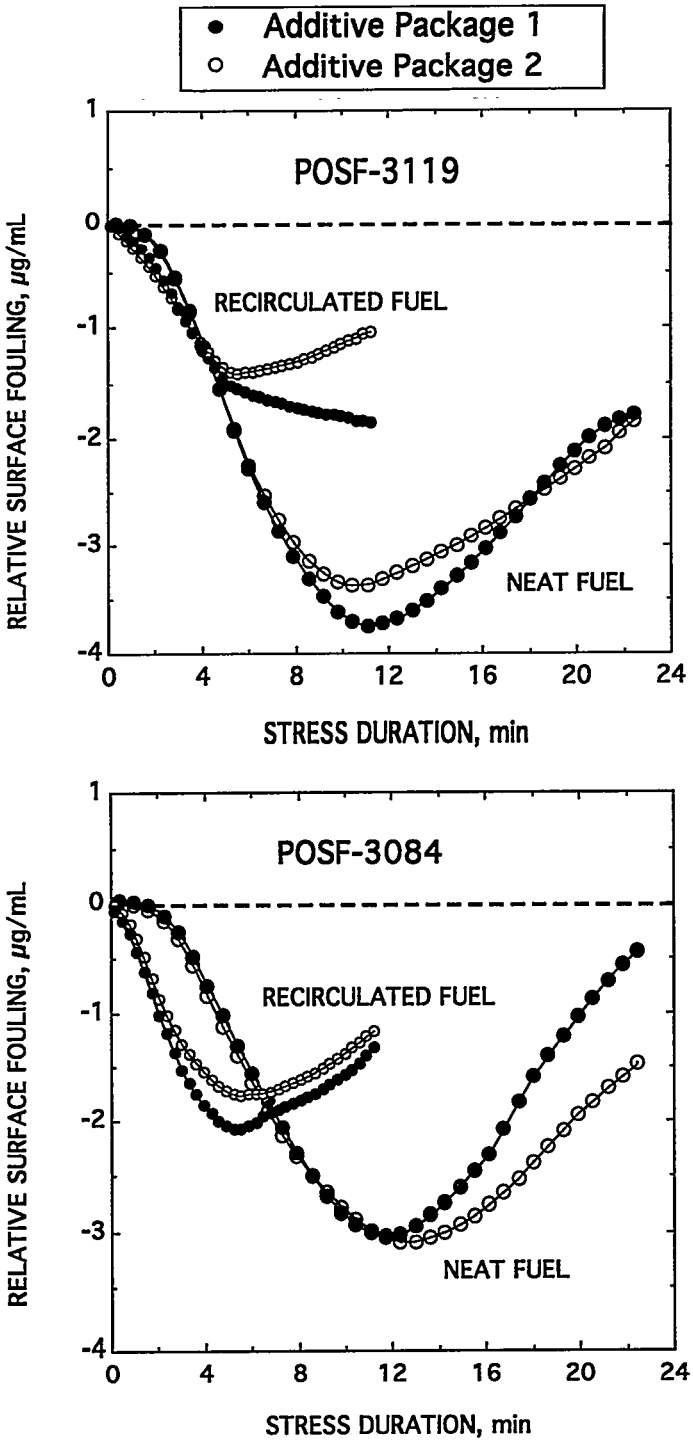


Figure 4. Effect of Additive Packages on Fouling

6th International Conference
on Stability and Handling of Liquid Fuels
Vancouver, B. C., Canada
October 13-17, 1997

COMPARISON OF THE EFFECTS OF STORAGE CONDITIONS, TYPE OF SOLUBLE COPPER, AND MDA ON JP-5 FUEL THERMAL STABILITY

Seetar G. Pande*[1] and Dennis R. Hardy[2]

[1]Geo-Centers, Inc., 4601 Presidents Drive, Lanham, MD 20706. [2]Code 6181, Naval Research Laboratory, Washington, D.C. 20375.

The effects of the type of storage and the source of soluble copper on fuel thermal stability were examined using five JP-5 fuels. The effects of the metal deactivator, MDA (N,N'-disalicylidene-1, 2-propane diamine) were also examined in the comparative studies using two of the five test fuels. Thermal stabilities were determined using the gravimetric JFTOT, which gives a quantitative measure of the total deposits formed. A copper concentration/storage effect was observed, which necessitated evaluations at *similar* copper concentrations. However, the source of copper appears not to be important. Instead, the main operative factor affecting the thermal stability of stored fuels appears to be the combined effect of long term ambient storage in the presence of copper. Good correlations were obtained between the thermal stabilities of fuels that were stored in the presence of 400 ppb copper from copper II ethyl acetoacetate (CuEA) at 90°C/50 psig air/24 hr versus comparable field conditions, which approximated an ambient storage period of six months in the presence of copper from 90:10 copper-nickel alloy. These results are significant for the following reasons: (1) they validate the use of the specified laboratory test conditions as being realistic; (2) they support our premise that the precursors that lead to thermal deposits are formed primarily on storage in the presence of copper; and (3) they offer a rigorous method for predicting the thermal stabilities of jet fuels. The MDA/Cu/storage studies also indicated good agreements between the thermal deposits of fuels stored using accelerated *vs* ambient conditions for periods equivalent to ~ six and twelve months in all the cases examined, which include with and without added copper from CuEA or Cu-Ni.

Introduction

Dissolved copper has been found to be the most reactive of the metals that catalyze fuel oxidation.[1,2] Consequently, due to the 90:10 copper-nickel (Cu-Ni) alloy used in the fuel piping systems of U.S. aircraft carriers and air capable ships,[3,4] copper contamination of JP-5 fuels is of particular interest to the U.S. Navy. From a commercial standpoint, copper contamination can also occur from other sources including the refinery copper sweetening process,[5] the copper bearings used in fuel pumps, and from the copper heating coils in many multipurpose tankers that are used to transport jet fuels. The adverse effects of metals, including copper, on jet fuel thermal stability have been reviewed by Nowack[6] and later by Hazlett.[5] As indicated in the reviews,[5,6] the deleterious effects of copper on fuel thermal stability are dependent on the fuel and the solubilized copper concentration.

Although long term storage is pertinent to U.S. Navy fuels (JP5s), all fuels are also subject to some storage effect when one includes the time interval from the time the fuel leaves the refinery to its combustion in the aircraft. Consequently, a study of the effects of fuel storage in the presence of copper, prior to determining its thermal stability, addresses realistic conditions.

The current study is a continuation of an earlier systematic investigation,[7] the results of which indicated that precursors that lead to thermal deposits are either formed, or their formation is accelerated, when the fuel is stored in the presence of copper. In the earlier study,[7] for convenience, fuel storage was accelerated in the Low Pressure Reactor (LPR) used by Hardy *et al.*[8] and the source of copper was a fuel-soluble copper compound, viz., copper II ethyl acetoacetate (CuEA). Consequently, because of the significance of the results of the earlier study[7] it was important to validate them with respect to storage using field conditions. However, identification of the precursors formed from the autoxidation effects of the copper II cation, is a task well beyond the scope of this paper.

The *objective* of this paper is to establish that a reliable agreement exists between the thermal stabilities of fuels that have been stored in the presence of copper using laboratory test conditions versus field conditions. In this context, laboratory test conditions are defined as accelerated storage in the LPR at 90°C/50 psig air/24 and 48 hours in the presence of known concentrations of soluble copper from CuEA. Field conditions are defined as storage at room temperature (~20°C) and atmospheric pressure in the presence of known concentrations of dissolved copper from 90/10 Cu-Ni alloy for a period of approximately six and twelve months, respectively. Also, MDA was likewise examined, with and without added copper, in a limited study. Thermal stabilities of the fuels, before and after storage, were measured using the Gravimetric JFTOT.[9]

In this paper, the results of two studies on the effects of the type of storage, the source of soluble copper, and copper concentration on thermal stability are presented. In the first study, the fuel set comprised three JP -5 fuels. In the second study, the fuel set comprised two freshly refined JP-5 fuels. The purpose of the second fuel set was to validate the results of the first set. In a third study, the comparative studies were extended to include a limited probe on the effects of the metal deactivator, MDA (N,N'-disalicylidene-1,2-propane diamine), because of its well-known benefit on fuel thermal stability.[4b]

Experimental Section

Test matrix. The overall broad test matrix for the studies conducted comprised two fuel sets, two types of storage, and two sources of copper, added at two concentrations/amounts (see Table 1). Adequate design of the test matrix, with respect to copper concentration, was obfuscated due to the unpredictability of the extent of copper solubilization in the Cu-Ni alloy dissolution studies.

Materials. All materials were used as received, unless otherwise specified.
Fuels. The two fuel sets employed are designated A and B. Fuel set A comprised three fuels and were *not* the same three fuels used in our earlier study.[7] Fuel set B, comprised two fuels. The

purpose for examining a second fuel set stemmed from the unexpected high concentration of solubilized copper (~2000 ppb) obtained on exposure of the fuels in set A, to Cu-Ni alloy.

As shown in Table 2, based on some pertinent compositional and properties data, the neat test fuels can be categorized as typical JP-5 field production jet fuels.[10] The inherent copper contents of the neat test fuels ranged from negligible (fuel set B: 2-4 ppb) to low (fuel set A: 18-22 ppb). Each fuel was obtained from a different location/refinery and for convenience they are thus identified. The three fuels included in set A are: Pax River (from Patuxent River Naval Air Station, VA), Norfolk (from the Defense Distribution Depot, in Norfolk, VA), and NAWC (from the Naval Air Warfare Center in Trenton, NJ). The two fuels included in set B are: TX from Texas and LA from Louisiana.

Copper. The two sources of copper used and the respective concentrations/amounts for the fuel sets employed are as follows:
(a) *copper II ethyl acetoacetate* (CuEA) from Eastman Kodak. For fuel set A, the copper concentration of CuEA initially employed for both the room temperature and accelerated storage studies was 400 ppb. This level was chosen because it depicts a median level of the range[5] in copper concentration found in JP-5 fuels aboard the U.S. Navy aircraft carriers. Significantly higher levels (1700-2000 ppb) were also examined in the LPR, to match the high levels of solubilized copper from the Cu-Ni alloy/room temperature storage studies. And, to validate the thermal stability results obtained from the fuels in set A, for fuel set B, the copper concentrations of CuEA employed were 400 and 2000 ppb in both the accelerated and room temperature storage studies.

(b) *90/10 copper/nickel alloy* from Hillman Brass and Copper Co. For fuel set A, the Cu-Ni alloy used was in the form of plates. The dimensions of each plate were: 7 cm x 10 cm x ~ 0.15 cm; ten plates were used per test fuel. For fuel set B, the alloy was used in the form of rods to facilitate mixing (see Procedures, Stirring). The dimensions of each rod were: 2.54 cm x 0.95 cm diameter. In an effort to obtain different concentrations of solubilized copper, six and eighteen rods were used.

N,N'-disalicylidene-1,2-propane diamine commonly known as MDA was obtained as a powder from Pfaltz and Bauer. In a limited study, MDA was added at 20 and 40 ppm concentrations to each fuel in set B (i.e., TX and LA).

Procedures
Pretreatment. The copper-nickel alloy plates and rods were cleaned by first immersing in a mixture of equal volumes of toluene, acetone, and methanol, then rinsed with hexane, and air dried.

Stirring. The copper-nickel plates were held in wedges made in a Teflon rack that was constructed from two parallel placed Teflon strips (13 cm x 1.5 cm x 0.5 cm). Teflon beading obtained from Atlantic Tubing Co., was threaded through holes bored near the ends of the rack, and used for suspension purposes. This facilitated periodic stirring of the fuel by manually rotating the rack, which housed the copper plates. Rods were used in the second fuel set instead of plates to

simplify mixing, which was effected simply by shaking the capped cans. Otherwise throughout storage, the epoxy coated one-gallon cans containing the test fuels were either loosely covered with aluminum foil (when plates were used), or covered with foil pierced with small holes for aeration purposes (when rods were used).

Copper analyses. The concentrations of fuel solubilized copper from the Cu-Ni alloy/room temperature storage studies were determined at periodic intervals. Copper analyses were performed using graphite furnace atomic absorption spectroscopy, at the Naval Air Warfare Center, Aircraft Division, Trenton, NJ.

Fuel storage. The two forms of storage used were: (1) at room temperature (approximately 20°C) and atmospheric pressure, hereafter referred to simply as ambient storage; and (2) accelerated storage, which was conducted at 90°C under a pressure of 50 psig air for 24 and 48 hours in a Low Pressure Reactor (LPR).[8] The accelerated conditions of 90°C/50 psig air/24 and 48 hours were intended to simulate room temperature storage for approximately six and twelve months, respectively.

Gravimetric JFTOT. Thermal stabilities of the fuels, before and after storage, were measured using the gravimetric JFTOT.[9] This method gives the weight of total thermal deposits formed, in mg/L, when a fuel flowing at 3 mL/min is heated at 260°C, under approximately 500 psi back pressure, for 2.5 hr. The filtered fuel flows over a stainless steel strip (grade 302 and approximately 7 cm x 0.5 cm x 0.025 mm), contained in a heated strip holder. The total deposit is the sum of the deposits formed on the stainless steel strip and the filterables contained in the effluent. The effluent was filtered using two Magna nylon membranes of 0.8 micron pore size. Further details of the method are described elsewhere.[7,9] In the gravimetric JFTOT method, the strip deposits are significantly lower than the filterables: on average, about 10% of the total weight. And, because the strip deposits track well with changes in the filterables, only the *total* thermal deposits are reported (Tables 3-9).

Repeatability. Thermal stability determinations of the room temperature-stored fuels were conducted in duplicate. The overall repeatability of the duplicate testings was within the average standard error (standard deviation estimate x 100/mean), which is approximately ±15% for the total thermal deposits in the gravimetric JFTOT. Duplicate determinations of the accelerated stored fuels were generally not done since earlier studies had indicated the repeatability had no subsequent effect on thermal stability tests.

Results and Discussion

Copper/Storage: Studies 1 and 2

Neat fuels. Based on the criterion by Hardy *et al.*,[11] that for stable fuels the maximum total deposit is 5 mg/L, the five test fuels may be described as thermally stable. For example, as shown in Tables 3 and 4, low total thermal deposits (approximately 0.1-0.9 mg/L) were formed from the individual effects of storage, and of added copper, *as well as* from their combined

effects, e.g., on storage in the presence of 400 ppb copper, the total deposits formed were approximately 0.6-3 mg/L (Table 4).

Effects Compared. The effects of accelerated *vs* room temperature storage on the thermal stabilities of the stored fuels were compared for storage conducted without and with added copper. When the source of added copper was CuEA, the effects of accelerated *vs* room temperature storage on fuel thermal stability were compared at similar copper concentrations. However, when the source of added copper was Cu-Ni, the effects of storage - using laboratory test conditions (accelerated storage: 24 hr LPR in the presence of CuEA) *vs* field conditions (storage at room temperature and pressure in the presence of 90:10 Cu-Ni for approximately six months) also at similar copper concentrations - on fuel thermal stability were determined (see Fuel storage using laboratory test *vs* field conditions).

Approximate Six Months Ambient Storage Period versus 24 hr LPR (90°C/50 psig air)

Fuel storage only: no copper added (Table 3). Both fuel sets exhibited good agreements between the thermal stabilities of the fuels stored at accelerated conditions (24 hr LPR) versus those stored at room temperature for approximately six months. The agreements are considered to be good because large percentage differences for such small amounts of deposits are not meaningful (i.e., compared to the maximum of 5 mg/L for stable fuels[11]).

Fuel storage in the presence of CuEA (Table 4):
At 400 ppb copper from CuEA, when one factors in the repeatability of the gravimetric JFTOT test method, the overall results for the five test fuels again indicate good agreements between the thermal stabilities of the accelerated and the room temperature stored CuEA additized fuels.

At 2000 ppb copper from CuEA, comparisons are pertinent only to fuel set B (see test matrix,Table 1). Of the two fuels in set B only the LA fuel exhibited good agreement between the thermal stabilities of the accelerated and room temperature stored CuEA fuels.

Fuel solubilization of copper from the Cu-Ni alloy ambient storage studies (Figures 1 and 2). In general, all the test fuels showed increases in copper levels with time, which were followed by a decrease. For the TX fuel (Figure 2), this trend is not apparent graphically because of the wide range in the scale of the ordinate. However, the extent of the increases, with time, differed significantly with the fuel, thereby suggesting a fuel dependency. For the fuels in set A (Figure 1), the maximum appears at ~2000-2400 ppb copper; whereas, for the fuels in set B (Figure 2), the maximum appears at approximately 100 ppb for the TX fuel, and at approximately 3500 ppb for the LA fuel.

Fuel storage using laboratory test vs field conditions (Table 5). The concentrations of solubilized copper from the Cu-Ni/room temperature storage studies differed significantly from the concentrations of soluble copper added as CuEA in the storage studies conducted. Due to a copper concentration effect that was identified (see Copper concentration/storage effect), these significant concentration differences necessitated comparisons of the thermal stabilities of the

stored fuels at *similar* copper concentrations. Consequently, direct comparisons between laboratory test versus field conditions were limited. Subject to the available data, direct comparisons at copper concentrations of approximately 400 ppb and 2000 ppb are subsequently described.

At ~400 ppb copper from Cu-Ni:

For fuel set A, the significantly high solubilized copper concentrations after approximately six months storage at room temperature (viz., 1800-2200 ppb, Figure 1) preclude a direct comparison between the thermal stabilities of fuels stored using laboratory test *vs* field conditions in the presence of 400 ppb copper. Nevertheless, an evaluation based on an indirect comparison is addressed later (see Evaluation of the Thermal Stabilities of Fuels Stored Under Laboratory *vs* Field Conditions).

For fuel set B, with respect to the extent of copper solubilization after approximately six months storage at room temperature, the converse effect was observed: the solubilized copper levels were considerably lower. For example, in the presence of six Cu-Ni rods, the copper levels were 70 and 169 ppb for the TX and LA fuels, respectively. In the presence of 18 Cu-Ni rods, the copper levels were 108 and 455 ppb, respectively.

Nevertheless, as shown in Table 5, for fuel set B, good agreements are exhibited between the thermal stabilities of the fuels that were stored using laboratory test conditions in the presence of 400 ppb copper from CuEA versus those stored using field conditions in the presence of approximately 100-400 ppb from Cu-Ni. The agreements are considered to be good based on their similarly small amounts of thermal deposits. The improved agreements at the higher levels of solubilized copper (cf. data for 6 *vs* 18 Cu-Ni rods) suggest that a threshold concentration effect may also be operative.

At ~ 2000 ppb copper from Cu-Ni. At this high level of solubilized copper from Cu-Ni, direct comparisons are applicable only to the fuels in set A (see Table 5). And, of the three fuels in this set, two (viz., Pax River and Norfolk) exhibited good agreements in their thermal stabilities on storage in the presence of similarly high concentrations of copper (~2000 ppb) using laboratory conditions (CuEA copper-doped/24 hr LPR accelerated storage) versus field conditions (Cu-Ni/6-7 months room temperature storage). The corresponding correlation for the NAWC fuel may be considered to be reasonable when one factors in the $\pm 15\%$ repeatability of the test method: on doing so, the total thermal deposits for the LPR stored fuel becomes 6 mg/L and for the room temperature stored fuel, 5 mg/L.

<u>Twelve-Fourteen Months Ambient Storage Period versus 48 hr LPR (90°C/50 psig air)</u>

On extended storage (Table 6), for the non copper doped fuels in set A, good correlations were obtained between the thermal stabilities of fuels that were stored using accelerated versus ambient conditions. Corresponding correlations for fuels that were stored in the presence of copper were consistently poor for all fuels in set A and for one of the two fuels in set B. For

example, for fuel set B, when one factors in the repeatability of the test method, only the LA fuel exhibited correspondingly good correlations in all the cases examined.

Factors that Impact on the Analysis of the Results

The objective of this study was to determine whether the thermal stabilities of fuels that were stored using laboratory test conditions were similar to those stored using field conditions. Complicating the analysis of the results is the copper concentration/storage effect that appears to be operative for these fuels. This effect as well as the source of copper/storage effect on total thermal deposits are discussed subsequently. Both these factors are discussed prior to evaluating the results obtained, because they are pertinent to, and impact on, the analyses of the data.

Copper concentration/storage effect. Although the effect of copper is reported to be catalytic,[5,12] increases in concentrations at low copper levels have been known to increase thermal deposits.[5] For the fuels examined, increases in total thermal deposits due to a combined copper concentration/storage effect are shown in Table 7. For example, the total thermal deposits of most of the fuels increased with increasing concentrations of added copper from CuEA, regardless of the type of storage. The increases in thermal deposits for the fuels in set A, and particularly so for the Pax River fuel - on storage in the presence of approximately 2000 ppb copper, from Cu-Ni plates, versus storage in the presence of 400 ppb copper from CuEA - are likely attributable to a copper concentration effect and not to the difference in the source of soluble copper used (see Copper source, below).

Note: For the fuels in set B, relative to the concentration effect at 2000 ppb *vs* 400 ppb copper from CuEA (Table 7), the concentration effect at 400 ppb *vs* 100 ppb copper from Cu-Ni is relatively small (see Table 5). This is likely attributable to the inherent thermal stabilities of the neat fuels, i.e., such stable fuels likely exhibit a higher copper concentration threshold effect in the copper promoted autoxidation reactions of jet fuels.

Copper source/storage effect. The *source* of copper does not appear to play a role in the thermal stabilities of fuels that were stored in the presence of copper. Supporting this premise are the similar amounts of total thermal deposits formed from both fuels in fuel set B (Table 8), after storage at room temperature, in the presence of approximately 100-400 ppb copper, whether copper was derived from CuEA or from Cu-Ni rods. Furthermore, the reasonable to good agreements obtained between the thermal stabilities of the fuels in set A that were stored in the presence of approximately 2000 ppb copper, using laboratory test versus field conditions (Table 8), suggest the following: based on the specific test matrix examined, it is the combined effect of storage in the presence of copper that is important, and not the type of soluble copper, nor the type of storage.

Based on the above results, the anion of the copper II compound in these tests (viz., ethyl acetoacetate in the case of CuEA, or possibly one derived from the organic acids present in the fuel, as would be the case for Cu-Ni alloy), does not appear to participate in the reactions that lead to thermal deposits. From an autoxidation aspect (see Role of copper, below), this interpretation is consistent with Morris[13] and Turner's results that the source of the anion in the copper compound appears not to be a factor in oxygen consumption. These overall results do not support

Datschefski[14] findings that, in addition to the copper concentration, the chemical structure of the dissolved copper compound is also important.

Role of copper. Copper is reported to catalyze the formation of thermal deposits via the initiation of free radicals during the autoxidation process.[12] Also, being a multivalent ion, copper likely plays a role in the decomposition of hydroperoxides formed from the free radicals.[15] Nevertheless, the copper concentration effect observed, focuses on the threshold level of copper being fuel dependent.[6]

Test matrix design. The amounts of copper that a particular fuel will dissolve under a given set of conditions from contact with Cu-Ni alloy on storage at room temperature appear to be dependent on the fuel, the copper surface area/fuel volume, and the length of storage (see Figures 1 and 2). Consequently, it is inherently difficult to adequately design the test matrix with respect to copper concentration. Furthermore, the unpredictability of the extent of copper dissolution from Cu-Ni alloy becomes a particularly significant factor due to the copper concentration effect that appears to be operative for these fuels.

Evaluation of the Thermal Stabilities of Fuels Stored Under Laboratory *vs* Field Conditions

400 ppb Copper/storage (equivalent to ~6 months at room temperature)
For the fuels in set A, the solubilized copper concentrations from Cu-Ni (~2000 ppb, see Figure 1), were significantly higher than the 400 ppb soluble copper from CuEA used in the accelerated storage studies. In the effort to compare the thermal stabilities of fuels that were stored using laboratory test *vs* field conditions in the presence of 400 ppb copper, we adopted the following indirect method of analysis:

First, we compared the total thermal deposits formed from the fuels that were stored in the presence of 400 ppb copper from CuEA using accelerated versus room temperature conditions equivalent to approximately six months storage (Table 4). Since these showed good agreement, we then examined the effect of the source of copper. And, as discussed earlier, since the source of copper appears not to be important, we conclude that, at 400 ppb, as at 2000 ppb copper, the fuels in set A exhibit good agreement among the thermal stabilities of the stored fuels, regardless of the source of copper or the type of storage, when the storage period is equivalent to six months at room temperature conditions.

For fuel set B, this indirect mode of analysis was not required. As mentioned earlier, both fuels in set B exhibited good agreements, i.e., between the thermal stabilities of fuels stored in the presence of 100-400 ppb copper, using laboratory test versus field conditions (Table 5).

Thus, based on direct and indirect modes of comparisons, the overall good agreements for all five typical JP-5 test fuels examined, validate the use of specified laboratory test conditions (90°C/50 psig air/24 hrs in the presence of 400 ppb copper from CuEA) as being representative of storage under specified field conditions (six months' storage at room temperature in the presence of copper from Cu-Ni at similar copper levels). Furthermore, accelerated storage of

the test fuels using these validated laboratory test conditions, prior to determining their thermal stabilities can further serve as a rigorous predictive test method for assessing the potential thermal stabilities of jet fuels.

2000 ppb Copper/storage (equivalent to ~6 months at room temperature)

The reasonable and good agreements in the thermal deposits obtained for the fuels in set A, when stored in the presence of approximately 2000 ppb copper, using laboratory test versus field conditions (Table 5), would have been particularly useful when designing a predictive test for differentiating fuel thermal stability because of the copper concentration effect. However, the relatively poor correlation in the thermal deposits of the TX fuel for storage conducted using accelerated *vs* ambient conditions at similarly high copper levels from CuEA (see Table 4) suggests a fuel dependency and consequently would not be advisable for such high copper levels. Nonetheless, because copper levels as high as 1200 ppb have been reported in JP-5 fuels aboard U.S. Navy aircraft carriers[3] it may be worthwhile to conduct further studies at 1000 ppb copper to establish the optimum copper concentration for predictive test purposes.

Storage conditions

Correlations between the thermal stabilities of fuels that were stored in the presence of similar copper concentrations, using laboratory versus field conditions, were good when the storage period was equivalent to approximately six months at ambient conditions. However, when storage was extended to a period equivalent to approximately one year (12-14 months) at ambient conditions, the corresponding correlations were poor. As shown in Table 6, for fuel set A (no comparable data available for fuel set B), the consistent significantly higher amount of thermal deposits formed - on accelerated storage in the presence of 2000 ppb copper from CuEA for 48 hr in the LPR *versus* ambient storage for 12-14 months in the presence of similar concentration of copper from copper-nickel - may well be attributable to a time/ temperature effect.

Copper concentration effect versus accelerated stress time

For the fuels in set A, the significantly greater amount of deposits formed - on accelerated storage in the presence of 400 ppb copper for 48 hours (Table 6) versus 1700 ppb copper for 24 hours (Table 4) - suggests that of the two effects, stress time is more dominant, and unrealistically so, due to the time/temperature effect mentioned above.

Precursors' formation on storage in the presence of copper

The good agreements in the thermal deposits of the test fuels that were stored using the specified laboratory *vs* field conditions, support our original premise[7] that precursors that lead to thermal deposits are primarily formed, or their formation is accelerated, on long term ambient storage in the presence of copper. In this study, this is exemplified by the increases in thermal deposits due to the interactive effects of storage in the presence of copper, relative to the individual effects of storage and of copper (see Table 7). However, the small magnitude of the increases due to the combined effects, e.g., storage in the presence of 400 ppb copper, versus the individual effects (copper only, or storage only), likely reflects the inherent thermal stabilities of the neat fuels.

MDA/Copper/Storage: Study 3

Fuel set B. Because of the limited quantity of available freshly refined fuels, the MDA studies conducted are based on a judicious design of the test matrix. The total thermal deposits of the fuels that were stored in the presence of MDA and added copper from either CuEA or Cu-Ni, in the studies conducted, are shown in Table 9. And, to evaluate the effects of MDA on fuel thermal stability for the test matrix examined, the total thermal deposit data of the corresponding neat, stored, and copper-doped stored fuels - with no MDA present - are also included in Table 9.

As shown in Table 9, both fuels in set B exhibited excellent agreements in the thermal stabilities of the test fuels that were stored in the presence of MDA in all the cases examined. These include the following:

(a) with and without added copper (one case was examined with no added copper).
(b) using accelerated *vs* ambient conditions.
(c) using laboratory test *vs* field conditions (one case examined, viz.,for storage period equivalent to approximately 12-14 months at ambient conditions).
(c) for storage periods equivalent to approximately 6 months (one case examined) and 12-14 months at ambient conditions.

The results also indicate that MDA consistently improved the thermal stabilities of the fuels that were stored in the presence of copper ranging from100-2700 ppb concentrations in conjunction with high concentrations of MDA (20 and 40 ppm). However, because of the overall stabilities of the neat test fuels, the improvements were generally not dramatic except in one case. Specifically, MDA significantly decreased the thermal deposits of the TX fuel that was stored in the presence of 2000 ppb copper *and* 40 ppm MDA for approximately 14 months at ambient conditions (cf., 0.5 mg/L versus 21 mg/L total thermal deposits, for the corresponding copper doped/no MDA/stored fuel). Also, for the *non-copper doped* 12-14 month stored fuels, at the high concentration employed (20 ppm), MDA was not detrimental. This evaluation is based on the rationale, described earlier, that large percentage differences of small amount of deposits are not meaningful.

Conclusions

A copper concentration effect was identified which necessitated evaluations at fairly similar copper concentrations. Based on direct and indirect modes of analyses, all five typical JP-5 field production test fuels exhibited good agreements in their thermal stabilities for fuels that were stored - with and without added copper - using specified laboratory test versus field conditions equivalent to six months ambient storage. Consequently, the specified laboratory test conditions, viz., accelerated storage at 90°C/50 psig air/24 hr in the presence of 400 ppb copper from copper II ethyl acetoacetate, simulate field storage conditions of approximately six months at room temperature in the presence of similar amounts of copper derived from 90:10 Cu-Ni alloy.

The MDA/Cu/storage studies also indicated good agreements between the thermal deposits of the fuels that were stored using accelerated *vs* ambient conditions, in all the cases examined.

These include storage in the presence of MDA with and without added copper from either CuEA or Cu-Ni for periods equivalent to approximately six and twelve months at ambient conditions.

The overall results further indicate that whereas the source of soluble copper does not appear to be important in the test matrix examined, the main operative factor appears to be the combined effect of long term ambient storage in the presence of copper. These results thus support our original premise that precursors that lead to thermal deposits are primarily formed, or their formation is accelerated, when copper is present during storage.

The increase in thermal deposits attributable to the combined copper concentration/storage effect is particularly relevant in designing a predictive test method for differentiating the thermal stabilities of jet fuels and needs to be explored further in future studies, i.e., accelerated storage of the fuel in the presence of copper prior to the determination of its thermal stability. Moreover, based on the variables examined in this study, interested users can construct laboratory conditions to reflect their own field conditions.

Acknowledgments

The authors thank the Office of Naval Research (M.Soto) for funding support, Dr. Robert Morris for helpful comments and valuable discussions, Dr. Alice Huang of the Naval Air Warfare Center, Trenton, NJ, for the great number of copper determinations, and Mr. Lindsay Hicks of the Defense Fuel Supply Center, in Alexandria, VA. for kindly providing the TX and LA test fuels.

Literature Cited

(1) Pedersen, C.J. *Ind. Eng. Chem.* **1949**, *41*, 924.

(2) Smith, J.D. *Aircraft Eng.* **1967**, *39*, 19

(3) Shertzer, R. "Investigation of the Reduction of Thermal Stability of Fuel by Copper Contamination on Aircraft Carriers," Naval Air Propulsion Test Center: NAPC-PE-14, January 1973.

(4) Morgan, R.; Berger, W.; Meehan, R. "Determine the Thermal Stability Properties of Fuel and Copper Concentration," Pratt and Whitney Aircraft Materials Development Laboratory Work Request, No. 15493; December 1970.

(5) Hazlett, R.N. *Thermal Oxidation Stability of Aviation Turbine Fuels*; ASTM Monograph 1, American Society of Testing and Materials: Philadelphia, 1991, chapter. VIII.

(6) Nowack, C.J. *CRC Literature Survey on the Thermal Oxidation Stability of Jet Fuel*; CRC Report 509, Coordinating Research Council, Inc: Atlanta, GA, April 1979, chapter VI.

(7) Pande, S.G; Hardy, D.R. *Energy Fuels*, **1995**, 9, 177.

(8) Hardy, D.R.; Hazlett, R.N.; Beal, E.J.; Burnett, J.C. *Energy Fuels,* **1989**, *3*, 20.

(9) Beal, E.J.; Hardy, D.R.; Burnett, J.C. In (a) Proceedings of the 4th International Conference on Stability and Handling of Liquid Fuels: Orlando, FL, Nov. 1991, pp245-259. (b) Aviation Fuels Thermal Stability Requirements, ASTM STP 1138; Kirklin, P.W.; David, P., Eds; American Society for Testing and Materials: Philadelphia, PA, 1992, pp138-150.

(10) Military specification, MIL-T-5624.

(11) Hardy, D.R.; Beal, E.J. Presented to CRC TS Test Methods Panel of the Oxidation Stability Group, 19 April 1993. Also: *Prepr.-Am. Chem.Soc., Div. Pet. Chem.* **1994**, *39*, 82.

(12) Kendall, D.R.; Mills, J.S. *Ind. Eng. Chem. Prod. Res. Dev.* **1986**, *25*, 360

(13) Morris, R.E.; Turner, N.H. *Fuel Science and Technology*, **1990**, *8*(4), 327.

(14) Datschefski, G. *Fuel Science and Technology*, **1988**, *6*(6), 609.

(15) Walling, C. *Free Radicals in Solution*; John Wiley and Sons: New York, 1957; p.427.

Table 1. Summary of the Test Matrix for the Three Studies Conducted

test matrix*	Cu/storage**		Cu/MDA/storage***
	study 1	*study 2*	study 3
fuel set: JP-5 fuels	A: Pax River, Norfolk, NAWC	B#: TX, LA	B#: TX, LA
CuEA,ppb: 24,48 hr LPR	400, 1700-2000	400, 2000	400, 2000
: ~6,12 mth Amb	400	400, 2000	400, 2000
90:10 Cu-Ni: Amb	10 plates	6,18 rods	6, 18 rods
MDA, ppm	nd	nd	20, 40

* LPR: accelerated storage using a low pressure reactor; Amb: ambient storage

** Storage in the presence of copper. The type of storage and the source of copper is, as identified; nd: not determined.

*** Storage in the presence of copper and MDA, as identified.

Fuels were freshly refined.

Table 2. Available Properties and Compositional Data for Four Fuels Examined*

properties/composition (ASTM method, MIL-T- 5624 specification limits)	Norfolk	NAWC	TX	LA
aromatics, vol% (D1319, max: 25)	16	19.6	19	14.9
olefin, vol% (D1319, max: 5)	1.1	1.7	0.8	1.1
mercaptan sulfur, wt% (D3227, max: 0.0020)	0.0011	- ve**	0.0001	0.0012
total sulfur, wt% (D4294, max: 0.40)	0.07	0.06	0.0069	0.09
total acid, mg KOH/g (D3242, max:0.015)	0.002	0.009	0.003	0.002
density, g/mL (D4052, min-max: 0.788 - 0.845)	0.818	0.811	na	0.819
flash point, °C (D93, min: 60)	64.4	67	62.2	64
freeze point, °C (D2386, max: - 46)	- 48	- 50	- 50.5	- 48.5
peroxide content, ppm (D3703, max: 8)	<0.001	na	<0.001	<0.001
antioxidant	✓	✓	✓	✓
corrosion inhibitor	✓	✓	✓	✓
fuel system icing inhibitor, vol% (0.15-0.20)	0.17	0.14	0.13	not stated
copper content, ppb	22	19	4	2

* Corresponding data for the Pax River fuel were not available; however its copper content was 18 ppb; na: not available.

** Based on Doctor test.

✓: added

Table 3. Effects of theType of Storage/No Added Copper on Total Thermal Deposits
Comparison of Accelerated vs Ambient Storage

test description	grav. JFTOT total deposit (mg/L)				
	fuel set A			*fuel set B*	
	PXRVR	NFLK	NAWC	TX	LA
neat: (reference)	0.1	0.5	0.1	0.3	0.3
accelerated storage (24 hr LPR)	0.2	0.6	0.2	0.3	0.5
ambient storage (~6 months)	0.4	0.9	0.7	0.2	0.4

Table 4. Effects of Storage in the Presence of Soluble Copper from CuEA
Comparison of the Type of Storage at Similar Copper Concentration on Total Thermal Deposits

test description	grav. JFTOT total deposit (mg/L)				
	fuel set A			*fuel set B*	
	PXRVR	NFLK	NAWC	TX	LA
neat (reference)	0.1	0.5	0.1	0.3	0.3
~400 ppb Cu(CuEA)/no storage	0.1	0.3	0.5	nd	nd
at ~400 ppb Cu as CuEA					
accelerated storage (24 hr LPR)	0.9	3.1	2.0	0.6	1.6
ambient storage (~6 months)	0.6	1.7	2.8	0.8	1.2
at ~1700-2000 ppb Cu as CuEA					
accelerated storage (24 hr LPR)	5.0	4.2	7.0	6.2	4.4
room temp storage (~6 months)	nd*	nd	nd	2.9	3.3

* nd: not determined.

Table 5. Effects of Storage Using Lab vs Field Conditions on Total Thermal Deposits
Comparison of CuEA/Accelerated Storage vs Cu-Ni/Room Temperature Storage at Similar Copper Concentrations

test description	grav. JFTOT total deposit (mg/L)				
	fuel set A			*fuel set B*	
	PXRVR	NFLK	NAWC	TX	LA
neat (reference)	0.1	0.5	0.1	0.3	0.3
~400 ppb Cu(CuEA)/no storage	0.1	0.3	0.5	nd *	nd
at ~100-400 ppb Cu:					
lab test condns: 24 hr LPR/CuEA: 400 ppb Cu	0.9	3.1	2.0	0.6	1.6
field condns: ~6 mths rm temp/(6 Cu-Ni rods): ~70 and 169 ppb Cu**	nd	nd	nd	0.4	1.0
field condns: ~6 mths rm temp/(18 Cu-Ni rods): ~108 and 455 ppb Cu**	nd	nd	nd	0.7	1.5
at ~1700-2300 ppb Cu#:					
lab test condns: 24 hr LPR/ CuEA: 1700-2000 ppb Cu	5.0	4.2	7.0	6.2	4.4
field condns: ~ 6 mths rm temp/Cu-Ni plates: 1900-2300 ppb Cu	4.3	4.8	4.2	nd	nd

* nd: not determined.

** the first Cu concentration pertains to the TX fuel, and the second, to the LA fuel.

range of added/solubilized copper levels for the test fuels as specified.

Table 6. For Storage Equivalent to ~ 12-14 months Ambient
Comparison of the Effects of Type of Storage and Soluble Copper on Thermal Stability

test description	grav. JFTOT total deposit (mg/L)				
	fuel set A			*fuel set B*	
	PX RVR	NFLK	NAWC	TX	LA
neat: no storage (reference)	0.1	0.5	0.1	0.3	0.3
storage only (12-14 mths ambient):					
accelerated (LPR)	0.3	2.1	1.1	nd	nd
ambient (amb)	0.1	0.8	0.6	0.2	0.4
~100-400 ppb Cu and above/storage:					
~400 ppb Cu (CuEA)/LPR	10.4	7.3	7.1	6.6	2.7
~400 pb Cu (CuEA)/Amb	0.4	2.5	3.3	0.6	2.3
100 and 1690 ppb Cu* (6 Cu-Ni rods)/Amb	nd	nd	nd	0.7	2.8
~2000 ppb Cu/storage:					
~2000 ppb Cu (CuEA)/LPR	14.6	7.2	10.4	nd	nd
2000 ppb Cu (CuEA)/Amb	nd#	nd	nd	21.1	3.5
~2000 and 2730 ppb Cu**(Cu-Ni)/Amb	3.2	4.1	4.7	na##	5.3

* the first Cu concentration pertains to the TX fuel and the second, to the LA fuel.

** the first Cu concentration pertains to the fuels in set A and the second, to the LA fuel in set B.

nd: not determined.

na: not applicable - the solubilized Cu concentration for the TX fuel was 210 ppb, which is significantly lower than the ~ 2000 ppb Cu solubilized by the other test fuels.

Table 7. Effect of Copper Concentration/Storage on Total Thermal Deposits

test description	grav. JFTOT total deposit (mg/L)				
	fuel set A			*fuel set B*	
	PX RVR	NFLK	NAWC	TX	LA
added copper as CuEA/accelerated storage (24 hr LPR)					
neat fuel: no storage/no added Cu (reference)	0.1	0.5	0.1	0.3	0.3
storage/no added Cu	0.2	0.6	0.2	0.3	0.5
~ 400 ppb Cu	0.9	3.1	2.0	0.6	1.6
1700-2000 ppb Cu	5.0	4.2	7.0	6.2	4.4
added copper as CuEA or Cu-Ni/room temp storage/~6 mths					
no added Cu	0.4	0.9	0.7	0.2	0.4
~ 400 pb Cu (CuEA)	0.6	1.7	2.8	0.8	1.2
1700-2000 ppb Cu (CuEA)	nd *	nd	nd	2.9	3.3
1900- 2300 ppb Cu: Cu/Ni plates	4.3	4.8	4.2	nd	nd

* nd: not determined.

Table 8. Effect of Source of Copper/Storage on Total Thermal Deposits

At Fairly Similar Copper Concentrations

test description	grav. JFTOT total deposit (mg/L)				
	fuel set A			*fuel set B*	
	PX RVR	NFLK	NAWC	TX	LA
~100-400 ppb Cu/type of storage					
~ 400 ppb Cu (CuEA)/room temp storage	0.6	1.7	2.8	0.8	1.2
108 and 455 ppb Cu** (18 Cu-Ni rods)/room temp storage	nd *	nd	nd	0.7	1.5
~1700-2300 ppb Cu#/ type of storage:					
1700-2000 ppb Cu (CuEA)/accelerated storage (lab)	5.0	4.2	7.0	6.2	4.4
1900- 2300 ppb Cu (Cu-Ni plates)/room temp storage (field)	4.3	4.8	4.2	nd	nd

* nd: not determined.

** the first copper concentration pertains to the TX fuel and the second, to the LA fuel

range of added/solubilized copper levels for the test fuels as shown.

Table 9. Limited Comparison of the Effects of MDA, the Type of Storage, and Soluble Copper on Thermal Stability For Two Typical JP-5 Fuels

test description *	grav. JFTOT total deposit (mg/L) *fuel set B* TX	LA
Storage: approx 6 months ambient/24 hr LPR		
neat: no storage	0.3	0.3
LPR	0.3	0.5
ambient storage	0.2	0.4
storage/~2000 ppbCu:		
2000 ppb Cu (CuEA)/LPR	6.2	4.4
1700-2000 ppb Cu (CuEA)/Amb	2.9	3.3
storage/~2000 ppbCu/MDA:		
2000 ppb Cu (CuEA)+ 40 ppm MDA/LPR	0.3	0.7
1500-1870 ppb Cu (CuEA)+ 40 ppm MDA/Amb	0.2	1.1
Storage: approx 12-14 months ambient/48 hr LPR		
ambient	0.2	0.4
storage/MDA (no Cu)		
20 ppm MDA/LPR	0.2	0.1
20 ppm MDA/Amb	0.3	0.1
storage/~400 ppbCu:		
398 ppb Cu (CuEA)/LPR	6.6	2.7
400 ppb Cu (CuEA)/Amb	0.6	2.3
75 and 2170 ppb Cu (6 Cu-Ni rods)/Amb	0.7	2.8
storage/~400 ppbCu/MDA:		
398 ppb Cu (CuEA) +20ppm MDA/LPR (lab conditions)	0.2	0.2
400 ppb Cu (CuEA)+ 20 ppm MDA/Amb	0.1	0.5
480 and 260 ppb Cu (6 Cu-Ni rods) + 20 ppm MDA/Amb (field conditions)	0.2	0.6
storage/~2000 ppbCu or as indicated:		
2000 ppb Cu (CuEA)/Amb	21.1	3.5
210 and 2730 ppb Cu (18 Cu-Ni rods)/Amb	0.5	5.3
storage/~2000 ppbCu/MDA:		
2000 ppb Cu (CuEA) + 40 ppm MDA/Amb	0.5	0.9
2090 and 1540 ppb Cu (18 Cu-Ni rods) + 40 ppm MDA/Amb	0.3	1.1

*Where two Cu concentrations are given, the first pertains to the TX fuel, the second to the LA fuel.

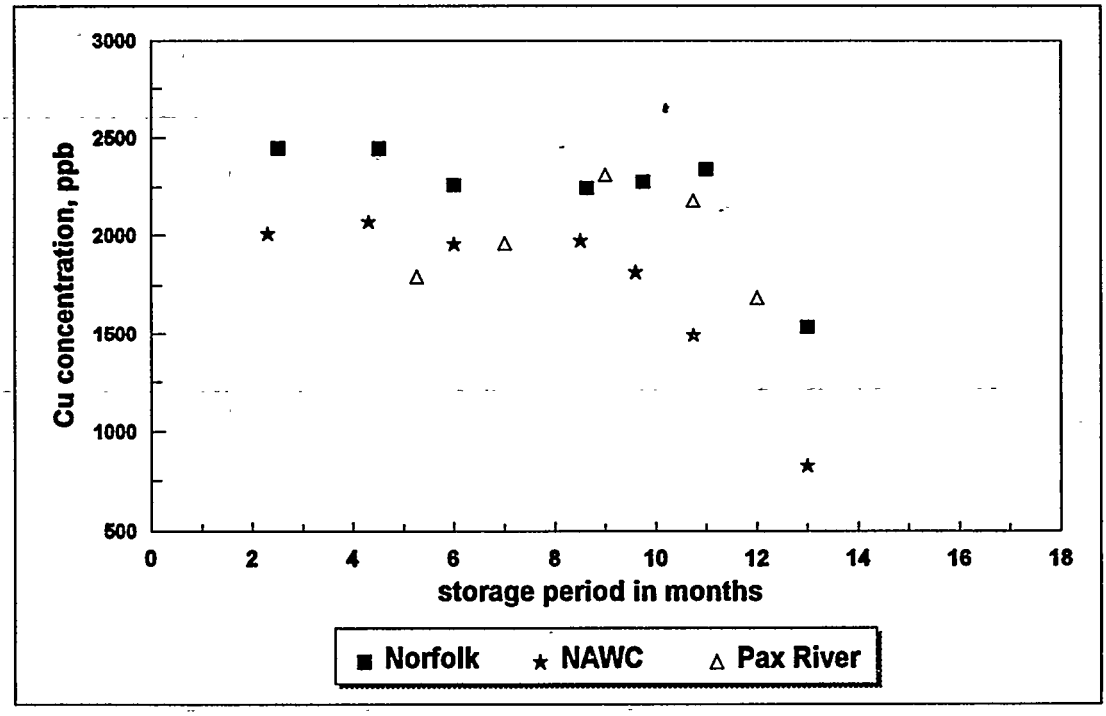


Figure 1. For fuel set A: fuel solubilization of copper from Cu-Ni plates on ambient storage for 0-13 months.

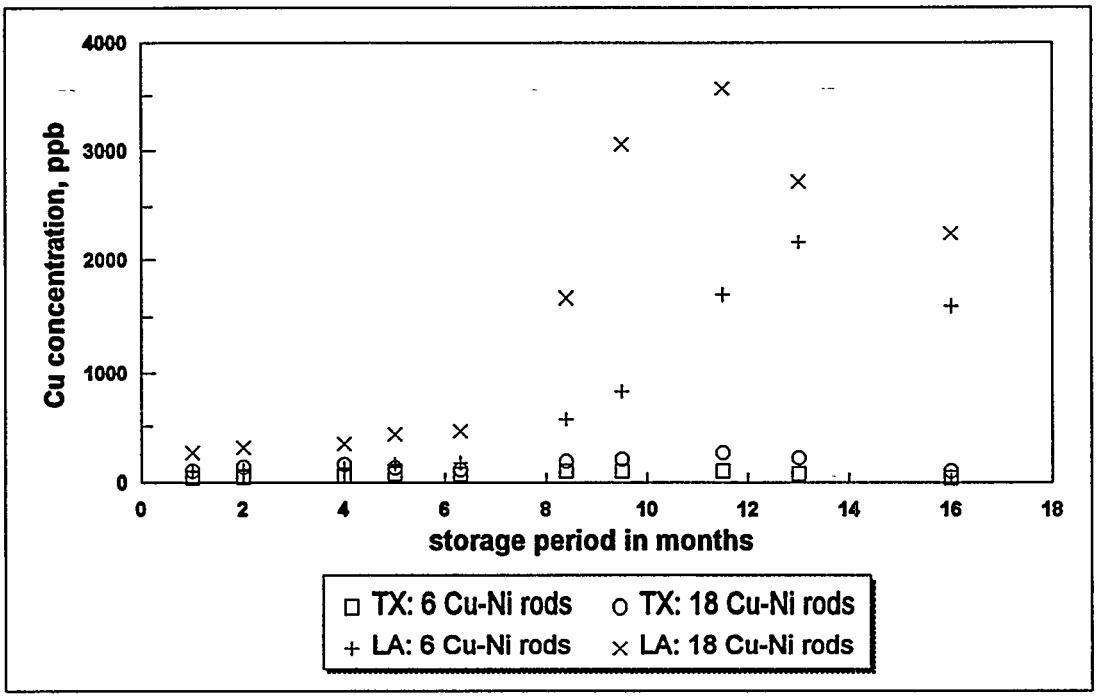


Figure 2. For fuel set B: fuel solubilization of copper from Cu-Ni rods on ambient storage for 0-16 months.

6th International Conference
on Stability and Handling of Liquid Fuels
Vancouver, B. C., Canada
October 13-17, 1997

INVESTIGATION OF THE EFFECTS OF TIME ON THE PHYSICAL COLLECTION OF AVIATION FUEL DEPOSITS IN A SCALED TURBULENT FLOW SYSTEM

John E. Colbert*[1] and Clarence J. Nowack[2]

[1]Naval Air Warfare Center, 1440 Parkway Avenue, Trenton, NJ 08628, USA;
[2]194 Teal Circle, Berlin, MD 21811, USA.

ABSTRACT

The Fuels & Lubricants Division of the Naval Air Warfare Center has developed and verified a hypothesis which models the collection and buildup of aviation fuel carbon deposits as a function of time in a turbulent flow simulator (i.e., fuel injector nozzle). These deposits are the result of thermal oxidative breakdown that typically occurs when aviation fuels are exposed to the different heat loads rejected into various parts of an aircraft fuel system (viz., fuel injector nozzles) during flight operations. This paper presents experimental data that supports the use of a proposed mathematical model used in describing the fuel thermal deposition process and provides theory upon which the model is based. Assumptions are made which enable this model to be used in calculating the deposition rate within a turbulent simulator over a wide range of typical temperature conditions of an aircraft fuel system. The intended use of this work is to develop a test protocol that will require less test time and fuel in order to study the effects of fuel thermal stability using a high fuel flow unit.

I. PURPOSE

The purpose of this research program is to propose and validate a hypothesis (via experimental data) which models the collection and buildup of aviation fuel deposits as a function of time in a turbulent flow simulator (i.e., fuel injector nozzle)[1].

In addition, it will be demonstrated how this hypothesis is fitted to the Arrhenius expression with a constant slope that is representative of all fuels operating at temperature conditions typically encountered in actual Naval aircraft fuel systems. It will be further demonstrated how this modified Arrhenius expression is used as the basis for the Navy's improved test protocol. This protocol will be used to estimate, on a relative basis, the coking tendencies of generic aircraft fuel injectors and will eventually assist in defining the coking behavior of various fuels operating under an actual aircraft temperature environment. The turbulent flow system used to conduct these experiments is the Naval Aviation Fuel Thermal Stability Simulator (NAFTSS) which is owned operated by the Fuels & Lubricants Division of the Naval Air Warfare Center (NAWC) currently located in Trenton, NJ. A flow schematic showing the major test sections of the NAFTSS is shown in Appendix 1 (p. A-1).

II. OBJECTIVES

1. Conduct time-controlled experiments to validate the preliminary theory addressing the deposition collection process that occurs in the fuel injector nozzle of the NAFTSS unit. To establish this hypothesis, experiments should include test conditions typically encountered in actual aircraft fuel systems.

2. Calculate a deposition constant at constant temperature and determine NAFTSS unit life expectancy from the experimental data using the following equation:

$$W = C * t^3 \qquad 1)$$

where,

W	=	Weight of the carbon deposit in the NAFTSS nozzle tube **(mg)**
t	=	NAFTSS test duration **(hours)**
C	=	Collection Constant which represents fuel quality with respect to the deposition collection behavior in the NAFTSS nozzle tube at a specific nozzle wetted-wall temperature between 350-600°F **(mg/hr^3)**

3. Incorporate the collection constant into the classical Arrhenius expression[2, 3] to achieve an expression with a slope that is assumed to be constant for all fuels. Select a representative fuel/operating condition and conduct experiments to calculate a range of collection constants for wetted-wall temperatures between 450 and 600°F. Use this data to calculate a constant slope for the modified Arrhenius expression.

III. THEORY ON SURFACE DEPOSITION

The deposition collection process that occurs inside a clean, unused (i.e., deposit-free) fuel injector nozzle under heat loads experienced during aircraft flight operations can be viewed as three (3) distinct time periods, described in detail in the sections that follow.

A. Deposition Collection Process for a Generic Fuel Injector

(1) *Pre-Induction Period*

As defined by the Shell-Thorton studies[4], the pre-induction period occurs when the virgin metal surface of a clean fuel injector becomes initially coated with deposits. This is evidenced by a low rate of surface deposition when the tiny deposit particles are released from the fuel. These particles are trapped within the microscopic crevices located on the inside surface of the fuel injector nozzle. These surface irregularities are the result of the injector's manufacturing process.

(2) ***Induction Period***

During this period the inside metal surface of the same fuel nozzle is covered with a mono-layer of deposits. This results in increased surface roughness which promotes better collection of subsequent deposits. This period represents a major transition in the deposition collection process.

(3) ***Post-Induction Period***

This post-transitional period is evidenced by a high rate of surface deposition which appears to be constant when extrapolated to some point in time. At this point the particle adhesion continues at a high rate until some theoretical failure point is reached. We arrive at this point when a reduction in the nozzle diameter affects the fuel flow path of the nozzle.

B. **Deposition Collection Process for the NAFTSS Nozzle Tube**

The test conditions in the NAFTSS are run at steady state conditions of constant wetted-wall temperature, heat transfer, and fuel flow rate. The chemical kinetic rate of deposit formation from the fuel can also be assumed constant.

At the beginning of a test when the nozzle tube is deposit-free, the amount of particles that adhere to the surface is only a small percentage of the total deposit particles released from the fuel and the collection sites are random. The remaining particles pass through the nozzle and into the NAFTSS Hot Filter Section, which contains a sintered steel filter with a nominal porosity of 60 μ. As the test progresses, the microscopic crevices that exist in the nozzle become randomly filled and a mono-layer of deposit begins to form. From this point on, a major transition period occurs whereby more and more particles adhere to the nozzle wall and fewer particles pass through the exit of the nozzle. This is referred to as the Induction Period and the deposit adhesion to the mono-layer increases dramatically.

Following this major transition period, the tube collection efficiency is at its maximum which initiates the Post-Induction Period. At this time the surface deposition rate inside the nozzle is very high and constant. This causes a major portion of the deposits to cling to the inside of the metal surface until the nozzle tube approaches some theoretical failure point. Before the tube reaches this point, a significant rise in the (measured) wetted-wall temperatures of the NAFTSS nozzle tube will be observed due to the insulating properties of the accumulated deposit particles. This large disturbance indicates the test should be terminated. Based upon the theory of deposit growth, it was perceived that a non-linear power equation would be best suited to model these events. It was not until actual data was collected and analyzed that the cubic equation (from equation 1) above was selected to best approximate the deposition process.

IV. ANALYSIS OF TEST DATA

(1) *Verification of Hypothesis ($W = C * t^3$)*

Contained in the table in Appendix 2 (p. A-2) is the entire test program designed to study the use of the collection model. Some of these experiments under the listed conditions are still in the process of being studied. The first three conditions, however, have been completed and are presented as follows:

(a) neat fuel at baseline conditions
(b) neat fuel at higher/lower wetted-wall temperature
(c) neat fuel with dissolved copper at baseline conditions

For NAWC JP-5 (Neat), a total of seven (7) tests were performed at baseline conditions. The data showed an excellent correlation using the equation $W = C * t^3$. The value of r^2 (coefficient of determination) is 0.935 and is shown in the graph in Appendix 3 (p. A-3). This can be interpreted as 93.5% of the variation in deposit (carbon) weight (W) is caused by the underlying variation in test duration (t). The value of the Collection Constant, C, obtained from

the equation can be used further to calculate deposit growth over any period of time for a wetted-wall temperature of 550°F.

The other two (2) conditions, i.e., NAWC JP-5 at higher/lower wetted-wall temperature and NAWC JP-5 + 250 ppb Copper, also demonstrate an excellent correlation to the model as shown by the graphs in Appendices 4 and 5 (pp. A-4 and A-5), with r^2 values of 0.915 and 0.904, respectively. Their respective C values are also shown in these graphs. For all other test conditions run, r^2 values and Collection Constant (C) data, as well as other pertinent data, are listed in the table in Appendix 6 (p. A-6).

(2) ***Arrhenius Expression (Ln C = Ln A - 16610/T)***

As shown in Appendix 7 (p. A-7), Collection Constant (C) values generated from NAWC JP-5 (Neat) are shown for wetted-wall temperatures at 450, 500, 550, & 600°F. This data was used to modify the Arrhenius expression for predicting deposition collection behavior at lower (extrapolated) wetted-wall temperature conditions. As shown in the this graph, this data fits the Arrhenius expression quite well, with an r^2 value of 0.9274, a y-intercept value for Ln A of 21.616, and a slope (E_a/R) of -16,610. This means that 92.74% of the variation in "the natural logarithm of the Collection Constant" (Ln C) can be explained by the variation in the reciprocal temperature, 1/T (in °K). Since these test conditions represent the baseline conditions and have the most Collection Constant (C) data with respect to wetted-wall temperature, the slope value of -16,610 will be an assumed constant representing the "Average Apparent Energy" of activation for all fuels/operating conditions. As more data becomes available, a new average will be used to adjust the slope.

For NAWC JP-5 + 250 ppb Copper, the Arrhenius expressions for this data is shown in Appendix 8 (p. A-8) for wetted-wall temperatures from 450 through 600°F, inclusive. As shown by the Least Squares equation for this data, an r^2 value of 0.8048 was established, thus indicating a strong correlation between C and 1/T. Since we have previously assumed that the same thermal oxidative breakdown mechanism will exist for all fuels/operating conditions (i.e., a constant slope

condition for the Arrhenius expression), this data can be adjusted to fit the slope of -16610. After this is accomplished the value of the y-intercept (Ln A) will also be adjusted accordingly as shown in Appendix 8 (p. A-8). After adjusting the slope, a fairly good correlation exists, thus verifying the validity of the hypothesis and the corresponding assumptions, viz., that of the kinetic rate of deposition remains the same for all fuels/conditions.

A summary of all pertinent parameters relating to the deposition collection model and the Arrhenius expression is shown in the table in Appendix 6 (p. A-6) for all the tests performed in this study to date. Once the hypothesis has been proven for all fuels/operating conditions, all other tests run at wetted-wall temperature between 450-600°F (inclusive) can be fitted to the modified Arrhenius expression with constant slope of -16610. Furthermore, the relative coking tendencies of any fuel/operating condition can determined by calculating the adjusted value of "A" for the condition of interest and dividing it by the value of "A" for NAWC JP-5 (neat) at baseline conditions. By definition the relative ranking of the baseline conditions would be "1".

V. CONCLUSIONS

1. The deposition collection model, $W = C * t^3$, has been validated for representative fuels and operating conditions typically encountered in actual Naval aircraft fuel systems. These conditions include fuel quality, fuel injector wetted-wall temperature, bulk fuel temperature, copper contamination, and thermal stability improving additives.

2. The deposition collection model, $W = C * t^3$, has been successfully fitted to the modified Arrhenius expression to predict coking tendencies of various fuels/operating conditions in the NAFTSS for wetted-wall temperatures from 350-600°F.

3. The NAFTSS test protocol, using the deposition collection model as its foundation, can evaluate the relative coking tendencies of any fuel/operating condition experienced in an actual

aircraft fuel system by performing one test to the post-induction period of the nozzle tube (see Appendix 9, p. A-9). This is equivalent to a nozzle carbon deposit of approximately 10-12 mg.

4. Collection Constant data from the NAFTSS, in conjunction with the modified Arrhenius expression (Ln C = Ln A - 16610/T), can be used to help better define and assess the impact of coking (i.e., thermal oxidative breakdown) that typically occurs at temperatures in actual fuel injectors. This can be accomplished by calculating the relative ranking of a given fuel/operating conditions from NAFTSS data by taking the value of "A" at the specific condition of interest and dividing it by the value of "A" for the baseline conditions.

5. Alternatively, relative coking tendencies of various fuels/operating conditions can be assessed with respect to "time to failure" of the NAFTSS nozzzle tube. This can be accomplished by calculating the failure time (t_f) in the NAFTSS for the specific condition of interest and dividing by the failure time for the baseline conditions. Assuming that a carbon deposit of 20 mg constitutes a failure in the NAFTSS nozzle tube, failure time at a specific wetted-wall temperature can be calculated as follows:

$$t_f = (W / C)^{1/3} \qquad 2)$$

6. The NAFTSS test protocol appears to be the best and most cost effective means of ranking the coking tendencies of various fuels/operating conditions.

REFERENCES:

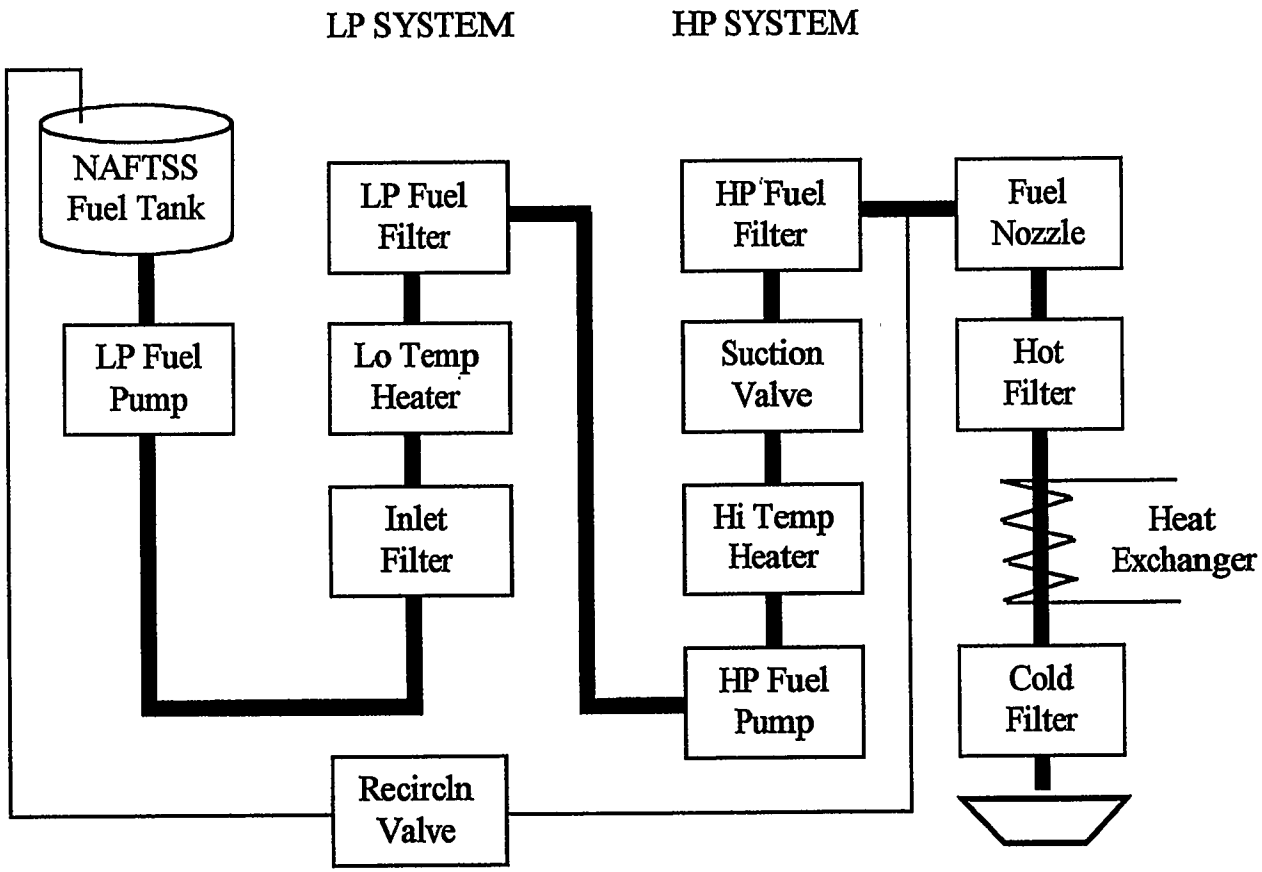
(1) "Investigation of Surface Collection Efficiency on System Performance," Proposal submitted by C.J. Nowack under AERA Contract No. N68335-94-D-0024, March 26, 1996.

(2) Por, Nahum, "Stability Properties of Petroleum Products," The Israel Institute of Petroleum and Energy, The School of Petroleum and Energy Sciences, March 1992.

(3) Hazlett, Robert N., "Thermal Oxidation Stability of Aviation Turbine Fuels," ASTM Publication Code Number (PCN) 31-001092-12, 1991.

(4) Clark, R.H. and Wolveridge, P.E., "Induction Periods: Are You Measuring the Right Rate?", Presented at CRC-Aviation Fuel Meeting, CRC Project No. CA-43-67, April 1993.

APPENDIX 1: NAFTSS FLOW SCHEMATIC



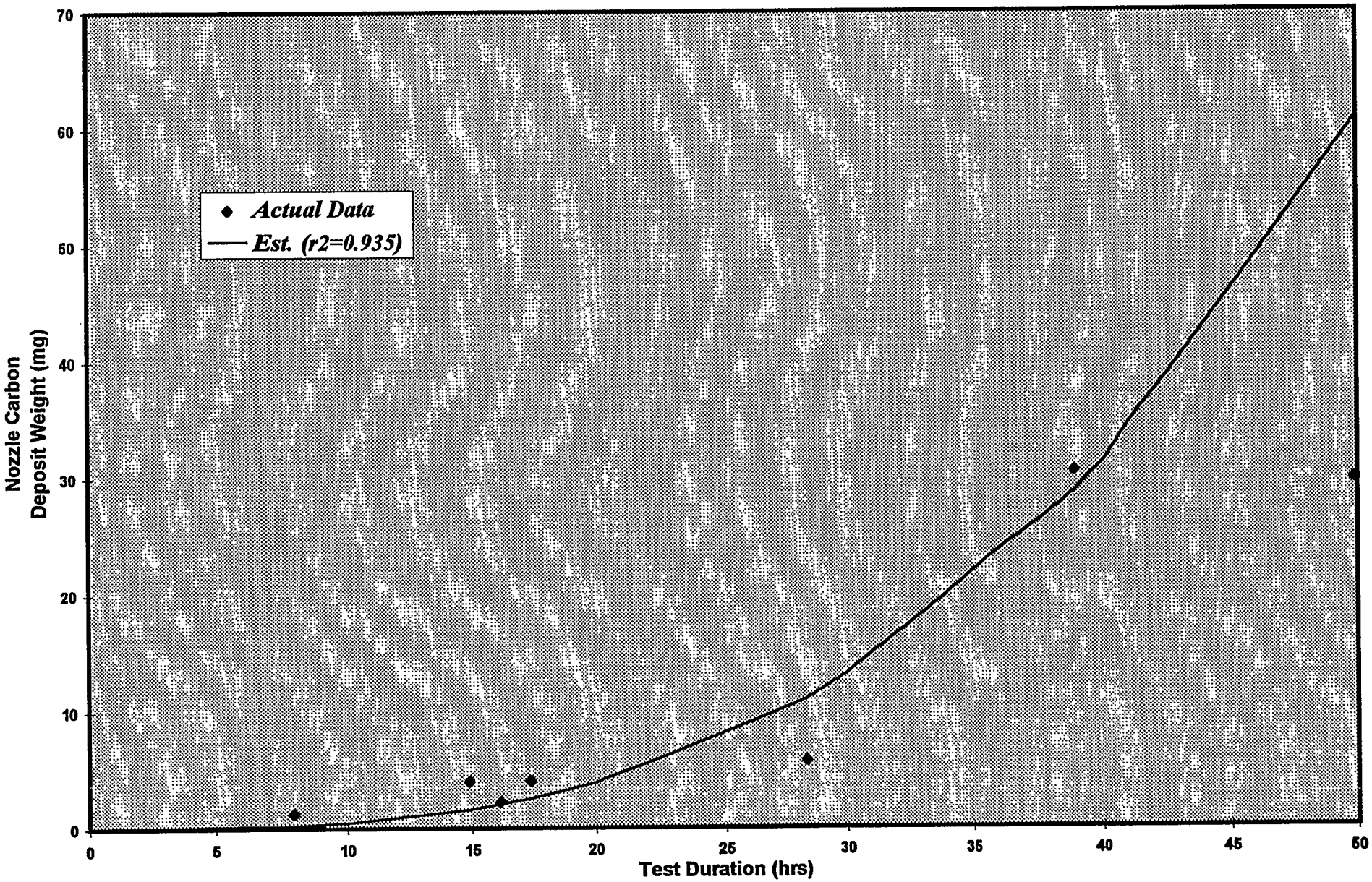
APPENDIX 2: NAFTSS TEST PLAN TO VALIDATE HYPOTHESIS

TEST CONDITION	FUEL TYPE	ADDITIVE TYPE	ADDITIVE CONCENTRATION (ppm)			JFTFT BPT	LP FILTER / AIRFRAME TEMP			HP FILTER / FMU TEMPERATURE			WETTED-WALL TEMP				NO. OF TESTS[1]
			Low	Effec.	High	°F	100°F	150°F	200°F	300°F	325°F	340°F	450°F	500°F	550°F	600°F	
Baseline Conditions	NAWC JP-5 (Neat)	N/A	N/A	N/A	N/A	520	X			X					X		7
Higher/Lower Wetted-Wall Temperature	"	"	"	"	"	"	X			X						X	3
Higher/Lower HP Filter Temperature	"	"	"	"	"	"	X				X				X		3
"	"	"	"	"	"	"	X					X			X		3
Copper Contamination	NAWC JP-5 + 250 ppb Cu	"	"	"	"	< 400	X			X					X		3
Thermal Stability Improving Additives	NAWC JP-5 (Neat)	MDA		5.8 (w/v)		> 575	X			X					X		3
"	"	Betz 8Q462		256 (v/v)		"	X			X					X		3
Hot Fuel Recirculation (future)	NAWC JP-5 (Neat)	N/A	N/A	N/A	N/A	520	X			X					X		3

NOTES:

(1) At least one (1) test should be run in each of the three (3) induction modes, i.e., Pre-, Regular, & Post-Induction periods

APPENDIX 3: BASELINE CONDITIONS
NAWC JP-5 (Neat)
LP Filter=100°F, HP Filter=300°F, Wall B=550°F
$W = 4.8777E\text{-}04 * t^3$

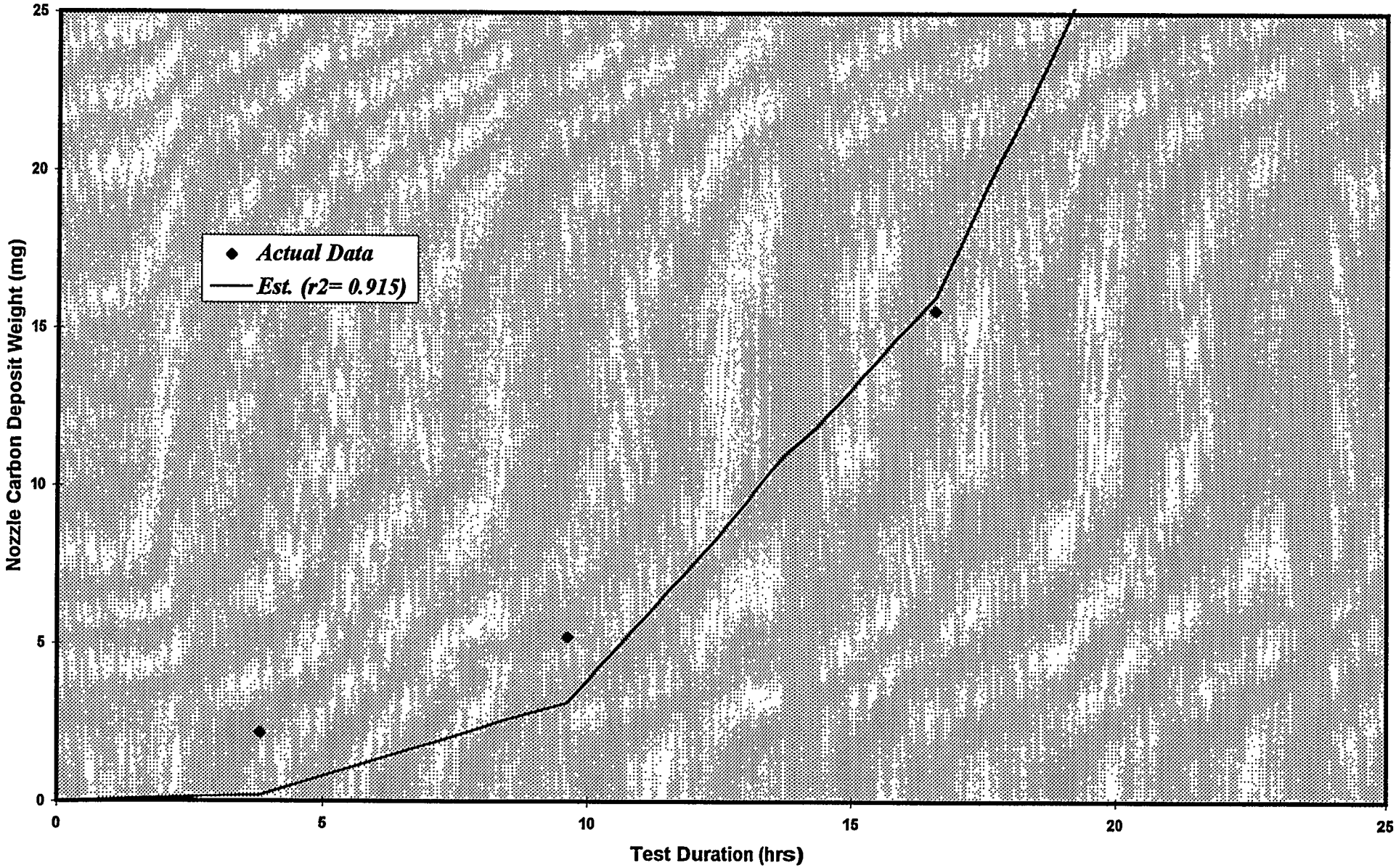


APPENDIX 4: EFFECT OF HIGHER/LOWER WALL TEMPERATURE

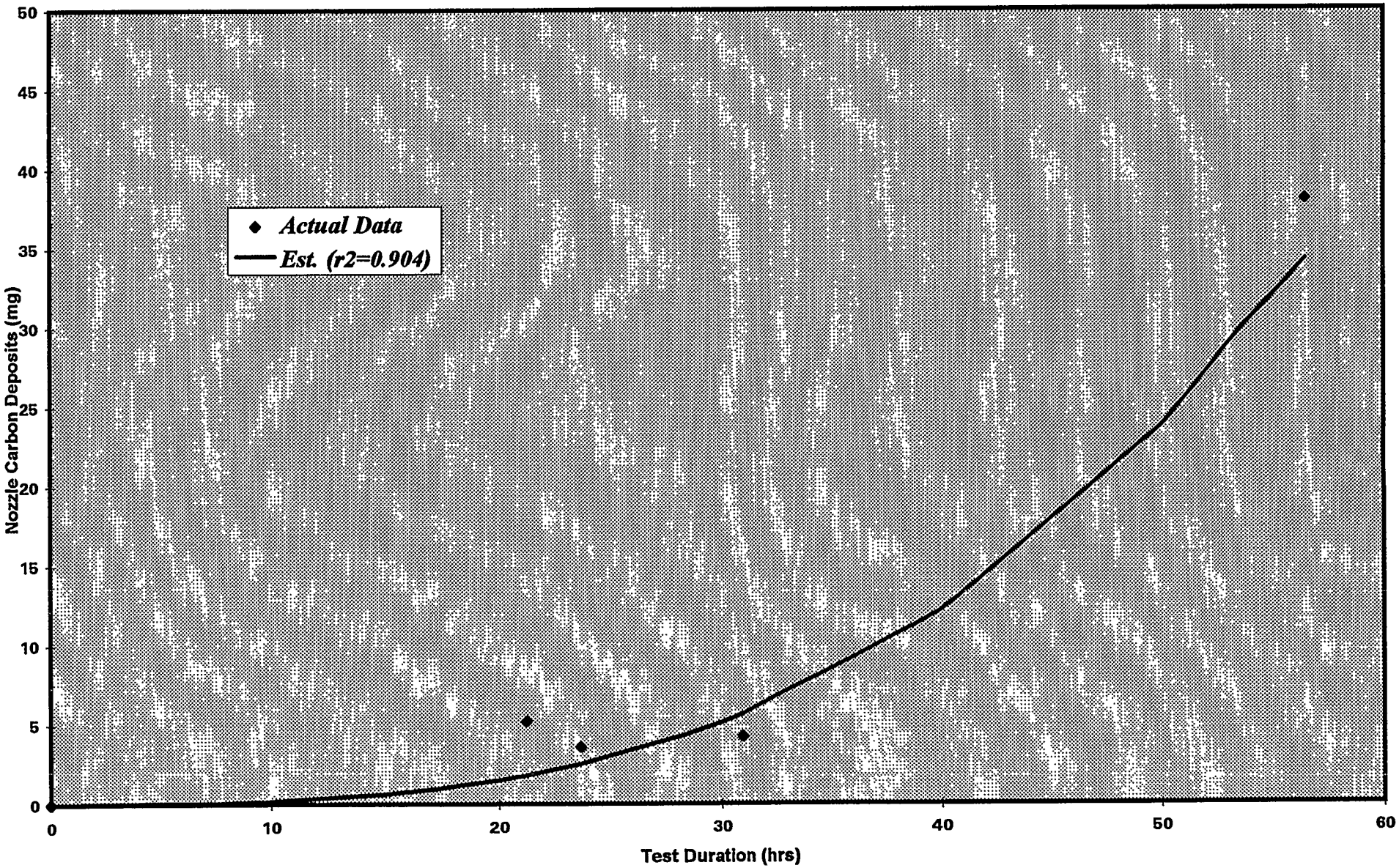
NAWC JP-5

LP Filter=100°F, HP Filter=300°F, Wall B=600°F

$W = 3.5184E\text{-}03 * t^3$



APPENDIX 5: EFFECT OF COPPER
NAWC JP-5 + 250 PPB COPPER
LP Filter=100°F, HP Filter=300°F, Wall B=550°F
$W = 1.90E\text{-}04 * t^3$

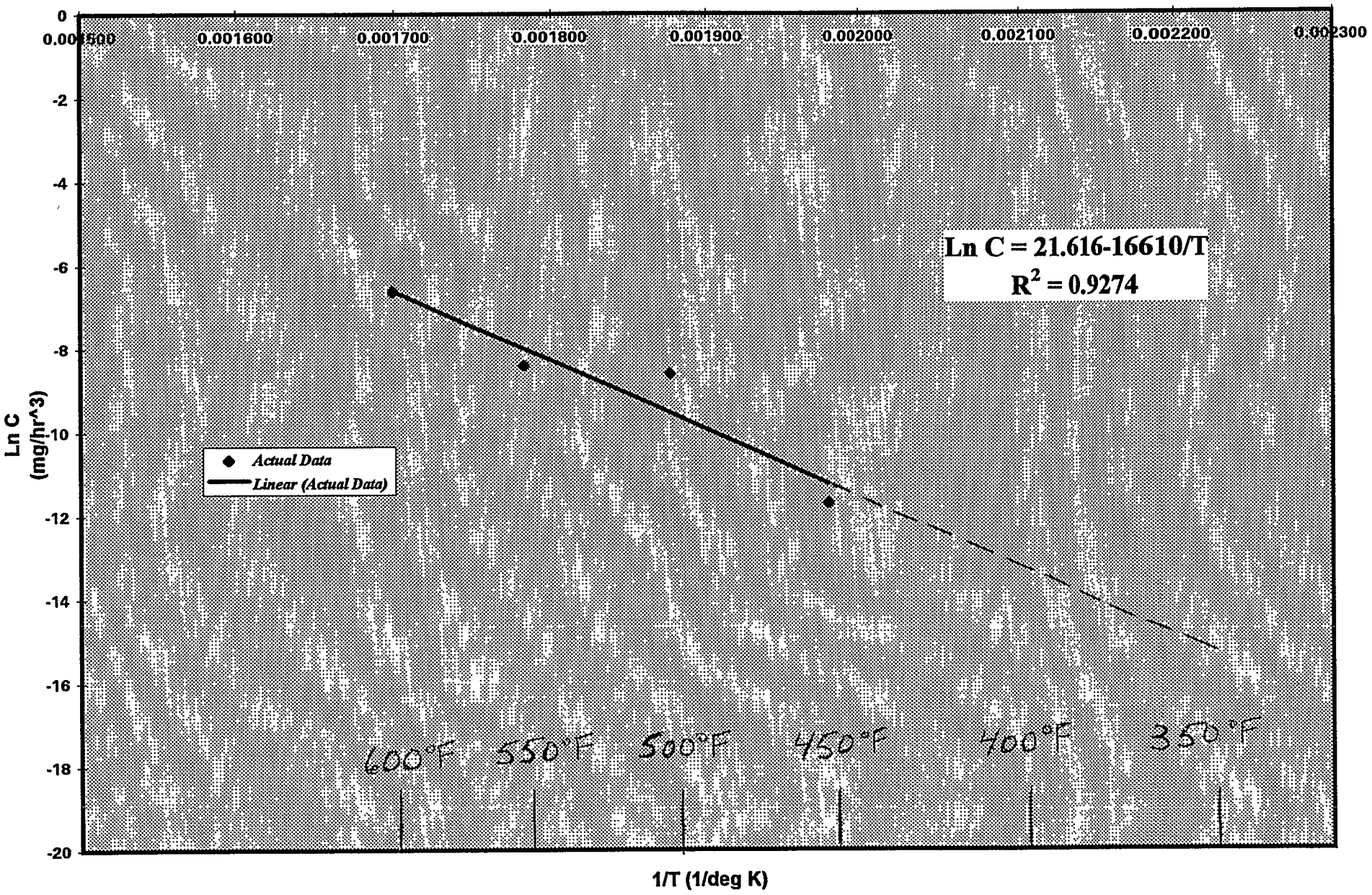


APPENDIX 6
NAFTSS TEST DATA TO VALIDATE HYPOTHESIS
$W = C * t^3$; $C = A * \exp(-16610/T)$
$\ln C = \ln A - 16610/RT$

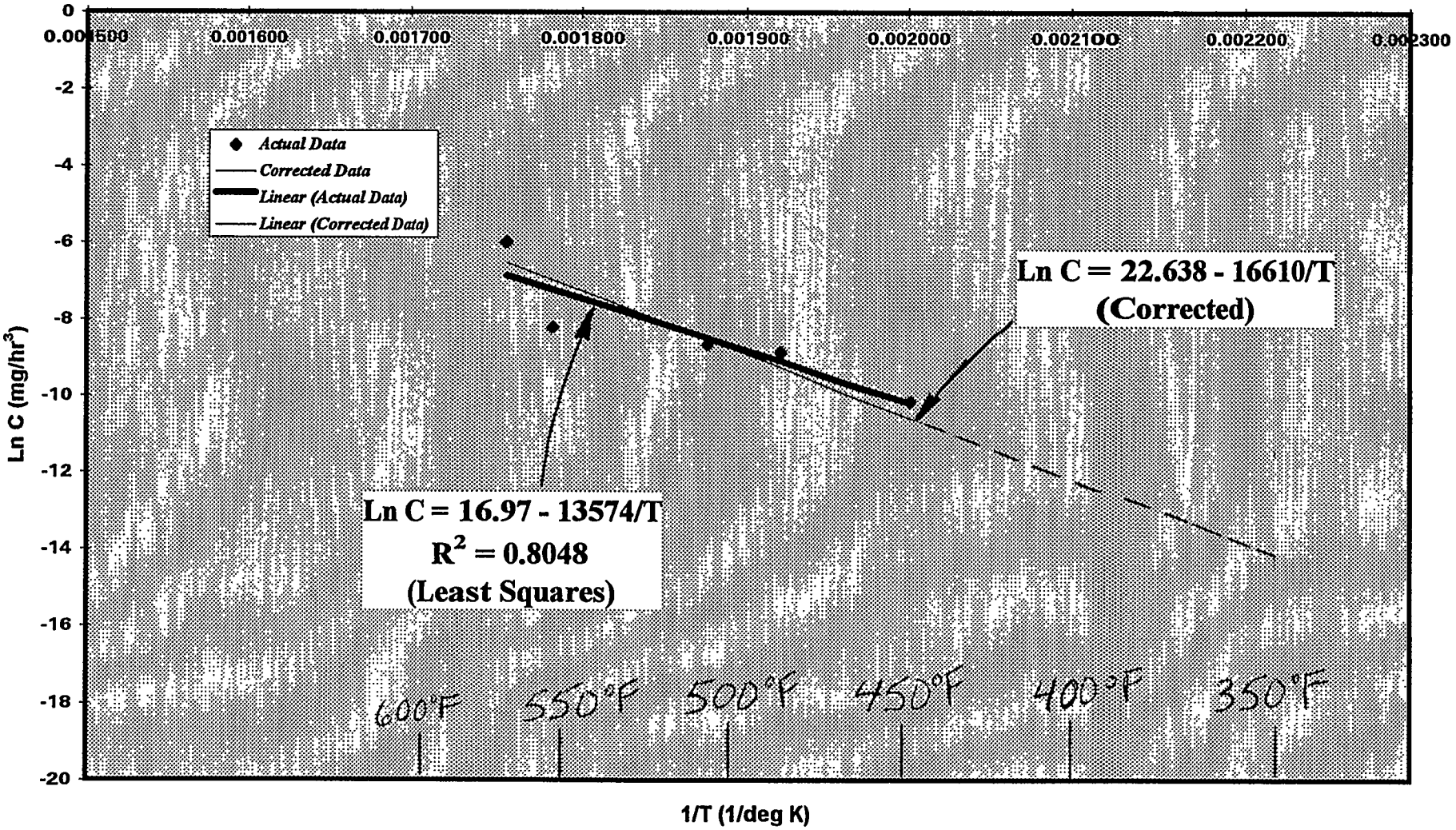
TEST CONDITION	FUEL TYPE	JFTPT BPT	LP FILTER/ AIRFRAME TEMP			HP FILTER/FMU TEMPERATURE			WETTED-WALL TEMP				$W = C * t^3$ C	$W = C * t^3$ r^2	ADJUSTED Ln A	RELATIVE RANKING (of 4)
		°F	100°F	150°F	200°F	300°F	320°F	340°F	450°F	500°F	550°F	600°F	mg/hr^3	(unitless)	mg/hr^3	(unitless)
Baseline Conditions	NAWC JP-5 (Neat)	520	X			X					X		4.8780E-04	0.935	21.616	1.00
Higher/Lower Wetted-Wall Temperature	"	"	X			X						X	3.5184E-03	0.915	22.572	2.60
Higher/Lower HP Filter Temperature	"	"	X				X				X		8.2440E-04	0.784	22.519	2.47
"	"	"	X					X			X		1.8654E-03	0.91	23.335	5.58
Copper Contamination	NAWC JP-5 + 250 ppb Cu	< 400	X			X					X		1.9000E-04	0.904	21.051	0.57
Thermal Stability Improving Additives	NAWC JP-5 + 5.8 mg/L MDA	> 575	X			X					X		5.4946E-05	0.984	19.810	0.16
"	NAWC JP-5 + 256 ppm (v/v) Betz 8Q462	> 575	X			X					X		N	N	N	N
Hot Fuel Recirculation (future)	NAWC JP-5 (Neat)	520	X			X					X		N	N	N	N

(1) "N" denotes that test has not been run yet.

APPENDIX 7: BASELINE CONDITIONS
NAWC JP-5 (Neat)
LP Filter=100 F, HP Filter=300 F, Wall B=350-600 F`



APPENDIX 8: EFFECT OF COPPER
NAWC JP-5 + 250 PPB COPPER
LP Filter=100°F, HP Filter=300°F, Wall B=350-600°F



APPENDIX 9: NAFTSS TEST PROTOCOL FOR EVALUATING FUELS/OPERATING CONDITIONS

1. Run tests under desired operating conditions (i.e., fuel type, bulk fuel temp, neat vs. additized, copper, hot fuel recirculation, etc.) at a NAFTSS nozzle wetted-wall temperature of 550°F.

2. Continue running test until the nozzle tube wetted-wall temperature (wall B) rises to the point that indicates that the beginning of the Post-Induction period has been reached. This is equivalent to a nozzle tube deposit of approximately 10-12 mg.

3. At the end of the test, perform surface carbon analysis on the nozzle tube using the LECO Carbon Analyzer. Calculate the Collection Constant, C, based on knowledge of the carbon deposit weight (W) in the nozzle tube and the test duration (t). This can be calculated by manipulating equation 1 to the following form:

$$C = (W / t^3) \qquad 3)$$

4. Using the calculated value of C from step 3 above and the initial wetted-wall temperature (wall B), find the value of A in the modified Arrhenius expression shown below:

$$\mathbf{Ln\ C = Ln\ A - 16610/T} \qquad 4)$$

Knowing the value of A will give you the value of C over the range of wetted-wall temperatures from 350-600°F for any fuel/operating condition.

5. Once the C value is determined for a specific fuel/operating condition, predictions can be made with respect to the expected life (in hours) of the NAFTSS nozzle tube. Predicted life expectancy can be determined using the assumption that 20 mg carbon is equivalent to a failure in the

NAFTSS nozzle tube. Thus, time to failure can be calculated by re-arranging equation 1 to the form of equation 2 as previously shown:

$$t_f = (W / C)^{1/3} \qquad 2)$$

5. Alternatively, fuels can be ranked by taking the ratio of the C value at the specific conditions of interest and comparing to some known baseline value.

6th International Conference
on Stability and Handling of Liquid Fuels
Vancouver, B.C., Canada
October 13-17, 1997

EVALUATION OF JP-8 + 100 FUEL COMPATIBILITY WITH AIRCRAFT FUEL SYSTEM MATERIALS: THE EFFECT OF DETERGENT/DISPERSANT ON AIRCRAFT MATERIALS

Dexter H. Kalt, University of Dayton Research Institute, 300 College Park, Dayton, OH 45469-0148

Abstract. Within airframe and engine fuel systems, materials including metallics, composites and non-metallics are found in contact with aircraft fuel. This paper describes a few of these materials and physical property changes observed in these materials after thermal aging in specific aircraft fuels in a laboratory setting. These changes are evaluated in comparison to physical properties of materials before fuel aging and with different test fuels and additives. The laboratory tests are designed to reasonably replicate temperatures to which the materials and the specific fuels would be subjected in airframes and engines. The 28 day aging test temperatures range from ambient to 400 ° F. The materials are identified according to use categories in aircraft fuel systems. The materials include those used in fuel system tanks and in associated components (bladders, sealants, locking devices) as well as alloys and sealing materials used in fuel lines and components up to the engine combustion chamber. Included in the test data points are the materials' effects on the fuel i.e. conductivity, elements, gums, acid number and hydroperoxides. This paper describes aircraft fuel system materials and their compatibility with a new higher thermal stability fuel. The improved thermal stability JP-8 fuel is obtained by incorporating a fuel additive package commonly referred to as JP-8 +100. The effects of this fuel additive on the aircraft fuel systems materials are measured and determined by comparing their effects to that of a baseline JP-8 fuel. The +100 refers to the increase in the expected thermal stability range of the fuel by 100 ° F over that of a JP-8 baseline fuel. The +100 fuel additive package incorporates dispersant / detergent, metal deactivators and antioxidant compounds which are incorporated to reduce the rate of oxidation and deterioration of fuel at higher temperatures.

Introduction. The stated objective of this evaluation is to: "Demonstrate by comparative thermal aging tests and analysis that JP-8 fuel, containing a thermal stability additive package (detergent and dispersant) does not deteriorate or oxidize the contacted fuel system materials to the extent that degraded system performance ultimately occurs; i.e., fuel leakage and/or component malfunction".

The scope of this paper includes not only an examination of the compatibility effects of the thermal stability fuel additive in normal and 4x (times) concentrations on certain fuel system materials, but also illustrations of the critical importance of the time/temperature selection criteria for fuel system materials which experience the temperature variances in the air vehicle

environment. The Department of Defense inventory includes an extensive number of both older and newer aircraft types and models. More than two hundred thirty-five materials which come in contact with fuel have been identified for the subject evaluation. Consequently, this paper can, as a practical matter, discuss only the results of a few material examples.

The material tests were designed to examine and document two fuel / fuel system materials compatibility issues. The first issue was whether the *physical properties* of the fuel system materials examined in this test were affected by the JP-8 fuel *with* the +100 TSA (thermal stability additive) *to any greater degree* than they were affected by JP-8 fuel *which did not contain* the additive. The second issue was identification of those fuel system materials physical properties which were affected by the time / temperature in JP-8 fuel in *any* or *all* of the tests. Materials which *"failed" any physical property test in JP-8 and / or JP-8 + 100* were considered for an evaluation in an aircraft component / system fuel flow dynamic test stand specifically designed for these tests.

The tests examined a wide range of physical properties. Identical material samples were immersed in JP-8 fuel and in JP-8 +100 fuel and subjected to aging at appropriate temperatures (see "Aging Temperatures"). Data for each material's physical properties was collected and recorded in laboratory data collection sheets. This data was compiled on individual test data sheets (where all test data for *one* material were recorded on *one* sheet). Thus, comparisons between pre- and post- test material physical properties could be made as well as comparisons between JP-8's and JP-8 + 100's impacts on the materials physical properties. In addition, the test data was compiled into test summary sheets (where *comparisons* between the effects of the JP-8 and the JP-8 +100 in the various test temperatures could be easily discerned).

The current methods for evaluating materials which come in contact with fuel are separated into two basic categories: those methods used for evaluating metallics and those used for evaluating non-metallics. The methods used to evaluate materials' physical properties in a free state (non-component system application) may not necessarily reveal the materials' performance in an actual aircraft application. For example, physical property loss, and/or corrosion which may ultimately result in fuel leakage and/or component malfunction may not be determined in this laboratory test series. The correlation of the materials' free state aging to an actual aircraft component / system fuel flow dynamic application is a part of the overall planned

program evaluation. One such material, "leaded bronze", was tested in an engine gear pump, the test and results are discussed in this paper. Additional testing of "O" ring seals is planned to correlate component application test results to the static tests results.

In the following discussions, two non- metallics and one metallic will be examined in some detail. The tests on the two non-metallics will examine the materials' thermal tolerance. The tests on a leaded bronze alloy material will show the effects of the fuel with and without the + 100 fuel additive. Fuel / temperature aging effects on the material are demonstrated by the data when compared to non-aged material. Improved properties resulting from the effects of the additive also will be demonstrated.

Test Materials Identity. An early vigorous investigative effort of both industry and governmental agencies resulted in a comprehensive list of the materials used in airframe and engine fuel systems.

Aging Temperatures. Test temperatures were determined as practical laboratory approximations of use conditions. Four primary test temperatures were selected for this fuel/material evaluation. The primary test temperatures chosen were: 160 ° F; 200 ° F; 325 ° F; and 400 ° F. The temperatures were determined as follows:

For existing airframe fuel systems, 160 ° F generally is an accepted "high" temperature range. However, new and future airframe systems which have fuel recirculation from the engine back to the airframe fuel tanks may require continued operation up to 200 ° F. This test temperature exposure would provide a list of materials which could safely operate in fuel systems at 200 ° F and those which could not be used. A 325 ° F fuel temperature exposure was chosen for most materials commonly found on the aircraft engine. A 400 ° F fuel temperature exposure was chosen for the higher temperature sections of the aircraft engine.

In a limited number of instances, test data indicated the usefulness of other temperature exposures as dictated by a particular aircraft application. These are noted where they were used.

Fuel and Fuel Additives. The baseline fuel used in the subject tests was Jet A with the additives (static dissipater, icing and corrosion inhibitors) which, when added to Jet-A, produce fuel appropriately designated as JP-8. The two test fuels were produced by adding Betz Dearborn additive (at 100 mg/l and 400 mg/l concentrations). The BETZ additive package 8Q462 has dispersant and detergent properties. In addition a metal deactivator (MDA) at 2 mg/l

concentration and antioxidant (BHT) additive at 25 mg/l concentration are part of the Betz additive package. The MDA and BHT already were qualified additives. The BHT was not added in a 4x concentration. However, the MDA, for this test evaluation, was in a 10 mg/l concentration, higher than current specifications which require a 2 mg/l concentration.

Test Duration. The test duration for each material was twenty-eight days with a fuel changeout cycle of seven days.

Materials Categories. Following is a list of categories of materials examined in the subject test series grouped according to their use in aircraft airframe and engine fuel systems and in ground tank and fuel storage systems. (Each category may include many different materials and types of materials from a variety of manufacturers.)

Adhesives; Fuel Bladder Materials; Coatings; Primers; Sealants; Composites (used in fuel tanks, vent lines and isolator tubes, etc.); Fuel Filter Materials; Explosion Suppression Materials (foams); "O"-Ring Materials; Gasket and Washer Materials; Hose Materials; Insulation /Electrical/Wire/Clamps/Misc; Joining Materials; Bearing Materials; Locking Device Materials; Airframe, Tank and Plumbing Materials; Engine, Fuel Line and Components Materials; Float Materials; Potting Compound Materials.

Material Properties Test Evaluation. The data pages selected for these materials represent non-metallics tests with two different "O"-ring elastomeric materials and illustrate material property changes i.e.: tensile, elongation, volume swell, hardness (shore) and compression set. The tests with these non-metallics also show changes in the fuels properties which include color, fuel acid number, gums, hydroperoxides and fuel conductivity.

The metallic tests show material property changes i.e.: weight, color, and pitting (visual and microscopic). The tests with the metallic materials also evaluate fuel property changes including color, fuel conductivity and fuel materials elemental changes by use of graphite furnace and/or inductive coupled plasma test equipment.

The evaluation of physical properties related to other categories of fuel system materials tested includes pencil hardness, lap shear, cohesion, tape adhesion, peel strength, laminar shear, resistivity and torque.

The data pages compare the materials' properties aged in a JP-8 baseline fuel and with the JP-8 fuel containing a thermal stability additive in a normal concentration and in X 4 concentration.

In order to facilitate the evaluation of the non-metallic materials property changes, control material tests at ambient temperatures (72 ° F) also are performed and recorded.

Allowable tolerance ranges for the material property changes were established based on each material's specification requirements tempered with the constraints and conditions of each test. These tolerance ranges provide the test evaluation criteria for judging the performance of the materials fuel temperature aging test results.

Discussion. Following is a brief discussion of some of the findings of the subject tests.

Nitrile (MIL-P-5315) "O"-Rings. Fuel seals are of vital importance to proper function and fuel containment of a fuel system and the components thereof. Seals/ gaskets normally are in the form of "O"-rings and are found throughout the fuel system both within the confines of the fuel tanks, and, perhaps most importantly, outside the fuel tanks. Outside the tanks, they are found extensively in fuel couplings, valves, pumps, fuel tank interconnects and in ground and aerial refueling lines and components. These "O" rings prevent fuel leakage, a paramount safety concern because of the fuel's inherent volatility. In addition "O"-ring failure can affect the proper functioning of fuel system components and sub-systems.

This material's (Nitrile, MIL-P-5315, "O"-Rings) post physical properties after a 28 day aging in JP-8 and with the + 100 and + 100 X 4 thermal stability additives generally performed fully satisfactorily at a temperature of 160 ° F as illustrated in Table #1. However, its physical properties were degraded to an unacceptable level at temperatures of 180 ° F with JP-8 and +100 additive as illustrated in Table #2. At temperatures of 200 ° F and 325 ° F, the material exhibited extreme degradation of its physical properties to the extent that they could not be measured (Tables #3 and #4). For some properties, in Table #1 it can also be noted that a significant improvement in the nitrile physical properties occurs with fuel containing the thermal stability additive over the baseline JP-8 fuel to the extent that they approach the control material which has had no temperature/fuel aging. This positive effect of the thermal stability (detergent and dispersant) additive has been noted with many other materials.

Fluorosilicone MIL-P-25968 "O"-Rings. The fluorosilicone "O"- ring materials' post physical properties after a 28 day aging in JP-8 and the +100 and +100 X 4 concentrations of fuel additive performed fully satisfactorily at a temperature of 200 ° F as illustrated in Table #5. At temperatures of 250 ° F and 325 ° F, the materials' physical properties were degraded to an unacceptable level in both the JP-8 fuel and in the fuel containing a thermal stability additive in both concentrations as shown in Tables #6 and #7.

Leaded Bronze (TAP MS 285). This material is used for the bearings in gear-driven fuel pumps on aircraft engines. This particular material showed excessive amounts of lead and copper being extracted from the bearing material into the fuel during initial static coupon testing. It was determined that this excessive extraction (depicted in Table #8, graphite furnace element measurements) was caused by improper mixing and by the saw cut surfaces of the coupons. Appropriate mixing and using polished surfaced coupons, which more nearly duplicated the material in use, corrected this excessive extraction of copper and lead. (See Table #9.) The JP-8 baseline fuel and the fuel containing the +100 additive in normal and X 4 concentrations exhibited similar effects.

Due to a concern for this copper and lead being extracted from the leaded bronze alloy material by the fuel, this effect was evaluated in a fuel recirculation test stand using an actual engine fuel pump with bearings of this same material and coatings. The evaluation included baseline JP-8 fuel and fuel containing the thermal stability additives in the X 4 concentrations at a temperature of 325 ° F for approximately 119 hours. The pump was evaluated to determine whether the fuel has resulted in degraded pump performance (measured by pressure and flow changes) and any fuel effects and/or thermal stability additive effects on the bearings and gear wear. Tables #10 and #11 show the performance comparison of the JP-8 effects on the leaded bronze bearing to that of the + 100 fuel x4 concentration (detergent and dispersant) additive. Note the weight delta.

Fuel/Material Selection Guide. As a result of the subject fuels and materials evaluations, acceptable temperature ranges are being established for many of the currently used and new fuel system materials. This list of materials will provide airframe, engine and component manufacturers with a valuable guide in selecting materials which should withstand the temperatures and fuel environments of both current and future aircraft applications.

Conclusions/Findings.

1. On the basis of a comparative evaluation with JP-8 and of the materials tested and evaluated, the Betz/Dearborn 8Q462 thermal stability fuel additive is compatible with the materials found in Air Force aircraft fuel systems.

2. The Betz/Dearborn 8Q462 thermal stability fuel additive actually improves the material properties of many non-metallic materials. In addition, the Betz/Dearborn 8Q462 thermal stability fuel additive generally results in cleaner metallics.

3. Numerous materials were determined to have temperature limitations after continuous exposure at temperature.

4. A fuel selected to be used for a particular fuel additive also should be used as the JP-8 comparative fuel, since different fuels may have significantly different oxidation characteristics.

5. Materials should not be used beyond temperature range. Examples, Fluorosilicone "O" rings, 225 ° F; Fluorocarbon "O" rings, 325 - 400 ° F; (note compression set limits); Nitrile (fuel compatible), 160 ° F.

6. Materials which should not be used in contact with fuel / fuel vapors are: Nitrile, "O" rings designed for hydraulic fluids and Polysulfides potting compounds (e.g. CS-3100).

7. Certain metallic materials should not be used in continuous contact with fuel. These are: copper, lead, zinc, and cadmium.

8. Materials which should be retested in component / application form as appropriate for correlation or results include: leaded bronze, nylon, "O" rings, and Teflon.

9. New research / development programs are needed for certain fuel system materials. These are: extended temperature range (- 45 ° F to 400 ° F) of "O" rings fuel applications; fuel bladder innerliners, 225 ° F minimum; and potting compounds, 225 ° F minimum.

Acknowledgments. This work was supported by the U. S. Air Force, Wright Laboratory, Fuels and Lubrication Division, Aero-Propulsion and Power Directorate, Wright-Patterson Air Force Base, OH under contract No. F33615-92-2207, with Mr. Charles W. Frayne serving as the Air Force Technical Monitor. Support was also provided by the University of Dayton Research Institute, Materials Engineering, Kettering Laboratories and by the Materials Directorate, Wright Laboratory, Wright Patterson Air Force Base, OH.

References:

1. ASTM D4054-81, Fuel Additives
2. ASTM Standard & MIL HDBK 149B, Military Standardization HandBook Rubber
3. ASTM D381, Gums
4. ASTM D3242MoD, Acid No.
5. ASTM D412, Tensile, Elongation
6. ASTM D395 Method B, Compression Set
7. ASTM D2240, Hardness (Pencil)
8. ASTM F483-90, Weight Loss/Gain
9. ASTM G1-90, Cleaning
10. SAE/AS5172, Peel Strength
11. ASTM D257, Resistivity
12. ASTM D790, Laminar Shear
13. FED STD 141, MTHE 6301) Tape Adhesion
14. MIL-S-22473, Torque
15. ASTM D1414, Tensile/Elongation
16. ASTM D2624, Conductivity
17. ASTM G46, Pitting Evaluation
18. ASTM F-995, SCC

FUEL / MATERIAL COMPATIBILITY TEST RESULTS

TEST PLAN I.D. NO.	I.G.3	MATERIAL / IDENTITY:	NITRILE, N 602-70 (PARKER) MIL-P-5315
TEST TEMPERATURE (°F)	160	USE:	AIRFRAME, FUEL SYSTEM GASKETS, "O" - RINGS
EXPOSURE TIME (DAYS)	28	TEST ADDITIVE/FUEL:	BETZ DEARBORN 8Q462 (Normal & x4 Concentrations)/93POSF 2980
TEST DATE START:	15 FEB 96	JP-8 BASELINE FUEL:	93 POSF 2980 +(JP-8 Additives)

MATERIAL PROPERTY TESTS (AVG. 5 SPECIMENS)	TEST MATERIAL / FUEL EXPOSURE RESULTS			TEST EVALUATION CRITERIA					EVALUATION OF TEST RESULTS					
					ALLOWABLE TOLERANCE REQUIREMENT				COMPARISON TO CONTROL & ALLOWABLE REQUIREMENTS			OVERALL EVALUATION		
	JP-8 POST	JP-8 +100 POST	JP8+100 (X4) POST	CONTROL MAT MEASURED AT AMBIENT TEMP	DECREASE	MIN VALUE	INCREASE	MAX VALUE	JP-8	JP-8+100	JP-8+100 x4	JP8	+100	X4
TENSILE (PSI)	1009	1526	1592	1712	25%				-41	-11	-7	O	W	W
ELONGATION (%)	199	199	202	264	25%				-25	-25	-23	W	W	W
VOLUME SWELL (%)	16	17	17	N/A		0%		25%	P	P	P	W	W	W
HARD'S; a) SHORE A (PTS)	57	65	65	66	5 PTS		5 PTS		-3	-3	-4	W	W	W
b) PENCIL														
COMP. SET (avg. 2 spcm's)	9	12	6	N/A				50%	P	P	P	W	W	W
LAP SHEAR (PSI)														
COHESION (%)														
TAPE ADHESION (P/F)														
PEEL STRENGTH (LB/IN)														
LAMINAR SHEAR (PSI)														
RESISTIVITY (OHM-CM)														
TORQUE (INCH -LBS.)														
RUPTURE PRESS. (IN.HG)														
VISUAL OBSERVATIONS														

FUELS PROPERTY TESTS*	TEST FUEL / MATERIAL EXPOSURE 4 X 7 DAY PERIODS (28 DAYS)			CONTROL FUEL PRE (NEW) VS. POST (STRESSED) 160°F 7 DAYS						SPECIFICATION RANGE FOR JP-8		GENERAL OBSERVATIONS		
				JP-8		JP-8 + 100		JP-8 + 100 x4						
	JP-8 POST	JP-8 +100 POST	JP8+100 (X4) POST	PRE	POST	PRE	POST	PRE	POST	MIN	MAX	JP8	+100	X4
COLOR (7 DAYS)	NE	NE	NE	C	C1	C	C1	C	C1			NE	NE	NE
ACID NO. mgKOH/gm	NE	.004	.004	.001	NE	.001	.002	.003	.003		0.015	NE	W	W
GUMS mg/100ml	NE	4.4	41.4	.6	NE	4.4	5.2	9.6	12.4		7	NE	W	O
HYDROPEROXIDES mM/l	NE	0	0	.001	NE	0	.01	0	ND			NE	W	W
CONDUCTIVITY pS/m @72°F	15	400	662	100	NE	248	NE	912	NE	150	600	O	W	NSR
VISUAL OBSERVATIONS														

NOTES:

Fuel Color: C = Clear C1 - C6 = Light to Dark

Designations: NE = Not Evaluated; ND = Not Detected; BD = Below Detection; P = Pass; F = Fail
W = Within Allowable Requirement; O = Outside Allowable Requirement
OT = Material Tested Beyond Temperature Range
N/A = Not applicable; NSR = No Spec. Req. and/or 4 (x) Additive Concentration

* Fuel Property Test Data Was Collected to Establish Whether Any Correlation Exists Between Material Degradation and Fuel Properties Degradation

DATE:
UDRI TECH: J. DUES
UDRI ENG: B. WILT
UDRI P.I. ENG: D.H. KALT
A.F. AUT. W./MLSE: A. FLETCHER
A.F. AUT. WL/POSF S. A. ANDERSON

FUEL / MATERIAL COMPATIBILITY TEST RESULTS

TEST PLAN I.D. NO.	LG.3	MATERIAL / IDENTITY:	NITRILE, N 602-70 (PARKER) MIL-P-5315
TEST TEMPERATURE (°F)	180	USE:	AIRFRAME, FUEL SYSTEM GASKETS, "O" - RINGS
EXPOSURE TIME (DAYS)	28	TEST ADDITIVE/FUEL:	BETZ DEARBORN 8Q462 (Normal & x4 Concentrations)/POSF 2980
TEST DATE START:	14 MAR 96	JP-8 BASELINE FUEL:	93 POSF 2980 +(JP-8 Additives)

MATERIAL PROPERTY TESTS (AVG. 5 SPECIMENS)	TEST MATERIAL / FUEL EXPOSURE RESULTS			TEST EVALUATION CRITERIA					EVALUATION OF TEST RESULTS					
	JP-8 POST	JP-8 +100 POST	JP8+100 (X4) POST	CONTROL MAT MEASURED AT AMBIENT TEMP	ALLOWABLE TOLERANCE REQUIREMENT DECREASE	MIN VALUE	INCREASE	MAX VALUE	COMPARISON TO CONTROL & ALLOWABLE REQUIREMENTS JP-8	JP-8+100	JP-8+100 x4	OVERALL EVALUATION JP8	+100	X4
TENSILE (PSI)	1163	1093	1320	1712	25%				-32	-36	-23	OT	OT	W
ELONGATION (%)	232	223	187	264	25%				-12	-16	-29	W	W	O
VOLUME SWELL (%)	18	17	17	N/A		0%		25%	P	P	P	W	W	W
HARD'S; a) SHORE A (PTS)	55	57	62	66	5 PTS		5 PTS		-11	-9	-4	OT	OT	W
b) PENCIL														
COMP. SET (avg. 2 spcm's)	19	24	25	N/A				50%	P	P	P	W	W	W
LAP SHEAR (PSI)														
COHESION (%)														
TAPE ADHESION (P/F)														
PEEL STRENGTH (LB/IN)														
LAMINAR SHEAR (PSI)														
RESISTIVITY (OHM-CM)														
TORQUE (INCH -LBS.)														
RUPTURE PRESS. (IN.HG)														
VISUAL OBSERVATIONS														

FUELS PROPERTY TESTS*	TEST FUEL / MATERIAL EXPOSURE 4 X 7 DAY PERIODS (28 DAYS)			CONTROL FUEL PRE (NEW) VS. POST (STRESSED) 180°F 7 DAYS						SPECIFICATION RANGE FOR JP-8		GENERAL OBSERVATIONS		
	JP-8 POST	JP-8 +100 POST	JP8+100 (X4) POST	JP-8 PRE	JP-8 POST	JP-8 + 100 PRE	JP-8 + 100 POST	JP-8 + 100 x4 PRE	JP-8 + 100 x4 POST	MIN	MAX	JP8	+100	X4
COLOR (7 DAYS)	C1	C1	C1	C	C1	C	C1	C	C1			W	W	W
ACID NO. mgKOH/gm	.006	.003	.004	.001	.003	.001	.003	.003	.007		0.015	W	W	W
GUMS mg/100ml	3.2	5.4	12.4	.6	6.0	4.4	4.0	9.6	8.4		7	W	W	O
HYDROPEROXIDES mM/l	.37	0	0	.001	ND	0	.022	0	.00			O	W	W
CONDUCTIVITY pS/m @72°F	149	376	604	100	NE	248	NE	912	NE	150	600	W	W	NSR
VISUAL OBSERVATIONS														

NOTES:

Fuel Color: C = Clear C1 - C6 = Light to Dark

Designations: NE = Not Evaluated; ND = Not Detected; BD = Below Detection; P = Pass; F = Fail
W = Within Allowable Requirement; O = Outside Allowable Requirement
OT = Material Tested Beyond Temperature Range
N/A = Not applicable; NSR = No Spec. Req. and/or 4 (x) Additive Concentration

* Fuel Property Test Data Was Collected to Establish Whether Any Correlation Exists Between Material Degradation and Fuel Properties Degradation

DATE:
UDRI TECH: J. DUES
UDRI ENG: B. WILT
UDRI P.I. ENG: D.H. KALT
A.F. AUT. W./MLSE: A. FLETCHER
A.F. AUT. WL/POSF S. A. ANDERSON

FUEL / MATERIAL COMPATIBILITY TEST RESULTS

TEST PLAN I.D. NO.	LG.3	MATERIAL / IDENTITY:	NITRILE, N 602-70 (PARKER) MIL-P-5315
TEST TEMPERATURE (°F)	200	USE:	AIRFRAME, FUEL SYSTEM GASKETS, "O" - RINGS
EXPOSURE TIME (DAYS)	28	TEST ADDITIVE/FUEL:	BETZ DEARBORN 8Q462 (Normal & x4 Concentrations)/93POSF 2980
TEST DATE START:	21 NOV 94	JP-8 BASELINE FUEL:	93 POSF 2980 +(JP-8 Additives)

MATERIAL PROPERTY TESTS (AVG. 5 SPECIMENS)	TEST MATERIAL / FUEL EXPOSURE RESULTS			TEST EVALUATION CRITERIA					EVALUATION OF TEST RESULTS					
				CONTROL MAT MEASURED AT AMBIENT TEMP	ALLOWABLE TOLERANCE REQUIREMENT				COMPARISON TO CONTROL & ALLOWABLE REQUIREMENTS			OVERALL EVALUATION		
	JP-8 POST	JP-8 +100 POST	JP8+100 (X4) POST		DECREASE	MIN VALUE	INCREASE	MAX VALUE	JP-8	JP-8+100	JP-8+100 x4	JP8	+100	X4
TENSILE (PSI)	174	991	1211	1970	25%				-91	-50	-39	OT	OT	OT
ELONGATION (%)	34	138	147	265	25%				-87	-48	-45	OT	OT	OT
VOLUME SWELL (%)	16	17	18	N/A		0%		25%	P	P	P	W	W	W
HARD'S; a) SHORE A (PTS)	76	63	63	69	5 PTS		5 PTS		+7	-6	-6	OT	OT	OT
b) PENCIL														
COMP. SET (avg. 2 spcm's)	37	41	40	N/A				50%	P	P	P	W	W	W
LAP SHEAR (PSI)														
COHESION (%)														
TAPE ADHESION (P/F)														
PEEL STRENGTH (LB/IN)														
LAMINAR SHEAR (PSI)														
RESISTIVITY (OHM-CM)														
TORQUE (INCH -LBS.)														
RUPTURE PRESS. (IN.HG)														
VISUAL OBSERVATIONS														

FUELS PROPERTY TESTS*	TEST FUEL / MATERIAL EXPOSURE 4 X 7 DAY PERIODS (28 DAYS)			CONTROL FUEL PRE (NEW) VS. POST (STRESSED) 200°F 7 DAYS						SPECIFICATION RANGE FOR JP-8		GENERAL OBSERVATIONS		
				JP-8		JP-8 + 100		JP-8 + 100 x4						
	JP-8 POST	JP-8 +100 POST	JP8+100 (X4) POST	PRE	POST	PRE	POST	PRE	POST	MIN	MAX	JP8	+100	X4
COLOR (7 DAYS)	NE	NE	NE	C	C1	C	C1	C	C1			NE	NE	NE
ACID NO. mgKOH/gm	NE	NE	NE	.001	.002	.001	.002	.003	.003		0.015	NE	NE	NE
GUMS mg/100ml	NE	NE	NE	2	4.8	4.4	2.8	9.6	8.6		7	NE	NE	NE
HYDROPEROXIDES mM/l	NE	NE	NE	.004	.037	0	.038	0	.018			NE	NE	NE
CONDUCTIVITY pS/m @72°F	NE	NE	NE	108	39	248	131	912	410	150	600	NE	NE	NE
VISUAL OBSERVATIONS														

NOTES:

Fuel Color: C = Clear C1 - C6 = Light to Dark

Designations: NE = Not Evaluated; ND = Not Detected; BD = Below Detection; P = Pass; F = Fail
W = Within Allowable Requirement; O = Outside Allowable Requirement
OT = Material Tested Beyond Temperature Range
N/A = Not applicable; NSR = No Spec. Req. and/or 4 (x) Additive Concentration

* Fuel Property Test Data Was Collected to Establish Whether Any Correlation Exists Between Material Degradation and Fuel Properties Degradation

DATE:
UDRI TECH: J. DUES
UDRI ENG: B. WILT
UDRI P.I. ENG: D.H. KALT
A.F. AUT. W./MLSE: A. FLETCHER
A.F. AUT. WL/POSF S. A. ANDERSON

FUEL / MATERIAL COMPATIBILITY TEST RESULTS

TEST PLAN I.D. NO.	I.G.3	MATERIAL / IDENTITY:	NITRILE, N 602-70 (PARKER) MIL-P-5315
TEST TEMPERATURE (°F)	325	USE:	AIRFRAME, FUEL SYSTEM GASKETS, "O" - RINGS
EXPOSURE TIME (DAYS)	28	TEST ADDITIVE/FUEL:	BETZ DEARBORN 8Q462 (Normal & x4 Concentrations)/93POSF 2980
TEST DATE START:	16 NOV 94	JP-8 BASELINE FUEL:	93 POSF 2980 +(JP-8 Additives)

MATERIAL PROPERTY TESTS (AVG. 5 SPECIMENS)	TEST MATERIAL / FUEL EXPOSURE RESULTS			TEST EVALUATION CRITERIA					EVALUATION OF TEST RESULTS					
				CONTROL MAT MEASURED AT AMBIENT TEMP	ALLOWABLE TOLERANCE REQUIREMENT				COMPARISON TO CONTROL & ALLOWABLE REQUIREMENTS			OVERALL EVALUATION		
	JP-8 POST	JP-8 +100 POST	JP8+100 (X4) POST		DECREASE	MIN VALUE	INCREASE	MAX VALUE	JP-8	JP-8+100	JP-8+100 x4	JP8	+100	X4
TENSILE (PSI)	132	(Broke)	111	1970	25%				-93	-100	-94	OT	OT	OT
ELONGATION (%)	35	(Broke)	23	265	25%				-87	-100	-92	OT	OT	OT
VOLUME SWELL (%)	19	15	15	N/A		0%		25%	P	P	P	W	W	W
HARD'S; a) SHORE A (PTS)	70	82	75	69	5 PTS		5 PTS		+1	+13	+6	W	OT	W
b) PENCIL														
COMP. SET (avg. 2 spcm's)	170	162	147	N/A				50%	F	F	F	OT	OT	OT
LAP SHEAR (PSI)														
COHESION (%)														
TAPE ADHESION (P/F)														
PEEL STRENGTH (LB/IN)														
LAMINAR SHEAR (PSI)														
RESISTIVITY (OHM-CM)														
TORQUE (INCH -LBS.)														
RUPTURE PRESS. (IN.HG)														
VISUAL OBSERVATIONS														

FUELS PROPERTY TESTS*	TEST FUEL / MATERIAL EXPOSURE 4 X 7 DAY PERIODS (28 DAYS)			CONTROL FUEL PRE (NEW) VS. POST (STRESSED) 325°F 7 DAYS						SPECIFICATION RANGE FOR JP-8		GENERAL OBSERVATIONS		
				JP-8		JP-8 + 100		JP-8 + 100 x4						
	JP-8 POST	JP-8 +100 POST	JP8+100 (X4) POST	PRE	POST	PRE	POST	PRE	POST	MIN	MAX	JP8	+100	X4
COLOR (7 DAYS)	C2	C2	C2	C	C2	C	C2	C	C2			W	W	W
ACID NO. mgKOH/gm	.005	.001	.006	.001	.007	.001	.006	.003	.008		0.015	W	W	W
GUMS mg/100ml	4.2	7.6	15.8	2	3	4.4	3.4	9.6	12.2		7	W	O	O
HYDROPEROXIDES mM/l	.016	NE	.011	.004	.017	0	.015	0	.008			O	NE	O
CONDUCTIVITY pS/m @72°F	10.75	99	403	108	123	248	141	912	555	150	600	W	W	W
VISUAL OBSERVATIONS														

NOTES:

Fuel Color: C = Clear C1 - C6 = Light to Dark

Designations: NE = Not Evaluated; ND = Not Detected; BD = Below Detection; P = Pass; F = Fail
W = Within Allowable Requirement; O = Outside Allowable Requirement
OT = Material Tested Beyond Temperature Range
N/A = Not applicable; NSR = No Spec. Req. and/or 4 (x) Additive Concentration

* Fuel Property Test Data Was Collected to Establish Whether Any Correlation Exists Between Material Degradation and Fuel Properties Degradation

DATE:
UDRI TECH: J. DUES
UDRI ENG: B. WILT
UDRI P.I. ENG: D.H. KALT
A.F. AUT. W./MLSE: A. FLETCHER
A.F. AUT. WL/POSF S. A. ANDERSON

FUEL / MATERIAL COMPATIBILITY TEST RESULTS

TEST PLAN I.D. NO.	I.G.5 / II.G.2	MATERIAL / IDENTITY:	FLUOROSILICONE, PARKER L 677, MIL-P-25988
TEST TEMPERATURE (°F)	200	USE:	AIRFRAME, FUEL SYSTEM GASKETS, "O" - RINGS
EXPOSURE TIME (DAYS)	28	TEST ADDITIVE/FUEL:	BETZ DEARBORN 8Q462 (Normal & x4 Concentrations)/93POSF 2980
TEST DATE START:	9 JUN 94	JP-8 BASELINE FUEL:	93 POSF 2980 +(JP-8 Additives)

MATERIAL PROPERTY TESTS (AVG. 5 SPECIMENS)	TEST MATERIAL / FUEL EXPOSURE RESULTS			TEST EVALUATION CRITERIA					EVALUATION OF TEST RESULTS					
				CONTROL MAT MEASURED AT AMBIENT TEMP	ALLOWABLE TOLERANCE REQUIREMENT				COMPARISON TO CONTROL & ALLOWABLE REQUIREMENTS			OVERALL EVALUATION		
	JP-8 POST	JP-8 +100 POST	JP8+100 (X4) POST		DECREASE	MIN VALUE	INCREASE	MAX VALUE	JP-8	JP-8+100	JP-8+100 x4	JP8	+100	X4
TENSILE (PSI)	856	857	852	984	45%				-13	-13	-13	W	W	W
ELONGATION (%)	199	201	194	231	35%				+2	+3	-1	W	W	W
VOLUME SWELL (%)	9	9	9	N/A		0%		25%	P	P	P	W	W	W
HARD'S; a) SHORE A (PTS)	63	63	63	69	20Pts				-2	-2	-2	W	W	W
b) PENCIL														
COMP. SET (avg. 2 spcm's)	6	9	10	N/A				30%	P	P	P	W	W	W
LAP SHEAR (PSI)														
COHESION (%)														
TAPE ADHESION (P/F)														
PEEL STRENGTH (LB/IN)														
LAMINAR SHEAR (PSI)														
RESISTIVITY (OHM-CM)														
TORQUE (INCH -LBS.)														
RUPTURE PRESS. (IN.HG)														
VISUAL OBSERVATIONS														

FUELS PROPERTY TESTS*	TEST FUEL / MATERIAL EXPOSURE 4 X 7 DAY PERIODS (28 DAYS)			CONTROL FUEL PRE (NEW) VS. POST (STRESSED) 200°F 7 DAYS						SPECIFICATION RANGE FOR JP-8		GENERAL OBSERVATIONS		
	JP-8 POST	JP-8 +100 POST	JP8+100 (X4) POST	JP-8		JP-8 + 100		JP-8 + 100 x4		MIN	MAX	JP8	+100	X4
				PRE	POST	PRE	POST	PRE	POST					
COLOR (7 DAYS)	C1	C1	C1	C	C1	C	C1	C	C1			W	W	W
ACID NO. mgKOH/gm	.002	.002	.003	.001	.002	.001	.002	.003	.003		0.015	W	W	W
GUMS mg/100ml	3.4	5.2	14.2	2	4.8	4.4	2.8	9.6	8.6		7	W	W	W
HYDROPEROXIDES mM/l	.09	.03	0	.004	.037	0	.038	0	.018			O	W	W
CONDUCTIVITY pS/m @72°F	42	231	399	108	39	248	131	912	410	150	600	W	W	W
VISUAL OBSERVATIONS														

NOTES:

Fuel Color: C = Clear C1 - C6 = Light to Dark

Designations: NE = Not Evaluated; ND = Not Detected; BD = Below Detection; P = Pass; F = Fail
W = Within Allowable Requirement; O = Outside Allowable Requirement
OT = Material Tested Beyond Temperature Range
N/A = Not applicable; NSR = No Spec. Req. and/or 4 (x) Additive Concentration

* Fuel Property Test Data Was Collected to Establish Whether Any Correlation Exists Between Material Degradation and Fuel Properties Degradation

DATE:
UDRI TECH: J. DUES
UDRI ENG: B. WILT
UDRI P.I. ENG: D.H. KALT
A.F. AUT. W./MLSE: A. FLETCHER
A.F. AUT. WL/POSF S. A. ANDERSON

FUEL / MATERIAL COMPATIBILITY TEST RESULTS

TEST PLAN I.D. NO.	II.G.2	MATERIAL / IDENTITY:	FLUOROSILICONE, L677 PARKER, MIL-R-25988
TEST TEMPERATURE (°F)	250	USE:	ENGINE / AIRFRAME, FUEL SYSTEMS GASKET
EXPOSURE TIME (DAYS)	28	TEST ADDITIVE/FUEL:	Betz/Dearborn 8Q462 ((Normal and x4 Concentrations) /93 POSF 2980
TEST DATE START:	20 JUN '95	JP-8 BASELINE FUEL:	92 POSF 2980 + (JP-8 Additives)

MATERIAL PROPERTY TESTS (AVG. 5 SPECIMENS)	TEST MATERIAL / FUEL EXPOSURE RESULTS			TEST EVALUATION CRITERIA					EVALUATION OF TEST RESULTS					
				CONTROL MAT MEASURED AT AMBIENT TEMP	ALLOWABLE TOLERANCE REQUIREMENT				COMPARISON TO CONTROL & ALLOWABLE REQUIREMENTS			OVERALL EVALUATION		
	JP-8 POST	JP-8 +100 POST	JP8+100 (X4) POST		DECREASE	MIN VALUE	INCREASE	MAX VALUE	JP-8	JP-8+100	JP-8+100x4	JP8	+100	X4
TENSILE (PSI)	162	546	562	984	45%				-84	-45	-43	OT	W	W
ELONGATION (%)	130	225	192	195	35				-33	+15	-2	W	W	W
VOLUME SWELL (%)	4	9	8	N/A		0		25	P	P	P	W	W	W
HARD'S; a) SHORE A (PTS)	44	54	58	65	20				-21	-11	-7	OT	W	W
b) PENCIL														
COMP. SET (%) (avg. 2 spcm's)	18	NT	NT	N/A				30	P	NE	NE	W	NE	NE
LAP SHEAR (PSI)														
COHESION (%)														
TAPE ADHESION (P/F)														
PEEL STRENGTH (LB/IN)														
LAMINAR SHEAR (PSI)														
RESISTIVITY (OHM-CM)														
TORQUE (INCH -LBS.)														
RUPTURE PRESS. (IN.HG)														
VISUAL OBSERVATIONS														

FUELS PROPERTY TESTS*	TEST FUEL / MATERIAL EXPOSURE 4 X 7 DAY PERIODS (28 DAYS)			CONTROL FUEL PRE-NEW) VS. POST (STRESSED) 250°F 7 DAYS						SPECIFICATION RANGE FOR JP-8		GENERAL OBSERVATIONS		
	JP-8 POST	JP-8 +100 POST	JP8+100 (X4) POST	JP-8		JP-8 + 100		JP-8 + 100 x4		MIN	MAX	JP8	+100	X4
				PRE	POST	PRE	POST	PRE	POST					
COLOR (7 DAYS)	NE	NE	NE	C	C1	C	C1	C	C1			NE	NE	NE
ACID NO. mgKOH/gm	NE	NE	NE	.001	.002	.003	.003	.003	.002		0.015	NE	NE	NE
GUMS mg/100ml	NE	NE	NE	.6	3.6	4.0	4	9.6	6.4		7	NE	NE	NE
HYDROPEROXIDES mM/l	NE	NE	NE	.001	.01	.22	.01	0	.01			NE	NE	NE
CONDUCTIVITY pS/m @72°F	NE	NE	NE	100	NE	248	NE	912	NE	150	600	NE	NE	NE
VISUAL OBSERVATIONS														

NOTES:

Fuel Color: C = Clear C1 - C6 = Light to Dark

Designations: N.E. = Not Evaluated; N.D. = Not Detected; B. D. = Below Detection; P = Pass; F = Fail
W = Within Allowable Requirement; O = Outside Allowable Requirement
OT = Material Tested Beyond Temperature Range
N/A = Not applicable; NSR = No Spec. Req. and/or 4 (x) Additive Concentration

* Fuel Property Test Data Was Collected to Establish Whether Any Correlation Exists Between Material Degradation and Fuel Properties Degradation

DATE:	
UDRI TECH:	J. DUES
UDRI ENG:	B. WILT
UDRI P.I. ENG:	D.H. KALT
A.F. AUT. W./MLSE:	A. FLETCHER
A.F. AUT. WL/POSF	S. A. ANDERSON

FUEL / MATERIAL COMPATIBILITY TEST RESULTS

TEST PLAN I.D. NO.	II.G.2/I.G.5	MATERIAL / IDENTITY:	FLUOROSILICONE "O" RING 1677 PARKER, MIL-R-25988
TEST TEMPERATURE (°F)	325	USE:	ENGINE COMPONENTS
EXPOSURE TIME (DAYS)	28	TEST ADDITIVE/FUEL:	Betz/Dearborn 8Q462 ((Normal and x4 Concentrations) /93 POSF 2980
TEST DATE START:	7 SEPT '94	JP-8 BASELINE FUEL:	93 POSF 2980 + (JP-8 Additives)

MATERIAL PROPERTY TESTS (AVG. 5 SPECIMENS)	TEST MATERIAL / FUEL EXPOSURE RESULTS			TEST EVALUATION CRITERIA					EVALUATION OF TEST RESULTS					
				CONTROL MAT MEASURED AT AMBIENT TEMP	ALLOWABLE TOLERANCE REQUIREMENT				COMPARISON TO CONTROL & ALLOWABLE REQUIREMENTS			OVERALL EVALUATION		
	JP-8 POST	JP-8 +100 POST	JP8+100 (X4) POST		DECREASE	MIN VALUE	INCREASE	MAX VALUE	JP-8	JP-8+100	JP-8+100x4	JP8	+100	X4
TENSILE (PSI)	121	131	139	896	45%				-86	-85	-84	OT	OT	OT
ELONGATION (%)	88	96	82	214	35				-59	-55	-62	OT	OT	OT
VOLUME SWELL (%)	11	10	10	N/A		0		25	P	P	P	W	W	W
HARD'S; a) SHORE A (PTS)	38	40	41	67	20				-29	-27	-26	OT	OT	OT
b) PENCIL														
COMP. SET (%) (avg. 2 spcm's)	60	60	57	N/A				30	F	F	F	OT	OT	OT
LAP SHEAR (PSI)														
COHESION (%)														
TAPE ADHESION (P/F)														
PEEL STRENGTH (LB/IN)														
LAMINAR SHEAR (PSI)														
RESISTIVITY (OHM-CM)														
TORQUE (INCH -LBS.)														
RUPTURE PRESS. (IN.HG)														
VISUAL OBSERVATIONS														

FUELS PROPERTY TESTS*	TEST FUEL / MATERIAL EXPOSURE 4 X 7 DAY PERIODS (28 DAYS)			CONTROL FUEL PRE-NEW) VS. POST (STRESSED) 325°F 7 DAYS						SPECIFICATION RANGE FOR JP-8		GENERAL OBSERVATIONS		
	JP-8 POST	JP-8 +100 POST	JP8+100 (X4) POST	JP-8 PRE	JP-8 POST	JP-8 + 100 PRE	JP-8 + 100 POST	JP-8 + 100 x4 PRE	JP-8 + 100 x4 POST	MIN	MAX	JP8	+100	X4
COLOR (7 DAYS)	C3	C3	C3	C	C2	C	C2	C	C2			W	W	W
ACID NO. mgKOH/gm	.003	.010	.004	.001	.007	.001	.006	.003	.008		0.015	W	W	W
GUMS mg/100ml	12.0	13.6	20.0	2	3	4.4	3.4	9.6	12.2		7	O	O	O
HYDROPEROXIDES mM/l	.025	.001	NE	.004	.017	O	.015	0	.008			O	W	NE
CONDUCTIVITY pS/m @72°F	343	1011	627	108	123	248	141	912	555	150	600	W	O	W
VISUAL OBSERVATIONS														

NOTES:

Fuel Color: C = Clear C1 - C6 = Light to Dark

Designations: N.E. = Not Evaluated; N.D. = Not Detected; B. D. = Below Detection; P = Pass; F = Fail
W = Within Allowable Requirement; O = Outside Allowable Requirement
OT = Material Tested Beyond Temperature Range
N/A = Not applicable; NSR = No Spec. Req. and/or 4 (x) Additive Concentration

* Fuel Property Test Data Was Collected to Establish Whether Any Correlation Exists Between Material Degradation and Fuel Properties Degradation

DATE:
UDRI TECH: J. DUES
UDRI ENG: B. WILT
UDRI P.I. ENG: D.H. KALT
A.F. AUT. W./MLSE: A. FLETCHER
A.F. AUT. WL/POSF S. A. ANDERSON

FUEL / MATERIAL COMPATIBILITY TEST RESULTS

TEST PLAN I.D. NO.	II.M.23.1	MATERIAL / IDENTITY:	LEADED BRONZE (TAP MS 285), SAW CUT
TEST TEMPERATURE (°F)	325	USE:	ENGINE FUEL PUMP GEAR BEARING
EXPOSURE TIME (DAYS)	28	TEST ADDITIVE/FUEL:	Betz Dearborn 8Q462 (Normal and x4 Concentrations) /93 POSF 2980
TEST DATE START:	7 SEP 94	JP-8 BASELINE FUEL:	93 POSF 2980 + (JP-8 Additives)

MATERIAL PROPERTY TESTS (AVG. 5 SPECIMENS)	TEST MATERIAL / FUEL EXPOSURE RESULTS						EVALUATION OF TEST RESULTS			
	JP-8		JP-8 +100		JP8+100 (X4)		OBSERVATIONS AND REFERENCES	OVERALL EVALUATION		
	PRE	POST	PRE	POST	PRE	POST		JP8	+100	X4
COLOR	L	L3	L	L3	L	L3	Discoloration / Surface Deposits All Samples	CN	W	W
PITTING (VISUAL)	ND	P	ND	P	ND	P		CN	W	W
PITTING (MICROSCOPY)	ND	P	ND	P	ND	P	Pitting All Samples	CN	W	W
AVG. WT. (gms)	14.8183	14.8123	15.0083	15.0061	16.0856	16.0818				
GAIN / LOSS (gms)		-.0010		-.0022		-.0038				
MICROSCOPY EVAL.										

FUELS PROPERTY TESTS*	TEST FUEL / MATERIAL EXPOSURE 4 X 7 DAY PERIODS (28 DAYS)						CONTROL FUEL PRE (NEW) VS. POST (STRESSED 7 DAYS @ 325°F)						SPEC. RANGE FOR JP-8	TEST RESULTS GENERAL OBSERVATIONS		
							JP-8		JP-8 + 100		JP-8 + 100 x4					
	7	28	7	28	7	28	PRE	POST	PRE	POST	PRE	POST	MIN / MAX	JP8	+100	X4
COLOR (7 DAYS)	C5	C5	C4	C4	C3	C3	C	C1	C	C1	C	C1		W	W	W
CONDUCTIVITY (AVG. of 4)	PRE	POST	PRE	POST	PRE	POST										
PS/M AT 72° F	104	6	227	97	764	480	108	123	248	141	912	555	150/600	O	O	W
GRAPHITE FURN/ICP (PPB)	7 DAY	28 DAY	7 DAY	28 DAY	7 DAY	28 DAY										
Cu	500	550	1800	800	3000	1200								O	O	O
Pb	2000	ND	7000	ND	10,000	ND								O	O	O
Sn	ND	ND	ND	ND	ND	ND								W	W	W

NOTES:

Metallic Color: L = *Light (No Deposit)* L1 - L2 = *Discoloration/Deposits*

Fuel Color: C = *Clear* C1 - C6 = Light to Dark

Designations: NE = *Not Evaluated;* ND = *Not Detected;* BD = *Below Detection* P = *Pitting*

Comparisons: W = *Within Allowable Requirement;*
OT = *Material Tested Beyond Temperature Range* O = *Outside Allowable Requirement*
N/A = *Not applicable;* CN = *Control*
GT = *Greater than 500 ppb* LT = *Less than 500 ppb*
NSR = *No Spec. Req. and/or 4 (x) Additive Concentration*

* Fuel Property Test Data Was Collected to Establish Whether Any Correlation Exists Between Material Degradation and Fuel Properties Degradation

DATE:	
UDRI TECH:	J. DUES
UDRI ENG:	B. WILT
UDRI P.I. ENG:	D.H. KALT
A.F. AUT. W./MLSE:	A. FLETCHER
A.F. AUT. WL/POSF	S. A. ANDERSON

FUEL / MATERIAL COMPATIBILITY TEST RESULTS

TEST PLAN I.D. NO.	II.M.23.2	MATERIAL / IDENTITY:	LEADED BRONZE (TAP MS 285), Cu, POLISHED EXCEPT D.F. END
TEST TEMPERATURE (°F)	325	USE:	ENGINE FUEL PUMP GEAR BEARING
EXPOSURE TIME (DAYS)	28	TEST ADDITIVE/FUEL:	Betz Dearborn 8Q462 (Normal and x4 Concentrations) /93 POSF 2980
TEST DATE START:	7 SEP 94	JP-8 BASELINE FUEL:	93 POSF 2980 + (JP-8 Additives)

MATERIAL PROPERTY TESTS (AVG. 5 SPECIMENS)	TEST MATERIAL / FUEL EXPOSURE RESULTS						EVALUATION OF TEST RESULTS			
	JP-8		JP-8 +100		JP8+100 (X4)		OBSERVATIONS AND REFERENCES	OVERALL EVALUATION		
	PRE	POST	PRE	POST	PRE	POST		JP8	+100	X4
COLOR	L	L2	L	L2	L	L2		W	W	W
PITTING (VISUAL)	ND	NOTE	ND	NOTE	ND	NOTE	Voids in Graphite Coating - All Fuels	W	W	W
PITTING (MICROSCOPY)	ND	ND	ND	ND	ND	ND	EDS Mapping Revealed Selective Leaching of Pb	CN	W	W
AVG. WT. (gms)	14.7343	14.7347	14.7221	14.7216	14.8250	14.8246	Not Present, No Noticeable effect on Cu or Sn			
GAIN / LOSS (gms)		+.0004		-.0005		-.0004		W	W	W
MICROSCOPY EVAL.										

FUELS PROPERTY TESTS*	TEST FUEL / MATERIAL EXPOSURE 4 X 7 DAY PERIODS (28 DAYS)						CONTROL FUEL PRE (NEW) VS. POST (STRESSED 7 DAYS @ 325°F)						SPEC. RANGE FOR JP-8	TEST RESULTS GENERAL OBSERVATIONS		
							JP-8		JP-8 + 100		JP-8 + 100 x4					
	7	28	7	28	7	28	PRE	POST	PRE	POST	PRE	POST	MIN / MAX	JP8	+100	X4
COLOR (7 DAYS)	C2	C2	C2	C2	C2	C2	C	C1	C	C1	C	C1		W	W	W
CONDUCTIVITY (AVG. of 4)	PRE	POST	PRE	POST	PRE	POST										
PS/M AT 72° F	105	9	442	35	751	334	108	39	248	131	912	410	150/600	O	W	W
GRAPHITE FURN/ICP (PPB)	7 DAY	28 DAY	7 DAY	28 DAY	7 DAY	28 DAY										
Cu	127	NE	130	NE	145	NE								W	W	W
Pb	565	NE	540	NE	620	NE								O	O	O
Sn	47	NE	53	NE	45	NE								W	W	W

NOTES:

Metallic Color: L = *Light (No Deposit)* L1 - L2 = *Discoloration/Deposits*

Fuel Color: C = *Clear* C1 - C6 = Light to Dark

Designations: NE = *Not Evaluated;* ND = *Not Detected;* BD = *Below Detection* P = *Pitting*

Comparisons: W = *Within Allowable Requirement;*
OT = *Material Tested Beyond Temperature Range* O = *Outside Allowable Requirement*
N/A = *Not applicable;* CN = *Control*
GT = *Greater than 500 ppb* LT = *Less than 500 ppb*
NSR = *No Spec. Req. and/or 4 (x) Additive Concentration*

* Fuel Property Test Data Was Collected to Establish Whether Any Correlation Exists Between Material Degradation and Fuel Properties Degradation

DATE:	
UDRI TECH:	J. DUES
UDRI ENG:	B. WILT
UDRI P.I. ENG:	D.H. KALT
A.F. AUT. W./MLSE:	A. FLETCHER
A.F. AUT. WL/POSF	S. A. ANDERSON

Table #10

LABORATORY TEST STAND
ENGINE GEAR PUMP BEARING
TEST EVALUATION
COMPARISON RESULTS

119 HOURS @ 325°F

	JP-8	JP-8 + 100 x4 (BETZ)
OVERALL PUMP PERFORMANCE *(FLOW)*	SOME FLOW LOSS (starting conditions)	NO DISCERNIBLE FLOW LOSS
GEARS *(2 EACH)*	CLEAN	VERY CLEAN
BEARINGS (LEADED BRONZE) *(4 EACH)*	SOME WEAR	MINIMUM WEAR

GEAR PUMP BEARINGS

BEARING WEIGHT CHART

PUMP MODEL 828200
S/N EX-1046

(USED FOR TESTING)

325°F / 119 HOURS

TYPE OF TEST	*BEARING SERIAL NO.*	*PRE-TEST WEIGHT-GRAMS*	*POST-TEST WEIGHT-GRAMS*	*BEARING WEIGHT DELTA*	*DATE WEIGHED*
JP-8 BASELINE	00004	336.288	336.269	- .019	6 / 20 /95 AND 9 / 11 / 96
JP-8 BASELINE	00004B	337.319	337.298	- .021	
JP-8 BASELINE	00014	367.003	366.964	- .039	
JP-8 BASELINE	00001	367.645	367.548	- .097	
JP-8 + BETZ X4	00005	336.774	336.770	- .004	9 / 11 96 AND 11 / 18 / 96
JP-8 + BETZ X4	00009	336.559	336.556	- .003	
JP-8 + BETZ X4	00007	366.888	366.891	+ .003	
JP-8 + BETZ X4	00002	367.423	367.417	- .006	

6th International Conference
on Stability and Handling of Liquid Fuels
Vancouver, B. C. Canada
October 13-17, 1997

JP-8+100: THE DEVELOPMENT OF HIGH THERMAL STABILITY JET FUEL

Shawn P. Heneghan*[1] and William E. Harrison III[2]

[1]Aerospace Mechanics Division, University of Dayton Research Institute Dayton, OH 45469-0151
[2]USAF Wright Laboratories; WL/POSF Bldg. 490, 1790 Loop Road North Wright Patterson AFB, OH 45433

Abstract

Jet fuel requirements have evolved over the years as a balance of the demands placed by advanced aircraft performance (technological need), fuel cost (economic factors), and fuel availability (strategic factors). These challenges include: maintaining availability while minimizing the cost; maintaining flammability and heat content while minimizing fire and explosion hazards; allowing cold weather and high altitude operations by restricting flow characteristics, improving storage lifetimes, improving handling and improving refueling safety. To meet these evolving challenges, the Air Force over the years has developed fuels and fuel additive packages for both general (JP-4 and JP-8 fuels) and specialized (JPTS and JP-7) use. In a modern aircraft, the jet fuel not only provides the propulsive energy for flight, but also is the primary coolant for aircraft and engine subsystems. To address this particular requirement, the U.S. Air Force, industry, and academia have teamed to develop a new additive package for kerosene jet fuels that offers increased heat sink and thermal stability. This advanced additive package when added to jet fuels enables improved aircraft design and decreases fuel system maintenance due to fuel fouling/coking. This paper describes the development of an improved JP-8, named "JP-8+100", that offers a 55C (100F) increase in the bulk maximum temperature (from 325F to 425F), wetted wall temperature (from 400F to 500F) and improves the heat sink capability by 50%. Included are sections that detail the problem definition, the additive selection and design process, and flight and field-testing and evaluation. Field-testing in current front line Air Force aircraft has shown that an improvement in thermal stability of JP-8 fuel reduces fuel-related maintenance, reduces replacement parts requirements and increases aircraft readiness. In studies of the design of future advanced aircraft, JP-8+100 has been shown to reduce fuel system complexity and weight.

Nomenclature

AFB	Air Force Base	**JFTOT**	Jet Fuel Thermal Oxidative Tester
CFDC	Computational Fluid Dynamics with Chemistry	**JP**	Jet Fuels
WRDC	Wright Research and Development Center	**TAC**	Total Accumulated Cycles

Introduction

High performance aircraft use fuel as the primary coolant for aircraft subsystems (i.e. gearboxes, hydraulic systems, generators, and environmental control systems) and to cool the lubricating oils in the engine. High performance, high thermal efficiency engines currently being designed will operate at significantly higher temperatures than current engines. These advanced engines will require more fuel cooling to preserve component life and integrity and also will have less fuel available with which to manage and transfer that heat since they are more fuel efficient. The end result is that jet fuel will be exposed to significantly higher temperatures for longer periods of time causing the fuel to degrade and foul aircraft and engine components.

In 1990, an Aircraft Thermal Management Working Group of Wright Research and Development Center (WRDC) investigated the cooling requirements for current, next generation, and future aircraft.[1] Figure 1 illustrates the maximum estimated heat loads for various future aircraft and aircraft subsystems. Also, Figure 2 provides the worst case temperatures, pressures, and residence times experienced by fuel in various engine and airframe components. The WRDC working group reached an alarming conclusion: "*aircraft development in the near future will suffer performance penalties as tremendous quantities of ram air or excess fuel will be required to meet the heat sink requirements.*" To resolve the problem, the WRDC working group recommended the development of high thermal stability fuels, such as: (i) a high temperature thermally stable JP-8+100 fuel which provides a 50% improvement in heat sink capability over conventional JP-8 fuel, and (ii) a new fuel JP-900 that has a 482C (900F) thermal stability and could eliminate the need to recirculate fuel on-board an aircraft. Recent studies conducted by the Air Force have also identified the need for an intermediate heat sink fuel (between JP-8+100 and JP-900) identified as JP-8+225 and for fuels with more heat sink than JP-900 identified as endothermic fuels. All these advanced high heat sink fuels will be based on the additive building block philosophy of JP-8+100 and will undergo similar testing as outlined in this paper.[2]

This paper presents a brief overview of the development of JP-8+100, with emphasis on current flight testing and evaluation. Included are descriptions of the following:

1. Challenges faced in the development of JP-8+100 thermally stable fuel including, test development, additive testing, and materials interactions evaluation,
2. Test assessment and selection of an additive package from screening to flight tests,
3. Evaluation of additive performance based on flight data.

JP-8+100 Program

In 1989, the U.S. Air Force initiated a research program to increase the thermal stability of JP-8 with the partnership of other government agencies, industry, and universities. Jet fuel development is the best compromise solution to engine performance requirements (technological

needs), fuel cost (economic factors), and fuel availability (strategic factors). These same factors were key to the development of JP-8+100. The main goal of this program was to increase the heat sink capacity of current JP-8 fuel by 50 percent (i.e., a 55C increase in fuel operating temperature from 163C to 218C) by developing additives to blend with the fuel at a cost of $1 per 1000 gallons. This fuel will alleviate the need for using expensive specialty fuels such as JP-7 and JP-TS in future aircraft, and decrease maintenance costs for existing aircraft. To meet this goal, the following *five* major research tasks were identified and completed:

1. Identify and develop new fuel thermal stability test techniques.
2. Advance fundamental understanding of fuel thermal stability.
3. Develop global chemistry models and a thermal stability scale.
4. Formulate effective thermal stability improving additive packages.
5. Demonstrate, in actual aircraft flight time and maintenance records, the performance and cost savings produced by the use of new JP-8+100 fuel.

Additives Testing

A prime goal of the "JP-8+100" development program was to find an additive or an additive combination that will improve the thermal stability of JP-8 fuel by 55C. Laboratory tests, while having significant advantages in assessing the development of an additive package, all have some inherent disadvantages. Not the least of which is that each test is limited as to the range of temperatures and times over which fuel heating (stressing) takes place. An initial analysis of showed that no one test (such as the accepted Jet Fuel Thermal Oxidation Tester, JFTOT) could replicate all of the temperature/times that fuels could undergo in a variety of airframes. Since little was known about modeling these effects, so as to extrapolate to other conditions, a variety of tests were planned. These tests have been grouped as screening tests, follow-on tests, and large-scale engineering tests (see Table 1.).

Since 1989, additive manufacturers have supplied over 400 additive candidates for testing. To accommodate such a large number of additives, a series of screening tests were used for initial additive evaluation. Tests were generally run at the manufacturer's recommended concentration. Screening tests are simple to operate; typically yielding results in less than a day. This allows many additives to be tested. However, these tests are operated under accelerated test conditions (i.e., excess oxygen or temperature). As a result, significantly more assumptions concerning the behavior of fuels and additives is needed to properly evaluate the test results. Those additives that performed "best" were tested in up to 12 fuels (see reference [3] for a description of the test fuels), and selected for follow-on testing including concentration optimization.

Follow-on tests more closely approach reality, but require significantly more time both in testing and turnaround thereby limiting the number of additives and fuel/additive combinations

TABLE 1: SUMMARY OF THERMAL STABILITY TEST RIGS AND CONDITIONS

Test	Temperature Range (C)	Miscellaneous
Screening Tests		
Quartz Crystal Microbalance[8]	140	Closed system - measures surface deposits
Isothermal Corrosion Oxidation Test[9]	180	Bubbling air - measures bulk deposits
Microcarbon Residue Test[9]	225	Distillation - measures residual deposits
Hot Liquid Process Simulator[10]	335	JFTOT flow system
Jet Fuel Thermal Oxidative Tester	~260	JFTOT flow system
Follow-on Tests		
Augmentor[11]	< 1000	Vaporization flow system - simulates afterburner and nozzle soak back
Phoenix[12]	200-300	Constant wall temperature with on-line dissolved O_2 measurement
Near Isothermal Flowing Test Rig[4]	140 - 210	Isothermal flow system with on-line dissolved O_2 measurement
Engineering Tests		
Extended Duration Thermal Stability Test[14]	160-200	Establishes fuel bulk and wetted wall temperatures
Advance Reduced Scale Fuel System Simulator[13]		Configured to simulate F-22

that can be evaluated. Isothermal flowing tests[4] have been used to not only evaluate additives, but also to develop an understanding of the chemistry involved in autoxidation, deposition, and additive performance. Much of the chemistry involved in the autoxidation of jet fuels in static and isothermal flowing chemistry has been successfully modeled.[5] The chemistry models have further been incorporated into computational fluid dynamics with chemistry modeling codes.[6,7] These test rigs have been crucial in developing the models, and have been used to assess the effectiveness of nearly a dozen additives in up to 4 fuels. After testing, the candidate additives with the best likelihood of success were extensively tested in large-scale engineering rigs.

The large-scale engineering rigs are the closest to reality in temperature, flow conditions, oxygen level, and recirculation, but require significant time to evaluate an additive and often produce results that are hard to evaluate. However, this is the first level of test that can be used to assess the actual improvement in operating temperature achieved by the additives.[14] The difficulty of maintaining baselines and the large times scale required for a single test have limited the evaluation in large-scale test rigs to a few additives.

Concurrent with the large-scale test rigs, a series of materials compatibility tests were also run to identify/correct any adverse materials impact. To accomplish this compatibility tests, over

400 material/temperature combinations have been identified. Materials tested in this program span more than 50 years of technology from materials first used in the late 1950's and early 1960's on aircraft such as the KC-135 tanker and the B-52 bomber to aircraft materials planned to be used on aircraft after the turn of the century. In addition, many materials that are widely used on aircraft were never thoroughly tested with JP-8 such that baseline performance of all materials with JP-8 was required. Once the baseline for the large number of material and temperature combinations was established with JP-8 and the Betz Dearborn JP-8+100 additive, a shorter list was compiled for other additives. The performance of new additives needs be evaluated against only those materials that are most susceptible to chemical attack by an additive. A complete list of materials, material/fuel test results, and evaluations criteria are detailed in reference.[15]

Despite the fact that screening tests were followed-up with additional tests in up to 12 fuels, there remained a large variety of fuels in which the additive may be used. Therefore, in addition to and concurrent with the large scale testing, we verified that the additive package would work in most fuels by studying the effects in a world fuel survey. This survey comprised the baseline fuel tests and fuel plus additive package tests for the basic battery of screening tests.[16]

To date, one package has been qualified for flight. Field-testing has begun at a variety of military air reserve and national guard bases throughout the US. This package comprises an antioxidant (butylated-hydroxy-toluene) a metal deactivator (n,n'-disalicydene-1,2,- propane diamine) and ă detergent/dispersant (proprietary, Betz Dearborn Corporation). Details of the actual testing results, evaluations, chemistry models, model development, statistical analysis, and complete reference list for JP-8+100 development are listed in.[17] A second additive distributed by Shell International has recently been approved and will be available for use by US and foreign allies in Europe.

Engine and Flight Tests

Although extensive laboratory testing of JP-8+100 was conducted, the true validation of the fuel is obtained by testing in actual aircraft hardware. Initial combustion tests of JP-8+100 were conducted in a CFM-56 combustor rig at Wright Laboratory. These tests showed excellent combustion behavior through a wide range of fuel to air ratios. Also, the fuel was tested in an F100-PW-200 engine in a 50 hour, 224 total accumulated cycles (TAC) test. The engine, prior to testing, was "dirty" with visible fouling typical of those found in the fleet. The JP-8+100 additive cleaned lightly fouled components, and improved overall engine performance by opening several small orifices such that the engine could operate at design conditions. Several other engines were tested (T63-A-700, F100-PW-200 (4000 TAC test), F100-PW-229 and in components of the F119-PW-100 engine) with similar improvements. Since these tests were successful, a flight test was conducted at Edwards AFB in September 1994. An F-16 with an F100-PW-220E engine was

flown for 4.4 hours throughout the entire flight envelope including 28 engine restarts. This test found no problems, which cleared the fuel for use in other aircraft, and field-testing. In May 1997, Air Education and Training Command (AETC) facilitated a flight test of the Raytheon T-1A at the Raytheon facility in Wichita KS. Prior to the flight test, Pratt & Whitney Canada conducted a ground test of the JT15D engine. The test lasted 107 hours and showed a gradual small improvement in the specific fuel consumption. Raytheon conducted a complete evaluation of the performance of the aircraft with JP-8+100 and compared it to the performance of JP-8. Raytheon found no aircraft performance differences and cleared the T-1A for the use of JP-8+100, thus facilitating the conversion of T-1A aircraft at all AETC training bases. In March to May 1997, the Air Force Flight Test Center at Edwards AFB CA conducted a flight test of a C-141A aircraft with JP-8+100 to determine aircraft cruise performance, fuel quantity gauging effects, engine airstarts and engine smoke and soot production. Approximately 10 flight hours were conducted on JP-8+100. No differences were found with JP-8+100 when compared to JP-8 on aircraft cruise performance, fuel quantity gauging, and engine airstarts. The visual analysis of smoke and soot production was inconclusive, however, the engine showed reduced levels of soot upon post test inspection.

Field Evaluation Results

Field evaluations are being conducted to quantify long term benefits of JP-8+100. Locations of the field evaluations, aircraft type, engine type and duration of the field evaluation are shown in Table 2. At all the bases except Westfield, all aircraft were converted to JP-8 + 100. At Westfield approximately one-half the aircraft were converted for the evaluation. The demographics of the aircraft numbers and types participating in the field evaluations are as follows: 73 F-16 aircraft, 70 F-15 aircraft, 97 T-37 aircraft, 114 T-38 aircraft, 30 C-130 aircraft, 16 helicopters and 8 OA-10 aircraft. Maintenance data for most locations was collected for a minimum of a 12 month period on JP-8+100 and compared to maintenance data collected during a prior 12 month period on JP-8. By analyzing data from a 12 month period, statistical sample size variations and season variations that effect engine performance are minimized. Results compared across several locations for the same aircraft and engine type also improve the statistical significance of the data collected.

Fuel fouling/coking was observed in fuel nozzles, fuel manifolds, augmentor sprayrings and spraybars on many of the engines that were using JP-8. The severity of the fouling/coking and the effect on engine maintenance varied from engine type to engine type and to a lesser extent from location to location. Some locations using JP-8 reported significant problems with augmentor no lights and bangs (augmentor turns on but doesn't light for a short period of time), engine stalls and flame-outs, premature failure of turbine blades and vanes, plugged manifolds, nozzles and augmentors, whereas others reported minor problems. Analysis of the problems with

JP-8 was complicated by variations between locations in maintenance trouble shooting procedures (within technical orders), maintenance practices to correct deficiencies, and data reporting into maintenance data bases. Because of these issues, data collected on the benefits of JP-8+100 required extensive manpower intensive analysis of the maintenance data to assure that maintenance reductions are carefully counted. Top level statistical analyses proved to be somewhat inconclusive since many non-fuel related factors (engine aging, non-fuel wetted parts failure, inspections etc.) can significantly effect maintenance actions and related costs.

Problems with statistical analysis

The statistical analysis of the occurrence of augmentor bangs presents an interesting problem. Because it is typically on the order of one to ten per 1000 hours of flight, The variation from one time period to the next can be large when compared to the average. If ordinary variance of analysis techniques (such as t-distributions) are used, the analysis shows real probabilities of negative rates of occurrence. That is, the analysis is not straightforward since the data set may not be large enough to use the central limit theorem, and a t-statistic may not be an appropriate distribution for analysis of the data. To correct this problem, a Poisson distribution can been assumed.

The Poisson distribution, $f(x) = \frac{\mu^x e^{-\mu}}{x!}$ for $x \geq 0$ and $x \subseteq$ integers (x is the number of occurrences in a specified time period), has at least one very interesting property; the mean = μ and the variance = μ. Even for small samples, the Poisson distribution can approximate a normal distribution fairly well. That is, the assumption that $\frac{\bar{x}-\mu}{\frac{\sigma}{\sqrt{n}}}$ is n(0,1) is valid. However, the assumption that $\frac{ns^2}{\sigma^2}$ is independent of $\frac{\bar{x}-\mu}{\frac{\sigma}{\sqrt{n}}}$ (a necessary condition for t-statistics analysis) is not valid, since the variance σ is equal to the mean μ. The problem is self-correcting though since if we believe the central limit theorem holds then the z-statistic for a Poisson is just $\frac{\bar{x}-\mu}{\frac{\sigma}{\sqrt{n}}}$. This z-statistic does not suffer from the same problem as the normally distributed z-statistic in that there is but one unknown parameter in Poisson z-statistic (there is no σ) and therefore no need to use a t-statistic analysis. Therefore we can solve for the distribution of this statistic immediately, and determine a 95% (1.96σ) confidence limit from n(0,1). That is, $-1.96 < \frac{\bar{x}-\mu}{\frac{\sigma}{\sqrt{n}}} < 1.96$.

TABLE 2: SUMMARY OF FIELD TEST AIRCRAFT AND LOCATIONS

Air Force Base	Aircraft type	Engine	Test Time (months)*
Kingsley Field ANGB OR	F-16A/B	F100-PW-200	36
Fargo ANGB ND	F-16A/B	F100-PW-200	15
Otis ANGB MA	F-15A/B	F100-PW-100	21
Portland ANGB OR	F-15A/B	F100-PW-100	14
Langley AFB VA	F-15A/B	F100-PW-100	4
Burlington ANGB VT	F-16C/D	F100-PW-220E	21
Westfield ANGB MA	OA-10	TF34-GE-100A	20
Sheppard AFB TX	T-37B, T-38	J69-T-25, J85-GE-5	30
Louisville ANGB KY	C-130H	T56-A-15	18
Nashville ANGB TN	C-130H	T56-A-15	16
Springfield ANGB OH	F-16A/B	F110-GE-100	15
Kirland AFB NM	UH-1	T400-CP-400	6
	MH-53	T64-GE-7	6
	HH-60	T700-GE-700C	6
	MC-130	T56-A-15	6

* As of Nov 97

This does not have a simple solution, but can be solved iteratively using an initial guess of $\mu = \bar{x}$ and calculating a new guess using $\mu = 1.96\sqrt{\frac{\mu}{n}} \pm \bar{x}$. The 95% confidence limits for a Poisson distribution are not evenly distributed about the mean, being truncated on the lower side, and as expected, as the number of flight hours increases, the interval for 95% confidence decreases. In these equations the "n" is the number of thousand hour flight intervals. We have checked our analysis and verified that the results do not depend on the size of this interval. The analysis has been shown to be robust except at extremely small n and $\bar{x}$, or $\bar{x} = 0$.

To verify a statistically significant decrease in occurrences as a result of JP8+100 usage, it suffices to show that the rate of failure with JP8, $\bar{x}_{JP8}$, is greater than the 95% confidence upper limit of the JP8+100 failure rate, $\bar{x}_{JP8+100}$. Or, conversely, that $\bar{x}_{JP8+100}$ is less than the 95% lower limit of $\bar{x}_{JP8}$. One can see from Figure 3 that there is a statistically significant decrease in the mean failure rate that is more than two per month. The decrease in the measured mean failure rate is nearly four per month.

Additional field and laboratory observations

Other analyses have involved the careful analysis of each maintenance action comparing the initial pilot indication of problems to the actual maintenance action taken to correct the problem. Using this time intensive process, non fuel related maintenance actions can be sorted out and actual numbers determined. Due to the time intensity of this analysis, detailed quantitative results are not complete at this time, however the following qualitative results have been found: In F-15's and F-16's with the Pratt & Whitney F100 series engine, JP-8+100 reduces fouling/coking in augmentor manifolds and sprayrings. In laboratory experiments JP-8+100 has been shown to reduce deposition in these components by approximately 50% and in the field similar results have been found. In some applications, no new deposition was reported in up to 300 operating hours with the thermal stability additive package. By reducing the formation of deposits, augmentor anomaly rates have dropped 40 to 50% resulting in fewer unscheduled engine removals and reductions in maintenance man-hours and parts. Engine hardware appears to be cleaner with the use of the additive and reductions in smoke and soot in the engines has been note. In C-130 aircraft with the Allison T56 engine, the maintainers have had to replace fewer fuel nozzles and turbine assembles with JP-8+100. Inspections of hot section components have been made easier with reduced levels of soot on these components. Reductions in nozzle fouling have been observed in T-37 aircraft with the J69 engine and nozzle and augmentor fouling has been reduced in the J85 engine on T-38 aircraft. Both aircraft have experienced reduction in engine no-lights. In helicopters engines, preliminary results show reduced fuel nozzle coking and reductions in smoke and soot. In F-16 aircraft with the General Electric F110 engine, few problems were noted with JP-8 fuel. Hardware looks somewhat cleaner with JP-8+100 and some reduction in coking in the fuel nozzle swirler cups has been noted on engines with several hundred operating hours on the additive. The General Electric TF34 had an excellent track record of few problems on JP-8. After more than one year of analysis, no significant improvements were noted and no operational deficiencies were found. Overall, in engines with known fouling/coking problems, JP-8+100 reduces the problem and saves the Air Force scarce maintenance dollars.

The Air Force has developed an implementation plan to have all fighters and trainers use JP-8+100 by FY99. Twelve fighter and trainer bases were stood up in 1997 beyond the locations that participated in the field evaluation. Currently over 1000 aircraft are realizing the benefits of JP-8+100.

Summary

This paper has discussed the development and field testing of a high thermally stability JP-8+100 fuel that provides a 50 percent improvement in the heat sink capability over

conventional JP-8 fuel at an increased cost of less than a halfpenny per gallon. Some principle advances made towards achieving this goal are:

1. New techniques to test additives were developed and have been demonstrated to simulate the actual environment that fuel is exposed to in aircraft. Positive results in actual engines and aircraft in the field validated the testing process.
2. Fundamental global reaction mechanisms were proposed and used in CFDC computer models to predict oxidation and deposition processes in jet fuels. These models guided experiments and helped increase the understanding related to chemical and physical aspects of fuel deposition.
3. An additive package was developed for JP-8 fuel that increases thermal stability by 100F. The additive is now part of the JP-8 specification and is currently being used in over 1000 Air Force Aircraft
4. Statistical techniques to analyze the field-test data have been developed. These analyses combined with detailed maintenance data tracking validate the benefits of JP-8+100.
5. Field evaluation of the thermal stability additive package has been successful and the benefits obtained have paid for the increased effort associated with the tests. In many aircraft, significant maintenance savings have been achieved and reductions in smoke and soot noted.
6. Implementation plans have been established such that all fighter and trainer aircraft will be using the fuel by FY99. Plans to extend the use to all Air Force aircraft have been initiated.

References

(1) Harrison III, W. E., "Aircraft Thermal Management: Report of the Joint WRDC/ASD Aircraft Thermal Management Working Group," WRDC-TR-90-2021, Wright Patterson AFB OH, 1990

(2) Edwards, T, "Prospects for JP-8+225; A stepping stone to JP-900," paper submitted for presentation at 34th Annual AIAA/ASME/SAE/ASEE Joint Propulsion Coinference, Cleveland, OH, July, 1998

(3) Grinstead, R. R., Heneghan, S. P., Striebich, R. C., and Zabarnick, S., "Jet Fuel Thermal Stability and Analytic Test Data," University of Dayton Technical Report: Dayton, OH, UDR-TR-94-20, 1994

(4) Jones, E. G., Balster, W. J., and Post, M. E., "Degradation of a Jet-A Fuel in a Single Pass Heat Exchanger," *Trans. ASME Jour. Eng. Gas Turb. Power*, Vol. 117, pg. 125.

(5) Zabarnick, S., 1993, "Chemical Kinetic Modeling of Jet Fuel Autoxidation and Antioxidant Chemistry," *Ind. Eng. Chem. Res.*, **115**, 1012, 1995

(6) Katta, V. R., Jones, E. G., and Roquemore, W. M., "Development of Global Chemistry Model for Jet-Fuel Thermal Stability Based on Observations from Static and Flowing Experiments," 81st AGARD Symposium on Fuels and Combustion Technology for Advanced Aircraft Engines, Collifero, Italy, AGARD-CP-536, Paper No. PEP-19, 1993

(7) Ervin, J. S., Williams, T. F., Heneghan, S. P., and Zabarnick, S. "The Effects of Dissolved Oxygen Concentration, Fractional Oxygen Consumption, and Additives on JP-8 Thermal Stability," presented at *ASME International Gas Turbine Institute* Birmingham Eng, 1996

(8) Zabarnick, S., "Evaluation of Jet Fuels and Jet Fuel Additives Using the Quartz Crystal Microbalance and Pressure Measurements," University of Dayton Research Institute, UDR-TR-94-63, 1994

(9) Grinstead, R. R., "Evaluation of JP-8+100 Additives by Isothermal Corrosion Oxidation Test and Microcarbon Residue Test," University of Dayton Technical Report: Dayton, OH, UDR-TR-94-85, 1994

(10) Biddle T. B., Hamilton, E. H., and Edwards, W. H., "United Technologies Corporation, Pratt & Whitney, R&D Status Reports to WL/POSF," Contract No. F-33615-90-C-2051, Wright Patterson Air Force Base, OH, 1994

(11) Edwards, J. T., "Deposition During Vaporization of Jet Fuel in a Heated Tube," 30th Aerospace Sciences Meeting, Paper No. AIAA 92-0687, Reno, NV, 1992

(12) Heneghan, S. P., Williams, T. F., Martel, C. R., and Ballal, D. R., "Studies of Jet Fuel Thermal Stability in A Flowing System," *Trans. ASME J. Eng. Gas Turb. Power*, Vol. 115, pp. 480-484, 1993

(13) Morris, R. W. And Binns, K. E., "Evaluation of Improved Thermal Stability Jet Fuels in an Advanced Reduced Scale Fuel System Simulator," *Abstract to 5th International Conference on the Handling and Stability of Liquid Fuels*, Rotterdam, the Netherlands, page 42, 1994

(14) Dieterle, G. L. and Binns, K. E. "Extended Duration Thermal Stability Test of Improved Thermal Stability Jet Fuel," ASME Paper No. 95-GT-69 presented at the ASME Turbo Expo '95, Houston, TX, June, 1995

(15) Kalt, D., "Fuel material and Additivity," UDR TR 97-01, University of Dayton Research Institute, Dayton, OH, 1997

(16) Zelesnik, P., "Studies of Jet Fuel Thermal Stability, Oxidation and Additives Using the Quartz Crystal Microbalance and Oxygen Monitoring," Master's Thesis, University of Dayton, Dayton, OH, 1995.

(17) Heneghan, S. P., Zabarnick, S., Ballal, D. R., and Harrison III., W. E., "JP-8+100: The Development of High-Thermal-Stability Jet Fuel" *Trans. ASME J. Energy Res. Tech.* Vol. **118**,. 170, 1996

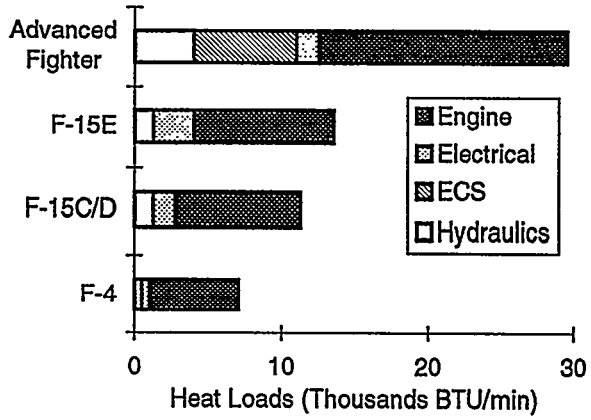
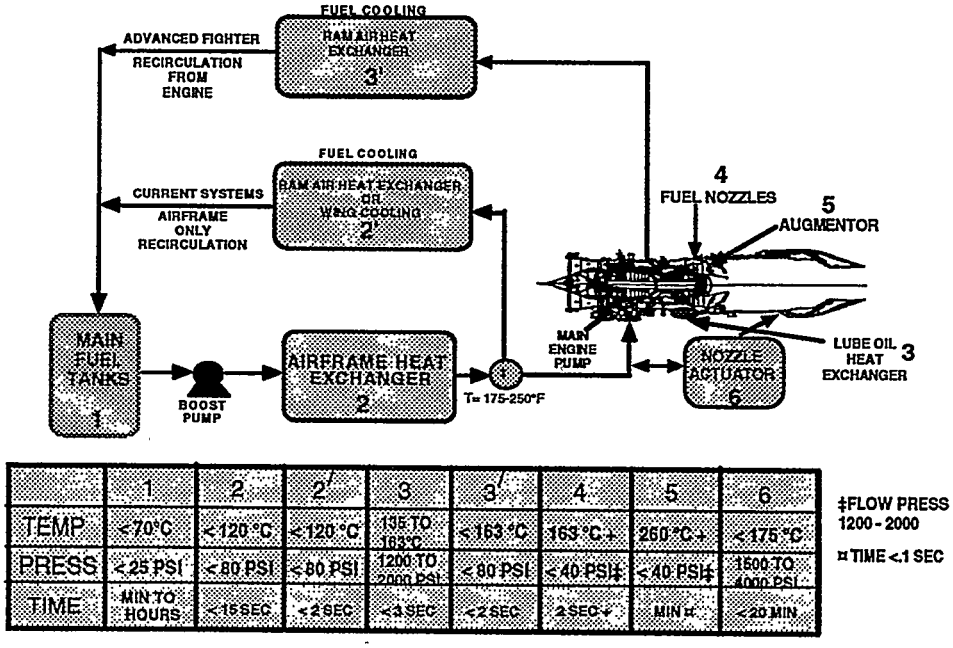


Figure 1: Maximum estimated excess heat loads for various aircraft.



	1	2	2'	3	3'	4	5	6
TEMP	<70°C	<120 °C	<120 °C	135 TO 163°C	<163 °C	163 °C +	260 °C +	<175 °C
PRESS	<25 PSI	<80 PSI	<80 PSI	1200 TO 2000 PSI	<80 PSI	<40 PSI‡	<40 PSI‡	1500 TO 4000 PSI
TIME	MIN TO HOURS	<15 SEC	<2 SEC	<3 SEC	<2 SEC	2 SEC +	MIN ¤	<20 MIN

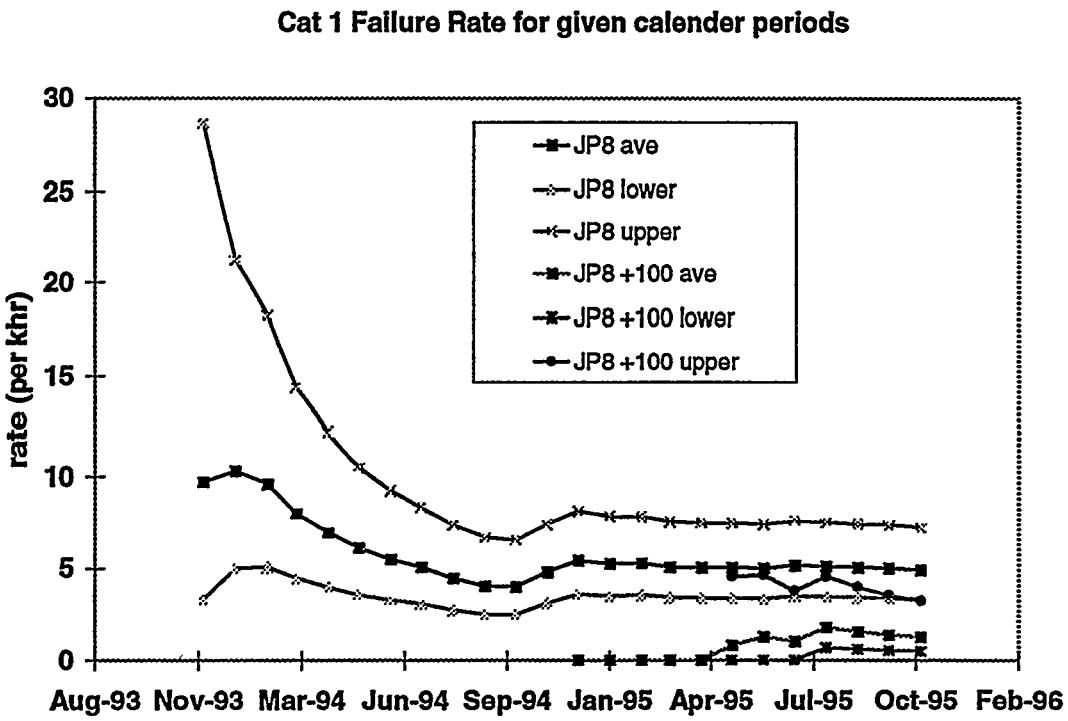


Figure 3: Mean rate of Category 1 failures with upper and lower bounds on the mean (2-sigma confidence limits) for JP8 and JP8+100 at Kingsley AFB.

6th International Conference
on Stability and Handling of Liquid Fuels
Vancouver, B. C., Canada
October 13-17, 1997

ADDITIVE STABILITY IN JP8 – METAL ALLOY SYSTEMS AT ELEVATED TEMPERATURES

Marlin D. Vangsness* and Shawn P. Heneghan

University of Dayton, 300 College Park, Dayton, OH 45469 - 0148, USA.

Abstract

We have developed a method to determine the concentration of the Betz/Dearborn 8Q462, know as SPEC-AID 8Q462, thermal stability additive in jet fuel samples. Betz 8Q405, the dispersant component, includes a proprietary amount of phosphorus. This technique utilizes the phosphorus content of Betz 8Q405 to estimate the concentration of the complete package in JP-8 +100. The precision depends on the availability of base fuel to correct for background and other matrix effects. If the base fuel is available the concentration can be measured with day to day or sample to sample variations less than 5%. Without the base fuel, but using a generic Jet-A or JP-8 as a standard, the sample to sample variations are within 17%. We have used this technique to study the effects of thermal aging in the presence of a variety of metallic materials. The change in additive concentration was studied over 28 day periods in three jet fuels, at 160F, 200F, and 350F, in the presence of Fe, Cu, Ni, Al and several stainless alloys. Preliminary results indicate that the concentration of BETZ 8Q405 remaining in solution is dependent on the storage temperature and type and condition of metal surfaces in contact with the fuel.

Introduction

For several years the US Air Force has been sponsoring research to improve the thermal stability of jet fuels. One additive in particular, SPEC-AID 8Q462, has shown promise in significantly reducing fuel deposits and increasing fuel thermal stability. Before complete field implementation of the new additives occur, the airframe/fuel system engineers need to be assured that the new additives are compatible with all existing and/or proposed materials. At a minimum, it is necessary to identify all adverse effects. As part of the overall approval process, the Air Force initiated research into fuel/material interactions. In this paper, we focus on the effect of the materials on the additive concentration, and the development of a simple laboratory technique to estimate the concentration of additive in jet fuels.

To accommodate large numbers of samples (literally hundreds of materials have been identified and several base fuels and temperatures are used) and to be of use in evaluating

unknown fuel additive concentrations, the analysis technique should have the following characteristics.

a. Minimal sample preparation

b. High sample throughput

c. Accurate analysis of field samples in the absence of base fuels for background correction

d. Environmentally benign (small sample size, minimal use of hazardous chemicals).

We have developed a technique using a Leeman Labs ICP-AES, (Inductively Coupled Plasma - Atomic Emission Spectrometer), to analyze fuels for phosphorus and scandium, Sc is used as an internal standard, to determine the concentration of BETZ 8Q405 in Jet-A or JP-8. We analyzed data obtained from ongoing fuel additive/material compatibility tests to describe additive stability during storage. These tests expose fuel system materials to neat fuel, normal additized fuel, and fuel additized at 4 times the normal concentration. The fuel soaked materials are stored at, 160F, 200F, and 325F for 4 weeks. Aged fuel is replaced each week and samples are analyzed from the first and last week. The fuel samples are analyzed for alloy metals and phosphorus while the metal test coupons are examined for evidence of corrosion. Smaller reductions in additive concentration on day 28 compared with day 7 are an indication of surface passivation. By analyzing alloy and additive concentrations from fuel/metal compatibility tests we hope to predict the interactions of additized fuel with the storage facilities and aircraft systems.

Fuels and Chemicals

Chemicals used in the analysis are listed in Table 1. Each day of testing, (40 to 50 samples), consumes 100 mg of 300 ppm S-21 , (S-21 is a Conostan calibration standard comprised of 21 elements in an oil base), 7 mg of 500 ppm Sc, 200 ml of Kerosene, and 7,000 – 9,000 L argon. Fuels were supplied by the US Air Force Fuels Branch (POSF) and are identified by a unique four-digit number. The fuel identifiers and origin are given in Table 2.

Instrumentation

A Leeman Labs ICP-AES is used to analyze test fuels for phosphorus and metallic corrosion products. This is an emission spectroscopy technique where the fuel sample is sprayed into an argon stream prior to its introduction into an argon plasma. Within the plasma the sample is completely disassociated into excited and ionized atoms. As the atoms regain their electrons

and return to ground energy states they emit light at characteristic wavelengths. This light is collected by the collection optics and dispersed onto the detector by a dispersing prism and an Echelle grating (a grating designed to operate at very high orders). Dispersing by color and order provides very high resolution along with excellent signal thru-put. With the exception of Sn, all of the metals in S-21 are detectable in kerosene at 50 ppb or less. Single point calibration at 1,500 ppb yields errors on the order of +/- 50 ppb for measurements in the 5,000 ppb range.

The plasma conditions used for phosphorus measurements:

Power	1.0 KW
Argon coolant flow	16 lpm
Auxiliary flow	1 lpm
Nebulizer (V grove)	34 psi
Sample	1.3 ml/min

Method

Phosphorus, a constituent of the Betz package, is normally found at very low concentrations in Jet-A fuels (typically less than 20 ppb). Since phosphorus can be detected by several techniques, its concentration is commonly used as an indicator of SPEC-AID 8Q462 concentration in JP8+100. The background signal produced by the bulk solvent and the solvent's effect on sample transport (termed matrix effects) along with lot to lot variation in additive production, limit the accuracy of additive concentration determinations. In order to base concentration determinations on a pure measurement, we chose to quantify phosphorus directly and apply our conversion assumptions to arrive at an estimate of SPEC-AID 8Q462 concentration. We analyzed a number of JP8 and JP8+100 samples taken from various AF bases for phosphorus content In order to test the usefulness of this method.

Initially kerosene was used for background measurements and dilution of calibration standards as it produces very little signal at wavelengths used for metal detection. A 300 ppm (each metal) standard of S-21 was diluted with Kerosene to 2 ppm, the high range expected for most dissolved metals. Measurements were taken on two different days on ten Jet-A fuel samples containing Betz additive. Two additional unadditized fuels along with three in-house additized fuels were also analyzed. Figure #1 displays the concentration of phosphorus, normalized by the average phosphorus concentration. The phosphorus content of the survey had a fuel to fuel standard deviation of 19% and 13% on the two test days with an average 6% standard deviation

in day to day measurements of the same fuel. Figure #2 shows the phosphorus content of 22 unadditized fuels taken from U.S. military bases throughout the United States and Europe. Clearly, an elevated level of phosphorus alone indicates the rough concentration of Betz 8Q405 where no other phosphorus containing additive is likely. However, the average phosphorus content measured was higher than the correct amount in a proper formulation. (The actual concentration constitutes proprietary information.)

A comparison of measured quantities of phosphorus in spiked samples of kerosene and Jet-A confirmed that some fuels delivered up to 60% more sample to the plasma than kerosene at the same sampling conditions. This was attributed to the different transport efficiency of kerosene as compared to JP8 or Jet-A. We then chose POSF-2926, (a particular Jet-A) as a background, or 'zero' standard, and to dilute the 300 ppm S-21 calibration standards to 1.5 ppm. Cobalt was added to each fuel sample at approximately 10 ppm to act as an internal standard for determining remaining transport effects. The percent recovery of Co indicated the net transport efficiency of the sample fuel compared with the standard fuel and was used to normalize the other metal concentrations.

Three fuel samples were prepared in the laboratory from Jet-A stock (POSF numbers 3250, 3272, and 3285). Each sample was mixed with the same amount of SPEC-AID 8Q462 and spiked with 100 µl of cobalt solution per 10 ml of sample. This produced three different Jet-A fuels with the same phosphorus concentration and 10 ppm Co. The samples were analyzed on Nov. 26 and 27 for P and Co. The phosphorus concentration was corrected by the percentage of Co recovered ($P_{measured}$ x $Sc_{spike}/Sc_{measured}$, see Figure #3) and normalized by the average phosphorus content. In addition to improving the day to day precision, the spike recovery (internal standard) technique helps to correct for sample transport property differences and environmental changes in the laboratory. While background differences (matrix effects) are still a problem whenever a neat fuel sample is not available for calibration, this method is sufficiently accurate to determine if a fuel has the Betz additive package in approximately the correct concentration.

Subsequent to this initial study we settled on the following method for metals and phosphorus measurements in standard fuel samples. Fresh standards are made up each day of 300 ppm calibration standard, S-21, diluted to 1 ppm with Jet-A (POSF 2926). For calibration, 20 ml of the 1 ppm S-21 in Jet-A is removed and spiked with 200 µl of 500 ppm Scandium (final

concentration of 5 ppm Sc). Scandium was chosen for its large signal to noise ratio at 361.384 nm, its absence of interference with our normal metallic measurements and its scarcity in common jet fuels. Phosphorus is determined by its peak at 213.618 nm. Fuel samples are prepared by spiking 10 ml of sample with 100 µl of the same 500 ppm Sc solution. By mixing calibration standards by weight and spiking both the cal standard and sample by volume we are able to quickly evaluate and correct for most sample delivery variations in the system. The Sc spike also functions as an internal check standard where less than 90% spike recovery indicates an equipment or optical alignment problem and these results are rejected. On Sept. 3, 1997, the three sample fuels were sampled and analyzed using Sc as the internal standard. The results show good agreement with previous determinations, Figure #3. Using spike recovery we measured phosphorus content with 7%-12% std. dev. across the well mixed fuel types on the same day while the std. dev. of measurements of the same fuels on 3 different days was only 2% - 4%. On Sept. 3, '97 another survey of JP8+100 fuels was taken. Figure #4 summarizes the phosphorus content (normalized by the average P concentration) using scandium as the internal standard. In this case the average P concentration agreed with the predicted value while the standard deviation of results across all fuels remained at 0.17%. The remaining scatter is a result of possible mixing variations and uncorrected background noise.

Material Compatibility Fuel Test Results

Metal coupons, 1" x 2" x 0.06", were soaked in fuel at 160F, 200F, or 325F for 28 days with weekly fuel changes. SPEC-AID 8Q462, was added to the base fuel in both the normal (1X) concentration and in 4 times the normal concentration (4X). One JP8 base fuel was used for all of the tests reported here. At the end of 28 days the metals were examined for evidence of corrosion and weight change to indicate a pass or fail. Fuel samples taken during the test were analyzed for alloy components to correlate with corrosion evidence and, phosphorus was measured to track changes in the 8Q405 concentration.

In broad metallic categories, the amount of phosphorus (detergent component of the Betz package) remaining in solution after the first and last 7-day test segment is shown in Tables 3 and 4. The values reported represent averages over several alloys in each classification. Data on all alloys at all temperatures does not exist for this study since many materials were not tested at 160 F and a considerable number of alloys had been evaluated before the arrival of our ICP.

The most obvious trend is for higher phosphorus retention at lower temperatures. While copper appears to affect the phosphorus level the least, it also shows the highest dissolved metal content of any of these test metals. Copper concentrations, (though not reported here, 15 metals are quantified sequentially on each sample), indicate that much of the phosphorus measured is active in keeping copper in solution and may not be free to aid in dispersing additional material. Iron also appears in higher concentrations in tests of iron and stainless alloys when Betz is present to aid in keeping it in solution. Aluminum is known to have a surface affinity for phosphorus and since we do not see Al in measurable quantities in solution we believe the dispersant is binding to the surface. When we analyze the fuel from tests on predominantly nickel alloys we do not see any metals in measurable quantities and would expect to find the missing dispersant on the alloy surface.

Conclusions

ICP-AES measurement of phosphorus content in jet fuels can provide a good indication of SPEC-AID 8Q462 additive concentration. Analysis of jet fuel field samples can be done without a true blank, however matrix effects can contribute more than 20% to measurement errors. The uniform addition of Scandium to calibration standards and to samples is a simple way to measure fuel to fuel variations in sample delivery efficiency and to monitor system performance. Preliminary results indicate that for fuel systems at elevated temperatures, Iron and Aluminum alloys have a significant effect on additive concentration, while alloys with high Nickel content have a minimum effect on Betz 8Q405.

Acknowledgement

This research was supported by the U.S. Air Force Wright Laboratory, Aero Propulsion and Power Directorate, Wright-Patterson Air Force Base, OH, under contract No. F33615-92-C-2207. Mr. C. W. Frayne was the technical contract monitor.

Table 1: Chemicals – Sources and Uses in this Study

Kerosene	Fisher Scientific	Used to dilute 5000 ppm Sc standard to 300 ppm, also used as rinse fluid in ICP sample path.
Argon (liquefied)	Air Products	Primary constituent of the plasma 'flame' and carrier for sample mist.
S-21	Conostan	Calibration standard containing 21 common metals at a concentration of 300 ppm by weight in oil matrix.
Sc	Conostan	Calibration standard containing 5000 ppm by weight of Scandium in oil matrix.
Co	Conostan	Calibration standard containing 5000 ppm by weight of cobalt in oil matrix.
Cobalt Solution	Locally Prepared	Internal Standard: 1Part cobalt Conostan standard, 10 parts Kerosene - nominally 500 ppm
Scandium Solution	Locally Prepared	Internal Standard: 1Part scandium Conostan standard, 10 parts kerosene - nominally 500 ppm

Table 2: Fuel Type and Origin

POSF #	Fuel	Date Rec.	Loc.
2827	Jet A	5/16/91	OH
2890	JPTS	11/12/91	OH
2926	Jet A	5/21/92	OH
2928	Jet A	6/4/92	OH
2934	Jet 50	9/21/92	AK
2962	JP-5	6/1/93	**
2976	JPTS	5/1/93	OH
2980	Jet A	6/1/93	**
3000	JP-5	9/1/93	TX
3049	JP-8	3/1/94	Greece
3082	JP-5	12/1/94	NY
3083	JP-8	12/1/94	HI

POSF #	Fuel	Date Rec.	Loc.
3102	JP-5	12/1/94	HI
3109	JP-8	12/1/94	VT
3110	JP-8	12/1/94	DE
3118	JPTS	12/1/94	**
3119	Jet A	2/1/95	OH
3166	Jet A	1/1/96	OH
3285	JP-8	7/1/96	TX
3325	JP-8	11/19/96	NM
3334	JP-8	1/7/97	MD
3389	JP-8	4/9/97	CA
3396	JP-8	4/21/97	CA
3413	Jet A	6/1/97	IL
3419	JP-8	6/6/97	NM

JP-8 +SPEC-AID 8Q462

POSF #	Date	Loc.
3060	5/1/94	TX
3229	2/23/96	VT
3233	2/25/96	MD
3250	5/1/96	OH
3261	5/1/96	KY
3272	6/1/96	OH
3273	6/1/96	OH
3286	7/1/96	TX
3289	7/1/96	OH
3295	8/1/96	OH

POSF #	Date	Loc.
3323	11/1/96	NM
3326	11/20/96	NM
3329	1/7/97	MD
3352	12/11/96	NM
3397	4/1/97	CA
3400	4/1/97	CA
3401	4/1/97	CA
3420	6/1/97	NM
3428	7/1/97	OH
3430	7/1/97	TX

Table 3: Phosphorus Remaining of 1X Betz Concentration

	325F		200F		160F	
	Day 7	Day 28	Day 7	Day 28	Day 7	Day 28
Aluminum	60%	40%	**	70%	**	**
Copper	80%	**	80%	80%	90%	70%
Iron	50%	60%	**	**	**	**
Nickel	60%	**	**	90%	**	**
Stainless	40%	60%	70%	90%	**	**

Table 4: Phosphorus Remaining of 4X Betz Concentration

	325F		200F		160F	
	Day 7	Day 28	Day 7	Day 28	Day 7	Day 28
Aluminum	70%	**	75%	66%	**	**
Copper	83%	**	88%	98%	100%	**
Iron	58%	100%	**	**	**	**
Nickel	79%	100%	**	**	**	**
Stainless	50 - 84%	66 - 100%	68 - 75%	100%	**	**

** Data unavailable.

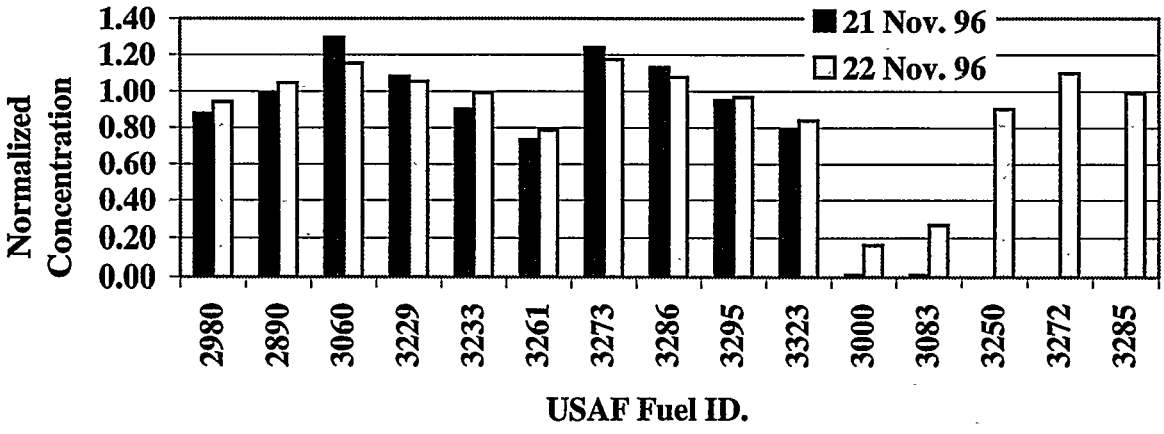


Figure 1: Normalized phosphorus content in Table #2 fuels.

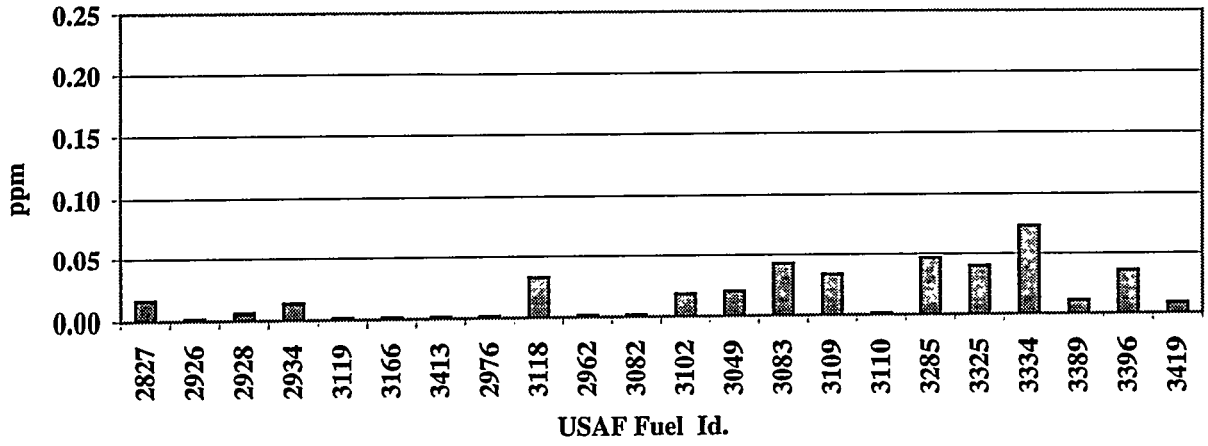


Figure 2: Phosphorus content of un-additized world survey fuels in Table #2.

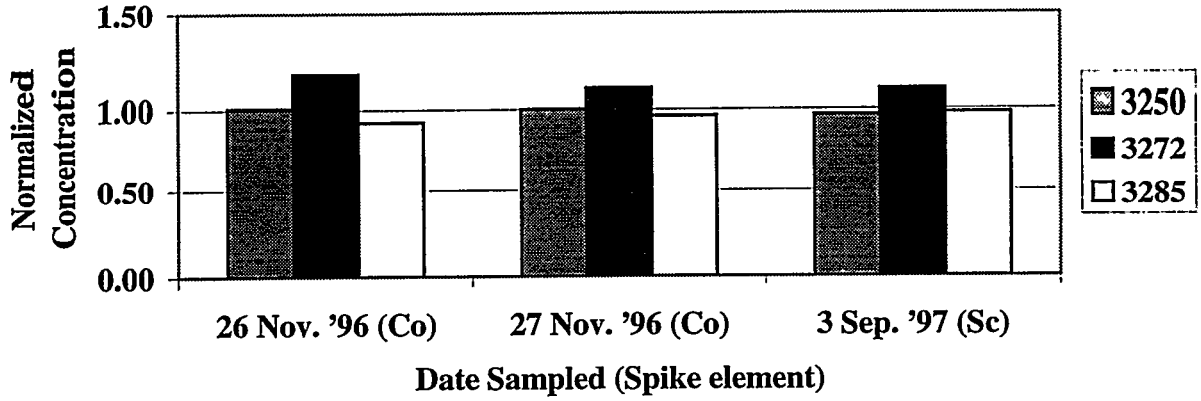


Figure 3: Normalized phosphorus content of laboratory additized fuels.

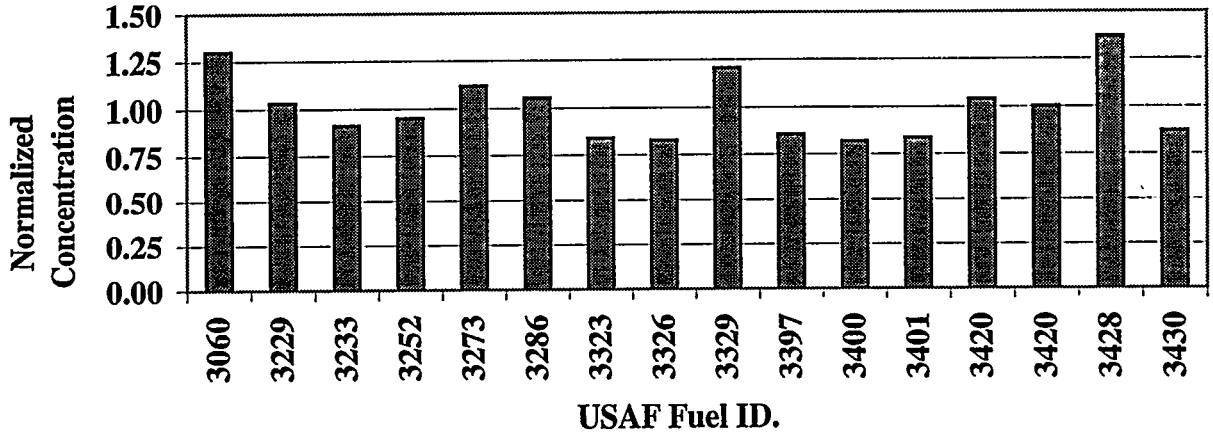


Figure 4: Normalized phosphorus content of Table #2 fuels containing SPEC-AID 8Q462.

6th International Conference
on Stability and Handling of Liquid Fuels
Vancouver, B.C. Canada
October 13-17, 1997

HIGH REYNOLDS NUMBER THERMAL STABILITY (HiReTS) RIG FOR REALISTIC, RAPID EVALUATION OF DISTILLATE FUEL THERMAL OXIDATIVE STABILITY

Joanna M. Bauldreay*, Richard J. Heins, Geoffrey Houlbrook, and Johanne Smith

Shell Research & Technology Centre, Thornton, P.O. Box 1, Chester, CH1 3SH, UK.

Shell Research Limited have developed a small-scale rig to evaluate jet fuel thermal stability under realistic test conditions. Pre-production prototypes of the HiReTS (High Reynolds number Thermal Stability) rig, known during its laboratory history as the Capillary JFTOT (C-JFTOT), have now been produced. Fuel passes through a stainless steel capillary tube at flow rates sufficient to ensure that turbulent conditions prevail. The tube is electrically heated and PC control ensures a fixed fuel outlet temperature. More power must be provided to maintain the fuel outlet temperature when deposits build up on the inner capillary surface. A non-invasive infrared thermometer monitors the tube outer surface during the, typically, two hour test. The more deposit produced, the higher the temperatures rise. The end-of-test result is the HiReTS or C-JFTOT number, the summation of final temperature rises at set scanning positions. C-JFTOT numbers have correlated well both with post-test carbon burnoff values and with results from large-scale rigs. 3-D displays of temperature changes provide dramatic pictures of temporal and positional differences in fuels' deposit-forming tendencies. HiReTS numbers for hydroprocessed fuels are up to an order of magnitude lower than those for specification-passing Merox fuels. Standard operating conditions were chosen to identify poor fuels, and differentiate between typical commercial fuels. Thermal stability improving additives can significantly lower HiReTS numbers and different flow/temperature/time conditions may be needed for the HiReTS to differentiate between high thermal stability fuels rather than to reject poor fuels. USAF are now evaluating a pre-production HiReTS machine, both as a possible specification test and as a research tool.

INTRODUCTION

The JFTOT uses 600 mL of fuel per 2.5 hour test[1] to assess thermal stability properties. Jet fuels with poor thermal stability produce heavily lacquered test pieces and/or bulk insolubles that tend to block the filter downstream of the heated test piece. Features such as short test time, small sample size and ease of operation make the method acceptable for the routine qualification of fuels. However, the JFTOT, its variants and most small-scale rigs operate in the unrealistic laminar flow regime. Various studies have highlighted this and other limitations of the JFTOT including tube rating technique and the test heater metallurgy[2,3]. Operating under laminar flow conditions means that the JFTOT will always be sensitive to reactant mass transport effects[4]; it will suffer from the dominance of mass-transfer limitations on deposition, particularly for fuels of low radical initiation rate.

By contrast, large-scale rigs such as Thornton's Single-Tube Heat Transfer Rig (STHTR)[2], Mini-Injector Feed-Arm Rig (MIFAR)[5] and, formerly, Injector Feed-Arm Rig (IFAR)[6] require a specialist trained operator but provide realistic simulations of aircraft fuel

systems. The STHTR test piece derives from a component of a fuel-cooled oil-cooler; the method monitors the loss of heat transfer efficiency, ΔHTC, as deposits build up on the test piece walls. Unfortunately, most large-scale rigs, whilst operating in (realistic) turbulent flow regimes, have large fuel appetites and long test durations; for the STHTR these would typically be 2000 litres and 100 hours, respectively. Such rigs tend to be "one-offs", totally unsuited for incorporation in jet fuel specifications.

This unsatisfactory position was the starting point for the current research, i.e. the designing of a small-scale rig using conveniently small samples, offering an accelerated test and yet incorporating the turbulent flow present in an aircraft fuel system. Initially, Kendall[7] examined the possibility of achieving a turbulent flow tester by modification of the JFTOT tube. His fluid dynamics calculations showed that the Reynold's number, R_e, for the JFTOT system under normal operations is about 11[8], assuming a bulk flow temperature of 170°C. This is clearly in the laminar flow regime since the minimum R_e for turbulent flow is about 5,000. Kendall concluded that, even by altering gap sizes, it would be impossible to achieve high enough R_e in a JFTOT for there to be turbulent flow. He then considered the design criteria for a capillary test section that would produce turbulent flow conditions. These covered: flowrate/diameter combinations necessary to achieve R_e of about 5,000; estimates of the pressure drop within the test region; consequences of different diameter/length combinations; impact of capillary size/test regimes on the feasibility of measuring the resultant deposition. These estimates indicated that a large diameter capillary was required to: minimise the pressure drop; prevent blockage; ensure an adequate area for sufficient deposits to be generated for burn-off. However, these factors tended to conflict with the desire to use small flowrates and hence a small sample size. Also a larger capillary would make it more difficult to resolve small changes in heat-transfer data. The calculations favoured the use of a short capillary to enable a high wall temperature (300°C minimum, to produce higher levels of deposit) to be used in conjunction with a moderate, i.e. realistic, fuel temperature. Heat-transfer data are also seen as a route to measuring the degree of fuel degradation, i.e. the build-up of an insulating layer of lacquer will result in a rise in metal wall temperature.

Kendall's work provided the starting point for the development of a radically different small-scale tester, known during development stages as the Capillary JFTOT (C-JFTOT) and now, at pre-production prototype stage, as the High Reynolds number Thermal Stability (HiReTS) rig. The development work on the rigs, including preliminary statistical analyses and correlations with results from other thermal stability tests, form the bulk of this report.

APPARATUS DEVELOPMENT

Overview. Early work concentrated on forming deposits under realistic conditions and detecting them properly; a prerequisite was that the device should distinguish between fuels of very different thermal stability. From the outset of the programme Shell aimed to assess

deposition by monitoring the rise in tube outer wall (TOW) temperature as this method would not require any further equipment to analyse deposits. Early design work focused on the capillary test section; specifically, how to obtain the required fuel flow, the most efficient method of heating the capillary, how to control the test temperature and, not least, the best method of quantifying fuel stability. In Phase 1 of the development, the basic kit was assembled: a fuel supply system, a test piece, deposition monitoring facilities, and a test control system. Capillary diameters and lengths were varied to achieve suitable fuel outlet temperatures. During Phase 2, deposit monitoring methods were changed and developed. Some experiments were performed with a differential pressure transducer fitted across the test section. Correlations were used to check whether the C-JFTOT results bore any relationship to test data from other, particularly large turbulent flow, rigs. By the start of Phase 3 (mid-1991), a novel small-scale tester had been produced that was able to monitor fuel degradation and subsequently rank fuels. The basic operating conditions in the C-JFTOT device had been established: tests were set to run at a fuel outlet temperature of 290°C for 2 hours. The software and deposition monitoring protocols were optimised for these conditions. Work then concentrated more on automation of the system, removing its dependence on expensive and specialist external equipment, introducing more safety trips and cut-outs, and thereby making it more acceptable as a potential specification test. Fuels used in these early studies are detailed in Table 1; all were produced as Jet A-1.

A final phase of tests were run under "standard" conditions to generate a limited results database. Phase 4 used a different suite of (newer) Jet A-1 and related fuels: seven, some with additives, were derived from Merox treatment (from at least 3 locations); two were straight run; two were hydroprocessed (one with additives); a poor thermal stability JP-5 fuel ex US Navy (unknown processing); and there were 7 fuels containing 15 to 100% of Shell Middle Distillate Synthesis kerosine blended with conventional jet fuels or blending components. After further correlation and crude statistical exercises, these design and operation features were adopted as the base of a pre-production model, the HiReTS. The following sections summarise the evolution of certain components, through various stages, to the final configurations used in the C-JFTOT and HiReTS devices.

Fuel supply. Initially fuel was delivered to the capillary test section by using a pressurised reservoir that attached to a JFTOT apparatus. This was soon superseded by the use of a Gilson variable flow HPLC pump capable of delivering up to 50 mL/min at up to 2000 psi. Pulsations in flow were largely damped out by fitting a small accumulator immediately downstream of the pump. System pressure during a test was set to approximately 400 psi using an in-line relief valve downstream of the cooler. An adjustable over-pressure cut-out was incorporated to stop the pump should pressure exceed a preset value, 1000 psi. A high pressure water-cooled fuel-cooler was fitted downstream of the capillary test section to

reduce the spent fuel temperature to ambient before the fuel went to waste at atmospheric pressure, thus preventing boiling.

Initially it was hoped to measure any build-up of deposits on a downstream test filter, much as is achieved by pressure drop (ΔP) measurements in the JFTOT. A differential pressure transducer was fitted, to measure ΔP across the test section. Unfortunately, it offered an easier electrical path than the capillary. When the transducer was insulated with high pressure Teflon tubing the bore was so narrow that the device had no sensitivity. Transducer and ΔP approach were rapidly dropped from the system.

Test Piece. Feasibility experiments used capillary tubing with outer and inner diameters (O.D and I.D) of 560 and 254μm, respectively. This was soon superseded with more robust commercially available 254 μm stainless steel capillary, with 1.59 mm O.D. Originally these capillary sections had sleeves silver-soldered to each end (to provide a large contact area for the electrical bus bars) and thermocouples spot welded at various points along the available test lengths. Thermocouples were abandoned when IR thermometry and carbon-burnoff approaches to deposit detection were introduced. Instead, test pieces were painted black to achieve better and uniform thermal emissivity.

Heating control. From the outset the capillary test section was heated electrically by applying power to bus bars that held the test section in place. Initially the operator adjusted the power of a simple transformer to produce a given initial tube outer wall (TOW) temperature at a given thermocouple on the test piece. A series of experiments were performed with 15 and 20 cm tubes, varying flow rates for different target TOW temperatures and measuring associated power, fuel outlet temperatures and capillary inlet pressures. 35 mL/minute, creating $R_e >> 10{,}000$ at the hottest part of the tube, produced the highest fuel outlet temperature for a given initial TOW temperature and was chosen as the "standard" flow condition. An off-grade Merox fuel W (see Table 1) was used in the capillary and fouling was monitored by pressure drop across the capillary and the rise in wall temperature for a constant fuel outlet condition. In the 6 hour test, ΔP was only 60 psi but the wall temperature rose by about 120°C. Tests with fuel W and with a very stable hydrotreated fuel, Y, soon showed that the intrinsic repeatability of this approach was poor.

The "start of test condition" was then redefined in terms of a fuel outlet temperature (FOT). Power was supplied to the bus bars until the capillary exit thermocouple reached a setpoint FOT. Initially, a 260°C FOT condition was used but 290°C produced more deposits. A Eurotherm 815 programmable temperature controller was introduced to automate this heating and was operated as a stand alone unit. Later, the controller was switched to operate in "Remote" mode from a PC which supplied the setpoint.

Deposition Monitoring. Earliest experiments used thermocouples to monitor deposits, much as was done for test sections in larger rigs (STHTR, MIFAR, etc.). Despite some promising results with a poor fuel, the approach had poor repeatability and was unable to

distinguish between very different stability fuels W and Y. The thermocouples may have been distorting the capillary cross-section and acting as a considerable heat drain on the system because of their relatively high masses compared to that of the capillary tube.

The second phase of work introduced a novel, non-invasive approach to temperature detection, infrared thermometry. A separate rig was also constructed to measure the low levels of carbon on the test pieces, representing 70-80% of the lacquers produced at such temperatures. Post-test, the test pieces were placed in the rig and the carbon was burned off and measured (10-200 μg) in a controlled fashion; see details later.

An Ircon Ltd infrared thermometer was attached to a data logger, aligned on the test piece and used to record TOW temperatures at a single position. The IR system showed excellent repeatability in measured TOW temperature but no variation in results between fuels W and Y. However, end-of-test carbon deposit measurements indicated that a difference was present. Raising the fuel outlet temperature from 260 to 290°C produced a 100°C difference in TOW temperature between two fuels after two hours which was in accord with differences in post-test carbon deposit weights. These results suggested that rises in outer wall temperature during the test, caused by the need to apply more power to maintain the fuel outlet temperature as deposits built up inside the capillary and changed thermal resistance, could be used to monitor the increasing impact of fuel degradation with time. The differing gradients for these very different thermal stability fuels demonstrated an ability to distinguish and rank fuels. Further tests identified the position of maximum deposit formation along the test piece, 10 mm below the top bus bar (fuel exit point), and examined how sample pretreatment affected the levels of deposition. The pretreatment had no significant effect but these tests once again showed poor correlation between temperature changes and carbon measurements. These difficulties led to a period when "off-line", end-of-test carbon determination was used as the primary measure of deposition though "on-line" temperatures were still recorded.

Early assessments. A limited set of correlations were attempted between the average carbon burn-off values for the C-JFTOT at 290°C and other thermal stability predictors such as JFTOT variants (Carbon burnoff value, CBO, and JFTOT breakpoint), the radical initiation rate, R_i, (from the Thornton flask oxidation test[9]), fuel total sulphur content and data from large-scale rigs. The CBO value is the amount of carbon burnt off a tube tested at 350°C in a modified JFTOT apparatus, and the JFTOT breakpoint is the highest temperature at which the fuel still passes the visual tube rating (VTR) requirements of the JFTOT test. Table 1 lists data used in a STATGRAF linear regressions analysis program.

Figure 2 summarises data from the correlation of ΔHTC results from the STHTR with C-JFTOT carbon data. Neglecting intercept and gradient errors, the related fit using carbon burnoff values obtained after a 350°C test using a conventional JFTOT was: $Log_{10}(HTC) = 1.31*Log_{10}(CBO) - 2.49$, with 99.49% correlation confidence, F value 15.78 and R^2 =

0.6636. While a significant correlation clearly existed between STHTR and C-JFTOT, the C-JFTOT parameter was no better than other more traditional predictors of rig performance. A possible explanation was that the 290°C condition was too accelerated and may not have been reflecting reactions dominating under more realistic (lower temperature) conditions. Repeating the exercise at 260°C did not improve the correlation with STHTR. On the other hand, the C-JFTOT data correlated well with radical initiation rates measured in the flask oxidation test[10] i.e., the C-JFTOT responded to fuel chemistry (radical initiation) rather than mass transport effects. The STHTR response, which might have been expected to be similar, was probably reflecting the stages of pre-heating which simulate wing-tank heating (low grade but long residence time). The conventional JFTOT's moderate ability to predict STHTR performance may have been because the stagnant layer in the JFTOT's laminar system could be considered as equivalent to pre-heating the fuel.

A limited series of tests investigated the impact of sample preheating in the C-JFTOT. An "Off-the-shelf" Alcor heated reservoir was modified to tolerate the high pressures in the rig. Its capacity allowed a preheating residence time of 30 minutes. Correlations did not improve so the preheater was removed. Better simulation of the complex heat history of fuel in the STHTR, either by increasing the severity of preheat or by increasing the residence time, was not a viable option at that stage either because of safety reasons or the need to commission more new equipment.

Earlier work had already shown that Ri was a modest predictor of performance in the MIFAR, a rig usually run without tank heating[5]. The C-JFTOT was used to test a further five fuels all previously tested in the MIFAR. Ten fuels with MIFAR data (see Table 1) were then used in a second set of correlations. Figure 3 shows that the C-JFTOT was a better predictor of MIFAR than it had been of STHTR. The correlation results in Table 2 also showed that C-JFTOT was marginally better than the conventional JFTOT (breakpoint or carbon burnoff mode) in predicting MIFAR performance. By this stage the feasibility of the C-JFTOT technique had been demonstrated. However, the labour and skill levels required, combined with the use of external equipment to make the carbon measurements, made impossible its use as a specification test in that configuration.

Earlier single point IR thermometry had probably failed because of fuel-to-fuel variations in the position of the thickest point of lacquer on the capillary. (Sectioning of test pieces from other rigs - JFTOT, STHTR and MIFAR - has also shown that lacquer patterns are fuel-dependent.) Choosing a single point for temperature determinations without being able to see the inside of the rig was, at best, an optimistic approach. Now scanning was tried. Two-hour tests were performed with a fuel outlet temperature of 290°C, manually adjusting the detector position throughout the test. Temperature changes (T_{final} - $T_{initial}$) were much larger for poor thermal stability fuels (high carbon burnoff) than for high stability fuels (very low carbon burnoff). Temperature profiling at six positions along the test piece provided

good measures of the amounts of deposit produced by three fuels of significantly different thermal stability. These fuels produced completely different amounts and patterns of lacquering. Summing end-of-test temperature change values along the tube length ($\Sigma\Delta T$) produced a number with which to rank the fuels:

Hydrocrackate	ranking number 7.25	±25%
Merox AD	ranking number 475	±7.5%
Merox S	ranking number 745	±3%

These numbers showed good repeatability and correlated well with the total mass of carbon deposited. Additionally, the pattern of fouling as time proceeded at any given position closely followed that seen in the MIFAR and other large-scale simulators, i.e. an induction period followed by constant deposition[5,6].

A PC was introduced to operate a mechanical scanner, collect and process the data, allowing the instrument to become "stand alone" and removing the need for "off-line" measurements of carbon weight. Scanning was fine-tuned. Standard conditions were chosen to provide adequate resolution in time and space in areas where there was significant deposition yet minimal distortion caused by heat drain from the upper bus bar. The change in outer wall temperature was an indication of the thermal resistance at that point and thus a representation of the lacquer thickness. Software was written to allow data to be captured continuously into an ASCII file for downloading into a spreadsheet at the end-of-test. The spreadsheet was set up to make an automatic search for the minimum recorded temperature at each position x, $T_{min}(x)$, which was not necessarily the first temperature recorded (see later). It then provided a 3-D display of a measure of deposition against position and time, and a numerical test result, the Capillary JFTOT number. This was the summation of the increase in surface temperature of the capillary at the n points of temperature recording (x =1 to n), on the last scan:

$$\text{C- JFTOT number} = \text{CJ\#} = \sum_{x=1}^{n} \Delta T(x), \text{ where } \Delta T(x) = T_{final}(x) - T_{min}(x).$$

The C-JFTOT apparatus developed by this stage was as shown in Figure 1. The following sections describe the experimental conditions used with it in Phase 4 testing and the results obtained.

EXPERIMENTAL

Test pieces. The test capillary consists of a commercially available[11] 152 mm length of HPLC stainless steel tube, with nominal 0.01" (254 μm) inner and 0.0625" (1.59 mm) outer diameters, respectively. To improve thermal emissivity for IR measurements the tubes are painted with two coats of high temperature matt black paint; spraying the capillary clamped stationary appears to give a consistent finish. Two commercially available paints, Rustolian B-B-Q Black and Wurth, have been used; the latter can degrade at high capillary temperatures.

The 20mm end sections, where the capillary is clamped in the bus bars, are masked off during this process. A batch of tubes are prepared in advance and then stored until needed. The capillaries are inspected prior to use for paint integrity and tube straightness. A "Swagelock" nut is then pre-swaged onto each end. The finished tubes are not cleaned with solvent but are flushed with test fluid prior to the main test.

Fuels. Fuels used in early development work are listed in Table 1. Phase 4 fuels were used to test the C-JFTOT in its "final" laboratory configuration. The first of these were chosen to cover a broad range of thermal stabilities; many were chosen because they already had full suites of analytical and test rig data, thus anticipating future correlation and checking exercises. Fuels with MDA, CI/LI or JP-8+100-type additives did not start to be tested until early 1995.

Most fuels are now routinely tested in the HiReTS unit, to establish a results database, irrespective of whether large rigs are run in parallel. Fuel for testing is sampled according to normal jet fuel testing protocols. About 5 litres are put into a clean stainless steel container, ready for testing. No pre-filtration is performed but the fuel passes through the HPLC pump's inlet sintered filter (20 μm pososity).

Test protocol. Figure 1 illustrates the complete C-JFTOT system. The test piece is electrically heated via bus bars, and fuel is passed through it via a 2000 psi HPLC pump. A dedicated IBM PS/2 40 controls the heating (via the Eurotherm unit) and temperature measurement protocols. It is interfaced to a "Time and Precision" stepper motor screw jack system to control the vertical tracking of the IR thermometer which records capillary wall temperatures at set positions and times. At the completion of the test, which is deemed to be the point at which the IR scanner returns to its start position following the recording of the final temperature on the last scan, power is switched off to the bus bars and the capillary is allowed to cool. Fuel flow is maintained until the fuel outlet thermocouple indicates the fuel temperature has fallen to 30°C or less. At this stage the HPLC pump is stopped and the disassembly of the test section can take place after a heptane flush. Post-test the data are presented in tabular and graphical formats using proforma spreadsheets. The C-JFTOT number is automatically calculated from these data. Most fuels are tested twice and the average C-JFTOT number is quoted.

The standard test protocol measures capillary wall temperatures every five minutes at 2.5 mm intervals 1 to 21 mm from the fuel outlet, for two hours. These nine positions are along the hotter section of the test piece. The fuel flow rate is 35 mL/minute; with pre-flushing and post-test cooling this means that the test requires just under 5 L of fuel.

Safety Features. High pressures and elevated temperatures have demanded that the machine has numerous safety cut-outs. Both in the final C-JFTOT and now in the HiReTS rigs, any safety trip operation stops heating to the capillary; fuel flow, etc. are continued until the conditions become safe. Almost all the HiReTS's safety features are under PC control.

Carbon burnoff. Post-test carbon burnoff values are usually established and also averaged. Pre-test cleaning and post-test rinsing of the capillary test piece are controlled to optimise the carbon burnoff method's sensitivity. The fuel inlet end of the used test capillary is connected to a low pressure oxygen (0.2 bar) supply, and the outlet is connected to a tube fed into the furnace of a Leco carbon analyser. The capillary, clamped between two electrical bus bars, is heated while oxygen is passed through it and the carbon dioxide evolved is measured. The amount of carbon in the deposit can then be calculated.

RESULTS

Spreadsheet statistical packages have been used to analyse most Phase 4 results. C-JFTOT method repeatability itself has yet to be formally assessed but there seems to be an increase (worsening) in test repeatability as the fuel quality worsens. Figure 4 shows how average CJ# varies with average post-test carbon burn-off values. In all cases, the carbon and C-JFTOT results for the best fuels are at the limit of detection, and at the other extreme, the limited results for poor fuels may have an undue influence on the plots. When only non-additivated fuels (i.e. no metal deactivator, no corrosion inhibitor/lubricity improver or JP8+100 additive) are included, the fit improves slightly ($R^2 = 0.90518$). Similar plots for the non-averaged results still give quite reasonable regression coefficients for rig data, $R^2 > 0.8$. The corresponding results for additivated fuels alone are not included as the dataset is not large enough and the whole question of testing additivated fuels needs more consideration (see below). Nevertheless, the above correlations between CJ# and carbon weight are good enough to rely on CJ# alone when seeking correlations with other rigs, i.e. when establishing the predictive capabilities of the C-JFTOT.

JFTOT and variants. C-JFTOT and JFTOT-type tests should not be expected to correlate very well with one another or to provide similar predictions of larger rig performances because they examine fuels under different flow, temperature and metallurgy regimes. The C-JFTOT's acceptance as a candidate specification test, however, demands that the two approaches be compared. Figure 5 shows how average C-JFTOT results compare with the VTR in the standard, 260°C JFTOT test, for all Phase 4 fuels. There is a directional link between the two sets of results, albeit that the datasets do not include many poor fuels. Only one fails the existing 260°C pass with the JFTOT, which requires a non-peacock, non-abnormal VTR less than 3. A CJ# of about 1000 provides almost the same cut-off as the standard JFTOT test.

JFTOT breakpoint is established to within 5°C and therefore provides a statistic more amenable to correlation exercises than does the standard JFTOT result. However, the step size means that a very good correlation between JFTOT breakpoint and any other measurement is unlikely. Figure 6 again shows a correlation limited by the shortage of bad fuels. Whether for all the fuels or just those without additives, fits between breakpoint and

CJ# are poor, with $R^2 = 0.3288$ and $F = 9.3$ for the full set. (The F-test is more appropriate than R^2 for non-linear data.) These data were also transformed to give plots of a) Log_eCJ# versus 1000/BP (in K) and b) 1000/BP (in K) versus CJ#. Of the three plots, 1000/BP versus CJ# gives the best correlation figure - $R^2 = 0.3819$ and $F = 11.7$ - but none provide convincing evidence for a good linear correlation.

Looking at Figures 6 and allowing for the scatter of the data, however, there appears to be some non-linear relationship between the two parameters. Since all fuels on or above the line at 260°C would pass the standard JFTOT test, the assumption that 1000 provides a reasonable pass/fail criterion still seems reasonable. (The 260°C JFTOT pass level has, historically, prevented obviously bad fuels being accepted despite the method's shortcomings, so this link-in has some justification.) Fuels which are destined to reach this level will have significant and measurable levels of deposits long before the end of the "standard" two hour test. Assuming that there is not much of an induction period before deposits build up, this suggests that a pass/fail specification test could be considerably shorter than the existing two hours and therefore require less fuel.

On the other hand Figure 6 also suggests that the C-JFTOT test may not discriminate adequately between very good fuels (say, breakpoints > 290°C). This was not, of course, what the C-JFTOT's standard operating conditions were chosen to achieve and does not mean that the apparatus cannot distinguish between very high thermal stability fuels. All that is required is a different set of operating conditions.

CBO experiments involve running a JFTOT test at 350°C and then measuring the amount of deposit created in terms of the weight of carbon that burns off. The condition is severe enough that practically all fuels produce deposit. Data are not shown here but there is not a straightforward relationship between CBO and the C-JFTOT results, either for the full set of fuels or for the fuels without additives.

Large scale rigs. Early correlations had suggested that the C-JFTOT was a good predictor of MIFAR performance. With a fuel appetite of at least 2000 litres, the MIFAR is not, however, used routinely for all fuels. The correlation between MIFAR and CJ# for just four fuels was good, as shown by Figure 7 which includes a regression line fitted to the points (R=0.9994). No very unstable fuels have been included; one could have been produced by deliberate doping of a good fuel but this approach might produce a systematic bias in the results. Figure 7 also shows results for a fifth fuel. Initially this Merox fuel had appeared too good for the ranking exercise - it had the same 290°C breakpoint as another Merox fuel already tested - but all the rig tests (STHTR, MIFAR and C-JFTOT) have shown it to be noticeably worse when tested under more realistic conditions. The two Merox fuels with the same breakpoint are shown. Including the fifth point in the regression fit decreases R slightly but the result remains very good compared with those for other correlation exercises, and is

better than seen for the earlier Log(MIFAR) versus Log(C-JFTOT by carbon) fit listed in Table 2.

In the STHTR the loss of heat transfer efficiency per hour, ΔHTC, is measured at one or more fuel outlet temperature once steady conditions have been achieved. The one FOT always used is 225°C. When there is sufficient fuel, multiple measurements are made and results are fitted to a pseudo-Arrhenius model; this then allows a "best fit" ΔHTC value at 225 °C to be quoted. The actual (raw) and best fit (where available) results at 225°C are plotted against CJ# in Figure 8. Except at lower CJ# values, where results from both methods relate to very low deposit levels, there is some relationship between the two measurements. Figure 9 provides a log-log display of the same data, and includes the best fit to Log(best fit data) and Log(CJ#), omitting the lowest CJ# result. The value of $R = 0.9097$ ($R^2 = 0.8277$) and the F value of 24.021 show that this is a much more convincing correlation than previously observed between STHTR and C-JFTOT carbon (Figure 2). It is also better than the correlations between C-JFTOT and the JFTOT variants, but not as good as that seen between C-JFTOT and MIFAR. Some of this difference in correlations with MIFAR and STHTR correlation may relate to more data points being used in the latter case. However, there is also the possibility that the C-JFTOT still cannot fully model the heating effects (heated tank, in particular) of the STHTR.

Additivated fuels. Large scale rigs such as the MIFAR and STHTR can provide real time rates of change of temperature (not just post-test ratings) and results from these two rigs relate to periods of constant rates of change of heat transfer when the induction period has passed. Generally, the more stable the fuel, the longer the induction period and the lower the rate of heat transfer change (deposit build up) when the induction period has been overcome[5,12]. This only stops being the case when the fuel contains additives such as metal deactivator (MDA). Such additives increase the induction period but do not reduce the ensuing rate of heat transfer exchange; they may even increase the deposition rate and thus the rate of heat transfer loss[5,6]. These additives are thus able to "fool" instruments, such as the JFTOT, which only look at an end-of-test result and so are unable to tell if they are still operating within induction period conditions.

None of the C-JFTOT development work was explicitly targeted at whether the C-JFTOT would also be fooled by additives. Few Phase 4 fuels were additivated, although it was clear that JP-8+100 additives had a dramatic impact on the performance of poor thermal stability fuels[13]. The C-JFTOT does at least provide real time measurements as part of its standard operation and could be operated over longer periods, say 10 hours, to check that the induction period had ended.

A JFTOT-failing JP-5 fuel was received in April 1995, from the US Navy at Trenton. It contained just under 40 ppb metal (20.5 ppb Cu and 15 ppb Fe), a level that could cause many fuels to fail the thermal stability criteria of specifications. N.B. JP-5 fuel contains FSII and

CI/LI performance additives; the CI/LI is surface active and may already affect the deposit-forming tendencies of the fuel. There was just sufficient fuel to run two standard C-JFTOT tests and to run a single test where the fuel had been doped with 5.7 ppm MDA to the fuel (the maximum allowable amount and far in excess of the amount required to chelate the copper and iron). 3-D temperature rise versus position versus time plots are shown in Figures 10 and 11. The average result for the JP-5 is 1540. (The capillary tube was glowing red at the end of the tests.) This fuel would be rejected by a CJ# "cut-off" of 1000. Addition of MDA has caused a considerable reduction in the amount of temperature rise and the result is 495. The MDA-doped fuel seems to produce a more even deposit along the test specimen (the profile is flatter along the distance axis). Data for the hottest positions are replotted in 2-D format (see Figure 12); this figure illustrates the temperature dip effect noted with the C-JFTOT. (Temperature dips have been seen in all SRTCT's large-scale simulators - STHTR, MIFAR and IFAR - being most apparent with high stability fuels. One explanation for this is that the small amounts of deposit laid down in the capillary at the start of test effectively roughen the surface, increasing the turbulence of the fuel and hence increasing the initial rate of heat transfer. Another explanation is that the early deposit lay down fills surface crevices and thereby improves thermal conductance. Either has the effect of lowering the surface temperature. The C-JFTOT proforma spreadsheet automatically searches for this lowest temperature reading and uses it as the baseline from which all ΔT values are quoted at that particular measuring position.) It is not clear if MDA addition has prolonged the induction period as has been noted in MIFAR and STHTR experiments in the past. The temperature/time gradients for the MDA test are not very different from those at during the induction periods of the base fuel but rates of deposition are worsening as time progresses. A longer test or one with much less MDA in the system (had fuel supplies been sufficient) might have clarified the situation.

DISCUSSION

The laboratory version of the C-JFTOT has been used in its existing format (see Figure 1) since early 1993 and appears to be a good predictor of large-scale rig, particularly MIFAR, performance. Shell Internationale Research Maatschappij B.V. has filed patent applications covering the basic design[14] (used in Phase 4 tests) and collaborated with a third party to produce a pre-production prototype, the HiReTS rig. The first machine was delivered in mid-1996 and a second was supplied at the end of 1996. Both machines have been commissioned and are producing results very similar to those obtained with the older C-JFTOT rig. Basic experimental details are similar to those already described for the C-JFTOT. Exact design details of the HiReTS rigs are proprietary, but the test section and its ancillaries are in a single unit (comparable in size to that of the JFTOT), with a PC controller system in a second unit. An on-screen display shows power readings and system pressure, as well as on-going

temperature measurements. A video camera assures detector alignment. All system safety trips come under the control of the computer monitoring system and additional safety control test parameters are monitored by the computer. A "hard-wired" emergency stop system allows unattended running of the machine.

Machines are now about to be or are actually in the process of being evaluated by third parties (under loan), both to establish the inherent reliability of the HiReTS (repeatability and reproducibility of results) and to identify the best test protocols to adopt. There will be some tests performed on fuels with known engine performance data.

The existing test protocol was established with a commercial/civilian specification test in mind. This means discriminating between fuels with good and bad thermal stability so that the latter will be rejected. A CJ# or HiReTS number greater than 1000 appears to be found for most fuels that fail the standard JFTOT at 260°C. A detailed appraisal of the data is planned but it is probable that a shorter "specification" test could be adopted to achieve the desired pass/fail outcome. The HiReTS apparatus also has the potential to be developed for research activities and other specification tests; these applications are not mutually exclusive. In particular, it is becoming increasingly important to understand how additives affect deposition in turbulent flow environments. Such knowledge is relevant to another application that has arisen over the last few years, i.e. differentiating between fuels of good and excellent thermal stability. USAF are achieving thermal stability improvements through additivation.

Existing jet fuel specifications allow (or demand, for military applications) the use of metal deactivator and corrosion inhibitor/lubricity improver additives. The increased flexibility of the pre-production HiReTS should prove useful in studies to investigate the impact of these and JP-8+100 additives on aviation kerosine thermal stability. An increased range of additivated fuels have started to be tested under the current conditions to see if additivated and non-additivated fuels fall on different regression lines in correlations against JFTOT breakpoint, MIFAR performance, etc.. A number of systems have shown major discrepancies between HiReTS and JFTOT results. One case involves a poor Merox fuel with negligible levels of copper and iron that has been doped with MDA. The JFTOT breakpoint increases dramatically while the HiReTS number only drops marginally and is still much greater than the arbitrary cut-off (pass/fail) value of 1000[13]. Increasing the test time beyond two hours may help establish whether HiReTS numbers are always being quoted after the induction periods has passed; the original MDA/JP-5 result did not answer that question clearly. A longer test time and/or a higher FOT and/or a different flow rate might then allow a second test protocol to be adopted, aimed at differentiating between very good fuels rather than discarding poor ones. This would be particularly relevant for USAF's JP-8+100 programme. Preliminary results with such additives do suggest that the protocol will need to be altered when the object is not just to reject poor fuels

In its role as a research apparatus, the HiReTS may help investigate such effects as fuel recirculation. It may provide mechanistic insights far more readily and rapidly than is possible with large, fuel hungry rigs such as the MIFAR and STHTR and comparable rigs used at other locations. Additionally, the apparatus may be suitable for testing fluids other than aviation kerosine. Its short term development, however, will be directed towards ensuring that only reliably good thermal stability fuels are loaded onto aircraft.

ACKNOWLEDGEMENTS

The authors thank Shell Research Ltd for their support of this work and co-workers, in particular Drs D.R. Kendall and R.H. Clark, for their original concepts, proving experiments and other assistance. They also thank Blue Chip Technology for their work in producing the prototype HiReTS machines.

REFERENCES & NOTES

(1) Details outlined in ASTM D3241/IP 323.

(2) Kendall,D.R.;Mills,J.S. *SAE Technical paper 851871.*

(3) Strauss, K.H. *SAE Technical paper SAE881532* and references therein.

(4) Clark,R.H.; Thomas, L. *SAE 881533.*

(5) Clark,R.H.; Stevenson,P.A. *Proceedings of 200th American Chemical Society meeting, Division of Fuel and Petroleum Chemistry* **1990**, *35(4)*, 1302- 1314.

(6) Kendall,D.R.; Houlbrook,G,; Clark,R.H.; Bullock,S.P.; Lewis,C. *The thermal degradation of aviation fuels in jet engine injector feed-arms. Part 1 - results from a full-scale rig,* International Gas Turbine Congress, Tokyo, October 1987.

(7) Kendall,D.R. Unpublished minutes of MoD(PE) Thermal stability steering group,1986.

(8) $R_e = LV\eta/\rho$ where L = characteristic linear dimension of the flow channel, V = linear velocity, η = fluid viscosity and ρ = fluid density. Frictional corrections can be applied.

(9) Kendall,D.R.; Clark,R.H.; Stevenson,P.A. *The influence of polar compounds on the stability of jet fuel,* 2nd International Conference on long-term storage stability, San Antonio, Texas July 29 - August 1, 1986.

(10) Unpublished work, Shell Research Ltd, 1989.

(11) Capillary part no. 550842 from Phase Separations UK.

(12) Clark,R.H.; Wolveridge, P.E. Paper presented at the Coordinating Research Council, Alexandria, Virginia 21/22 April 1993.

(13) Bauldreay,J.M.; Blundell,W.G.; Heins,R.J.; Houlbrook,G.; Smith,J. *Testing JP-8+100 packages in European jet fuels - Evaluating and understanding benefits and drawbacks.* In these proceedings.

(14) International patent application publication No. WO 95/0281, published on 26 January 1995.

Table 1 - Test data for fuels used in first two correlation exercises using STATGRAF package

		C-JFTOT	STHTR HTC	JFTOT CBO	JFTOT BP	Ri x 10^7	Sulphur content	MIFAR deposit rate
	Units	*µg*	*%/h*	*µg*	*°C*	*mol/L/s*	*%w*	mg/cm²/h
	STATGRAF coding =>	*CAP*	*HTC*	*CBO*	*BP*	*RI*	*Sul*	MIFAR
Fuel	*Processing*							
I	Merox	214	1.1	146.0	295	4.7	0.11	
M	Merox	457	7	228.0	275	10.7	0.13	
O	Merox	12	5.4	86.0	285	0.5	0.13	0.22
Q	Merox	44	1.3	143.0	285	2.5	0.03	0.33
R	Hydrocracked	8	1.9	90.0	290	4.9	0.01	0.15
S	Merox	122	0.6	138.0	265	5.8	0.10	0.27
T	Merox	97	1.28	307	250	12.30		0.105
V	Merox +LCCCO	1277	12.3	553.0	245	4.9	0.30	0.41
W	Merox	699	28	714.0	210	25.5	0.10	
Y	Hydrotreated	7	0.19	54.0	285	0.93	0.002	0.049
HC-1	Hydrocracked	8	0.58	31.0	270	2.55	0.004	
HC-12	Hydrocracked	4	0.2	30	300	0.54		0.046
AD	Merox	67	0.68	117.5	275	8.26		0.166
AL	Merox	35	7.3	179	275	7.14		0.137

where: HTC = STHTR loss of heat transfer efficiency at 225°C, CBO = Carbon burnoff value, BP = JFTOT breakpoint, Ri = Radical initiation rate, from flask oxidation test. C-JFTOT uses average carbon weight data recorded for 290°C fuel outlet temperature. MIFAR results quoted for fuels Q, S and T are the average of two determinations.

Table 2 - STATGRAF analyses of correlations. Large scale rigs versus carbon deposit weights from conventional and capillary JFTOTs, for fuels with MIFAR data in Table 1. All Logs are to base 10.

Dependent	Log(MIFAR)	Log(MIFAR)	Log(MIFAR)	Log(MIFAR)	Log(HTC)
Independent	Log(CJFTOT)	Breakpoint	Log(BP)	Log(CBO)	Log(CJFTOT)
Mean square error	0.0562	0.0890	0.0899	0.0612	0.3105
Correlation confidence, %	98.06	84.1	83.35	97.18	88.77
F value	8.5	2.41	2.32	7.15	3.17
R-squared	0.515	0.232	0.225	0.472	0.284
Intercept +/-1 standard error	-1.3047+/-14%	1.607+/-97%	12.33+/-70%	-2.104+/-23%	-0.5599+/-77%
Gradient +/-1 standard error	0.3103+/-34%	-0.0088+/-64%	-5.389+/-65%	0.6134+/-37%	0.4454+/-56%

Figure 1. Laboratory Capillary JFTOT apparatus, used as basis of development of pre-production HiReTS machines.

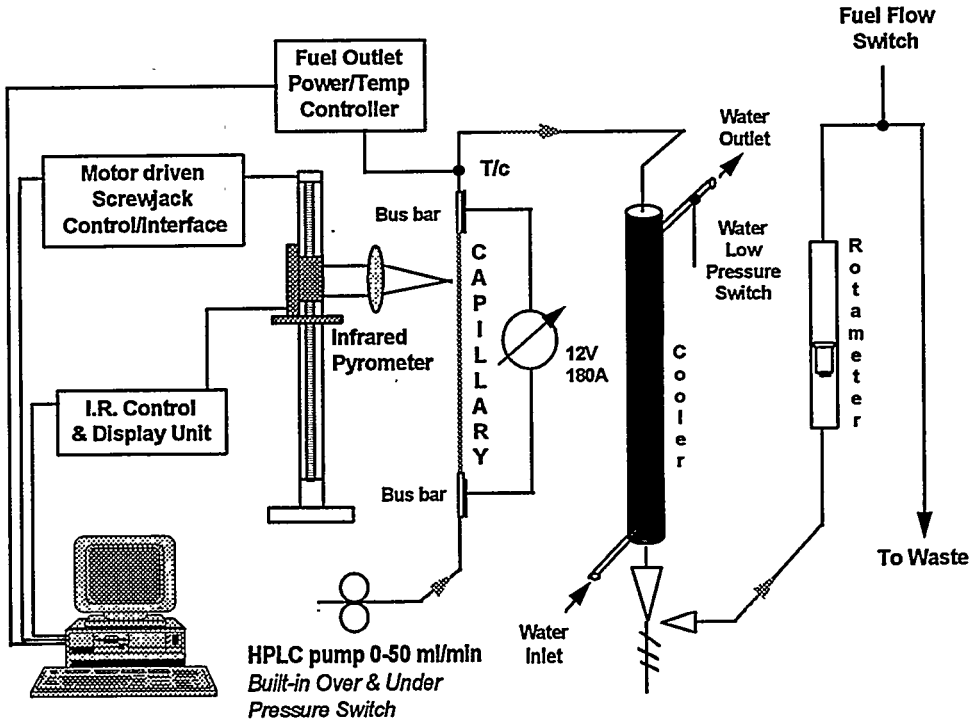


Figure 2. First correlation between fouling rate in the STHTR and carbon deposited in C-JFTOT at 290°C condition. $R^2 = 0.4507$, $F = 6.56$ and 95% confidence limits are shown.

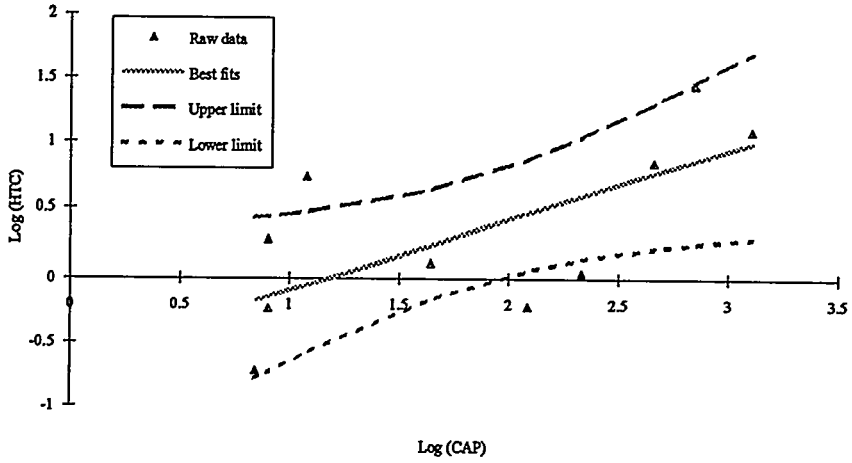


Figure 3. Correlation between deposition rate in the MIFAR and carbon deposited in C-JFTOT at 290°C condition, including 95% confidence limits. $R^2 = 0.5150$ and $F = 6.50$.

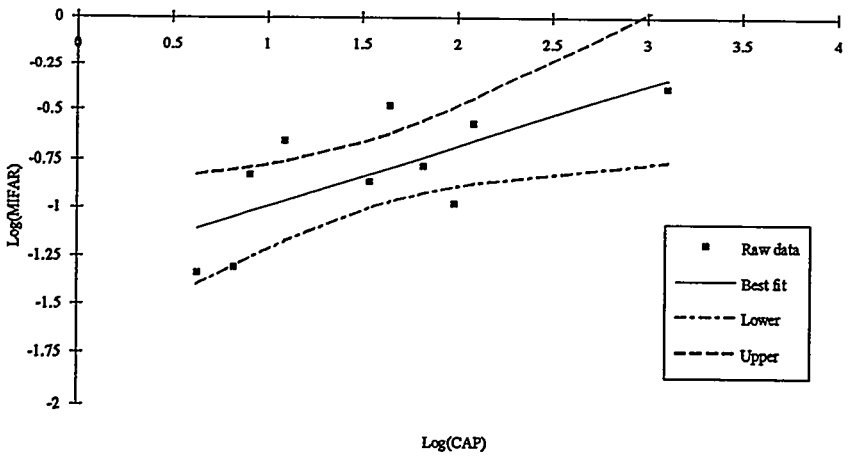


Figure 4. Average carbon deposit weight versus average C-JFTOT number (Phase 4 fuels).

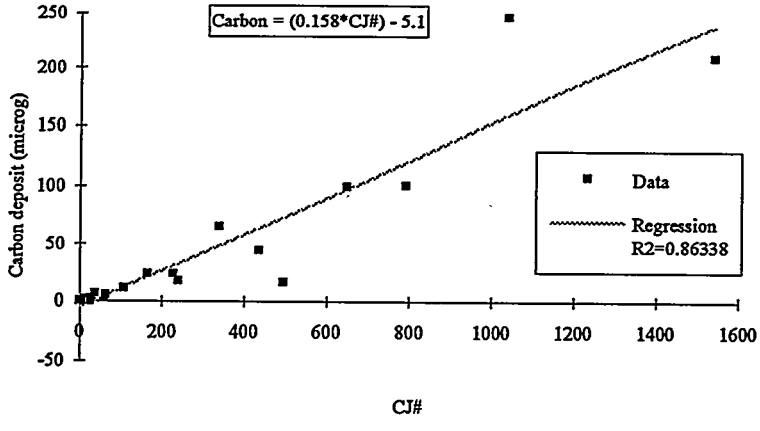


Figure 5. CJ# versus visual tube ratings from standard JFTOT tests for Phase 4 fuels.

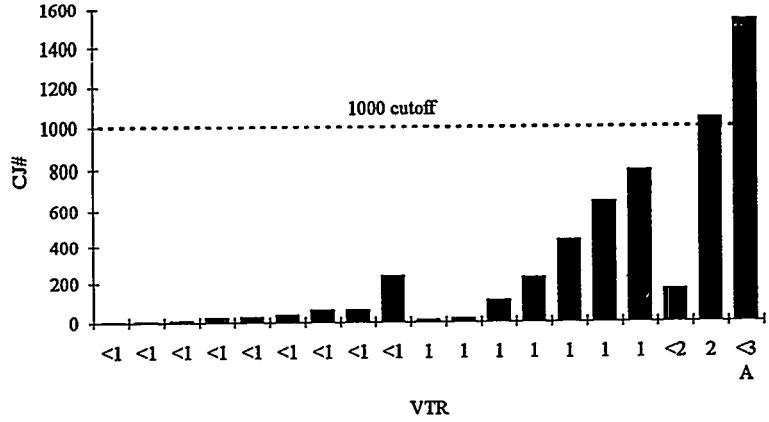


Figure 6. JFTOT breakpoint versus C-JFTOT number showing linear regression fit for Phase 4 fuels; omitting those with additives, Breakpoint = 292 - (0.0239*CJ#) with $R^2 = 0.4387$.

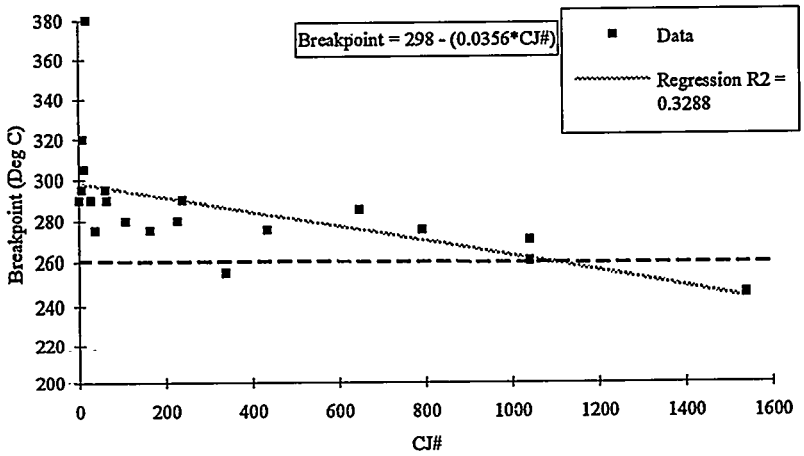


Figure 7. MIFAR deposit rate versus C-JFTOT number for Phase 4 fuels.

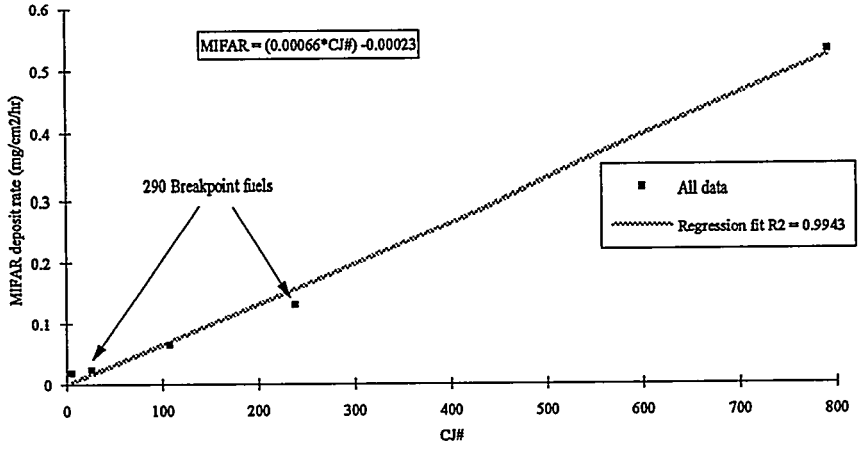


Figure 8. STHTR heat transfer coefficient ΔHTC at 225°C versus CJ# for Phase 4 fuels. STHTR data may be "raw" or from fitting data obtained at several temperatures.

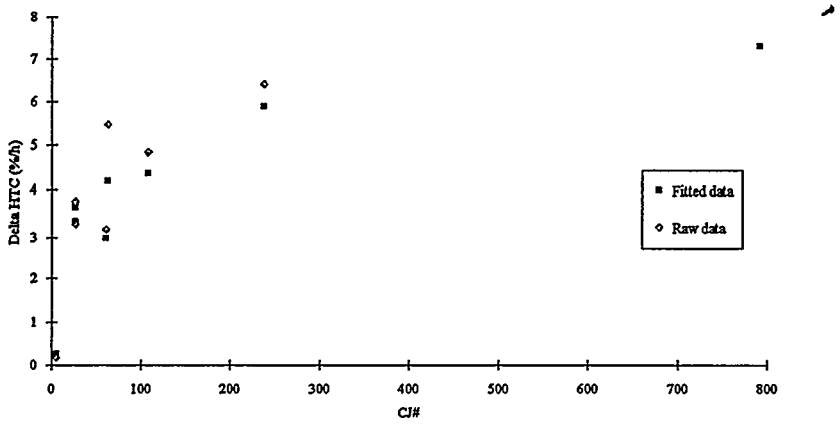


Figure 9. Log (ΔHTC) versus Log (CJ#), and regression fit (omitting lowest CJ# point).

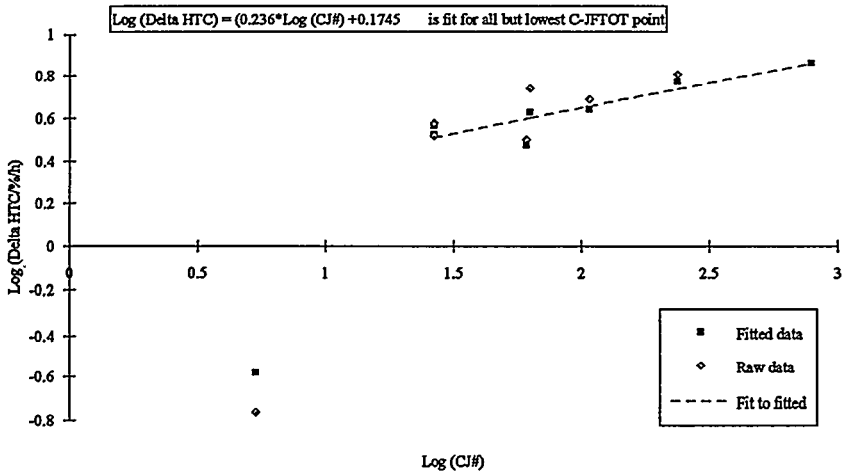


Figure 10. Trace for poor thermal stability JP-5 fuel received from US Navy, using C-JFTOT

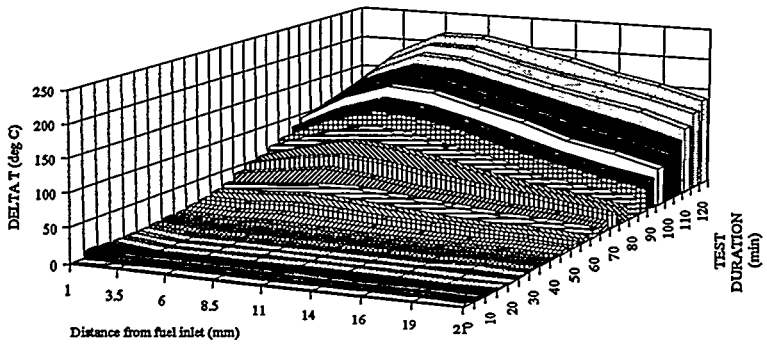


Figure 11. Same fuel with maximum allowable concentration of metal deactivator additive.

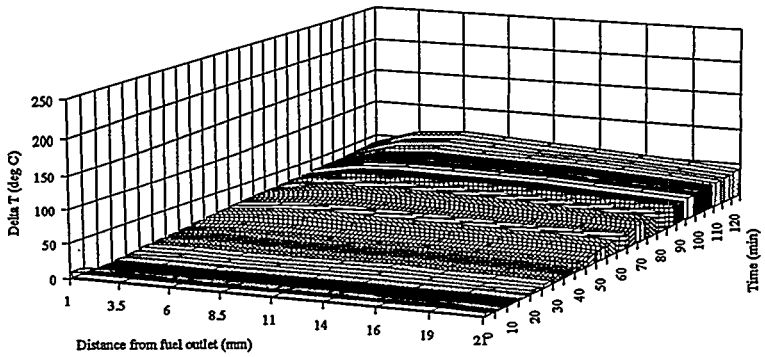
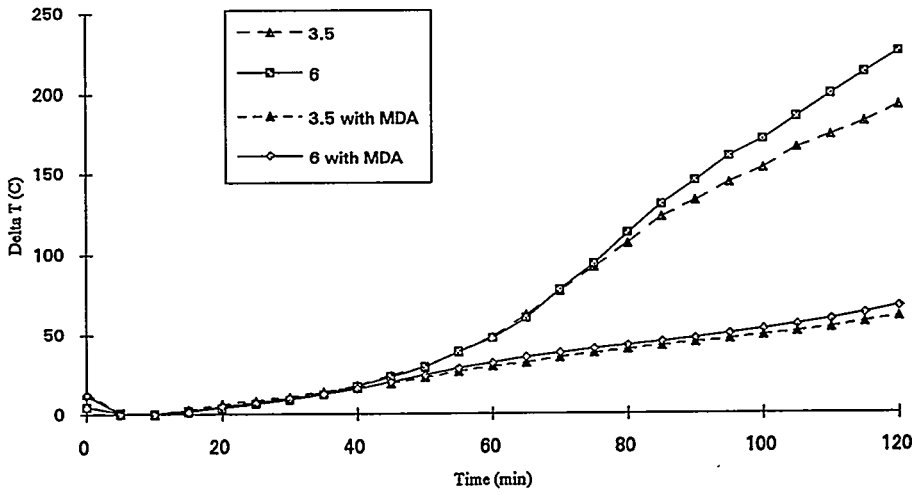


Figure 12. 2-D temperature change (Delta T) versus time at two hottest positions (3.5 and 6 mm from fuel outlet) for US Navy JP-5 fuel, as received and with 5.7 mg/L active matter MDA. Both show initial drop in Delta T followed by temperature rise.



6th International Conference
on Stability and Handling of Liquid Fuels
Vancouver, B. C., Canada
October 13-17, 1997

ELECTRICAL CONDUCTIVITY OF HITTS ADDITIVE PACKAGES FOR THE JP8+100 PROGRAMME

Brian Dacre* and Janice I. Hetherington

Rutherford Laboratory, Royal Military College of Science, Shrivenham, Swindon, Wilts SN6 8LA, UK.

ABSTRACT

The behaviour of two HITTS high temperature additive packages has been studied to examine possible interference with existing conductivity improver and also to assess their potential as conductivity improvers. The HITTS additives are shown to impart sufficient conductivity to fuels to meet certain fuel conductivity specifications without the addition of Stadis. Use of the HITTS additives with Stadis is shown to produce values of conductivity above the fuel specification. The conductivity performance of the HITTS additives is unaffected by the presence of phenolic or sodium salt impurities in the fuel which have been shown to have a detrimental effect on the performance of Stadis. The conductivity behaviour of the individual components of the HITTS additives is discussed. The dispersant is the main conducting component in the additive packages, but there are variations in the magnitude of the conductivity observed.

1. INTRODUCTION AND AIMS

The major objective of the JP8+100 programme is to improve the thermal stability of jet fuel using carefully selected additives. However, in this paper we examine the effects of such additives on properties which are unrelated to thermal stability characteristics, but which can have important consequences for the handling characteristics of the fuel.

In earlier papers[1,2,3] we examined the effects of a wide range of compounds, representative of naturally-occurring fuel components, on the performance of static dissipators (conductivity improvers). The work identified highly polar species capable of substantially reducing their effectiveness.

Certain HITTS packages are known to impart some conductivity to fuel. This work investigates the magnitude of this conductivity effect, on a model fuel and on three real fuels, for two Betz JP8+100 additives based on SPEC-AID 8Q405. SPEC-AID 8Q405, alone, at a concentration of

100mgl^{-1}, has been reported to produce an average conductivity increase of ~140pSm^{-1} in three reference fuels[4]. The spread of values in these fuels was not stated. The two fully formulated HITTS packages NB 345 S286 and SPEC-AID 8Q460 have been examined and components of the packages have been studied separately to identify components contributing to the conductivity.

The sensitivity of these HITTS packages to model impurities, phenols and sodium salts,has been determined and is compared with that of Stadis450. The effects of the HITTS additives on Stadis450 have also been measured.

Brief comments are made on the potential for the use of such additives as conductivity improvers.

2. EXPERIMENTAL

2.1 Materials: The composition of the HITTS additive packages NB 345 S286 and SPEC-AID 8Q460 are given in Table 1. The fully-formulated additives , SPEC-AID 8Q460 and NB234 S286A, the partially formulated package SPEC-AID8Q406 and the components SPEC-AID 8Q405(dispersant batch-1) and SPEC-AID8Q400(Betz metal deactivator) were supplied directly via Wright Patterson AFB by Betz Process Chemicals Inc. A second sample of SPEC-AID 8Q405 (batch-2), was supplied via British Petroleum. The additive BHT (2,6-diter-butyl-4-methyl phenol) was obtained from Aldrich Chemical Co Ltd., "conventional" metal deactivator (NN disalicylidene 1,2-propane diamine - abbreviated to c-MDA) from Pfalz and Bauer Inc., m-cresol from British Drug Houses and octylamine from Fluka Chemica.

Stocks of the HITTs fuels were held by and supplied to us by Shell. These were, an additive-free Merox base fuel (Merox-AF), having a kinematic viscosity of 3.698 mm^{2}s^{-1} at -20C , and two fuels produced from this to JetA1 and JP8 specification. These are designated Jet A1-MA1, which contains 1.87mgl^{-1} reformulated Stadis450 and JP8-MA2 which contains 1.87mgl^{-1} reformulated Stadis450 plus AL-48 to give a concentration of 1300mgl^{-1} of FSII and 27mgl^{-1}of Nalco 5403.

The sources and purification procedures employed for materials used previously, have been described[1,2,3].

2.2 Equipment and measurements: All measurements were made with the apparatus described previously[2,3] and made at 25C. The series of measurement was as follows:

i) time dependence of conductivity for NB 345 S286 and SPEC-AID8Q460 in dodecane.

ii) the conductivity of NB 345 S286 and SPEC-AID 8Q460 in dodecane and HITTS Fuels over

a concentration range of 10 mgl^{-1} to 800 mgl^{-1}.

iii) the conductivity of NB 345 S286 and SPEC-AID 8Q460, over a range 10mgl^{-1} to 800mgl^{-1}, in dodecane containing 3mgl^{-1} Stadis450

iv) *m*-cresol and 2,6-di-*tert*-butyl-4-methylphenol were added separately over the concentration range 50-1000 mgl^{-1} to solutions of 135mgl^{-1} NB 345 5286 in dodecane and HITTS Fuels and 127mgl^{-1} SPEC-AID 8Q460 in dodecane and HITTS Fuels. The conductivity was measured after each addition of the phenol.

v) sodium naphthenate was added, over the concentration range 0.3 to 18 mgl^{-1}, to solutions of 135mgl^{-1} NB 345 S286 in dodecane and 127mgl^{-1} SPEC-AID 8Q460 in dodecane. Conductivity measurements were made after each addition of sodium naphthenate.

vi) components of the additive packages namely SPEC-AID8Q405, SPEC-AID8Q400 and c-MDA were added separately to HITTS Fuels and the conductivity measured.

vii) test of the variability of samples of SPEC-AID8Q405 dispersant between batches (where impurity levels could be different) by measurement of the conductivity of batch 2 SPEC-AID,8Q405 in the three HITTS fuels to compare with similar results from batch 1.

viii) neutralisation of possible acidic impurities using SPEC-AID 8Q406 (SPEC-AID8Q405 + BHT antioxidant) was shaken for five minutes with finely divided $CaCO_3$ diluted with hexane, then separated and the solvent removed by evaporation. A control sample was treated in a similar way but without the $CaCO_3$.

Acid and Base Additions: In a preliminary attempt to investigate ion production mechanisms we have examined the effects of an amine and an acid on the conducting species. Octylamine, diluted in toluene, was added to a solution of 100mgl^{-1}dispersant SPEC-AID 8Q405 in the Merox-AF and the conductivity was measured after each addition. Similar measurements were made using dodecylbenzenesulphonic acid.

3. RESULTS AND DISCUSSION

3.1 The Time dependence of the Conductivity of Fully-Formulated Additives, NB345 S286 and SPEC-AID8Q460 in Dodecane Solutions

The time dependence of conductivity has been examined in a limited series of measurements over a three-hour period. These measurements were required in order to see if any large drifts in conductivity occurred during the time-scale of the experiments. The conductivity of the NB345 S286 solution(135mgl^{-1}) increases slowly with time whereas that for SPEC-AID8Q460 (127mgl^{-1})

shows a slow decrease. However in neither case were the changes sufficient to warrant detailed corrections to data obtained during the period of the experiments-normally about an hour.

3.2 Effect of Concentration of Fully-Formulated Additives on the Conductivity of Dodecane Solutions

Data in dodecane were required to provide a baseline for comparison with behaviour in real fuels. In these experiments only the the fully-formulated HITTS additive packages SPEC-AID 8Q460 and NB345 S286 were examined.

Figure 1 shows the effect of these packages on dodecane and demonstrates their ability to impart conductivity. We note also that the conductivity varies approximately linearly with concentration of the additive package, with the NB345 S286 giving a larger gradient than SPEC-AID8Q460. The recommended in-fuel concentrations of these additives are 135mgl^{-1} for the former and 127mgl^{-1} for the latter .

The behaviour of these packages in dodecane containing 3mgl^{-1} of original Stadis450 is shown in figure 2. The results of repeat runs, undertaken after an interval of nineteen months show a measurable change in behaviour. The fact that the stadis450/dodecane solution had a conductivity close to that in the original experiments suggests that the observed changes are due to ageing effects in the Hitts additives. The cause of the low concentration behaviour is not yet clear, however at concentrations >200mgl^{-1} the variation of conductivity with concentration for each package is similar to that observed in the absence of Stadis450. These low concentration effects are reminiscient of the effects of salts on Stadis450.

3.3 Effects of Polar Fuel Components on the Conductivity of Hitts Additives in Dodecane

Figure 3 shows the influence of m-cresol concentration on the conductivity of solutions containing given concentrations of (i) original-Stadis450, (ii) NB345 S286 and (iii) SPEC-AID8Q460. The concentrations chosen are recorded on the figures and correspond approximately to those used in jet fuels.

We previously reported on the influence of m-cresol on original-Stadis450[3] and this is also further discussed in an accompanying paper[5]. For SPEC-AID8Q460 we observe a small decrease in conductivity with concentration which is probably insignificant from a user viewpoint. For NB345 S286 conductivity appears to increase gradually with m-cresol concentration and the increase, after allowance for a small time correction, would be ~ 30pSm^{-1} at 1000mgl^{-1} m-cresol. For comparison figure 4 shows the effects of a highly hindered phenol of the type employed as

antioxidants. This is a good example of an almost complete lack of any antagonistic interaction with any of the three additives.

Earlier results on the effects sodium salts of a naphthenic acid, a phenol and dodecylbenzenesulphonic acid, on the behaviour of original-Stadis450, showed strong antagonistic effects on conductivity response[3] and these were qualitatively similar for all three types of salt. Sodium naphthenate was chosen as representative of these and its influence on the additive packages is shown in figure 5. For each HITTS package the concentration dependence of conductivity is quite different from that of Stadis solutions. There is no minimum, the conductivity remains approximately constant up to a concentration of ~ $2mgl^{-1}$ and then increases with concentration. We note that sodium naphthenate alone imparts some conductivity[3] , but this cannot account for the total observed increase. However, in this case, because the concentration of such compounds in fuels is likely to be low-probably $<1mgl^{-1}$, the practical effect of this will be very small.

3.4 Effects of Fully-Formulated Additives on the Conductivity of Hitts Fuels

We note that the conductivities of Jet A1-M1A and JP8-M2A, measured at the start of the study, are very similar, having values of ~ 500 pSm^{-1}. However , during the period of the work conductivity is seen to decrease for each fuel, with that for JP8 showing a fall of ~34% and for JetA1 a fall of ~20% over 250 days. This is taken into account in our comparisons of behaviour. The only difference between these fuel solutions is the presence of AL-48 in JP8-M2A. We know that in short-duration experiments AL-48 has no measurable effect on the performance of Stadis450[6]. No long-duration experiments ie up to ~250 days have yet been done.

Figure 6 shows the response of HITTs fuels to NB345 S286. This is represented by the increase in conductivity over the initial conductivity of the fuel. Dodecane data are shown for comparison. Clearly there are differences in response which follow the order : JP8 > Jet A1 > Merox-AF > Dodecane. Likewise figure 7 shows the response of HITTs fuels to SPEC-AID8Q460. In this case the differences in response are much less clear cut, though JP8 and Jet A1 again show greater resonse than Merox-AF and Dodecane. ie JetA1 ~ JP8 > Dodecane ~ Merox-AF. The lower viscosity for Merox-AF($1.45mm^2s^{-1}$) compared with dodecane($1.86mm^2s^{-1}$) at 25C would lead us to expect a higher conductivity in Merox-AF. Mixtures of aromatic and alkane liquids of a given viscosity are expected to promote a higher conductivity than an isoviscous pure alkane at the same temperature. Therefore the presence of aromatic components in Merox-AF(19%) will

raise the conductivity[6]. To these effects must also be added those due to interactions between additives. The net result on ion production is seen in the measured conductivity. Paradoxically the low concentration behaviour observed with these additivesin Stadis/dodecane mixtures is not observed in the more complex real fuel systems. In these cases however, the ageing effect has not yet been examined.

A practical point is that, at the recommended dosing concentration for HITTs additives in JP8 and JetA1, the total conductivities, as shown in table 2, are above the upper limit specification values of 600pSm^{-1} and 450 pSm^{-1} respectively. We also note that the conductivity of Merox-AF, containing the recommended concentrations *is* within the specification conductivity range for JetA1 without the addition of Stadis 450, but 8Q460 falls slightly short of the minimum value for JP8. However we feel that more data is required on batch-to-batch variations and on fuel composition effects.

3.5 Effect of Model Phenolic Impurities on the Conductivity of HITTS Additives in HITTS Fuels

Figure 8 shows that the total measured conductivities of SPEC-AID 8Q460 in Merox-AF are *insensitive* to the presence of *m*-cresol "impurities". Results for NB345 S286 are similar. The apparent sensitivity to *m*-cresol in the JP8 and JETA1 fuels can therefore be attributed to the interaction of the *m*-cresol with the Stadis450 in these fuels and not to any interaction of the *m*-cresol with NB 345 S286 or SPEC-AID8Q460.

3.6 Effects of Additive Components on the Conductivity of HITTS Fuels

Work on a range of phenol types[5] in dodecane has shown that highly hindered phenols have little or no effect on the conductivity of hydrocarbons nor do they adversely affect the performance of Stadis450. We have confirmed that BHT does not contribute to the conductivity of the additive package in any of the HITTS fuels.

Earlier measurements on conventional-MDA in dodecane showed it had no effect on conductivity[1]

Figure 9 shows that this is also true for solutions in Merox-AF and JP8. For Jet A1 a small decrease of ~10% is observed in the concentration range 0 to 100 mgl^{-1}.

In marked contrast, the Betz MDA, see figure 10, although it contributes only a small amount to the conductivity of Merox-AF, nevertheless has a considerable enhancing effect on the conductivity of Jet A1 and causes a modest reduction in the conductivity of JP8. These effects are clearly indicative of interaction between this MDA and components present in these fuels.

Repeat runs with this additive, after an ageing period of eighteen months, demonstrated an increased response. However, during this period the USAF decided not to consider a new MDA but to continue with conventional MDA. For this reason work on Betz MDA was discontinued. Figure 11 shows that the dispersant SPEC-AID8Q405 imparts significant conductivity to each of the fuels and conductivity varies linearly with concentration above ~50mgl^{-1}. We note the response follows the order JP8 > Jet A1 > Merox-AF as observed for the fully-formulated additive packages. In view of the results for BHT and c-MDA discussed above, it is clear that SPEC-AID8Q405 is the only conducting component in SPEC-AID8Q460 and is the main, but not the sole conducting component in NB345 S286.

3.7 Effect of Batch Variation on the Behaviour of SPEC-AID 8Q405

Figure 11, also demonstates batch to batch variation on the conductivity-improving ability of SPEC-AID 8Q405 with Batch 2 giving generally lower conductivity values. At a concentration of 100mgl^{-1}, batch-1 in Merox-AF meets the Jet-A1 and JP8 conductivity specifications, without Stadis, whereas batch-2 meets that for Jet-A1 only. Either batch added to Jet-A1 fuel causes the conductivity to be out of specification. This is also the case for addition of batch-1 to JP8 fuel. The magnitudes of some of the observed effects seems also to be influenced by ageing of the fuels and we hope to examine this further.

3.8 Preliminary Investigation of the Conducting Species

The conductivities of both carbonate-treated and untreated SPEC-AID8Q406 samples (see para 2.2) are identical. This suggests that participation of acidic species in the conduction process is unlikely.

Figure 12 shows that both dodecylbenzenesulphonic acid n-octylamine interact to increase the conductivity. Repeat experiments after an interval of sixteen months show, that apart from some small apparent differences at very low concentrations, the behaviour is generally unchanged within the experimental uncertainty. In the case of the sulphonic acid the effect is partly due to the acid itself[4,3]. However, this cannot be the explanation for the effect of the amine which alone has no effect on the conductivity[6]. More information is required before much speculation can be justified.

4. SUMMARY AND CONCLUSIONS

4.1 CONDUCTIVITY BEHAVIOUR OF HITTS PACKAGES

4.1.1 In Model Fuel (Dodecane) with Model Impurities

1 Both the HITTS packages impart conductivity which shows a small time dependence.

2 Both the HITTS packages can impart conductivity to fuel, without the use of Stadis450.

3 The conductivity response of both the HITTS packages is insensitive to phenolic impurities.

4 The conductivity response of both the HITTS packages is insensitive to sodium salts.

5 The HITTS packages have the advantage of imparting the required conductivity to fuels without the sensitivity to fuel impurities, such as phenols and sodium salts, which is detrimental to Stadis450.

4.1.2 In HITTS Fuels

1 Both the HITTS additive packages used at the recommended concentration in the HITTS fuels JP8 MA2 and JETA1 M1A, gave conductivities *above* the fuel specification.

2 The conductivity of the MeroxA-F containing the recommended levels of both HITTS packages was within the fuel conductivity specification for Jet-A1 *without* the use of Stadis450. For JP8 with the additive 8Q460, conductivity falls slightly short of the minimum conductivity specification

3 There is a simple linear relationship between conductivity and the concentration of the HITTS additives.

4 Both the HITTS additive packages appear to be unaffected by the presence of phenolic impurities in fuel.

5 Reduction in conductivity in the HITTS JP8 and JET A1 with the HITTS additives in the presence of phenolic impurities is attributed to interaction of the phenol with the Stadis 450 in these fuels.

6 The HITTS additives show potential as conductivity improvers. Additional work is required on batch-to batch variation, ageing effects and on the temperature dependence of conductivity before these additives can be given serious consideration as sole conductivity improvers.

4.2 CONDUCTIVITY BEHAVIOUR OF *INDIVIDUAL COMPONENTS* OF HITTS ADDITIVES

1 The c-MDA contributes little to the conductivity of the HITTS additive.

2 The contribution of the Betz MDA to conductivity is complex. In the Merox-AF the Betz MDA contributes a small increment to the conductivity. In the JP8 it produced a reduction in conductivity and in the JETA1 it produced an increase in conductivity. The reasons for the variations could be due to interaction with Stadis450 and/or water in the fuels. Recently the Betz MDA has ceased to be of interest to USAF.

3 The BHT antioxidant does not contribute to the conductivity of the HITTS additives.

4 The dispersant SPEC-AID8Q405 is the main conducting component in the HITTS additives. At 100mgl^{-1} in the presence of Stadis, conductivity will generally exceed the specification upper limit. In the absence of Stadis it is likely that the Jet-A1 specification will be met but there is uncertainty with respect to JP8.

5. ACKNOWLEDGEMENTS

The authors wish to thank additive manufacturers and oil companies, in particular BP, for their constructive cooperation and for supplies of additives and fuels. Especially they would like to thank BP and DRA for many helpful and enjoyable discussions during the course of this work. They also wish to express their thanks to the DRA for its funding support provided under DRA Contract LSF/E 20093.

6. REFERENCES

1.Dacre,B.; Abi Aoun, W.G. The Effects of Fuel Components on the Behaviour of Conductivity Improvers in Jet Fuel, 4th International Conference on Stability and Handling of Liquid Fuels, Orlando, Florida,USA, November 1991.

2.Dacre,B.; Abi Aoun, W.G. Effects of Fuel Components on the Performance of Conductivity Improvers in Hydrocarbons, Journal of Electrostatics,39(1997)89-110.

3.Dacre,B.; Hetherington, J.I. Behaviour of Conductivity Improvers in Jet Fuel, 5th International

Conference on Stability and Handling of Liquid Fuels, Rotterdam, The Netherlands, October 1994.

4.Anderson, S.D.; Harrison,W.E.; Edwards,T.; Morris,R.W.; Shouse,D.T. Development of Thermal Stability Additive Packages for JP-8, 5th International Conference on Stability and Handling of Liquid Fuels, Rotterdam, The Netherlands, October 1994.

5.Dacre,B.; Hetherington, J.I. The Effect of Phenolic Impurities in Jet Fuel on the Behaviour of Conductivity Improvers, 6th International Conference on Stability and Handling of Liquid Fuels Vancouver, B. C., Canada, October 13-17, 1997 .

6.Dacre,B.; Hetherington, J.I. Preliminary unpublished work.

Commercial Additive	Description	Concentration Added to Fuel	Comments
BHT	Antioxidant 2,6-di-*tert*-butyl-4-methylphenol	25mgl^{-1}	
MDA (conventional)	Metal Deactivator NN'disalicylidene-1,2-propanediamine	10mgl^{-1}	
8Q405	Dispersant BETZ (proprietory)	100mgl^{-1}	
Spec Aid 8Q400	Betz Metal Deactivator	10mgl^{-1}	Different chemistry from conventional DuPont MDA
Spec Aid 8Q406	8Q405 / BHT dispersant / antioxidant	125mgl^{-1}	
NB 345 S286A	Experimental 8Q405/BHT/8Q400 Dispersant / Antioxidant / Betz MDA	135mgl^{-1}	Assumed composition: 8Q405 100mgl^{-1} BHT 25mgl^{-1} MDA 10mgl^{-1} (Betz)
Spec Aid 8Q460	8Q405 / BHT /MDA Dispersant / Antioxidant / MDA (conventional chemistry)	127mgl^{-1}	Assumed composition: 8Q405 100mgl^{-1} BHT 25mgl^{-1} MDA 2mgl^{-1} (conventional)

Table 1 **Composition of HITTS High Temperature Additive Packages**

FUELS	SPEC AID8Q460 127mgl^{-1}	NB 345 S286 135mgl^{-1}
Merox-AF	123	221
Jet-A1	666	817
JP8	668	864
Dodecane	132	200

Values taken from data in figures 7 and 8.

Specification Conductivity ranges: Jet-A1 50--450pSm^{-1}
JP8 150--600pSm^{-1}

Table 2 Measured Conductivities (pSm^{-1}) in HITTS Fuels

Fuel	Batch-1 100mgl^{-1}	Batch-2 100mgl^{-1}
Merox-AF	158	115
Jet-A1	689	584
JP8	671	557

Values taken from data in figure 11.

Table 3 Measured Conductivities (pSm^{-1}) of 8Q405 in HITTS Fuels

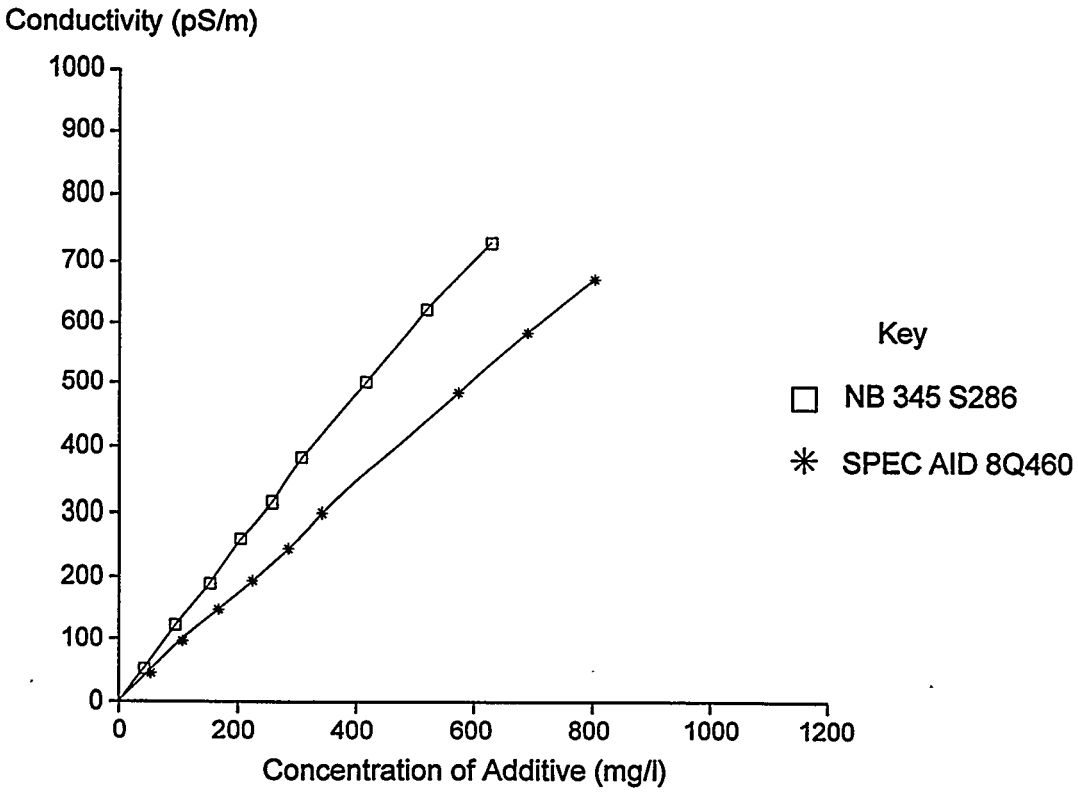


Fig. 1 Conductivity vs. Concentration for High Temperature Additive Packages in Dodecane

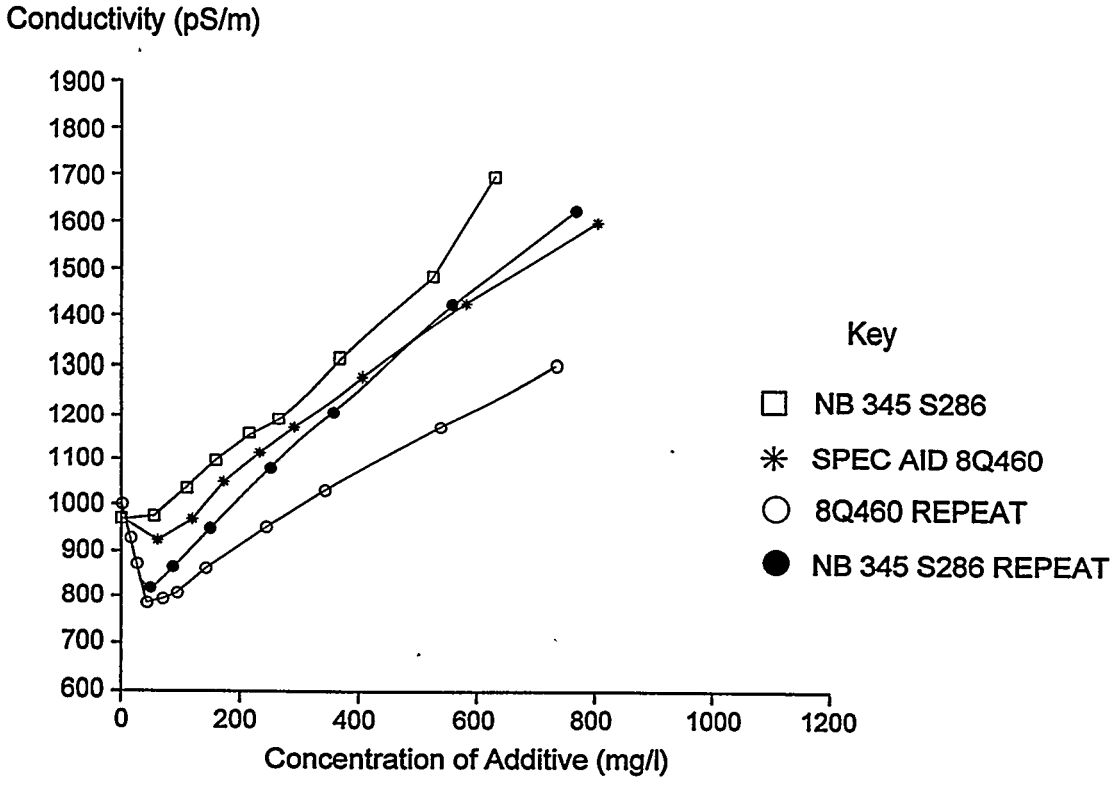


Fig. 2 Effect of High Temperature Additive Packages on Conductivity of 3mg/l STADIS 450 in Dodecane

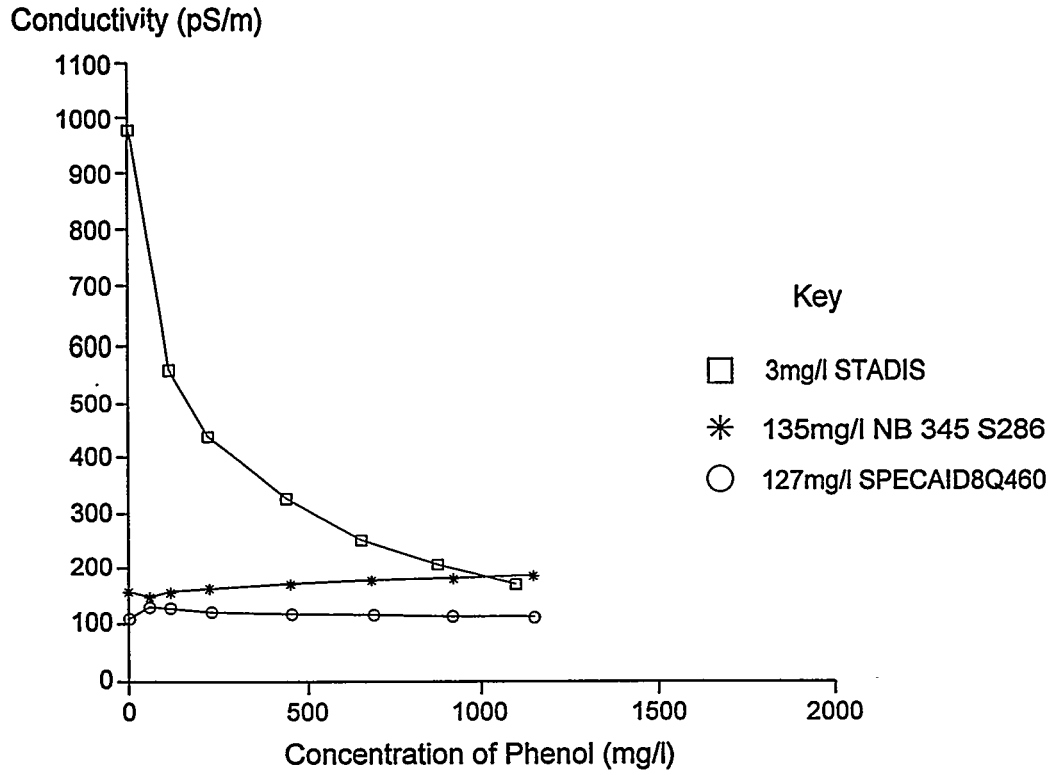


Fig. 3 ffect of m-Cresol on Conductivity of Stadis 450 and High Temperature Additive Packages in Dodecane

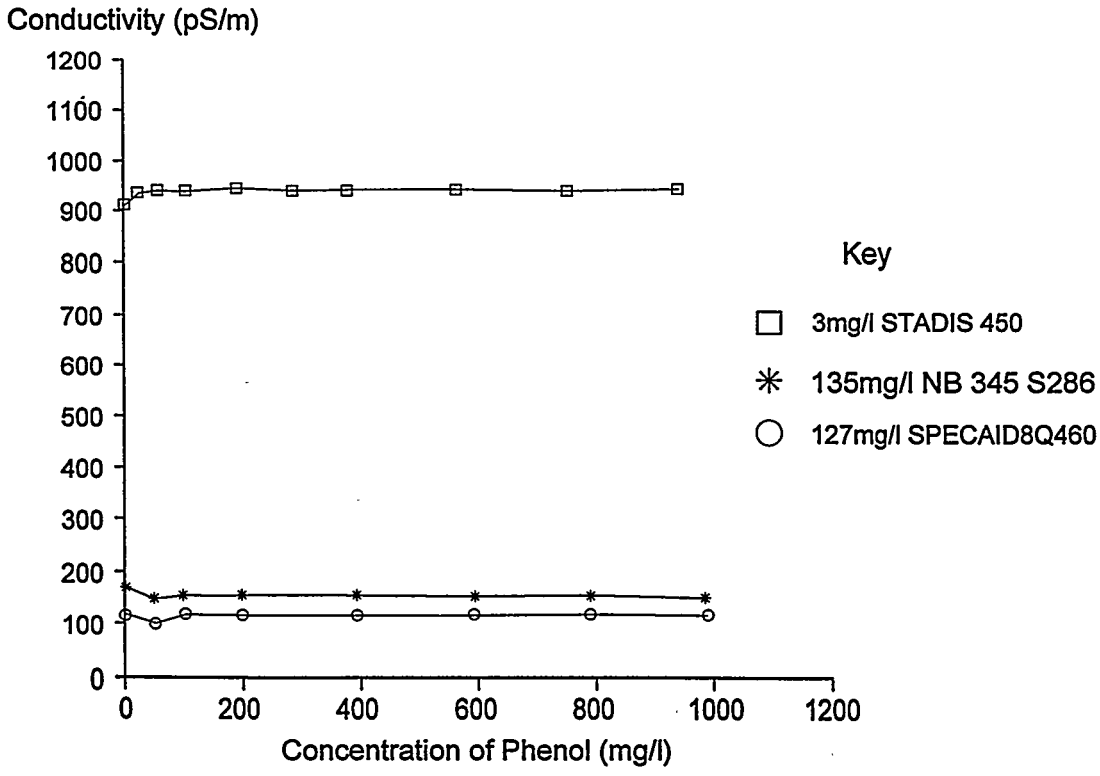


Fig. 4 Effect of 2,6di(tert)butyl-4-methylphenol on Conductivity of Stadis 450 and High Temperature Additive Packages in Dodecane

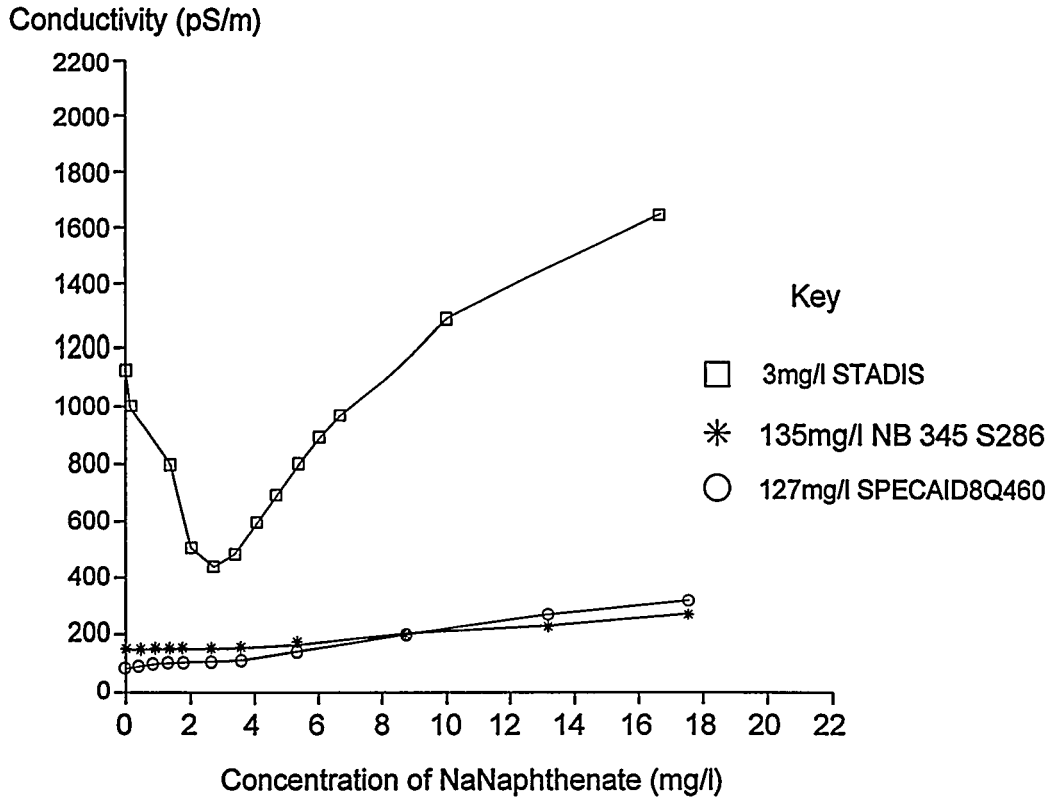


Fig. 5 Effect of Sodium Naphthenate on Conductivity of Stadis 450 and High Temperature Additive Packages in Dodecane

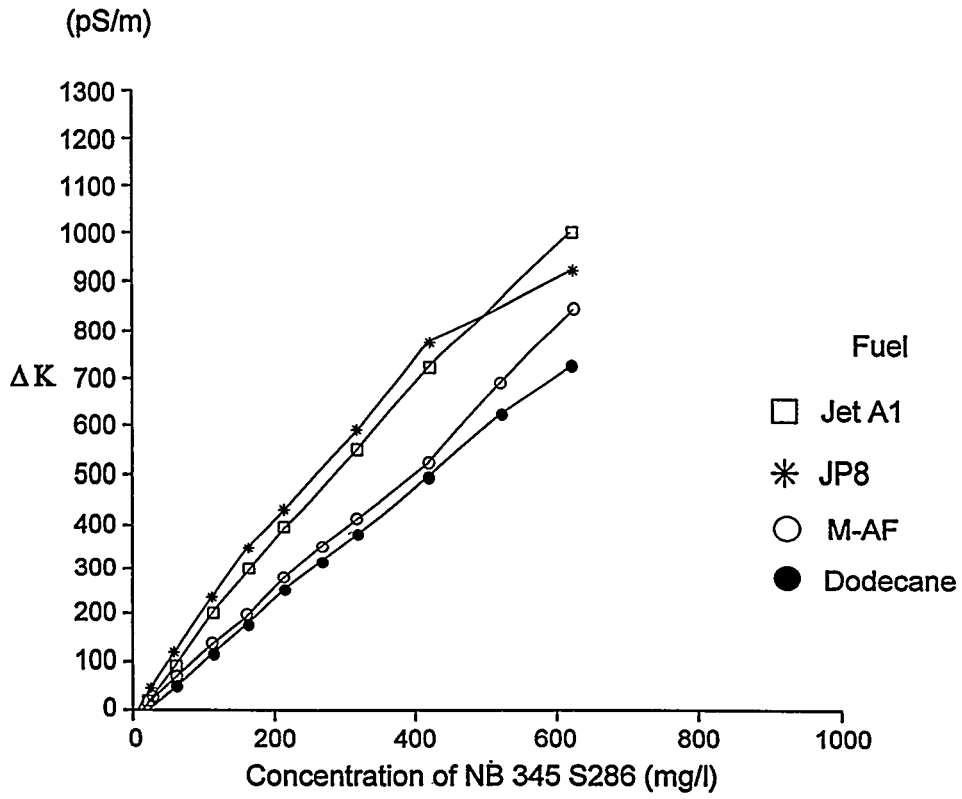


Fig. 6 Effect of NB 345 S286 on the Conductivity of HITTS Fuels

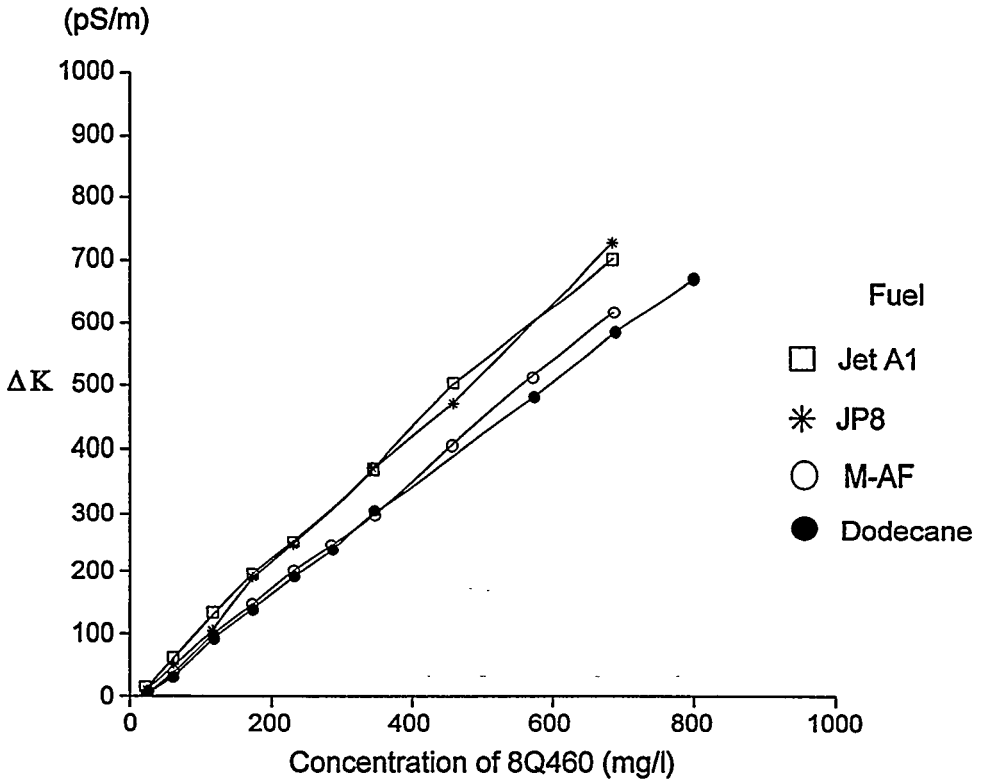


Fig. 7 Effect of 8Q460 on the Conductivity of HITTS Fuels

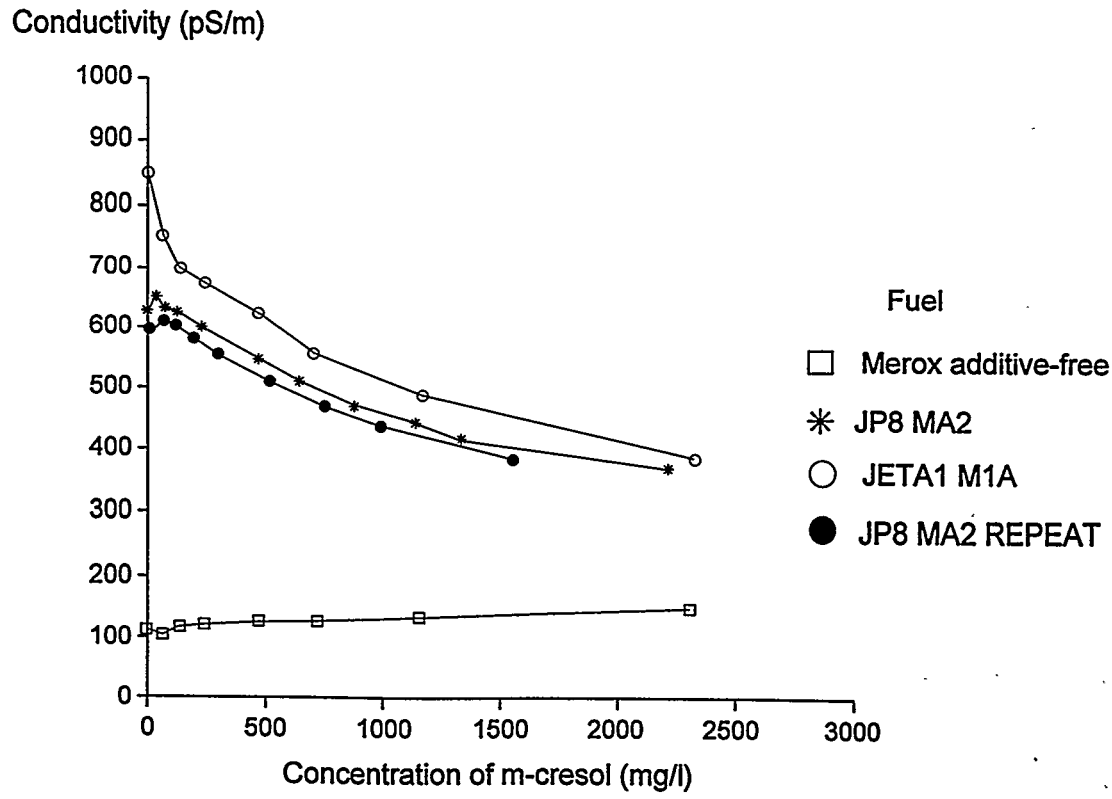


Fig. 8 Effect of m-cresol on Conductivity of 127 mg/l SPECAID 8Q460 in HITTS Fuels

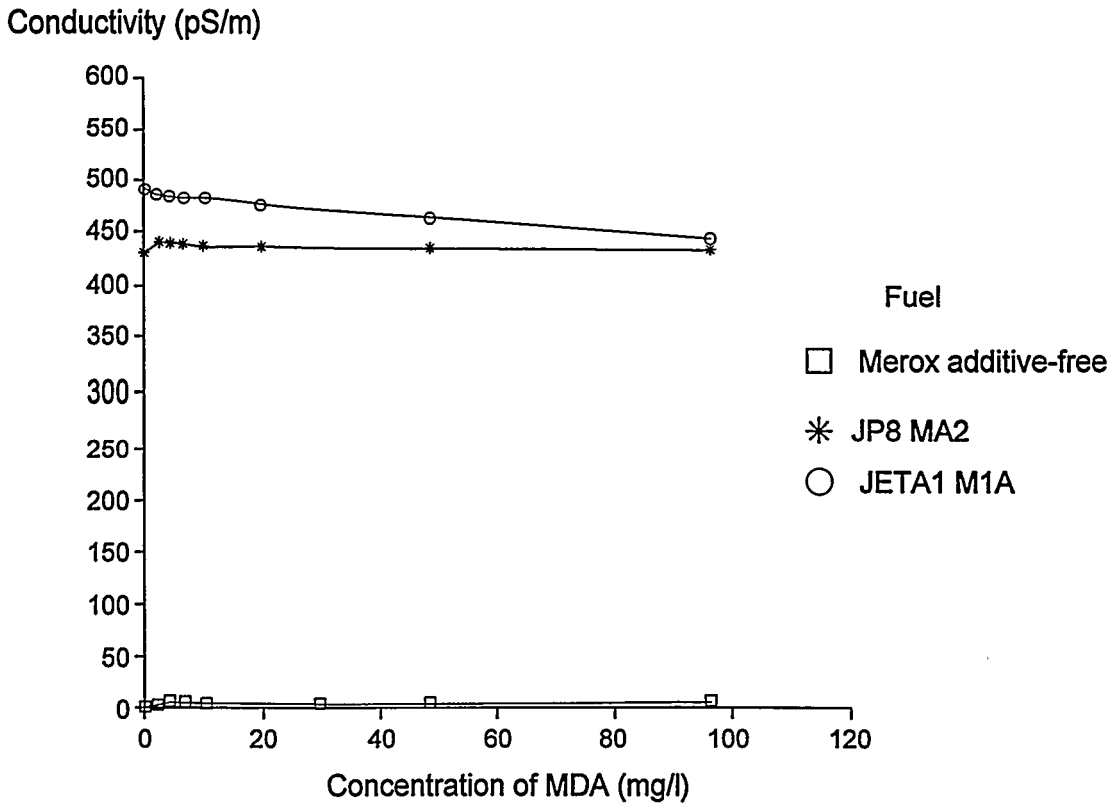


Fig. 9 Effect of MDA (conventional) on Conductivity of HITTS Fuels

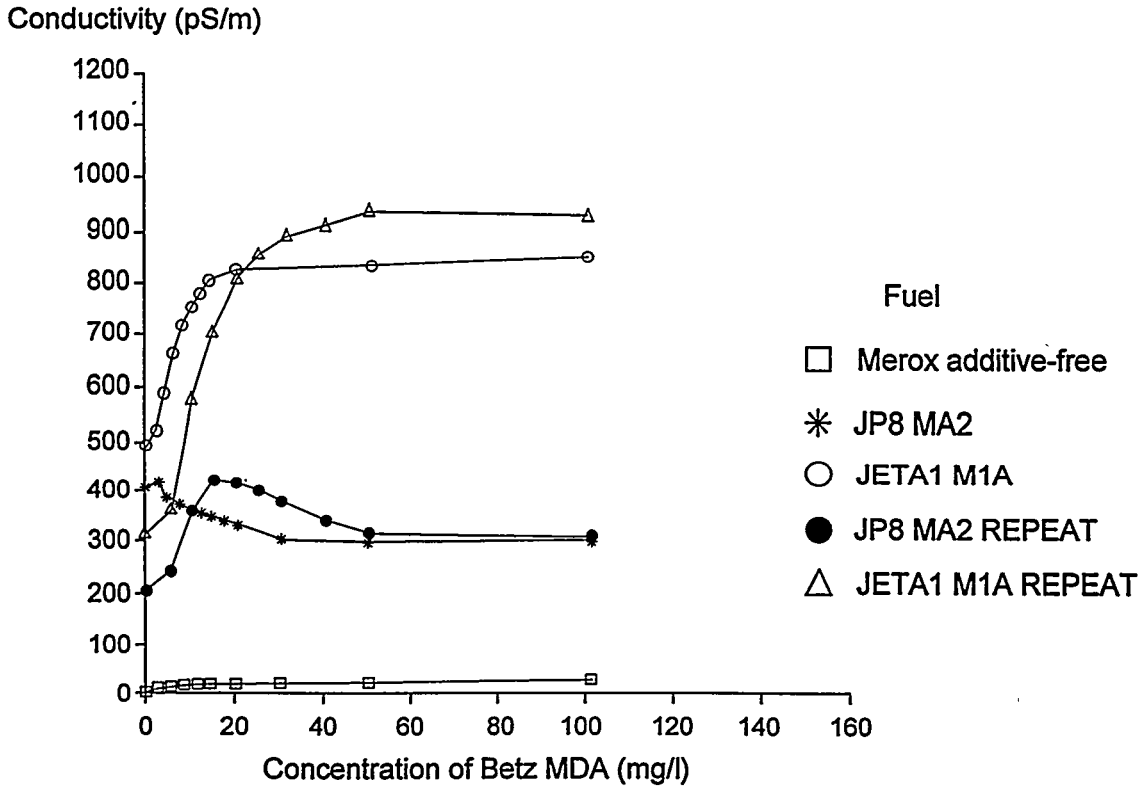


Fig. 10 Effect of Betz MDA on Conductivity of HITTS Fuels

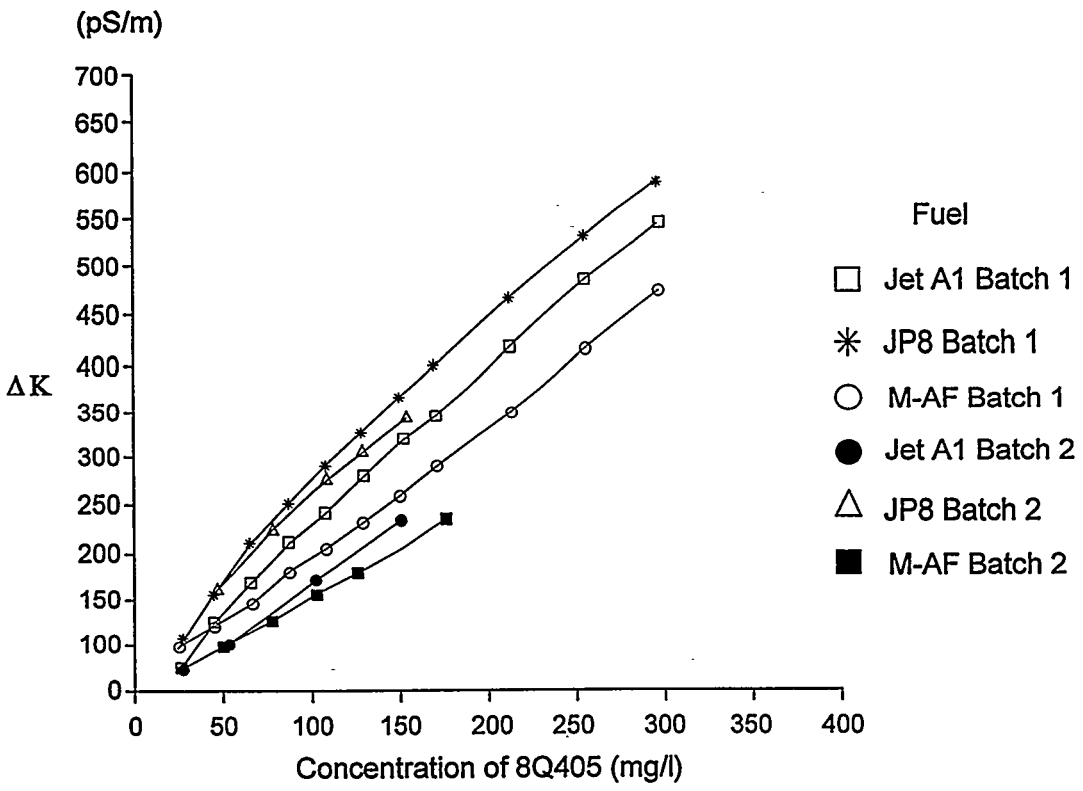


Fig. 11 Effect of 8Q405 and Batch Variation on the Conductivity of HITTS Fuels

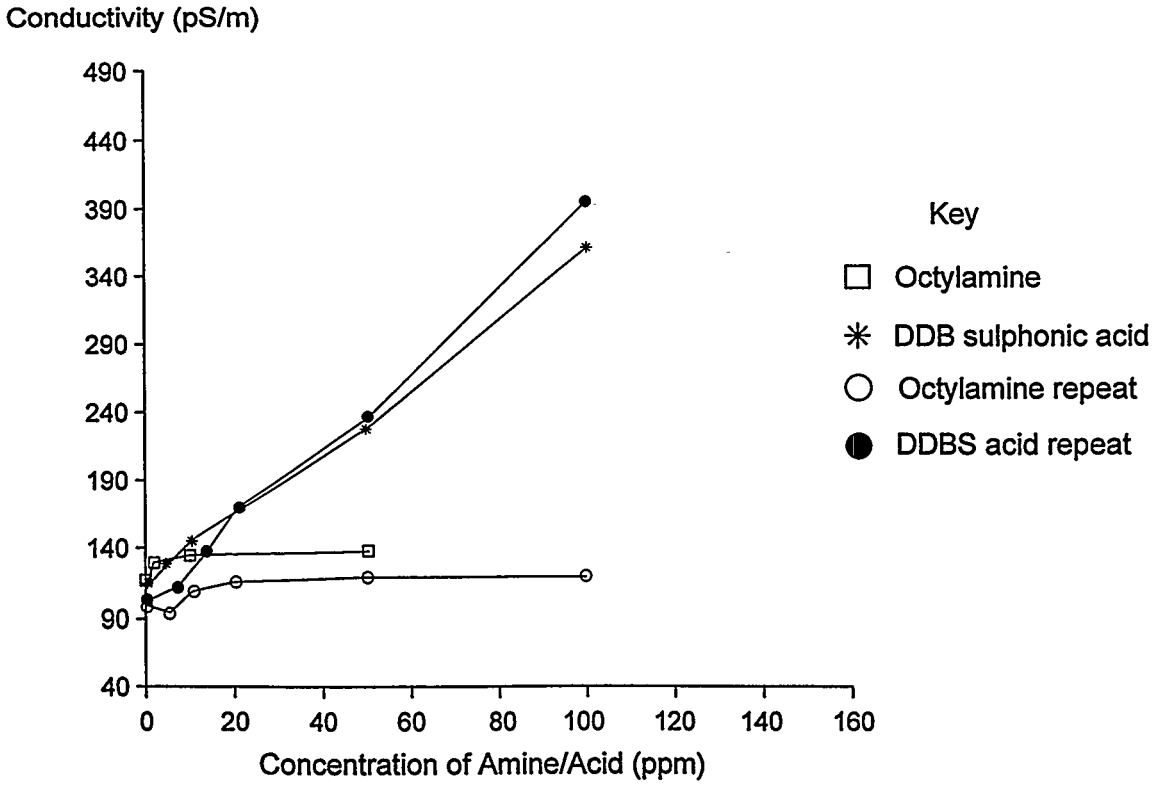


Fig. 12 Betz Dispersant 8Q405(Batch 2) 100mg/l in HITTS Additive-free Merox
Effect of Acid or Amine on Conductivity

6th International Conference
on Stability and Handling of Liquid Fuels
Vancouver, B.C. Canada
October 13-17, 1997

TESTING JP-8+100 PACKAGES IN EUROPEAN JET FUELS - EVALUATING AND UNDERSTANDING BENEFITS AND DRAWBACKS

Joanna M Bauldreay*, William G Blundell, Richard J Heins, Geoffrey Houlbrook and Johanne Smith

Shell Research & Technology Centre, Thornton, P.O. Box 1, Chester, CH1 3SH, UK.

The UK's Ministry of Defence (MoD) has instigated a European extension of the JP-8+100 programme, testing front-runner USAF additive packages and other additives from UK companies in European-sourced jet fuels. Shell Research Ltd have provided Jet A-1 fuels and upgraded them to military specifications (JP-8 = NATO F-34) by the use of fuel system icing inhibitor and corrosion inhibitor/lubricity improver (CI/LI) additives. Fundamental, analytical, small-scale and large-scale rig tests have been used to examine how and if the additives improve thermal stability performance. A Flask Oxidation Test investigates the first stages of fuel oxidation and indicates that none of the additives has a significant impact on this step. Later stages in the fuel degradation are affected as evidenced by higher JFTOT breakpoints, lower levels of deposit in a carbon burn-off version of the JFTOT, and lower levels of deposition in Shell's new HiReTS (High Reynolds number Thermal Stability) rig. Fuels containing both CI/LI and JP-8+100 additives produce the greatest apparent improvements in thermal stability performance. Other performance characteristics have been tested in parallel: lubricity, handling (e.g. water shedding), low temperature and storage stability. CI/LI additives alone improve fuel lubricity (JP-8 better than Jet A-1) but lead to a drop in handling performance. None of the JP-8+100 additives significantly affects lubricity performance but results for water shedding tests are further worsened. Low temperature behaviour is insensitive to the presence of the additives while accelerated storage tests indicate that the JP-8+100 additivated fuels produce higher levels of gums than the base fuels.

INTRODUCTION

The United States Air Force and its collaborators have established that the thermal stability performance of military jet fuels can be improved by using additive packages. Many papers and presentations have been made in the last six years, for instance, at the last conference in this series[1]. In the UK, the Ministry of Defence (MoD) has instigated a European extension of USAF's JP-8+100 programme, managed by the Defence Evaluation & Research Agency (DERA), Pyestock. Additives have been tested in fuels, produced from a different slate of crudes to those used in North America, and which are supplied as Jet A-1 to DEF STAN 91-91 specification (or to the AFQRJOS "Checklist"). Such fuels must contain a static dissipator additive (SDA) and, if hydroprocessed, an antioxidant (AO).

Testing "same batch" additives in a common set of fuels is allowing MoD-sponsored companies to maximise the read across between experimental results. Experiments range from

small-scale fundamental tests to specification tests to large-scale rig operations. Various in-house methods have been used thereby providing new insights into how and if particular additives affect performance. Shell Research Ltd have been concentrating on small-scale tests covering not only thermal stability performance but also side-effects and storage stability evaluations. The performances of Jet A-1 and JP-8 fuels with additive packages or single components are now compared with those of the baseline fuels.

EXPERIMENTAL

Reagents. Large volumes of three fuels have been procured for the MoD programme: JPTS (provided by USAF via RAF Killingholme); a deliberately marginal thermal stability Merox base fuel (AT); and a hydroprocessed Jet A-1 (HT-1A). JPTS is the "target" fuel whose thermal stability performance JP-8+100 fuels are intended to approach. Two tanks of AT have been upgraded to Jet A-1 (M-1A), by the addition of 2 mg/L of new formulation Stadis 450 static dissipator, the dosage level having been advised by S.D. Anderson of USAF Dayton. Table 1 lists additives and additive packages used to upgrade or modify the fuels. It includes mandatory and JP-8+100 performance and component additives such as DMD-2, a 50% active matter metal deactivator additive (MDA). Samples of both Jet A-1 fuels, in 200-litre epoxy-lined steel drums, have been further upgraded to JP-8 fuels by the addition of mandatory fuel system icing inhibitor (FSII) and corrosion inhibitor/lubricity improver (CI/LI) additives (Table 1). Originally this conversion was achieved by adding AL-48 to the Jet A-1 but the concentration chosen led to 20% overdosing of the CI/LI component so all subsequent blends have been made by adding FSII and CI/LI separately. Unless otherwise indicated non-mandatory and "performance" additives have been doped singly or as packages directly into 25 to 50L batches of Jet A-1 and JP-8 fuels at the levels indicated in Table 1. (Most of the work relates to fuels treated with some or all of the components of the Betz Spec Aid 8Q462 package that has formed the basis of most JP-8+100 field trials by USAF.) BHT blends have been prepared by first dissolving the BHT powder in a small portion of fuel before making up to the final volume. M-1A has also been used to prepare a 200L stock of 2 mg/L active matter MDA, WF, to match the 8Q462 concentration of MDA. Aliquots of this stock have been diluted to produce the 25L blends WG and WH described in Table 4. BP have supplied four fuels (based on AT) that they have doped with their candidate additives A to D.

Apparatus and Procedures. Four classes of tests have been performed on the fuels: Certificate of Quality, CoQ, or specification tests; industry standard tests not required by specifications; non-industry tests using specification apparatus in non-standard modes; in-house (IH) analytical or "rig" tests using non-specification apparatus. All CoQ tests are performed according to the ASTM and/or IP methods required by, e.g. DEF STAN 91-91 Issues 1 & 2. Most industry tests are performed according to the indicated ASTM or IP method. Particulate contaminants have been measured using a modified version of ASTM D2276/IP 216; only 1L of fuel is filtered through a 0.22 μm filter. Low temperature flow

properties have been measured by an in-house variant upon ASTM D 4305-83 that uses a Mark I Setapoint apparatus modified to automate some of the heating and cooling stages.

Analytical. Copper and iron contents of fuels have been measured by an in-house quantitative ICP-MS method which compares signals with those from a standard solution of the two metals in metal-free Jet A-1. Other metal contents are measured using a semi-quantitative ICP-MS method which relies on a S21 Conostan mixed element standard diluent doped into Jet A-1. This gives approximate elemental concentrations in the sample to within a factor of three of the true value but results are only reported if the isotope signals are significantly above fluctuations on a blank solution.

Thermal stability. Two more quantitative versions of the JFTOT test have been performed using standard model 203 or 240 apparatus. JFTOT breakpoint has been established by identifying, to the nearest 5°C, the highest temperature at which the fuel still passes the rating and pressure drop restrictions of ASTM D3241/IP 323. The JFTOT carbon burn-off (CBO) method uses stainless steel test pieces and operates the JFTOT at 350°C. A Leco analyser measures the carbon content of the resultant deposit. A flask oxidation test[2] has been used to investigate the very early stages of fuel degradation that precede deposit formation. Oxygen uptake is measured as air is passed through samples held at 160°C, and the oxidation rate versus time profile allows induction periods and/or radical initiation rates to be calculated. A new apparatus, the High Reynolds number Thermal Stability rig, HiReTS,[3] (or its laboratory forerunner, the Capillary JFTOT (C-JFTOT)) has been used to measure the amount of deposit formed under turbulent flow conditions. Standard two hour tests have been performed, with a 290°C fuel outlet temperature condition. Quoted HiReTS (or C-JFTOT) numbers and, where appropriate, end-of-test carbon weights in the capillary test pieces refer to averages of duplicate determinations unless otherwise indicated. (C-JFTOT numbers can be compared from table to table, but at this stage, it is only appropriate to compare HiReTS results obtained in a restricted series of tests, invariably displayed in a single Table.)

Lubricity and water shedding tests. The Thornton Aviation Fuel Lubricity Evaluator (TAFLE) establishes the highest load a fuel can bear before a cylinder-on-cylinder contact starts to break down because of scuffing wear. The rig operates in a one-pass mode and measures the friction and wear generated as contacts are made with progressively higher loads between two different hardness EN31b steel discs, one fixed and one rotating. Unless indicated otherwise, TAFLE loads are the average of duplicate determinations. WASP, an in-house test[4], involves preparing a fine 1000 ppm water-in-fuel emulsion then measuring the water content at a fixed depth after a 45 minute settling period. The lower the water content the better the water shedding properties, and experience shows the fuel is less likely to cause problems such as coalescer disarming.

Storage stability. Two 5L portions of each fuel have been stored in epoxy-lined cans in a thermostatically controlled cabinet held at 45°C to accelerate processes that might occur in

sample storage at ambient conditions. Cans have been removed after 6 or 12 weeks of storage and certain small-scale (CoQ, analytical and rig) tests have been repeated to check for product degradation. (These conditions are not as severe as those required for the JPTS specification, MIL-T-25524D.) Where a particular fuel has been stored in more than one large tank, samples from each have been taken for storage tests.

RESULTS

JPTS. CoQ tests have confirmed that the JPTS sample meets MIL-T-24424D. Its freeze point is -63.5°C, well within the specification. Several properties have changed slightly after storage: Saybolt colour, total acidity and the level of filterable particulates. Its behaviour in non-standard tests is summarised in Table 2. Poor WASP and MSEP test results are consistent with the high levels of surfactant additives in the fuel and which are at least partially responsible for the excellent thermal stability performance. The flask oxidation test induction period is about twice the length observed for normal hydrotreated fuels indicating excellent resistance to the first stages of oxidation. Those tests that look at the later stages of degradation, when deposits are laid down, show the fuel to be very stable. Whether this is wholly because of reduced radical initiation rates or whether it is because the additives prevent adhesion of fuel deposits (in the bulk or on surfaces) is not clear. Figure 1 shows a trace for JPTS in the laboratory C-JFTOT apparatus; with the standard operating conditions, the result is at the lower limit of deposit detection.

Merox Jet A-1. Table 3 records key CoQ and other test results for the base fuel, AT, and the Jet A-1 produced from it, M-1A. AT meets the Jet A-1 specification except in the area of conductivity; there had not been any SDA addition to this moderately high sulphur content fuel at the refinery. It is borderline on flash point and smoke point performance, with quite low IBP and FBP. Metals contents, except lead, are fairly insignificant. M-1A, with SDA, passes the conductivity requirements of DEF STAN 91-91 but its water shedding properties have degraded; the fuel would be expected to have borderline handling properties. The first breakpoint measured for AT was 270°C. Breakpoints measured for M-1A started at a similar level but, as with those for AT, have degraded over time; samples now give results of 260±5°C. A TAFLE failure load of 102.5 kg for AT is very good, consistent with the fuel's moderately high total sulphur content though perhaps better than one might first have anticipated from its BOCLE result. Previous work at Thornton, however, has shown that scuffing resistances of high sulphur fuels are underestimated by the BOCLE which operates under a different, milder wear regime.

Approved additives (WF, WG, WH & WI). Fuels have been tested that just contain MDA or BHT, two already approved components in the USAF front-runner 8Q462 package. MDA is an additive with a reputation for "fooling" the JFTOT[5]. BHT would normally only be added to hydroprocessed fuel on run down at the refinery, to provide antioxidancy at ambient temperatures. Preliminary results are in Table 4 as are results for the base fuel, M-1A,

retested in parallel. Few of the simple analytical tests show any significant change upon the additivation and none of the additives affect BOCLE performance. Thermal stability tests do respond to the additives, though differently. HiReTS numbers for WF and WI are only slightly lower than those for M-1A. By contrast, the JFTOT breakpoint for WF is at least 340°C.

Jet A-1+100 (VX, VY and WW). M-1A (not from same tank as above) has been doped with 8Q405 and 8Q406 to produce fuels VX and VY, respectively. WW has been produced by doping another M-1A tank sample with the "full" 8Q462 package. Table 5 lists the current status of analytical and small-scale tests. BOCLE results for these three fuels and M-1A are not significantly different. Additivation notably worsens performances in the handling tests - MSEP, WASP and water reaction - consistent with the presence of the dispersant/detergent additive that makes up 8Q405. Conductivities of all three fuels exceed the limits for Jet A-1. All three additives or packages also produce significant (approximately 30°C) rises in JFTOT breakpoint; the presence of antioxidant in VY has not produced any further improvement over the performance of VX but MDA in WW provides a 5°C increase. The appropriate M-1A was tested in the HiReTS before and after the two additivated fuels; before, the average HiReTS result was 840 while a single run at the end of the series gave a result of 621. Results for VX and VY are very low, at the limit of detection of the apparatus, suggesting excellent thermal stability improvements have been achieved. Storage stability results for VX, VY and M-1A are in Table 6 and show that the fuels have deteriorated slightly with respect to Saybolt colour and MSEP (albeit that this last test is of dubious worth for additivated fuels). Conductivities have decreased in every case, more markedly for the base fuel than the additivated ones, and now all are within Jet A-1 specification limits. WASP ratings and water reaction test results for VX and VY have remained bad, and existent gum levels have worsened. None of the fuels have deteriorated in JFTOT or corrosion tests.

Merox JP-8 (M-2A). Table 3 includes test results for an early (i.e. CI/LI overdosed) batch of M-2A. Compared with the base and Jet A-1 fuels there are slight increases in thermal stability performance and a worsening with respect to existent gum, total acidity and water shedding properties. These changes and the improved lubricity (BOCLE) performance are directly ascribable to the addition of the acidic CI/LI component which is a surfactant designed to adsorb onto metal surfaces. The first flask oxidation test result for M-2A indicated that the radical initiation rate for JP-8 was lower than for the base fuel, AT. A second FOT result, about a year later, was greater for M-2A than for AT. The later result indicates fuel deterioration has taken place and/or that the original difference in radical initiation rate was not significant. M-2A has a breakpoint 5°C higher than that first measured for AT and M-1A; bigger differences are apparent in the C-JFTOT. AT has a single test result of 1040 while the average result for M-2A is 434. Figure 2 shows one of the C-JFTOT traces for M-2A.

JP-8+100 (VO and M-4A). Table 7 lists test results for the CI/LI overdosed JP-8 doped with 8Q405 and 8Q406. MSEP, WASP and water reaction results are very bad for both fuels,

again consistent with the presence of a highly surface active dispersant/detergent additive. As expected from work at Thornton and elsewhere[6] the additives further boost the fuel conductivities, in this case above the Jet A-1 maximum limit of 450 pS/m; one of the VO results would also fail the F-34 (JP-8) specification[7] limit of 600 pS/m maximum.

Flask oxidation test results for the two fuels are similar, and only slightly lower than the latest result for JP-8, suggesting that the additives have no significant impact on the early stages of fuel oxidation. Breakpoints for both fuels, however, are significantly increased over the JP-8 result of 275°C. M-4A shows a further dramatic improvement in C-JFTOT number over that seen for M-2A (Figure 3), with the average C-JFTOT number being very similar to that obtained for JPTS. CBO deposit weights are much lower for these fuels than for the JP-8; differences between the results for VO and M-4A are not very large. These suggest that the apparent thermal stability improvements are achieved mainly by dispersant/detergent action and not by antioxidant action.

Lubricity results for VO and M-4A are similar but may just be significantly different from the JP-8 BOCLE result of 0.53 mm. There may be some interaction in the bulk fuel or at the metal surface between the dispersant/detergent and the CI/LI or the results may be an indication of the BOCLE's sometimes dubious response to additives. Storage stability tests have been completed for a new, second batch of JP-8 fuels, with and without Betz additives (Table 8). Saybolt colour and conductivity results have changed for the JP-8 but all fuel handling related test results have stayed similar, all pointing towards a fuel with high surfactant content and poor water shedding properties. Corrosion and thermal stability test results have remained satisfactory. VO and M-4A have shown less dramatic decreases in Saybolt colour and have slightly higher existent gum levels than M-2A.

Hydrotreated Jet A-1. CoQ, simple analytical test results and additive details for a sample from one of the three HT-1A tanks are in Table 9. These data show that the fuel meets all specification requirements for Jet A-1, with freeze point close to the maximum acceptable value. Table 9 also includes JFTOT breakpoint values, metals contents and WASP results. Breakpoints have varied slightly from tank to tank (results are shown for all three tanks in this case) and are at the low end for hydrotreated fuels. They still indicate a more thermally stable fuel than the Merox fuel in the programme. All UK participants have noted problems in rating the JFTOT tubes for this fuel and some derived from it; unusual white deposits have been observed. Oxidation rate profiles in the flask oxidation test have also been unlike those seen for most hydroprocessed fuels. After an induction period, the oxidation rate increases (as normal) but then falls again suggesting that the system has produced its own antioxidancy. (This may or may not have some link to the odd JFTOT deposits and rising breakpoints, and to the fuel's relatively high sulphur content compared with previous samples from the same refinery). The behaviour warrants investigation, but in the meantime the traces have been analysed according to normal rules for hydroprocessed fuels: induction times have been

measured and radical initiation rates have then been calculated given known antioxidant dose rates. The radical initiation rates are about an order of magnitude lower than those for the Merox fuels, consistent with the better JFTOT performance of HT-1A. HT-1A also produces much lower levels of deposit in the HiReTS; Figure 4 provides an example of a typical trace. The fuel does not deteriorate significantly in 12 weeks of accelerated storage, indicating that the mandatory antioxidant has been effective. WASP ratings for HT-1A are moderate rather than good; the fuels are not excellent water shedders but one would not anticipate undue handling problems with them. MSEP values, though not required because of the added SDA, are satisfactory. BOCLE results for the two samples taken are similar to those of the Merox base and Jet A-1 fuels and, taken on their own, do not indicate that any lubricity problems should be experienced. The TAFLE results, however, show the fuels to have considerably less lubricity than the Merox fuels.

Jet A-1+100 (VT and VU). Table 9 shows small-scale and storage stability test results for fuels derived from one of the HT-1A tanks. Rig tests show that the performance additives have no significant impact on lubricity performance. JFTOT breakpoints have improved by 20 to 25°C on the Jet A-1, and limited HiReTS test results show the additives give about half as much deposit as HT-1A (see Figure 5). Neither test shows a significant difference between the 8Q405 and 8Q406 packages. CBO deposit weights for VT fuels are, if anything, greater than a Jet A-1 result of 38 µg; maybe at 350°C the deposit is a combination of fuel and additive. After storage, changes in Saybolt colour, acidity, JFTOT and peroxide number are small. All fuels still produce poor MSEP and water reaction test results. WASP results have improved numerically (though not significantly) but still show all the fuels to have poor handling characteristics. All have acceptable thermal stability and conductivity performance, though the latter test values have decreased.

JP-8 (HT-2A). HT-2A has a breakpoint significantly higher than that of the Jet A-1, and higher than that achieved by using Betz additives; see Table 10. The impact of CI/LI additive is also shown by the higher total acidity and improved BOCLE performance; the fuel has marginally worse lubricity performance than the CI/LI overdosed Merox-based JP-8 but both results are still "good". A single TAFLE result confirms the improvement in fuel lubricity. The WASP result is worse than that for the Jet A-1 and indicates a fuel of borderline handling properties. Conductivity is well within specification. Storage stability results for the JP-8 are given in Table 11. MSEP and WASP ratings worsen, though water reaction results remain unchanged. Black fibres (not analysed) have been seen in the aged product, consistent with the unusually high levels of filterable deposits.

JP-8+100 (VZ and WA). Most tests results for the two additivated JP-8s are different from those for the JP-8 (Table 10). Existent gum levels are higher, WASP and MSEP ratings are worse, and both fuels exhibit increased conductivity. Breakpoints are significantly higher than those for the JP-8, and are higher than for the additivated Jet A-1s and corresponding

Merox-based fuels. HiReTS test numbers show a small reduction with the additives but the differences are probably not significant for these already thermally stable fuels. The same is true for the BOCLE results for the additivated fuels; all give good performances. Storage stability test data in Tables 11 show few significant changes for the additivated fuels. Saybolt numbers appear to cycle with time. Water reaction test results worsen, with no clear trend for the already poor MSEP and WASP performances of the two fuels.

Assessment of BP candidate additives. Small samples of Merox base fuel, M-1A, additivated with candidate BP additives A to D have been tested as a small suite in the HiReTS production prototype unit 1. A sample of M-1A fuel was also included in the test suite; it has given borderline performance in the JFTOT (260°C breakpoint at best). There was insufficient fuel to perform other tests. Results from duplicate tests are summarised in Table 12, and Figures 6 and 7 are examples of the HiReTS profiles. One test ended prematurely so the result for additive C is not the average of duplicate tests. All four candidates produce very significant improvements in the thermal stability of the Merox fuel. The HiReTS repeatability at these levels means, however, means that the additives cannot be considered as having significantly different thermal stability improving properties.

DISCUSSION

The two base fuels chosen for the programme have considerably less thermal stability than the target JPTS, and are amenable to showing thermal stability improvements produced by additives. The Merox fuel has been consistently less stable than the hydrotreated fuel. Thermal stabilities and lubricities of both improve in at least one test just with the addition of JP-8 packages though these same packages then worsen fuel handling properties; this is not surprising since CI/LI additives are strong surfactants. Addition of Betz additives to the Jet A-1 and JP-8 fuels improves thermal stability and tends to further worsen handling properties; the dispersant/detergent component is the most potent component in this respect. BHT and MDA additions make, at best, small improvements in thermal stability and none of the additivated fuels match the JPTS fuel in terms of JFTOT performance.

A full suite of fuels have yet to be tested in all the pertinent rigs, and new types of performance additives are currently being tested. Nevertheless, some trends or features are clear and findings can be carried forward. Certain CoQ categories are unaffected by the presence of the additives. None has yet affected corrosion, combustion or volatility properties. Likewise, none of additives tested has affected the low temperature performance features - low temperature viscosity, freeze point, Setapoint flow temperatures - of the Jet A-1 or JP-8 into which they are doped. This means that most JP-8+100 fuels will not match the low temperature performance of JPTS, for which maximum freeze point requirement is -53°C, 6°C lower than Jet A-1 specifications demand. If JPTS-like low temperature performance is needed for a particular application, the operator either will have to use JPTS or will have to specially procure lower freeze point Jet A-1/JP-8 fuels. Only fuels derived from naphthenic

crudes or produced by hydrocracking are likely to meet these criteria. Storage stability tests have not identified any unexpected or particularly worrying or trends; handling properties have tended to worsen and the additive packages have not obviously slowed down fuel degradation processes.

Conductivity data for the additivated Merox fuels may be misleading. The performance additives (directly or indirectly) boost the conductivities significantly, to above specification levels. The Jet A-1 already had a high conductivity because of the high SDA dope rate; refinery dope rates are typically 1 to 1.5 mg/L SDA and the performance additives might not cause failures if added to a Jet A-1 with an optimised SDA dosage. Corresponding hydrotreated fuels, with 1.0 mg/L of SDA, do not give such high conductivities and the Jet A-1 has a higher conductivity than the JP-8, the reverse of the Merox fuel cases. This may be because of the lower additive levels or because the old Stadis 450 and the CI/LI may have interacted in a different manner in the hydrotreated JP-8 to that seen between the new Stadis 450 and CI/LI combination in the Merox JP-8. There may be some interesting fuel:additive, CI/LI:additive, SDA:CI/LI:additive combinations to investigate in more detail. Conductivity and lubricity studies could be performed in parallel; lubricity data do not yet show signs of any significant synergies or antagonisms between the components. None of the Betz additives provide Merox or hydrotreated Jet A-1 with a boost in lubricity performance or significantly degrade the performance of the JP-8 fuels. This suggests that the CI/LI additives are more strongly adsorbed to the metal surfaces than the Betz additives over the range of temperatures experienced in the BOCLE's ball-on-cylinder contact zone. BOCLE data have yet to be obtained for Jet A-1 or JP-8 with MDA in the full 8Q462 package to see if MDA might be another additive that can affect lubricity performance. The mean wear scar diameter of 0.66 mm for JPTS, while good, is higher than one might have anticipated for a fuel with mandatory CI/LI additives. This may indicate some interaction between the many additives in JPTS which include the multi-component JFA-5 additive, which itself contains MDA.

Only in the area of prime interest, thermal stability, are there any large issues to be sorted out. The HiReTS rig, operated in its standard format, certainly appears to differentiate between fuels of different thermal stability. (Without longer time data, it is not possible to establish whether the system may have been fooled by CI/LI and other additives, i.e. whether effects are only short-lived.) As performances improve, the scope for differentiation becomes smaller; the deposits approach the IR camera's limit of detection of temperature changes. Used with a poor fuel, the HiReTS can certainly identify additives which can improve other fuels' performances. The protocol should probably be altered to produce a more severe test if it is to rank performances of "good" additives, e.g. to differentiate between the various BP additives or to compare the BP additives with the Betz packages.

In its standard mode, the HiReTS rig has been a good predictor of at least one large rig simulator. Some of the additivated systems are now starting to be ranked differently in the

HiReTS to the way the JFTOT tests would rank them. Planned large-scale rig tests may clarify why this is happening but in the short term it suggests that traditional measurements of thermal stability should be treated with caution when additives are introduced into fuels. One case to illustrate the problem is the work with MDA-doped M-1A which, though not yet complete, shows that 2 mg/L MDA significantly improves JFTOT breakpoint whereas the HiReTS result is only marginally improved. The effect of the same level of MDA in the full 8Q462 package in the same Jet A-1 is nowhere near as dramatic - the breakpoint is 295° rather than >340°C. Has the HiReTS been responding, correctly, just to a slightly reduced radical initiation rate caused by the chelation of low levels of copper and iron in the fuel while the JFTOT test piece responds to differing levels of MDA adsorption from the two fuels?

Discussions with USAF and other MoD-sponsored companies suggest that the bulk of the findings of the Shell work do not contradict results obtained with other rigs and fuels. There are fuel-to-fuel variations in the performances of additivated fuels, and fuel handling properties are invariably degraded as thermal stability properties are improved. If the differences and new findings in this report can be resolved, real progress will have been made.

ACKNOWLEDGEMENTS

The authors thank other colleagues, past and present, at Shell Research Ltd for their contributions to the project which has been funded jointly by Shell International Oil Products and DERA Pyestock.

REFERENCES

(1) See *Proceedings of 5th International Conference on Stability and Handling of Liquid Fuels*, Rotterdam, The Netherlands, October 3-7, 1994. Papers by, e.g. Anderson,S.D,. Zabarnick,S., Binns, K. and colleagues.

(2) Kendall,D.R.; Clark,R.H.; Stevenson,P.A. *The influence of polar compounds on the stability of jet fuel,* 2nd International Conference on long-term storage stability, San Antonio, Texas July 29 - August 1, 1986.

(3) Bauldreay,J.M.; Heins.R.J.; Houlbrook,G.; Smith,J. *High Reynolds number Thermal Stability (HiReTS) rig for realistic, rapid evaluation of distillate fuel thermal stability.* In these proceedings.

(4) Hughes,V.B. Paper presented at the Coordinating Research Council, Alexandria, Virginia April 22-26, 1996.

(5) Clark,R.H. *Proceedings of 3rd International Conference on Stability and Handling of Liquid Fuels,* London, UK, September 13-16, 1988.pp 283-293.

(6) Dacre,B.; Hetherington,J. *Electrical Conductivity of HiTTS Additive Packages for the JP8+100 Programme.* In these proceedings.

(7) Interim DEF STAN 91-87/Issue 1 23 December 1994.

TABLE 1 - Additives for HiTTS/JP-8 programme and Fuels containing them

Additive name (type)	*Type*	*Dope rate*	*Main blends:*
"New" Stadis 450	SDA	2 mg/L	M-1A (& VX,VY,WW,WF, WG,WH,WI) and M-2A (& VO,M-4A)
AL-48 Type 6 (see DEF STAN 68-150/Issue 1)	FSII + CI/LI (Nalco 5403)	0.13%vol	M-2A, 1st blends (& VO,M-4A 1st blends)
AL-41 (NATO code S-1745) (see (Interim) DEF STAN 68-252/Issue 1) Nalco 5403	FSII CI/LI	0.13% vol 22.5 mg/L	M-2A, 2nd blends (& VO,M-4A 2nd blends); HT-2A (& VZ,WA)
DMD-2 (50% Active matter)	MDA	2 mg/L max, AM (see Table 4)	WF, WG, WH
BHT = 2,6-di-tert-butyl-p-cresol	AO	25 mg/L	WI
Betz Spec Aid 8Q405	"Dispersant/detergent"	100 mg/L	VX, VO, VT, VZ
Betz Spec Aid 8Q406 = 8Q405 + BHT	Disp/det + AO	125 mg/L	VY, M-4A, VU,WA
Betz Spec Aid 8Q462	(Disp/det + AO + MDA) + Aromatic solvent = 1:1	254 mg/L	WW

TABLE 2 - In-house tests on JPTS[1]

Specification Description	*Method*	*Units*	*Value*
CONTAMINANTS			
WASP rating	SMS 2772	(mg/kg)	1080
Metals	PT/71:GM08		
Copper		(ppb)	6
Iron		(ppb)	<3
(THERMAL) STABILITY			
Breakpoint	SEM/004	(°C)	≥ 380
Flask oxidation test	SEM/008		
Induction time		(minutes)	137.5
Capillary JFTOT	Under dev		17.8
CBO Deposit weight	SEM/003	(µg/C)	21.1
LUBRICITY			
Wear scar diameter (BOCLE)	D 5001	(mm)	0.66

[1] *In this and following tables: * = Not a specification test; RT = retest; (xw) = test result after x weeks accelerated storage at 45°C; # = Retest on 2nd blend.*

TABLE 3 - Progress on tests with Merox-based fuels for HiTTS

Fuel Code:			AT (Base)	M-1A(Jet A-1)	M-2A (JP-8)
PT/A Test Results:	Method	Units	Value	Value	Value
APPEARANCE					
Appearance	UK 1636		B&C	Satisfactory	Satisfactory
Saybolt Colour*	D 156		28		26
COMPOSITION					
FIA Aromatics	D 1319/IP 156	(%V)	19.3		
Mercaptan sulphur	D 3227/IP 342	(%m/m)	0.0008		0.0009
Total sulphur	D 1266/IP 107	(%m/m)	0.18		
	D 2622/Inhouse	(%m/m)	0.170		0.175
Total acidity	D 3242/IP 354	(mg KOH/g)	<0.001	0.004	0.004
VOLATILITY					
Distillation (partial) IBP/FBP	D 86/IP 123	(°C)	144.0/245.0		
Flash point, Abel	IP 170	(°C)	38.5		
Density @ 15°C	D 1298/IP 160	(kg/m3)	792.2	792.6	793.0
FLUIDITY					
Freezing point	D 2386/IP 16	(°C)	-52.0		-50.5
Viscosity @ -20°C	D 445/IP 71	(cSt)	3.698		3.710
COMBUSTION					
Specific energy	D 4529/IP 381	(MJ/kg)	43.339		
Smoke point	D 1322	(mm)	25		
(THERMAL) STABILITY					
JFTOT - Pressure drop/VTR	D 3241/IP 323	(mm Hg/-)	0.0/2	<1/1	<1/1
CORROSION					
Copper Corrosion (2h/100°C)	D 130/IP 154		1A		1A
Silver Corrosion (4h/50°C)	IP 227		0		0
CONTAMINANTS					
Existent gum	D 381/IP 131	(mg/100mL)	1		4
Particulate contaminant*	D 2276/IP 216 mod	(mg/L)	0.8	0.4	0.30
Water reaction, interface rating	D 1094/IP 289		1B	1B	1B
MSEP	D 3948		98	93	49
WASP rating*	SMS 2772	(mg/kg)	220	720	1200
Metals* - Copper, Iron	PT/71:GM08	(ppb)	<8, 5.5	4, 6	3, <4
Other (semi-quantitative)		(ppb)	Pb 164	Pb 124	Pb 200, Zn 7
OTHER TESTS					
Peroxide number*	D 3703	(ppm)	1	1	<1
Conductivity	D 2624/IP 274	(pS/m @ °C)	3 @ 20.5	325 @ 21.0	430 @ 23.0
IH FLUIDITY					
Flow/No-flow temp (Setapoint Mk 0)	SEM/024	(°C)		-48.7/-51.4	
IH (THERMAL) STABILITY					
Breakpoint	SEM/004	(°C)	270 then 260	270, 260, 260	275
CBO Deposit weight	SEM/003	(µg/C)	77.2	146	102.6
Total acidity (inc retests)	TMS 448/93	(mg KOH/g)	0.0009	0.0018, 0.0021	0.0036, 0.0042
Flask oxidation test, Ri	SEM/008	(Mol/L/s)	3.82E-7		2.66E-7, 5.26E-7
C-JFTOT number	Under dev		1039.6(1)		434.15
IH LUBRICITY					
Wear scar diameter (BOCLE)	D 5001	(mm)	0.75	0.74	0.53
Failure load (TAFLE)	SEM/013	(kg)	102.5		

TABLE 4 - Analytical & small scale test results for approved additives in Merox Jet A-1

Fuel Code/Additive:			M-1A	WF/MDA	WG/MDA	WH/MDA	WI/MDA
		mg/L:	0	2	1	0.5	25
Specification Description	*Method*	*Units*	*Value*	*Value*	*Value*	*Value*	*Value*
COMPOSITION							
Total acidity	D 3242/IP 354	(mg KOH/g)	0.001	0.001			0.001
(THERMAL) STABILITY							
JFTOT- Pressure drop/VTR	D3241/IP 323	(mm Hg)/-	<1/1	<1/1			<1/1
Breakpoint	SEM/004	(°C)	~260	≥340	325	305	260
CBO Deposit weight	SEM/003A	(µg/C)	146				
HiReTS	"Standard"						
HiReTS number (start/end)			>1697/ >1617	1468.5			1418.1
Carbon burn-off (start/end)		(µg)	238/229	103			173
CONTAMINANTS							
Existent gum	D 381/IP 131	(mg/100mL)	<1	1	<1	<1	1
Particulate contaminant	D2276/IP 216	(mg/L)		0.4			0.6
Water reaction, interface rating	D 1094/IP 289		1B	1B	1B	1B	1B
MSEP	D 3948		63	54			71
WASP rating*	SMS 2772	(mg/kg)	350	480	440	770	540
OTHER TESTS, LUBRICITY							
Conductivity @ 20°C	D 2624/IP 274	(pS/m)	253	298	300	314	285
Wear scar diameter (BOCLE)	D 5001	(mm)	0.74 (4)	0.76 (4)	0.76 (4)	0.755 (5)	0.755 (4)

TABLE 5 - Main small scale & analytical test results for additivated Merox Jet A-1 fuels

Fuel Code/Additive:	Method	Units	VX/8Q405	VY/8Q406	WW/8Q462
APPEARANCE, COMPOSITION					
Saybolt Colour*	D 156		+20	+20	+18
Total acidity	D 3242/IP 354	(mg KOH/g)	0.004	0.004	0.007
FLUIDITY					
Freezing point	D 2386/IP 16	(°C)	-51.5	-51.0	
Viscosity @ -20°C	D 445/IP 71	(cSt)	3.736	3.792	
COMBUSTION, CORROSION					
Specific energy	D 4529/IP 381	(MJ/kg)	43.371	43.368	
Copper Corrosion (2h/100°C)	D 130/IP 154		1A	1A	1A
(THERMAL) STABILITY					
JFTOT- Pressure drop/VTR	D 3241/IP 323	(mm Hg)	1/1	<1/1	<1/1
CONTAMINANTS, OTHER TESTS					
Existent gum	D 381/IP 131	(mg/100mL)	1	2	2
Particulate contaminant	D 2276/IP 216	(mg/L)	0.5	0.4	1.1
Water reaction, interface rating	D 1094/IP 289		2	2	4
MSEP	D 3948		55	54	49
WASP rating*	SMS 2772	(mg/kg)	920	812	560
Peroxide number*	D 3703	(ppm)	0.2	0.2	<0.1
Conductivity	D 2624/IP 274	(pS/m @ °C)	587 @ 18	475 @ 19	458 @ 22
IN-HOUSE TESTS					
Flow/No-flow temp (Setapoint Mk 0)	SEM/024	(°C)	-51.55/-51.8	-51.35/-51.65	
Breakpoint & CBO Deposit weight	SEM/004/003	(°C)/(µg/C)	290	290	295/58.0
HiReTS number/Carbon burn-off	"Standard"	- (µg C)	18.8(3)/1.48	11.95/0.8	
Wear scar diameter (BOCLE)	D 5001	(mm)	0.7275	0.7525	0.76

TABLE 6 - Storage stability tests - Merox Jet A-1 and with Betz additives.

Test	Fuel: Method	Units	M-1A Initial	M-1A 6 wk	M-1A 12 wk	VX 8Q405 6 wk	VX 8Q405 12 wk	VY 8Q406 6 wk	VY 8Q406 12 wk
APPEARANCE									
Saybolt Colour*	D 156		+21	+19	+11	+14	+14	+18	+14
COMPOSITION									
Total acidity	D 3242/IP 354	(mg KOH/g)	0.002	0.003	0.002	0.002	0.002	0.004	0.002
(THERMAL) STABILITY									
JFTOT Presure drop/VTR	D 3241/IP 323	(mm Hg)/-	<1/1	<1/1	1/1	<1/1	<1/1	<1/1	<1/1
CONTAMINANTS									
Existent gum	D 381/IP 131	(mg/100mL)	2	3	2	6	6	7	5
Particulate contaminant	D 2276/IP 216	(mg/L)	0.8	0.8	1.9	0.4	1.1	0.4	0.5
Water reaction, interface rating	D 1094/IP 289		1B	1B	1B	2	1B	2	2
MSEP	D 3948		88	60	46	0	46	0	0
WASP rating*	SMS 2772	(mg/kg)	685	480	1040	1005	1100	935	1070
OTHER TESTS									
Conductivity	D 2624/IP 274								
Conductivity		(pS/m @ °C)	478 @ 21	380 @ 18	111 @ 17	430 @ 18	440 @ 15	450 @ 18	410 @ 17
Conductivity		(pS/m @ °C)	380 @ 16#						
Peroxide number*	D 3703	(ppm)	1, 0.3#	1.4	0.9	1.5	0.6	0.8	0.5

TABLE 7 - Small scale and analytical test results for additivated Merox JP-8 fuels

Fuel code/ mg/L Additive:			VO (100 8Q405)	M-4A(125 8Q406)
Test Description:	*Method*	*Units*	*Value*	*Value*
APPEARANCE, COMPOSITION				
Saybolt colour*	D 156		+24	+24
Total acidity	D 3242/IP 354	(mg KOH/g)	0.006	0.007
Total sulphur	PT/71:IH09	(%m/m)		0.175
FLUIDITY				
Freezing point	D 2386/IP 16	(°C)	-51.0	-50.5
Viscosity at -20°C	D 445/IP 71	(cSt)	3.755	3.659
(THERMAL) STABILITY				
JFTOTPressure drop/VTR	D 3241/IP 323	(mm Hg)/-	<1/1	<1/1
CONTAMINANTS, OTHER TESTS				
Existent gum	D 381/IP 131	(mg/100mL)	3	<1.0
Particulate contaminant	D 2276/IP 216	(mg/L)	1.8	0.9
Water reaction, interface rating	D 1094/IP 289		2	4
MSEP	D 3948		43	0
WASP rating*	SMS 2772	(mg/kg)	1210	1225
Metals* - Copper/Iron	PT/71:GM08	(ppb)	4/<6	4/10
Other (semi-quantitative)		(ppb)	Pb 133, Zn 40, Mn 6	Pb 95.5, Zn 15
Conductivity	D 2624/IP 274	(pS/m @ °C)	734 @ 26.5	540 @ 21
Conductivity (pre-storage)	D 2624/IP 274	(pS/m @ °C)	476 @ 17	457 @ 17
Peroxide number	D 3703	(ppm)	0.9	
IH (THERMAL) STABILITY				
Breakpoint/CBO Deposit weight	SEM/004/003	(°C)/(µg/C)	300/53	305/35.75
FOT, radical initiation rate	SEM/008		4.45E-7	4.32E-7
C-JFTOT number	Under dev			11.95
IH LUBRICITY				
Wear scar diameter (BOCLE)	D 5001	(mm)	0.595	0.575

TABLE 8 - Storage stability tests - Merox JP-8 and JP-8+100 fuels.

		Fuel:	M-2A		8Q405	VO	8Q406	M-4A
Test	*Method*	*Units*	*6 week*	*12 week*	*6 week*	*12 week*	*6 week*	*12 week*
APPEARANCE								
Saybolt Colour*	D 156		+14	+7	+18	+12	+19	+14
COMPOSITION								
Total acidity	D 3242/IP 354	(mg KOH/g)	0.005	0.006	0.003	0.015	0.004	0.006
CORROSION								
Copper Corrosion (2h/100°C)	D 130/IP 154		1A	1A	1A	1A	1A	1A
Silver Corrosion (4h/50°C)	IP 227		0	0	0	0	0	0
(THERMAL) STABILITY								
JFTOT Pressure drop/VTR	D 3241/IP 323	(mm Hg)/-	<1/1	<1/1				
CONTAMINANTS								
Existent gum	D 381/IP 131	(mg/100mL)	5	2	3	3	3	4
Particulate contaminant	D 2276/IP 216	(mg/L)	1.2	2.7	0.5	0.6	0.9	0.3
Water reaction, interface rating	D 1094/IP 289		1B	1B	2	2	2	4
MSEP	D 3948		48	57	45	0	0	41
WASP rating	SMS 2772	(mg/kg)	960	1110	900	410	935	975
OTHER TESTS								
Conductivity	D 2624/IP 274	(pS/m @ °C)	283 @ 18	155 @ 22	544 @ 20	550 @ 18	503 @ 20	412 @ 18
Peroxide number*	D 3703	(ppm)	2.1	0.6	3.5	1.6	3.3	1.1

TABLE 9 - CoQ, Small-scale & storage tests for Hydrotreated Jet A-1 &/- additives

Fuel/additive			HT-1A	VT/8Q405	VU/8Q406
Test Description	*Method*	*Units*	*Value*	*Value*	*Value*
APPEARANCE, COMPOSITION					
Appearance	UK 1636		Satisfactory		
Saybolt Colour * (0,6,12 weeks)	D 156		27, 23, 22	27, 23, 21	26, 22, 22
Total acidity (0,6,12 weeks)	D 3242/IP 354	(mg KOH/g)	0.002, 0.002, 0.003	0.003, 0.001, 0.003	0.003, 0.001, 0.002
FIA Aromatics	D 1319/IP 156	(%V)	17.1		
Mercaptan sulphur	D 3227/IP 342	(%m/m)	0.0002		
Total sulphur (also ran IP 336)	IP 373	(%m/m)	0.0175	0.0152	0.0148
VOLATILITY, FLUIDITY					
Distillation (partial), IBP/FBP	D 86/IP 123	(°C)	153/256		
Flash point, Abel	IP 170	(° C)	44		
Density @ 15°C	D 4052/IP 365	(kg/m3)	793.4	793.5	793.4
Freezing point	D 2386/IP 16	(°C)	-48	-47	-47.5
Viscosity @ -20°C	D 445/IP 71	(cSt)	4.000	4.023	4.021
COMBUSTION, CORROSION					
Specific energy, net	D 4529/IP 381	(MJ/kg)	43.403	43.394	43.395
Smoke point	D 1322	(mm)	26	24	24
Copper Corrosion (2h/100°C)	D 130/IP 154		1A (0&12w)	1A (0&12w)	1A (0&12w)
Silver Corrosion (4h/50°C)	IP 227		PASS (0)		
(THERMAL) STABILITY					
JFTOT at 260°C	D 3241/IP 323				
Pressure drop/VTR		(mm Hg)/-	<1/1	<1/1	<1/1
Pressure drop/VTR		(mm Hg)/-	<1/1 (6w)	<1/1 (6w)	<1/1 (6w)
Pressure drop/VTR		(mm Hg)/-	<1/1 (12w)	2/1 (12w)	<1/1 (12w)
CONTAMINANTS					
Existent gum (0,6,12 weeks)	D 381/IP 131	(mg/100mL)	<1, <1, 1	2, 6, 2	2, 2, 2
Particulate contaminant* (0,6,12 weeks)	D 2276/IP 216	(mg/L)	0.5, 0.7, 0.4	1.6, 0.4, 1.0	1.2, 0.6, 0.8
Water reaction, interface rating	D 1094/IP 289		1B	2	2
MSEP	D 3948		93	44	43
WASP rating* (0,6,12 weeks)	SMS 2772	(mg/kg)	570,615, 470	860, 975, 870	925, 1020, 920
Metals* - Cu/Fe&Sn(Semi-Q)	PT/51:GM08	(ppb)	4/2 & 6(SQ)		
OTHER TESTS, ADDITIVES					
Conductivity	D 2624/IP 274				
Conductivity & temp		(pS/m @ °C)	345 @ 20	321 @ 22	278 @ 22
Conductivity & temp		(pS/m @ °C)		340@20#	300@20#
Conductivity & temp (12weeks)		(pS/m @ °C)	380 @ 17	267 @16	238 @17
Peroxide number* (0,6,12 weeks)	D 3703	(ppm)	<1, 0.3, 0.3	<1, 0.5, 0.2	<1, 0.3, 0.2
Antioxidant	RDE/A/609	(mg/L)	22.7	22.7	22.7
Static dissipator additive	RDE/A/621	(mg/L)	1.0	1.0	1.0
IH FLUIDITY					
Setapoint Flow/no-flow temp	SEM/024	(°C)	-46.65/-49.3	-46.95/-49.5	-49.1/-40.55
IH (THERMAL) STABILITY					
Breakpoint* (2nd figure is repeat)	SEM/004	(°C)	280, 275	300	300
CBO Deposit weight	SEM/003A	(µg Carbon)		72.9	
HiReTS number/Carbon burn-off	"Standard"	- /(µg)	64.0/0.2 & 62.8/0(1)	17.25/0	33.7/0
FOT - Induction period & Radical initiation rate	SEM/008A	(min) & (Mol/L/s)	65.2 & 5.96E-8		
IH LUBRICITY					
Wear scar diameter (BOCLE)	D 5001	(mm)	0.76	0.76, 0.81#	0.76
Failure load (TAFLE)	SEM/013	(kg)	30		

TABLE 10 - Analytical data and small scale tests on hydrotreated JP-8 and blends

MOD Code:			HT-2A	VZ	WA
Fuel & additive type:			JP8	JP8+8Q405	JP8+8Q406
Specification Description	*Method*	*Units*	*Value*	*Value*	*Value*
APPEARANCE					
Appearance	UK 1636		Satisfactory		
Saybolt Colour*	D 156		+21	+23	+23
COMPOSITION					
Total acidity	D 3242/IP 354	(mg KOH/g)	0.006	0.005	0.005
Mercaptan sulphur (potentiometry)	IP 342	(%m/m)	0.0004		
Total sulphur (also ran IP 336 - 0.02)	IP 373	(%m/m)	0.0160	0.0145	0.0149
VOLATILITY					
Density @ 15C	D 4052/IP 365	(kg/m3)	793.7	793.8	793.8
FLUIDITY					
Freezing point	D 2386/IP 16	(Deg C)	-48	-48.5	-48
Viscosity	D 445/IP 71				
Viscosity @ -20°C		(cSt)	4.018	4.055	4.043
Viscosity @ 40°C*		(cSt)	1.243	1.242	1.238
Flow temperature (Setapoint Mark 0)*	SEM/024				
Flow temperature (endpoint)		(Deg C)	-47.45	-47.65	-47.35
No-flow temperature		(Deg C)	-49.90	-49.85	-49.65
CORROSION					
Copper corrosion (2h/100°C)	D 130/IP 154		1A		
(THERMAL) STABILITY					
JFTOT at 260C	D 3241/IP 323				
Pressure drop		(mm Hg)	<1	<1	<1
Visual tube rating			1	1	1
Breakpoint*	SEM/004	(Deg C)	~310	325	320
HiReTS* - HiReTS number	"Standard"				
HiReTS number			25.55	15.5	14.4
Carbon burn-off		(µg C)	0.15	0.05	0
CONTAMINANTS					
Existent gum	D 381/IP 131	(mg/100mL)	<1	3	3
MSEP	D 3948		85	46	43
Particulate contaminant*	D 2276/IP 216	(mg/L)	0.6	1.1	0.7
Water reaction, interface rating	D 1094/IP 289		1B	2	2
WASP rating*	SMS 2772	(mg/kg)	743	965	925
OTHER TESTS					
Conductivity	D 2624/IP 274	(pS/m@ °C)	168@22	250 @ 17.5	230 @ 17
Peroxide number*	D 3703	(ppm)	<0.1	<0.1	<0.1
LUBRICITY*					
Wear scar diameter (BOCLE)	D 5001	(mm)	0.57	0.57	0.605
Failure load (TAFLE)	SEM/013	(kg)	60(1)		

TABLE 11 - Storage stability test results for hydrotreated JP-8 and JP-8+100 variants.

See also Table 10.

			HT-2A		8Q405	VZ	8Q406	WA
Test	*Method*	*Units*	*6 week*	*12 week*	*6 week*	*12 week*	*6 week*	*12 week*
APPEARANCE								
Appearance	UK 1636		Satis	Black fibres	Satis	Satis	Satis	Satis
Saybolt Colour*	D 156		+25	+16	+9	+14	+13	+18
COMPOSITION								
Total acidity	D 3242/IP 354	(mg KOH/g)	0.005	0.004	0.003	0.006	0.004	0.005
(THERMAL) STABILITY								
JFTOT at 260°C	D 3241/IP 323							
Pressure drop		(mm Hg)	<1		<1	<1	<1	<1
Visual tube rating			1		1	1	1	1
CONTAMINANTS								
Existent gum	D 381/IP 131	(mg/100mL)	<1	3	7	3	5	3
Particulate contaminant*	D 2276/IP 216	(mg/L)	0.6	8.6	0.5	0.4	1.2	0.5
Water reaction, interface rating	D 1094/IP 289		1B	1B	2	4	2	4
MSEP	D 3948		59	48	46	0	47	49
WASP rating*	SMS 2772	(mg/kg)	645	970	930	960	965	1110
OTHER TESTS								
Conductivity	D 2624/IP 274	(pS/m @ °C)	75 @ 23	212 @ 17	324 @ 21	320 @ 20	301 @ 20	280 @ 19
Peroxide number*	D 3703	(ppm)	<0.1	<0.1	1.8	3.8	1.6	0.2

TABLE 12 - Results for BP HiTTS candidates in HiReTS unit 1

Fuel code	HiReTS numbers	Carbon burn-off (µg C)
Merox Base fuel, AT, ex tank 248	Test 1 - 1100.48 Test 2 - 1006.7 Average 1055.8	Test 1 = 102 Test 2 = 74.4 Average 88.2
A	Test 1 - 10.7 Test 2 - 28.1 Average 19.4	Test 1 = 0 Test 2 = 0.2 Average 0.1
B	Test 1 - 18.7 Test 2 - 29.1 Average 23.9	Test 1 - 0 Test 2 - 0 Average 0
C	Test 1 - 4.1 - Stopped early Test 2 - 17.7 Report: 17.7 (1)	Test 1 = NA Test 2 = 1.89 Report: 1.89 (1)
Base fuel - check run	Test 3 - 1040.3	Test 3 - 112
D	Test 1 - 11.6 Test 2 - 20.1 Average 15.9	Test 1 = 0.3 Test 2 = 0.75 Average 0.53

Figure 1. 3-D C-JFTOT trace for JPTS, the JP-8+100 "target" fuel.

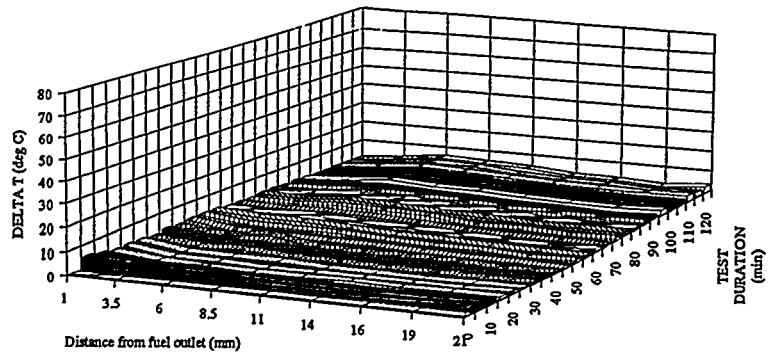


Figure 2. On same scale, trace for Merox JP-8 (M-2A).

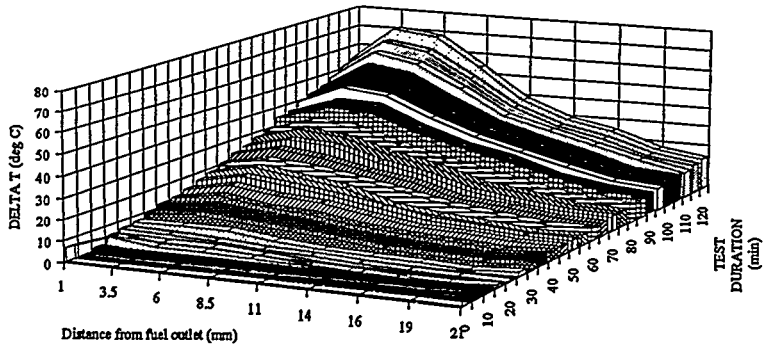


Figure 3. M-2A plus 125 mg/L 8Q406, = M-4A, again on same scale.

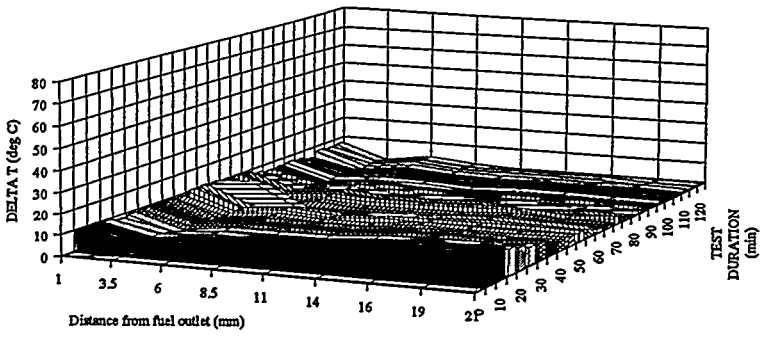


Figure 4 - HiReTS trace for Hydrotreated Jet A-1, HT-1A

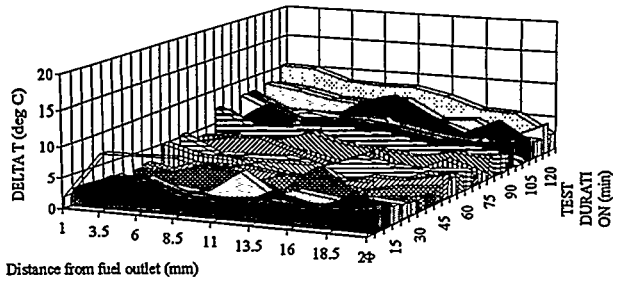


Figure 5 - HiReTS trace for above Jet A-1 plus Betz 8Q405 = VT.

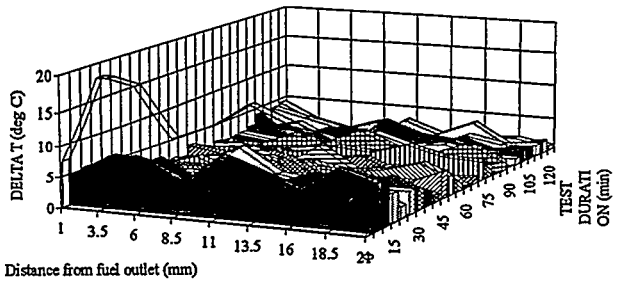


Figure 6 - A HiReTS 3-D profile for the base fuel used in the BP additive tests

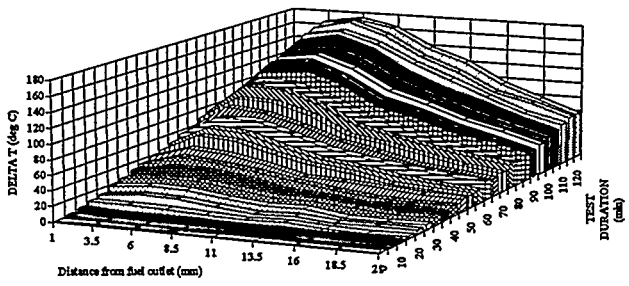
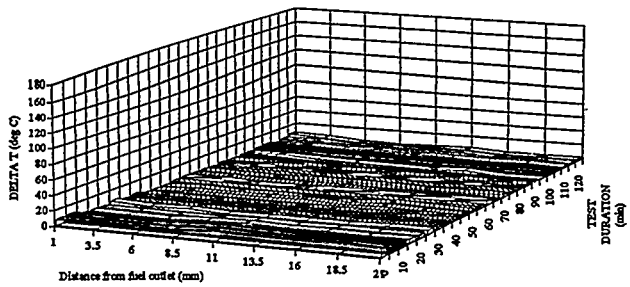


Figure 7 - Same base fuel with BP additive A, on the same scale as Figure 6



6th International Conference
on Stability and Handling of Liquid Fuels
Vancouver, B. C., Canada
October 13-17, 1997

EXPERIMENTAL EVALUATION OF THE TWO-TIERED JFTOT TEMPERATURE PROVISION FOR JET A FUEL

Cliff Moses*[1], Stan Seto[2], and Steve Anderson[3]

[1]Southwest Research Institute, P.O. Drawer 28510, San Antonio, TX 78228-05210. [2]General Electric Aircraft Engines, 1 Neumann Way, Cincinnati, OH 45215-6301. [3]WL/POSF, Wright-Patterson AFB, OH 45433-7521.

ABSTRACT

An experimental program is being conducted to assess the potential impact to fuel-nozzle fouling life of using Jet A fuels which pass the JFTOT at 245°C but not at 260°C. Since the JP-8 fuel specification allows only the 260°C minimum temperature, this is an important consideration for military aircraft which upon occasion refuel with Jet A at commercial airports. The methodology of accelerated fuel-nozzle fouling tests and subsequent analysis follows previous projects for the US Navy to answer similar questions on the effect of reductions in thermal stability. Although the project is underway, unforseen delays precluded the presentation of actual results at this meeting. Anticipated results are presented and discussed.

INTRODUCTION

Aircraft of the US Air Force on occasion are refueled at commercial airports with fuel meeting the ASTM D 1655 fuel specification for Jet A, but not necessarily meeting the MIL-T-83133D fuel specification for JP-8. Specifically, there is a two-tiered temperature provision for thermal stability in ASTM D 1655 that allows for a fuel that does not pass the JFTOT test at 260°C to be retested at 245°C and approved for use if the fuel passes the test at the lower temperature, providing both results are reported. MIL-T-83133D requires that all fuels pass the JFTOT at 260°C. Many military aircraft engines have less margin available for thermal stability than do commercial engines, and there is concern that operating on fuels with a 245°C pass on the JFTOT may compromise reliability and mission readiness.

It is generally not possible to predict the effect of using a fuel with a JFTOT breakpoint temperature between 245 and 260°C since, with some exceptions as discussed below, there are no correlations

between JFTOT results and fouling rates in real engine hardware. It is therefore important to develop data on the fouling tendency of an atomizer from an Air Force engine when operated on fuels of marginal or "off-spec" thermal stability. It is also desirable to determine the effect of the "+100" additive package on atomizer fouling with such fuels to determine if that is a viable means of "upgrading" the fuel.

PREVIOUS RELATED STUDIES

During the late 1970's and early 1980's, some atomizer fouling tests were conducted for the US Air Force and US Navy as part of their alternative fuel programs. Some of these fouling tests were conducted by the engine manufacturers[1-6] while others were conducted at Southwest Research Institute (SwRI)[7-9].

The purpose of the fouling tests sponsored by the US Navy [7-9] was to determine the impact of using JP-5 that had been contaminated either by diesel fuel, i.e. DFM/NATO F-76, or by copper so as to cause the jet fuel to fail the JFTOT test for thermal stability, a problem very similar to the Air Force concern described earlier.

The nozzle fouling tests in the Navy program were conducted at SwRI. Test nozzles were immersed in an air flow which simulated the thermal environment of the engine installation. The surface temperature of the nozzle and the fuel flow rate were that of the beginning of idle-descent, which is considered to be the worst-case flight condition for deposition since the fuel and engine parts are still hot, but the fuel flow rate has been greatly reduced. The fuel inlet temperature was a variable among tests and was higher than normal engine experience to accelerate the tests. Fuels of different thermal stability, as determined by JFTOT breakpoint temperature, T_{BP}, were tested at three fuel inlet temperatures each. The test nozzle was instrumented for surface temperatures, inlet fuel temperature, flow rate, and pressure drop. A new nozzle was used for each test. The fuel was discarded after passing through the nozzle, and was not recirculated or reused.

Figure 1 illustrates typical fouling histories for five fuels of varying T_{BP}; these data came from the Navy program to determine the effect of contamination of JP-5 by diesel fuel and by copper on nozzle

fouling[8]. In this comparison, the inlet fuel temperature was constant. It is evident from these results that fouling takes place rather linearly with time and that fuels of lower thermal stability, i.e., lower T_{BP}, cause fouling at a higher rate.

From test results such as these, it is possible to compare the fouling rates caused by the fuels and develop expressions of equivalent fouling life, i.e., number of hours on a good fuel that it would take to produce the same amount of flow degradation in the nozzle. Figure 2 illustrates such results by comparing the equivalent fouling life for several different fuel nozzles as the breakpoint of the fuel is reduced beyond the minimum of 500°F (260°C)[7]. Considering one extreme, nozzle "a", the results indicate that a decrease in T_{BP} of 75°F(42°C) would cause about a 10-fold increase in fouling rate, i.e., one flight would produce the same deposit as 10 flights on a fuel of minimum acceptable thermal stability of 500°F (260°C). For the other extreme, nozzle "b", the effect of a 75°F (42°C) decrease in T_{BP} would be negligible.

The methodology used in the tests just described has been incorporated into a project for the US Air Force to determine the following while avoiding the expense of multiple engine endurance tests:

- the effect of the two-tiered JFTOT on military aircraft
- the effect of the "+100" additive package on fuels of marginal or sub-standard thermal stability

The test schedule has been delayed, so only the project description and anticipated results will be discussed.

OBJECTIVE

The objectives of this project are to experimentally determine the effect of using fuels with JFTOT breakpoint temperatures less that 260C on the fouling rate of a relevant fuel atomizer and subsequently determine the effect of the JP-8+100 additive on fuels of marginal or sub-standard thermal stability.

APPROACH AND SCOPE

Accelerated fuel-nozzle fouling tests are being conducted on a candidate nozzle using three fuels of different JFTOT breakpoint temperature to quantify the effect of breakpoint temperature on fouling rate. These results will then be used to evaluate the effect of using a fuel with a 245°C breakpoint. The tests will then be rerun with the "+100" additive added to the test fuels.

The three test fuels were supplied by the Fuels Branch at Wright-Patterson AFB following an initial screening of five fuels to select three JP-8 type fuels with the following thermal stability characteristics as determined by JFTOT breakpoint (T_{BP}):

- $T_{BP} \approx 245°C$
- $T_{BP} \approx 260°C$
- $T_{BP} >> 260°C$

The fouling rates are accelerated by raising the fuel inlet temperature. Test times of 25 to 75 hours are desirable, representing a compromise between excessively high temperatures and long test times. Nozzle tests are being conducted at three inlet temperatures.

The nozzle being tested is a dual-orifice pressure atomizer of the type used in the General Electric F108 and F110 engines. Figure 3 shows an outline schematic of the nozzle along with the locations of the thermocouples used to monitor test conditions.

EXPERIMENTAL CONDITIONS

The nozzle fouling tests are conducted by suspending the test nozzle in a heated air flow so as to reproduce surface temperatures on the nozzle that are typical of engine-installed conditions. The fuel flow rate is that of the beginning of idle-descent, which is considered to be the worst-case flight condition for deposition since the fuel and engine parts are still hot, but the fuel flow rate has been greatly reduced. The test nozzle is instrumented for surface temperatures, flow rate, and pressure drop.

Figure 4 presents a flow schematic of the experiments. The test nozzle is submerged in a heated fluidized bed of sand which serves to increase the heat transfer between the heated air and the nozzle body. The temperature of the air flowing through the bed is adjusted to maintain a constant temperature at the tip of the test nozzle for all the tests. Since the fuel flow rate and pressure drop across the nozzle are constantly monitored, it is possible to see the results of the fouling occur in real time.

The fuel inlet temperatures are being chosen to achieve test times on the order of 25 to 75 hours. The test time is the time required to develop a 10 percent increase in pressure drop across the nozzle. This is a value that is large enough to be significant and easily measured without extending test times unnecessarily.

ANTICIPATED RESULTS

Figure 5 illustrates the type of data results that are anticipated to determine the effect of fuel thermal stability on fouling rate for the three test fuels. Each of the lines will be a least-squares fit to data at three temperatures. Figure 6 illustrates the possible analyses of the data of Figure 5 in a manner similar to the results presented in Figure 2; a large increase represents a significant reduction in fouling life. If the three lines of Figure 5 are very close together, there will be little effect of a decrease in breakpoint temperature. The larger the separation of the three lines, the greater the effect will be on the equivalent-life analysis of Figure 6.

If the "+100 additive package" performs as expected, the lines of Figure 5 should be shifted to the right to higher fuel temperatures. The degree of the shift and whether or not the effect will be the same on all three fuels can not be predicted.

REFERENCES

1. Gleason, C.C., et al., "Evaluation of Fuel Character Effects on J79 Engine Combustion System," US Air Force AFAPL-TR-79-2015, June 1977.

2. Gleason, C.C., et al., "Evaluation of Fuel Character Effects on F101 Engine Combustion System," US Air Force AFAPL-TR-79-2018, June 1979.

3. Vogel, R.E. et al., "Fuel Character Effects on Current High Pressure Ratio, Can-Type Turbine Combustion Systems," US Air Force AFAPL-TR-79-2072, April 1980.

4. Gleason, C.C., et al., "Evaluation of Fuel Character Effects on J79 Smokeless Combustor," US Air Force AFAPL-TR-80-2092, November 1980.

5. Oller, T.L., et al., "Fuel Mainburner/Turbine Effects," US Air Force AFAPL-TR-81-2100, May 1982.

6. Russell, P.L., "Fuel Mainburner/Turbine Effects," US Air Force AFAPL-TR-81-2081, September 1982.

7. Moses, C.A., et al., "An Alternate Test Procedure to Qualify Fuels for Navy Aircraft: Phase II," US Navy NAPC-PE-145C, August 1984.

8. Tyler, J.C. et al., "An Alternate Test Procedure to Qualify Fuels for Navy Aircraft: Phase II Continuation," US Navy NAPC-PE-176C, August 1987.

9. Moses, C.A., "Effect of a Metal Deactivator Fuel Additive on Fuel Deposition in Fuel Atomizers at High Temperature," US Army BFLRF Report No. 281, AD A260915, August 1992.

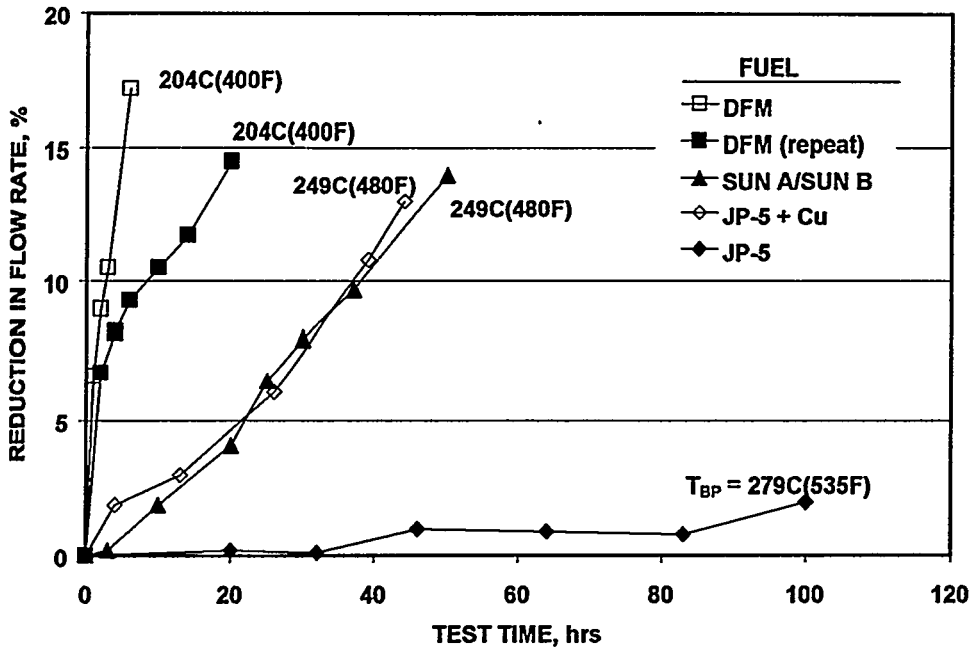


FIGURE 1. EFFECT OF JFTOT BREAKPOINT TEMPERATURE ON NOZZLE FOULING (from Ref. 8)

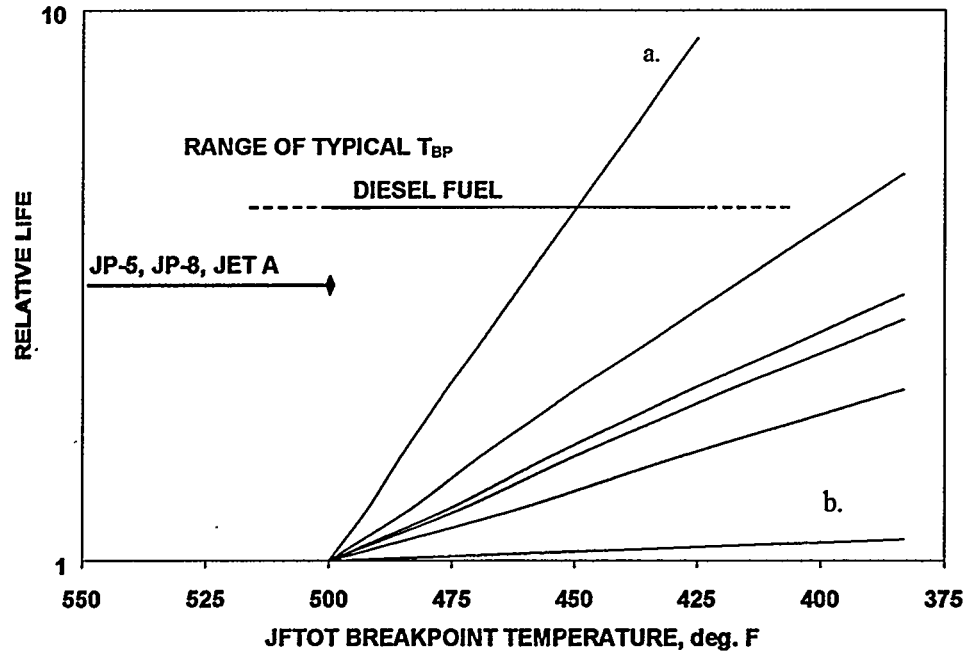


FIGURE 2. EFFECT OF BREAKPOINT TEMPERATURE ON RELATIVE FOULING LIFE (from Ref. 7)

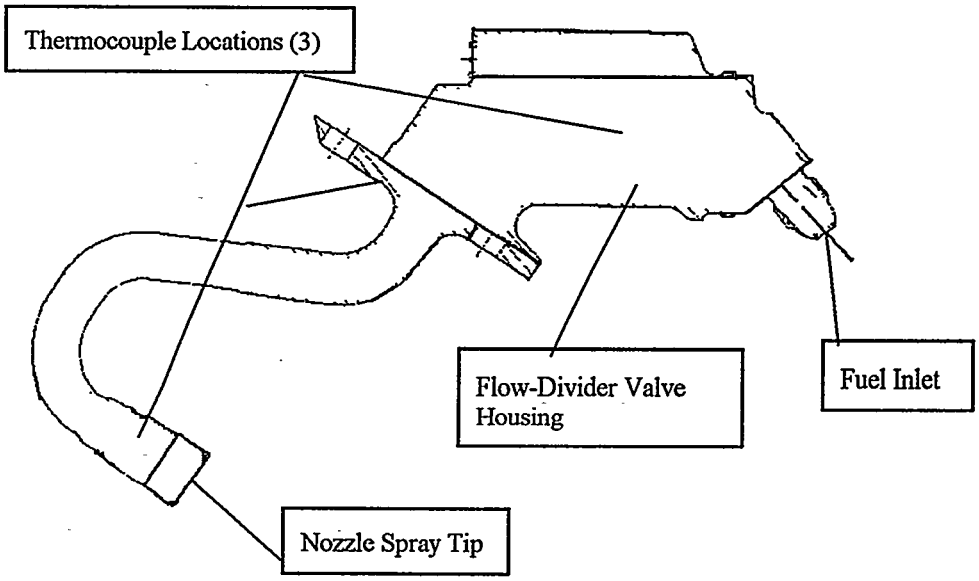


FIGURE 3. TEST ATOMIZER SHOWING THERMOCOUPLE LOCATIONS

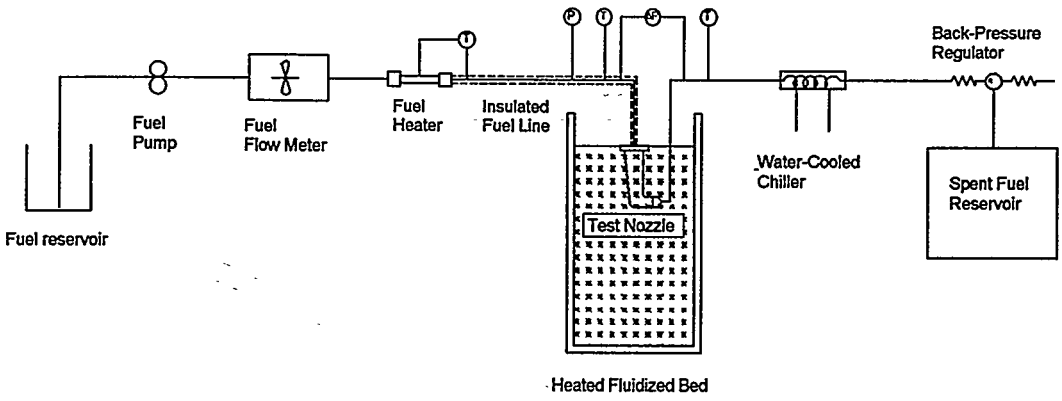


FIGURE 4. FLOW SCHEMATIC OF NOZZLE FOULING TESTS

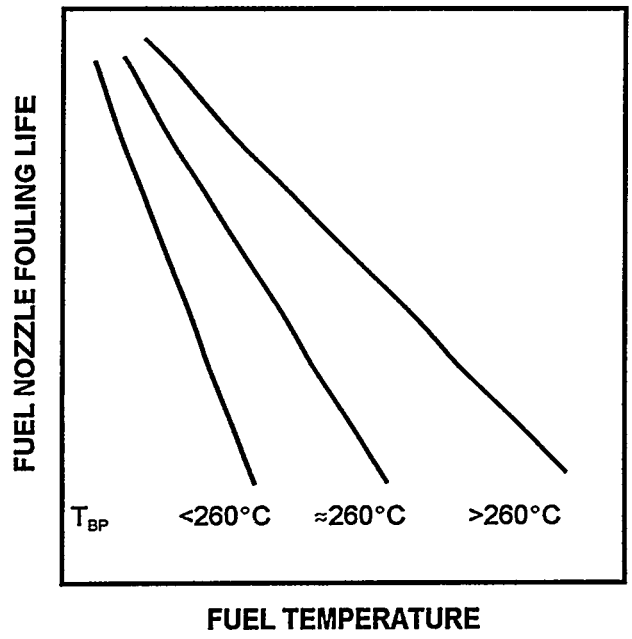


FIGURE 5. ANTICIPATED RESULTS FROM FUEL-NOZZLE FOULING EXPERIMENTS

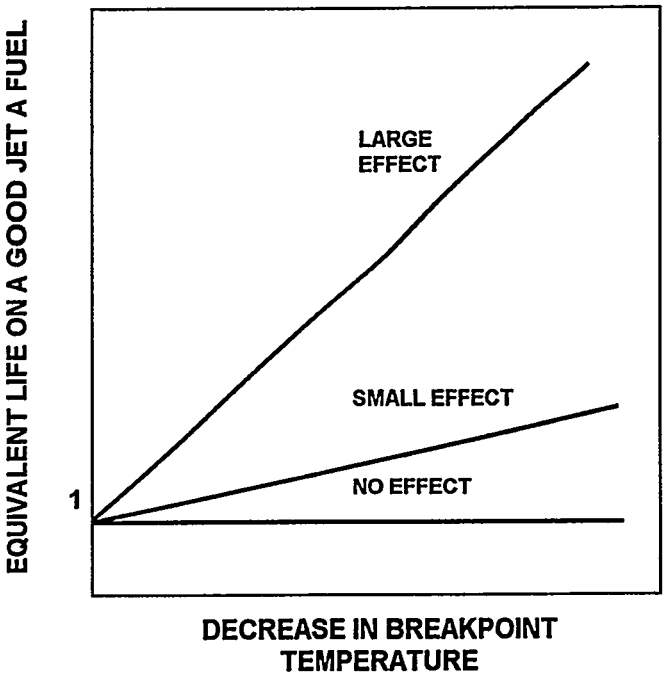


FIGURE 6. POSSIBLE RESULTS FROM THE ANALYSIS OF NOZZLE FOULING DATA TO QUANTIFY THE EFFECT OF BREAKPOINT TEMPERATURE ON FOULING LIFE

6th International Conference
on Stability and Handling of Liquid Fuels
Vancouver, B. C., Canada
October 13-17, 1997

STUDIES OF JET FUEL OXIDATION USING OXYGEN MONITORING AND CHEMICAL KINETIC MODELING

Steven Zabarnick*, Shawn D. Whitacre, Mark S. Mick, and Jamie S. Ervin

University of Dayton Research Institute, Aerospace Mechanics Division, 300 College Park, KL-463, Dayton, OH 45469-0140, USA.

A quartz crystal microbalance (QCM)/Parr bomb system with a headspace oxygen sensor is used to measure oxidation and deposition during thermal oxidative stressing of jet fuel. In studies of jet fuel antioxidants, we find that rapid increases in oxidation rate occur upon consumption of the antioxidant. The antioxidant appears to be consumed by reaction with alkylperoxy radicals. In studies of metal deactivator (MDA) additives, we find that MDA is consumed during thermal stressing, and this consumption results in large increases in the oxidation rate of metal containing fuels. Mechanisms of MDA consumption are hypothesized. Chemical kinetic modeling was used to simulate the autoxidation of jet fuel including the chemistry of peroxy radical inhibiting antioxidants and hydroperoxide decomposing species. Recent experimental measurements of oxygen concentration during autoxidation of jet fuel were used to "calibrate" the rate parameters of the mechanism. The model showed excellent agreement with oxygen profiles of static measurements at 140°C. At 185°C, the model predicts that peroxy radical inhibiting antioxidants and hydroperoxide decomposers both slow and/or delay oxidation, but the resulting oxygen profiles display different characteristics. We have shown that comparison of these profiles with fuel blending and fuel dilution measurements have the potential to differentiate between the two types of oxidation slowing species. The modeling predicts that the presence of both types of species in a fuel results in a synergistic slowing of the oxidation rate.

Introduction

Jet fuel undergoes oxidative chemistry upon being heated in the fuel systems of advanced military aircraft. Besides being heated by heat transfer from the hot turbine compressor air (or in the afterburner by combustor exhaust), the fuel is also heated while being used as a coolant for various engine and airframe components.[1] It has been predicted that this coolant usage will become even more important in future advanced aircraft.[2] Air saturated fuel typically contains

≈60 ppm (w/w) or 1.8×10^{-3} M of oxygen. This very small amount of oxygen can result in the formation of gums and deposits which are capable of impairing proper performance of the fuel system and grounding of the aircraft. In a flowing fuel system, the mass of deposits formed per volume of fuel is small, on the order of 1 μg/mL (≈1.2 ppm w/w) for complete oxygen consumption;[3] but, the volumes of fuel used in military aircraft are extremely large over the lifetime of an aircraft. Thus the small amounts of deposits which form can build up over time, ultimately resulting in filter plugging, fouling of close tolerance valves, valve hysteresis, and other problems.

Antioxidants have been used for many decades to slow and/or delay autoxidation. Indeed, the development of antioxidants has been so successful that they are used routinely in many industrial and consumer products, including foods and gasoline. There are many types of antioxidants that have been used in hydrocarbon liquids: hindered phenols, phenylenediamines, peroxide decomposers, and metal deactivators. It is believed that hindered phenols and phenylenediamines slow oxidation by intercepting the alkylperoxy free radicals that carry the autoxidation chain. Peroxide decomposers react with hydroperoxides and prevent their decomposition into free radicals. Metal deactivators complex with metal ions and prevent their catalysis of processes which form free radicals. Thus each of these antioxidant types is thought to lower the concentration of free radicals either by preventing their formation or rapidly removing them after they are formed.

Although antioxidants are widely used and have proven very successful in preventing the formation of detrimental products, chemical kinetic modeling of the chemical mechanism of antioxidant action has received little attention. Fortunately, the primary reactions by which hindered phenol antioxidants intercept alkylperoxy radicals have been studied extensively. Previously, we have performed chemical kinetic modeling of antioxidant action for jet fuel applications.[4] This study was limited to relatively short reaction times before significant consumption of the antioxidant species occurred. Also, because of the lack of suitable experimental data, no comparison with laboratory measurements was included. Recent measurements of oxygen concentration during the autoxidation of jet fuel, jet fuel mixtures, and

model jet fuel species have provided reasonable data for comparison with modeling.[5-8] In the present study we utilize these experimental data for "calibration" of the kinetic parameters of the model. Also, we compare the predicted and measured oxygen profiles to provide insight into the antioxidant mechanism. In addition, we explore the type of behavior expected by the presence of peroxide decomposing species. This study will also address relatively long reaction times, where the antioxidant species may become completely consumed. In experimental studies, we also explore the mechanisms by which metal deactivators and hindered phenols slow and/or delay the autoxidation process.

Experimental

The QCM/Parr bomb system has been described in detail previously and will only be outlined briefly here.[9,10] The Parr bomb is a 100 mL stainless steel reactor. It is heated with a clamp-on band heater and its temperature is controlled by a PID controller through a thermocouple immersed in the fuel. The reactor contains an rf feedthrough, through which the connection for the quartz crystal resonator is attached. The crystals are 2.54 cm in diameter, 0.33 mm thick and have a nominal resonant frequency of 5 MHz. The crystals were acquired from Maxtek Inc. and are available in crystal electrode surfaces of gold, silver, platinum, and aluminum. For the studies reported here gold crystal electrodes were used. The QCM measures deposition (i.e., an increase in mass) which occurs on overlapping sections of the two sided electrodes. Thus, the device responds to deposition which occurs on the metal surface and does not respond to deposition on the exposed quartz.

The device is also equipped with a pressure transducer (Sensotec) to measure the absolute headspace pressure and a polarographic oxygen sensor (Ingold) to measure the headspace oxygen concentration. Previous studies have demonstrated the value of determining the oxidation characteristics of fuels and fuels with additives. A personal computer is used to acquire data at one minute intervals during the experimental run. The following data are recorded during a run:

temperature, crystal frequency, headspace pressure, headspace oxygen concentration, and crystal damping voltage.

BHT (2,6 di-*tert*-butyl-4-methylphenol) was quantified by gas chromatography-mass spectrometry (GC-MS). 500 μL fuel samples were withdrawn from the reactor through a GC septum and extracted with 500 μL of methanol. 2 μL samples of the methanol solution were injected into a Hewlett-Packard GC-MS operating in single-ion monitoring (SIM) mode. The mass spectrometer was set to follow the intensity of the 205 amu fragment ion and the 220 amu parent ion of BHT. Calibration curves were obtained by injecting standard solutions of BHT in methanol.

MDA was quantified by a procedure developed by Striebich.[11] 10 mL of fuel is passed through a silica gel solid phase extraction cartridge. The polar components, including MDA, are retained on the cartridge and subsequently eluted with methanol. The methanol is evaporated and the remaining condensate is dissolved in 200 μL of toluene. This toluene solution is injected into a GC/MS operated with base deactivated injector liner and column. Single ion monitoring of the 161 amu fragment ion and the 282 amu parent ion were used for quantitation.

Chemical Kinetic Modeling Methodology

The methodology used in the chemical kinetic modeling reported here has been reported previously,[4] and therefore will only be described briefly. The chemical kinetic modeling was performed using the modeling package REACT.[12] This is a relatively simple package that integrates the multiple differential equations that result from a detailed chemical kinetic mechanism and yields species concentrations as a function of time. The following is input to the code: reaction mechanism with rate constants, initial concentrations for each species present in the mechanism, reaction time and time intervals for output, and various tolerances for the precision of the computation. The code outputs the individual species concentrations at each time interval.

As jet fuels are mixtures of hundreds of chemical species, it is impractical to model the chemical changes of all components of the mixture. Instead we have chosen to model the bulk fuel as a single compound, RH. RH has the chemical properties of a straight-chain alkane, such as n-dodecane; this is a reasonable simplification as alkanes comprise a large proportion of a jet fuel mixture. This single compound "fuel" can also contain dissolved oxygen (O_2), an antioxidant species (AH), and a peroxide decomposer (SH). The reaction mechanism used in the present study is shown in Table 1. The mechanism is a modification of that used previously.[4] Modifications involve adjustment of rate parameters to better match experimental measurements and the inclusion of a "peroxide decomposer" species.

Results and Discussion

Studies of peroxy radical intercepting antioxidants

Peroxy radical intercepting antioxidants are widely used in the petroleum industry to slow the oxidation of petroleum distillates. Military jet fuels which are hydrotreated require the addition of antioxidants to prevent the formation of gums and peroxides during storage and handling. In addition the US Air Force is considering the use of an antioxidant additive in the JP-8+100 thermal stability additive package. We have noted, in rapidly oxidizing fuels stressed at 140°C in the QCM system,[10] that the addition of an antioxidant additive can significantly delay oxidation and deposition. But, in such fast oxidizing fuels, after some time the oxygen removal process will begin.

This behavior is illustrated in Fig. 1 for a hydrocarbon solvent, Exxsol D-110. Exxsol D-110 is a dearomatized, narrow-cut aliphatic solvent with <1% aromatics and 3 ppm sulfur. As it is highly refined, it contains few naturally occurring antioxidants and therefore oxidizes quite rapidly. The figure shows that complete oxygen consumption occurs in two hours at 140°C. As it contains few naturally occurring antioxidants, Exxsol D-110 is an ideal model fuel in which to study antioxidants. We have added the antioxidant BHT over the concentration range 4.2 to 50

mg/L and measured the headspace oxygen concentration. Deposition is not reported as it is quite low for this solvent. The figure shows that as the concentration of added BHT is increased the oxidation process is delayed. But, after the delay period, oxidation occurs at a very similar rate to the neat fuel. Chemical kinetic schemes can reproduce this delay in oxidation;[4] but, it is not clear why the oxidation rate increases at longer times. One possible explanation is that the antioxidant molecule is consumed during the slow oxidation time until it is reduced below some critical level, then the oxidation process can proceed. This explanation is supported by the concentration dependence of the oxygen curves of Fig. 1. The more antioxidant that is present the longer is the delay before rapid oxidation occurs. A second explanation is that oxidation products build up slowly during the slow oxidation, and reach a critical level at which point they can help initiate faster oxidation.

To test the first theory, we have measured the concentration of BHT during a run by withdrawing 500 μL samples and performing the GC-MS analysis for BHT described in the experimental section. These experiments were performed in fuel F-3139, a fast oxidizing Jet A fuel. The results are shown in Fig. 2. The neat fuel consumes all of the headspace oxygen in three hours, and the addition of 25 mg/L of BHT delays the time of complete oxygen consumption out to seven hours. The figure shows that the BHT concentration decreases to near zero over the first 5 hours of the run. The oxidation rate increases when the BHT concentration begins to get quite low (<5 mg/L). Unfortunately, not enough data were taken during the 3 to 6 hour range to better determine the critical BHT concentration below which the oxidation rate increases. We believe that these BHT concentration measurements support the first explanation hypothesized above. Recently performed chemical kinetic modeling also supports the supposition that the consumption of the antioxidant will precipitate rapid oxidation.[13] Presumably the antioxidant is being consumed by reaction with peroxy radicals in its role as a peroxy radical inhibitor.

Studies of metal deactivator additives

Metal deactivator species have been used for many years in the petroleum industry to inhibit the catalytic effect of metals in petroleum distillates.[14] These metals, and copper in

particular, act to catalyze the autoxidation chemistry thereby greatly increasing oxidation and deposition rates. This catalytic effect occurs at the part per billion level of dissolved metal. It was realized early on that the presence of these metals in petroleum distillates had the effect of greatly reducing the antioxidant capabilities of peroxy radical inhibiting antioxidant species. Thus, metal deactivator additives were developed as an inexpensive solution to suppressing the catalytic activity of the metals without removing them from the system. The metal deactivators, N,N'-disalicylidene-1,2-propanediamine and N,N'-disalicylidene-1,2-cyclohexanediamine, are optional additives in the JP-8 military specification (MIL-T-83133D). In the jet fuel community the use of metal deactivators is controversial due to their possible over response in the JFTOT thermal stability fuel specification test.[15]

Although originally designed to chelate metal ions in solution, it has been proposed that these metal deactivators may also act by surface passivation of exposed metal surfaces and as antioxidants by radical inhibition.[16] To further explore the nature of metal deactivators as thermal stability additives we have performed a series of experiments in the QCM system. In these studies we use fuel F-3145, which has been doped with 285 ppb copper, and the metal deactivator, N,N'-disalicylidene-1,2-propanediamine, hereafter referred to simply as MDA. In Figs. 3a and 3b are shown plots of deposition and headspace oxygen at 140°C for fuel F-3145 neat and with 3.0, 5.8, and 12.0 mg/L added MDA. The neat fuel produces deposition during the first four hours, after which the deposition levels. The oxygen sensor data show that oxidation occurs during this initial four hour period, and oxygen is completely consumed at five hours. The addition of MDA delays both the oxidation and deposition processes. Increasing amounts of MDA allow longer delays in oxidation and deposition. With 3 mg/L added MDA, these processes are delayed for one hour, with 5.8 mg/L the delay is five hours, and with 12 mg/L the delay is 10 hours. The final deposit amounts for all of the MDA concentrations are near 4 $\mu g/cm^2$, reduced from the 7 $\mu g/cm^2$ produced by the neat fuel.

As fuel F-3145 contains 285 ppb copper, a delay in the oxidation and deposition process is fully expected. Clark[15] reported a chelation ratio for MDA:Cu of 1.1:1 mol/mol or 5:1 w/w.

Thus all of the copper can be complexed by the addition of approximately 1.1 mg/L MDA. Therefore even the smallest amount of added MDA shown in Fig. 3, 3 mg/L, is enough to completely complex all of the copper in the fuel. If MDA acted only as a simple complexing agent of copper and was not depleted during the test, we would expect the oxidation and deposition results to be identical for these three concentrations of MDA, because addition of excess MDA (>1.1 mg/L) should have no effect on oxidation or deposition. But instead we see that the oxidation delay is a function of the concentration of MDA.

The two previously reported secondary behaviors of MDA, surface passivation and free radical inhibition, may be able to yield the observed behavior. In addition, if MDA is consumed by chemical reaction, the observed behavior would be expected. To date, we are not aware of any previous reports of MDA consumption during thermal stressing of a fuel. To test this third mechanism we have measured the concentration of MDA present during an experimental run and the results are shown in Fig. 4. A separate experimental run was used for each MDA concentration point shown in the figure, as the analysis required 10 mL of fuel. The figure shows that the MDA concentration drops during the entire run, resulting in an MDA concentration below the detection limit at 15 hours. The figure also shows that oxygen consumption is moderately slow until seven hours, after which the oxidation rate increases substantially. The time of rapid increase in the oxidation rate occurs when the MDA concentration drops below approximately 1 mg/L. This is close to the predicted concentration requirement (1.1 mg/L) for chelation of all of the copper as determined by the binding ratio. It would appear that when the MDA concentration falls below this level, unchelated copper becomes available to catalyze the initiation reactions and thereby accelerates the oxidation process. These results clearly show that the consumption of MDA controls the time delays observed from MDA addition to fuel.

However, the mechanism by which MDA is depleted is uncertain. We are not aware of any MDA consumption reactions reported in the literature. Presumably MDA could be removed by chemical reaction, complexation with reaction products, or adsorption to the reactor walls. MDA contains phenolic hydrogen atoms which may be amenable to attack by peroxy radicals. Complexation of acidic reaction products is also a possible pathway for MDA consumption.

Chemical kinetic modeling

Modeling of BHT addition at 140°C

Recent measurements of the antioxidant behavior of jet fuel, jet fuel mixtures, and model jet fuel species have shown a distinctive behavior of the oxidation profiles as the antioxidant concentration is varied.[6-8] An example of this behavior is shown in Figure 1 for the autoxidation of Exxsol D-110 with various levels of added BHT at 140°C in a Parr bomb reactor.[6] It is apparent from the figure that increasing levels of added BHT result in increasing delays in the oxidation process. The oxidation behavior with added antioxidant is characterized by a slow initial oxidation followed by a sudden rapid increase in the oxidation rate.

Previous chemical kinetic modeling of antioxidants in jet fuel concentrated on relatively short reaction times, where significant consumption of the antioxidant species had not occurred.[4] In the present work, we extend the modeling to longer times to determine if the model can predict and corroborate the sudden increase in oxidation rate upon antioxidant consumption. The results at various levels of added BHT antioxidant are shown in Fig. 5. The figure shows plots of oxygen concentration versus time for modeling performed at 140°C. The rate parameters of Table 1 were used and the concentration of the peroxide decomposing species, SH, was held at zero to "turn off" reaction 17. The plot shows that without added antioxidant the "fuel" oxidizes rapidly, completely consuming the available oxygen in less than one hour. In the presence of added antioxidant there is an initial slow oxidation followed by a change to a more rapid loss of oxygen. As the antioxidant concentration is increased, the delay until the onset of rapid oxidation increases. This qualitative behavior is remarkably similar to the experimental measurements of Figure 1. As the antioxidant concentration is varied over the range 0 to 50 mg/L the time at which the oxidation rate rapidly increases, matches the measurements quite well. Note that a direct quantitative comparison between Figs. 1 and 5 cannot be performed as the Parr bomb technique is complicated by the presence of headspace oxygen and diffusional effects.[9] Also the first 45 minutes to one hour of the measurements in Figure 1 corresponds to the heat-up period of the reactor, and thus significant reaction does not occur during this time.

Modeling of autoxidation at 185°C

Figure 6 shows results for the modeling at a temperature of 185°C. Without antioxidant the "fuel" oxidizes rapidly, completely consuming the oxygen in 60 seconds. As at 140°C, at relatively low concentrations of added antioxidant (0.5 to 8 x 10^{-4} M) there is an initial slow oxidation followed by a change to a more rapid oxygen loss. The figure also shows predicted oxygen profiles at relatively high concentrations of added antioxidant, up to 3.2 x 10^{-3} M (704 mg/L based on the molecular weight of BHT). As the antioxidant concentration is increased above 8 x 10^{-4} M, the rate of the initial oxidation increases significantly, eroding the gains in slowing the oxidation at lower concentrations of antioxidant. This increase in oxidation rate with added antioxidant is similar to that observed in the blending of slow and fast oxidizing fuels.[8] These workers progressively diluted a slow oxidizing fuel with Exxsol D-80 and measured the oxidation profiles at 185°C. They observed that as the fuel was diluted to a 1:1 fuel:solvent ratio, that oxidation slowed. Upon further dilution the oxidation rate increased. We have previously argued that the dilution of a slow oxidizing fuel, i.e., one which contains a significant quantity of naturally occurring antioxidants, is effectively the same as lowering the concentration of these antioxidants.[7] Thus, the present modeling predicts that at relatively high concentrations of antioxidant, increases in the oxidation rate will be observed relative to lower, more optimum levels. Indeed, the blending experiments showed such behavior, implying the slow oxidizing fuel contained a concentration of antioxidant greater than optimum. Thus, dilution slows oxidation until the optimum concentration is reached, and further dilution decreases the time to complete oxygen consumption due to a lower than optimum antioxidant concentration. This behavior, where there exists an optimum antioxidant concentration above and below which the oxidation rate increases, was also predicted by the previous modeling study.[4]

Figure 6 also shows that as the concentration of added antioxidant is varied over the range 0.5 to 8 x 10^{-4} M, the time at which complete oxygen consumption occurs appears to increase in approximately even increments as the antioxidant concentration is doubled. This behavior is remarkably similar to that observed in the blending of fuels.[8] Balster et al. observed an approximate even spacing in increasing oxygen consumption time as the dilution factor is doubled

for the blending of a fast oxidizing fuel with a slow oxidizing fuel. This occurred over the range 2.5 to 20% of the slow oxidizing fuel. This agreement lends further support to the validity of the chemical kinetic model. It also supports the view that dilution of a slow oxidizing fuel with a fast oxidizing fuel is, in effect, a dilution of the naturally occurring antioxidants present in the slow oxidizing fuel.

The good qualitative agreement observed between the chemical kinetic model employed here, and measurements of fuel and hydrocarbon oxidation, provides evidence of the correctness of the assumptions in the mechanism. In particular, the interception of peroxy radicals by the antioxidant species, reaction 5, and subsequent antioxidant product chemistry is successful in reproducing both the observed slowing in oxidation at short times and the subsequent increase in oxidation rate at long times. On the other hand, Jones et al.[5] have hypothesized that the primary mechanism for the relatively slow autoxidations observed in some jet fuels is the reaction of hydroperoxides with sulfur species to produce non-radical products, reaction 17. We have shown above that the presence of peroxy radical inhibiting species can provide significant slowing of oxidation and the modeling of these reactions shows excellent qualitative agreement to the measured oxygen profiles. In order to explore the role that hydroperoxide decomposers may play in the autoxidation process, we will set the AH concentration to zero and vary the concentration range of the SH over the range 0 to 2×10^{-2} M for oxidation at 185°C. In order to maximize the importance of reaction 17, we have used a "fast" A-factor and an activation energy of zero for the rate parameters of this reaction. The results are shown in Figure 7. The figure shows that over the range of SH concentrations 2 to 200×10^{-4} M, significant delays in oxidation are predicted. Complete oxygen consumption is delayed to 670 seconds upon addition of 2×10^{-3} M of SH. No further changes in oxidation are predicted at higher concentrations of SH. With increasing SH concentration, the oxygen profiles appear to approach a limiting oxygen profile which is near linear in time. This is due to hydroperoxide consumption via reaction 17 completely preventing unimolecular hydroperoxide decomposition via reaction 11.

Can we now use these modeled oxygen profiles to determine if the observed laboratory oxygen behavior during fuel/solvent blending[8] is due to a peroxy radical inhibitor or a peroxide

decomposer? The behavior of the calculated oxygen profiles of Fig. 7 with increasing peroxide decomposer, SH, is different from those observed with increasing peroxy radical interceptor, AH (Figure 6), in three respects. First, the delays observed, a maximum of 670 seconds, are significantly smaller than for the addition of AH. Second, as the SH concentration is doubled over the range 2 to 16 x 10^{-4} M, the time for complete oxygen consumption is not evenly spaced. And third, at large SH concentrations the oxidation profile reaches a limiting rate. In contrast, the measured oxygen profiles of fuel blends of Balster et al. have oxygen consumption times greater than 1500 seconds, show evenly spaced consumption times with a doubling of the AH concentration, and do not reach a limiting profile. It is apparent that the predicted effects of a peroxide decomposer addition on oxidation are not similar to the laboratory measurements of Balster et al., while the peroxy radical inhibition mechanism does represent the data well.

In a separate work, Jones et al.[5] studied the effects of blending two jet fuels, one of which (the slower oxidizing fuel) is the same fuel as in the Balster et al. study. This study reports maximum oxygen consumption times of 840 seconds and the oxygen profiles do reach a limiting value at blends approaching 100% of the slow oxidizing fuel. But as the slow oxidizing fuel is added to the fast oxidizing fuel, as the slow oxidizing fuel is doubled the time to complete oxygen consumption does appear to be evenly spaced. Thus, it would appear that in this study the oxygen decay behavior has some, but not all, of the characteristics of the peroxide decomposer mechanism. Unfortunately, this study is complicated by the probable presence of naturally occurring (and possibly refinery added) antioxidants in the relatively fast oxidizing fuel. The blending of these two fuels is not a true dilution of the antioxidant concentration of the slow oxidizing fuel because the fast oxidizing fuel contains these additional inhibitors. Balster et al. point out that dilution of a jet fuel which contains approximately 20% aromatics with another jet fuel of similar aromatic content is different from dilution with a solvent which is devoid of aromatics. They posit that the initiation rate is proportional to the aromatic content and attribute the differences in the two studies to these changes in aromatic content.

This modeling study shows that the fuel/solvent blending behavior matches the behavior predicted by the peroxy radical interception mechanism and is therefore the most likely

mechanism for the observed oxygen profiles in these fuel blends. The fuel/fuel blending study exhibits behavior that has some of the characteristics of both the peroxy radical inhibition and hydroperoxide decomposition (reaction 17) mechanisms. As the slow oxidizing fuel is the same in the two studies, it is likely that the same oxidation slowing pathways are important in both studies. It must be emphasized that the mechanism used here is an oversimplification of the complex chemistry that occurs during the oxidation of real fuels. In particular, the peroxide decomposer reaction, reaction 17, is a simplification of a poorly understood mechanism in which oxidized sulfur species that are produced from the reaction may provide additional peroxide decomposition pathways.[17,18] Also, as jet fuel is a complex chemical mixture which likely contains both naturally occurring peroxy radical inhibitors and peroxide decomposer compounds, it is likely that both mechanisms occur in real fuels. To determine the behavior predicted for the simultaneous occurrence of the two inhibition pathways we have modeled the case at 185°C in which equal concentrations of the two compounds, AH and SH, are present at a concentration of 1×10^{-4} M. The results are shown in Fig. 8, along with the predicted oxygen profiles in the presence of the individual compounds at 2×10^{-4} M. It is apparent from the figure that the model predicts the two compounds acting together display a synergistic effect on the oxidation profile. The oxidation rate is drastically slowed by the presence of both species, much more than would occur from just the sum of the two effects. Indeed, this type of synergism between peroxy radical inhibiting antioxidants and peroxide decomposing species has been observed experimentally.[19] Apparently, the presence of the peroxide decomposer lowers the radical production rate enough to significantly slow the consumption of the peroxy radical inhibiting antioxidant. Thus, AH survives longer and the change to faster oxygen consumption occurs later. Another view is that the peroxy radical inhibiting antioxidant slows the production of hydroperoxides and thus the peroxide decomposer is able to survive longer. These processes occur simultaneously as both SH and AH are removed simultaneously during the run.

Conclusions

This study has utilized the QCM/Parr bomb system with a headspace oxygen sensor to simultaneously measure oxidation and deposition during thermal oxidative stressing of jet fuel. We find that rapid increases in oxidation will occur upon consumption of an added antioxidant to a fast oxidizing fuel. The antioxidant appears to be consumed by reaction, presumably with alkylperoxy radicals. We find that MDA is consumed during thermal oxidative stressing, and this consumption results in large increases in the oxidation rate in metal containing fuel. Mechanisms for MDA consumption have been hypothesized. The consumption of antioxidants and MDA have important implications in the design of jet fuel thermal stability improving additive packages, particularly in the additive concentration optimization process. We also used chemical kinetic modeling to simulate the autoxidation of jet fuel including the chemistry of peroxy radical inhibiting antioxidants and hydroperoxide decomposing species. Recent experimental measurements of oxygen concentration during autoxidation of jet fuel were used to "calibrate" the rate parameters of the mechanism. The model shows excellent agreement for oxygen profiles of static measurements at 140°C. At this temperature the model predicts large increases in oxidation rate upon peroxy radical inhibiting antioxidant consumption to below 1×10^{-5} M. At 185°C we have shown that peroxy radical inhibiting antioxidants and hydroperoxide decomposers both slow and/or delay oxidation, but the resulting oxygen profiles display different characteristics. We have shown that comparison of these profiles with fuel blending measurements has the potential to differentiate between the two types of oxidation slowing species. The modeling predicts that the presence of both types of species in a fuel results in a synergistic slowing in the oxidation rate.

References

(1) Hazlett, R. N. *Thermal Oxidation Stability of Aviation Turbine Fuels*; ASTM: Philadelphia, 1991.
(2) Heneghan, S. P.; Zabarnick, S.; Ballal, D. R.; Harrison, W. E. *J. Energy Res. Tech.* **1996**, *118*, 170-179.
(3) Edwards, T. *Prepr.-Am. Chem. Soc., Div Pet. Chem.* **1996**, *41*, 481-487.
(4) Zabarnick, S. *Ind. Eng. Chem. Res.* **1993**, *32*, 1012-1017.
(5) Jones, E. G.; Balster, L. M.; Balster, W. J. *Energ. Fuels.* **1996**, *10*, 509-515.
(6) Zabarnick, S.; Whitacre, S. D. "Aspects of Jet Fuel Oxidation," ASME 97-GT-219, 1997.
(7) Zabarnick, S.; Zelesnik, P.; Grinstead, R. R. *J. Eng. Gas Turbines Power.* **1996**, *118*, 271-277.
(8) Balster, L. J.; Balster, W. J.; Jones, E. G. *Ind. Eng. Chem. Res.* **1996**, *10*, 1176-1180.
(9) Zabarnick, S. *Ind. Eng. Chem. Res.* **1994**, *33*, 1348-1354.
(10) Zabarnick, S.; Grinstead, R. R. *Ind. Eng. Chem. Res.* **1994**, *33*, 2771-2777.
(11) Striebich, R. **1996**, unpublished results.
(12) Whitbeck, M. *Tetrahedron Comput. Methodol.* **1990**, *3*, 497-505.
(13) Zabarnick, S. *Energ. Fuels.* **1997**, submitted.
(14) Downing, F. B.; Clark, R. G.; Pedersen, C. J. *Oil & Gas J.* **1939**, *38*, 97-101.
(15) Clark, R. H., Presented at the 3rd International Conference on the Stability and Handling of Liquid Fuels, London, 1988.
(16) Clark, R. H.; Delargy, K. M.; Heins, R. J. *Prepr.-Am. Chem. Soc., Div. Fuel Chem.* **1990**, *35*, 1223-1230.
(17) Holdsworth, J. D.; Scott, G.; Williams, D. *J. Chem. Soc.* **1964**, 4692-4699.
(18) Denison, G. H.; Condit, P. C. *Ind. Eng. Chem.* **1945**, *37*, 1102-1108.
(19) Scott, G. *Chem. and Ind.* **1963**, 271-281.

Table 1
Reaction Mechanism for Chemical Kinetic Modeling

Reaction	Arrhenius A-Factor (moles, liters, and secs units)	Activation Energy (kcal/mole)	Reaction Number
$I \Rightarrow R\cdot$	1×10^{-3}	0.0	(1)
$R\cdot + O_2 \Rightarrow RO_2\cdot$	3×10^{9}	0.0	(2)
$RO_2\cdot + RH \Rightarrow RO_2H + R\cdot$	3×10^{9}	12.0	(3)
$RO_2\cdot + RO_2\cdot \Rightarrow$ termination	3×10^{9}	0.0	(4)
$RO_2\cdot + AH \Rightarrow RO_2H + A\cdot$	3×10^{9}	5.0	(5)
$AO_2\cdot + RH \Rightarrow AO_2H + R\cdot$	3×10^{5}	10.0	(6)
$A\cdot + O_2 \Rightarrow AO_2\cdot$	3×10^{9}	0.0	(7)
$AO_2\cdot + AH \Rightarrow AO_2H + A\cdot$	3×10^{9}	6.0	(8)
$AO_2\cdot + AO_2\cdot \Rightarrow$ products	3×10^{9}	0.0	(9)
$R\cdot + R\cdot \Rightarrow R_2$	3×10^{9}	0.0	(10)
$RO_2H \Rightarrow RO\cdot + \cdot OH$	1×10^{15}	42.0	(11)
$RO\cdot + RH \Rightarrow ROH + R\cdot$	3×10^{9}	10.0	(12)
$RO\cdot \Rightarrow R_{prime}\cdot$ + carbonyl	1×10^{16}	15.0	(13)
$\cdot OH + RH \Rightarrow H_2O + R\cdot$	3×10^{9}	10.0	(14)
$RO\cdot + RO\cdot \Rightarrow RO\cdot$ termination	3×10^{9}	0.0	(15)
$R_{prime}\cdot + RH \Rightarrow$ alkane $+ R\cdot$	3×10^{9}	10.0	(16)
$RO_2H + SH \Rightarrow$ products	3×10^{9}	0.0	(17)

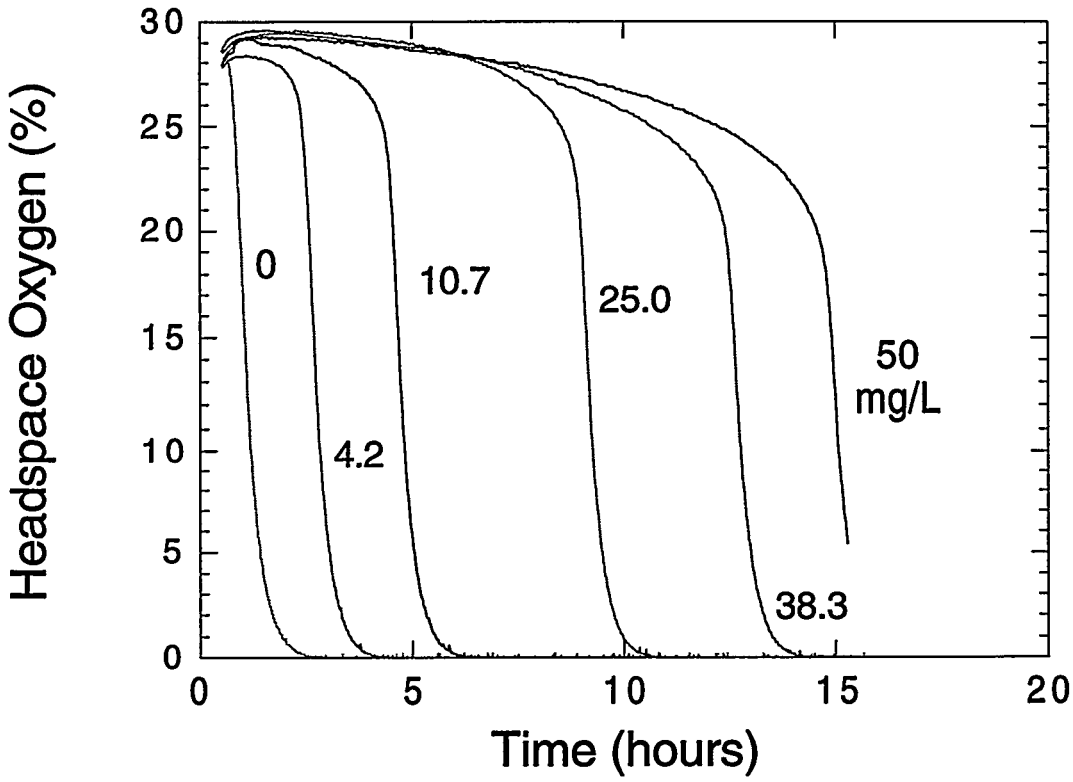


Figure 1. Plots of headspace oxygen concentrations versus time for Exxsol D-110 at various concentrations of added BHT at 140°C.

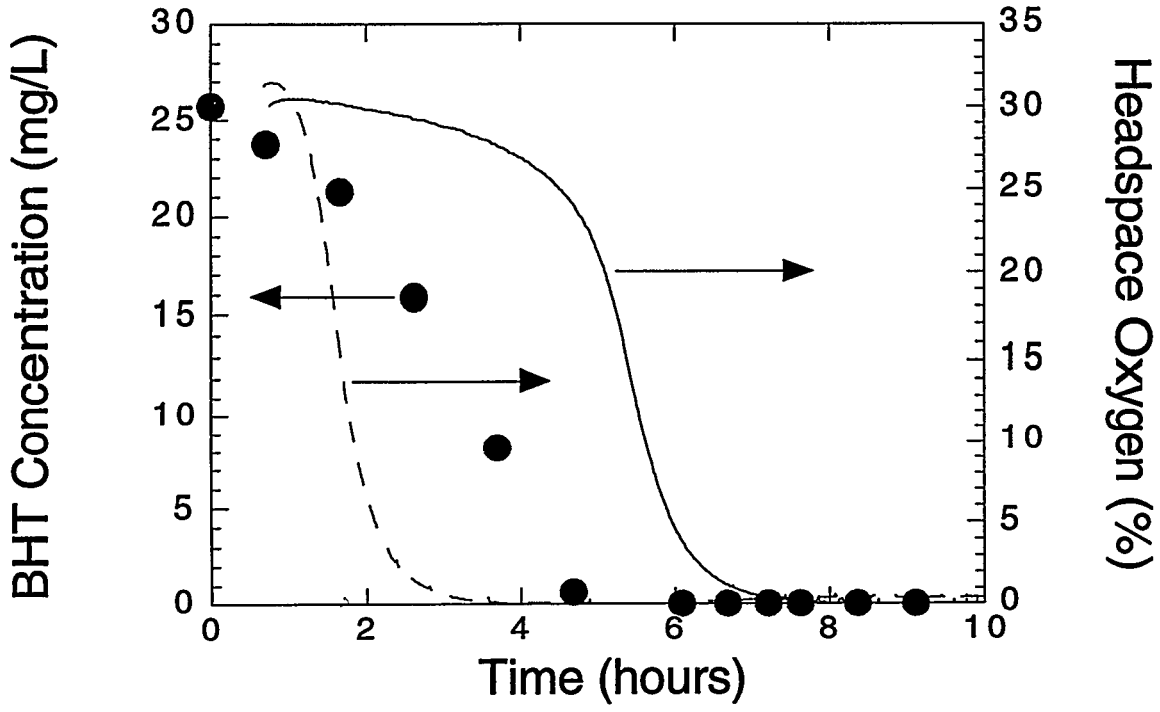


Figure 2. Plots of BHT (●) and headspace oxygen concentrations versus time for fuel F-3139 neat (dotted line) and with 25 mg/L BHT (solid line) at 140°C.

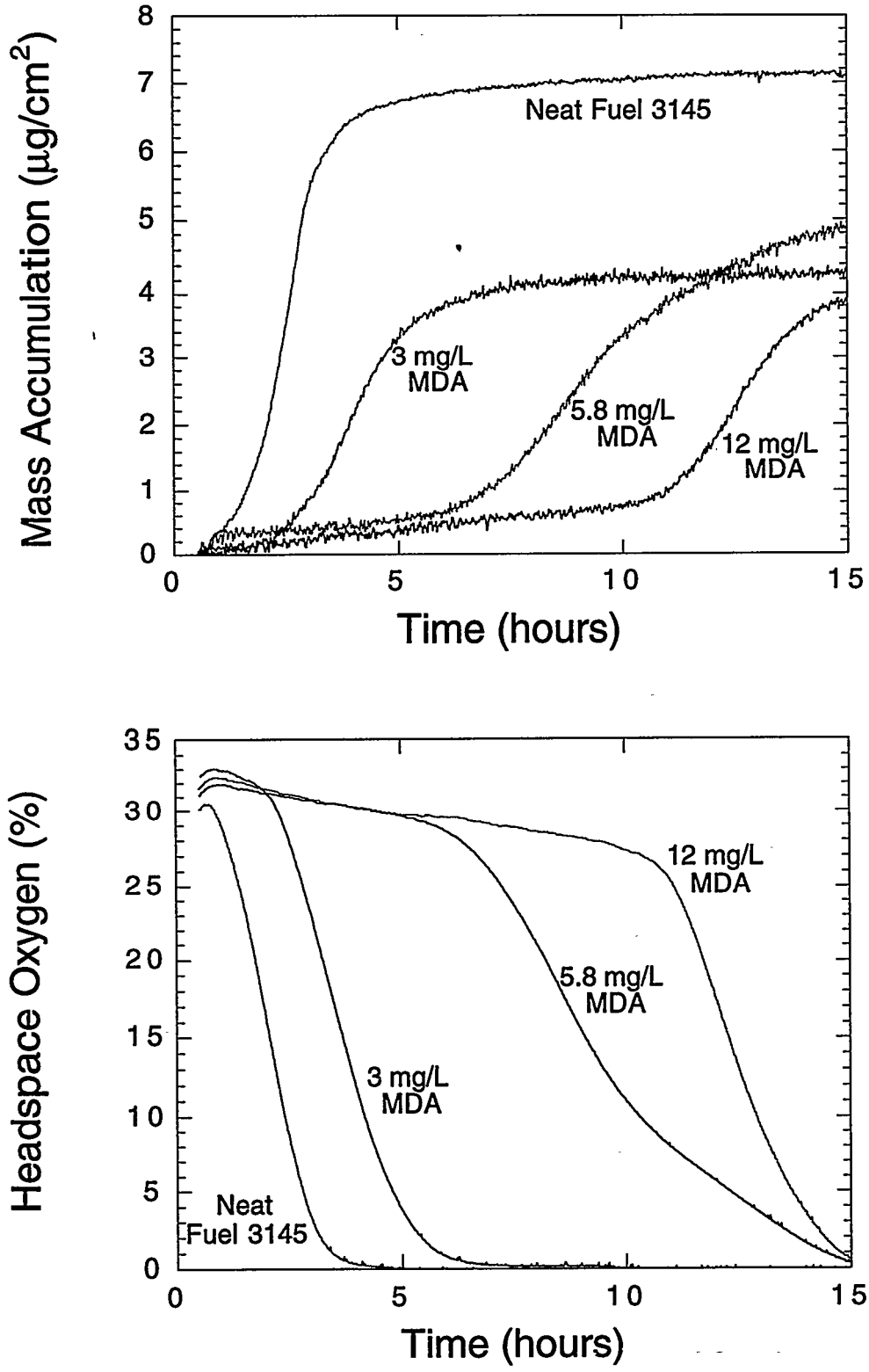


Figure 3. Plots of mass accumulation (a, top) and percent oxygen (b, bottom) for fuel F-3145 at various concentrations of added MDA at 140°C.

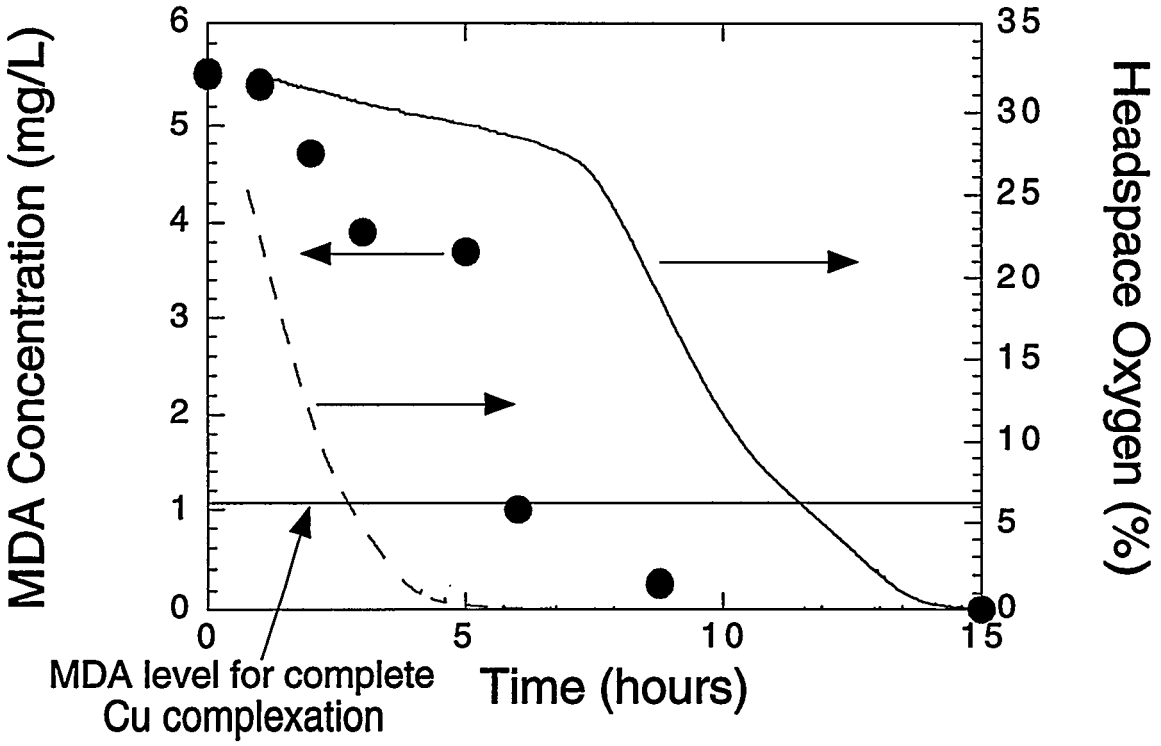


Figure 4. Plots of MDA (●) and headspace oxygen (line) concentrations versus time for fuel F-3145 with 5.8 mg/L MDA at 140°C.

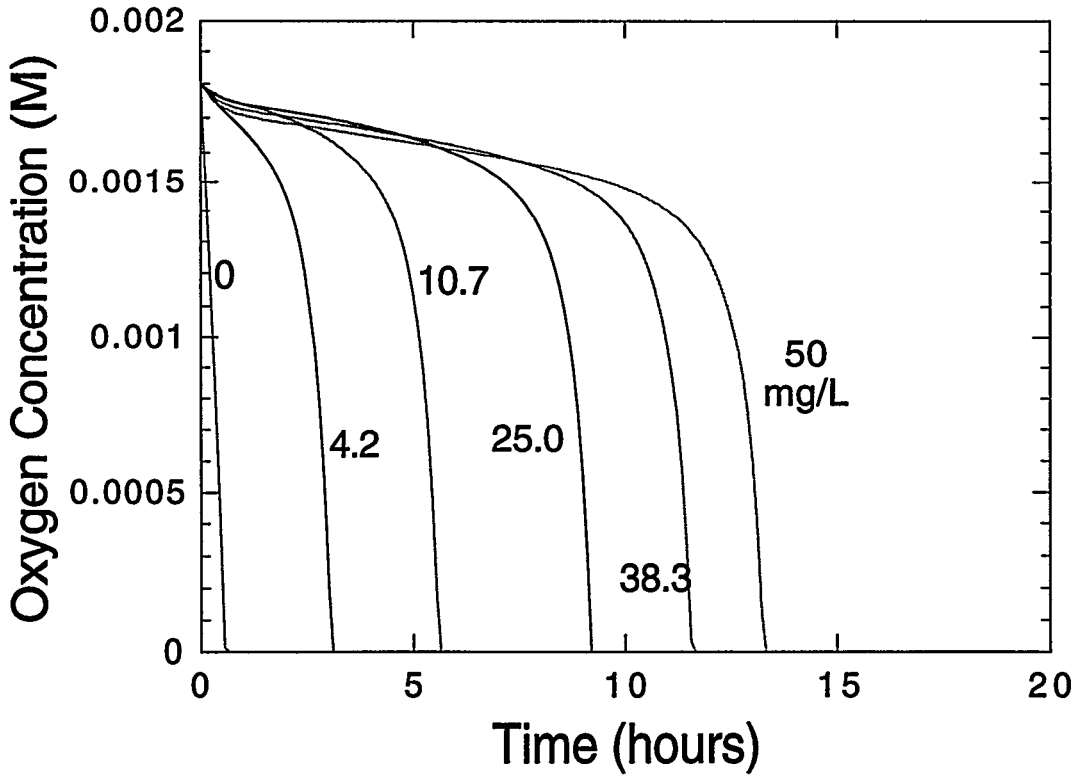


Figure 5. Plots of calculated oxygen concentration versus time at various concentrations of added antioxidant BHT at 140°C.

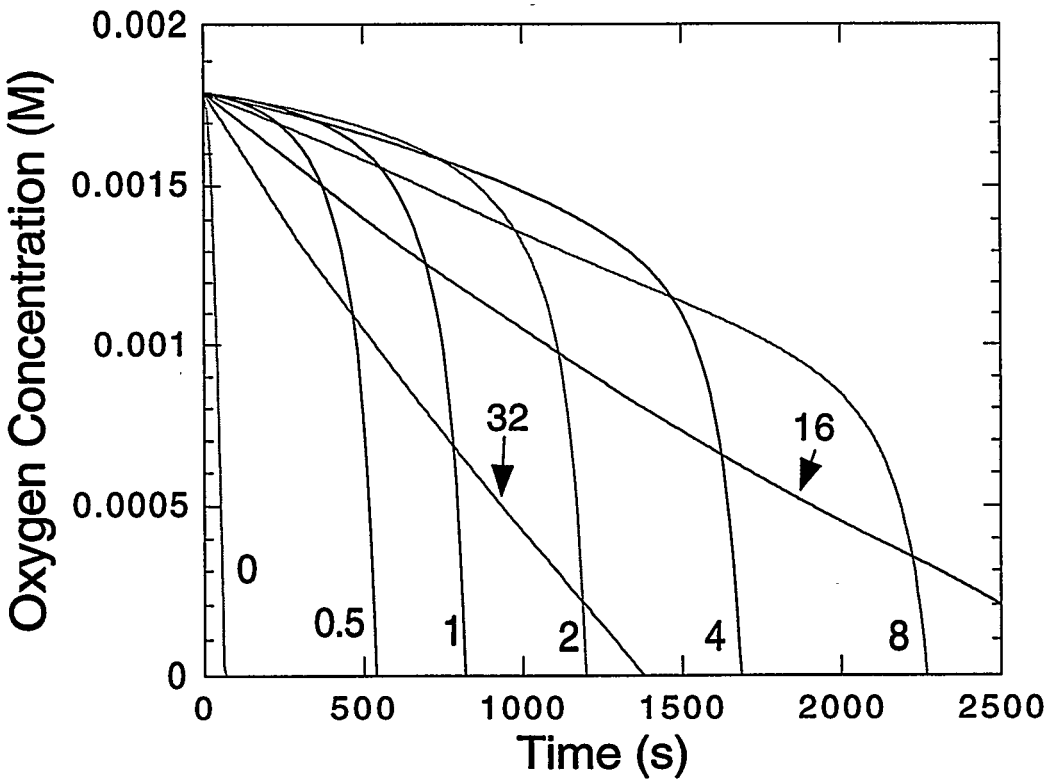


Figure 6. Plots of calculated oxygen concentration versus time for various concentrations of added antioxidant AH (x 10^{-4} M) at 185°C.

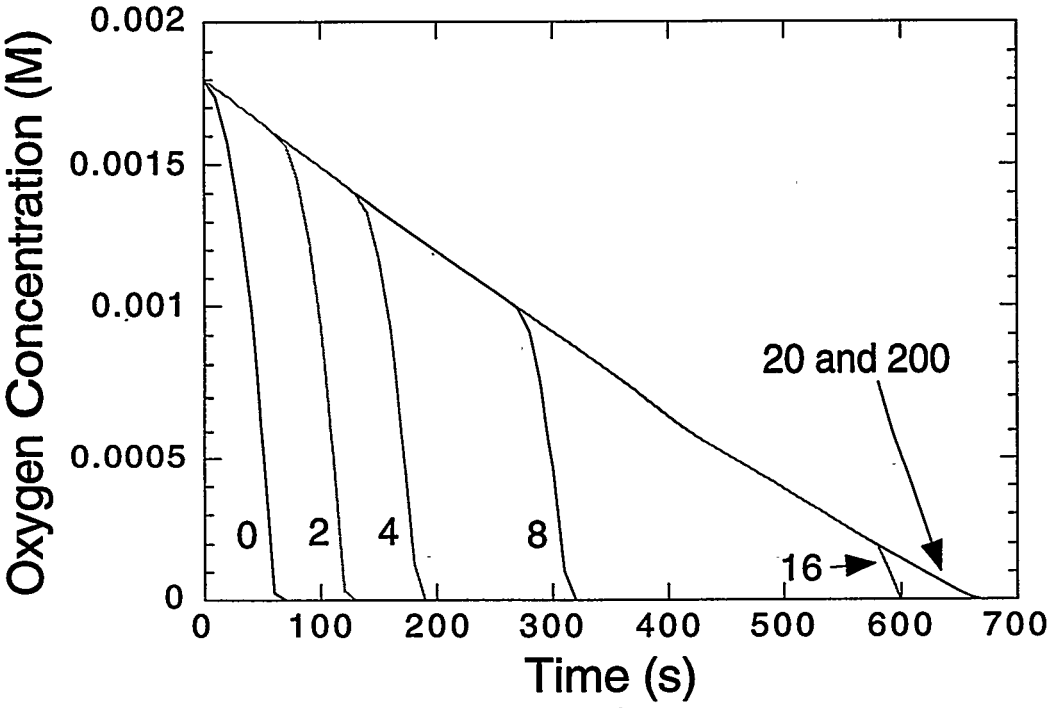


Figure 7. Plots of calculated oxygen concentration versus time for various concentrations of hydroperoxide decomposer, SH (x 10^{-4}) at 185°C.

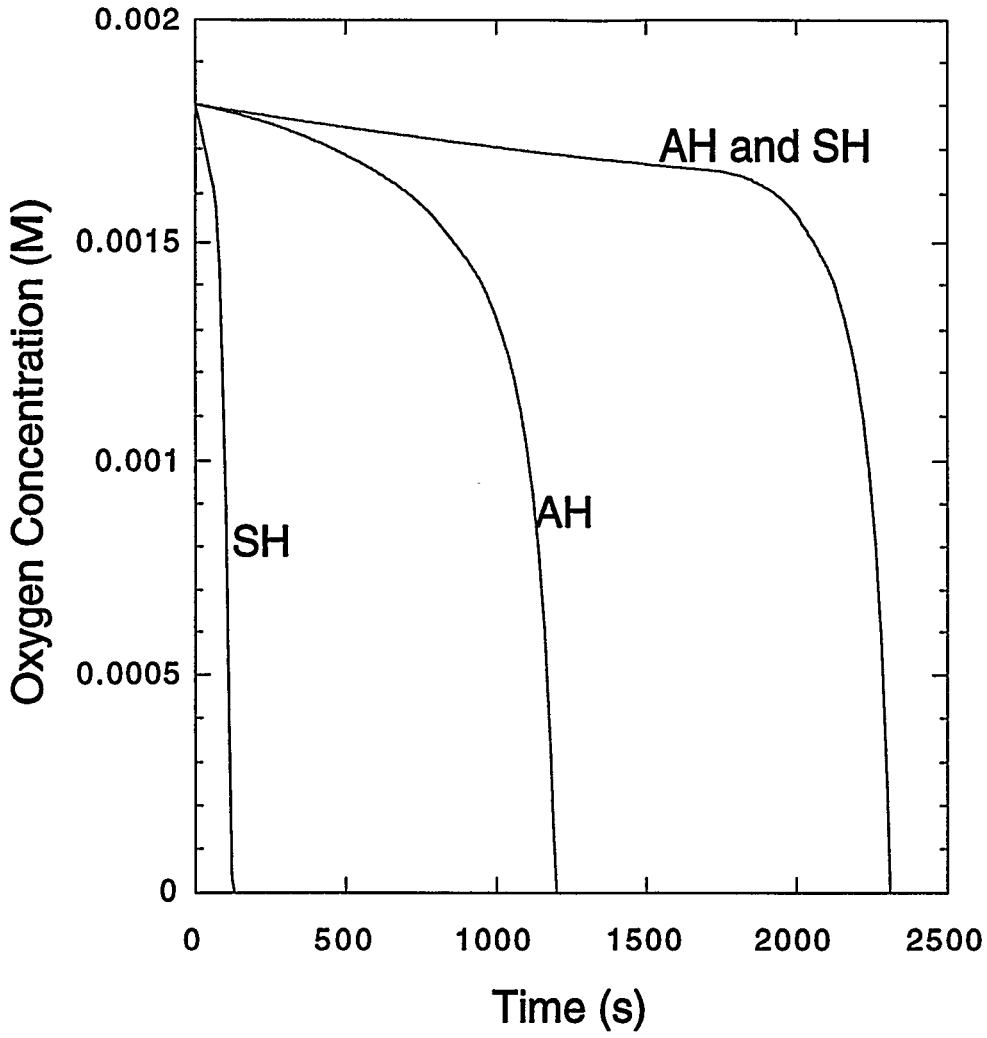


Figure 8. Plots of oxygen concentration versus time at 185°C for AH and SH both at 1×10^{-4} M and each compound individually at 2×10^{-4} M.

6th International Conference
on Stability and Handling of Liquid Fuels
Vancouver, B.C., Canada
October 13-17, 1997

NUMERICAL SIMULATIONS OF JET FUEL OXIDATION AND FLUID DYNAMICS

J.S. Ervin* and S. Zabarnick
University of Dayton Research Institute, Dayton, OH 45469-0210

A pseudo-detailed kinetics model which considers antioxidant chemistry was employed in a computational fluid dynamics code, and concentration profiles of various species along a stainless-steel tube were calculated for both nearly isothermal and non-isothermal flowing systems. Flowing experiments were performed with both a severely hydrotreated fuel and a straight-run fuel, and the predicted dissolved oxygen and hydroperoxide profiles agreed well with the measured profiles over a range of bulk fuel temperatures and flow conditions. Favorable comparison was also found between model predictions and measurements taken from the literature. The model was found to be capable of simulating a synergistic reduction in the oxidation rate that is sometimes observed among different fuel antioxidants. The present model offers an improved understanding of jet fuel oxidation, antioxidant chemistry, and the involved fluid dynamics.

Introduction

Jet fuel is circulated in military aircraft as a coolant. In the presence of heat and dissolved O_2, jet fuel degrades through a complex sequence of chemical reactions forming oxidized products and fouling surfaces. Fouling can disrupt normal fuel flow within fuel system components and may potentially lead to catastrophic failure.[1] Since the reactions in which dissolved O_2 is consumed comprise a portion of the fouling process, an understanding of dissolved O_2 removal is imperative for aircraft design.

Computational simulations which use the mass, momentum, energy, and species conservation equations along with an appropriate chemical kinetics model can be used to predict O_2 consumption for different flow conditions. However, jet fuels are mixtures of numerous compounds and, thus, it is impractical to model the chemical changes of all components. To add to the complexity of numerically simulating O_2 removal, military jet fuels come from many different geographical sources and their compositions change while in storage. Since fuel oxidation is complex, global-chemistry kinetics have been used in previous computational

simulations.[2,3,4,5] The global mechanisms used in computational fluid dynamics simulations generally employ one reaction to represent fuel autoxidation:

$$\text{Fuel} + O_2 \rightarrow \text{Products} \quad (1)$$

The underlying assumption of equation 1 is that the overall reaction of a mixture of compounds can be represented by a single rate equation that is comprised of a rate constant multiplied by concentrations with simple order dependence.[6] It is further assumed that the rate constant is defined by the product of an Arrhenius A-factor and an activation energy term.

The approach taken here is to model the oxidation of hydrocarbon fuels by means of pseudo-detailed chemical kinetic modeling. The model is pseudo-detailed in the sense that the chemical kinetics of O_2 consumption are described using several reactions which represent the dominant chemistry rather than using hundreds of reactions as might be found in a detailed model or a single oxidation reaction as found in previous studies. The current work employs the first computational fluid dynamics code which uses pseudo-detailed kinetic modeling of dissolved O_2 consumption and antioxidant chemistry in jet fuel. The numerical model permits the study of the effects of naturally occurring antioxidants and antioxidant additives. It is highly desirable to have the capability to predict the effects of additives on fuels because experiments involving the additive testing of fuels are costly.

Two groups of antioxidants are considered. The first, denoted by AH, represents hindered phenols which slow oxidation by removing alkyl peroxy free radicals from the autoxidation chain.[7,1] Hydroperoxide decomposers, represented by SH, comprise the second group. SH is thought to be some sulfur (or other) species which provide alkyl hydroperoxide (ROOH) decomposition pathways as an alternative to unimolecular ROOH decomposition reactions.[7,8,9] The objective of this paper is to study jet fuel oxidation and the behavior of these two groups of antioxidants in flowing systems using computational fluid dynamics and pseudo-detailed chemical kinetic modeling.

Experimental

For model verification, experiments were conducted using a heat exchanger which simulated a complex thermal and flow environment approaching that of an aircraft. Profiles of dissolved O_2 and ROOH concentrations along the tube length for both a rapidly-oxidizing

hydrotreated fuel and a slowly-oxidizing straight-run fuel were compared to numerical predictions which used a pseudo-detailed kinetic model. Table 1 lists characteristics of neat F2827 and F2747 jet fuels used in the experiments. F2827 produces relatively low hydroperoxide concentrations and oxidizes relatively slowly when heated in the presence of dissolved O_2. On the other hand F2747, which has very low sulfur and naturally occurring antioxidant components and produces relatively high concentrations of ROOH, oxidizes relatively rapidly when oxidatively stressed. Based on the measurements of Striebich and Rubey,[10] the dissolved O_2 concentration (air saturated value) at the flow rig inlet was 65 ppm (w/w) for F2827 and 73 ppm for F2747.

Fuel at ambient temperature enters the heated tube[11] at a pressure of 2.48 MPa. At this pressure level, the fuel remains as a liquid everywhere within the system. Bulk dissolved O_2 levels were measured on-line at the flow inlet and exit by means of a modified gas chromatograph.[12] The ROOH concentrations of the aged fuel were measured by cyclic voltammetry techniques.[13]

A heated copper block envelopes the 316 stainless-steel tubing (45.8-cm long by 2.16-mm ID by 3.18-mm OD) through which the fuel passes. Calibrated thermocouples (20 gage) are welded to the outer surface of the stainless-steel tubing to provide the outer tube wall temperatures with an uncertainty of ± 2 °C. The bulk fuel temperature at the exit of the heated tube was also measured, and the uncertainty in its measurement was $\pm$ 10 °C. The stainless-steel tubes (ASTM grade A269/A213) have a surface roughness (arithmetic average) of 8 to 15 micro inches and are cleaned with Blue Gold alkaline solution in an ultrasonic bath, rinsed with deionized water, and dried with flowing laboratory-grade nitrogen gas prior to use.

The tests conducted in the present apparatus are usually conducted under conditions of relatively high flow rates and temperatures. In the present work, with a volumetric flow rate of 16 ml/min, the flow was laminar at the entrance of the heated block but became turbulent. Buoyancy forces normal to the flow direction increased the heat and mass transport, rendering the flow turbulent.[4] The study of turbulent flow is important because it is normally encountered in the fuel systems of military aircraft.

Fluid dynamics and heat transfer strongly influence jet fuel oxidation, but the nature of this influence is not well understood.[1] For this reason, numerical simulations of dissolved O_2

consumption were performed for the present flow conditions as well as for the flow conditions reported by Jones et al.[8,14] in a near-isothermal flowing test rig (NIFTR). In contrast to the conditions of our apparatus, the NIFTR experiments are conducted at lower temperatures and flow rates in order to attain near-isothermal conditions in a minimum length of tube. In both experiments, the temperature of the copper block used to heat the tube and the flow rate are varied to produce different oxidation rates and residence times, respectively. Figure 1 shows calculated bulk fuel temperature and measured tube wall temperature profiles along the heated tube length for both the present experiments and the NIFTR experiments. The NIFTR experiments use a 81.3 cm-long heated tube, whereas the current experiments use a 45.8 cm-long heated tube. The maximum wall temperature for both experiments of Figure 1 is near 200 °C. Figure 1 shows that for a flow rate of 16 ml/min and a maximum tube wall temperature near 200°C, the calculated bulk fuel temperature increases along the entire heated tube length, never reaching the wall temperature. Although not shown, similar experiments performed at greater wall temperatures were characterized by bulk temperature profiles which also never attained the wall temperature. In contrast in the NIFTR for a flow rate of 0.125 ml/min, the fuel temperature reaches the tube wall temperature near the flow entrance.

Numerical Simulations

Pseudo-detailed chemical kinetic modeling was performed using the mechanism of Table 2 which is based on the mechanism of Zabarnick.[7] It is extremely difficult, if not impossible, to model the multitude of compounds present in jet fuel. Thus, the fuel is represented by the single compound RH. The initiation step (reaction 1 of Table 2) is assumed to occur by unimolecular decomposition of an initiating species, I. Reaction 1 is a simple representation of complex process that initiates the autoxidation chain with a low production rate of $R^{\bullet}$ radicals.[7,15] Reactions 1 through 4 and reaction 10 represent a simple chain mechanism for the oxidation of a hydrocarbon fuel. Reactions 5 through 9 represent the antioxidant chemistry associated with AH, which is a species with an easily abstracted H atom. Reactions 11 through 16 are associated with ROOH decomposition which occurs at sufficiently high temperatures and is believed to play an important role in accelerated O_2 consumption.[9,15] Reaction 17 is used to model the effects of hydroperoxide-decomposing species (SH). Zabarnick[7,15] estimated the rate parameters

(Arrhenius "A-factors" and activation energies) for the pseudo-elementary reactions largely by comparison with measured rate constants and Benson style "thermochemical kinetics" analysis.[16]

With the exception of three rate parameters, those listed in Table 2 are taken from Zabarnick[7] where a similar mechanism was used to study the antioxidant chemistry of hydrocarbon fuels in a non-flowing isothermal system. In the present study, the pre-exponential factor for the initiation reaction (Reaction 1) is 1×10^{-10}, whereas in Zabarnick[7] this pre-exponential factor is given as 1×10^{-3}. A smaller pre-exponential factor is used here such that the production rate of $R^{\bullet}$ becomes negligible once the chain begins. In the current work, the activation energies of reactions 11 and 17 are different from those originally given in Zabarnick.[7] For reaction 11, Zabarnick[7] used an activation energy of 42 kcal/mole, which is a representative value for a homogeneous ROOH decomposition reaction. However, metals have long been suspected of being involved in catalytic decomposition of hydroperoxides.[1,8,9] Thus, in the presence of a metal surface and/or dissolved metals, it is reasonable for the activation energy for the ROOH decomposition reaction to be less than 42 kcal/mole. In the present work, the activation energy for reaction 11 was taken as 37 kcal/mole. This value provided predictions of O_2 consumption which agreed well with flowing experiments which used fuel F2747 over a large temperature range. Fuel F2747 has very low concentrations of AH and SH and is nearly a pure solvent. Thus, Fuel F2747 was chosen for the "calibration" of the activation energy corresponding to reaction 11 because it is desirable to make the "calibrated" activation energy independent of the AH and SH concentrations. The activation energy for reaction 17 was chosen to be zero in Zabarnick.[7] In the present work, the activation energy for reaction 17 is selected to be 16 kcal/mole. It was observed here that an activation energy less than 16 kcal/mole removed ROOH too rapidly at lower temperatures for various concentrations of AH and SH. As a result, for activation energies less than 16 kcal/mole, the predicted dissolved O_2 concentration was nearly always greater than the measured concentration at the exit of the heated tube for the straight-run fuel (F2827). In the modeling performed here, it is assumed for simplicity that all fuels have the same initiating species concentration (I) of 4×10^{-8} moles/liter. With the activation energies and pre-exponential factors of Table 2, it is then possible to define different fuels in terms of their initial AH and SH concentrations.

The species concentrations were found numerically by a finite difference solution[4,18] of the coupled equations that arise from the mechanism of Table 2 and the transport equations. The following were input to the numerical code: the activation energies and pre-exponential factors of Table 2, concentrations (O_2, AH, RH, SH, and I) for each species at the entrance of the heated tube, tube wall temperature profile, and the grid resolution. Individual jet fuel samples are known to possess a range of oxidation and deposition characteristics which results from varying source petroleum and refinery processing. To provide the range of oxidation properties that a fuel may possess, we have chosen to modify the antioxidant, AH, and hydroperoxide decomposer, SH, concentrations for individual fuel samples. In simulations of fuel oxidation, two kinds of computations were performed: those for a naturally inhibited system (F2827 fuel) and those for a relatively non-inhibited system (F2747 fuel). For the inhibited fuel, AH and SH concentrations were chosen to match experimentally determined oxidation rates and measured hydroperoxide concentrations. The initial AH concentration was assumed to be 1.62×10^{-3} moles/liter which is a reasonable value for jet fuels,[7] and the initial SH concentration was assumed to be 1.21×10^{-3} moles/liter. For the completely uninhibited case, both the AH and SH concentrations were set equal to 0 moles/liter. For both the severely hydrotreated fuel (F2747) and the straight-run fuel (F2827), an identical initial I concentration was used for simplicity. The normal air saturation concentration was used for the initial O_2 concentration. Table 3 summarizes the initial O_2, AH, SH, and I concentrations used in the simulations. Ultimately, this model will be most useful if an analytical chemistry test could be used to determine an "effective" AH and SH concentration for individual jet fuel samples. Thus, a measure of the "effective" AH and SH concentration could be measured in the laboratory and entered into the model to provide a method to predict the oxidation properties of the fuel over a range of temperature, residence times, and flow properties.

Results and Discussion

Simulations of Flowing Fuel F2747. Figure 2 shows measured and predicted fractions of remaining dissolved O_2 at the exit of the heated tube for F2747 fuel (zero AH and SH concentrations) flowing at 16 ml/min for different bulk temperatures. Figure 2 shows that as the temperature approaches 170 °C, the dissolved O_2 concentration decreases rapidly until near 210

°C where the O_2 is nearly depleted. This rapid increase in oxidation rate with increasing temperature has been observed previously[17] for similar flow conditions and different fuel types.

The rate of ROOH decomposition has been shown to be important in understanding jet fuel oxidation.[1,9,15] Figure 3 shows measured and predicted ROOH concentrations at the heated tube exit for F2747 fuel for the same range of bulk temperatures described in Figure 2. Figure 3 shows a maximum in both the predicted and measured hydroperoxide concentrations at 210 °C, which is near the temperature associated with the dissolved O_2 depletion of Figure 2. In addition, the ROOH concentration of Figure 3 increases to levels near the initial dissolved O_2 concentration. This means that the initial dissolved O_2 concentration reacts nearly entirely to form ROOH. After the dissolved O_2 is fully consumed and as the bulk temperature continues to rise, ROOH decomposition by unimolecular reaction (Reaction (11) of Table 2) becomes increasingly significant. Figure 3 shows a relatively large maximum concentration of ROOH for fuel F2747 in contrast to the ROOH concentration produced with fuel F2827 (described later) for otherwise identical conditions. This was expected as the hydrotreating process removes heteroatomic species which may decompose hydroperoxides.

Simulations of Flowing Fuel F2827. Figure 4 shows predicted and measured dissolved O_2 fractions at the exit of a heated tube for fuel F2827 flowing at 0.125 ml/min (laminar flow) and for different constant wall temperatures. The experimental measurements[8,14] are for fuel F2827 passing through stainless-steel tubes. At a constant mass flow rate, any position along the tube may be directly related to the reaction time through the average velocity which, in turn, can be found from the known inner tube diameter, mass flow rate, and fuel density. Thus, Figure 4 shows the dissolved O_2 fraction as a function of residence time. Figure 4 shows that as the tube wall temperature is increased, the reaction time required for complete O_2 depletion decreases. The initial AH and SH concentrations were adjusted to give an O_2 consumption history which followed the O_2 measurements at 185 °C. Oxygen consumption histories of F2827 at the other temperatures and in our experiments were then predicted reasonably well using these initial concentrations of AH and SH.

In contrast to the constant wall temperatures associated with Figure 4, the imposed wall temperatures vary along the tube length for the present experiments (fuel F2827 flowing at 16 ml/min). The bulk fuel temperature (275 °C) at which the O_2 is fully consumed is greater than

that observed with fuel F2747 (210 °C) for similar flow conditions. This depletion of O_2 at the greater temperature for F2827 might be expected because F2827, unlike F2747, contains relatively large concentrations of AH and SH. After heating of the fuel, the ROOH concentrations measured for F2827 were much smaller than those produced with F2747. Calculated ROOH concentrations at the exit of the heated tube lie in a range between 0 mole/liter and 0.0004 mole/liter and agree reasonably with measured values.

Figure 5 shows the simulated consumption of dissolved O_2, AH, and SH together with the ROOH concentration for turbulent, non-isothermal flowing F2827 fuel at 300 °C maximum wall temperature. The O_2, AH, and SH concentrations drop slowly until near 0.28 m, where there is increased O_2 consumption. As a result of increased fuel oxidation, the ROOH concentration begins to rise. Consequently, the rate of disappearance of SH increases due to the increase in the ROOH concentration. In addition at 0.28 m, the fuel temperature (251 °C) is relatively high which means that reaction 17, based on its activation energy, will proceed more readily than at lower temperatures. Beyond 0.28 m, the ROOH concentration profile rises rapidly to a maximum at a location of 0.33 m, which coincides with the location of O_2 depletion. There, $RO_2^{\bullet}$ is no longer produced by means of reaction 2. Later in the tube as the $RO_2^{\bullet}$ concentration decreases to zero (reactions 3 and 5), the AH concentration profile becomes flat because AH is no longer consumed (reaction 5). The ROOH concentration profile decays by both the unimolecular decomposition reaction (reaction 11) and the ROOH-SH decomposition reaction (reaction 17) beyond the location of 0.33 m. For the initial conditions of Figure 5, the acceleration in O_2 consumption is controlled by ROOH decomposition rather than by depletion of the antioxidants. Although occurring later in the tube, similar behavior in consumption profiles for O_2, AH, and SH was observed at lower wall temperatures of 270 °C and 265 °C.

Temperature Effects. Using a flow rate of 16 ml/min and the heated copper block of the present experiments, the fuel temperature continuously rises along the tube. Thus, the interpretation of AH and SH concentration changes is complicated by the fact that the increasing temperature decreases the fuel density and increases the rates of reactions with high activation energies. Thus, to further explore the antioxidant chemistry associated with F2827 fuel, the more simple conditions of isothermal walls and laminar flow are used. Figures 6 and 7 show simulations of the consumption of dissolved O_2, AH, and SH together with the depletion of

ROOH for F2827 fuel flowing at a rate of 0.125 ml/min and an imposed constant tube wall temperature. For reference, O_2 removal profiles are also shown for the situation where there are no initial antioxidants present in the fuel. At 175 °C (Figure 6), the O_2 and SH profiles are parallel over much of the tube length, until the O_2 is depleted. At this location, the AH is no longer consumed, and the AH profile is horizontal. As the ROOH concentration approaches 0.0001 moles/liter, SH is consumed at an accelerated rate by means of reaction 17 until the ROOH concentration is sufficiently decreased by both reactions 11 (unimolecular ROOH decomposition reaction) and 17 (SH-ROOH decomposition reaction). Once the available ROOH is consumed, Figure 6 shows that there is negligible consumption of SH. Figure 7 shows that with a wall temperature of 205 °C, the AH and O_2 profiles appear less linear than those observed at 175 °C. Again, as with the wall temperature of 175 °C of Figure 6, Figure 7 shows an increased rate of consumption of SH as the ROOH concentration approaches 0.0001 moles/liter. As the tube wall temperature is increased from 175 °C to 205 °C, the location of dissolved O_2 depletion moves in the upstream direction.

Simulations of Flowing Fuel in Which the Concentration of AH or SH Is Individually Varied. As the proposed mechanism of Table 2 has been shown capable of predicting measurements of dissolved O_2 consumption for real fuels under conditions of laminar and turbulent flow over a wide temperature range, it is reasonable to use the mechanism to explore the effects of varying the initial concentration of one antioxidant while the initial concentration of the other is zero. For these simulations, it was decided to use the well-defined conditions of laminar flow with the tube walls held at constant temperature. Two tube wall temperatures (185 °C and 205 °C) and a flow rate of 0.125 ml/min were chosen.

For a constant wall temperature of 185 °C (not shown), O_2 concentration profiles were calculated for different initial concentrations of AH and zero SH. In the initial portion of the heated tube (upstream of 0.0025 m), the O_2 concentration decreases because of changes in fuel density associated with heating. As the AH concentration at the entrance of the tube is varied from 0 moles/liter to 16.2×10^{-4} moles/liter, the location of dissolved O_2 depletion moves downstream. This downstream shift in the location of complete O_2 removal with increasing AH concentration demonstrates that the predicted oxidation rate decreases significantly with increasing AH. For the same initial AH concentrations but at a higher wall temperature of 205

°C (Figure 8), the locations of complete O_2 removal are upstream from those calculated using a wall temperature of 185 °C. As the temperature is increased, the rates of reactions which have non-zero activation energies tend to increase. Reactions (reactions 3, 6, 11, 12, 13, 14, and 16) which either directly or indirectly produce R• and propagate the oxidation chain have greater rates at 205 °C. Thus relative to 185 °C, there is increased oxidation prior to O_2 depletion at 205 °C.

Figure 9 shows O_2 consumption along the heated tube length for a wall temperature of 205 °C. Here the initial SH is varied between concentrations of either 0 or 16.2 x 10^{-4} moles/liter in the absence of AH. As the initial SH concentration is increased above zero, the location of complete O_2 removal moves slightly further from the tube entrance. The profiles of dissolved oxygen removal corresponding to the nonzero inlet SH concentrations (0.81 x 10^{-4}, 8.1 x 10^{-4}, and 16.2 x 10^{-4} moles/liter) essentially overlay each other. At a tube wall temperature of 185 °C (not shown), the dissolved oxygen profiles again nearly lie on each other, but the individual curves are less distinguishable near the tube inlet than those observed for an imposed wall temperature of 205 °C. For the same flow and temperature conditions, a comparison of Figures 8 and 9 reveals that SH is significantly less effective in delaying dissolved O_2 depletion for identical initial concentrations of SH and AH. Similarly at a lower tube wall temperature of 185°C (not shown) and with the same initial concentrations of SH and AH, AH is substantially more effective in delaying dissolved O_2 removal.

Synergistic Effects. Although the pseudo-detailed model presented here is an oversimplification of the complex chemistry that occurs during the oxidation of fuels, the model has been shown to correctly predict measured O_2 consumption and ROOH production and, as a consequence, may be used to further study the simultaneous presence of both AH and SH antioxidants. To this end, autoxidation under conditions of a constant wall temperature of either 185 or 205 °C and a flow rate of 0.125 ml/min has been modeled. Figure 10 shows that the presence of both AH and SH, each at a concentration of 8.1 x 10^{-4} moles/liter and at a wall temperature of 185 °C, is much more effective in delaying O_2 consumption than that occurring from the sum of the two effects of the antioxidants acting individually. The synergism between peroxy radical inhibiting antioxidants and peroxide-decomposing species shown in Figure 10 and

with a wall temperature of 205 °C (not shown) has been observed experimentally[9] and in an isothermal non-flowing model.[7]

Conclusions

A pseudo-detailed kinetics model has been incorporated into a computational fluid dynamics code to predict species concentrations for both non-isothermal and isothermal flows. With this pseudo-detailed model, experimental measurements such as hydroperoxide measurements in addition to dissolved oxygen measurements are used to characterize fuels over fairly wide temperature ranges. No assumption of a value for the over-all reaction order for oxygen consumption needs to be made with the current model. Since pseudo-detailed kinetic modeling relies on rate parameters which are more physically realistic than simpler global parameters, it is believed that pseudo-detailed kinetic modeling offers more promise to extend current simulation capabilities to include the effects of fuel additives. Experiments were conducted using a heat exchanger which simulated a complex thermal and flow environment. Oxygen consumption and the production of hydroperoxides were measured for a rapidly oxidizing hydrotreated jet fuel and for a slower oxidizing straight-run jet fuel. The predictions from the numerical simulations compared well with the experimental measurements.

Acknowledgments

This work was supported by the U.S. Air Force, Fuels and Lubrication Division, Aero Propulsion and Power Directorate, Wright Laboratory, WPAFB, under Contract Numbers F33615-92-C-2207 and F33615-97-C-2719 (Technical Monitor: C.W. Frayne). The authors would like to thank V.R. Katta of Innovative Scientific Solutions, Inc. for many helpful comments.

References

(1) Hazlett, R. N. *Thermal Oxidative Stability of Aviation Turbine Fuels*; ASTM: Philadelphia, 1991.

(2) Krazinski, J. L; Vanka, S. P.; Pearce, J. A.; Roquemore, W. M. *ASME Jour. Eng. Gas Turb. Power.* **1992**, *114*, 104-110.

(3) Chin, L. P.; Katta V. R.; Heneghan, S. P. *Am.Chem. Soc., Div. Pet. Chem. Preprints.* **1994**, *39*, 19-25.

(4) Katta, V.R.; Blust, J.; Williams, T.F.; Martel, C.R. *J. of Thermophysics and Heat Transfer.* **1995**, *9*, 159-168.
(5) Ervin, J.S.; Williams, T.F.; Katta, V.R. *Ind. Eng. Chem. Res.* **1996**, *35*, 4028-4032.
(6) Ervin, J.S.; Heneghan, S.P. International Gas Turbine Institute Turbo Expo: Orlando, Florida, 1997; Paper No. 97-GT-224.
(7) Zabarnick, S. Chemical Kinetic Modeling of Antioxidant Chemistry for Jet Fuel Applications, Submitted *Energy and Fuels.*
(8) Jones, E.G.; Balster, L.M.; Balster, W.J. *Energy and Fuels.* **1996**, *10*, 509-515.
(9) Scott, G. *Chem. and Ind.* **1963**, 271-281.
(10) Striebich, R.; Rubey, W. *Am.Chem. Soc., Div. Pet. Chem. Preprints.* 1994, *39*, 47-50.
(11) Heneghan, S.P.; Williams, T.F.; Martel, C.; Ballal, D.R. *ASME J. Eng. Gas Turb. and Power.* **1993**, *115*, 480-485.
(12) Rubey, W.A.; Striebich, R.C.; Tissandier, M.D.; Tirey, D.A.; Anderson, S.D. *J. Chromatogr. Sci.* **1995**, *33*, 433-437.
(13) Kauffman, R.E. *Am.Chem. Soc., Div. Pet. Chem. Preprints.* 1994, *39*, 42-46.
(14) Jones, E.G.; Balster, W.J.; Post, M.E. *ASME J. Eng. Gas Turb. and Power.* **1995**, *117*, 125-131.
(15) Zabarnick, S. *Ind. Eng. Chem. Res.* **1993**, *32*, 1012-1017.
(16) Benson, S.W. *Thermochemical Kinetics*; Wiley: New York, 1976.
(17) Heneghan, S.P.; Martel, C.M.; Williams, T.F.; and Ballal, D.R. *ASME J. Eng. Gas Turb. and Power.* **1995**, *117*, 120-124.
(18) Katta, V.R.; Jones, E.G.; Roquemore, W.M. 81st AGARD Symposium on Fuels and Combustion Technology for Advanced Aircraft Engines: Colliferro, Italy, May 1993; Paper No. PEP-19.

Table 1. Characteristics of F2747 and F2827 Jet Fuels

	F2747	F2827
fuel type	Jet A-1	Jet A
refinery treatment	hydrotreated	straight-run
total sulfur (%)	0.004	0.079
mercaptan sulfur (%)	0.000	0.001
aromatics (vol %)	19	19
JFTOT breakpoint (°C)	332	266
copper (ppb)	< 5	< 5
iron (ppb)		8
zinc (ppb)	18	<5

Table 2. Pseudo-Detailed Reaction Mechanism for Chemical Kinetic Modeling[7]

Reaction	Arrhenius A-factor (mol, L, and S)	Activation Energy (kcal/mol)	Reaction No.
$I \rightarrow R^{\bullet}$	1×10^{-10}	0	(1)
$R^{\bullet} + O_2 \rightarrow RO_2^{\bullet}$	3×10^{9}	0	(2)
$RO_2^{\bullet} + RH \rightarrow R\,O_2H + R^{\bullet}$	3×10^{9}	12	(3)
$RO_2^{\bullet} + RO_2^{\bullet} \rightarrow$ termination	3×10^{9}	0	(4)
$RO_2^{\bullet} + AH \rightarrow R\,O_2H + A^{\bullet}$	3×10^{9}	5	(5)
$AO_2^{\bullet} + RH \rightarrow AO_2H + R^{\bullet}$	3×10^{5}	10	(6)
$A^{\bullet} + O_2 \rightarrow AO_2^{\bullet}$	3×10^{9}	0	(7)
$AO_2^{\bullet} + AH \rightarrow A\,O_2H + A^{\bullet}$	3×10^{9}	6	(8)
$AO_2^{\bullet} + AO_2^{\bullet} \rightarrow$ products	3×10^{9}	0	(9)
$R^{\bullet} + R^{\bullet} \rightarrow R_2$	3×10^{9}	0	(10)
$RO_2H \rightarrow RO^{\bullet} + {}^{\bullet}OH$	1×10^{15}	37	(11)
$RO^{\bullet} + RH \rightarrow ROH + R^{\bullet}$	3×10^{9}	10	(12)
$RO^{\bullet} \rightarrow R_{prime}^{\bullet}$ + carbonyl	1×10^{16}	15	(13)
${}^{\bullet}OH + RH \rightarrow H_2O + R^{\bullet}$	3×10^{9}	10	(14)
$RO^{\bullet} + RO^{\bullet} \rightarrow$ termination	3×10^{9}	0	(15)
$R_{prime}^{\bullet} + RH \rightarrow$ alkane + $R^{\bullet}$	3×10^{9}	10	(16)
$RO_2H + SH \rightarrow$ products	3×10^{9}	16	(17)

Table 3. Initial Concentrations of Species

Species	Initial Concentration (moles/liter)
I	4.0×10^{-8}
RH	4.4
AH	Varied, 0-16.2 x 10^{-3}
SH	Varied, 0-16.2 x 10^{-3}
O_2	1.8×10^{-3}
remaining species	0

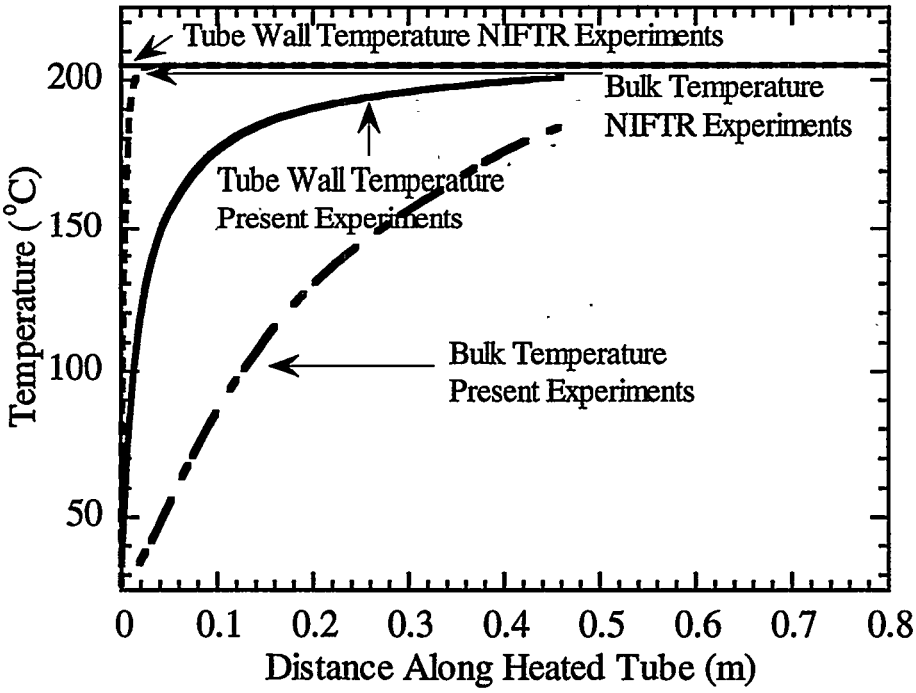


Figure 1. Bulk and tube wall temperature profiles along heated tube length. Present experiments (16 ml/min & 0.46 m length) & NIFTR experiments[14] (0.125 ml/min & 0.8 m length).

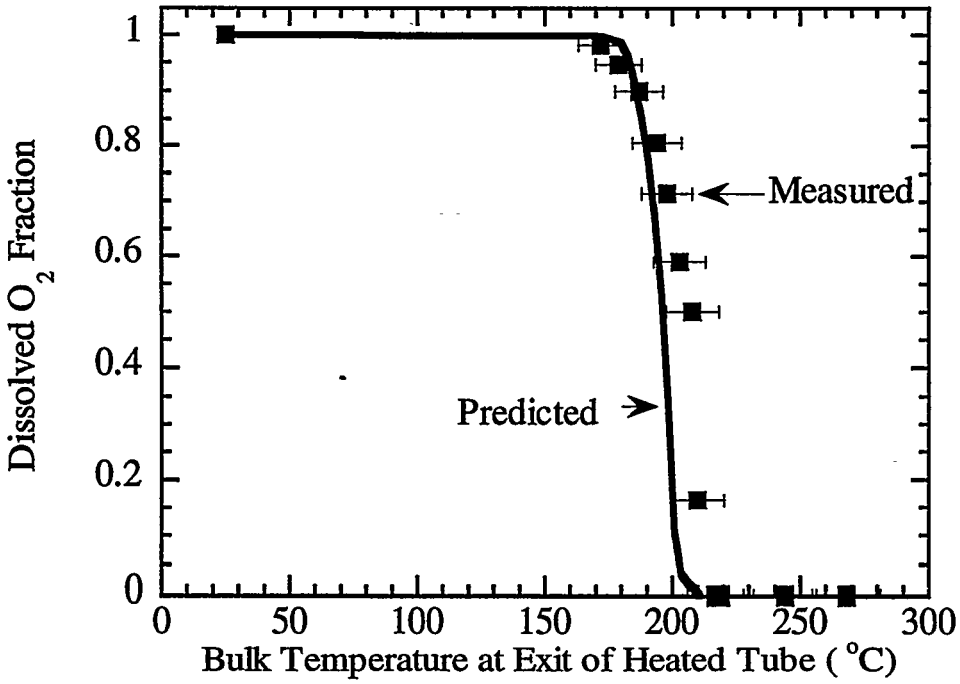


Figure 2. Dissolved O_2 concentration at tube exit. 16 ml/min & F2747 fuel.

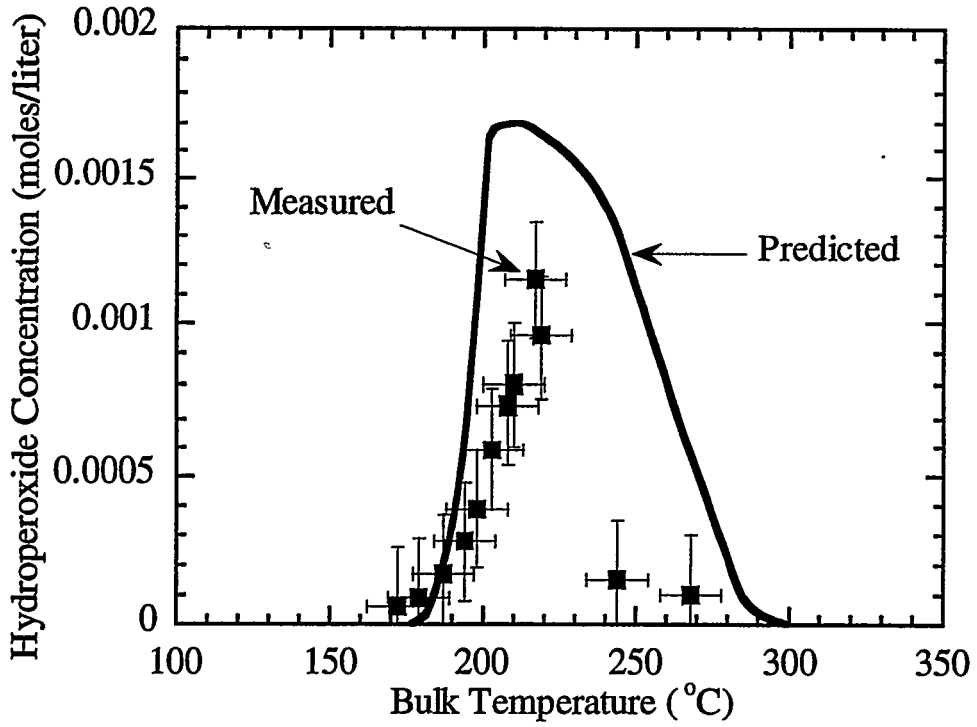


Figure 3. Hydroperoxide concentration at tube exit. 16 ml/min & F2747 fuel.

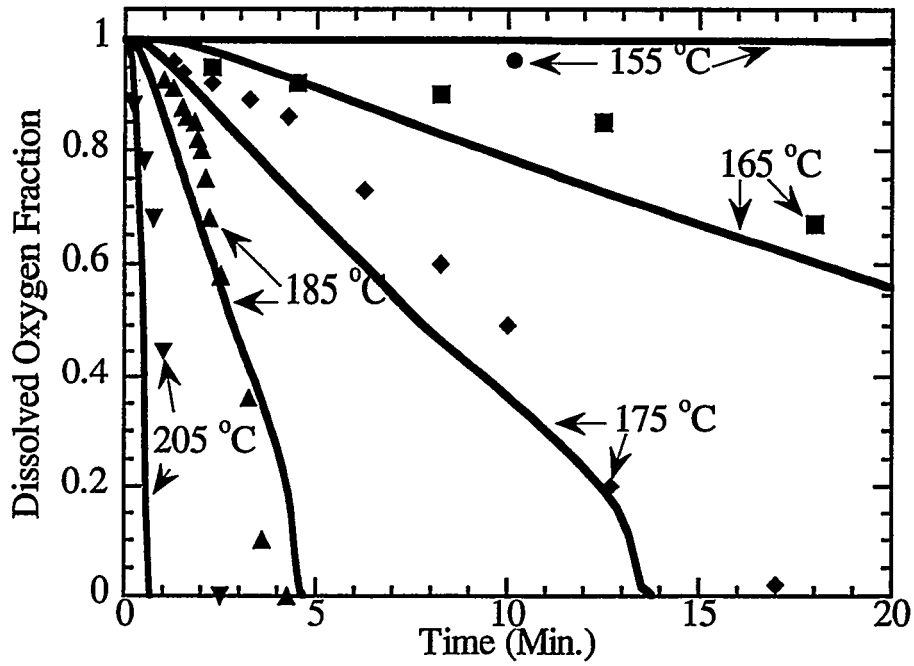


Figure 4. Predicted & measured[8,14] dissolved O_2 removal for nearly isothermal flow. 0.125 ml/min & F2827 fuel. Curves represent predictions.

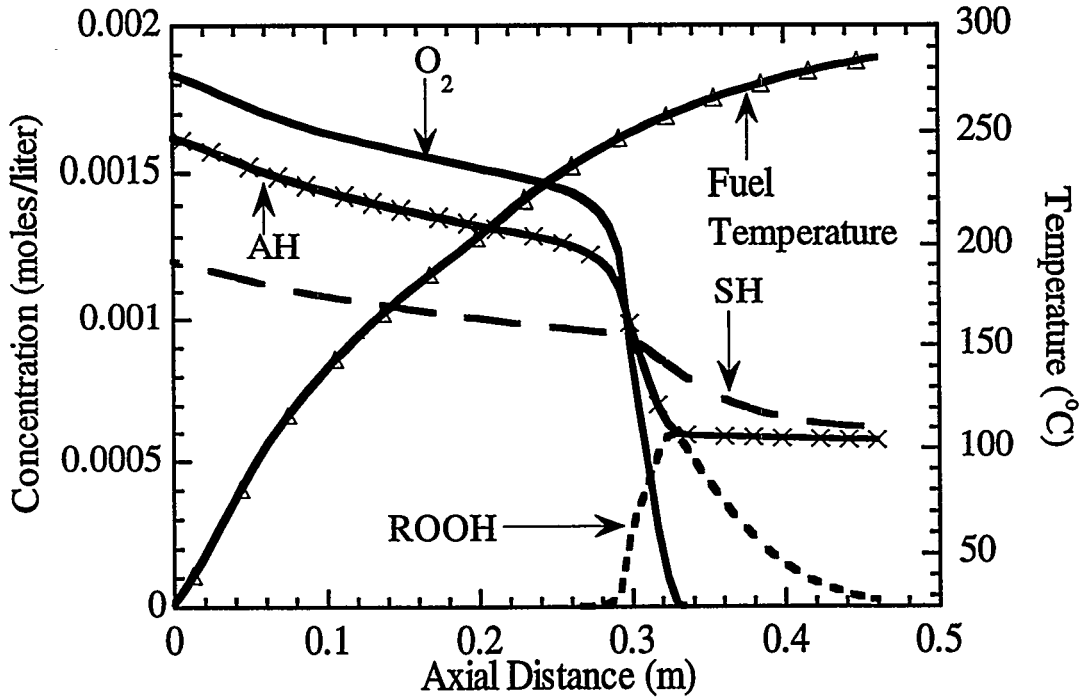


Figure 5. Calculated profiles of dissolved O_2, ROOH, AH, SH, & fuel temperature for F2827 fuel. 16 ml/min & 300 °C wall temperature.

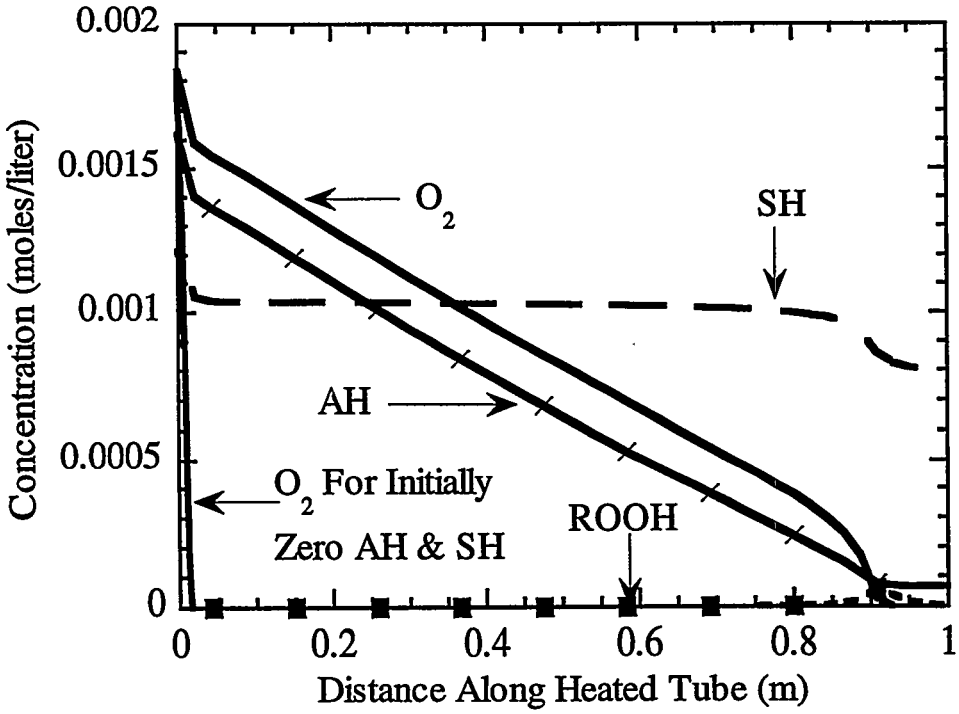


Figure 6. Calculated profiles of dissolved O_2, ROOH, AH, & SH. F2827 fuel, 0.125 ml/min, & 175 °C wall temperature.

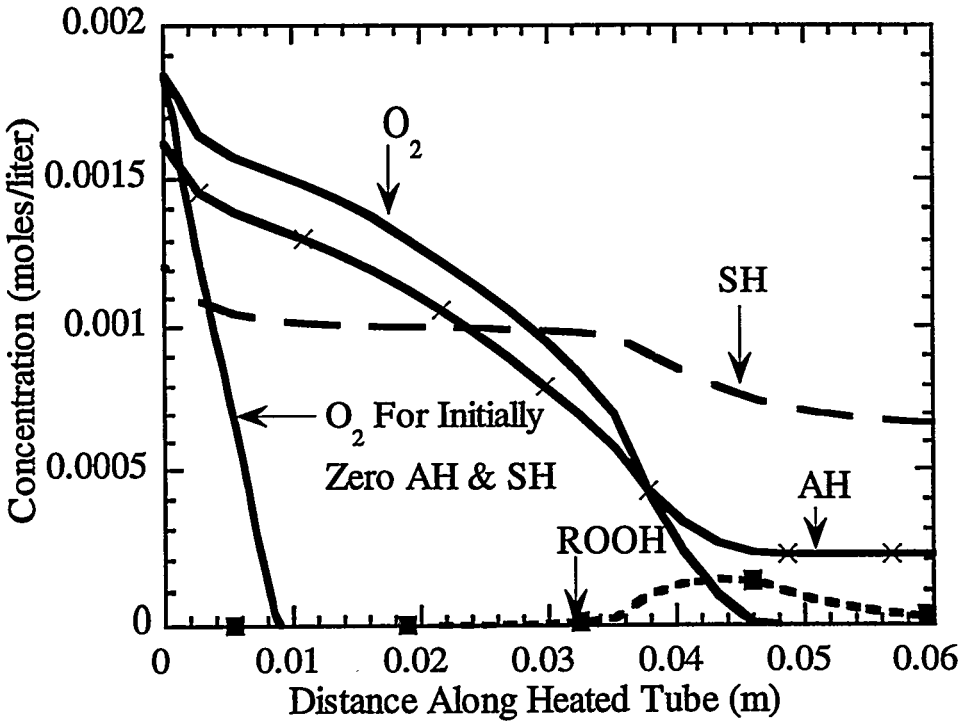


Figure 7. Calculated profiles of dissolved O_2, ROOH, AH, & SH for F2827 fuel. 0.125 ml/min & 205 °C wall temperature.

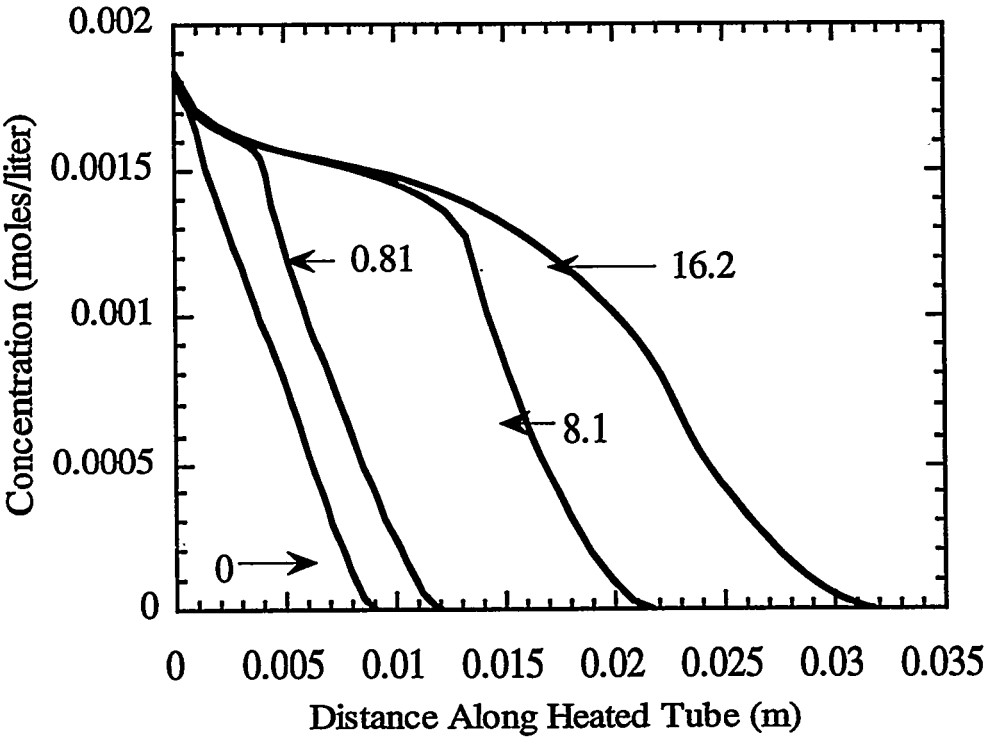


Figure 8. Calculated O_2 concentration profiles for different inlet concentrations of AH (x 10^{-4} moles/liter) in the absence of SH. 0.125 ml/min & 205 °C wall temperature.

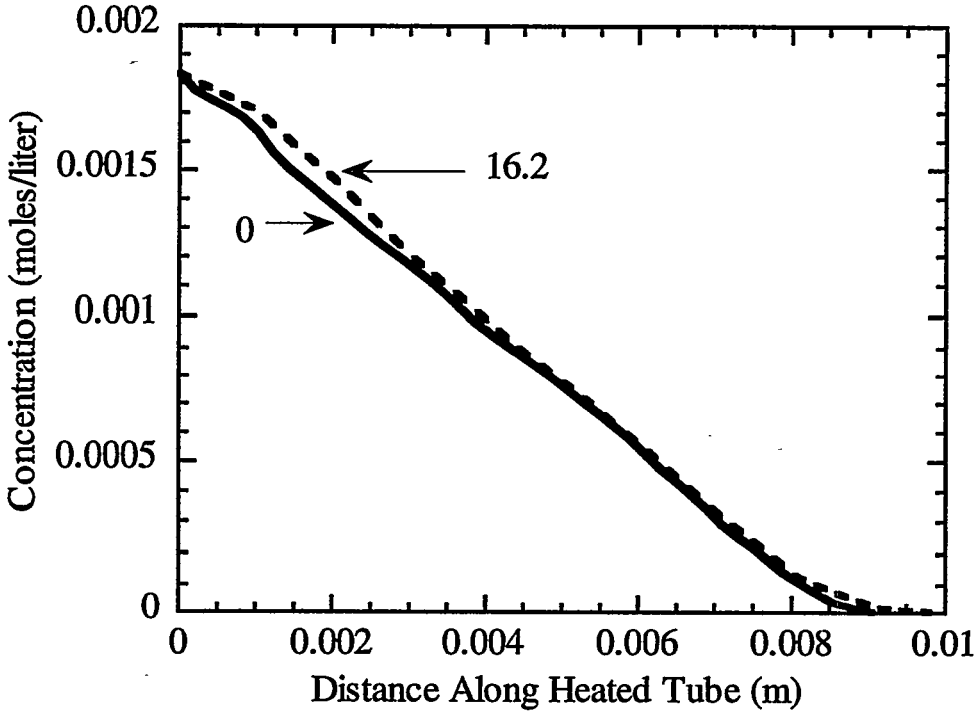


Figure 9. Calculated O_2 profiles along tube for different inlet concentrations of SH (x 10^{-4} moles/liter) in the absence of AH. 0.125 ml/min & 205 °C wall temperature.

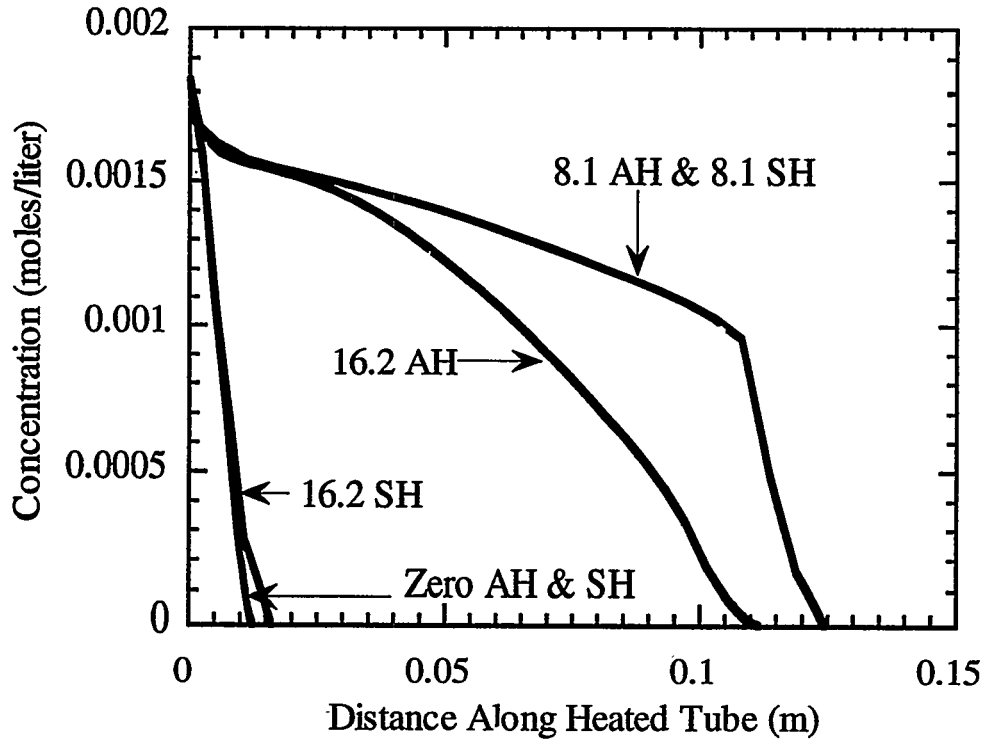


Figure 10. Synergism between AH & SH antioxidants. Calculated O_2 profiles for different initial concentrations (x10^{-4} moles/liter) of AH & SH. 0.125 ml/min & 185 °C wall temperature.

6th International Conference

on Stability and Handling

of Liquid Fuels

Vancouver, Canada October 13-17, 1997

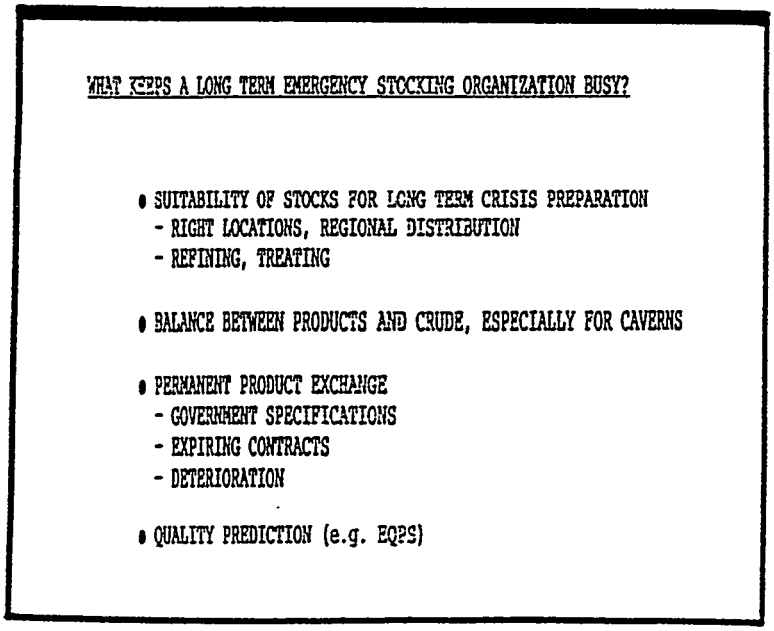
Eighteen Years of EBV's Handling and Quality Experience

J.W. Joachim Koenig
ERDÖLBEVORRATUNGSVERBAND
(German Strategic Petroleum Reserve)
Jungfernstieg 38
20354 Hamburg, Germany

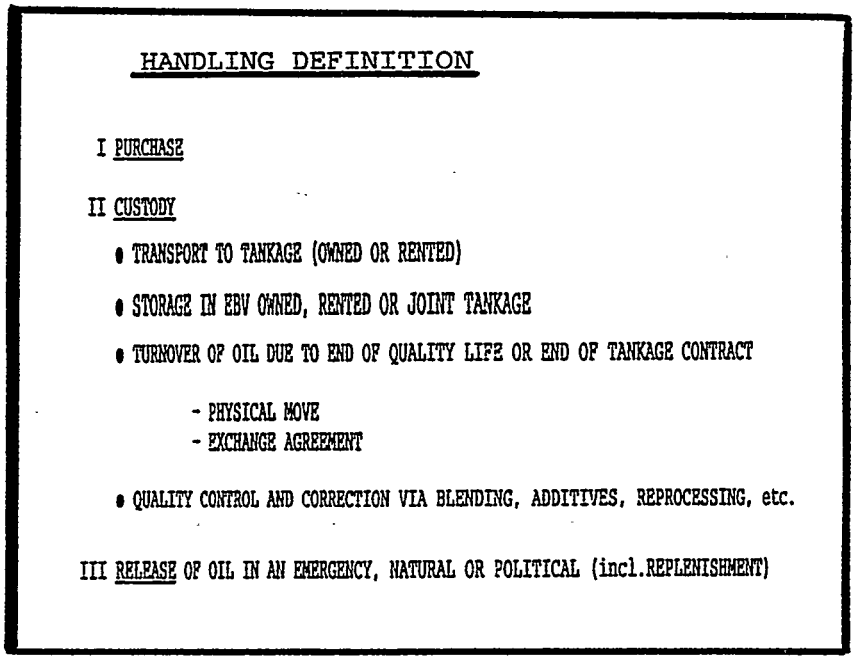
Chairman, Ladies and Gentlemen,

It is hard to imagine an oil company to report on spectacular handling events over the last 18 years of her existance, as those events are probably mainly problems and in the competitive business it can be quite damaging to talk about ones past difficulties.

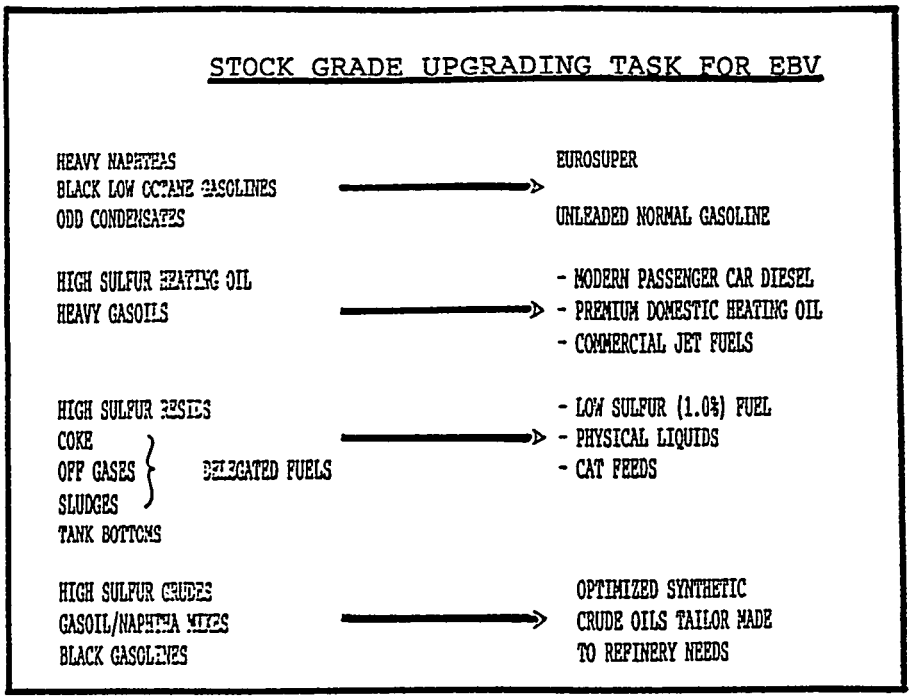
As an entity of public law we do not have competitors to watch out for and thus can talk more frankly about the difficulties conducting our business, of which the main is the handling of oil and its quality maintenance, as well as the financing. Though we will not talk about the latter today.



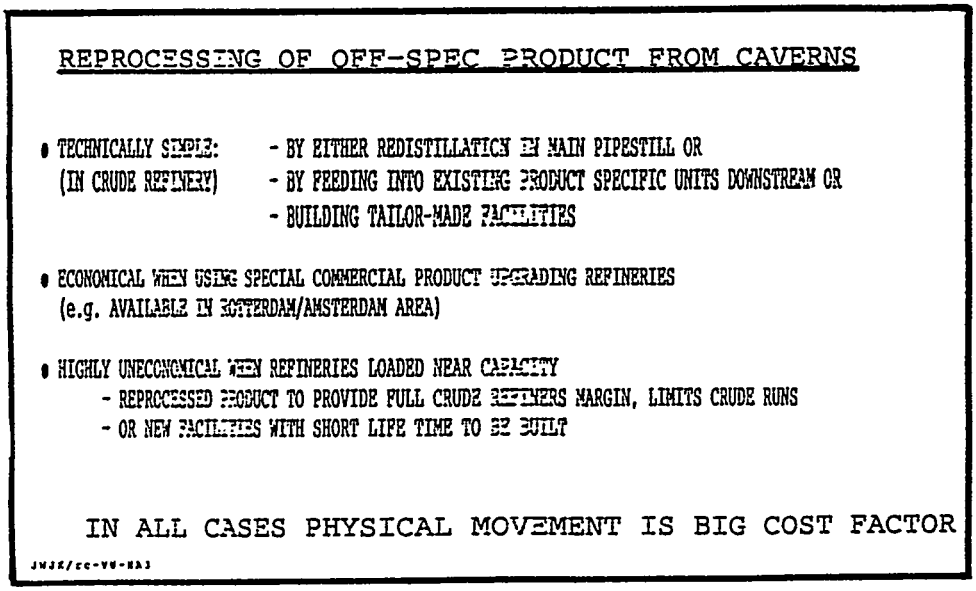
Let us first define what we mean by handling: handling comprises transport to our (own or rented) tankage facilities, storage in tankage while the oil is in our responsibility, turnover of the oil due to the end of the oil's natural lifetime or ending of a storage contract requiring to exchange, sell off or move the oil from the storage vessel, and finally the efficient release of oil in a minor/or major oil shortage period or crisis, for which the reserve has been created.



In a wider sense I would like to include even the oil purchase and quality surprises at a later date. The law allows the purchase of various products in three category groups like aviation and motor car gasolines, naphthas and naphtha based jet fuel as category I, all diesel, heating oils, kerosenes, kerosene based jet and gasoils as category II and all residual fuels, vaccum gasoils (incl. cat cracker feeds) and heavy oils as category III. Besides this, crude oil can substitute for product in a typical previous year manufacturing ratio, thus the internal flexibility to economize the mix is enormous. As a result EBV found itself with off-spec naphthas and gasolines, poor gasoils and home heating oils, practically no diesel or jet fuel, very high sulfur and high metal resids and heavy cheap Arabian Gulf crude oils, at the outset when after official foundation by law it had to take over all the left-overs companies wanted to get rid of fast.

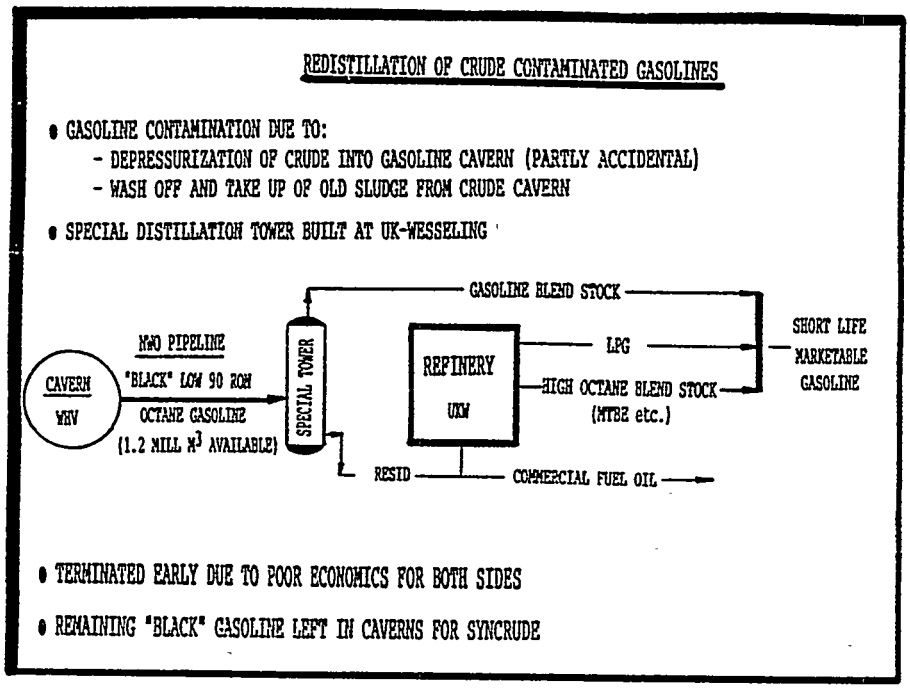


A joke of the time was that EBV harbours dangerous chemicals to be disposed of by special environmental permit. EBV has struggled ever since to improve its mix to a quality customers would expect from us in a crisis.

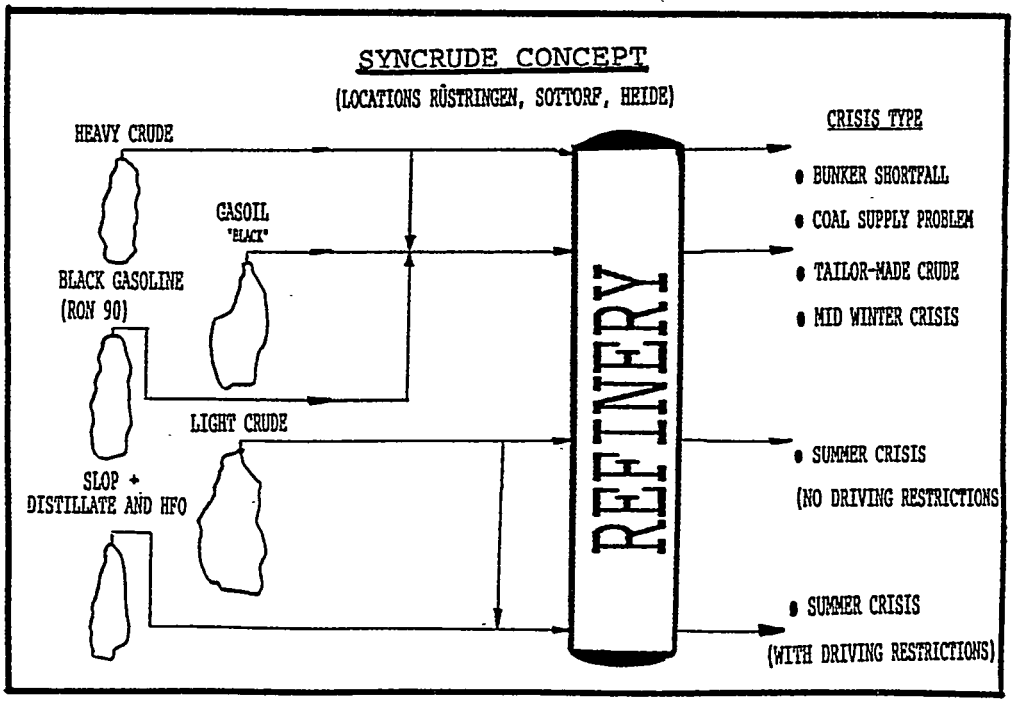


At the outset it was assumed that reprocessing in refineries would be a realistic option for off-spec gasolines and gasoils, it proved to be extremely costly and logistically difficult. In order to get rid of ca. 400 000 m^3 of crude

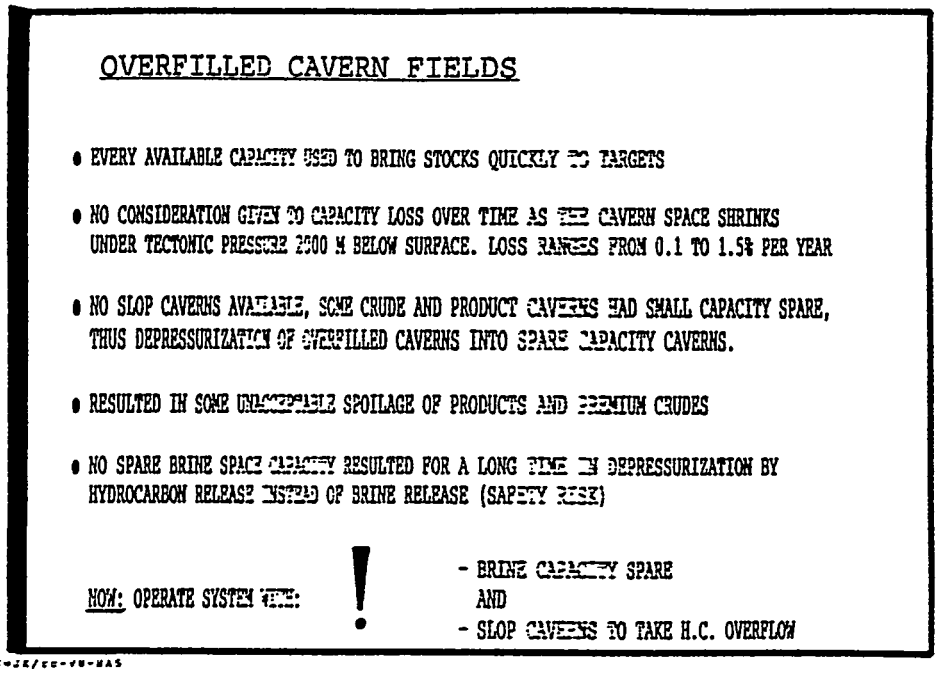
oil contaminated low octane gasoline, a special distillation tower had to be erected at a member's refinery site and a crude oil pipeline to be used to get it there. Neither EBV nor the refinery were happy with this handling and the contract was terminated prematurely.



Left over black gasoline volumes were integrated into the syncrude concept. Care had to be taken to avoid the overloading of syncrude with gasoline, which had seen catalytic reformers and thus contained aromatics, which would starve the reformers after re-distillation and a second go-through of hydrogen partial pressure. The syncrude concept has many advantages.

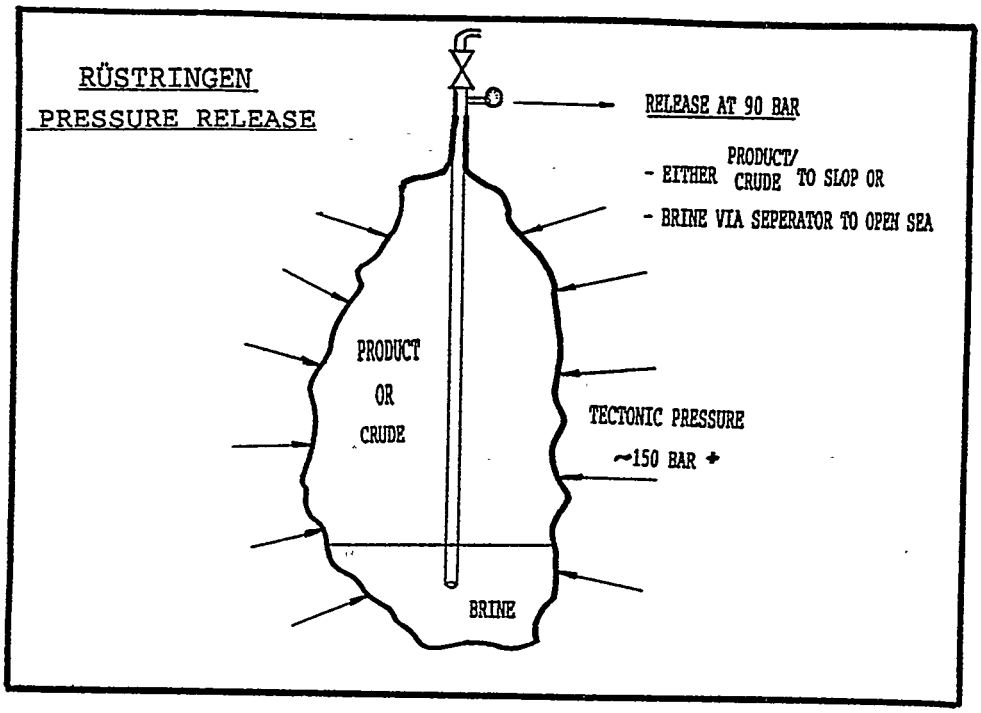


holds crude oils, contaminated naphthas and gasoils as well as cavern slop at several cavern sites. If all is available at one site including tanks for blending, any kind of "synthetic" tailor-made crude oil can be manufactured to suit the refinery type and a specific oil crisis situation.



When EBV started product storage in caverns, clean new caverns were not always available. When large quantities of low octane Romanian gasoline (so called RON 90) were purchased, they had to be stored in caverns which previously contained crude oil, thus they turned quickly black and at the time no one seemed to worry about the fact that this gasoline would not only be too low in RON and MON for German cars but would also block carburators and/or injection nozzles. Gasoils were generally purchased into caverns previously used to store naphthas, jet and middle distillate components by adjacent refineries, but when in stock, accidental decompression of crude caverns into the gasoil caverns caused again spoilage resulting in dark distillates.

The cavern fields had been overfilled in order to use every available capacity to reach EBV's stock targets as quickly as possible. No spare slop caverns were left aside nor built-in cavern spare by leaving substantial amounts of brine at each cavern bottom was provided for; so decompression, for each cavern in Rüstringen more than once a year required, had to use above ground tankage at the jetty tank terminal or accidental spare in a few large caverns. Now the system has been relieved by slop cavern spare, tank terminal capacity and a brine margin in each cavern for up to 5 years.



OTHER EBV EXPERIENCED HANDLING ISSUES WITH CAVERNS

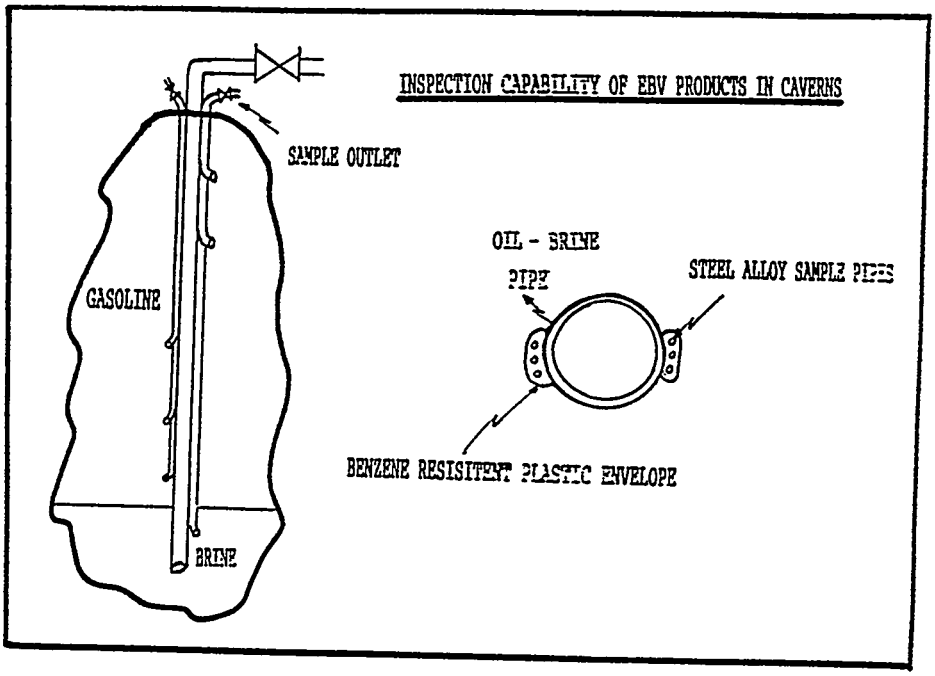
- VAPOR PRESSURE OF DIESEL SPOILED BY PREFILL WITH GASOLINE
  - NEEDED IN BETWEEN WASH STEP WITH GASOIL
- PRODUCT QUALITY TO BE SUPERVISED LOW COST
  - PRODUCT TO STAY IN CAVERN 10 YEARS
  - INSPECTION LOW COST AT ANY TIME NECESSARY
  - LOST INSPECTION TUBES BY ROCK FALL IN ONE OUT OF THREE BLEXEN CAVERNS
- PRODUCT ADDITIVATED AGAINST
  - OXYDATION
  - METAL CATALYTICS
  - CORROSION

  ACHIEVE STILL 10 YEARS IN SPITE OF HIGH CONVERSION CRACKERS
- AROMATICS AND LIGHT H.C. WASH-OUT FROM GASOLINE INTO BRINE
  - BENZENE WASH-OUT ALSO FROM CRUDE
- CAVERN TURNOVER
  - SIZE INCREASE
  - LOGISTICAL PROBLEMS

JWJE/cc-VU-HA6

But also diesel fuel at one time had to use an old gasoline cavern. The vapor pressure of the diesel would have become unacceptable so that an expensive wash-out step with gasoil returned to a nearby refinery for stabilization had to be taken before the low sulfur diesel could enter. In spite of early spoilage experience when starting product storage in caverns, the low cost option for large volumes being totally environmentally sound was further explored with some great success.

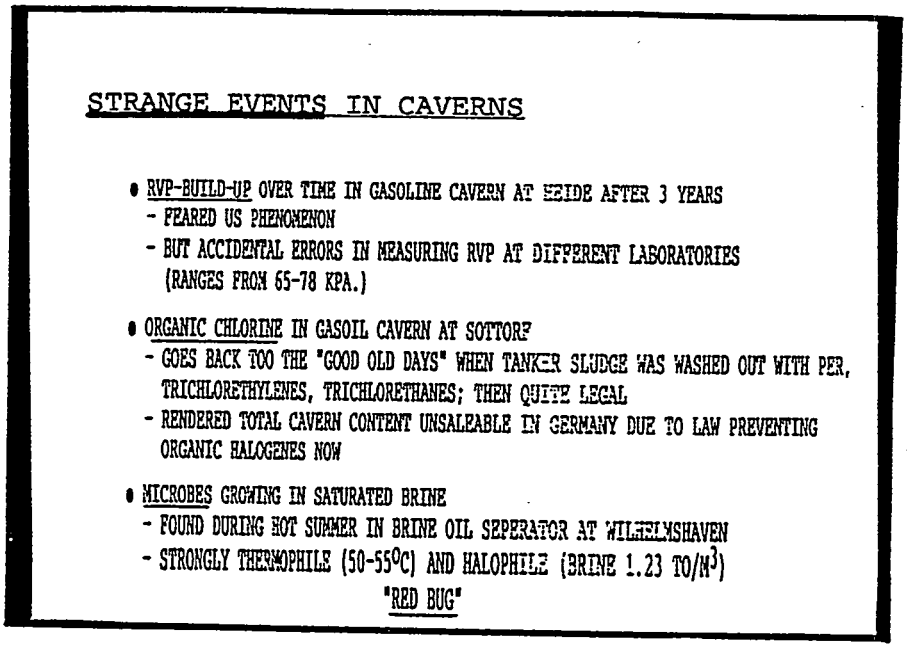
At Heide we managed to empty two gasoline caverns after 7 and 9 years of storage directly into DEA's retail system without any quality problems. Admittedly there are precaution steps necessary to achieve such storage results. Today we plan for 10 years at least, for both middle distillates and gasolines. Special additivation and tight quality restrictions when purchasing the fuel are employed to avoid surprises. Although the old Heide gasoline caverns could not be inspected on a routine basis, we bought all the



gasoline to cover the new eastern territories after German unification for storage in caverns at Blexen (Wintershall). We equipped three caverns of 350 000m^3 each with inspection tubes, which allow to test the product quality at various cavern horizons at any time. Normally 6 inspection tubes of ca. 1/2 inch diameter are flanged to the main pipe and are open at different levels. Ball valves on top of the cavern prevent the product outflow. When opened the cavern overpressure ejects the samples automatically. Before we had this device the main pipe had to be pulled out first at a cost of >100 000 US $ prior to sampling. Unfortunately we lost the device in one Blexen cavern due to a major rock fall sheering off the main pipe.

The only draw back of product storage over brine is the loss of benzene and toluene as well as some other light H.C. into the brine, whose solubility is higher than in sweet water. In the lower zone near the oil/brine interface normally about one RON number is lost due to the aromatics drain. Logistically a major problem of product storage in salt caverns is the mere size of those cavities. As the fill is part of EBV's reserves which by law have to be available at all times, product in large volumes has to be stored in above ground tankage temporarily when a cavern is emptied.

Such stand-by storage - especially for gasoline - is difficult to find in Germany and definitely not near the caverns. Therefore a complex system of delegations has to be activated with refineries and bulk plants elsewhere in the country.

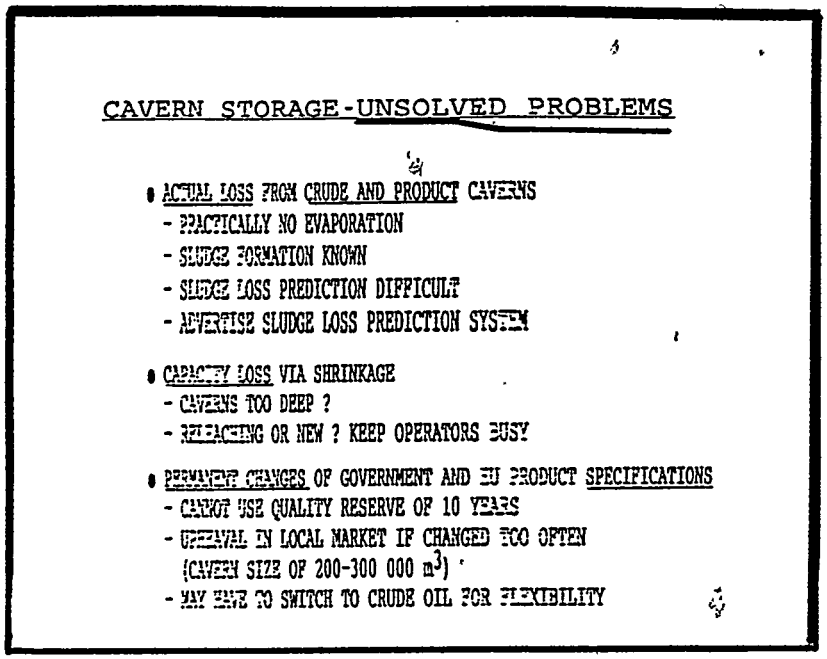


We also had our share of "strange events" with cavern storage. We observed a gradual increase of RVP-pressure in gasoline at Heide over the last 3 years. Since this was almost a straight line increase since filling time from 65 - 78 kpa we suspected intrusion of gas through the salt like it happened with the SPR in the USA. In the end it turned out to be a laboratory problem, a coincident of obviously wrong RVP measurements.

Another spectacular event, which unfortunately proved real was the organic chlorine content in one of our Sottorf gasoil/diesel caverns. Halogenated H.C. in middle distillates are strictly forbidden in Germany on environmental/health grounds. But 15 years ago when the gasoil was purchased it was quite common - and still legal - to wash tankers and vessels with PER, trichlorethylene, trichlorethane or tetra chlorcarbon and similar agents. A final definite explanation was never found, disposal was not without problems and loss of market value.

Since we use caverns for crude and products we have worried about the possibility of microorganisms not only entering but growing deep down in the caverns. It was shown by others (e.g. NIPER for SPR) that sludge in caverns contains microbes which will actively start multiplying again once conditions on the surface are right; no evidence was found that real metabolism takes place at the oil/brine interface at high cavern temperatures. In the hot summer of 1995 we found a rich biomass in the brine/oil seperator at Wilhelmshaven cleaning our brine before discharge into the sea, obviously very viable.

When exposing/adapting those bacteria to cavern conditions, we isolated a "red bug" which is strongly halophile and thermophile. It dies at low temperatures (e.g. 20°C) and low salinity. The biosurfactance and biomass capabilities are still being investigated.



Some cavern storage problems remain unresolved for EBV. While product losses through leakages and/or evaporation are negligible, we still do not have a clear understanding how much oil can be recovered when finally emptying caverns. Cavern losses are a function of:

- the cavern shape (oil lost in traps)
- the type of material stored:
  - o solubility
    (e.g.: benzene losses in brine)
  - o occluded waxes/asphaltenes at cavern walls
  - o sludge formation capability
- the type of technical equipment at the cavern head (e.g. pumps etc.)

EBV is conducting an active research programme in this field and fosters a sludge prediction technology development, of which we report elsewhere in this conference.

Further, the continuous loss of cavern capacity through shrinkage and the balancing of it through additional leaching of existing or new caverns in the same field still requires economic optimization. The questions of depth and type of salt are important influencing factors. While in some of our cavern fields the capactity loss is minimal, in deep fields like WHV-Rüstringen it is a real headache keeping an operating organization pretty busy.

Finally the biggest issue however is influenced by government regulations. While we are quite capable and successful to extend a normal 2-3 years product life time towards 10 years in caverns, the ever changing mainly environment driven product spec alterations since about 5 years (and expected to last at least until the year 2010) render the technical ageing control almost nonsensical. So far we were not successful to get permission to keep our products in stock until the end of their natural storage life and then sell under a special licence into the local markets.

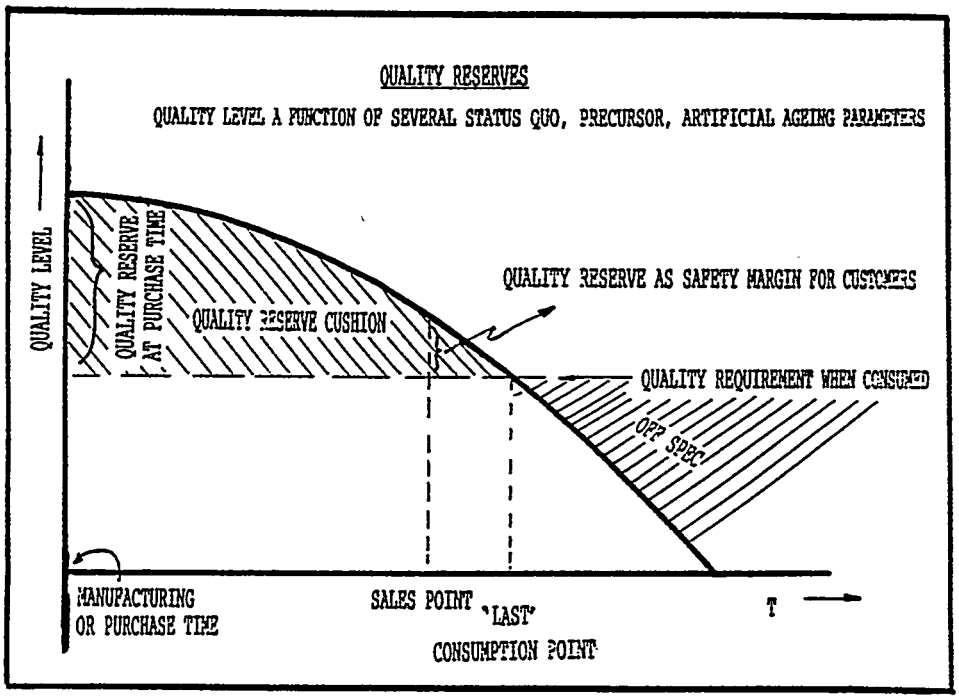
Since German caverns are built to allow in average about 7-8 turnovers only until the size gets too big and danger exists that one dissolves the support pillars between them, a too frequent exchange can ruin the whole cavern field. We do not operate brine lakes but displace the oil with sea water. The logistical cost of frequent changes also become quickly prohibitive, so that we actively consider to terminate product cavern storage in favour of crude oil or syncrude stocks. This would be a most unfortunate result of the wrongly understood environmental consciousness.

AGE QUALITY DEFINITION PARAMETERS (TYPICAL TESTS)

GASOLINES	DIESEL/GASOILS/DOMESTIC HEATING OIL
EXISTENT GUM	OXYDATION IN AIR } GUM
POTENTIAL GUM/INDUCTION TIME	OXYDATION IN OXYGEN }
UV-LIGHT STABILITY	- AMBIENT TEMPERATURE
BROMINE NUMBER	- RAISED TEMPERATURE
DIENE NUMBER	- OVERPRESSURE
	- W/W.O. CATALYSTS
	COLOR
	EXISTENT GUM
	UV-LIGHT STABILITY
	THERMAL STABILITY
	SEDIMENTS (ORGANIC/UNORGANIC)
	ACIDITY
	NITROGEN (TOTAL AND BASIC)

Lets now say a few words about quality. Manufacturers and consumers are mainly interested in performance and/or environmental specifications. While this must be of course also the basis for a strategic petroleum reserve, there are however additional considerations of susceptability to ageing, previous ageing, quality reserves etc. Since the age of an oil is not in itself a quality parameter, age and longevity can be characterized by sets of indicators like the ones in this vu-graph. Measurements of this kind on their own do not allow any predictions of how long the fuel may still be fit for use, but the results of such measurements can be used in ageing prediction models or

expert systems. EBV and its European sisters of the ACOMES group have built such an ageing predicton system called EQPS, which was presented at the Rotterdam IASH conference 3 years ago. The main difference between performance/environmental specifications and those for ageing/life prediction is the change over time, a phenomenon one finds generally with biological deterioration/degradation only. However the oil product is like a living organic system, which changes chemically and physically over time. This change effects seldom the performance unless one approaches "fit-for-use" limits and filters start plugging or deposits occur.



Since this change can be detected and predicted, there is a need to build a quality reserve, which is being consumed over time. This reserve often means special manufacturing and thus additional cost. The art of course is to quantify the quality reserve need and to sell the product into consumption before "fit-for-use" limits are approached, keeping in mind that most products spend a fair amount of time still in bulk/retail terminalling and customer tanks. These quality control and ageing predictions are major efforts of long term storage organizations holding finished or blend products. The problem does not really present itself when storing crude oil, other than the unpleasant crude oil sludging issue.

EBV EXAMPLES OF HISTORICAL PROBLEMS ARISING FROM LONG TERM STORAGE

- WAX FALL-OUT IN COLD WINTERS, EFFECTING MAINLY SMALL TANKS
  - WAX CRYSTALS TAKE OUT COLD PROPERTY ADDITIVES IN GASOIL
  - BUT ALSO AS HEAVY EMULSIONS IN CRUDE OIL TANKS
- TANK CONTENT CONTAMINATIONS
  - UNAUTHORIZED CHEMICAL DISPOSALS
  - SALT CARRY-IN FROM CAVERNS
  - ORGANIC CHLORINE FROM WASTE OILS (WRONGLY UNDERSTOOD SLUDGE CONCEPT)
  - BIODIESEL BLENDING
  - BIOLOGICAL INFECTIONS
- DEBLENDING
- SLUDGE FORMATION AND SLUDGE AGEING IN CRUDE OILS
- AGEING PROMOTION AND PERFORMANCE DETERIORATION CAUSED BY ENVIRONMENTAL IMPROVEMENTS
  - LOW SULFUR LUBRICITY
  - PEROXYDE PROBLEM THROUGH HYDROCRACKING/LOW SULFUR
  - BY-BLENDING OF OXYGENATES, MAINLY RME
- ADDITIVE 'POISONING'
  - BIOCIDES, - OVERADDITIVATION, - BIOLOGICAL FERTILIZATION

Allow me now to point out briefly also some typical long term storage issues for above ground steel tank storage. Strong winters occur in Germany about twice in 10 years. If the cold period is short, it mainly affects small tanks, if in very rare cases temperature stays below freezing point for more than 4 months even medium (>20 000 m^3) and large tanks (70 000 - 120 000 m^3) may be affected. The main problem is a fall-out of waxes, which in theory improves the cold properties of the fuel, in reality however it takes with the waxes most of the cold property improver additives (like WASA: wax antisettling additive) out as well, leaving behind a rather poor winter diesel or home heating oil. The fallen out waxes are hard to reblend back even in warm summers and often have to be sold under value as slop. As temperatures decrease water will also fall out and together with existing condensation water at tank bottoms and in pipes causes all sorts of damage in lines and pumps. In too cold crude oil tanks heavy emulsions at tank bottoms may solidify to permanent sludge prematurely, which then can be removed by physical "mining" methods only.

Great headaches have caused accidental or illegal contaminations like disposals of chemicals, waste oils, salt carry-ins from caverns or tankers and biological infections - mainly from poor house keeping in Eastern Europe. A static tank in a tank farm used by others seems to attract all sorts of junk; we once found the disposal of a whole gas station including rubber, nuts and bolts, stones wood, tools etc. in one of our naphtha tanks. Somebody tried to avoid polluting the environment by giving all this to us without permission.

As of recently the "trace contaminations" of the logistics system play a major role in handling and quality control. Luckily the "lead poisoning" gradually disappears, but biodiesel oxygenates and dozends of additives appear, many of which are detrimental to long term storage.

Also "smart blending" by Rotterdam "harbour artists" have bothered us in the past. They not only left unorganic acids from so called "tax crackers" in the product but used incompatible components to "tailor-meet" specifications. Unfortunately deblending in tanks occured after some time so that one customer got the front end, the other the back end octane. In gasoils it can be even more pronounced than in gasolines.

Not quite fully understood is the phenomenon of crude sludging in steel tanks, which we try to tackle by a special research programme. It sometimes even happens in gasoils, where in most cases however it is a wax shedding.

Even the blessing of improved environmental products proved often to create additional performance problems. A typical example is the poor lubricity of very low sulfur fuels or the peroxyde problems of hydrocracked blend stocks or the combustion improvement by oxygenates, which trigger off microbial spoiling in middle distillates.

Finally, cost pressures and competition forces companies more and more into joint terminalling of base stock products and brand differentiation by numerous additives at the loading racks prior to delivery into retail stations. Some of those additives at the time find their ways into cargoes offered to EBV, which then contain biocides dangerous to human health, or fertilize microbes in tanks or accumulate at lower tank parts after long term storage and form deposits in engines or burners, problems which do seldom occur if sales go immediately into consumption.

SPECTACULAR MICROBIAL CASES

- RUSSIAN GASOIL AND OVERADDITIVATION
- WRONG BIOCIDES, ESSO CASE, KICK-OUT OF KATHON
- CONTAMINATED JOINT BULK PLANTS, RHINE BARGE CASE
- RME ISSUE, BIOVULNERABILITY TEST
- ALCOHOL AND MTBE VULNERABILITY OF GASOLINE
- WATER DECLINE IN EBV-INSPECTED TANKAGE

Let me close my historical review of long term storage problems with a few important case studies of microbial spoilage, which occured in recent years in Germany, with direct or indirect influence on EBV. Microbiological problems - especially in kerosenes and diesel/home heating oils have been gradually increasing over the years in Germany with a major boost after the fall of the iron curtain, when large volumes from poor housekeeping tank farms - often in military hands - flooded western Europe. EBV was thought to be overexposed due to its normally high average storage times. However experience showed, that joint terminals and trading/transfer bulk plants are much more vulnerable due to continuous reinfection and carry-in of nutrition for microbes and water.

When the first highly infected Russian and East German cargoes arrived, traders used biocides at almost every trading step even before import into Europe, so that the German logistics system continued for quite some time a biocide level of at least 20 ppm or more. As a result this was delivered to end-consumer tanks, where sometimes even today thousand ppm of biocides can be found. (note that end-consumer tanks have no water drainage point by government order and thus biocides concentrate there over time with every refill). Even EBV in an overall survey found traces of biocides in almost every one of its tanks then, in spite of EBV's policy not to use them on a routine but rather in severe exceptional cases only.

A major oil company case excited everybody in North Germany and danger existed, that some of the highly contaminated Russian oil would also be traded to EBV. In the end, in desperation the company used the wrong emulsifying biocide which prevented the biomass to settle to tank bottom, and the oil was delivered with this biocide to retail customers. In their tanks the biocide emulsified the bottom water, carried all the deposits into the oil which then ruined the burners. Over one thousand customers had a heating
system failure and had to be "tank-cleaned", an enormous economic damage.

We had cases where barges stalled on the river Rhine and police boats failed when trying rescue operations, all had refuelled at the same "lousy" diesel tanks.

With biocides gradually on the decline (Kathon, the world's most popular was declared illegal in Germany) now gradually the logistics systems gets contaminated with biodiesel - mainly Rape Methyl Ester - an oxygenate which strongly heats up biomass production and speeds up biodeterioration, with start of major biological growth reduced from 2 years to 2-4 weeks.

We have evidence that alcohols and MTBE render unleaded gasolines vulnerable to microbial attack, even though any major outbreak has not been observed yet. With the historical biocides of TML/TEL lead and halogen-containing scavangers now gradually leaving the logistics system, the small amount of normal heptane, a strong biocide (as it dissolves the cell walls of microbes), still offers some protection. But as nc, as a low octane blendstocks is being converted to better components, this will not last long any more.

Finally a dramatic decline of water in tanks has resulted from an educational EBV-programme (naturally helped by spectacular incidents) at all of our contractual tank farms keeping microbial spoilage at bay.

HANDLING AFFECTS AGEING OF PRODUCTS

HOUSE KEEPING	DIRT AND RUST: CATALYTIC, MICROBIAL FOOD
	WATER: LEAKAGES OF ROOF, STARTS MICROBIAL SPOILAGE, DEWATERING A MUST
	SECURITY: AVOIDS DUMPING
CLIMATE	DEEP AND HIGH TEMPERATURE AS WELL AS SUDDEN TEMPERATURE SHOCKS PROMOTE AGEING REACTIONS
QUALITY OF TANKAGE	MODERN COATED, CLOSED CIRCUIT TANKS ARE BASIS FOR AGEING PREVENTION
CARE WITH BLENDING AND MIXING, TRANSPORT, DUMPING AND OVERADDITIVATION	INCOMPATIBILITY, DEBLENDING, FALL-OUTS, DEPOSITS BLOCKING OF FILTERS, UNCONTROLLED CHEMICAL AND PHYISICAL REACTIONS

→ ADDITIVES MAY HELP PERFORMANCE BUT MAY RUIN STABILITY AND LONGEVITY

As any long term storage organization has to worry about product ageing, the main message I would like to leave with you is, that not only the products chemistry, but to a very large extent the handling of products may contribute or prevent or at least slow down ageing processes significantly.

Poor housekeeping, lack of protection from an extreme climate, the overall quality of the tankage (underground is by far better than above ground) and wrong product blending, mixing, improper transport and by-blending/additivation play a major role precursing ageing reactions.

And please note that many additives good for performance may ruin stability and longevity.

Thank you ladies and gentlemen for your patience and attention.

6th International Conference on
Stability and Handling of Liquid Fuels
Vancouver, B.C., Canada
October 12-17, 1997

LONG-TERM STORAGE STABILITIES OF CRUDE OIL RESERVED BY JAPAN NATIONAL OIL CORPORATION

Takao Hara*[1], Naoyuki Hinata[2], Yutaka Imagawa[2], Masataka Kawai[3], Yoshiyuki Imai[3], Yoshihiko Kon[3] and Tatsuo Seiki[3]

[1]Department of Chemical Engineering, Faculty of Engineering, Yokohama National University, 79-5, Tokiwadai, Hodogaya-ku, Yokohama Japan 240

[2]Japan National Oil Corporation, 2-2-2, Uchisaiwaicho, Chiyoda-ku, Tokyo, Japan 100

[3]Japan Marine Surveyors & Sworn Measurers' Association, 1-9-7, Hachoubori, chuou-ku, Tokyo, Japan 104

Japan National Oil Corporation has been practicing the long-term strategic stockpiling of crude oil since 1978. The total amount of reserved crude oil now exceeds 48 million kl, corresponding to near 80 days' suply in Japan. Storage stabilities of crude oil, including formation of organic sludge, have been surveyed on four kinds of stockpiling systems (on-ground tank system, in-ground tank system, floating tank system and under-ground cavern tank system). Depositing sludge formed during stockpiling is removed periodically by the particular sludge sampler to clarify the physical and chemical properties. Depositing sludge is found to form W/O type oil-water emulsion and to be composed of crystalline n-paraffins of substantially higher carbon numbers. The amount of depositing sludge settled on the bottom of the tank has been carefully monitored during stockpiling for emergent dischaging. The efficiency of operational control against sludge accumulation is evaluated for various mixing device adopted in the on-ground and in-ground tank systems. In some occasional case, a slight amount of residual sludge is recovered after crude oil washing procedure (COW) during tank cleaning inspection. The residual sludge forms quite stable W/O emulsion, water content of which reaches 33 wt%. Minimum pour point of the sludge is found to be 52.5 ℃. In such case, hot water washing should be necessary in addition to the ordinary COW procedure. The mechanism of sludge formation is discussed and numerical analysis is applied to the relationship between amounts of accumulated sludge and stockpiling period. In further investigation, the coefficients of the assumed function could be expressed as variables of storage system, crude source, storage temperature, temperature drop, experienced condition on previous tank storage and so on.

1. INTRODUCTION

Japan National Oil Corporation (JNOC) has been practicing the long-term strategic stockpiling of crude oil since 1978. The total amount of reserved crude oil now exceeds 48 million kl, corresponding to near 80 days' suply in Japan. Four kinds of storage systems, namely on-ground tanks, in-ground tanks, floating tanks and under-ground caverns, have been adopted by JNOC. National oil srorage bases are located in ten places in Japan and most suitable storage system is adopted in each base, in keeping with the characteristics of the site location. It is, therfore, indispensable that the stability of the stored crude oil should be known to identify appropriate quality assurance after a certain period of storage. There are only few compilatory comprehensive informations on the long-term storage stabilities of crude oil either in Europe or in USA (1-5). The strategic stockpiling being in progress in Japan is the very unique and specific experience for the comprehensive understanding of chemistry involved in long-term storage of crude oil.

2. EXPERIMENTAL

2-1. Crude-Oil Source

The crude oil is basically stockpiled as pure base and the residual content in the pipeline is carefully replaced when the crude oil is transferred. JNOC reserves 31 kinds of crude-oil sources, as shown in Table 1. The densities of crude-oil sources vary in wide range from super light to super heavy (Fig. 1). The storage stabilities of the marked crude-oil sources in Fig.1 are carefully monitored throughout the storage period in this investigation. In the earlier stage of stockpiling project, some mixed crude oil were transferred in the on-ground storage system for the reason of the limitation of the storage vessels. The composition of mixed crude oil for stockpiling reserved by JNOC is listed in Table 2. The storage stabilities of these mixed crude oil are monitored in particular interest as well.

2-2. Stockpiling Systems Adopted by JNOC

Four kinds of storage systems are adopted by JNOC and the characteristic of each system is summarized in Table 3 with percent share of reserved crude oil among four systems.

2-3. Measurement of Depositing Sludge and Sludge Sampling

A steel tape and specified bob (disk-type weight) are used to determine the oil/sludge interface when the bob is grounded on the bottom deposit. The depositing sludge is defined in this investigation as the bottom deposit formed below the interface. Three-dimensional graphic aspect of depositing sludge formed on the bottom of the tank system can be drawn by use of the 20-200 inspection holes. The amount of depositing sludge is estimated for the contour-line aspect by the aid of computer. The depositing sludge is removed from the storage systems periodically and is subjected to determine the physical and chemical properties. The sludge sampler is designed and developed by Japan Marine Surveyors & Sworn Measurers' Association, as shown in Fig.2.

Table 1 Crude-Oil Sourse Reserved by JNOC

Classification		Kind of crude oil	Symbol	Number	Average Density
Light	Super Light	Marib Light	MR	2	0.8055
		Attaka	AT		0.8096
	Light	Qatar Dukhan	QD	5	0.8262
		Qatar Land	QL		0.8266
		Lower Zakum	LZ		0.8269
		Murban	MB		0.8273
		Zakum	ZK		0.8308
Medium	Light Medium	Umm Shaif	UM	6	0.8418
		Qatar Marine	QM		0.8485
		Arabian Light Berri	ALB		0.8494
		Mexican Crude	MC		0.8497
		Champion	CP		0.8508
		Oman	OM		0.8515
	Medium	Kirkuk	KC	9	0.8546
		Mexican	MX		0.8549
		Upper Zakum	UZ		0.8552
		Isthmus	IS		0.8577
		Arabian Light	AL		0.8600
		Iranian Light	IL		0.8602
		Hout	HT		0.8607
		Basrah	BS		0.8613
		Orient	OR		0.8638
Heavy	Heavy	Dubai	DB	7	0.8691
		Mexican Light	ML		0.8693
		Iranian Heavy	IH		0.8713
		Kuwait	KW		0.8733
		Suez Blend	SB		0.8735
		Arabian Heavy	AH		0.8764
		Khafji	KF		0.8784
	Super Heavy	Mexican Heavy	MH	2	0.8955
		Maya	MY		0.9085
		Total		31	0.8545

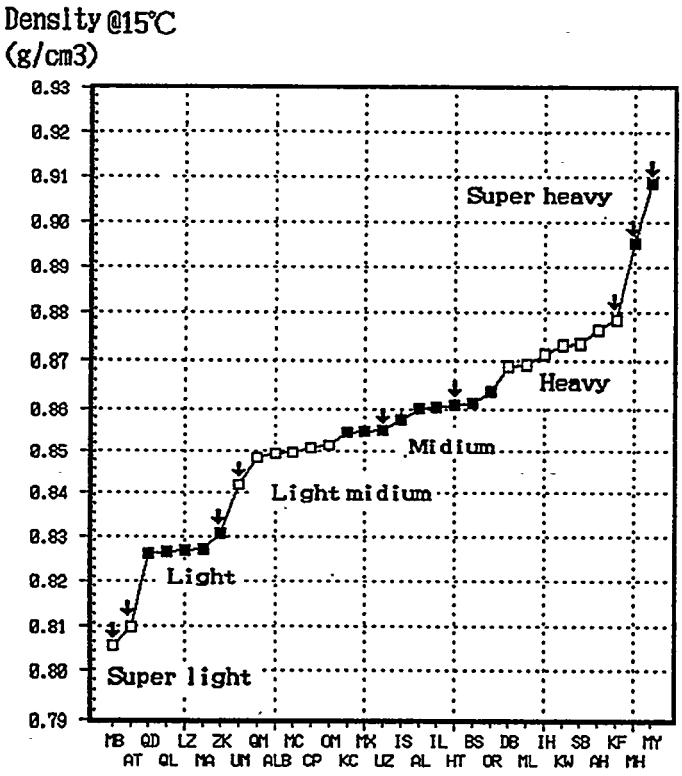


Fig. 1 Density of Crude Oil Reserved by JNOC

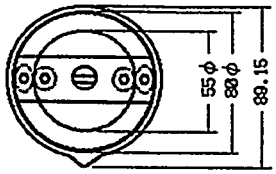
Table 2 Composition of Mixed Crude Oil for Stockpiling by JNOC

Crude Oil	Composition (vol%)
HT : AL	99.7 : 0.3
HT : AL: ZK : KF	78.8 : 17.2 : 2.4 : 1.6
KF : UM: ZK	16.7 : 47.5 : 35.8

HT: Hout, AL: Arabian Light, ZK: Zakum,
KF: Khafji, UM: Umm Shaif

Table 3 Stockpiling Systems Adopted by JNOC

Storing System (percent share of reserved oil)	Outline
On-Ground Tank System (60.5 %)	Floating Roof Tank (FRT) Capacity: 110,000-120,000 kl Equipped with a center-mount type of stirring device or side mixer.
In-Ground Tank System (11.7 %)	Under-ground FRT (diameter 97m, oil depth 48m) Capacity: 300,000-350,000 kl A submerged type pump is adopted for discharging. A center-mount type of stirring devise is equipped for agitation
Floating Tank System (11.6 %)	Dimensions of a floating vessel: (390m in length, 97m in width and 27.6m in height) Capacity: 880,000 kl Each vessel is divided into 9 compartments. An agitaion line and nozzle is equipped as mixing device.
Under-Ground Cavern System (16.2 %)	Each unit of artificial cavern tank consists of 2-4 tunnels, dug in the bedrock and each tunnel has 555m in length, 18m in width and 22m in height. Capacity of each unit: 350,000-740,000 kl Natural and/or artificial underground water is stored on the tank bottom, sealing the crude oil by groundwater pressure. A submerged type pump is adopted for discharging and for agitation as well.



Material : Brass
Spring : SUP4
Surface : Crome
Redused scale : 1/2

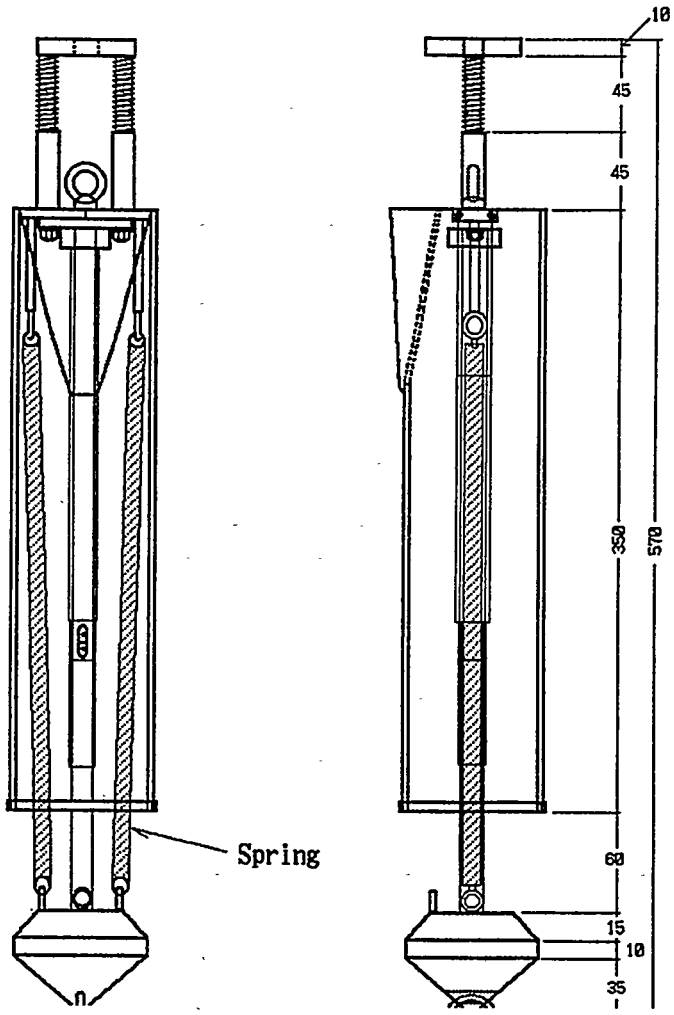


Fig. 2 Sludge Sampler

The sludge samples can be removed from the storage systems at the desirable positions by this sophisticated instrument.

2-4. Chemical Composition of Crude Oil and Sludge

The removed sample of crude oil as well as sludge from the storage systems is separated into volatile, saturates, wax, aromatics, resin and asphaltene by the conventional method, as shown in Fig.3.

3. RESULTS AND DISCUSSION

3-1. Formation of Depositing Sludge during Stockpiling

The formation of depositing sludge can be observed during stockpiling period among three storage systems (on-ground tank system, in-ground tank system and floating tank system), whereas, in under-ground cavern system, the substantial formation of sludge can not be detected even in the oil/water interface so far. The three-dimensional aspect of depositing sludge is sensitively influenced by the storage period, the seasonal change, the presence or absence of agitation and/or heating operation, the regional site of location, the crude oil source, the historical conditions (if the crude oil is transfered from one storage base to another because of the tank safety inspection), and so on. The typical aspect of depositing sludge is shown in Fig.4, where newly imported Kahfji crude oil (heavy-density: 0.8784) is stockpiled in on-ground floating-roof tank of 81.5 m in diameter at Mutsu-Ogawara storage base, located in northern Japan. The amount of depositing sludge is gradually increased along with the storage period, where agitation and heating operation is not carried out in this storage period. After two years of storage period, the maximum height of depositing sludge reachs to 2.97 m from the bottom of the tank. The surface of the accumulated sludge is quite complecated and shows mobile structure along with the seasonal change.

The maximum amount of depositing sludge reported from each storage base in the period of 1990-1992 is summarized in Fig.5. In general, the sludge amount is larger in the northern storage sites than in southern sites and is not necessarily larger along with the increase of density of crude source.

3-2. Physical and Chemical Properties of Depositing Sludge

Kinetic viscosity of crude oil and depositing sludge removed from the storage systems is shown in Fig.6. The usual depositing sludge is found to be so-called soft sludge. The kinetic viscosity of the soft sludge at 30 ℃ is quite similar with that of crude oil itself, but along with the decrease of temperature the kinetic viscosity of soft sludge increases substantially, as shown in the case of sample 4 and 5 in Fig.6. In quite occasional case, the depositing sludge is found to be so-called hard sludge, as shown in the case of sample 3 in Fig. 6. The kinetic viscosity of hard sludge reaches 31,000 cSt at 30 ℃. The optical microscopic photograph of both soft and hard sludge shows the formation of W/O-type oil-water emulsion, in which crystalline structure of n-paraffins can be observed. The difference between soft and hard sludge is only dependent on the degree of emulsification.

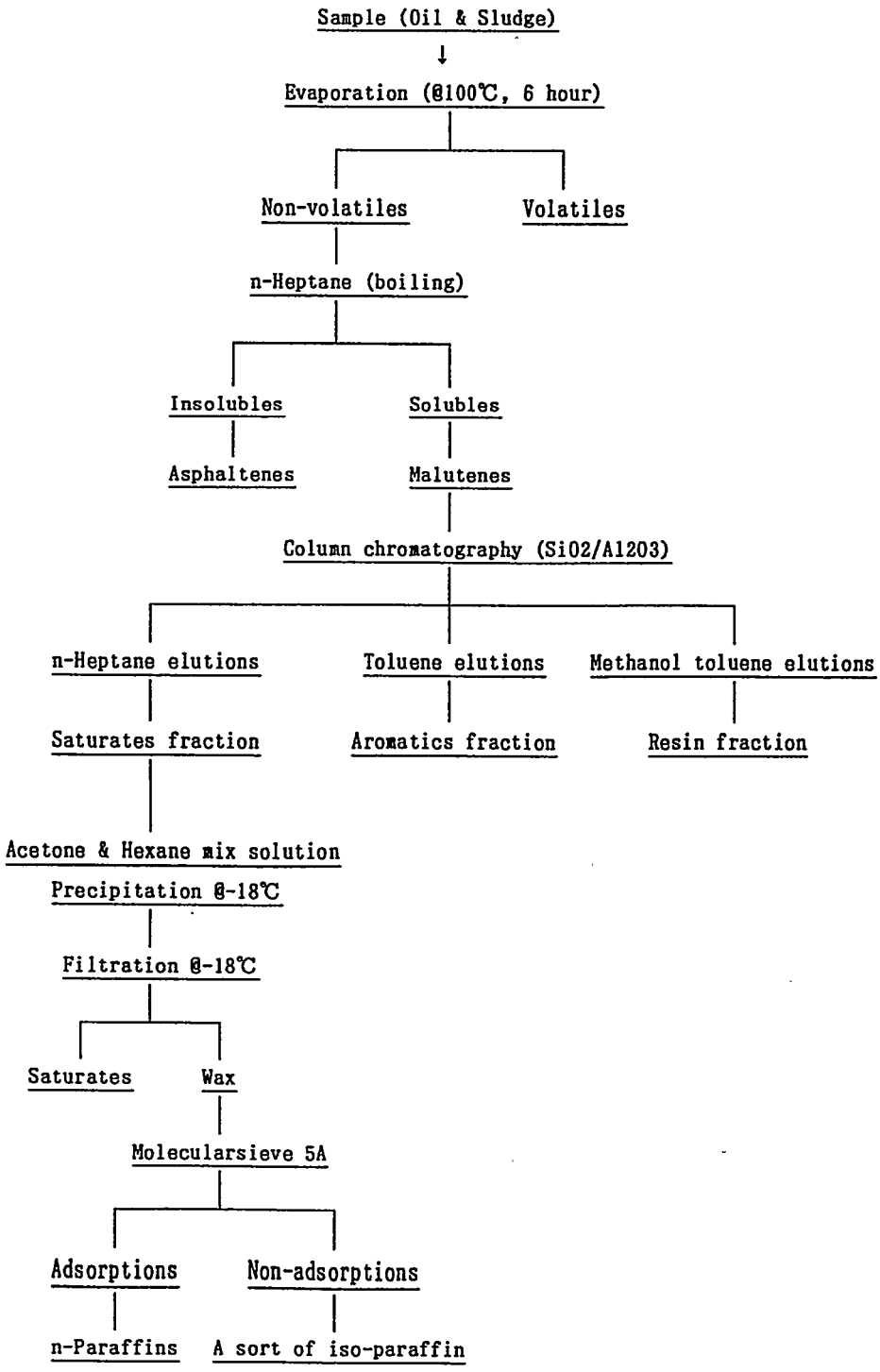
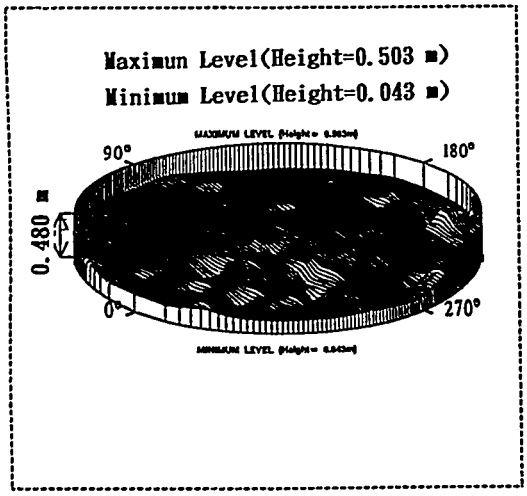


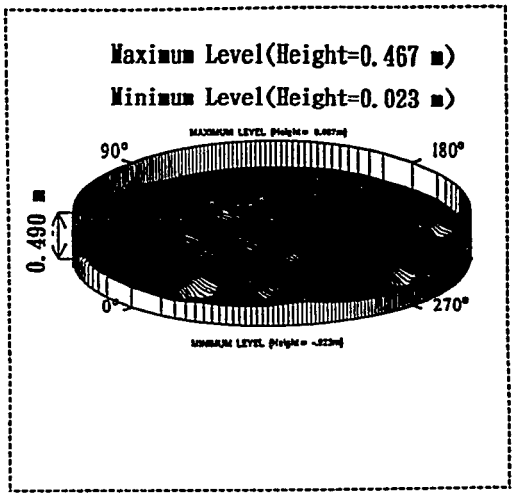
Fig. 3 Separation Scheme for Hydocarbon Composition

FRONT VIEW

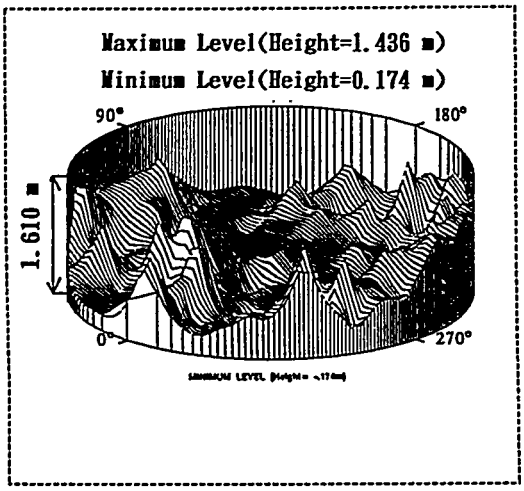
JULY 1989



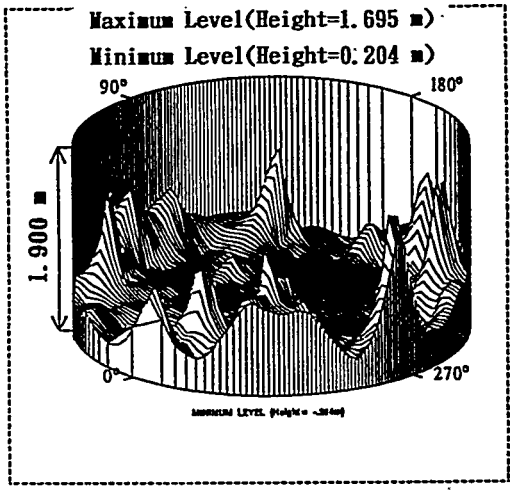
NOVEMBER 1989



JULY 1990



NOVEMBER 1990



JULY 1991

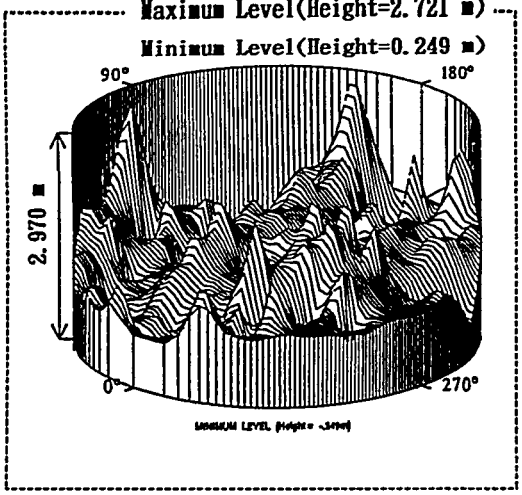


Fig. 4 Three-Dimensional Aspect of Depositing Sludge

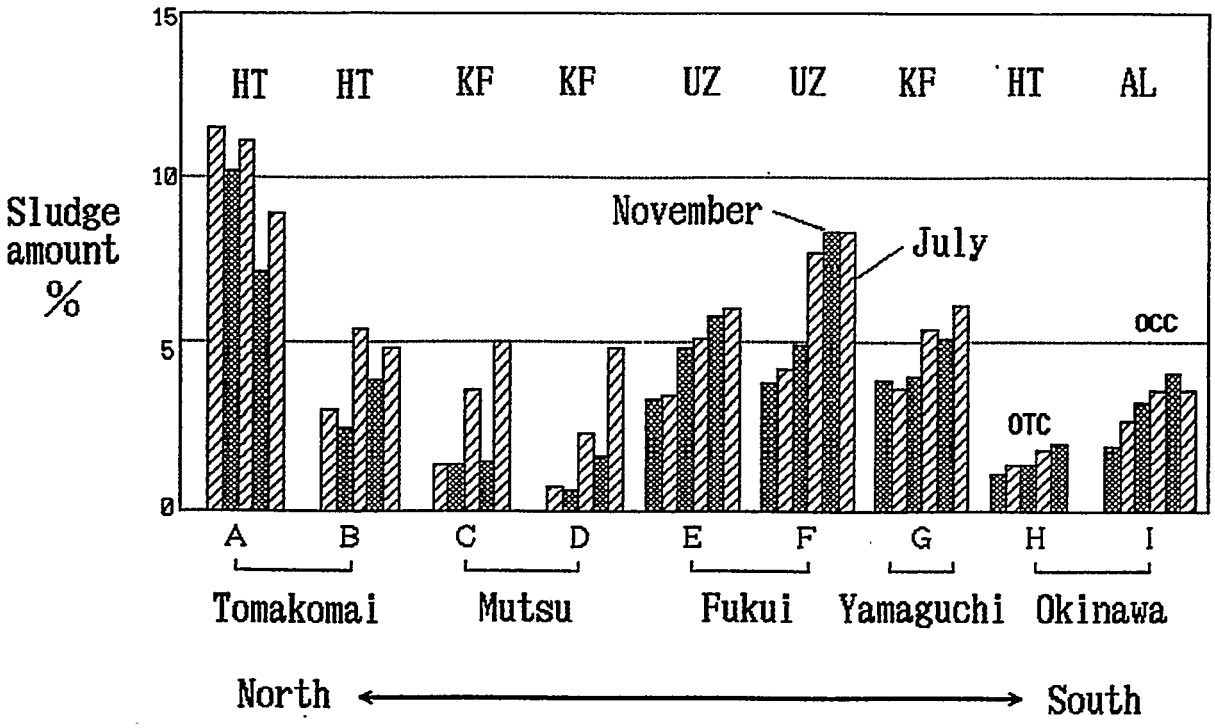
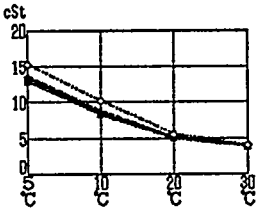


Fig.5 Maximum Amount of Depositing Sludge Reported by Each Storage Base during Stockpiling Period from 1990 to 1992

1. Zakum (Mutsuogawara No.23) ····· Bottom sample

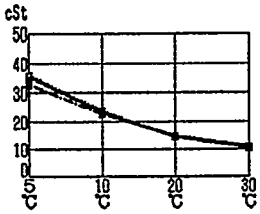
Temperature		5℃	10℃	20℃	30℃
when received		—	—	—	—
Crude	upper	13.41	8.360	5.118	3.936
	midle	13.60	8.736	5.163	3.956
	lower	12.91	8.129	5.011	3.860
Sludge	upper	12.83	8.259	5.097	3.922
	lower	15.25	10.15	5.569	3.987



North

2. Hout (Tomakomaitobu No.ST-T24) ··· Bottom sample

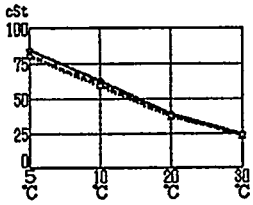
Temperature		5℃	10℃	20℃	30℃
when received		—	—	—	10.34
Crude	upper	35.23	23.50	14.30	10.52
	midle	34.93	23.36	14.28	10.36
	lower	35.73	23.69	14.36	10.66
Sludge	—	32.73	22.74	14.62	10.70



North

3. Hout (Shibushi No.40D-17) ····· hard sludge

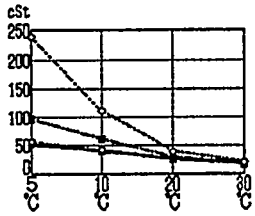
Temperature		5℃	10℃	20℃	30℃
when received		—	—	—	33.56
Crude	upper	84.47	62.83	38.97	24.35
	midle	81.07	59.86	37.47	23.55
	lower	79.70	58.75	36.55	23.43
Sludge	upper	—	—	—	5,700
	lower	—	—	—	31,000



South

4. Khafji (Mutsuogawara No.04) ·····soft sludge

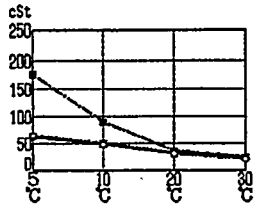
Temperature		5℃	10℃	20℃	30℃
when received		—	—	—	17.54
Crude	upper	50.23	41.16	25.89	19.39
	midle	55.27	38.81	25.84	17.83
	lower	55.87	40.33	25.33	18.50
Sludge	upper	97.12	60.71	28.25	18.44
	lower	238.8	111.9	38.86	20.37



North

5. Kafji (Mutsuogawara No.46) ·····soft sludge

Temperature		5℃	10℃	20℃	30℃
when received		—	—	—	20.46
Crude	upper	62.49	48.94	31.26	23.71
	midle	63.03	48.66	31.17	23.83
	lower	64.48	50.30	32.15	22.27
Sludge	upper	175.1	90.53	36.03	23.28
	lower	65.08	48.29	30.53	21.08



North

Fig.6 Kinetic Viscosity of Crude Oil and Depositing Sludge

In case of tank safety inspection, the whole researved crude oil is transferred from one storage system to another, accompanied by the crude oil washing (COW) procedure. The consecutive operation of COW procedure is shown in Fig.7. In some occasional cases, a slight amount of residual sludge (0.004 vol%) is recovered after crude-oil-washing in gas-phase (Fig.7), as shown in Table 4. The amount of sludge is estimated in each discharging step, as summarized also in Table 4. The properties of crude oil, depositing sludge (removed before mixing and heating operation) and residual sludge (recovered after COW in gas-phase) are clarified in Table 4. The residual sludge forms quite stable W/O emulsion as shown in Fig.8, water content of which reaches 33 wt%. Hydrocarbon composition (SARA components; saturates, aromatics, resin and asphaltene) is not changed substantially among three samples, whereas the content of wax component is quite larger in the residual sludge. According to the capillary GC profile of separated wax from three samples (Fig.9), the residual sludge is composed of crystalline n-paraffins of substantially higher carbon numbers including micro-crystal wax. The minimum pour point of the residual sludge is found to be 52.5 ℃, resulting in the complete disappearance of fluidity at ambient temperature. In order to avoid the formation of such residual sludge, hot-water-washing operation should be necessary in addition to the ordinary COW procedure, as shown in Fig.7. Moreover, the appropriate operational control against the excessive emulsification should be necessary during stockpiling period.

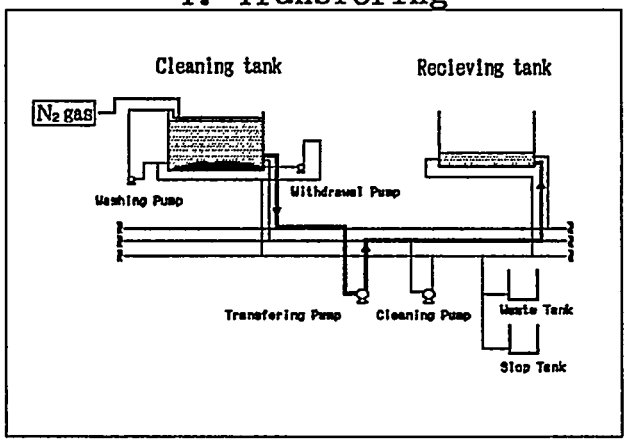
3-3. Operational Control against Sludge Precipitation

The efficiency of operational control against sludge precipitation is evaluated for various mixing devices adopted in the on-ground and in-ground tank systems. A center-mount rotary jet mixer is equipped in Shibusi (located in southern Japan) No.36 on-ground floationg roof tank. The effect of 24 hours mixing on the dispersion as well as on the dissolution of dipositing sludge is quantitatively investigated (Fig.10). The inspection hole 2 is located nearly in the center of the tank and the inspection hole A is in the side position. The distribution of temperature and the wax content along with the vertical position of the tank is measured before and after 24 hrs mixing operation. Before mixing operation, both distributions show quite large difference toward the bottom of the tank owing to the accumulation of depositing sludge. After mixing operation, both distributions are changed to uniform structure, indicating that the depositing sludge is effectively dispersed and dissolved in crude oil phase.

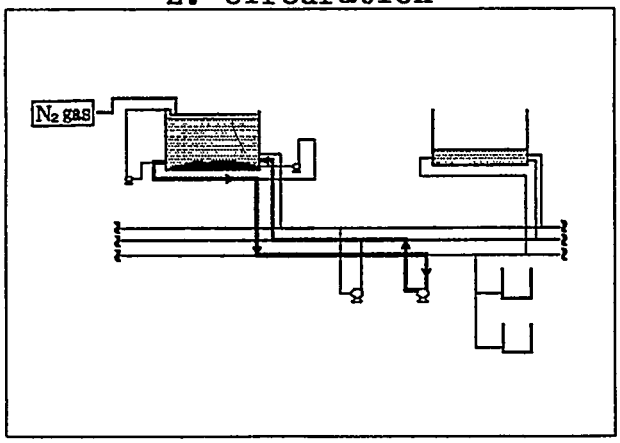
3-4. Mechanism of Sludge Formation

The amount of depositing sludge is quite sensitively influenced by various stockpiling conditions, as mentioned in 3-1. However, the sludge accumulation pattern can be classified into four types, as shown in Fig.11. Numerical analysis is applied to elucidate the relationship between sludge accumulation and stockpiled period (Fig.12). When the Gompertz function is applied, accumulation curves (Pattern I-Ⅲ) are well fitted with the calculated lines,

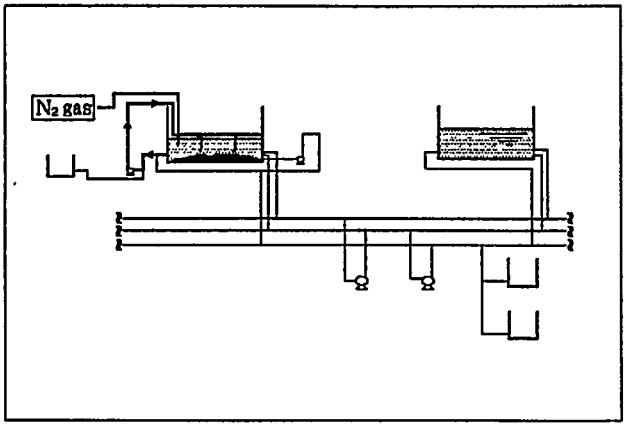
1. Transfering



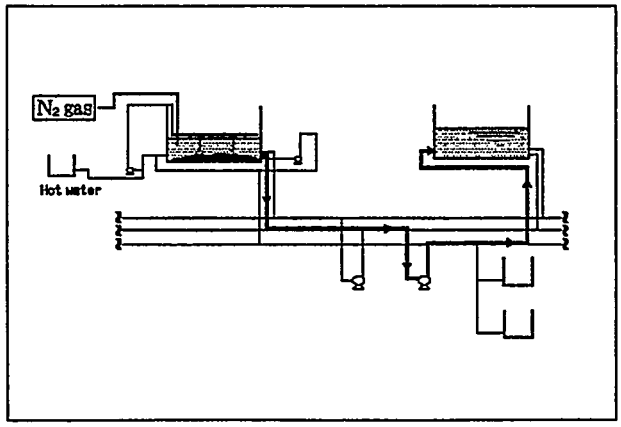
2. Circuration



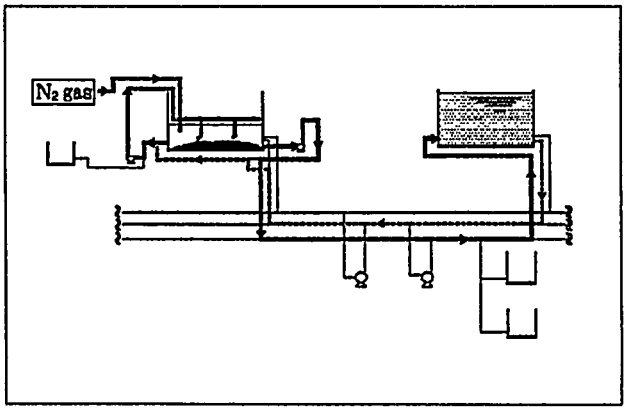
3. Crude Oil Washing
(In Oil phase)



4. Stripping



5. Crude Oil Washing
(In Gas phase)



6. Washing by Hot Water

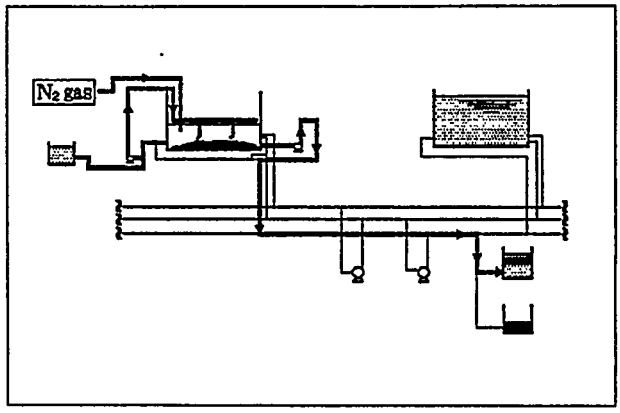


Fig.7 Procedure for Cdude Oil Washing (COW)

Table 4 Residual Sludge Recovered after COW Procedure

Crude oil: 97,800 kl (HT : KF = 95.8 : 4.2 vol%)

Step for Discharging		Amount of Sludge
Mixing and Heating	before	5,250 kl (5.4 vol%)
	after	2,230 kl (2.3 vol%)
COW	after	4 kl (0.004 vol%)

Properties of Crude oil, Depositing Sludge and Residual Sludge

Test Items	Crude Oil	Depositing Sludge	Residual Sludge
Water Content, wt%	0.75	1.70	33
Hydrocarbons, wt%			
Volatile	34.0	32.9	24.8
Saturates	28.4	25.7	26.9
Wax	3.1	6.8	13.1
Aromatics	24.8	24.5	24.3
Resin	7.7	8.2	8.4
Asphaltene	2.0	1.9	2.5
Density@15℃, g/cm³	0.8656	0.8678	0.9400
Fluidity Temp, ℃			
Minimun Point*1	<-20	<-20	52.5
Maximum Point*2	12.5	22.5	42.5
Kinetic @ 0℃, cSt	73.6	90,000	—
Viscosity @10℃	22.9	5,000	—
@20℃	15.6	1,300	—
@30℃	11.2	54	100,000

Depositing Sludge: Precipitated Sludge Settled on the bottom of the Tank before Mixing Procedure.

*1: Cooling down after heating at 80 ℃.

*2: Cooling down after heating at 45 ℃.

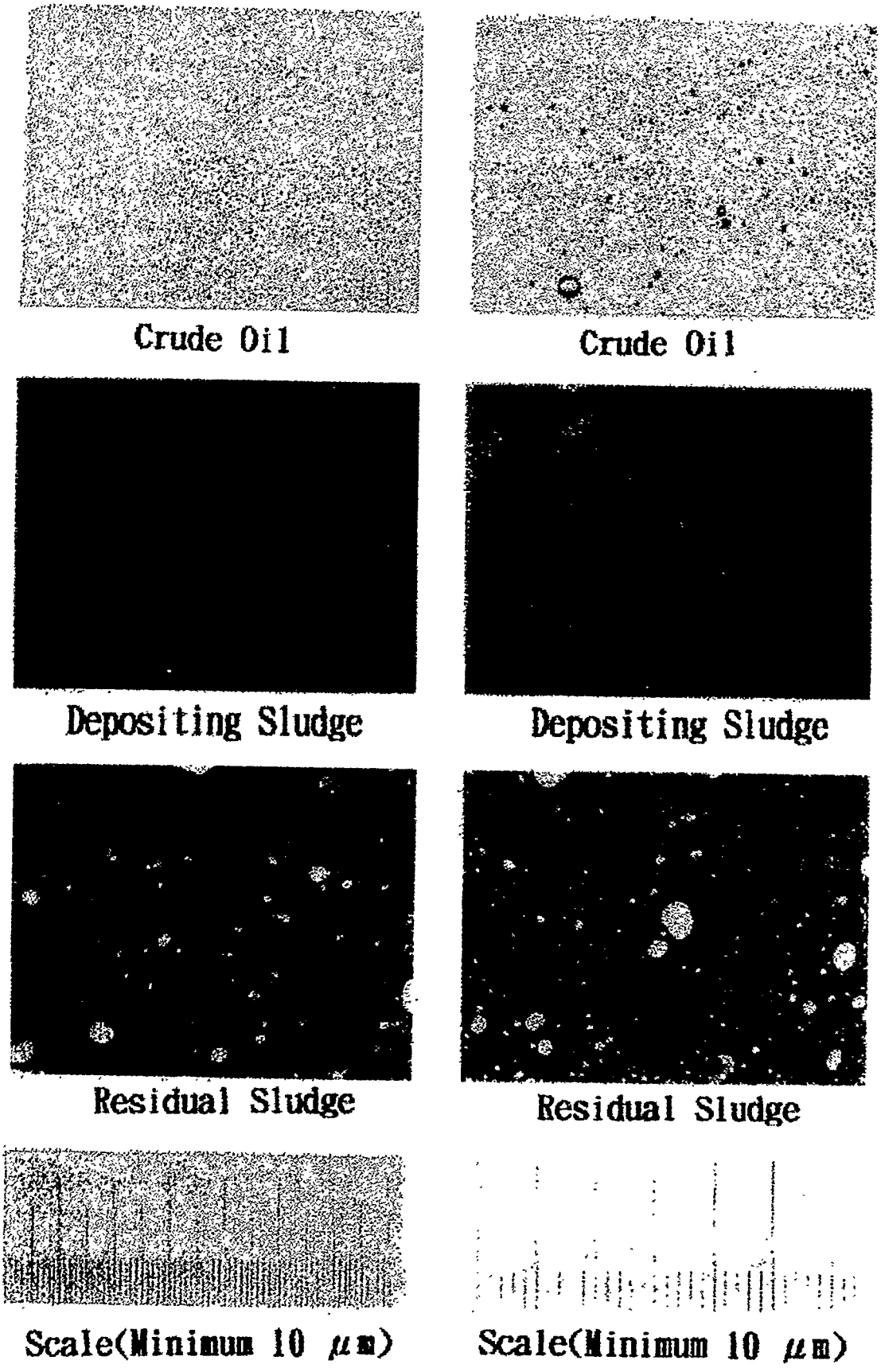


Fig.8 Optical Microscopic Photograph for Crude Oil, Depositing Sludge and Residual Sludge

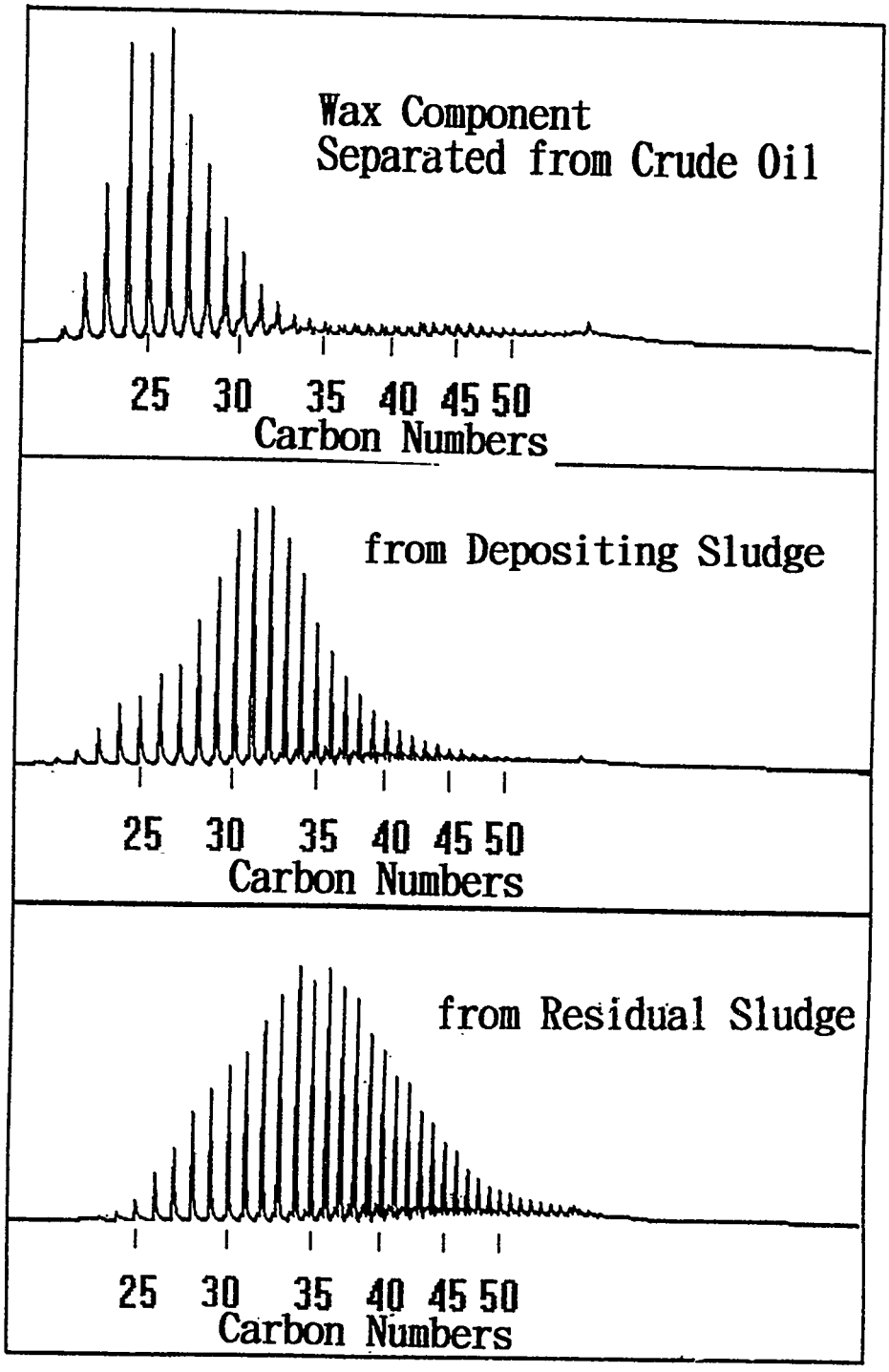
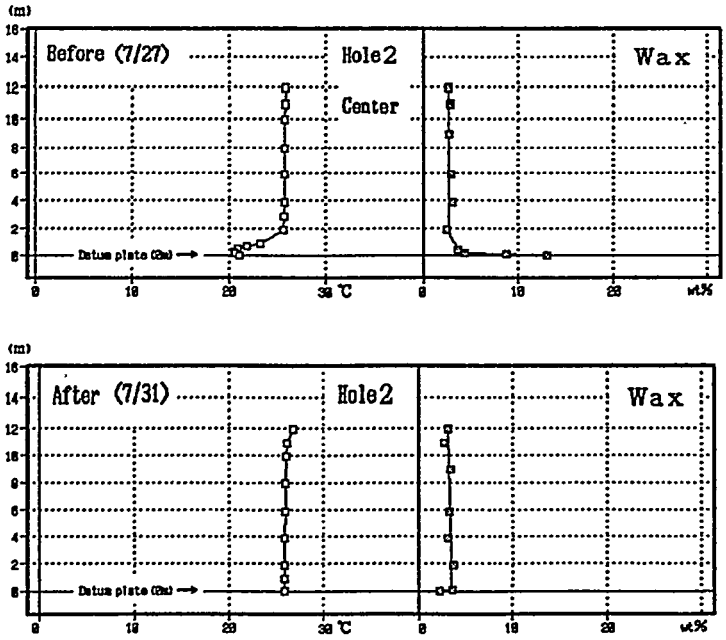


Fig.9 Capillary GC Profile of Separated Wax from Crude Oil, Depositing Sludge and Residual Sludge

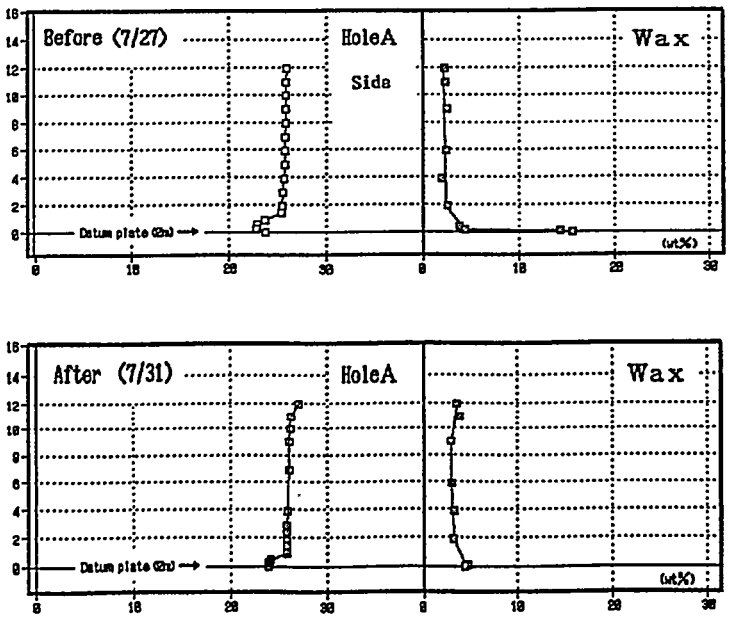
Mixing Procedure: Center Mount Rotary Jet Mixer

Mixing Time: 24 hours

Crude Oil: Upper Zakum



Shibushi No. 36 Tank Hole2(Center Location)



Shibushi No. 36 Tank HoleA(Side Location)

Fig.10 Evaluation of Operational Control against Sludge Accumulation

Pattern Ⅰ (some) : Generally, the sludging amount is some. (< 3 %)

Pattern Ⅱ (gradual increase) : The sludging amount increases gradually.

Pattern Ⅲ (rapid) : Sludge is deposited rapidly at the first stage of the storage, and then remains steady.

Pattern Ⅳ (gradual decrease) : Sludge is deposited rapidly at the first stage of storage, and the sludging amount decreases gradually afterwards.

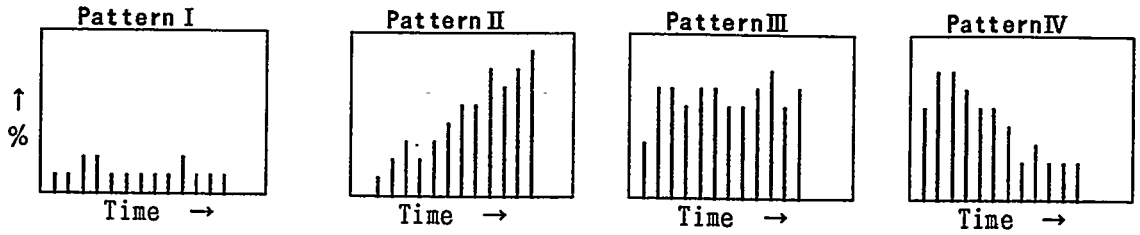
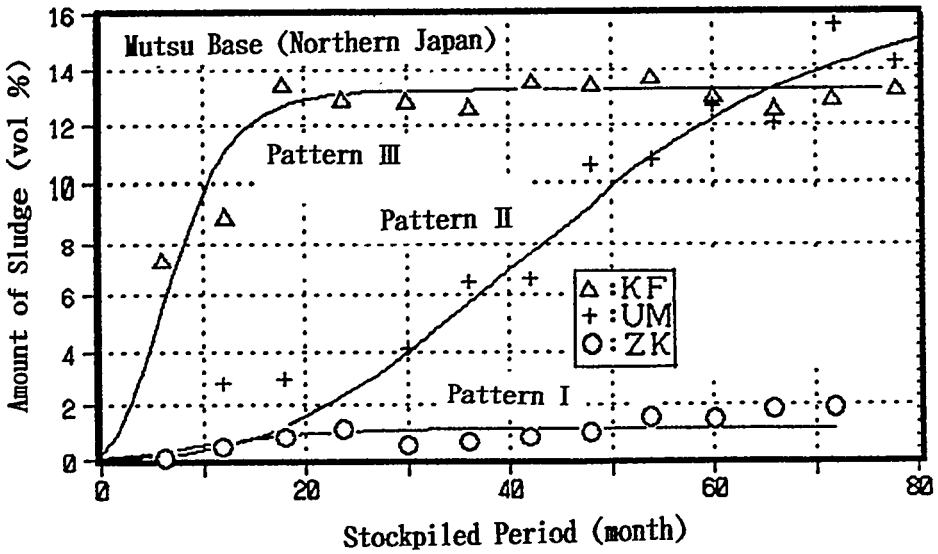
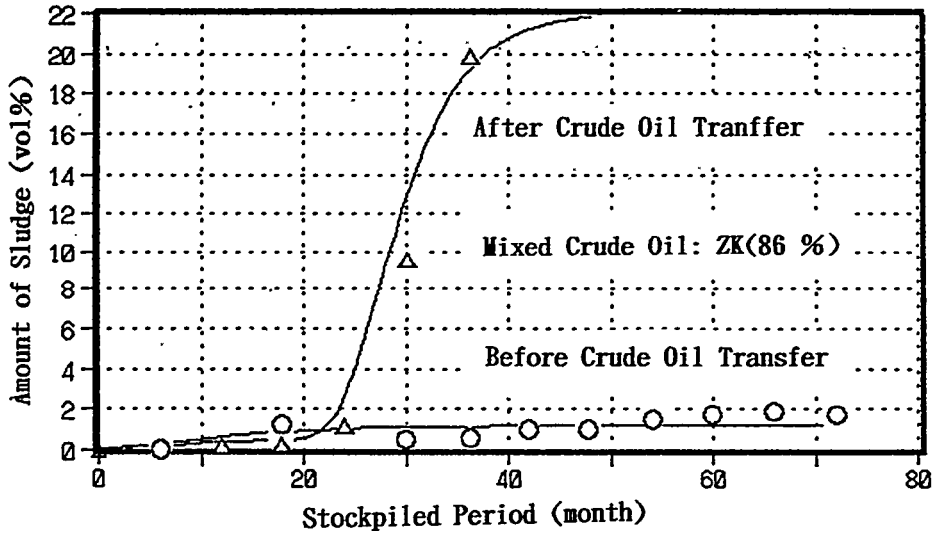


Fig.11 Accumulation Pattern for Depositing Sludge





$$Y = K \times A^{b^t}$$

Y = Amount of Sludge t= Stockpiled Period

K, A and b = Coefficient

Variables: Properties of Crude Oil,
Method of Stockpiling System,
Temperature and Temperature Drop,
Operational Control for Sludge
Historical Stockpiling Condition
and so on.

Fig.12 Numerical Analysis for Relationship between Sludge Accumulation and Stockpiled Period

as shown in Fig.12. As for Pattern Ⅳ, a linear combination of Gompertz function can be applied. In the case of mixed crude oil mainly composed of light-density Zakum crude oil (86 vol%), accumulation curve shows typical Pattern I. After the mixed crude oil is transferred to another storage base, the pattern is changed into Pattern Ⅲ in the presence of certain induction period (Fig.12). The fact can be expressed as the dependence of coefficients A and b on storage conditions, namely temperature and/or temperature drop. Therefore, multi-variates analysis of three coefficients (K,A and b) should be necessary to clarify the dependence on storage variables, listed in Fig.12, in further investigation.

4. CONCLUSION

(1) Organic sludge formed during stockpiling is exclusively waxy sludge and is not asphaltic one.

(2) Any degradation reaction could not be detected throughout the stockpiling period, including oxidation, oxygenation, biochemical degradation and so on.

(3) Depositing sludge contains crystalline structure of waxy molecules and forms stable W/O type emulsion. In some case, the content of water reaches more than 30 wt% to decrease fluidity drastically.

(4) Operational control against sludge accumulation adopted by JNOC works effectively and efficiently, so far.

(5) Prediction system for accumulation of sludge should be developed to improve the eficiency of stockpiling operation.

References

(1) Hara,T.; 2nd Conference Proceedings on Long-Term Storage Stabilities of Liquid Fuels, p 39-50, San Antonio, Texas 1986.

(2) Stavinoha,L.L.; Bowden,J.N.; Westbrook,S.R.; Giles,H.N.; AFLRL Report No.121 (1979).

(3) Brinkman,D.W.; Bowden,J.N.; Giles,H.N.; BETC/RI-79 (1979).

(4) Report on "Long-Term Storage Stabilities of Crude Oil", by Fuel Society of Japan, 1984-1986.

(5) Proceedings of 1st Conference on Long-Term Storage Stabilities of Liquid Fuels, Tel Aviv, Israel (1983).

6th International Conference
on Stability and Handling of Liquid Fuels
Vancouver, B.C., Canada
October 13-17, 1997

LONG TERM GASOLINE STORAGE AT GEOSEL MANOSQUE SALT CAVERN FIELS

Emmanuel David[1] and Gilles Le Ricousse[2]

[1]SAGESS, Société Anonyme de Gestion des Stocks de Sécurité, 3, rue E. et A. Peugeot - BP 282 - 92505 Rueil-Malmaison Cedex, FRANCE
[2]GEOSTOCK, 7, rue E. et A. Peugeot - 92500 Rueil-Malmaison, FRANCE.

1 - INTRODUCTION

GEOSTOCK, an engineering company subsidiary of ELF, TOTAL, BP and TRACTEBEL, specialized in design, construction and operation of underground storages, has built the storage of Manosque. GEOSTOCK, on behalf of GEOSEL MANOSQUE the owner of the site, is now operating this storage in salt leached caverns in which a long term storage of gasoline was performed between 1989 and 1996.

2 - MANOSQUE

The site is located in southeastern part of France near Marseilles and the Mediterranean coast. The storage was created in Manosque area, which is very sensitive in the field of environmental protection, because of the existence of an underground salt deposit dated 35 million of years (Oligocene period) and rearranged during Alpine formation. The salt layer is 200 - 1,000 m thick.

The MANOSQUE underground storage complex consists of 28 salt leached caverns having an available capacity of 6,5 million m3 used for the storage of crude, diesel oil, premium and naptha.

The storage system includes pipelines for the supply of fresh water and the transport of hydrocarbons and brine, and two holding ponds at LAVALDUC and ENGRENIER (owned by Salins du Midi) where brine can be stored for the local salt and petrochemical industries and for destroying.

The whole complex is controlled by one operator at a central control station using a computer interfaced system.

The system is interlinked with three refineries, two chemical plants, the port of LAVERA and the S.P.L.S.E and S.P.M.R pipelines.

3 - CHARACTERISTICS OF THE STORAGE

The storage caverns were made by drilling a short distance into the top of the salt dome and cementing in a main casing over the whole length. The hole was then deepened to the required position for the bottom of the caverns, and two concentric wash pipes installed. Fresh water pumped down the center pipe dissolves the salt and brine is forced up the annular space to the surface. The shape of the resulting cavern can be controlled by moving the wash pipes upwards in steps while monitoring the progress of the solution mining by sonar.

The stability of the caverns is ensured by their shape and the fact that they are kept full of liquid - brine or hydrocarbons - at all times.

Containment of stored product is rigorously checked by Mines department inspectors. The storage method is entirely safe because the product is kept out of contact with the atmosphere, lightning cannot reach it, and there are none of the dangers of leakage from accidental holing or corrosion attendant on surface storage tanks.

4 - BRIEF STATISTICS ON MANOSQUE

- Cavities vary in capacity from 100,000 to 425,000 m3. They are approximately 300 m high (the Eiffel Tower is 321 m high) and have a maximum diameter of 80 m (Notre Dame Cathedral in Paris is 48 m wide). The cavities are 400 m to 1,200 m below ground level.

- Brine buffer ponds with a capacity of 100,000 m3 each are provided at the storage site

- The main pumping station at MANOSQUE has 23 pump groups

- About 100 million m3 of fresh water will be used to mine the designed 10 million m3 of storage capacity.
  This would be sufficient water to meet the annual needs of a town of 600,000 to 700,000 people.

- About 12 million tons of salt will be removed, two of three times the annual salt production in France.

- More than 20,000 tons of steel pipe were used.

- Products are pumped in at a speed of 2 m per sec.

- The MANOSQUE facility uses a ground area of only 8 hectares. An equivalent surface tank farm would require 300 hectares

- Operational power requirement is 24,000 kva.

5 - GEOSEL OBJECTIVES FOR MANOSQUE STORAGE

MANOSQUE storage, whose creation was initiated after the first SUEZ crisis in 1956, was first intended to face supply crises. Therefore, its first aim is strategic.

This objective, which was first restricted to crude oils, was recently extended to refined products (gas oil and gasoline).

The integration of this specific storage (operated on behalf of its shareholders) in the logistic chain of the refineries of the South of France makes it a very important part of the French network of strategic petroleum storages.

Running this facility, integrated into the interlinked refineries, enables to meet seasonal requirements of some petroleum products, such as gasoil, and besides to assure an emergency function, in case of problems on the proper storages of the refineries or on those of petroleum installations in the South of France area.

Finally, the important capacity of this storage enables to operate it as a buffer storage in the framework of adjustments made by petroleum companies on their stocks because of circumstances due to the current conjuncture.

6 - THE V CAVERN

The V cavern in which the long term storage was performed is located in a multiproducts (diesel oil, premium, naphta) branch of the storage.

Its capacity is 195,000 m3 and it is now dedicated to gasoline after having stored diesel oil and naphta before 1989.

The particular shape of this cavern is *(see attachment 1)* due to the presence of insoluble banks broken up into pieces scattered throughout the mass of the salt.

SAGESS EXPERIMENT OF LONG TERM GASOLINE STORAGE IN MANOSQUE SALT CAVERN

1 - BACKGROUND

SAGESS is a private company which holds and controls strategic reserves of petroleum products on behalf of the French Government authorities. SAGESS stocks -5,5 million m3 of gasolines, diesel and heating fuels, jet fuels and crude oils- represent one fourth of the French reserves *(see attachment 2).*

SAGESS found attractive the possibility to store gasolines, then distillates and crudes in the MANOSQUE salt caverns rent to GEOSEL. In 1989, a joint SAGESS-GEOSTOCK venture was decided to set aside cavern «V» with a view to experiment the effects, on gasoline ageing, of a long-term storage in a salt cavern.

2 - SAGESS INCENTIVES

From a technical point of view, the salt caverns should provide a better protection of gasolines than above ground tanks against ageing *(see attachment 3)* for the following reasons :

- the cavern is entirely filled, thus ensuring the absence of air and UV, responsible for most of ageing processes,
- this close structure does not allow any volatility losses,
- the temperature inside the salt cavern is kept very stable due to the thermal inerty of the salt mine and depth of the cavern. GEOSTOCK estimated it should be within the 30 to 35°C range.

In addition, GEOSTOCK forbids the preliminary incorporation of any additive, dye or oxygenates in the virgin gasoline before storage to prevent it from ageing side effects. This additivation/blending treatment which aims to tailor the product to the retail specifications takes place in the refinery where it is returned in any case after storage for unexpected but possible need of reprocessing.

On the overall, the balance of technical/economical factors for this experiment looked attractive to SAGESS, taking in account the more economical storage costs in caverns and the possibility contemplated to extend storage times due to lower ageing processes.

3 - CAVERN « V » FEATURES

The so-called cavern « V » is a typical pear-shape structure of 180,000 m3 capacity leached by water in salt dome in 1971, at a depth between 590 and 660 meters. Between 1971 and 1989, the cavern «V» contained successively diesel fuel, naphtha, base gasoline for leaded *(see attachment 4)*.

4 - FILL / DISCHARGE HISTORY

Between January 1989 and January 1991, the cavern was filled, on behalf of SAGESS, with 11 batches supplied from the three refineries for a total volume of 175,926 m3 of a lead-free virgin gasoline. The material was considered to be a base stock for the later production of a leaded premium containing 0,25 g/l lead. The different lots were pumped sequentially into the cavern over 2 years. Between January 1991 (end of cavern fill) and March 1996 (beginning of discharge), no gasoline was added or withdrawn from the « V » cavern.

Discharge history

The injection of brine into the bottom of the cavern has displaced the filled-in lots in reverse order. Between March and September 1996, a total volume of 175,926 m3 was pumped out of the cavern in 8 sequential lots with volumes ranging from 15 to 31,000 m3.

Each delivering refinery got about one third of the cavern fill for entering it into their own blending/additivating logistic system. As already noted by GEOSEL in their previous fill/discharge operations of cavern «V», a volume of about 5,000 m3 product is permanently kept in vertical traps.

Storage time

As shown by the histogram of cumulated volumes in the cavern *(see attachment 5)*, 88,5 % of the gasoline volume had a storage time between 7 years 5 months and 7 years 8 months. The remaining share (11,5 %) corresponding to the volume of 20,000 m3 introduced in January 1991 stayed for 5 years and 2 months.

The average storage time, calculated on weighted volumes, was found to be of 6 years and 9 months.

5 - QUALITY CONTROL ANALYSIS

There is no documentation on the control data issued by the 3 supplying refineries on their respective production batches (before cavern fill-in, and at receipt of the lots after cavern discharge) which were kept for internal use. The control data available were obtained from the external independent laboratory which inspected the cumulated samples obtained by GEOSEL in recipes fed from the cavern fill-in and discharge lines.

The present report could not include the detailed quality control results on individual lots of gasoline but retained the most significant ranges of values and averages in the *attachments 6 and 7* and the corresponding graphs *(attachment 8).* They can be commented as follows :

Analysis of fill-in qualities

The individual quality control results appear typical of a virgin product including cat cracked gasoline, with few abnormal values identified :

- one batch (4,004 m3) exceeded the max. spec. of density at 15°C (778 versus 720-770 kg/m3),
- two batches (totalling 24,643 m3) were noted with a yellow colour (all others were rated yellow pale),
- one batch (10,170 m3) was noted with a copper corrosion of 1 b for a spec. of 2 max (others 1 a) and an existent gum value of 6 mg/dl (spec. 10 max).

The reported RON and MON results are clear, lead-free octane values. They cannot therefore be compared to the specifications of 97 min for RON and 86 min for MON which pre-suppose TML addition of 0,25 g/l lead. However, the clear values indicate good potential.

The discrepancies of results noted between several sequential batches and noticeable on the attached graphs, must be considered normal taking in account the supply from 3 different refineries and the effect of seasonal refinery production (e.g. P.V.R. and distillation) since gasoline delivery spread over 2 years (Jan 89 to Jan 91).

Analysis of pump-out qualities

The ranges of values obtained on the samples of the 8 consecutive lots are considerably narrower. They indicate that a mixing of the original batches took place in the cavern probably due to mixes induced by the superposition of the gasoline layers during filling-in operations and also from the convection moves during the nearly 7 years storage time. A more uniform gasoline has evolved during storage :

All characteristics illustrate this, but more especially :

Density at 15° C		range	reduced	from	32	to	4	units,
Distillation	E100	„	„	„	19	to	4	„
	FBP	„	„	„	28	to	7	„
RON (clear)		„	„	„	4,2	to	1,1	„
MON (clear)		„	„	„	6,4	to	0,8	„

The control results on the 8 sequential lots of the discharged gasoline fully meet the quality specifications originally established for its intended application.
An increase of colour level and existent gum values point out a moderate ageing but within reasonable limits.

New outlets for base gasoline

During the 7 years storage period, the French market demand has moved towards unleaded gasolines and gasolines containing lower contents of lead (0.25 g/l grade replaced by 0.15 g/l grade). This brought the refiners to consider the possible use of the stored gasoline in these new outlets.

The gasoline quality was found suitable by the refiners to manufacture both the premium leaded grade and the 95 unleaded Europremium. It went into their respective blending processes and their retail systems without any reprocessing and raised no quality complaint. How and to what extent each company upgraded their batches is not known to SAGESS. The only indication received was that the sulfur content of the gasoline (≅ 600 ppm) required a preliminary dilution with another low-sulfur gasoline stock to meet the 500 ppm limit of the Europremium grade.

6 - STUDY OF AGEING CHARACTERISTICS

The determination of ageing characteristics aimed to appraise better the interest of the underground salt caverns for long term storage of gasolines and other petroleum products.

SAGESS requested EBV partner's help to analyse the Manosque experience and learn lessons for their own cavern stocks of gasoline in Blexen and Heide (North Germany).

- **Composite samples**

EBV obtained cumulated samples (remainder of quality control) which were pooled into 3 representative composite samples for the top, middle and bottom sections and analysed by a Dutch expert laboratory, leading to the following conclusions :

1. The product after storage is very uniform but a slight density increase can be identified towards the bottom.

2. There is an aromatic increase from top to bottom in line with the density increase. The bottom section shows reduced olefins content, possibly due to the reaction with oxygen from the brine : under ultra-violet light, the top and middle sections are more reactive than the bottom section, as there are more reactive olefins left.

3. The product has formed no additional gum over the storage period : the available gum is not resin-like and easily washed away by normal heptane. The little amount of washed gum is dry and of uncritical consistency for modern injection engines.

4. The potential gum values show that substantial further and possibly faster ageing could have occurred, had the product been stored in a less protected environment like above ground ' el tankage.

   The above measurements allow the conclusion that the original gasoline probably contained some 20-30 % of light cat crack naphta but definitely no pyrolysis material and was more reactive than normal hydroskimming type gasoline, but as a conversion gasoline very suitable for cavern storage and long residence time.

- **Spot samples / Cavern segment analysis**

Analysis of spot samples *(see attachment 9)* performed by ETS Mont-Saint-Aignan on behalf of SAGESS revealed the following :

1. The existing gum values show a very consistent picture from top to bottom of the cavern.

2. While induction periods reach generally times over 1,000 minutes, they fall dramatically for the last m3 before interface with a corresponding big increase in oxygen reactivity and thus potential gum formation.

3. The aromatic increase going in hand with density increase reaches a peak value then decreases again with density at the cavern bottom, due to wash-out effects of light aromatics (mainly benzene) into the brine. The last liters of gasoline show this drastically. The loss in benzene and other aromatics explains the loss of research/motor octane numbers by at least one point.

4. The brine analysis *(see attachment 10)* shows a significant content of benzene and other aromatics as well as some other light hydrocarbons ; no bacteria contamination was detected.

7 - EQPS ASSESSMENT

EBV have operated EQPS, an expert system based on artificial intelligence, they have designed to predict ageing processes in oil products and calculate a further storage time during which the product use is still possible without significant risk.

Although the relevant ageing data were available only for the discharge batches and not for the fill-in batches the computer system labelled the gasoline after the storage time of 6 years 9 months as :

« A normal average product which may be very suitable for consumption within 18 months. Not ideal (anymore) for long term storage but risk of surprise is low -You may plan (even) for 2 years- ».

There was no difference in the predictions between the top, middle and bottom sections for the gasoline in the cavern. Please note that EQPS does not comment on changes of performance data, e.g. loss of RON due to benzene wash-out.

This would mean to say that the material could have been stored at least 2 years more in the cavern and still have been suitable for sale on the retail market, without reprocessing.

8 - MAIN CONCLUSIONS

Batches of base gasolines, intended for manufacture of 0,25 g/l leaded premium, were supplied from three refineries located in Marseilles area, and stored for nearly 7 years on behalf of SAGESS, in a salt cavern of Manosque site, rent to GEOSEL.

The gasoline analysis carried out at fill-in and after discharge of the cavern led to the following conclusions :

1. A mixing of the gasoline batches has resulted from the combined effect of their superposition in layers together with temperature convection moves. At discharge, the discrepancy of control values noted on original batches has disappeared to give a more uniform product.

2. An organized distribution of hydrocarbon families was noted from top to bottom of the cavern supported by a correlation of densities. The content of aromatics increases steadily to reach a max. peak at 130,000 m3 pumped, then followed by a fall until gasoline-brine interface. The balance of aromatics is made by olefins and isoparaffins. The drop in aromatics is especially sensitive at the near interface where 1 point fall of octane values is noted and a presence of light aromatics detected by GC in the brine.

3. Gasoline ageing after storage was rated as moderate as illustrated by limited increases of colour, contents of existent and potential gums, still matching quality specifications.

   Subsequently, the gasoline discharged from the cavern could be fully re-introduced in the gasoline pools of the 3 supplying refineries without requiring any re-processing. The product received was blended with octane improvers and adjusted with other available gasolines to match for the retail market either the specifications of 0,15 g/l leaded premium (0,25 g/l cancelled for environmental reasons) or the unleaded Europremium 95.

4. The potential gums in gasoline which normally turn into some existent gums for the products stored in above-ground tanks did not get through because of the privileged maintenance conditions in the cavern (no air, no UV, stable temperature, no volatility loss). This specific protection enhances the choice of salt caverns for the long storage of petroleum products.

5. The Manosque cavern findings confirmed previous experiments made in the German salt caverns of Blexen and Heide including the migration of aromatics at the interface from the gasoline layer into the brine layer.

6. A simulation program fed with gasoline ageing characteristics enabled to predict a further possible storage of at least 2 years in salt cavern without compromising its acceptable quality for sale on the domestic market.

9- FURTHER SAGESS EXPERIMENTS

The interesting results on the gasoline of cavern «V» encouraged SAGESS to extend this first experiment to cavern «P», another salt cavity filled with 313,000 M3 of an unleaded base gasoline (intended for 0,15 g/l leaded premium), supplied from the same refineries. Product which was stored in cavern «P» between March 1992 and March 1996 (3,5 years residence time) is currently being discharged for sale on the retail market.

Analysis of the so far discharged gasoline consolidated the basic conclusions for cavern «V» experiment :

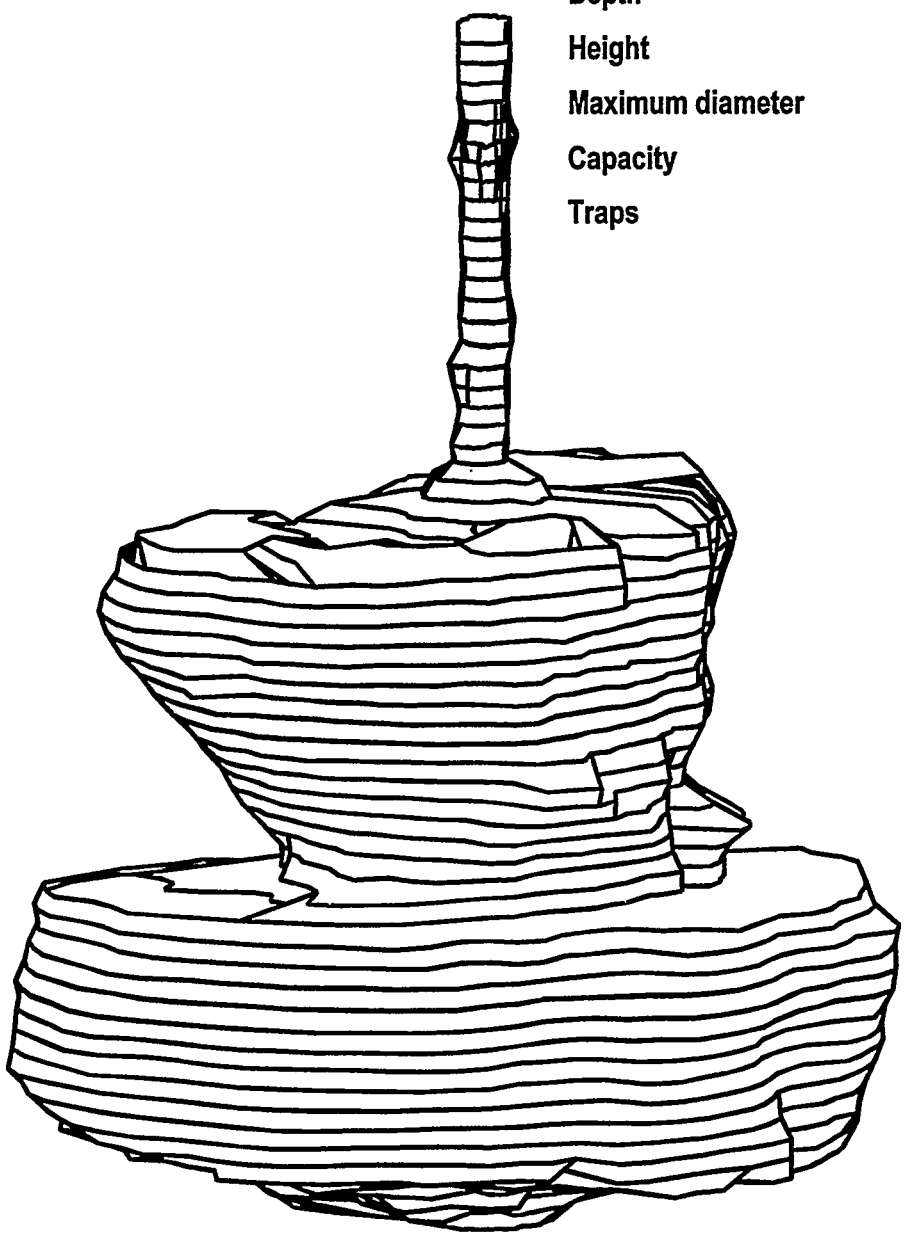
- Trouble-free introduction into refineries gasoline pools (without reprocessing) after suitable quality control,
- Mix of original batches but gradual increase of densities and aromatics with balanced decrease of naphtenics/isoparaffins followed by a decrease,
- Little evolution of ageing characteristics.

GÉOSEL MANOSQUE - CAVERN V

EASTERN OVERHANGING VIEW

Cavern characteristics

Depth	590 - 660 m
Height	125 m
Maximum diameter	91 m
Capacity	195,000 m^3
Traps	5,000 m^3



géostock

IASH '97
VANCOUVER - OCT - 1997

sagess

S.A.G.E.S.S.

Société Anonyme de GEstion des Stocks de Sécurité

☞ **A private company which fulfills a public service duty :**

Holding and controlling 1/4 of the French strategic petroleum reserves

SAGESS Strategic Stocks	Million m3
Gasolines	1.2
Diesel / Home Heating Fuels	3.8
Jet Fuels	0.2
Crude Oils	0.3

géostock

sagess

WHY STORING GASOLINE IN A SALT CAVERN ?

BALANCE OF TECHNICAL / ECONOMICAL FACTORS IS ATTRACTIVE

Technical

Salt cavern protects gasoline better than aboveground tanks

☛ No air, no UV responsible for ageing

No volatility loss

Storage temperature is stable (30 to 35° C range)

Economical

Storage times can be extended and costs are cheaper

géostock

CAVERN GASOLINE FEATURES

Fill history

PRODUCTS	STORAGE PERIODS
Diesel fuel	1971 ⇨ 1980
Naphta	1980 ⇨ 1981
Base gasoline for leaded	1981 ⇨ 1989
Base gasoline for leaded	1989 ⇨ 1996

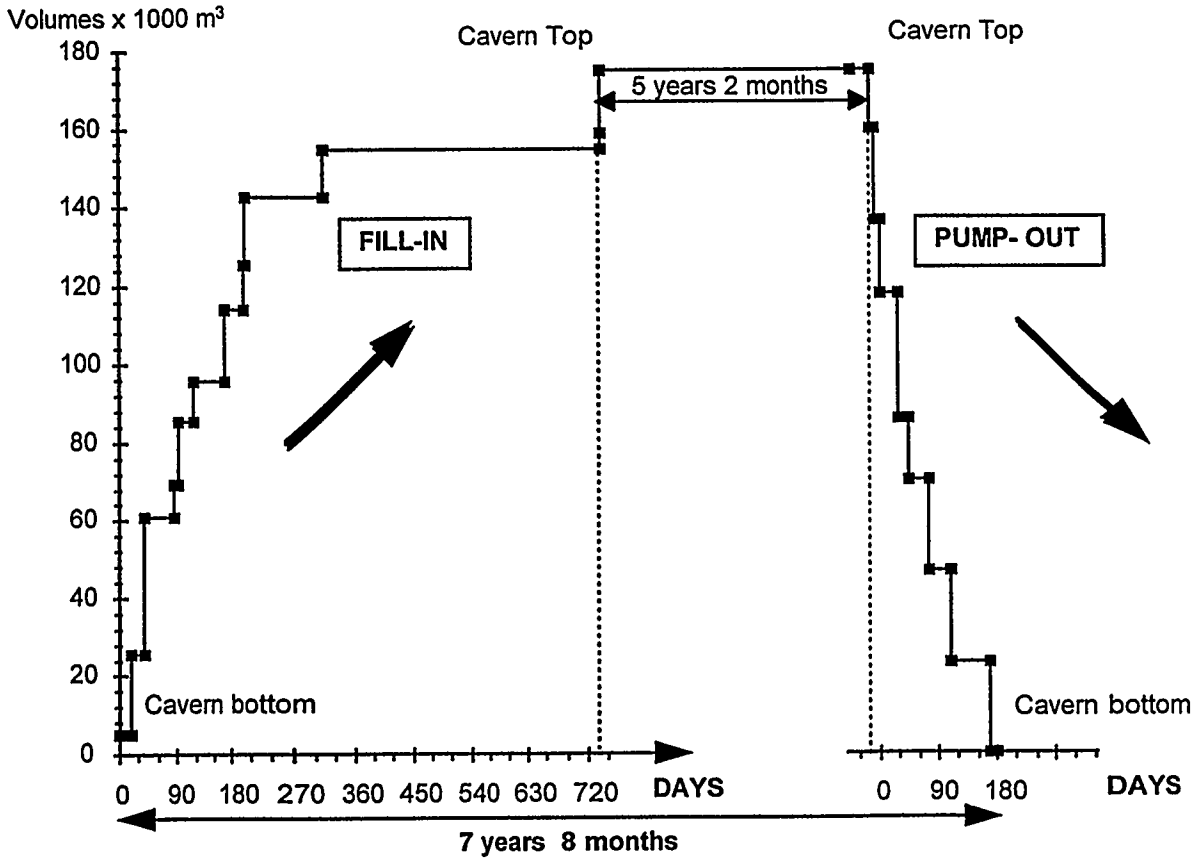
Gasoline : 11 batches, 3 CAT - cracking refineries (base for leaded premium)

Storage time

Between 5 years 2 months and 7 years 8 months

Average # 7 years

HISTOGRAM OF CAVERN GASOLINE CONTENTS



géostock

IASH '97
VANCOUVER - OCT - 1997

sagess

QUALITY CONTROL ANALYSIS

PRODUCT : LEAD-FREE GASOLINE STOCK FOR LEADED PREMIUM (0.25 G/L LEAD)

STORAGE TIME : 5-7 YEARS

		FILL-IN (11 BATCHES)			PUMP-OUT (8 LOTS)	
PROPERTY	**UNIT**	**RANGE OF VALUES**	**AVERAGE** *(weighted values)*	**SPECIFICATION**	**RANGE OF VALUES**	**AVERAGE** *(weighted values)*
Aspect	-	Clear and Bright		CaB	Clear and Bright	
Colour	-	Yellow pale	-		Light amber	
Density at 15°C	Kg/m3	746-778	757	720-770	754-758	756
DISTILLATION						
IBP	°C	27-38	34	-	33-41	37
50 %	°C	93-121	103	-	98-104	101
85 %	°C	138-167	152	180 max	143-154	148
90 %	°C	146-178	161	210 max	152-163	157
PF	°C	178-206	192	215 max	183-200	193

géostock

sagess

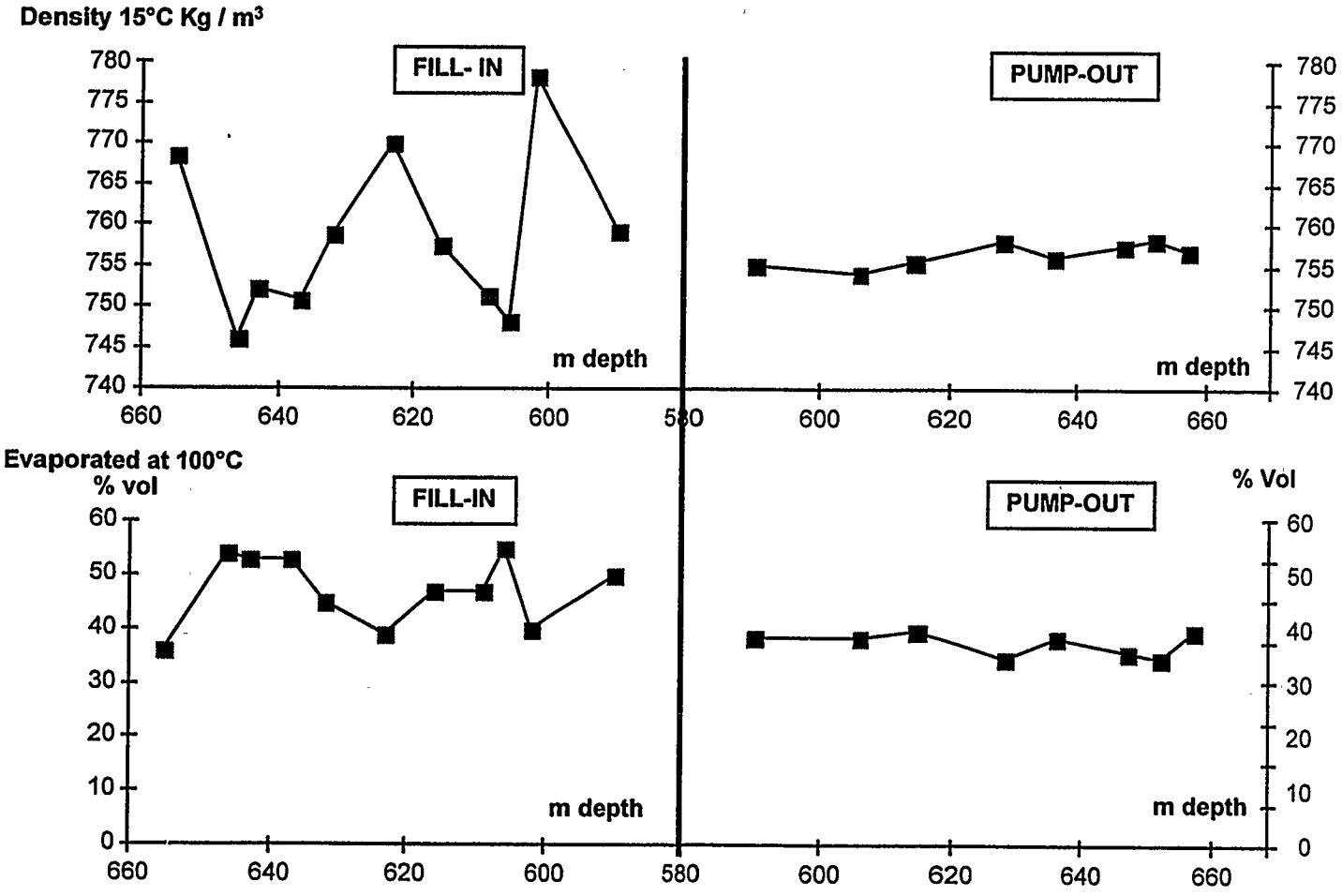
QUALITY CONTROL ANALYSIS

		FILL-IN (11 BATCHES)			PUMP-OUT (8 LOTS)	
PROPERTY	**UNIT**	**RANGE OF VALUES**	**AVERAGE** *(weighted values)*	**SPECIFICATION**	**RANGE OF VALUES**	**AVERAGE** *(weighted values)*
% Evaporated at 70 °C	% vol	15-30	24	10-47	24-30	26
% Evaporated at 100 °C	% vol	36-55	47	40-70	47-51	49
Residue	% vol	1-2	1,3	2 max	1-1,4	1,2
PVR at 37,8° C	HPa	500-720	590	450-790	484-731	604
Doctor test	-	Negative	-	Negative	Negative	-
Copper corrosion	Scale	1A-1B	1 A^+	1 B max	1A - 1B (1 out of 8)	$1A^+$
RON (clear)	Rating	92-96,2	94,9	-	94,5 - 95,6	95
MON (clear)	Rating	81,3-87,7	83,3	-	83 - 83,8	83,4
Existent Gum	mg/dl	0,5-6,0	2,0	10 max	1,1 - 5,5	3,5

NARROWER RANGES OF RESULTS ON GASOLINE AFTER STORAGE INDICATE MIXING

géostock

D15 AND DISTILLATION (E 100) VERSUS CAVERN DEPTH



géostock

IASH '97
VANCOUVER - OCT - 1997

sagess

SEGMENT ANALYSIS

- AGEING CHARACTERISTICS -

	UNIT					
VOLUME AT DISCHARGE PUMP	**x 1,000 m3**	**10**	**55**	**110**	**166**	**INTERFACE**
EXISTENT GUM WASHED	mg / dl	4.3	5.8	4.4	4.3	4.0
INDUCTION PERIOD	minutes	> 1000	> 1000	> 1000	> 1000	84
POTENTIAL GUM WASHED (6 hours)	mg / dl	426	46	58	60	344
AROMATICS (FIA)	% Vol	43.0	47.7	51.9	44.5	36.2
RON (PIONA)	-	93.9	94.8	95.0	93.7	91.5
MON (PIONA)	-	82.2	83.0	83.0	82.0	80.3

géostock

sagess

BRINE ANALYSIS *

DENSITY 15°C	Kg/l	1.2005	ASTM D 4052
SALINITY	Kg/l	0.3	CALCULATION
TOTAL HYDROCARBONS	mg/l	6.2	GC ANALYSIS
BENZENE	mg/l	2.4	„
TOLUENE	mg/l	0.1	„
OTHER LIGHT AROMATICS	mg/l	< 0.1	„
OXYGEN	mg/l	0.4	„
BACTERIA CONTAMINATION	RLU**	NIL	LUMAC

* At gasoline/brine interface, at the end cavern discharge

** Relative Luminescence Unit

☛ **A limited migration of benzene and other light aromatics from gasoline into brine is confirmed by analysis**

géostock

6th International Conference
on Stability and Handling of Liquid Fuels
Vancouver, B. C., Canada
October 13-17, 1997

ASSESSING THE POTENTIAL FOR OXIDATIVE CRUDE OIL DEGRADATION DURING LONG-TERM STORAGE

J. B. Green*[1], J. Y. Shay[1], K. Q. Stirling[1], and H. N. Giles[2].

[1]BDM-PT, P.O. Box 2543, Bartlesville, OK 74005
[2]U.S. DOE, Strategic Petroleum Reserve Headquarters, Department of Energy, FE-43, 3G-070 Forrestal Building, 1000 Independence Ave., S.W., Washington, DC 20585-0340

Alteration of crude oil composition and properties is a major concern for those involved with its long-term storage or strategic stockpiling. Significant alteration of crude oil could potentially occur via any of several pathways: microbial degradation, contamination, precipitation of slightly soluble components, or oxidative degradation. Over the course of an ongoing program for support of the U.S. Strategic Petroleum Reserve (SPR), the authors have examined each of the pathways listed above. This paper will focus on assessing the potential for oxidative degradation of crude oil. In order to assess the maximum extent of degradation likely to occur, three crude oils were subjected to a modified version of the oxygen overpressure test used to test diesel fuel storage stability (ASTM D 5304). Hot (85°C) filtration and sediment washing were employed to avoid wax precipitation. The crude was aged for 16, 40, and 90 hours under pure oxygen using conditions prescribed in the test method. Additional tests were also carried out under air and inert (N_2) atmospheres. The resulting aged crude oil samples and sediments were subjected to a variety of analyses. Aging under pure oxygen at 90°C for 90 hours produced maximum sediment levels of 2.3–23 g/L for the range of crude oils tested. Sediment levels obtained under air or nitrogen were much lower, typically <0.3 g/L. Maximum sediment formation was directly proportional to either asphaltene or vanadium content of the crude oils examined. Both of these parameters correlate with the proportion of high molecular weight, slightly soluble crude oil components present. Sediments from oxidized crude oil exhibit atomic H/C ratios near 1.0, moderately elevated heteroatom contents compared to the respective >1,050°F resid, and relatively low (<1 wt%) levels of carbonyl and sulfoxide functional groups. Based on the results obtained, it was concluded that oxidative degradation of crude in SPR caverns is of minimal concern.

Introduction

Shortages of crude oil experienced in the 1970's led to establishment of crude oil reserves within the U.S. and other major oil importing nations. The U.S. Strategic Petroleum Reserve (SPR) was authorized by the Energy Policy and Conservation Act signed into law on December 22, 1975. This act provided for storage of more than 500 million barrels of oil that could be readily retrieved and refined in case of a crude oil supply interruption or other emergency.

Since that time, the SPR Headquarters of the U.S. Department of Energy has been actively engaged in preparation, filling, and monitoring of crude oil storage caverns. The caverns are formed in salt deposits located in Texas and Louisiana via solution mining; i.e., by injection of fresh or brackish water to form cavities within a given deposit. Movement of crude oil into or out

of caverns is accomplished by lowering or raising brine levels within each cavern. Periodic monitoring is carried out to ensure that no significant degradation of oil occurs during storage. An overview of the SPR caverns and monitoring program was published previously.[1]

Earlier, a significant effort was expended on determining factors contributing to buildup of minor amounts of an emulsion layer ("sludge") in selected SPR caverns over time. These results were presented in part at the *4th International Conference on Stability and Handling of Liquid Fuels*.[2-5] In short, sludge formation was found to largely result from natural settling phenomena and not from significant chemical or microbial degradation. Workers investigating sludge formed in crude oil stored above ground in Japan implicated asphaltene precipitation, wax precipitation, and oxidative condensation as potential mechanisms/causes for sludge buildup.[6,7]

Although oxidation or oxidative condensation was not found to be a significant factor causing sludge formation in SPR caverns, measurable oxygen infusion into caverns could occur via air dissolved in water used to displace oil in cavern operations as well as from air in purchased crude used to fill caverns. In order to assess the maximum potential for crude oil degradation via oxidation, samples of SPR crudes were aged under severe conditions using the oxygen overpressure storage stability test developed for diesel fuels (ASTM D 5304). Pure oxygen, air and inert atmospheres were employed during the testing. In addition to measurements of insolubles formation resulting from accelerated aging, analyses of aged oils and the insolubles themselves were carried out. The objectives of the work were to determine the extreme upper limit of crude oil degradation possible from storage under high concentrations of oxygen, as well as to obtain a realistic assessment of the potential for crude oil oxidation during long-term storage in SPR caverns under typical conditions (45°C, <10 ppm O_2).

Experimental

Three crude oil samples were selected. One was from a SPR cavern containing a mixture of sweet crude oils (BM113). A second was from another SPR cavern containing a mixture of sour crude oils (BM110). The third sample, from the Naval Petroleum Reserve (NPR1), was of intermediate quality. The storage stability of each sample was evaluated using a modified version of ASTM D 5304 (Standard Test Method for Assessing Distillate Fuel Storage Stability by Oxygen Overpressure). This is a short term test normally used to determine the stability of diesel fuels. The crude oil was filtered at ~85°C rather than the ambient temperature normally used. The isooctane used to rinse the filter was also heated. Heating was required because of the paraffinic nature of the crudes. The samples were stored at 90°C under 100 psig oxygen, air, or nitrogen for 16, 40, and 90 hours.

Filtered aliquots of crude recovered from each storage condition were tested for: specific gravity, carbon residue, acid number, viscosity, heptane insolubles, and loss of light ends via GC simulated distillation. Standard ASTM procedures were used for each test. Particulates obtained after storage were analyzed by infrared spectroscopy. For this analysis, nominal 10 mg/mL dichloromethane solutions were prepared, placed in 0.5 mm KBr cells, and scanned using a conventional dispersive infrared instrument. Determination of sulfoxides from infrared spectra is described elsewhere.[8] Calculation of carbonyl compound types was similar, except that a molar absorptivity of 620 $Lm^{-1}cm^{-1}$ was used. If sufficient quantities of particulate were available, elemental analyses for C, H, N, S, Ni, and V were also performed.

Results

Table 1 summarizes results from the accelerated storage stability tests. Test results are reported for three time periods for each of the three atmospheres (N_2, air, O_2) used. The reported insolubles include adherent (coatings formed on the test vessel) as well as filtered sediments.

Under a pure oxygen atmosphere, each of the crudes produced significant insolubles. However, the crude from the sweet cavern (BM113) required 90 hours to generate insolubles in excess of 1 g/L; it produced significantly less insolubles than the other two crudes at any given condition. The BM110 crude produced much higher levels of insolubles under air than either of the other two crudes. Formation of insolubles under nitrogen was uniformly low for all the crudes.

Table 2 summarizes properties of the vacuum resid (>1,050°F) obtained from each crude. Properties of the resids, instead of the whole crudes, have been selected in this case because most of the precursors for insolubles are present in the >1,050°F fraction. Inspection of the table reveals that the only properties which follow the trends in insoluble formation listed above in Table 1 are vanadium (V) and asphaltene contents. Figures 1 and 2 illustrate correlations between total insolubles formed under the most severe storage condition (90 hours under 100 psig O_2) with vandium and asphaltene contents, respectively. In each figure, V and asphaltene contents are expressed both on whole crude as well as >1,050°F resid bases. For vanadium (Figure 1), a better correlation was obtained whenever results were expressed on a resid basis. For asphaltene content (Figure 2), expression of data on a whole crude basis provided the better correlation.

Correlation of insoluble formation during aging with asphaltene content is not surprising since asphaltenes, by definition, comprise the least soluble components in a given crude. The correlation of insolubles with vanadium content may be fortuitous, since V content often tracks asphaltene content in many crudes. In any case, either parameter may prove useful toward predicting the

oxidation susceptibility and/or storage stability of crude in a given SPR cavern. Further work will be needed to establish the general applicability of either correlation, however.

Tables 3–5 list properties of unaged crudes as well as for liquids recovered from each storage condition. The higher specific gravity (lower API gravity) and higher viscosities (77° and 100°F) observed for the aged crudes can largely be attributed to losses of light ends incurred during storage and handling. Figures 3–5 show correlations of those properties with light end loss for NPR1, BM110, and BM113 crudes, respectively. Out of all the plots shown, only those corresponding to viscosity for BM110 crude (Figure 4) exhibit any significant nonlinearity attributable to compositional changes beyond simple evaporation of volatile constituents. As evident from the larger quantities of insolubles formed from BM110 crude compared to the others (Table 1), its composition may have been altered the most during storage, particularly from aging under pure oxygen.

Figure 6 illustrates insoluble formation under 100 psig oxygen as a function of time for each crude. As noted above, the BM110 crude formed the most insolubles at any given time, in accordance with its higher V and asphaltene contents. Under an oxygen atmosphere, insoluble formation is approximately linear with time for each crude. Figure 7 shows acid number data determined on filtered crudes in Tables 3–5. In contrast to insoluble formation, increases in acid number tended to level off with time, particularly for NPR1 and BM113 crudes. Also, acid number increased the most for the NPR1 crude, which exhibited only intermediate levels of insoluble formation during aging.

Figure 8 shows the relationship between acid number versus insoluble formation for each crude. The exponential increase in insolubles with acid number for NPR1 and BM113 crudes suggests that insoluble formation may be acid catalyzed, or otherwise accelerated. However, the linear relationship evident for BM110 indicates that for it, the two processes occur independently. In any case, it should be borne in mind that acid number may simply coincide with a host of other oxidation-induced compositional changes which have equal or greater effect on insoluble formation.

Tables 6–8 list results from infrared analysis of sediments obtained from determination of insolubles. Table 9 shows elemental analyses of selected sediments. Neither the oxygen nor sulfur contents determined from infrared analysis account for major proportions of the total elemental contents shown in Table 9. This finding in turn indicates that the bulk of sediment S and O exists in other types of functional groups.

In the case of sulfur, most of the total S probably exists in thiophenic structures which are carried more or less incidentally into the sediment through actions of other structural moieties present. The fact that the sediment with the highest sulfoxide content (NPR1, Table 6) contained only moderate levels of total sulfur (2 wt%) illustrates the prevalence of thiophenic or other inert

forms of sulfur in crudes and corresponding sediments. This in turn prevents total sulfur (Table 2) from being a useful predictor of insoluble formation. The very moderate and relatively uniform levels of sulfoxide groups observed in all sediments suggests that their formation via oxidation of sulfide groups is not a key element in the process of insoluble formation.

Similarly, although nitrogen is somewhat enriched in sediments compared to levels in whole >1,050°F resids (by a factor of 2 or less, compare Tables 2 versus 9), its degree of enrichment is similar to that of sulfur—thereby indicating incidental incorporation. However, although total nitrogen does not correlate with insoluble formation, a subset of nitrogen containing-species could conceivably be activated toward insolubles formation (e.g., vanadyl porphyrins).

Incorporation of significant levels of acids (presumably carboxylic acids) in sediment should result in much higher levels of carbonyl groups in sediments than those actually observed in the infrared analyses (Tables 6-8). Although the levels of total oxygen estimated by difference in Table 9 are admittedly approximate, they surpass those determined by infrared by a great enough degree that precipitation of acids or other carbonyl types can effectively be ruled out as the major mechanism for insoluble formation. However, the "catalysis" or promotion of insoluble formation by acids suggested by exponential plots for NPR1 and BM113 crudes in Figure 8 cannot be refuted (or confirmed) by the infrared data.

Discussion

Based on the available data, the most likely mechanism for insoluble formation during crude storage is one where molecular oxygen acts as a free radical initiator, hydrogen acceptor, or otherwise as a promoter of condensation/agglomeration reactions yielding species too large to be soluble in crude oil. Quite likely, reactive species such as phenols undergo oxidative coupling via schemes analogous to that proposed by Mochida, etal.,[6] for crude oil stored above ground, or White, etal.,[9] for coal liquids. The insolubles produced are highly aromatic (H/C~1, see Table 9) and somewhat enriched in heteroatoms compared to the whole >1,050°F resid.

The hypothesis that molecular oxygen "chews up" selected crude oil components to the point where they contain sufficient polar functional groups to become insoluble is totally inconsistent with the experimental data. In fact, direct oxidation of functional groups like sulfides (to sulfoxides) very likely retards insoluble formation by consuming available oxygen in a manner analogous to conventional antioxidant additives. This explains the disproportionately low degree of insolubles formation observed under air compared to pure oxygen (except for BM110 crude, see Table 1), as well as the induction time usually required (except for BM110 crude–see Figure 6).

The exceptional behavior for BM110 crude may result from a deficiency in oxidizable functionalities which could provide it comparable protection to that of the other crudes.

Vanadium or asphaltene contents are useful indicators of a given crude's potential toward insolubles formation. This is likely the case because both of these parameters indicate/correlate with levels of large molecules with inherently lower solubility in crude oil.

Finally, the "problem" of insolubles formation during crude oil storage should be placed into perspective. First, the highest level of insolubles observed was 23 g/L, or approximately 2.5 wt%. This result was obtained under a completely unrealistic condition of 100 psig (115 psia) pure O_2. The dissimilarity of insolubles produced from diesel fuel at such extreme conditions of temperature and oxygen partial pressure to those formed under actual long-term storage was noted earlier by Power and Davidson.[10] Secondly, the likelihood of achieving even a 1 psia oxygen partial pressure inside a SPR cavern is extremely remote. As noted above, most crudes are capable of consuming moderate levels of oxygen, through sulfoxide formation and analogous mechanisms, with no formation of insolubles. By far, the conditions employed here which best represent actual crude storage in SPR caverns are those employing inert (N_2) gas. Therefore, the impact of oxidation or oxidative coupling on crude oil composition or insolubles formation over time periods of even several decades should be negligible. This finding is in agreement with earlier studies of sludge formation and composition which indicated the absence of significant chemical or microbial degradation of SPR crude in storage.[2-5]

Acknowledgment. This work was supported by the U.S. Department of Energy, SPR Headquarters. The authors thank Susan Howard and Cheryl Dickson for manuscript and figure preparation, respectively.

References

(1) Giles, H. N.; Koenig, J. W. J.; Neihof, R. A.; Shay, J. Y.; Woodward, P. W. *Energy Fuels* **1991**, *5*, 602–608.

(2) Green, J. B.; Woodward, P. W.; Thomson, J. S.; Shay, J. Y.; Giles, H. N. In *Proceedings of the 4th International Conference on Stability and Handling of Liquid Fuels*; Giles, H. N., Ed.; vol. 1, DOE/CONF-911102; NTIS: Springfield, VA, 1992; pp 50–64.

(3) Thomson, J. S.; Grigsby, R. D.; Doughty, D. A.; Woodward, P. W.; Giles, H. N. *ibid*, pp 65–78.

(4) Green, J. B.; Yu, S. K.-T.; Woodward, P. W.; Giles, H. N. *ibid*, pp 79–93.

(5) Bryant, R. S.; Chase, K. L.; Stepp, A. K. *ibid*, pp 94–108.

(6) Mochida, I.; Sakanishi, K.; Fujitsu, H. *Oil Gas J.* **1986**, *Nov. 17*, 58–63.

(7) Hara, T. In *Proceedings of the 2nd International Conference on Long-term Storage Stabilities of Liquid Fuels*; Stavinoha, L. L., Ed.; vol. 1, Southwest Research Institute: San Antonio, TX, 1986; pp 1–12.

(8) Green, J. B.; Yu, S. K.-T.; Pearson, C.D.; Reynolds, J. W. *Energy Fuels* **1993**, *7*, 119–126.

(9) White, C. M.; Jones, L.; Li, N. C. *Fuel* **1983**, *62*, 1397–1403.

(10) Power, A. J., Davidson, R. G. *Fuel* **1986**, *65*, 1753–1755.

Table 1. Storage Stability of Crude Oil Aged at 90°C under 100 psig Gas Pressure

Crude	Aging Time (hours)	Total Insolubles (g/L)		
		Nitrogen	Air	Oxygen
NPR1 (94SPR021)	16	0.03	<0.01	0.26
	40	<0.01	0.06	5.7
	90	0.10	0.15	15
BM113 (95SPR094–095)	16	0.07	0.08	0.17
	40	0.07	0.12	0.41
	90	0.06	0.27	2.3
BM110 (95SPR027–028)	16	0.29	0.22	4.9
	40	0.33	3.1	9.1
	90	0.22	6.7	23

Table 2. Properties of Vacuum Resids (>1,050°F)

Crude	NPR1 (94SPR021)	BM113 (95SPR094–095)	BM110 (95SPR027–028)
>1,050°F resid[a]			
wt%	13.4	13.1	18.5
vol%	11.1	11.2	15.4
API Gravity	6.1	10.8	5.3
wt% S	1.58	1.19	3.61
wt% N	1.55	0.68	0.57
MCR, wt%	25.2	14.6	24.3
Viscosity, cSt			
180°F	235,682	2,844	45,470
210°F	33,861	885	8,458
Metals, ppm			
Ni	201	27.2	73.5
V	218 (29.2)[a]	32.0 (4.2)[a]	318 (58.8)[a]
Fe	138	10.4	5.1
C_7-asphaltenes, wt%	11.9 (1.6)[a]	3.85(0.50)[a]	14.1(2.6)[a]

[a] Yield or concentration on a whole crude basis.

Table 3. Properties of NPR1 Crude as a Function of Aging

Aging time	0 hours		16 Hours			40 Hours			90 Hours		
Atmosphere	U[a]	F[b]	N_2	Air	O_2	N_2	Air	O_2	N_2	Air	O_2
Specific gravity 60/60°F	0.852	0.877	0.886	0.885	0.888	0.883	0.888	0.887	0.882	0.884	0.885
API° gravity	34.5	29.9	28.2	28.4	27.8	28.8	27.9	28.0	28.9	28.6	28.4
Carbon residue, wt%	3.53		3.82	3.89	4.25	3.78	3.87	4.13	3.50	3.81	3.77
Acid number, mg KOH/g	0.22		0.25	0.29	0.90	0.25	0.40	1.80	0.25	0.53	2.50
Viscosity, cSt @ 77°F	5.93	13.37	19.22	20.27	21.34	17.04	22.75	24.02	21.10	20.57	20.17
Viscosity, cSt @ 100°F	4.37	8.33	11.55	11.11	12.55	10.39	12.53	12.09	9.91	10.88	11.42
C_7-asphaltenes, wt%			1.46	2.43	3.45	2.32	2.82	3.11	1.50	2.57	2.89
Distilled, % @ 200°F	8	2	1	1	1	1	<1	1	1	1	1
Distilled, % @ 300°F	21	13	9	10	9	11	9	9	10	9	10
Estimated light end loss, %	0	7	12	11	12	10	12	12	11	12	11

[a] Unfiltered
[b] Filtered

Table 4. Properties of BM113 (Sweet) Crude as a Function of Aging

Aging time	0 hours		16 Hours			40 Hours			90 Hours		
Atmosphere	U[a]	F[b]	N_2	Air	O_2	N_2	Air	O_2	N_2	Air	O_2
Specific gravity 60/60°F	0.846	0.869	0.873	0.878	0.877	0.875	0.876	0.879	0.876	0.877	0.878
API° gravity	35.7	31.3	30.5	29.7	29.8	30.3	30.0	29.4	30.1	29.8	29.7
Carbon residue, wt%	2.20	2.58	2.56	2.72	2.79	2.57	2.73	2.84	2.60	2.86	2.84
Acid number, mg KOH/g	0.09	0.09	0.10	0.14	0.33	0.10	0.28	0.65	0.10	0.53	0.95
Viscosity, cSt @ 77°F	7.20	14.21	16.05	19.49	24.09	20.51	18.55	21.03	19.05	19.63	19.02
Viscosity, cSt @ 100°F	4.88	8.98	10.31	12.11	12.06	11.07	11.33	12.78	11.76	11.77	12.10
C_7-asphaltenes, wt%	0.96	0.71	0.50	0.77	0.47	0.34	0.53	0.67	0.38	0.64	0.51
Distilled, % @ 200°F	8	2	1	<1	<1	<1	<1	<1	<1	<1	<1
Distilled, % @ 300°F	18	9	7	5	6	6	5	5	6	6	6
Estimated light end loss, %	-	9	11	13	12	12	13	13	12	12	12

[a] Unfiltered
[b] Filtered

Table 5. Properties of BM110 (Sour) Crude as a Function of Aging

Aging time	0 hours		16 Hours			40 Hours			90 Hours		
Atmosphere	U[a]	F[b]	N_2	Air	O_2	N_2	Air	O_2	N_2	Air	O_2
Specific gravity 60/60°F	0.864	0.886	0.895	0.898	0.897	0.894	0.901	0.902	0.896	0.904	0.897
API° gravity	32.3	28.2	26.6	26.0	26.2	26.7	25.5	25.3	26.4	25.0	26.2
Carbon residue, wt%	4.57	5.12	5.44	5.70	5.58	5.35	5.64	5.29	5.41	5.67	4.94
Acid number, mg KOH/g	0.11	0.13	0.16	0.13	0.34	0.16	0.29	0.63	0.16	0.40	1.17
Viscosity, cSt @ 77°F	11.53	20.11	28.69	32.17	31.97	27.56	37.51	39.17	29.79	45.40	32.84
Viscosity, cSt @ 100°F	7.33	12.86	17.41	19.74	19.42	16.77	22.69	23.67	17.98	26.81	19.94
C_7-asphaltenes, wt%	1.78	2.04	1.32	2.97	3.30	2.61	3.76	2.87	1.79	4.65	2.01
Distilled, % @ 200°F	7	1	<1	<1	<1	<1	<1	<1	<1	<1	<1
Distilled, % @ 300°F	16	8	4	4	3	5	2	2	3	1	3
Estimated light end loss, %	-	8	12	12	13	11	14	14	13	15	13

[a] Unfiltered
[b] Filtered

Table 6. Infrared Analysis of Sediments from Aged NPR1 Crude

Aging time (hours)	Atmosphere	Carbonyl oxygen (wt%)			Sulfoxide sulfur (wt%)
		Ketone type	Amide type	Total	
0	-	0.06	0.14	0.20	0.12
16	N_2	0.24	0.45	0.69	0.61
40	N_2	0.20	0.32	0.52	0.33
90	N_2	0.18	0.37	0.55	0.29
16	air	0.29	0.39	0.68	0.46
40	air	0.32	0.41	0.73	0.56
90	air	0.38	0.42	0.80	0.51
16	O_2	0.43	0.47	0.90	0.88
40	O_2	0.45	0.42	0.87	0.92
90	O_2	0.57	0.50	1.07	0.86

Table 7. Infrared Analysis of Sediments from Aged BM113 Crude

Aging time (hours)	Atmosphere	Carbonyl oxygen (wt% O)			Sulfoxide sulfur (wt% S)
		Ketone type	Amide type	Total	
0	-	ins[a]			
16	N_2	ins[a]			
40	N_2	ins[a]			
90	N_2	ins[a]			
16	air	ins[a]			
40	air	ins[a]			
90	air	0.45	0.28	0.73	0.42
16	O_2	0.40	0.32	0.72	0.31
40	O_2	0.43	0.32	0.75	0.34
90	O_2	0.51	0.36	0.87	0.54

[a] Insufficient sediment available for analysis.

Table 8. Infrared Analysis of Sediments from Aged BM 110 Crude

Aging time (hours)	Atmosphere	Carbonyl oxygen (wt% O)			Sulfoxide sulfur (wt% S)
		Ketone type	Amide type	Total	
0	-	0.10	0.19	0.29	0.19
16	N_2	0.07	0.18	0.25	0.23
40	N_2	0.08	0.17	0.25	0.21
90	N_2	0.08	0.19	0.27	0.23
16	air	0.17	0.21	0.38	0.19
40	air	0.22	0.21	0.43	0.25
90	air	0.25	0.25	0.50	0.41
16	O_2	0.23	0.23	0.46	0.26
40	O_2	0.28	0.25	0.53	0.53
90	O_2	0.45	0.33	0.78	0.60

Table 9. Elemental Analysis of Selected Sediments (wt%)

Crude	Aging Condition	C	H	N	S	O[a]
NPR1	40 hrs-O_2	82.3	7.96	1.66	2.00	6.1
NPR1	90 hrs-O_2	82.3	7.92	1.67	2.07	6.0
BM113	90 hrs- O_2	81.7	7.13	0.952	2.05	8.2
BM110	40 hrs-air	77.0	6.87	0.870	5.07	10.2
BM110	40 hrs-O_2	81.1	7.03	1.048	5.63	5.2
BM110	90 hrs- O_2	80.0	6.85	0.914	5.70	6.5

[a] O calculated by difference.

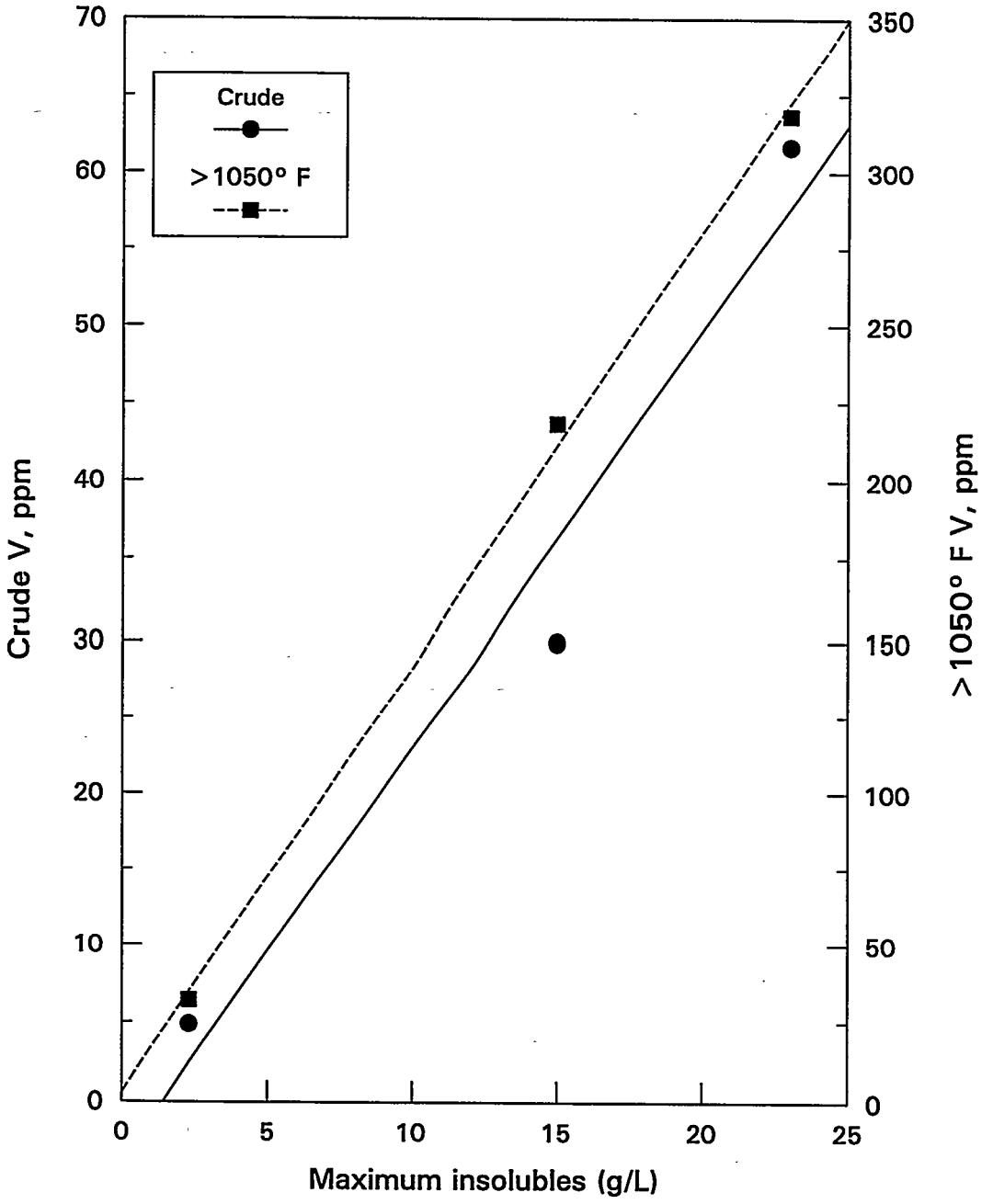


Figure 1. Correlation of maximum formation of insolubles (90 hrs, 100 psig oxygen) with vanadium content

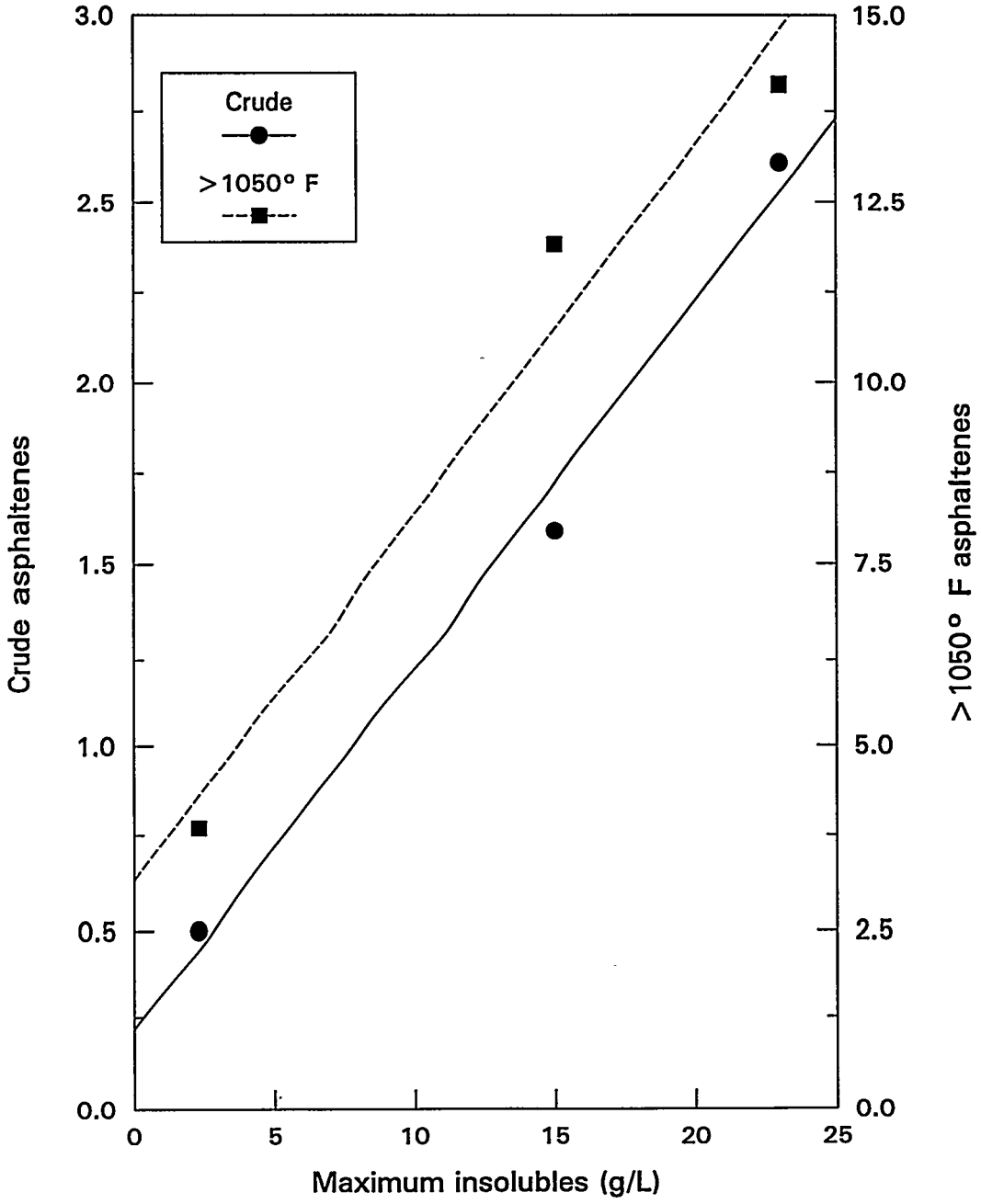


Figure 2. Correlation of maximum formation of insolubles (90 hrs, 100 psig oxygen) with asphaltene (heptane) content

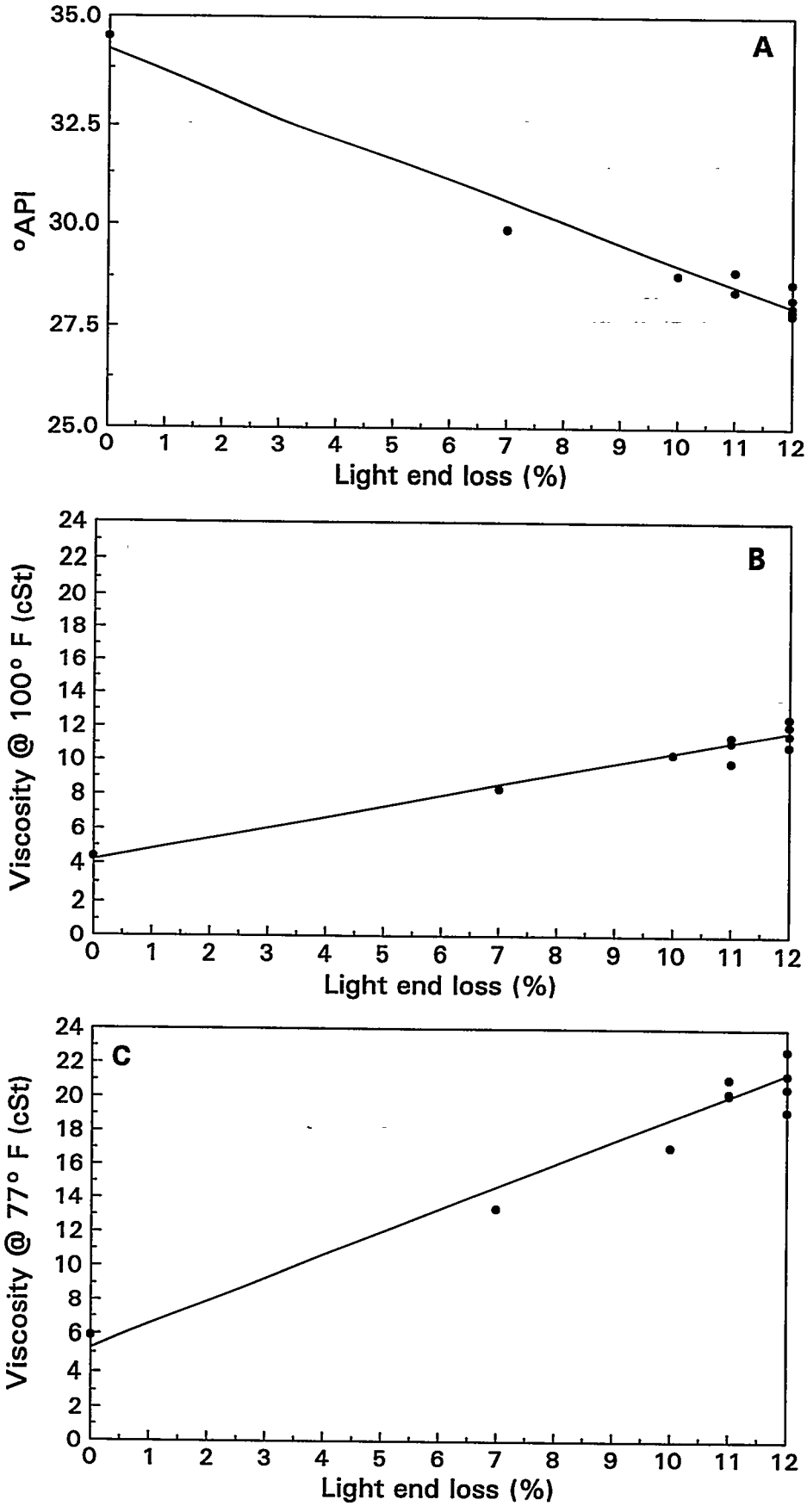


Figure 3. Correlations of light end loss with gravity and viscosity - NPR1

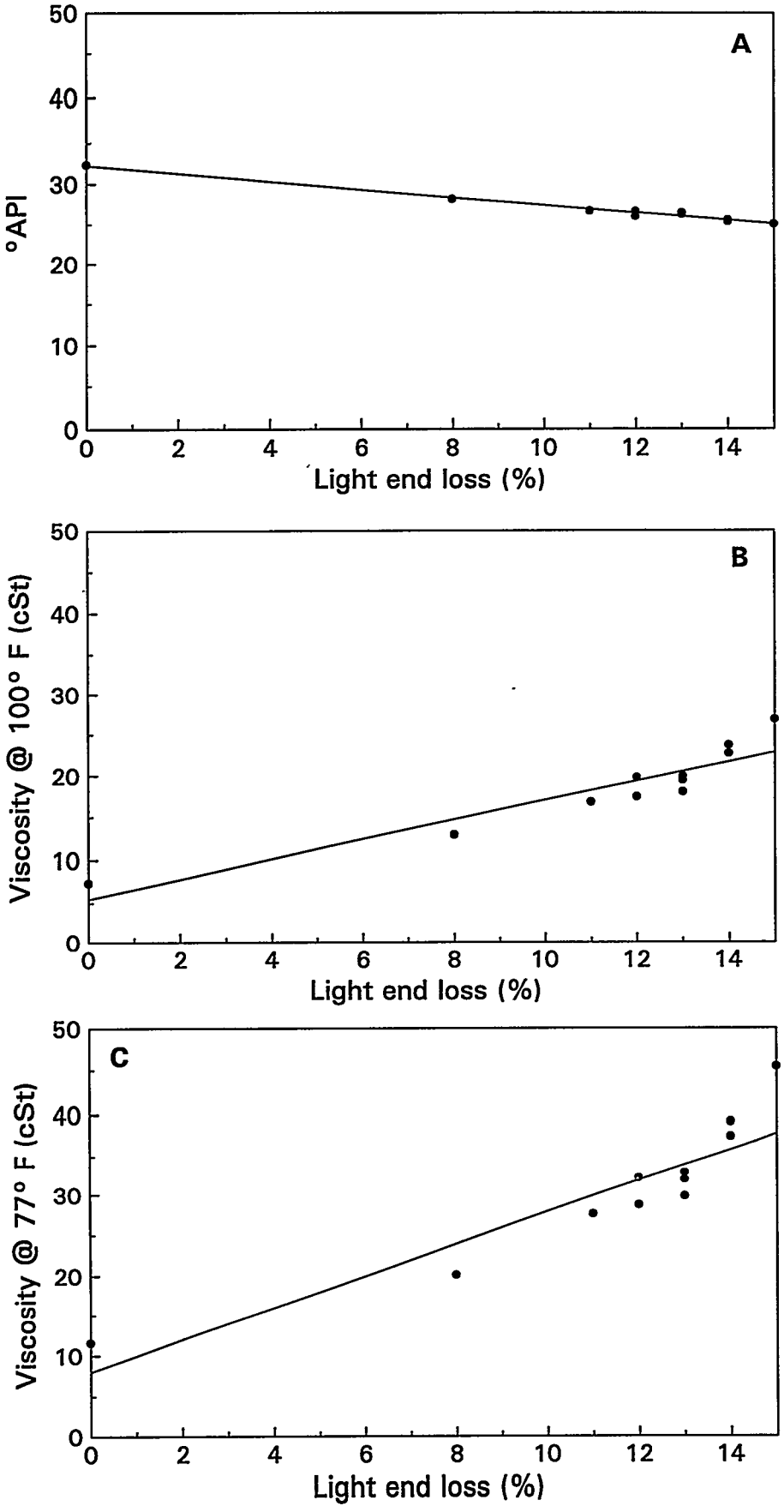


Figure 4. Correlations of light end loss with gravity and viscosity - BM110

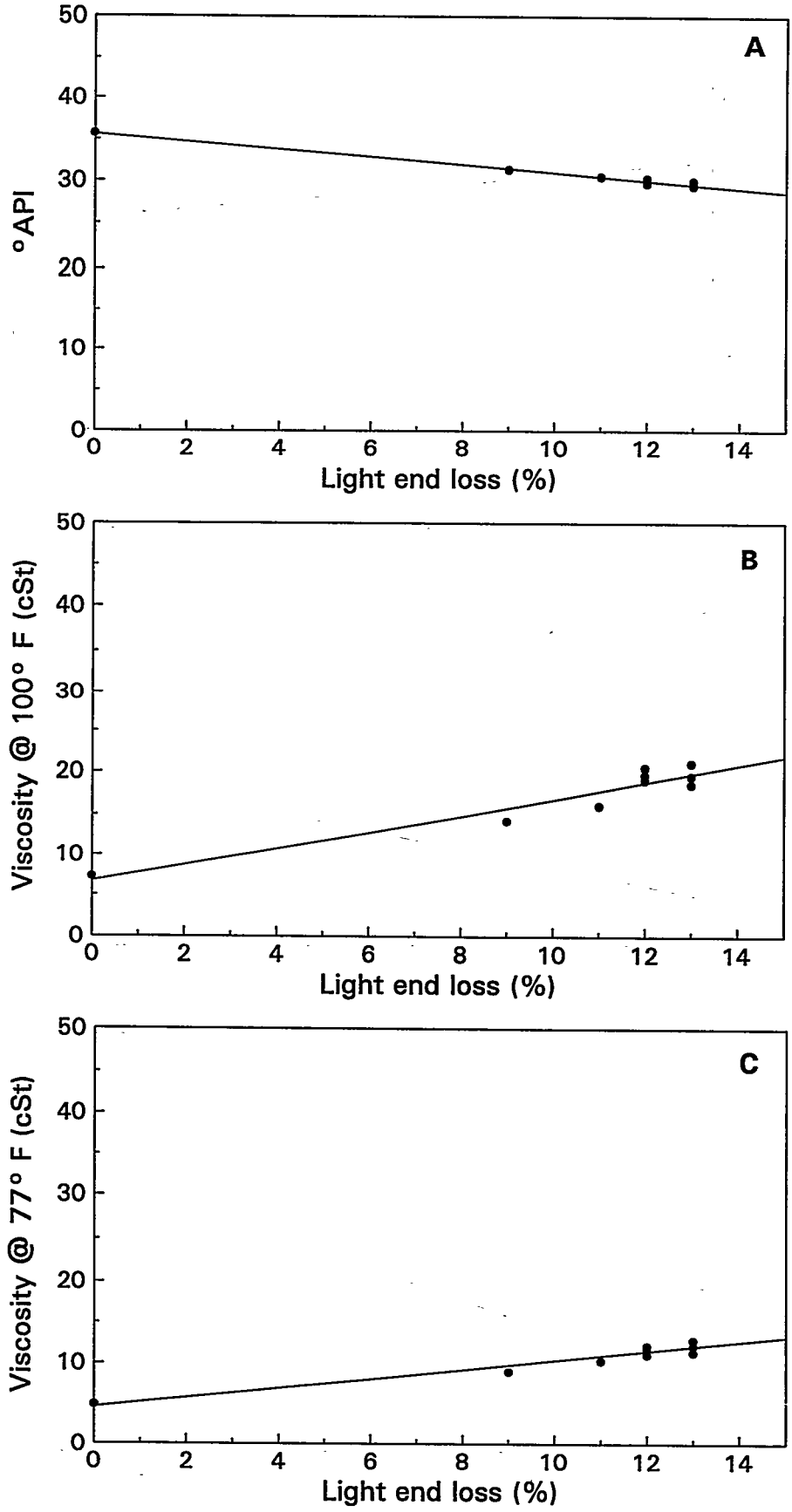


Figure 5. Correlations of light end loss with gravity and viscosity - BM113

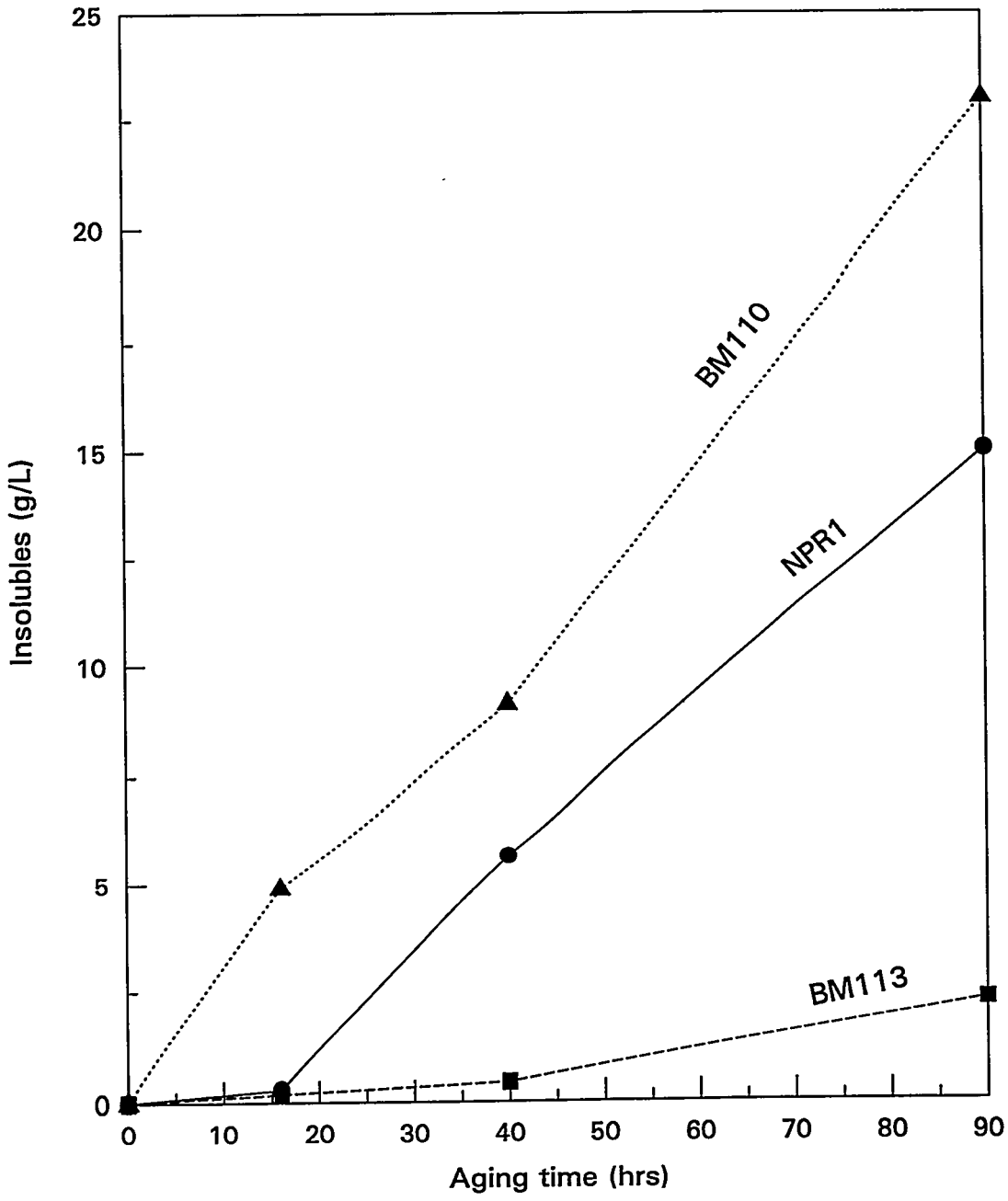


Figure 6. Formation of insolubles at 90° C, 100 psig oxygen as a function of time

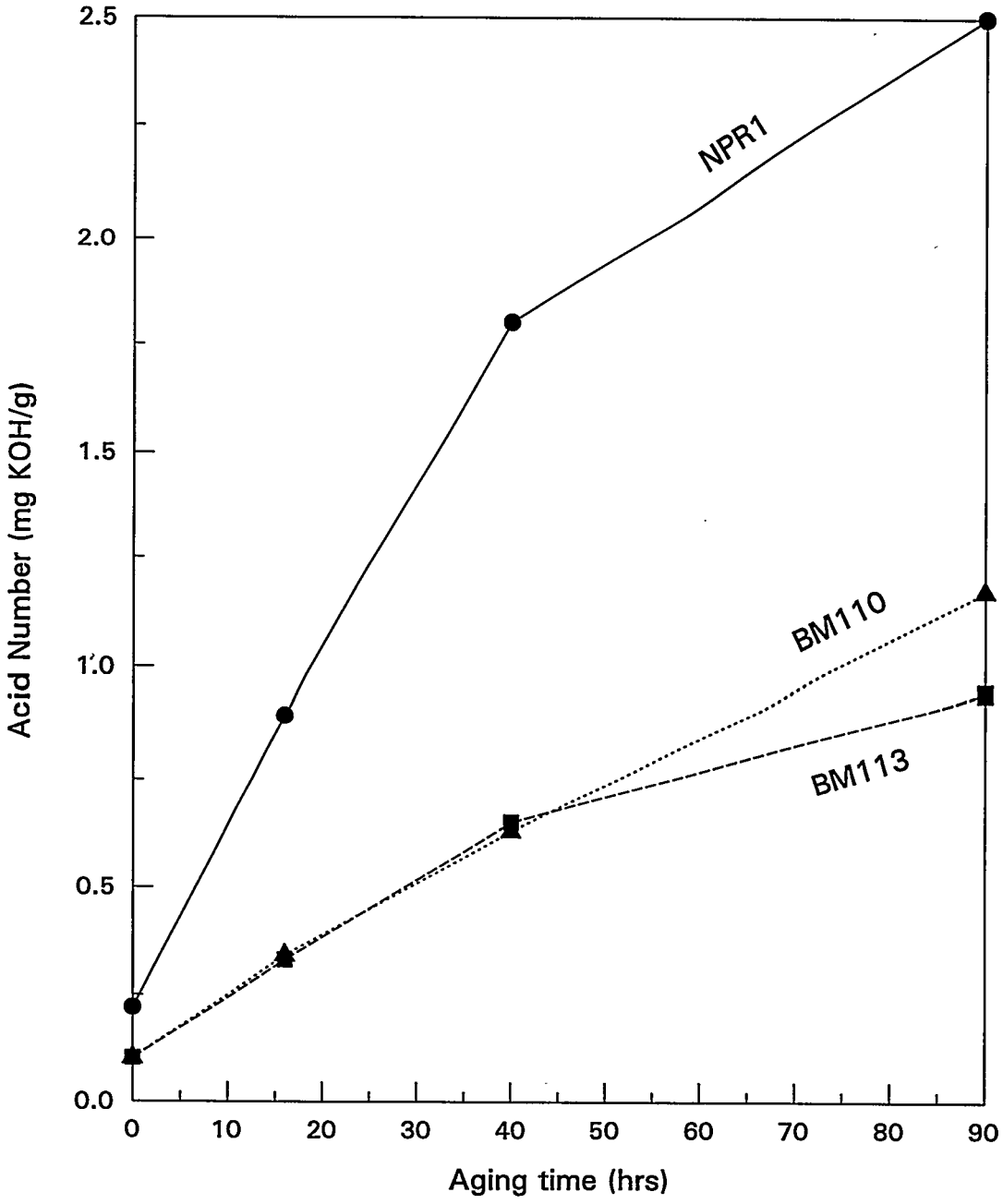


Figure 7. Increase in acid number with aging at 90° C, 100 psig oxygen

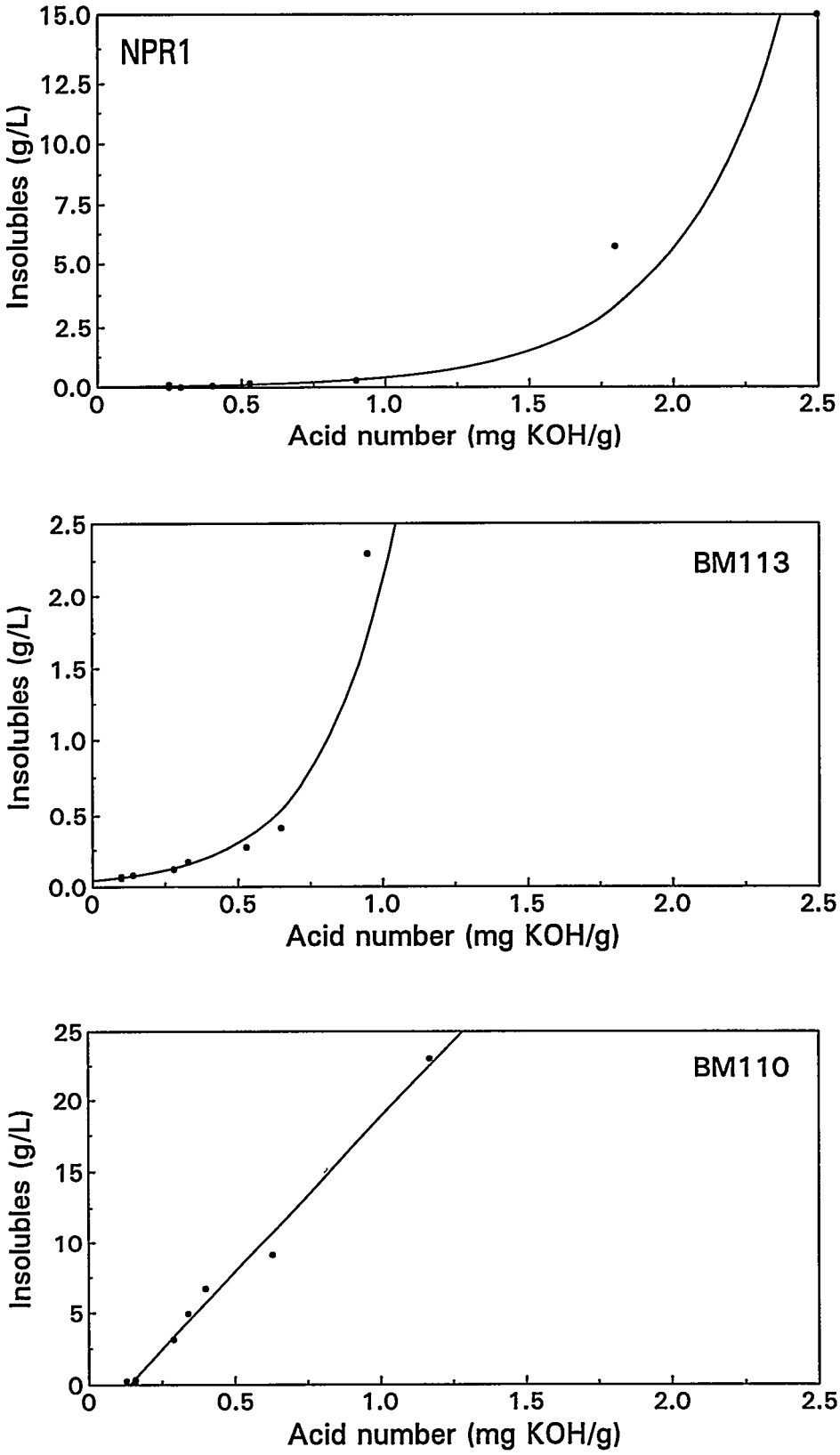


Figure 8. Correlation between acid number and formation of insolubles